



University
of Glasgow

<https://theses.gla.ac.uk/>

Theses Digitisation:

<https://www.gla.ac.uk/myglasgow/research/enlighten/theses/digitisation/>

This is a digitised version of the original print thesis.

Copyright and moral rights for this work are retained by the author

A copy can be downloaded for personal non-commercial research or study,
without prior permission or charge

This work cannot be reproduced or quoted extensively from without first
obtaining permission in writing from the author

The content must not be changed in any way or sold commercially in any
format or medium without the formal permission of the author

When referring to this work, full bibliographic details including the author,
title, awarding institution and date of the thesis must be given

Enlighten: Theses

<https://theses.gla.ac.uk/>
research-enlighten@glasgow.ac.uk

DEGRADATION OF POLYMERS

BASED ON

STYRENE AND BUTADIENE.

by

WILLIAM THOMAS KIRKWOOD STEVENSON

A thesis submitted in partial fulfilment of the requirements
for the degree of PHILOSOPHIAE DOCTOR in the Faculty of
Science at the University of Glasgow, Scotland.

NOVEMBER 1980

SUPERVISOR : DR. I.C. M^CNEILL

ProQuest Number: 10984231

All rights reserved

INFORMATION TO ALL USERS

The quality of this reproduction is dependent upon the quality of the copy submitted.

In the unlikely event that the author did not send a complete manuscript and there are missing pages, these will be noted. Also, if material had to be removed, a note will indicate the deletion.



ProQuest 10984231

Published by ProQuest LLC (2018). Copyright of the Dissertation is held by the Author.

All rights reserved.

This work is protected against unauthorized copying under Title 17, United States Code
Microform Edition © ProQuest LLC.

ProQuest LLC.
789 East Eisenhower Parkway
P.O. Box 1346
Ann Arbor, MI 48106 – 1346

FOREWORD

The work described was carried out between October, 1977 and October, 1980 in the Physical Chemistry department, which is under the general supervision of Professor G.A. SIM, and was supported during this period by a grant award to the author by the Science Research Council.

ACKNOWLEDGEMENTS

I am grateful to my supervisor Doctor I.C. M^CNeill for his firm yet restrained guidance which enabled me to express myself freely, extend my capabilities, and enjoy myself within a very carefully planned programme of research.

I would also like to thank Messrs. J. Gorman and G. M^CCuuloch for their sound technical assistance.

Finally, I would like to thank my wife, Laura, without whom none of this would have been possible.

SUMMARY

This discussion is concerned with the preparation, characterisation and subsequent degradation of some high polymers based on styrene and butadiene. It also considers some refinements to existing high vacuum techniques of thermal analysis and in addition, the development of a set of techniques able to identify and manipulate quantitatively the noncondensable product fraction associated with thermal degradation under open pumping conditions of polymer systems.

It was observed that the degree of adsorption of noncondensable gases, which could be produced in the thermal decomposition of polymer systems, onto synthetic zeolites held at -196°C , was a function of the nature of the gas. This led to the development of the Adsorption Thermal Volatilisation Analysis (ATVA) technique which is used to fractionate noncondensable gases in a manner analogous to that of the established TVA technique for condensable gas analysis. It was found that the condensed gas fraction could be quantitatively manipulated by using molecular sieve to pump it from one location to another. This effect was used to collect material for quantitative analysis by i.r. spectroscopy.

Polystyrene, polybutadiene and a 50/50 by weight A/B block copolymer of the two monomers were prepared under vacuum by anionic polymerisations at near ambient temperatures. Polymerisations were initiated by organolithiums and performed in inert solvent under the dry conditions required of this type of work.

Both polymers were degraded in the absence of oxygen isothermally at 380°C and under conditions of programmed temperature rise. The usual thermoanalytical techniques were applied to the problem and extensive product analyses were performed to ascertain the mechanisms of, and rate profiles of, the thermal degradation

processes. In particular, the hitherto uninvestigated high temperature decomposition reactions of polybutadiene were characterised and a reaction sequence able to explain the experimental data was postulated.

The 50/50 block copolymer was degraded in a similar manner and the same analyses performed with a view to comparing its degradative behaviour with that of the corresponding polymer blend system and the homopolymer mixture with no interaction. The block copolymer was found to be considerably more stable to volatilisation than both of the other systems. This extra stability was shown to be associated with the polystyrene portion of the system which was stabilised by radical transfer to a range of volatile materials produced in both the decomposition reactions of the polybutadiene component of the system.

Polystyrene was shown to give less volatile material when degraded under closed system conditions in the presence of 4-vinylcyclohexene - a typical product of the low temperature volatilisation reaction of polybutadiene. 4-Vinylcyclohexene and cyclised rubber - the cold ring product fraction produced in high temperature decompositions of polybutadiene were shown by the usual dilatometric techniques to be able to take part in chain transfer processes with the polystyryl radical.

Polybutadiene was modified by reaction with oxygen in the temperature range 0 - 300°C. The residue of oxidative degradation was examined and subjected to thermal degradation in an attempt to ascertain the mechanisms operative in the oxidation of the pure polymer and in the thermal degradation of oxidised polymer. A range of analyses were performed and it was concluded that, on a qualitative basis, the mechanisms of oxidation are insensitive to the temperature of oxidation in the range 0 - 300°C. The oxidation

reaction was shown to introduce to the polymer material which thermally decomposed in a reproducible manner to yield a range of oxygenated products. Mechanisms of oxidation and thermal degradation consistent with the experimental data were postulated.

The following conventions will be observed :-

(1). References to published material will be numbered consecutively.

A list of references is included at the end of the discussion.

(2). A reference to a figure contained in the same Chapter will be given in the form fig. y, where y is the figure number. A reference to a figure contained in another Chapter will be given in the form fig. x - y, where x is the Chapter number and y is the figure number.

(3). A reference to a Table will be in the form Table y or Table x - y where x and y are as in (2) above.

CONTENTS

	<u>PAGE</u>
<u>CHAPTER 1 INTRODUCTION</u>	1
A THE COMMERCIAL DEVELOPMENT OF POLYMERS BASED ON STYRENE AND BUTADIENE	1
B DEGRADATION OF POLYMERS	4
(i). GENERAL CONSIDERATIONS	4
(ii). MECHANISMS OF THERMAL DEGRADATION	5
(iii). THERMAL DEGRADATION OF POLYMER BLEND SYSTEMS	6
C AIMS OF THIS WORK	7
 <u>CHAPTER 2 ANALYTICAL TECHNIQUES</u>	 8
A TECHNIQUES OF THERMAL ANALYSIS	8
1. THERMAL VOLATILISATION ANALYSIS (TVA)	8
2. DIFFERENTIAL CONDENSATION TVA	10
3. PRODUCT FRACTIONATION IN THE TVA EXPERIMENT	12
4. OVEN ASSEMBLY	13
5. OVEN CALIBRATION	15
6. SAMPLE PREPARATION AND SIZE	15
7. SUB-AMBIENT THERMAL VOLATILISATION ANALYSIS (SATVA)	18
8. THERMOGRAVIMETRY (TG)	23
9. DIFFERENTIAL SCANNING CALORIMETRY (DSC)	24
10. PYROLYSIS GLC	24
B TECHNIQUES OF SEPARATION	25
1. GAS LIQUID CHROMATOGRAPHY (GLC)	25

	<u>PAGE</u>
2. PREPARATIVE THIN LAYER CHROMATOGRAPHY	28
C SPECTROSCOPIC TECHNIQUES	29
1. INFRARED (i.r.) SPECTROSCOPY	29
2. PROTON MAGNETIC RESONANCE (^1H n.m.r.)	
SPECTROMETRY	31
3. ULTRA-VIOLET (u.v.) SPECTROMETRY	32
4. MASS SPECTROMETRY	32

CHAPTER 3 ADSORPTION THERMAL VOLATILISATION

	<u>ANALYSIS (ATVA)</u>	34
A	INTRODUCTION AND LITERATURE REVIEW	34
1.	PREPARATION AND STRUCTURE OF SYNTHETIC	
	ZEOLITES	35
2.	ZEOLITE ACTIVATION	36
3.	ADSORPTION ISOTHERMS	36
4.	PUMPING SPEEDS	39
B	EXPERIMENTAL	41
1.	ADSORPTION AND DESORPTION OF STATIC GAS	
	VOLUMES AT SUB-AMBIENT TEMPERATURES	41
2.	DYNAMIC ADSORPTIVE BEHAVIOUR	47
3.	GAS GENERATION	49
4.	EXAMINATION OF CONDENSED MATERIAL	50
5.	QUANTITATIVE ANALYSIS OF CARBON MONOXIDE	51
(i).	DECOMPOSITION OF OXALIC ACID	51
(ii).	QUANTITATIVE ANALYSIS OF CARBON DIOXIDE	51
(iii).	SMALL VOLUMES BY GAS EXPANSION	53
(iv).	CONDITIONS OF DEGRADATION	55
(v).	PRODUCT SEPARATION AND ANALYSIS	55
(vi).	CELL CALIBRATION	57

6.	ATVA CURVES FOR NONCONDENSABLES USING 5A MOLECULAR SIEVE	60
 <u>CHAPTER 4 POLYMER PREPARATION AND CHARACTERISATION</u>		78
A	INTRODUCTION AND LITERATURE REVIEW	78
B	EXPERIMENTAL	82
1.	VACUUM MANIFOLD DESIGN AND OPERATION	82
2.	CLEANING OF GLASSWARE	84
3.	REMOVAL OF CHEMICALLY ADSORBED WATER	84
4.	REAGENT AGITATION	84
5.	LEAK DETECTION	85
6.	n-HEXANE MANIPULATION	85
7.	STYRENE MANIPULATION	87
8.	BUTADIENE MANIPULATION	88
9.	sec-BUTYLLITHIUM MANIPULATION	91
10.	POLYMERISATION PROCEDURE	92
C	POLYMER CHARACTERISATION	96
1.	OSMOMETRY	96
2.	INFRARED (i.r.) SPECTROMETRY	96
3.	PROTON MAGNETIC RESONANCE SPECTROMETRY	101
4.	ULTRA-VIOLET (u.v.) SPECTROMETRY	105
5.	POLYMER CHARACTERISATION	105
(i).	POLYSTYRENE	105
(ii).	POLYBUTADIENE (LOW MOLECULAR WEIGHT)	106
(iii).	POLYBUTADIENE (MODERATE MOLECULAR WEIGHT)	106
(iv).	DIBLOCK COPOLYMER	107

<u>CHAPTER 5</u>	<u>POLYSTYRENE DEGRADATION</u>	108
A	LITERATURE REVIEW	108
B	PROGRAMMED DEGRADATIONS	114
1.	TG UNDER NITROGEN	114
2.	DSC UNDER NITROGEN	114
3.	TVA	114
C	PRODUCT ANALYSIS (PROGRAMMED AND ISOTHERMAL DEGRADATIONS)	118
1.	VOLATILE PRODUCT ANALYSIS	118
2.	COLD RING PRODUCT ANALYSIS	120
D	ISOTHERMAL DEGRADATIONS AT 380°C	127
1.	INTRODUCTION AND DESCRIPTION OF APPARATUS	127
2.	EXPERIMENTAL RESULTS	129
(1).	TG UNDER NITROGEN	129
(11).	TVA	129
(111).	GRAVIMETRIC ANALYSIS UNDER VACUUM	131
3.	DISCUSSION	131

<u>CHAPTER 6</u>	<u>POLYBUTADIENE DEGRADATION</u>	135
A	INTRODUCTION AND LITERATURE REVIEW	135
B	PROGRAMMED DEGRADATIONS	141
1.	TG OF POLYBUTADIENE A UNDER NITROGEN	141
2.	DSC OF POLYBUTADIENE A UNDER NITROGEN	141
3.	TVA OF POLYBUTADIENE A	144
4.	ATVA OF POLYBUTADIENE A	147
C	PRODUCT DISTRIBUTION IN PROGRAMMED DEGRADATIONS	150
1.	VOLATILE PRODUCT DISTRIBUTION IN PROGRAMMED DEGRADATIONS	150

(i).	SATVA OF VOLATILE PRODUCTS OF PROGRAMMED DEGRADATIONS	150
(ii).	GLC SEPARATION OF VOLATILE PRODUCTS OF PROGRAMMED DEGRADATION	155
(iii).	VOLATILE PRODUCT IDENTIFICATION BY n.m.r. SPECTROSCOPY	155
2.	COLD RING FRACTION OF PROGRAMMED DEGRADATIONS	155
3.	RESIDUES OF PROGRAMMED DEGRADATIONS	162
D	MECHANISMS OF DEGRADATION	167
1.	THE EXOTHERMIC DECOMPOSITION REACTION	167
2.	THE ENDOTHERMIC DECOMPOSITION REACTION	174
E	ISOTHERMAL DEGRADATION AT 380°C	178
1.	TVA OF POLYBUTADIENE A	178
2.	TG OF POLYBUTADIENE A UNDER NITROGEN	178
3.	THE RESIDUE OF DEGRADATION	178
4.	VOLATILE PRODUCTS OF DEGRADATION	181
5.	THE COLD RING FRACTION OF DEGRADATION	181
6.	MECHANISMS OF DEGRADATION	181
7.	GRAVIMETRIC ANALYSIS UNDER VACUUM	186
<u>CHAPTER 7</u>	<u>THERMAL DEGRADATION OF BLOCK COPOLYMER</u>	188
	INTRODUCTION	188
7 - 1	PROGRAMMED DEGRADATION	189
A1	TG UNDER NITROGEN	189
A2	DSC UNDER NITROGEN	189
A3	TVA	193
A4	ATVA	196
B	VOLATILE PRODUCT FORMATION IN PROGRAMMED DEGRADATIONS	199

B1	SUB-AMBIENT TVA FRACTIONATION OF THE CONDENSABLE VOLATILE PRODUCT FRACTION OF DEGRADATION	199
B2	YIELDS OF STYRENE DURING PROGRAMMED DEGRADATIONS (BY GLC)	199
C	COLD RING PRODUCT FRACTION OF PROGRAMMED DEGRADATIONS	203
D	RESIDUE OF PROGRAMMED DEGRADATIONS TO 450°C	209
E	DISCUSSION	211
7 - 2	ISOTHERMAL DEGRADATION AT 380°C	215
A1	ISOTHERMAL TG UNDER NITROGEN	215
A2	ISOTHERMAL TVA	215
A3	GRAVIMETRIC ANALYSIS UNDER VACUUM	215
B	VOLATILE PRODUCTS OF ISOTHERMAL DEGRADATION AT 380°C	220
C	COLD RING PRODUCT FRACTION OF ISOTHERMAL DEGRADATION AT 380°C	226
D	RESIDUE OF ISOTHERMAL DEGRADATION AT 380°C	231
E	DISCUSSION	232

CHAPTER 8 POLYSTYRENE DEGRADATIONS IN THE PRESENCE
 OF 4-VINYLCYCLOHEXENE

		235
A	INTRODUCTION	235
B	EXPERIMENTAL	236
1.	REACTOR DESIGN AND OPERATION	236
2.	QUALITATIVE PRODUCT DISTRIBUTION	241
3.	QUANTITATIVE VOLATILE PRODUCT ANALYSIS	243

4.	SEMI-QUANTITATIVE ANALYSIS OF RESIDUAL MATERIAL	243
C	DISCUSSION	250

<u>CHAPTER 9</u>	<u>CHAIN TRANSFER TO 4-VINYLCYCLOHEXENE</u>	252
A	INTRODUCTION AND LITERATURE REVIEW	252
B	EXPERIMENTAL	257
1.	REAGENT PREPARATION AND PURIFICATION	257
2.	CONDITIONS OF POLYMERISATION	257
C	DISCUSSION	259

<u>CHAPTER 10</u>	<u>BULK DECOMPOSITION OF AZOBISISOBUTYRONITRILE</u>	264
A	INTRODUCTION AND LITERATURE REVIEW	264
B	PROGRAMMED OPEN SYSTEM DEGRADATIONS	268
1.	DSC AND TG UNDER NITROGEN	268
2.	TVA	268
3.	PRODUCT DISTRIBUTION	268
C	ISOTHERMAL OPEN SYSTEM DEGRADATIONS AT 90°C	273
1.	TG UNDER NITROGEN	273
2.	TVA	273
3.	PRODUCT DISTRIBUTION	273
D	PYROLYSIS - GLC	276
E	ISOTHERMAL CLOSED SYSTEM DECOMPOSITIONS AT 90°C	278
1.	PROCEDURE	278
2.	QUALITATIVE PRODUCT DISTRIBUTION	278
3.	QUANTITATIVE PRODUCT DISTRIBUTION	278
F	DISCUSSION	282

CHAPTER 11 THERMAL DEGRADATION OF POLYBUTADIENE

	<u>MODIFIED BY OXIDATIVE DEGRADATION</u>	283
A	INTRODUCTION AND LITERATURE REVIEW	283
B	PREPARATION OF OXIDISED MATERIAL	291
(i).	MATERIAL OXIDISED AT 0°C AND ROOM TEMPERATURE	291
(ii).	MATERIAL OXIDISED AT ELEVATED TEMPERATURES	291
C	THERMAL DEGRADATION OF OXIDISED MATERIAL (TECHNIQUES)	293
D	TG AND DSC	295
(i).	TG AND DSC OF PURE POLYBUTADIENE UNDER OXYGEN	295
(ii).	TG AND DSC OF POLYBUTADIENE MODIFIED BY OXIDATION AT 0°C UNDER NITROGEN	295
E	MICROSTRUCTURAL CHANGES ASSOCIATED WITH THE PROCESSES OF OXIDATION OPERATIVE AT ROOM TEMPERATURE	301
F	PROGRAMMED DEGRADATION UNDER VACUUM OF POLYBUTADIENE MODIFIED BY OXIDATION AT 0°C	310
(i).	TVA	310
(ii).	ATVA	310
G	PRODUCTS FORMED IN THE PROGRAMMED THERMAL DEGRADATION OF POLYBUTADIENE MODIFIED BY OXIDATION AT 0°C	315
1.	PRODUCTS GENERATED IN THE TEMPERATURE RANGE 100 - 200°C	315
(i).	NONCONDENSABLE VOLATILE MATERIAL	315
(ii).	CONDENSABLE VOLATILE MATERIAL	315
(iii).	COLD RING MATERIAL	315
(iv).	RESIDUAL MATERIAL	320
2.	PRODUCTS GENERATED AT TEMPERATURES ABOVE 200°C	320
(i).	NONCONDENSABLE VOLATILE MATERIAL	320

(ii).	CONDENSABLE VOLATILE MATERIAL	320
(iii).	COLD RING MATERIAL	322
(iv).	RESIDUAL MATERIAL	322
H	MICROSTRUCTURAL CHANGES ASSOCIATED WITH THE PROCESSES OF OXIDATION OPERATIVE AT 100°C	327
I	PROGRAMMED DEGRADATION UNDER VACUUM OF POLYBUTADIENE MODIFIED BY OXIDATION AT ELEVATED TEMPERATURES	328
(i).	ATVA	328
(ii).	COMBINED TVA/ATVA	329
J	PRODUCTS FORMED IN THE PROGRAMMED THERMAL DEGRADATION OF POLYBUTADIENE MODIFIED BY OXIDATION AT ELEVATED TEMPERATURES	333
(i).	NONCONDENSABLE VOLATILE MATERIAL	333
(ii).	CONDENSABLE VOLATILE MATERIAL	334
(iii).	COLD RING MATERIAL	334
K	DISCUSSION	336

<u>CHAPTER 12</u>	<u>GENERAL CONCLUSIONS AND SUGGESTIONS FOR FURTHER WORK</u>	347
-------------------	---	-----

CHAPTER 1.

INTRODUCTION.

A. THE COMMERCIAL DEVELOPMENT OF POLYMERS BASED ON STYRENE AND BUTADIENE.

Styrene monomer was first isolated in the early eighteenth century as a product of the thermal decomposition of some natural products. Its structure was deduced (1) and it was noted (2) that the material solidified during storage. The pioneering work of Staudinger which established the existence of the macromolecule chain, provided an explanation for the above process and gave impetus to commercial groups to exploit this new branch of Chemistry. Attempts were made to accelerate the polymer forming reaction of styrene under more precisely defined conditions by the use of selected additives. Initial advances in this direction were frustrated by the inability of the then current methods of organic synthesis to prepare styrene monomer of sufficient purity to eliminate the incorporation into the polymer of materials deleterious to its subsequent stability. The development of efficient catalyst systems, able to alkylate benzene and dehydrogenate the product to yield styrene has overcome this obstacle and has led to the production in bulk of very pure styrene.

Butadiene monomer was first isolated as a product of the thermal decomposition of some small molecules (3). The material can be produced by many laboratory reactions (4). It is, however, almost exclusively produced in bulk by the catalytic dehydrogenation of C_4 hydrocarbons.

In the infancy of the plastics industry, the incentive towards a commercial development of the polybutadiene system was removed by the availability in quantity of inexpensive natural

polyisoprene polymers. The shortages of natural rubber generated in the first and especially the second world war prompted massive investigations into the preparation and subsequent fabrication of synthetic polyelastomers. Butadiene emerged as the most successful "feed" material for these polymers and has retained its popularity as an isoprene substitute to this day.

The most successful synthetic elastomer was a random copolymer of styrene (in trace quantities) and butadiene. In the early stages of its development the material compared poorly with natural rubber in terms of its absolute "performance". The situation was, however, reversed with the advent of "cold" polymerisation techniques which enabled the polymer to be produced with a minimum of structural abnormalities, with the result that the styrene - butadiene copolymer (SBR) is today produced in quantities which rival that of natural rubber.

In recent years the production of styrene homopolymer has increased markedly. It is cheap, easily fabricated, and possesses excellent insulating properties. The major obstacle to the use of this material is its tendency to fragment when exposed to sudden mechanical stress. This has led to the development of the "high impact polystyrene" systems which in general are composite materials of styrene, along with a small quantity of butadiene, formed by a physical blending of the two homopolymers, a random copolymerisation of the two monomers, or a grafting of one homopolymer onto the other. The excellent physical properties of this material have led to its production in large quantity.

The polystyrene and polybutadiene homopolymer systems are chemically incompatible with the result that the extent of dispersion in a mixture of the two is limited by their tendency to form separate phases on a microscopic scale when cooled from the melt.

An important consequence of this is a loss of optical clarity as a result of light scattering at the microphase boundary. Another disadvantage of the blend system is the necessity of vulcanising the rubber component in situ . This transforms the composite to a resinous insoluble material which is difficult to process.

In recent years the styrene/butadiene A : B : A block copolymer system has gained in commercial importance. The polystyrene and polybutadiene components of this system remain incompatible. The degree of microphase dispersion is, however, greatly enhanced with the result that the optical clarity of the polymer is increased. The polybutadiene chains are chemically bound to the semi-crystalline polystyrene domains with the result that they are anchored with respect to slippage. This effect can be thought of as a physical analogue of the normal vulcanisation process. It can be eliminated by melting the polymer and be regenerated upon its subsequent cooling, with the result that the polymer is well suited to those uses which require a lengthy process of fabrication.

B. DEGRADATION OF POLYMERS.

(i). General Considerations.

In general the term "degradation" may be applied to those processes which operate within the polymer matrix, as a result of interactions with its environment, which lead to a deterioration of the polymer. A complete examination of these processes is beyond the scope of this work. Suffice it to say that, in general, the degradation of most fabricated polymers is effected by contact with oxygen in its various forms (molecular, singlet and ozone), by reactions directly promoted by light, and by the application of heat to the polymer. The degradation of most real polymer systems is usually induced by these three processes acting in concert. Although this has been recognised for some time, the complexity of the systems involved have usually limited any scientific study to the effect on the polymer of one degradation process, the most widely studied of which is that of thermal degradation.

The first polymer pyrolysis experiments were performed in an attempt to isolate and identify simple derivative materials. The deductive axioms of organic chemistry were then applied in reverse in an attempt to gain some insight into the structure of the polymer.

The importance of this type of work decreased with the advent of simpler techniques of microstructural characterisation such as i.r. and n.m.r. spectroscopy. More recently, the techniques of thermal degradation have been used to directly ascertain the resistance of polymers to thermal degradation and in some cases the mechanisms of thermal degradation with a view to establishing correlations between structure and thermal stability.

It may be argued that a study of the effect on a polymer of heat stress in the absence of other degradation agents is a poor approximation to reality. This is, however, not the case. For example, machine sealing gaskets are often subject to very high

temperatures in the absence of oxygen and light while plastics used in the space industry - admittedly a small fraction of the output of the plastics industry, are often subjected to very high temperatures in the absence of oxygen. Perhaps the greatest impetus to work of this kind has come from a realisation that the burning processes operative in polymer systems are restricted to material which has been volatilised from the surface of the polymer - in fact the polymer surface is often devoid of oxygen. If this is the case then the processes which are operative within the "burning" polymer closely approximate those which lead to its thermal degradation.

If the oxygen supply is limited, as is often the case in sealed volumes, large concentrations of the primary volatile products of thermal degradation can be accumulated. It is essential that knowledge be made available both of the nature of these materials and of their oxidised or partially oxidised derivatives in order that future polymers may be modified to be as safe as possible in a fire situation. The bulk of such knowledge can only be obtained from thermal degradation studies.

(ii). Mechanisms Of Thermal Degradation.

It is convenient to classify the mechanisms by which vinyl polymers are thermally degraded into the two categories shown below.

(a). Reactions which result in main chain scissions and/or depolymerisation to the monomer unit.

(b). Reactions which modify or remove pendant substituents from the polymer.

The chain scission reaction has been studied in some detail. It has been shown (5) that it can be completely described by a free radical chain reaction which includes the possibility of inter- and intra-molecular transfer of radical activity. As expected, the formation of monomer is encouraged in systems which do not possess

labile atoms dispersed throughout the polymer.

The latter processes must be facile at a lower temperature than that required for the chain fragmentation reaction of the polymer. In general they do not lead to a main chain scission.

These modifications to the polymer microstructure may stabilise or destabilise the polymer with respect to further weight loss. A good example of the former occurs during the thermal degradation of polyacrylonitrile (6,7) in which the formation of cyclic backbone units block the subsequent chain fragmentation reaction. The dehydrochlorination reaction of polyvinylchloride (8) is a good example of the latter situation. The generation of main chain unsaturation encourages the elimination of hydrogen chloride.

(iii). Thermal Degradation Of Polymer Blend Systems.

A systematic study of the thermal degradation of a range of polymer blend systems has been performed in this department under the supervision of Dr. I.C. McNeill. It has been found, in general, that the microphase separation effect persists to high temperatures with the result that direct contact with, and therefore reactions attributable to interactions between dissimilar macromolecules are discouraged.

The mechanisms of cooperative degradation, if any, can almost universally be explained in terms of interactions between polymer in one phase and a small molecule or radical produced in the other phase able to diffuse across the phase boundary. Specific examples of this effect have been discussed (9).

C. AIMS OF THIS WORK.

The work reported in this discussion was performed with four objectives in mind, the first and most important of which was to gain a more complete insight into the processes of thermal degradation in the polystyrene and polybutadiene homopolymer systems. The second objective was to compare the thermal degradative behaviour of the polystyrene/polybutadiene blend system with that of the corresponding A : B block copolymer system in an attempt to ascertain the effect (if any) of the differences in polymer morphology of the two systems on the degradation process. The third objective was to attempt to use the available techniques of thermal degradation to gain some insight into the mechanisms of oxidative degradation of polybutadiene and the effect of oxidation on the thermal stability of the polymer. The fourth and final objective was simply to refine and improve some techniques of thermal analysis in order that the first three objectives might be better achieved.

CHAPTER 2

ANALYTICAL TECHNIQUES

A 1 THERMAL VOLATILISATION ANALYSIS (TVA).

In the TVA technique described by McNeill (10), material involatile at room temperature under high vacuum is subjected to heat stress. A low molecular weight sample may undergo the physical processes of volatilisation or sublimation to the most accessible cold zone in the system. In high polymer systems, however, enthalpies of evaporation are prohibitive, with the result that instead of this physical change there is usually a complex sequence of chemical processes. The TVA technique is applicable to that product fraction which is volatile at room temperature and is based upon the following principle.

Material evolved under high vacuum maximises its entropy by expansion. If backward diffusion is eliminated by a liquid nitrogen trap or diffusion pump, material can be quantitatively removed at a rate dependent on the geometry of the degradation line. For a fixed pathway, the pressure exerted by a volatile species at a point between the oven and the pump is a measure of its rate of production.

This arrangement can be seen in schematic form in fig. 1. The environment of the pressure gauge is standardized by the inclusion of a 0°C foretrap. The use of a multichannel recorder permits the simultaneous recording of temperature and pressure curves.

Sometimes discrete volatile producing reactions can be followed by TVA. In most cases, however, an additive trace arising from overlapping reactions is obtained.

Before the applications of the TVA technique are discussed it is necessary to define clearly its limitations. A Pirani gauge output is a measure of the thermal conductivity of its environment. This is directly proportional to dynamic gas densities up to an

FIGURE 2 - 1

BASIC TVA APPARATUS

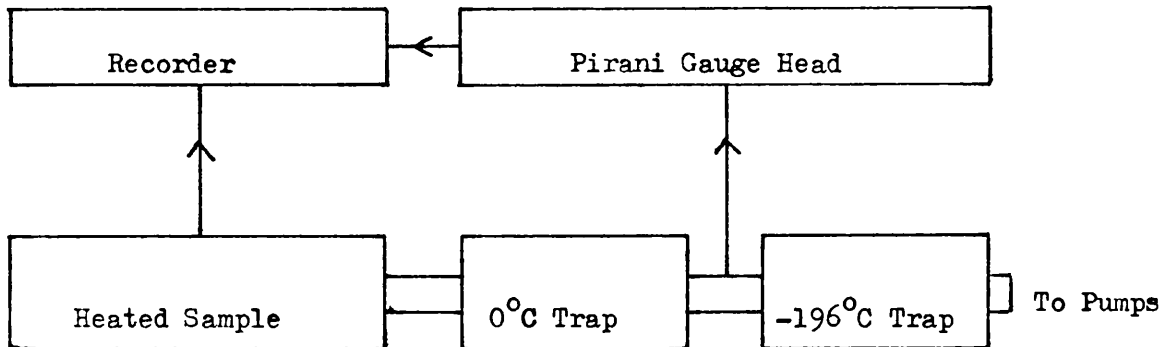
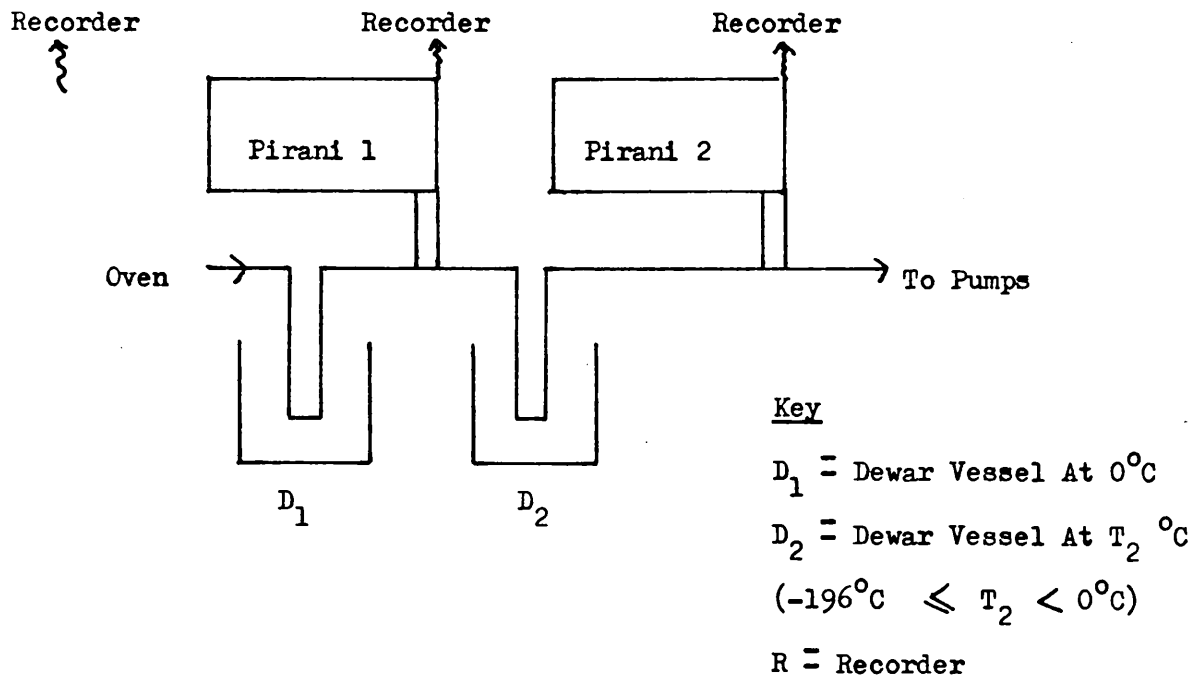


FIGURE 2 - 2

SINGLE LINE DIFFERENTIAL CONDENSATION TVA SYSTEM



output of approximately one millivolt. Hindered motion at higher pressures reduces conductivity and compresses the Pirani output. This "drawback" is put to good use in semi-quantitative work and allows both predominant and trace volatile producing reactions to be clearly seen on the same recorder scale.

Thermal conductivity is related to molecular structure and varies from compound to compound. For this reason calibrations must be carried out for each substance in quantitative work. Because the measured pressure is so dependent on the rate of volatile removal in dynamic systems a set of calibration curves is valid only for the degradation line which provided the data on which they are based.

A 2 DIFFERENTIAL CONDENSATION TVA.

Most TVA traces are "resultant" in that they arise from an addition of pressure curves from a range of processes often producing different materials. The differential condensation TVA experiment ⁽¹¹⁾ provides an indication of the range of product volatility at each temperature of a programmed degradation.

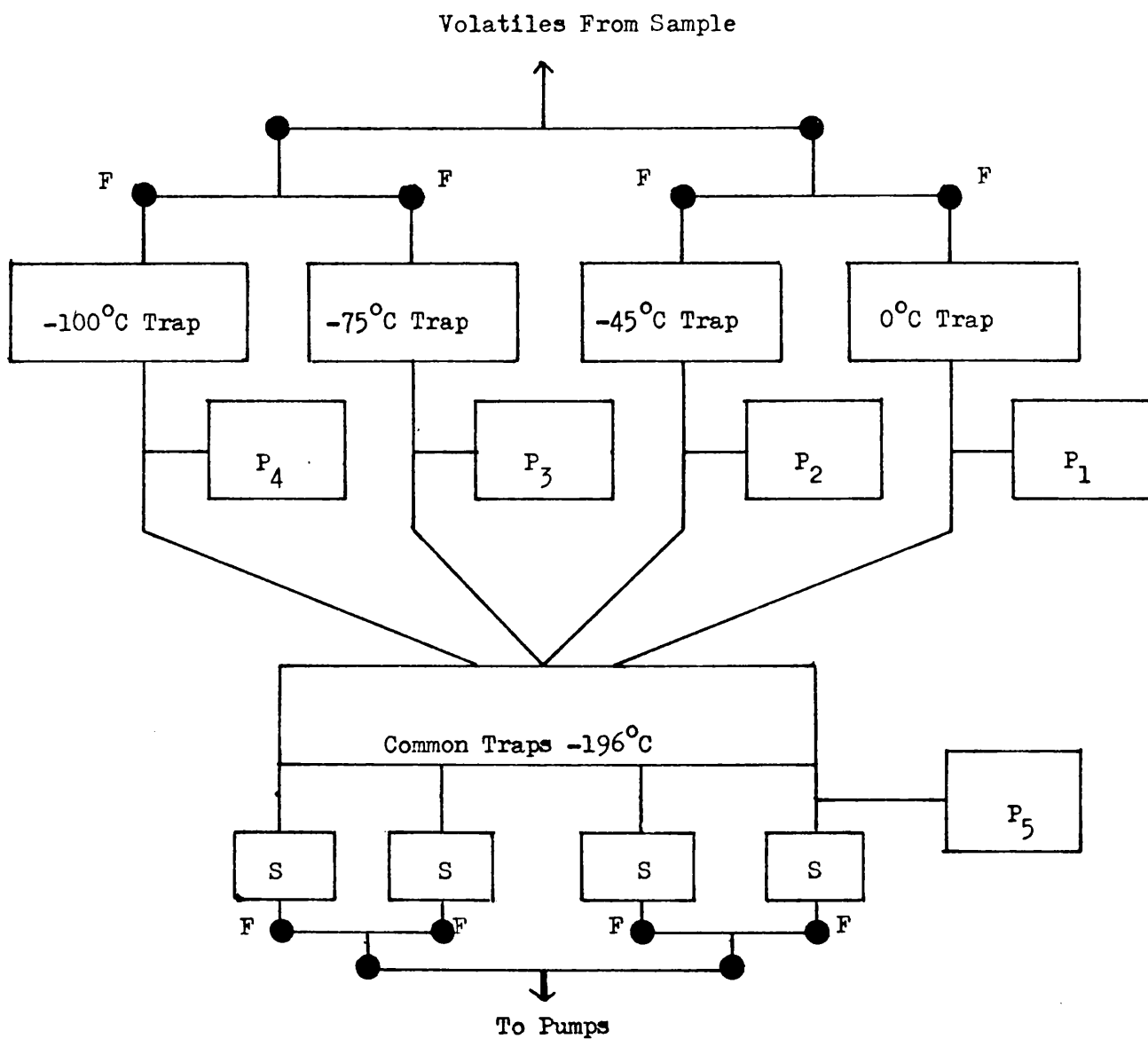
The basic apparatus is shown in fig. 2 . Pirani outputs one and two are recorded simultaneously with oven temperature. Output one measures the total volatile pressure while output two measures the pressure of material volatile at temperature T_2 . By repeating the experiment with different values of T_2 , in turn, the range of product volatility may be estimated.

If T_2 is in the temperature range where a component of the mixture exists as a liquid in equilibrium with its vapour then its distillation to the pumping system is at a "limiting rate". This effect can sometimes be used to identify the material (See Chapter 5).

By using the parallel line system of fig. 3 this

FIGURE 2 - 3

PARALLEL LINE DIFFERENTIAL CONDENSATION TVA SYSTEM



Key

P Pirani Gauge Heads

S Sample Collection Points

● Stopcocks

F● Stopcocks To Enable Line To Double As Sub-ambient TVA
Fractionating Grid

information may be collected in a single experiment for four values of T_2 .

Volatile pressure as measured by Pirani output was found to decrease with increasing path length to the oven. To eliminate this variable from the apparatus all the path lengths from the oven to the foretraps and from the foretraps to the liquid nitrogen traps were equalized. The Pirani output was also found to vary in a small way with the foretrap temperature - this effect possibly arising from a reduction in internal energy of material passing through the sub-ambient zone. To eliminate this variable, Piranis 1-4 were brought into coincidence with Pirani 5 under the conditions of the experiment using simple voltage dividing circuits. Pirani coincidence was checked periodically by following the oxygen evolution from degrading potassium permanganate.

A 3 PRODUCT FRACTIONATION IN THE TVA EXPERIMENT.

Products of degradation in the TVA experiment are fractionated according to volatility in the manner outlined below.

(1). The Residue of Degradation comprises material involatile at degradative temperatures. Analysis is often hindered by its insolubility. When it is to be examined it is convenient to carry out the degradation in a removable Pyrex boat.

(2). The Cold Ring Fraction of Degradation consists of products which are volatile at degradative temperatures but involatile at room temperature. In the basic TVA apparatus it can be removed from the upper section of the TVA tube by a tissue and eluted in a suitable solvent which can be pumped off under vacuum prior to analysis. The simple modification outlined in Chapter 5 allows the weight of cold ring fraction to be directly measured.

(3). The Condensable Volatile Fraction of Degradation consists of material volatile at room temperature but involatile at -196°C .

It can be condensed into a collecting vessel or subjected to sub-ambient fractionation prior to analysis.

(4). The Noncondensable Volatile Fraction of Degradation comprises the permanent gases H_2 , O_2 , N_2 , CO , CH_4 which are all volatile at $-196^\circ C$. The newly developed technique of Adsorption TVA (discussed subsequently) is important in their analysis.

It must be stated that fractions (1), (2), and (3) are not always precisely defined. For example, volatile material exhibiting a "limiting rate" of distillation at room temperature and material prone to sublimation at ambient temperatures are often also detected in the cold ring product fraction along with traces of high molecular weight polymeric material.

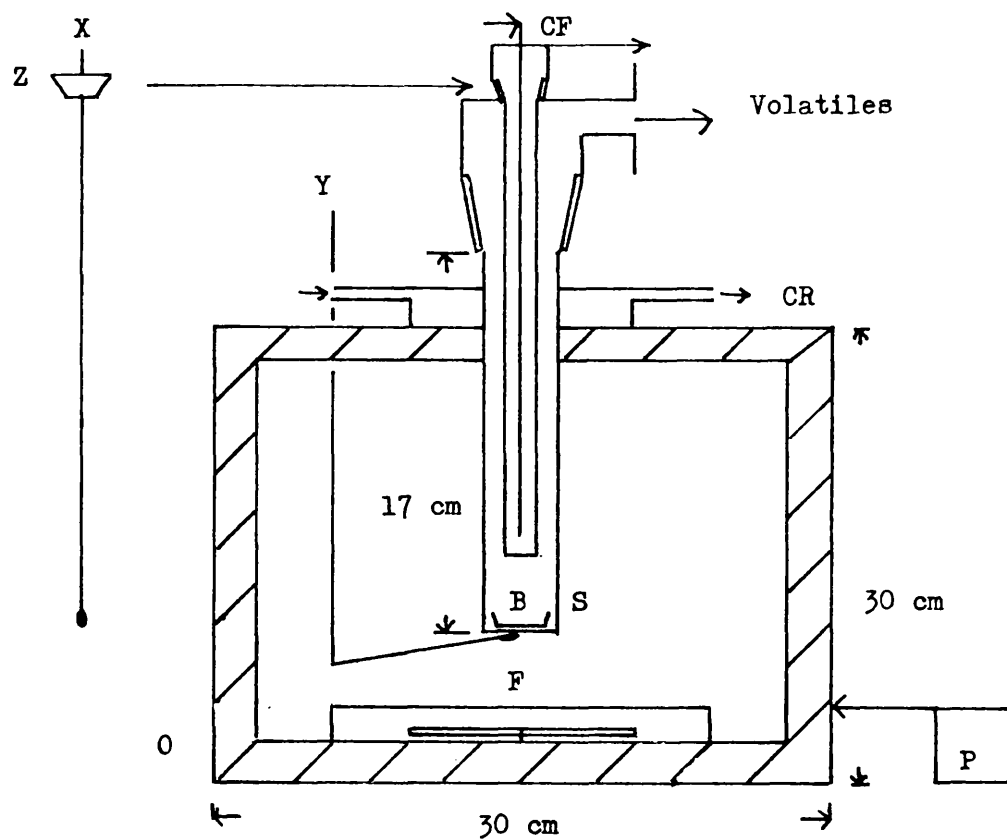
Ancillary techniques of separation can be employed. For example, residual material can be solvent extracted while the cold ring and condensable volatile fractions are amenable to preparative thin layer chromatography and GLC separation as discussed in this chapter.

A 4 OVEN ASSEMBLY.

Degradations were performed in the oven assembly shown in fig. 4. Samples were placed in a heavy walled pyrex degradation tube of base area 10 cm^2 ; connected to the vacuum line by the adaptor as shown. Heating to temperatures up to $500^\circ C$ isothermally or at programmed rates between $1^\circ C/\text{min}$ and $40^\circ C/\text{min}$ was effected by a Perkin Elmer model F11 precision oven with linear temperature programmer. Oven temperature was recorded using a Chromel - Alumel thermocouple pressed firmly onto the underside of the base of the degradation tube.

The high mass and heat capacity of the degradative assembly eliminated the problem of temperature overshoot in isothermal work and minimised temperature fluctuations due to sample endotherms

FIGURE 2 - 4
OVEN ASSEMBLY



Key

- B Pyrex Boat (Optional)
- CF Cold Finger
- CR Cold Ring/Water Jacket
- F Fan
- O Oven
- P Temperature Programmer
- S Sample Tube
- X Calibration Thermocouple
- Y Oven Thermocouple
- Z Serum Cap

and exotherms in isothermal and programmed work.

A 5 OVEN CALIBRATION.

The TVA tubes used were of high mass. This coupled with efficient "blackbody" internal heat loss produced a temperature gradient across the base of the tube. For a fixed oven assembly this temperature lag was found to be reproducible and could be measured by simultaneously recording inside and outside thermocouple readings at the base of the tube.

Thermocouple "X" (fig. 4) was coated with grease to ensure good thermal contact and pressed firmly onto the base of the tube prior to warm up. Its output (mv) during the run was recorded simultaneously with thermocouple "Y".

Calibration curves can be inspected in figs. 5 and 6. These indicate that the temperature lag is larger in programmed than in isothermal work. This effect was even more pronounced with faster warm up rates (20, 30, 40°C/min).

In all cases thermocouple output was converted to temperature by using standard conversion tables for Chromel - Alumel thermocouples.

A 6 SAMPLE PREPARATION AND SIZE.

Samples for degradation were added to the TVA tube in small pieces. This minimised exposure times of the rubber to the atmosphere and eliminated the requirement of sample preheating, necessary with solvent cast films. In fact the low molecular weight polymers under examination all melt-flowed before the onset of degradation to produce a thin film.

TVA and SATVA pressure curves were obtained with samples in the weight range 25 - 100 mg. The main criterion used in the determination of sample size was the production of moderate Pirani response sensitive to \pm pressure changes. In sub-ambient

FIGURE 2 - 5

OVEN CALIBRATION CURVES (PROGRAMMED RUN $10^{\circ}\text{C}/\text{min}$)

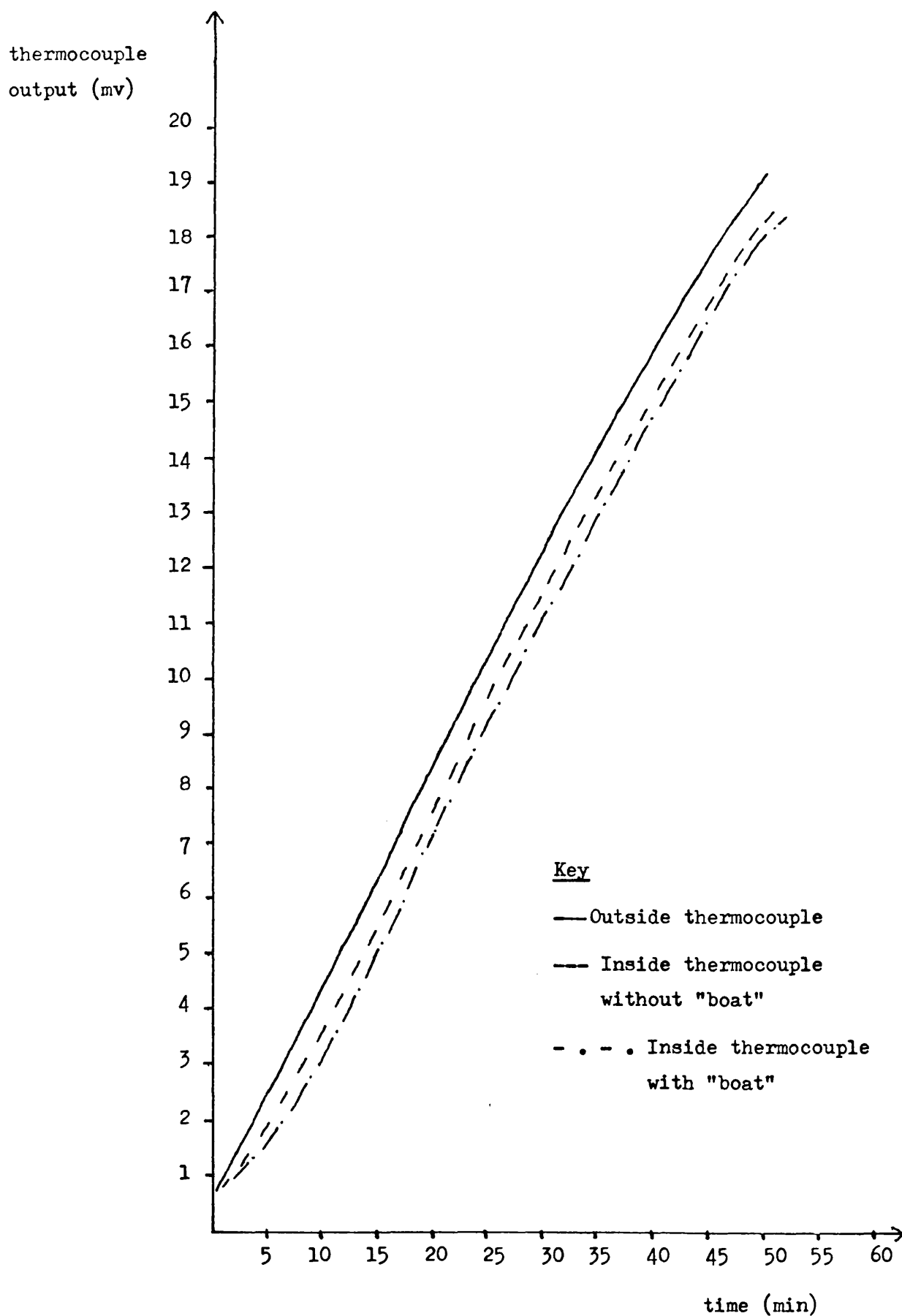
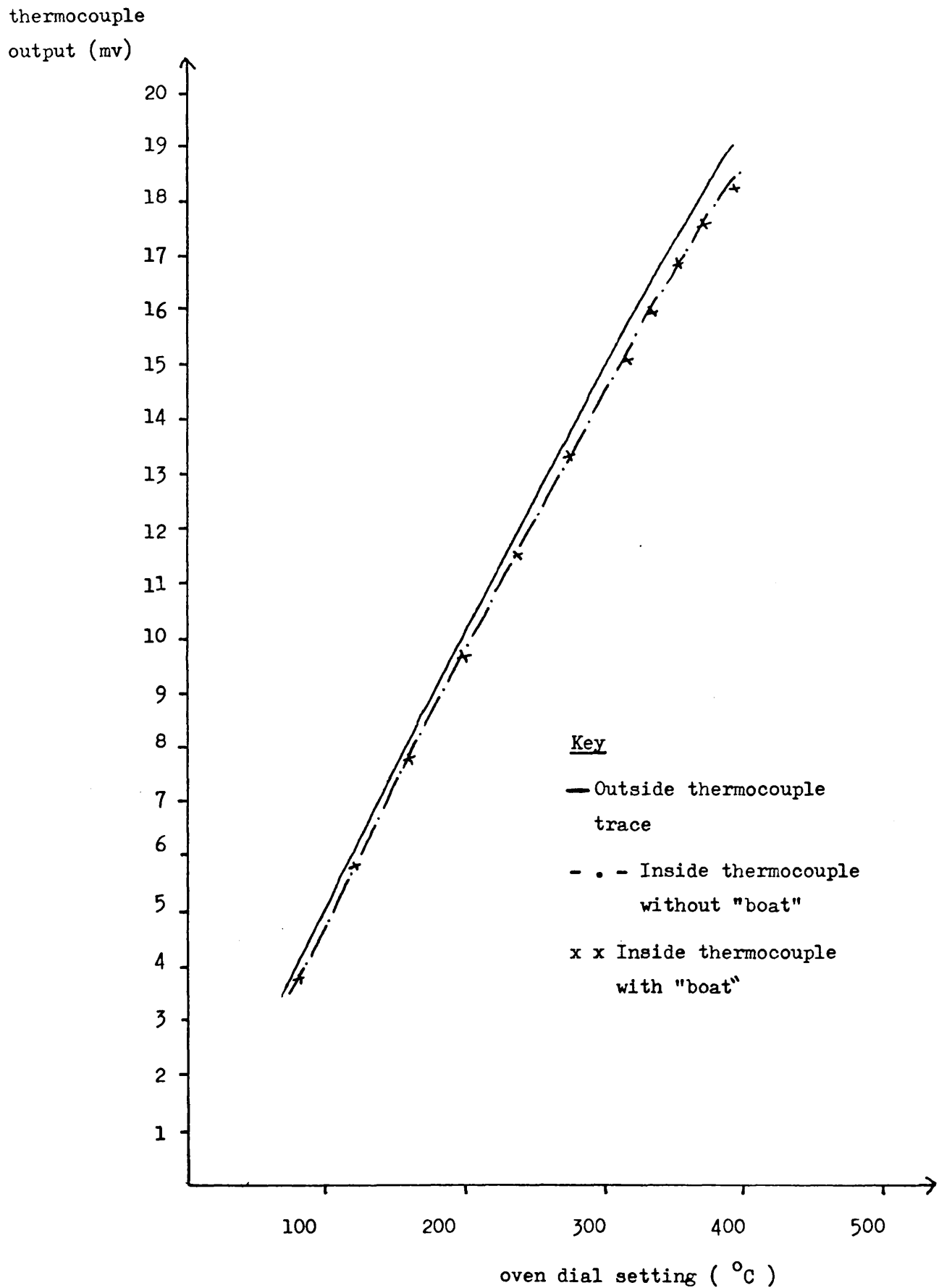


FIGURE 2 - 6

OVEN CALIBRATION CURVES (ISOTHERMAL WORK)



TVA experiments adherence to this approach eliminated the problem of peak movement.

In experiments designed for product analysis a range of sample sizes were required. Major volatile products could be detected in samples as small as 25 mg whereas the detection of minor products required samples of up to 250 mg. Sample sizes required to detect major and minor components of the cold ring fraction of degradation were in the same weight range of 25 - 250 mg.

A 7 SUB-AMBIENT THERMAL VOLATILISATION (SATVA).

TVA is applicable to any material involatile under high vacuum conditions. With polymeric samples volatile production is the result of chemical reactions within the sample. In principle, however, TVA could be used to volatilise successively the components of an oligimeric mixture on a molecular weight basis. The mixture would however reform by condensation onto the "cold ring" portion of the apparatus.

By shifting the temperature limits of the experiment to -196°C and 0°C it becomes possible to volatilise selectively a condensable volatile mixture. The SATVA technique developed by McNeill and co-workers (12) is based on this principle.

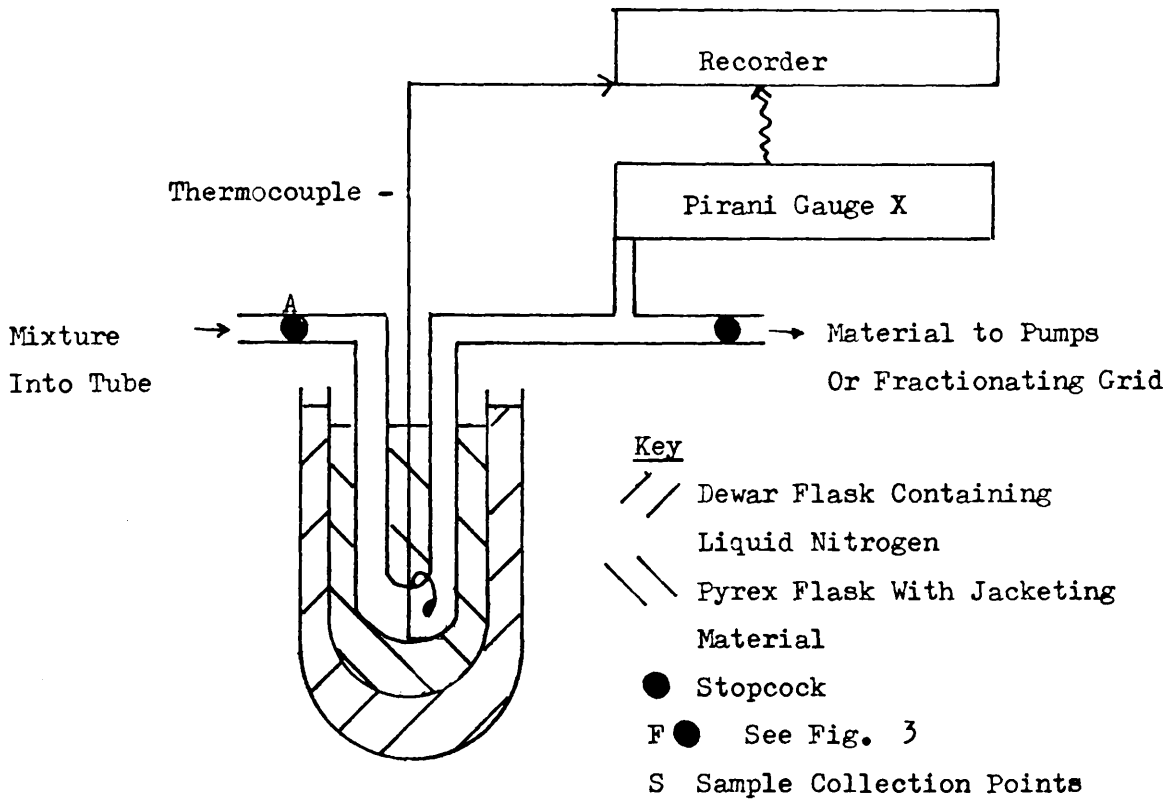
The SATVA assembly shown in fig. 7 is cooled to -196°C by surrounding it with liquid nitrogen. The sample is then condensed into the tube by through pumping in the direction shown. Stopcock "A" is closed, the liquid nitrogen is removed and the jacketing material allowed to warm to room temperature. This has been found to occur in a reproducible though non-linear manner. As evolved material distills to the most accessible trap the pressure curve is recorded simultaneously with the Chromel - Alumel thermocouple output producing together the SATVA trace.

If only the SATVA trace is required, material can be

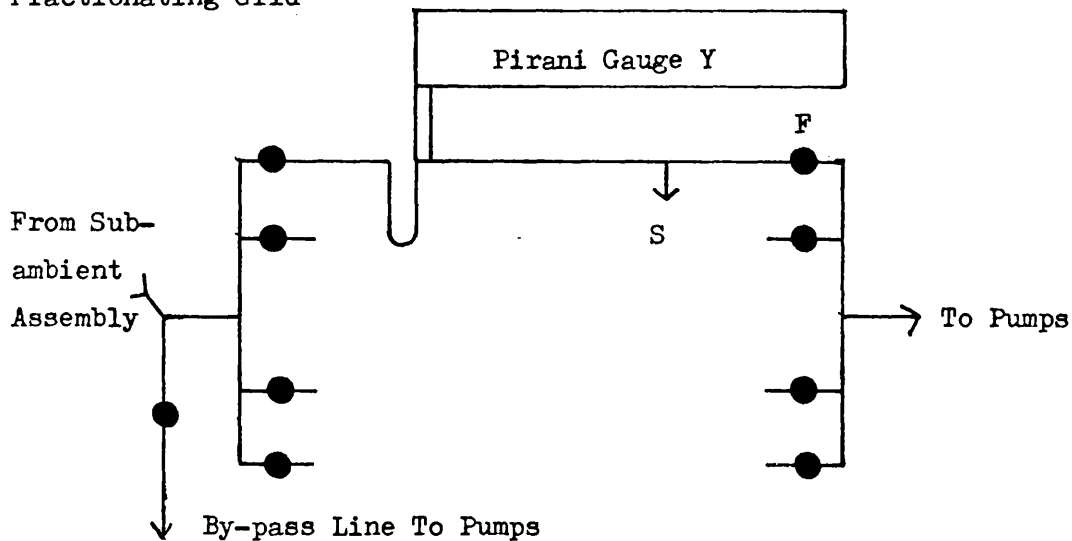
FIGURE 2 - 7

APPARATUS FOR SATVA FRACTIONATION

Sub-ambient Assembly



Fractionating Grid



directly routed into the fractionating grid shown in fig. 7 where up to four volatility bands can be separated for subsequent transfer, monitored by Pirani gauges "Y", to sample flasks "S".

In the SATVA assembly outlined in⁽¹²⁾ the fractionating grid was separate from the main TVA apparatus. A considerable simplification in design was obtained in this work by combining the two by the incorporation of stopcocks "F" into the TVA assembly and employing a manifold design which allowed volatiles to be "back pumped" from the TVA grid to the sub-ambient assembly and subsequently to be redistilled to the TVA grid for collection. A manifold schematic diagram is shown in fig. 8 .

In ⁽¹²⁾ the sub-ambient assembly consisted of a "cold finger" surrounded by p-xylene. Product collection in the cryozone was of a necessity under closed system conditions. When a large portion of the collected material exhibits a limiting rate of distillation at ambient temperatures the efficiency of transfer by closed system distillation can be low. Large quantities of such material are formed in rubber decompositions. For this reason the through pumping assembly shown in fig. 7 was used.

p-Xylene exhibits a heating discontinuity at its melting point of $+7^{\circ}\text{C}$. It was felt that peak shapes, corresponding to the "limiting rate" material already mentioned, would be better resolved if this was removed. The most successful alternative jacketing material used was solid paraffin wax (M.Pt. 50°C). A comparison with p-xylene can be seen in fig. 9 . Possibly due to its amorphous nature, $\frac{dT}{dt}$ is smaller for the wax at lower temperatures, early SATVA peaks are therefore better resolved. Another advantage of using this material is that, being solid and involatile, its mass is fixed upon solidification. This coupled with the fixed thermocouple position results in more reproducible warm up curves.

FIGURE 2 - 8

DEGRADATION MANIFOLD SCHEMATIC DIAGRAM

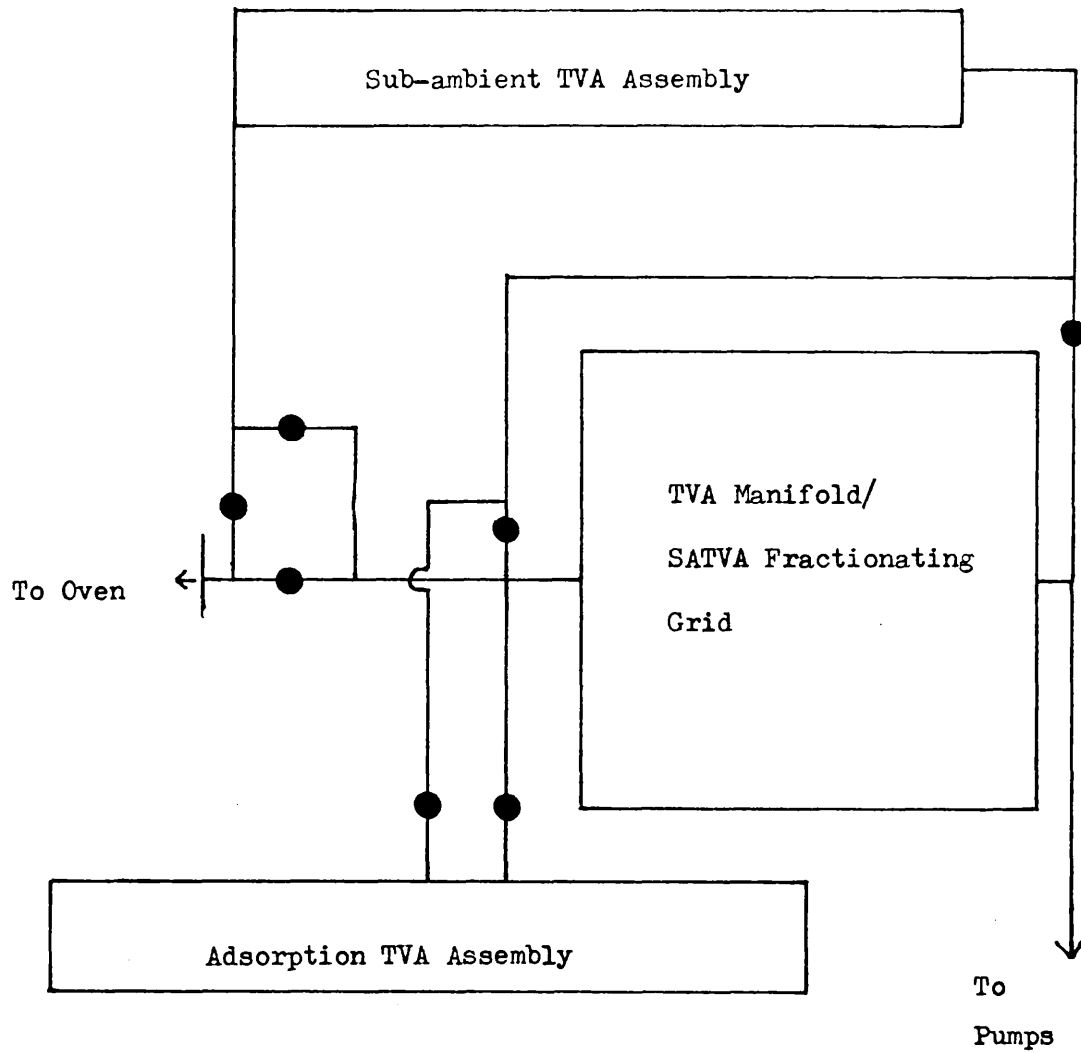
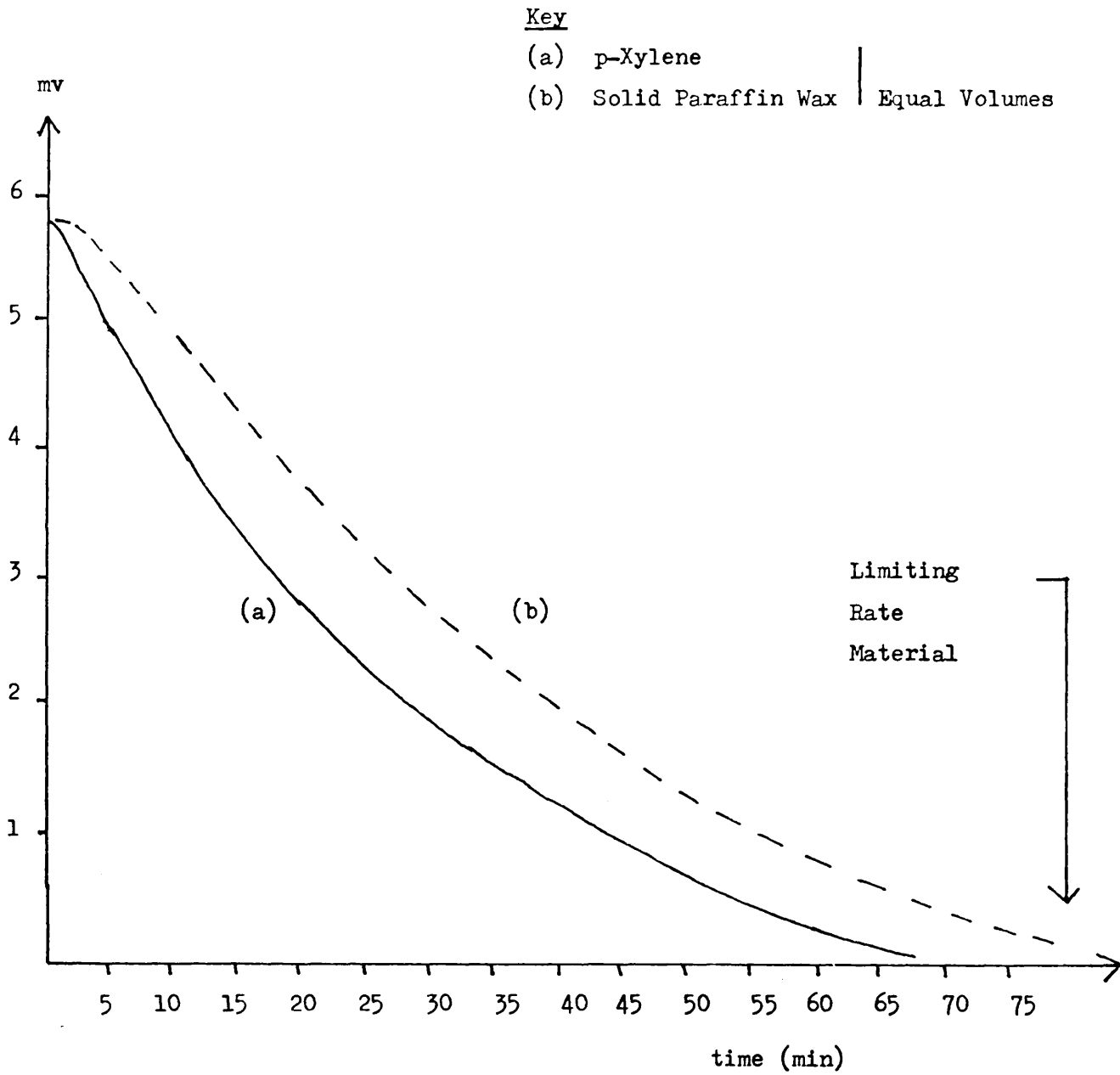


FIGURE 2 - 9

SATVA WARM UP CURVES



The effect of sample size on the SATVA trace has been discussed in section A6 of this chapter. Trace shape is also dependent on the rate of sample warm up. In general when the warm up is slowed down the peaks become less sharp, better separated and move to lower temperatures. This can be explained by assuming a limiting rate of heat transfer to the sample. The larger the time interval between the temperatures T and $T + dt$, the greater the heat transfer to and subsequent volatilisation of the sample between the two temperatures.

In the latter stages of warm up $\frac{dT}{dt}$ is small and material evolved in this region is often free of contaminants. At lower temperatures, however, $\frac{dT}{dt}$ is large and peaks can be close together. Often improved separation of this type of material can be achieved by jacketing the sub-ambient flask with a warm or cold Dewar flask to reduce convection and slow down the warm up rate.

A 8 THERMOGRAVIMETRY (TG).

Thermogravimetric measurements on samples degraded under a dynamic nitrogen atmosphere at flow rate 40 ml/min were carried out on a Du Pont thermal analyser.

Samples for analysis were contained in a boat shaped platinum sample holder of dimensions (1 x 0.5 x 0.25) cm held approximately 0.1 cm below the temperature measuring thermocouple. All sample weights were in the range (5-10) mg - large enough to eliminate vibrational noise and (hopefully) small enough to be free of sample bubbling and diffusion effects.

Isothermal measurements were made at temperatures indicated in the accompanying script, while programmed runs were carried out, unless otherwise stated, at a heating rate of 10°C/min from room temperature to 500°C. In the latter situation simultaneous

rate traces of the form $\frac{dw}{dT}$ were obtained, all on the same proportional scale to make possible a direct comparison of peak size and position for different polymers.

A 9 DIFFERENTIAL SCANNING CALORIMETRY (DSC).

Calorimetric measurements were made on a Du Pont 900 DSC module using programmed heating rates of 10°C/min from room temperature to 500°C.

Samples for analysis were contained in one of a matched pair of lightly crimped aluminium pans, positioned above the two heater blocks and temperature-measuring thermocouples. The whole assembly was housed under a dynamic nitrogen atmosphere of flow rate 40 ml/min.

Feedback from the sample pan thermocouple enabled the sample heater to compensate for heat flow to or from the sample by adjusting its output. These fluctuations were recorded as endotherms or exotherms respectively.

DSC facilities were used in preference to the Differential Thermal Analysis (DTA) facility also available because of superior baseline stability and the possibility of quantitative as opposed to qualitative estimation of peak sizes.

A 10 PYROLYSIS - GLC.

Materials to be pyrolysed were dissolved in volatile solvents and injected into a Perkin Elmer F11 assembly with injection block temperature set substantially higher than the breakdown range of the material.

The efficiency of breakdown was qualitatively measured by peak sharpness while possible solvent effects were examined by comparing product ratios using different solvents.

The conditions of product separation are given at the appropriate point in the discussion.

B 1 GAS LIQUID CHROMATOGRAPHY (GLC).

All GLC separations were carried out on a Perkin Elmer F11 single column assembly equipped with flame ioniser.

Carrier gas flow rates were set at 40 ml/min using a bubble flow meter, while solute concentrations were adjusted to keep the amplifier in a linear range where the quantity of material eluted is directly proportional to the weight of its cut out trace.

Toluene was chosen as the internal standard (where applicable) because it was found to be miscible with the materials under study and could be separated from them and eluted before the last component of the mixture. Methylene chloride and chloroform were used as solvents because of their low boiling point and subsequent clean separation from the first eluent peak.

Isobutyronitrile (IBN) was prepared as discussed below. Other GLC standards were of the highest purity available and were distilled before use if polymerisable (styrene, methacrylonitrile).

The technique was quantitatively applied in the following manner. The mixture, usually from the oven, was condensed into the U-tube of the TVA assembly and subsequently flash distilled to a "cold finger" prior to removal from the line. Before the distillate could melt the appropriate volume of toluene was added and a few microlitres of the mixture were added to 0.5 ml of solvent. After GLC separation has been performed the weight ratios of the peaks corresponding to the unknown and toluene were obtained. By application of the appropriate "sensitivity factor" this was expressed as a volume ratio. As the volume of toluene initially added to the mixture was known, the mass of unknown in the mixture could easily be calculated.

Most of the errors in this approach arise due to incomplete product transfer from the U-tube to the "cold finger" and

FIGURE 2 - 10

STANDARD GLC CALIBRATION CURVES

Internal Reference - Toluene

Key

(a) Methacrylonitrile

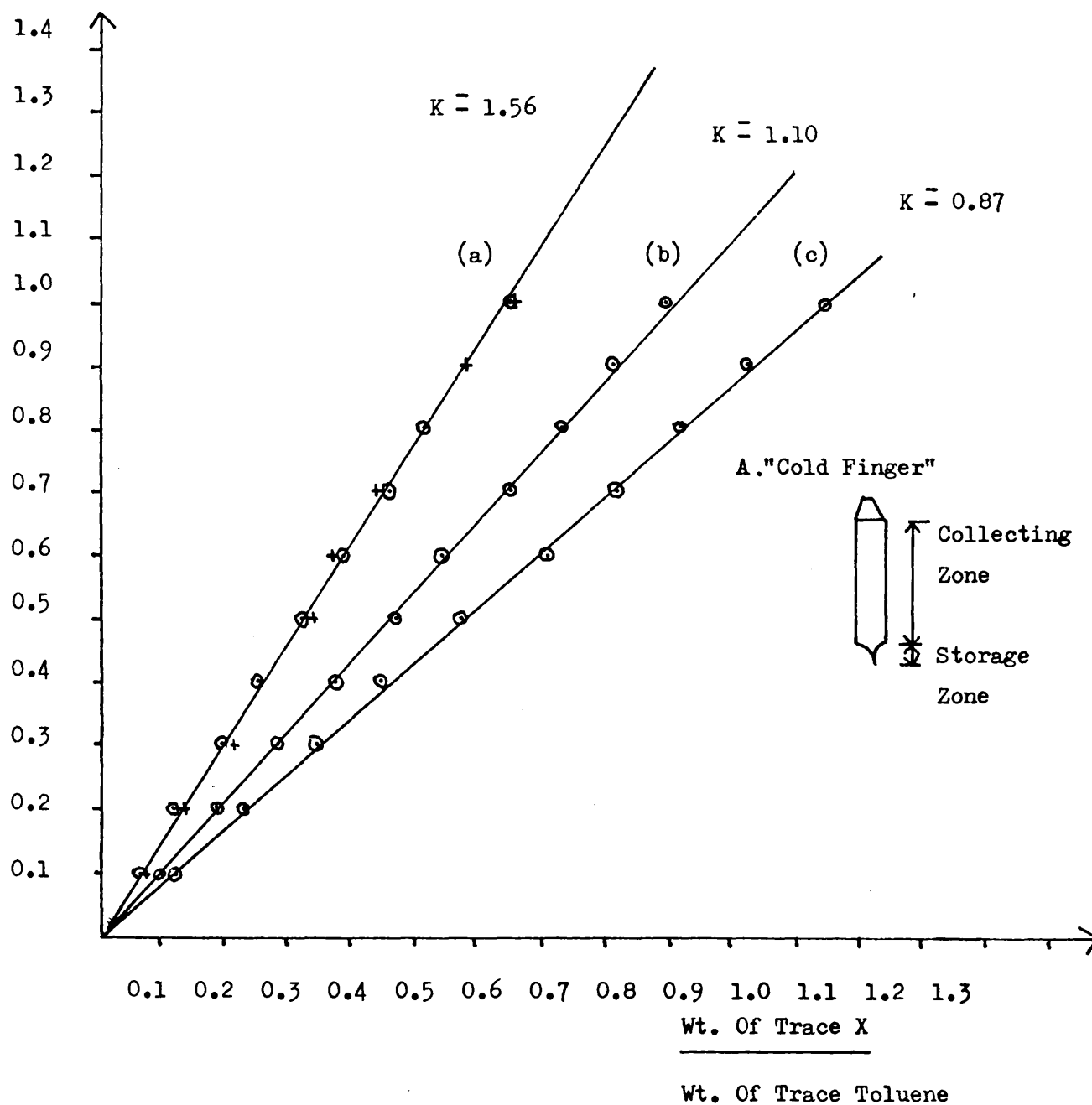
Isobutyronitrile (+)

(b) 4-Vinylcyclohexene

(c) Styrene

Volume X

Volume Toluene



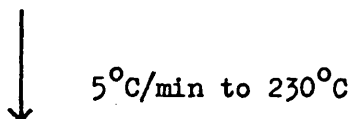
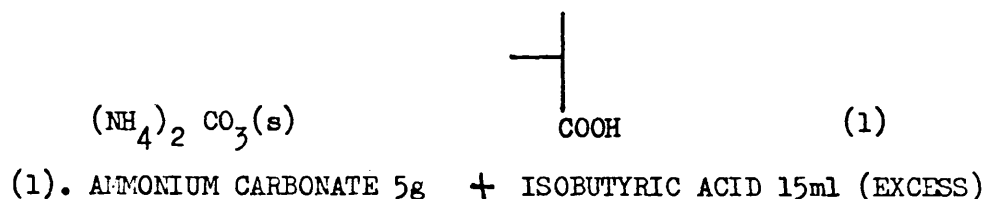
resultant losses by evaporation after removal from the line. These were minimised by consistently monitoring, by Pirani gauge, the distillation into "cold fingers" of the type shown in fig. 10 .

Sensitivity factors were obtained as follows. GLC traces of ten solutions of differing unknown/toluene volume ratios were obtained and the corresponding weight trace ratios measured. These were plotted as shown in fig 10 . The volume ratio of any unknown/toluene mixture could subsequently be obtained by multiplying its area ratio by the gradient (K) of the appropriate graph.

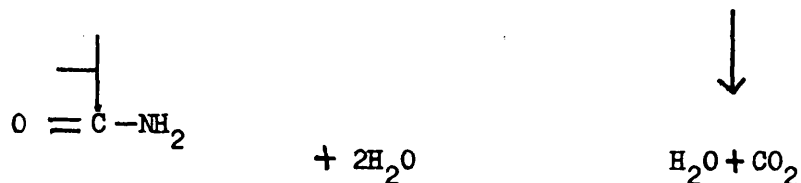
Details of the materials separated along with corresponding column compositions and temperatures of operation can be found in the appropriate chapters.

Isobutyronitrile Preparation.

IBN was prepared as outlined below under nitrogen in a vessel with a Teflon stopcock.

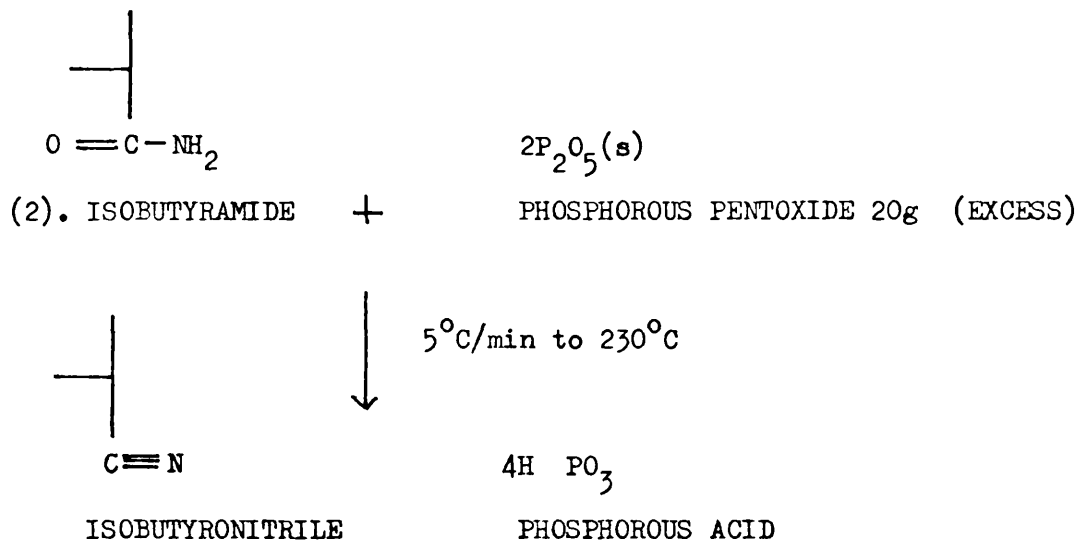


AMMONIUM SALT (INTERMEDIATE) + CARBONIC ACID



ISOBUTYRAMIDE

Water was removed by overnight pumping.



The IBN so produced was flash distilled from the vessel, stored overnight over ammonium carbonate and flash distilled to another vessel to remove residual acid. Its purity was estimated at 98% by n.m.r. spectroscopy.

B 2 PREPARATIVE THIN LAYER CHROMATOGRAPHY.

Components of the cold ring fraction of degradation were separated, when necessary by preparative thin layer chromatography.

Large samples of up to 250 mg were degraded and the cold ring produced, dissolved in a good solvent and painted across the base of a preparative thin layer chromatography plate.

The mixture was developed in n-hexane, separating material on a polarisability and molecular weight basis. Component bands were identified by their effect on the plate fluorescence under ultraviolet light and eluted in a suitable solvent. Filtration under pressure was followed by concentration by pumping to remove solvent.

Semi-quantitative i.r. and n.m.r. spectra were obtained by making all solutions up to a fixed volume prior to analysis.

C 1 INFRARED (i.r.) SPECTROMETRY.

The spectra referred to in the following notes were all obtained on a Perkin Elmer 257 grating spectrophotometer.

Spectra were obtained of both the parent polymers and their products of thermal degradation. Undegraded polymers were examined, whenever possible, as thin films cast on salt plates from volatile solvents. Polybutadiene was also subjected to liquid phase analysis (Chapter 4). Techniques applied to each of the TVA fractions are listed below.

(i). The Residue of Degradation.

Total residues were examined by the KBr disc method (3mg + 300mg salt). When necessary, soluble material was eluted, filtered and cast onto salt plates for examination.

(ii). The Cold Ring Fraction of Degradation.

Spectra of cold ring mixtures were obtained by smearing the material onto salt plates. After elution, filtration, and concentration by pumping, material separated by preparative thin layer chromatography was treated in a similar manner.

(iii). The Condensable Volatile Fraction of Degradation.

Depending on the volatility of the material, liquid and/or gas phase spectrometry was used.

Whenever possible, solution spectra were obtained in diluents of high symmetry - usually carbon tetrachloride, sometimes chloroform in 0.5 mm cells. Polar materials were examined in 0.1mm cells without solvent.

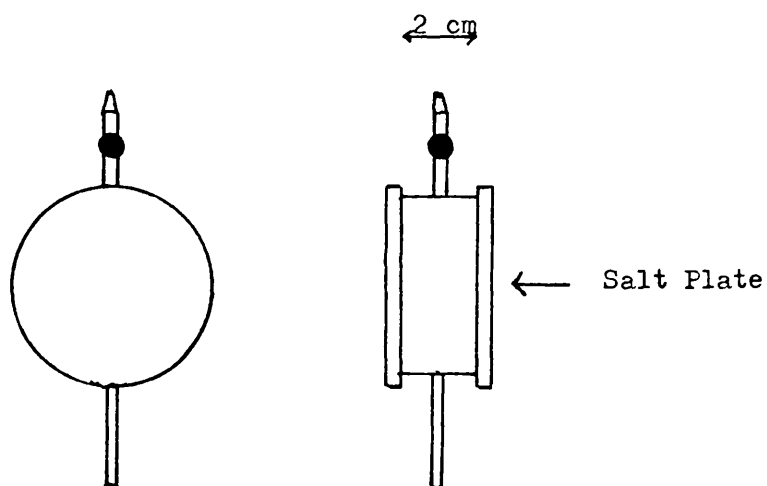
The gas phase i.r. cell developed during this work is shown in fig. 11B along with the old design (fig. 11A). The condensable volatile cell enabled the gas phase and liquid phase (after removal from the cell) spectra to be obtained of the same mixture.

Often a crude product fractionation could be observed in the two

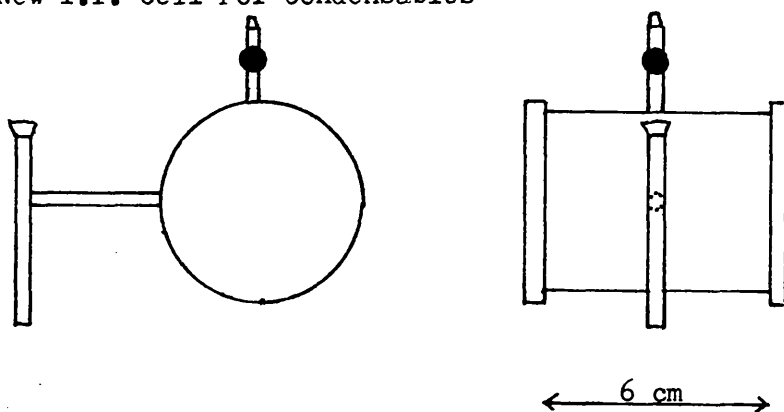
FIGURE 2 - 11

INFRARED GAS CELLS

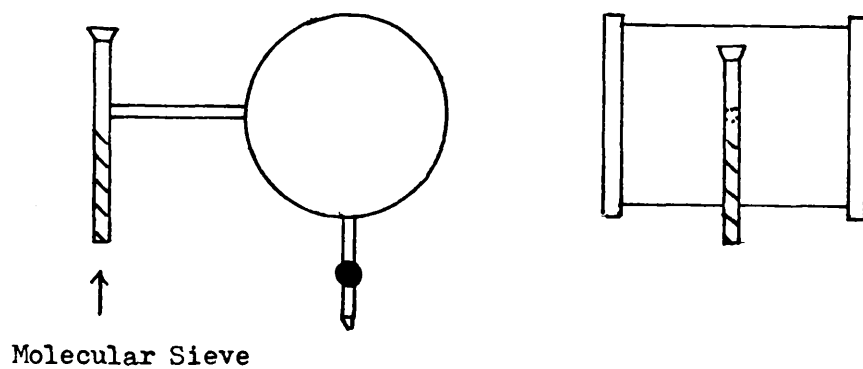
A. Old i.r. Cell For Condensables



B. New i.r. Cell For Condensables



C. New i.r. Cell For Noncondensables



spectra. This reduced analysis time and enabled gas phase reference spectra to be obtained without first distilling in the material. The staggered cold finger design also eliminated the problem of window breakage in the cooling cycle caused by the close proximity to the cold zone of the salt plates and "Powerpack" glue with their differing coefficients of thermal contraction .

(iv). The Noncondensable Volatile Fraction of Degradation.

Spectra were obtained in gas cell C of fig.11 after gas manipulation by the adsorption TVA method (Chapter 3).

C 2 PROTON MAGNETIC RESONANCE (H'n.m.r.) SPECTROMETRY.

All spectra were obtained on a Perkin Elmer R32, 90 MHz spectrometer with signal locking, integral and spin decoupling facilities. The spectrometer probe was at all times thermostatted at 35°C.

Carbon tetrachloride was used as solvent whenever possible. When solubility problems arose the appropriate deuterated solvent was substituted. Unless otherwise stated all spectra were obtained on a 0 - 10 δ scale "locked" onto tetramethylsilane (TMS) at 0 δ .

Many conclusions from this work are based upon information obtained by this method. It therefore becomes necessary to clarify its advantages over other spectral methods and also its limitations when applied to the polymer and mixed component systems under observation.

All polymer systems suffer n.m.r. signal broadening, usually from segmental motion and microscopic unhomogeneity. This allied to the additive "ring current" broadening effects observed in polystyrene containing samples, preclude the use of spin decoupling, and make electronic signal integration unreliable. Peak positions at constant temperature are however reproducible and signal areas, proportional to the relative proton count, can be obtained by the cutting out and weighing of traces.

More specifically, the reliance of the n.m.r. technique upon complete sample solubility for magnetic homogeneity, limits its use in the detection of microstructural changes in rubber containing systems. This is more than offset by its ability, whenever applicable, to separate completely for analysis aromatic, olefinic and saturated signals.

The analysis of small molecule mixtures is beset by similar problems - spin decoupling and signal integration are possible but always misleading unless the sample is amenable to some form of separation prior to analysis. Samples are rarely insoluble but component mass ratios in the mixture may be changed due to selective solvation effects.

These drawbacks are again more than offset by the advantages of signal separation outlined above.

C 3 ULTRAVIOLET (u.v.) SPECTROMETRY.

U.v. solution spectra of undegraded polymers were obtained on a Pye Unicam S.P. 800 spectrophotometer using 1 cm matched quartz cells.

Chromophore development in oxidised rubber was monitored with the material as a thin film on a quartz window.

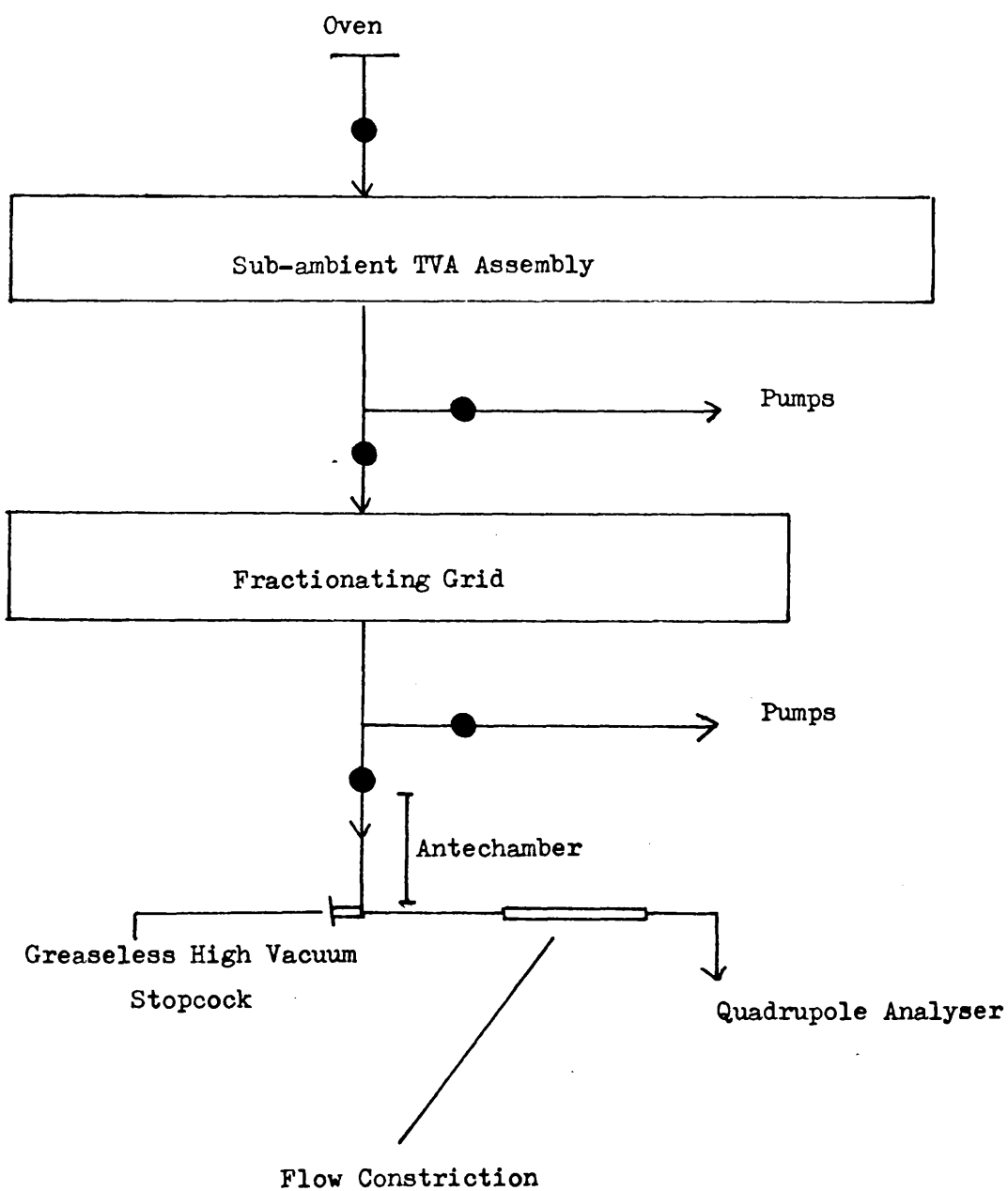
C 4 MASS SPECTROMETRY.

The low resolution cracking pattern and the parent masses of condensable volatile products of degradation were obtained via an on-line Micromass QX 200 Quadrupole analyser incorporated into the TVA manifold as shown in fig.12 .

The material was first separated into volatility bands using the sub-ambient TVA technique. These fractions were then expanded one by one into the spectrometer antechamber and subsequently into the analyser itself.

FIGURE 2 - 12

COUPLED SATVA - MASS SPECTROMETER SYSTEM



ADSORPTION THERMAL VOLATILISATION ANALYSIS (ATVA).

A. INTRODUCTION AND LITERATURE REVIEW.

A major disadvantage of all open-pumping vacuum degradation techniques, including TVA, is the inability of readily available cryogenic materials such as liquid nitrogen or oxygen to trap for analysis the noncondensable fraction of degradation products, which in theory may consist of mixtures, in any proportions, of the gases hydrogen, oxygen, nitrogen, methane and carbon monoxide.

"Closed system" degradations only partially solve this problem because of the uncertainty of product origin in this type of system. Observed volatile material may originate as a direct product of reactions within the polymer, or as a result of a rearrangement or reaction involving a primary decomposition product, unstable to prolonged exposure to degradative temperatures.

Primary noncondensables can, however, be trapped for examination in open system work by allowing them access to a number of surface-active solids, usually held at sub-ambient temperatures by a cooling medium. Three types of material were studied in this work, activated alumina, amorphous carbon and the "A" type synthetic zeolites. The first two proved unsuitable for use in a greased high-vacuum manifold. To maximise the efficiency of surface adsorption they had to be used in a finely powdered form which regularly fouled and scratched neighbouring stopcocks. On the other hand, adsorption of gas onto the surface of synthetic "A" type zeolites is followed by adsorption into the bulk of the material, leaving the surface open to more gas. For this reason the surface area did not have to be maximised and the material could be used in pellet form. Other advantages of the material included its chemical stability, its

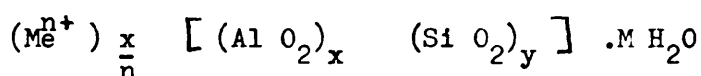
(proved) high capacity for adsorption of noncondensables, and its precisely defined structure which enabled conclusions drawn from the testing of one batch of material to be applied to all others.

The literature review which follows summarises work by other authors of direct relevance to this discussion.

A 1 PREPARATION AND STRUCTURE OF SYNTHETIC ZEOLITES (13-17).

Zeolites are best prepared by the controlled crystallisation of solutions of metal aluminates, silicates and hydroxides.

Stoicheometrically they can be represented by the formula



The most important quantity in the above formula is the ratio $\frac{x}{y}$. In "A" sieves it takes the value of two. The incorporation of aluminium into the lattice results in a charge imbalance which is removed by the inclusion of the mobile alkali or alkine earth cation Me^{n+} .

For reasons only partly understood, the nature of Me^{n+} has a subtle effect on the mean "pore" diameter. The newly prepared sieve contains sodium ions and has a pore diameter 4\AA . Ion exchange to calcium, increases this to 5\AA while a 50% ion exchange to potassium reduces the diameter to 3\AA .

X-ray crystallographic studies have established that the structure of the "A" type zeolites consists of three dimensional arrays of Si O_4 and Al O_4 tetrahedra in which oxygen sharing has produced the ratio $\frac{\text{O}}{\text{Al} + \text{Si}} = 2$.

The mobile cation Me^{n+} is held in an interstitial void, usually completely hydrated with M water molecules. Ion and molecule migration usually takes place via the interconnecting "pores" already mentioned.

A 2 ZEOLITE ACTIVATION.

The adsorption of small molecules into synthetic zeolites takes place by activated diffusion via the pore network to structural voids within the material. The nature and quantity of preadsorbed material greatly influence both the capacity for and kinetics of further adsorption. To ensure reproducible adsorptive behaviour it is necessary to remove as much of this material as possible.

Unactivated zeolites are saturated with water, up to 50% by weight. The enormous heats of water adsorption result in a concentrating effect at room temperature even under high vacuum conditions.

It was found by Stern and Di Paulo (18) however, that the equilibrium capacity of zeolites for water, in units of molecule/cage, decreased as the temperature of the sieve was raised. The high lattice energy of the material induces stability, even in oxidising atmospheres, at temperatures up to 700°C. For this reason, complete dehydration could be induced without lattice distortion, by heating under vacuum. The TG rate curves of fig. 1 and the TVA curves of fig. 2 suggest that water concentrations can be reduced to workable levels by prolonged heating at 150 - 200°C under vacuum.

Of passing interest is a conditioning effect which the authors propose to account for the increased reproducibility of successive gas adsorption/desorption cycles. This presumably arises via a displacement of preadsorbed species.

A 3 ADSORPTION ISOTHERMS (13,14, 18,19).

Much work has been carried out to relate equilibrium isothermal sieve capacities, in units of molecules/cage, to the gas pressure exerted on the sieve, usually at sub-ambient temperatures

FIGURE 3 - 1

TG RATE CURVES FOR WATER EVOLUTION UNDER
NITROGEN IN ZEOLITES

Sample Size 5 mg

Heating Rate $10^{\circ}\text{C}/\text{min}$

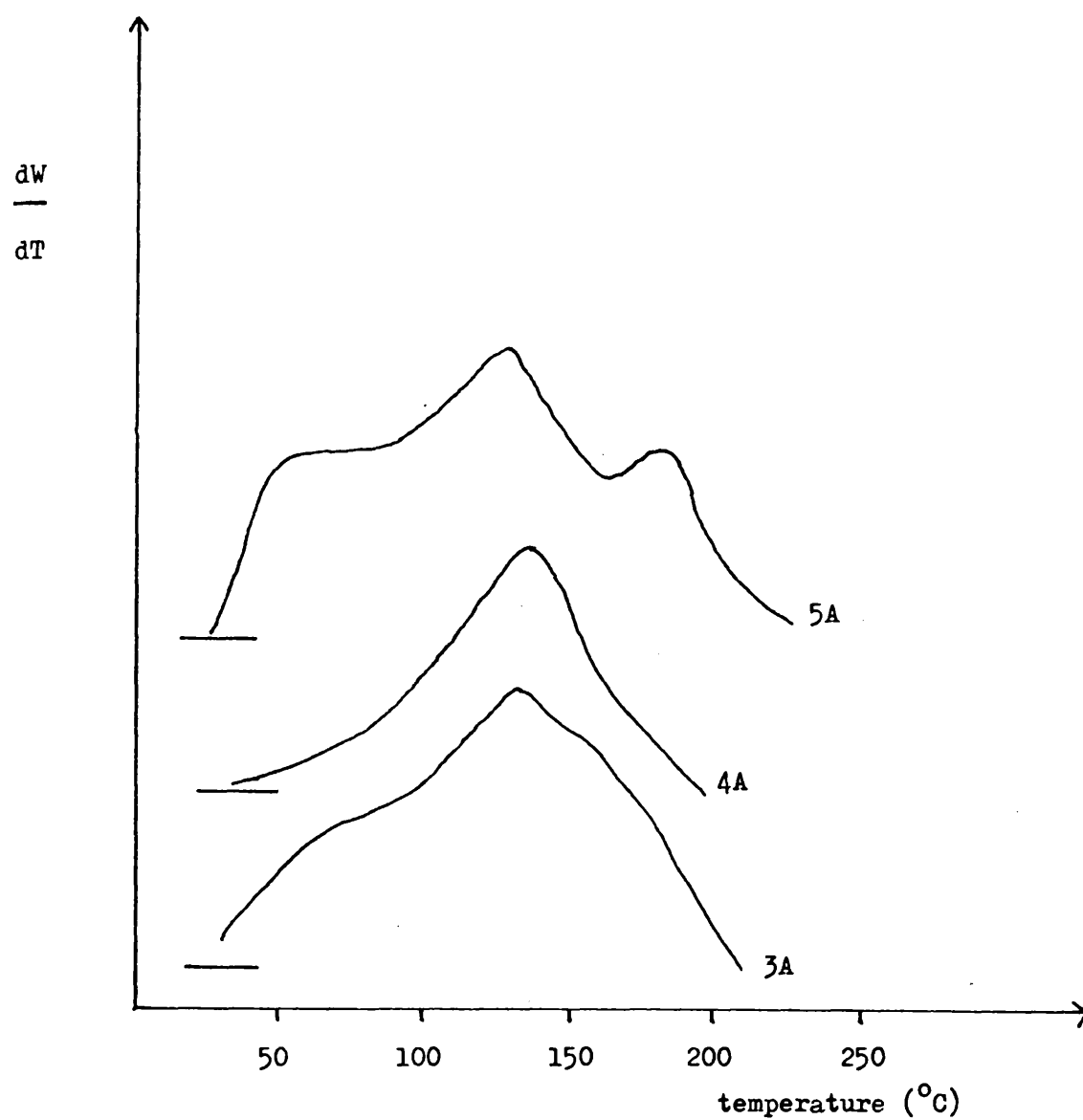
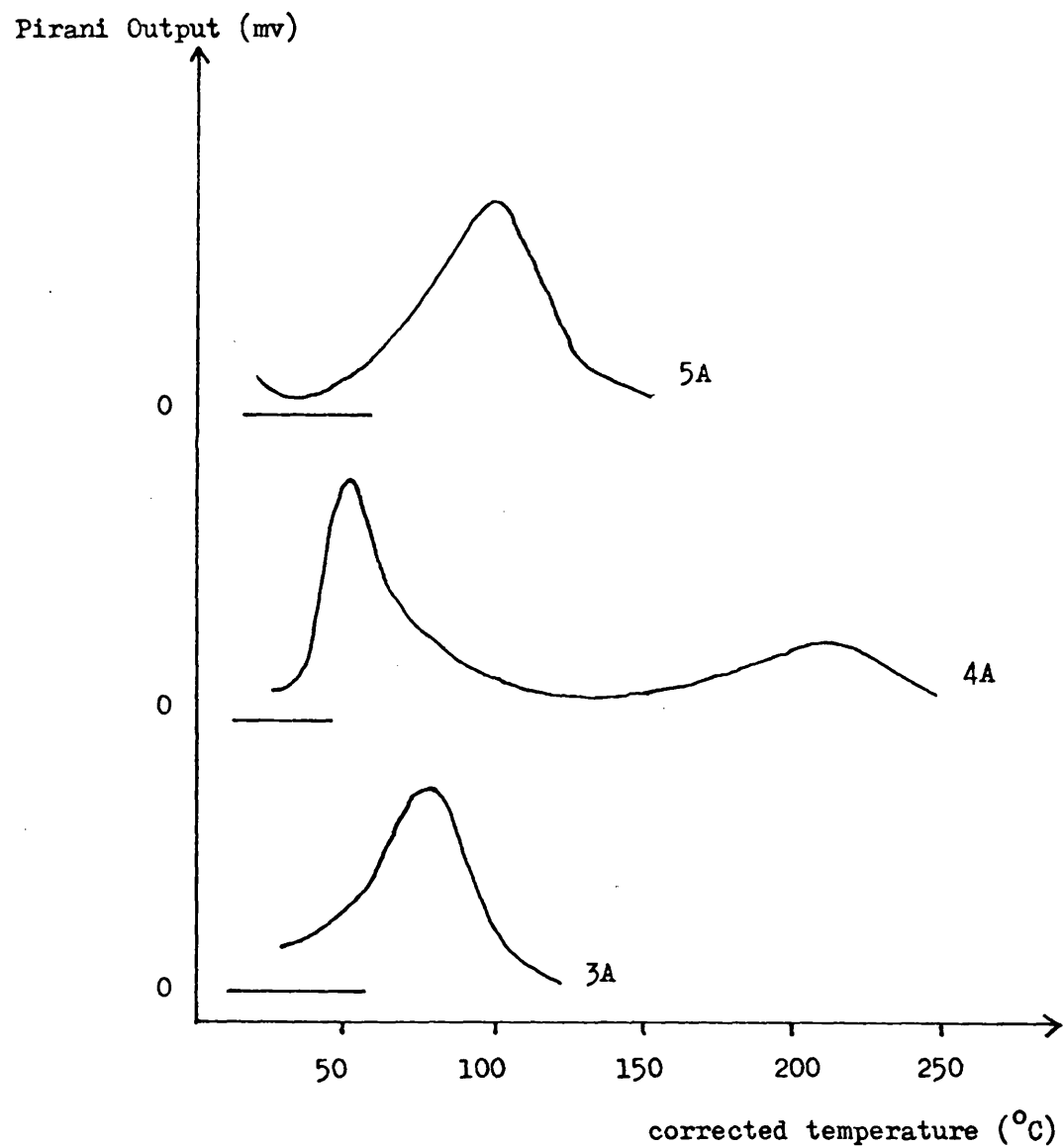


FIGURE 3 - 2

TVA WATER EMISSION CURVES FOR ZEOLITES

Sample Size 10 mg

Heating Rate $10^{\circ}\text{C}/\text{min}$



between 0°C and -196°C .

By themselves, such measurements do not explain the ATVA experiment (discussed subsequently) in which gas is partially or fully condensed onto a batch of sieve which is far from its equilibrium capacity, under conditions where non-condensed material is efficiently removed by the pumping system. They do, however, lead to the development of mathematical models (19) from which can be obtained an estimation of the effective molecular dimensions of the adsorbate (β) at the sieve temperature. Such values are tabulated below and will be used to rationalise the ATVA effect.

TABLE 3 - 1

EFFECTIVE NONCONDENSABLE GAS DIMENSIONS AT -196°C .

ADSORBATE	β (Å)
H_2	/
O_2	40 - 50
N_2	65 - 75
CH_4	50 - 60
CO	50 - 60

A 4 PUMPING SPEEDS.

Work has also been carried out to ascertain the rate of attainment of sieve/gas equilibrium at -196°C by measuring gas pumping speeds at low pressures, usually by a combination of ion gauge or mass spectrometer, and flow-calibrated gas orifice.

From this type of work (20 - 23) there emerges a set of "sticking probabilities" (\bar{S}) which measure the ability of freshly activated sieve to hold irreversibly the gas at -196°C .

Values of \bar{S} (tabulated below) are obtained from the standard equation used to calculate the mass of gas striking a surface per unit time, modified by the inclusion of \bar{S} to represent the quantity of gas irreversibly held per unit time.

$$S_{\text{eff}} = 3.6 F \bar{S} \sqrt{\frac{T}{M}}$$

Where

S_{eff} = EFFECTIVE PUMPING SPEED AT THE SURFACE (1/sec)

F = ADSORBANT SURFACE (cm^2)

T = TEMPERATURE (K)

M = GAS MOLECULAR WEIGHT

TABLE 3 - 2

EFFECTIVE GAS STICKING PROBABILITIES (\bar{S}) AND PUMPING SPEEDS ONTO

5A MOLECULAR SIEVE AT -196°C .

ADSORBATE	PUMPING SPEED (1/sec at 10^{-4} torr)	\bar{S} (10^{-3} cm $\sqrt{\frac{M}{T}}$)
H_2	0.35	3.6×10^{-5}
AIR ($\text{O}_2 + \text{N}_2$)	7.8	2.7×10^{-3}
CH_4	15.0	4.3×10^{-3}
CO	77.0	5×10^{-2}

It is of interest to note that oxygen, which is adsorbed in enormous quantities under equilibrium conditions (13), possesses a small \bar{S} value. This may result from a combination of its small \bar{P} value and high affinity for the oxide matrix which would result in a low activation energy of diffusion into (and out of) the sieve. This effect was illustrated by Chan and Anderson (24).

As expected "A" type zeolites were not found to pump hydrogen to any great extent at -196°C . This effect probably arises from the extremely small effective volume of the gas.

B 1 ADSORPTION AND DESORPTION OF STATIC GAS VOLUMES AT SUB-AMBIENT TEMPERATURES.

The following was carried out using the apparatus illustrated in fig. 3 . Noncondensable gases were admitted to section A of the apparatus which was subsequently opened to the rotary pump. This process was repeated to purge the pumping system of oxygen and nitrogen. A final volume of gas was admitted to section A, of volume 245 ± 3 ml (by gas expansion), and pumped down to a pressure of (usually) a few mm Hg.

Dewar vessel D_1 was filled with liquid nitrogen and used as shown to remove condensable impurities from the gas, which was then introduced to section B of the apparatus. It was found that small quantities of the gases O_2 , CH_4 , and CO were condensed into the U-tube during this process and were subsequently removed by pumping at a limiting rate. To eliminate this type of gas transfer to section B of the apparatus, stopcock 2 was immediately closed.

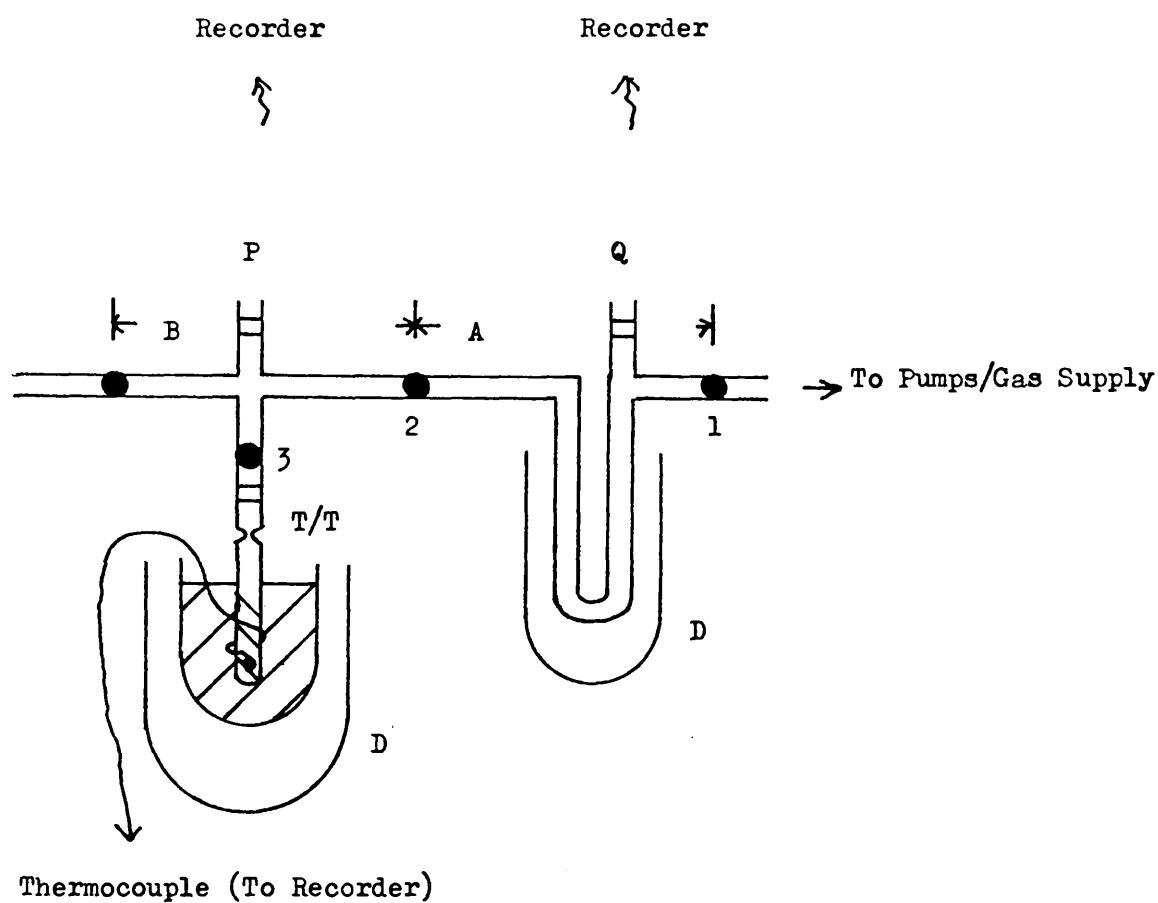
Stopcock 3 was next opened and the noncondensable gas fraction was allowed access to approximately 1g of freshly activated sieve held at 196°C . Condensation curves were obtained by measuring Pirani P output as a function of time.

This work was carried out on volumes of hydrogen, oxygen nitrogen, carbon monoxide and methane. To avoid repetition, results for nitrogen (representative) and hydrogen (the exception) are quoted.

Some typical pump-down curves are illustrated in fig. 4 . In curves 1 and 2 condensed material was not evolved by subsequent pumping on the sieve. However in situations of the type illustrated in curve 3A where the material is close to saturation, subsequent pumping on the sieve produces a limiting rate of gas evolution (curve 3B). This latter situation is better thought of as an

FIGURE 3 - 3

APPARATUS FOR ADSORPTION/DESORPTION OF STATIC GAS VOLUMES



Key

P,Q Pirani Gauges

T/T Test Tube With Constriction Containing 1 g "A" Sieve

A,B Sections Of The Apparatus

/// p-Xylene Jacketing Material

D Dewar Flasks Containing Liquid Nitrogen

FIGURE 3 - 4

PUMP DOWN CURVES FOR NITROGEN AND HYDROGEN OVER 3A SIEVE

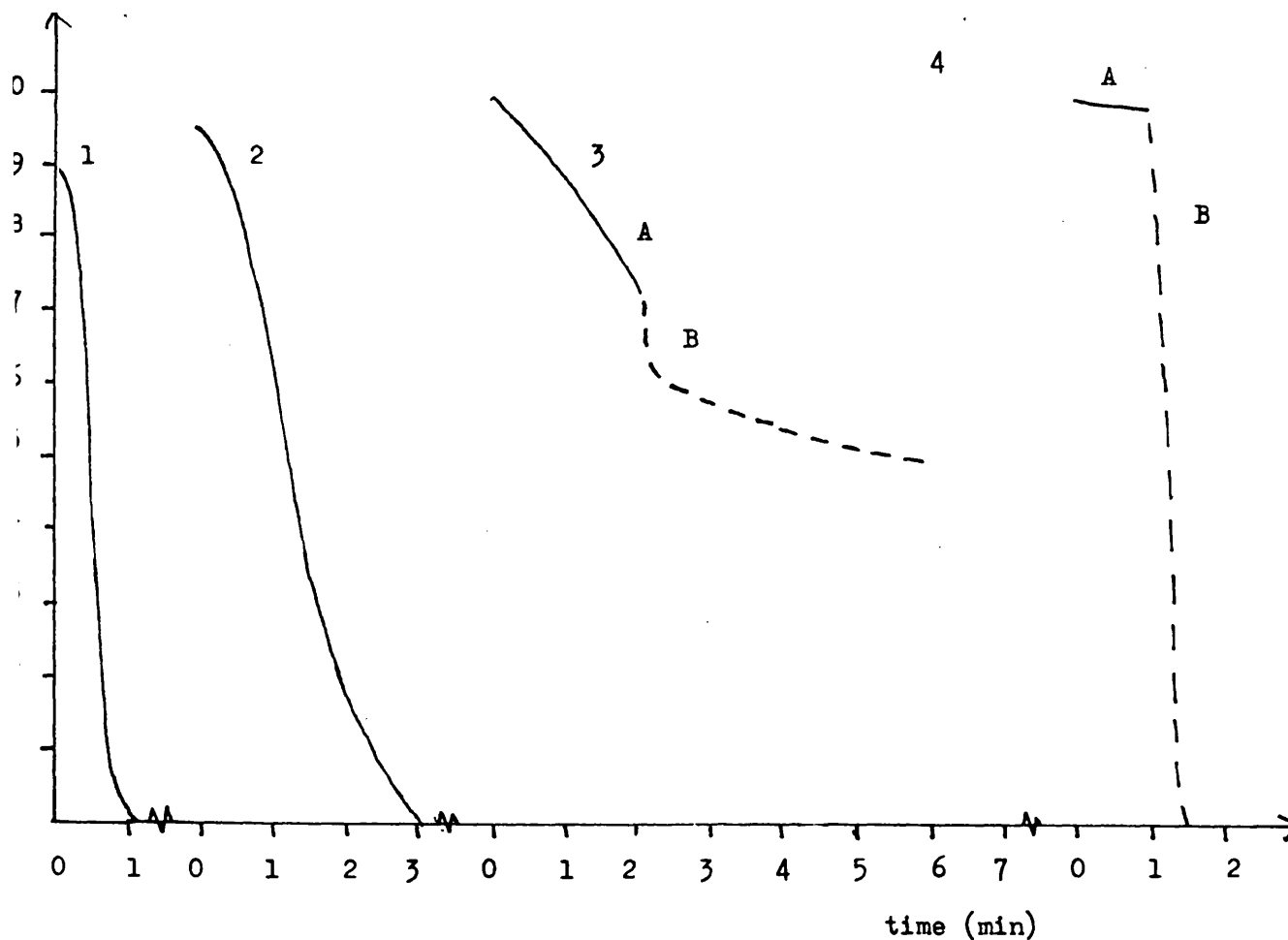
For Complete Adsorption

$$n \text{ (Moles Adsorbed)} = 1.3 \times 10^{-4} \cdot P \quad \text{Where } P = \text{True Gas Pressure In cmHg}$$

Key

- 1 Nitrogen $n = 3.3 \times 10^{-6}$ Mole
- 2 Nitrogen $n = 10^{-4}$ Mole
- 3 Nitrogen $n = 10^{-3}$ Mole
- 4 Hydrogen

Pirani Output (mv)



extension of the effect, illustrated in fig. 5 and discussed in the next paragraph, of sieve gas loading on the shape and position of the programmed warm up gas evolution curve. The pressure curve for hydrogen is best explained by an ideal gas contraction on exposure to liquid nitrogen temperatures followed by complete removal by pumping.

Programmed desorptions of completely adsorbed gas samples were carried out as follows. The system was opened to the pumps as illustrated in fig. 3 . Dewar vessel D_2 was removed and the p-xylene was allowed to warm up to ambient temperatures as in the normal sub-ambient TVA experiment. The volatilisation curve was obtained by simultaneously recording the temperature and pressure profile. It was established that evolved material was noncondensable in nature by recording also Pirani Y output with Dewar vessel D_1 containing liquid nitrogen in position.

The dependence of peak position on loading is illustrated in a qualitative manner in fig. 5 . The appearance of only one peak at a time indicates that binding sites act collectively in the desorption process. The direction of peak movement as loading is increased indicates that bound gas is destabilised by neighbouring gas molecules.

Fig. 6 illustrates the situation where a programmed warm up is interrupted at point C by immersing the jacketing material in liquid nitrogen. The dotted line indicates the curve shape of a normal sub-ambient TVA peak during this process. It can be seen that the efficiency with which the molecular sieve responds to the recooling process is low, possibly because of poor contact with the glass tube. It is therefore not possible to relate peak positions directly to the temperature of the jacketing material. The effect will vary from system to system.

FIGURE 3 - 5

PROGRAMMED SUB-AMBIENT DESORPTIONS OF NITROGEN GAS FROM 5A

MOLECULAR SIEVE

Variation Of Sub-ambient Peak Position With Gas Loading ($1 > 2 > 3 > 4$)

$n_1, n_2 \doteq 10^{-4}$ Mole

$n_3 \doteq 10^{-5}$ Mole

$n_4 < 10^{-5}$ Mole

Key

--- (-) Thermocouple Reading
 -.-.- Pirani Output Q
 — Pirani Output P

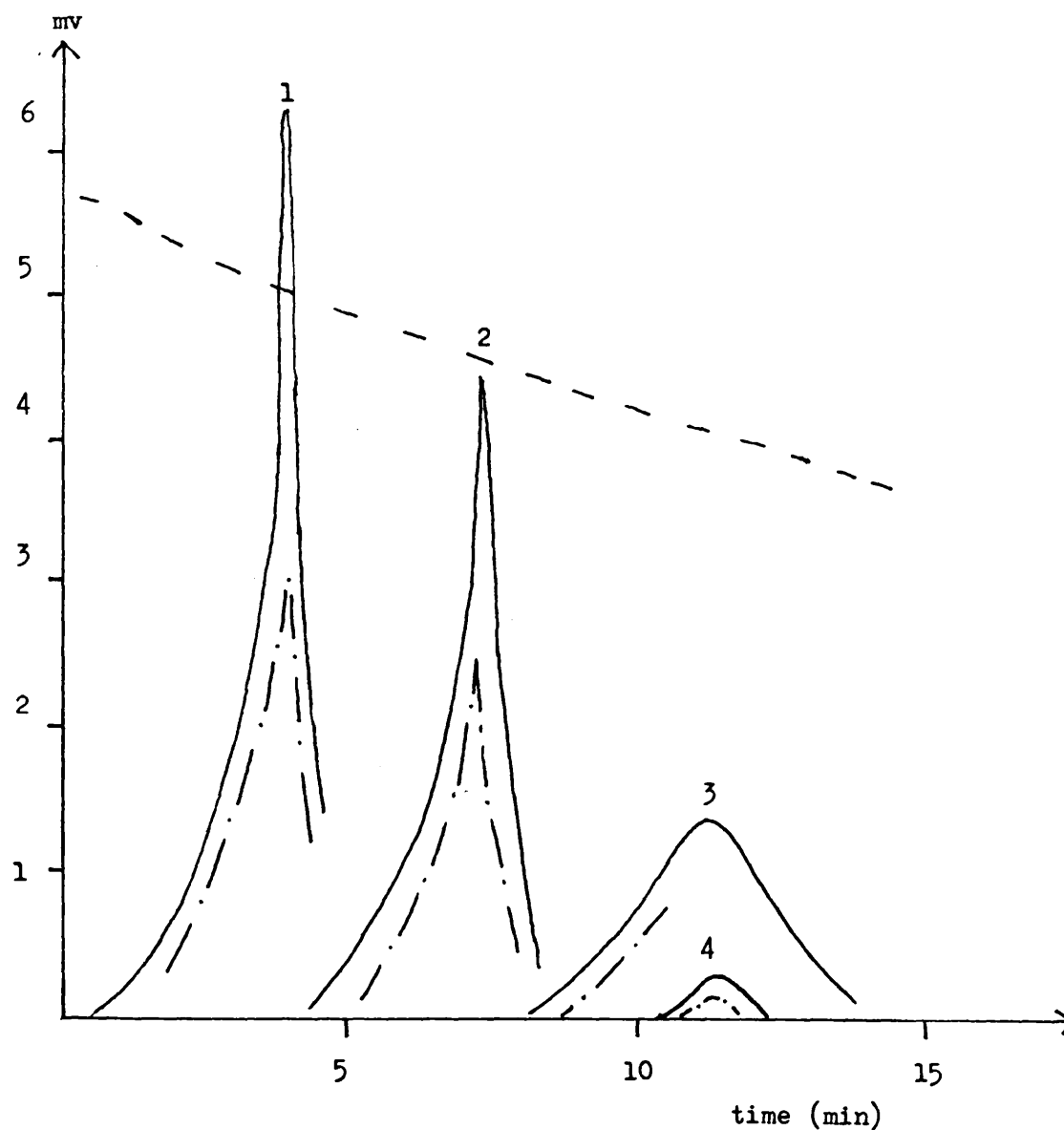


FIGURE 3 - 6

INTERRUPTED SATVA OF NONCONDENSABLE GAS

Gas Loading, $n \dot{=} 10^{-4}$ Mole

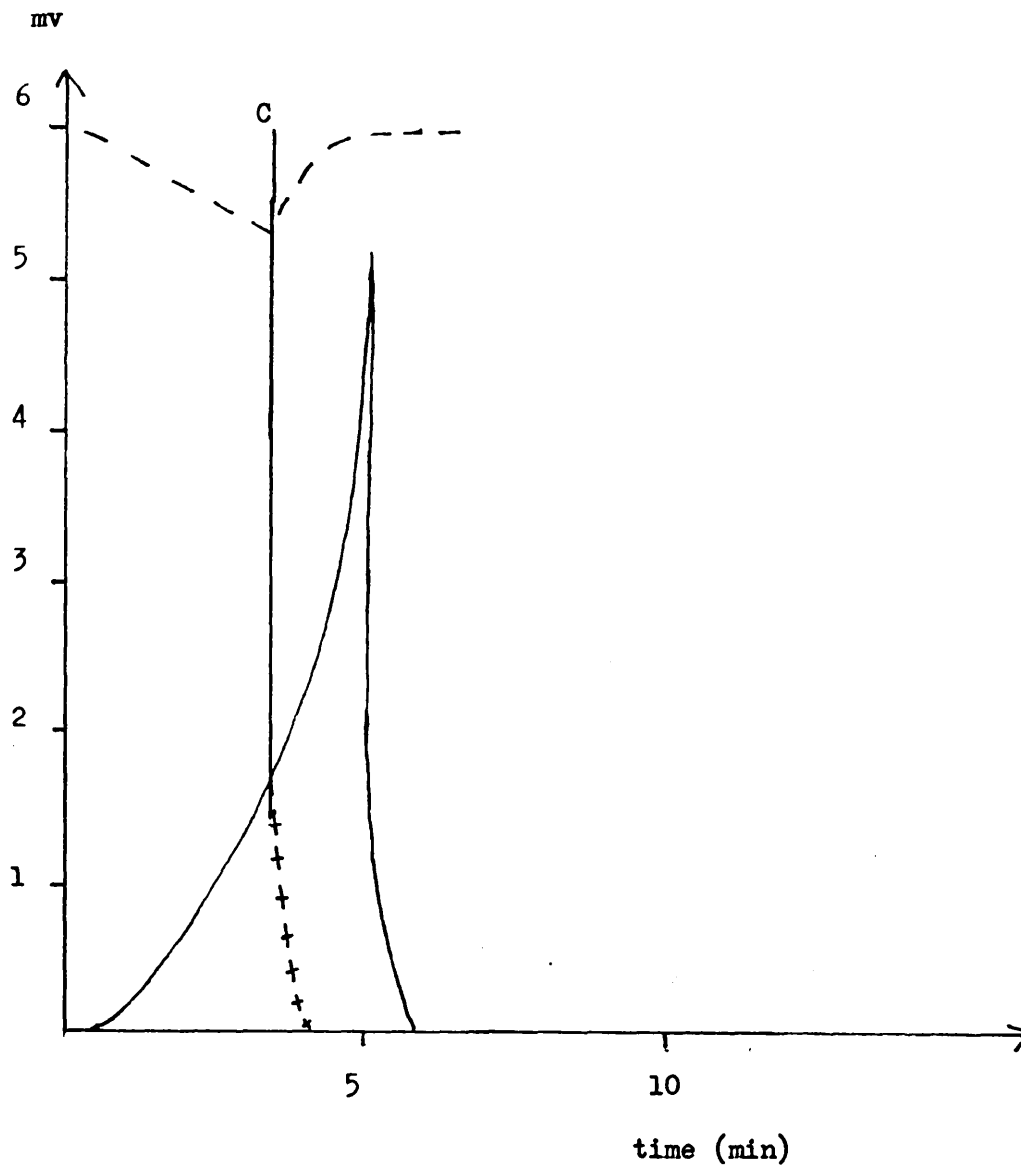
Key

---(-) Thermocouple Reading

— Pirani Output P

+ + + + Normal SATVA Peak Behaviour

C Point At Which Jacketing Material Is Surrounded With Liquid Nitrogen



The above two effects prevent the use of the method, in an analogous fashion to the normal TVA experiment, to separate and identify noncondensable gas mixtures. However, provided it is known that a pure gas is to be examined, peak areas may be used to measure quantitatively small samples of adsorbate.

B 2 DYNAMIC ADSORPTIVE BEHAVIOUR.

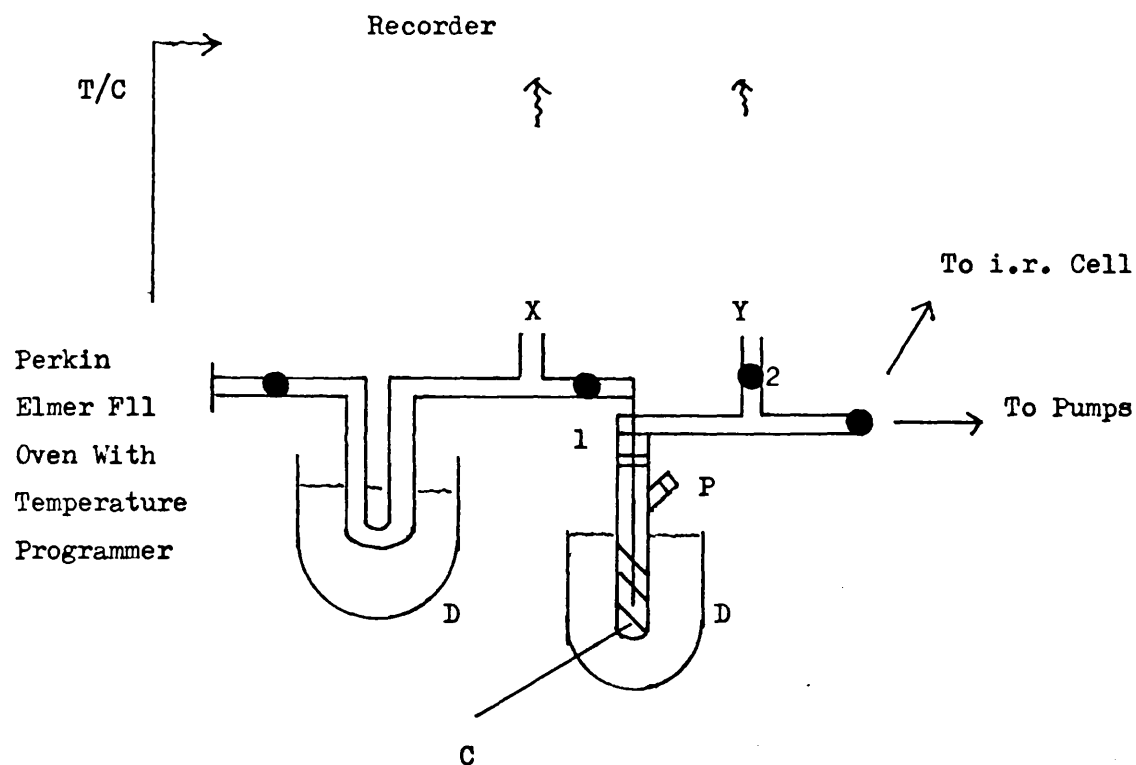
In the normal TVA experiment Pirani gauges are used to measure the effect on a gas flux of a cryozone through which the gas is forced to pass. It was felt desirable to ascertain the effect on a noncondensable gas flux of passage through cooled molecular sieve in the same manner.

Such work was carried out on the assembly illustrated in fig. 7. The cold trap was charged with 5A molecular sieve at port P. To eliminate fouling by vacuum grease during activation, all neighbouring seals were of silicone grease which is stable in the temperature range 150 - 200°C. Stopcocks 1, 2 and 3 were incorporated to minimise the risk of contamination of sieve by condensable vapour which must eventually be routed to the pumping system.

The gas mixture generated by a programmed degradation in the oven assembly, was freed of condensable impurities by passage through Dewar vessel D₁ containing liquid nitrogen. It was then passed through the sieve trap which had been precooled with liquid nitrogen in Dewar vessel D₂ to ensure temperature homogeneity. The degree of gas adsorption was measured by simultaneously recording Pirani X and Y outputs. The nature of the process did not allow X to be normalised to Y under the conditions of the experiment. Instead the outputs were equalised using static gas pressures above the sieve held at 0°C by an ice/water bath.

FIGURE 3 - 7

APPARATUS FOR ADSORPTION TVA



Key

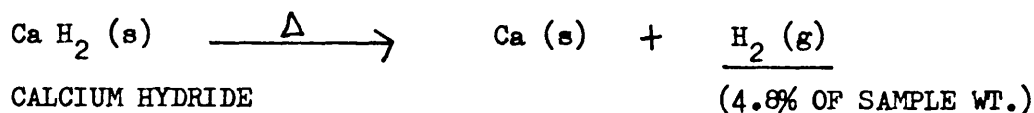
- T/C Oven Thermocouple Output (mv)
- C Cold Trap Charged With 10 g 5A Sieve
- P Port For Charging With Sieve
- D Dewar Vessels Containing Liquid Nitrogen
- X Pirani Gauge Before Sieve
- Y Pirani Gauge After Sieve
- \\ 5A Sieve

response at a TVA peak is increased if it is measured prior to a section of vacuum manifold which restricts the gas flow. The Pirani response after the restriction should be reduced. This argument is used to explain the large pressure gradient found to exist between Piranis X and Y under conditions where the material comprising the TVA peak does not interact with the sieve, for example with hydrogen passing through the trap held at 0°C. This effect was minimised by placing X and Y as close to the trap as possible.

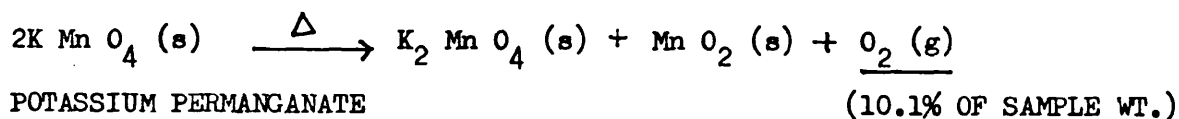
B 3 GAS GENERATION.

To simulate as far as possible the TVA experiment a continuous gas flux had to be generated. With the apparatus available this was most easily achieved by thermally degrading under vacuum, materials known to produce a single component noncondensable flux. In the case outlined below, decompositions were brought about using a heating rate of 10°C/min.

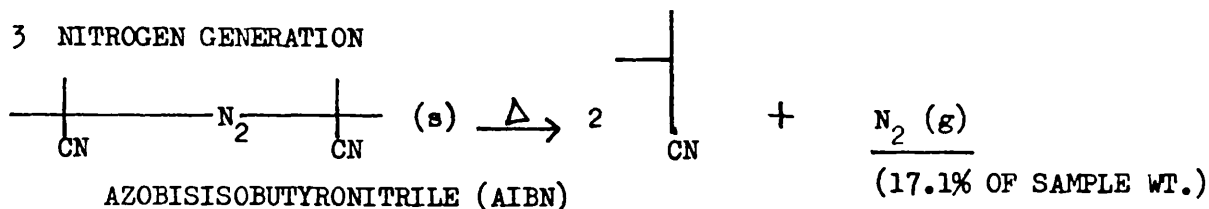
1 HYDROGEN GENERATION



2 OXYGEN GENERATION

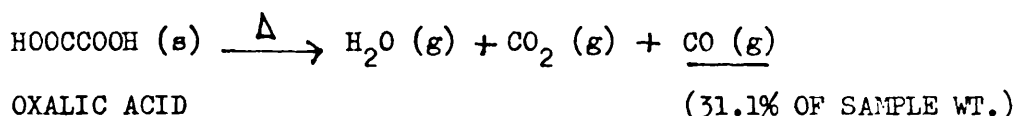


3 NITROGEN GENERATION



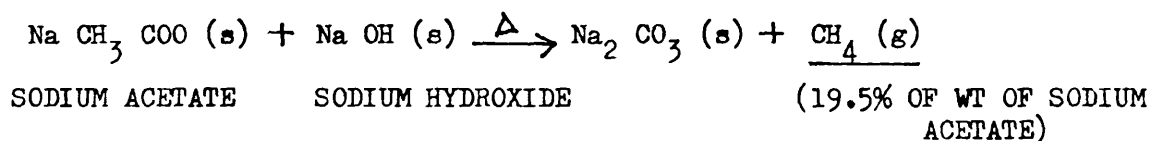
To reduce sublimation of the AIBN it was finely dispersed into 400 mg of 13X molar sieve which was pressed into pellet form.

4 CARBON MONOXIDE GENERATION



To reduce sublimation of the oxalic acid it was treated in the same manner as 3 above.

5 METHANE GENERATION



Because of the corrosive nature of the reacting mixture, degradations were carried out in a removable Pyrex boat.

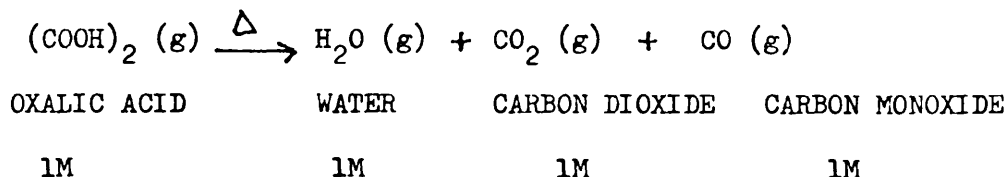
B 4 EXAMINATION OF CONDENSED MATERIAL.

At the end of the ATVA experiment the sieve chamber was isolated from the manifold and warmed to room temperature. Evolved material was monitored using Pirani Y. Working on the basis that material condensed onto 5A sieve could be recondensed onto it, the i.r. cell shown in fig.2-11 was constructed, positioned as shown in fig. 7 and used to concentrate the material for analysis. The efficiency of gas condensation was monitored by Pirani Y. It was found that provided the capacity of the sieve in the i.r. cell was not exceeded, the efficiency of transfer was superior to that obtained using Toepler pumping. In fact pressures of upwards of a few torr could be easily reduced to below 10^{-3} torr. This results in an efficiency of transfer of more than 99% .

A procedure was developed to calibrate the molecular sieve-containing i.r. cell already mentioned for carbon monoxide analysis by using the products of decomposition of oxalic acid.

(i). Decomposition of Oxalic Acid.

Oxalic acid was assumed to decompose by the reaction outlined below.



If a sample of oxalic acid could be degraded and its products of degradation efficiently manipulated, then the quantity of carbon monoxide condensed into the molecular sieve-containing cell could be assumed to be equal to the quantity of carbon dioxide condensed into a calibrated, condensable gas i.r. cell. A calibration chart of carbon monoxide absorbance at 2150 cm^{-1} versus gas content could then be constructed.

(ii). Quantitative Analysis of Carbon Dioxide.

The cell to be calibrated for carbon dioxide was attached to the gas handling manifold depicted in fig. 8 . Carbon dioxide was admitted to the storage bulb and thoroughly degassed. Gas at a range of pressures was admitted to the i.r. cell and the i.r. spectrum corresponding to each gas pressure was obtained. The wavenumber 3710 cm^{-1} was selected for quantitative work and a list of data points (absorbance (A), pressure (P)) was drawn up. A linear least squares procedure was used to determine the best straight line through the points to give the graph shown in fig. 12 .

The pressure P was converted to the molar gas content, n, of the cell by an application of the ideal gas law in the form :-

FIGURE 3 - 8

APPARATUS USED TO OBTAIN PRESSURE VERSUS i.r. ABSORPTION CURVE FOR CO₂ CELL

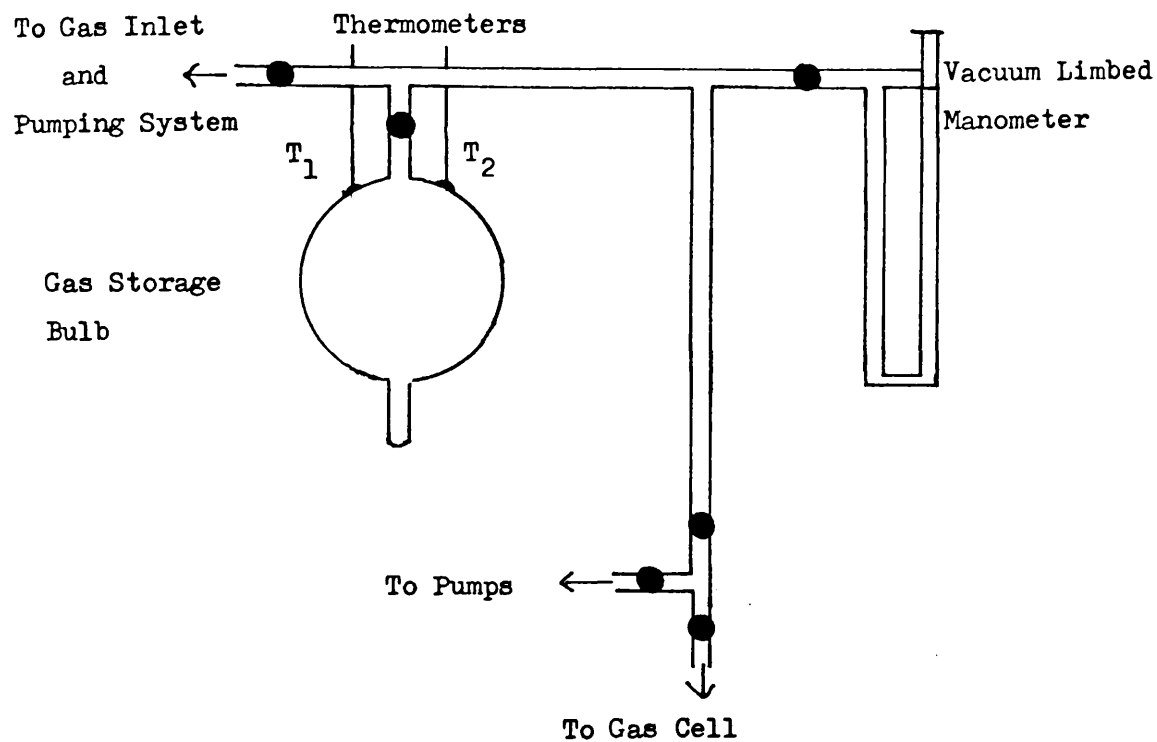
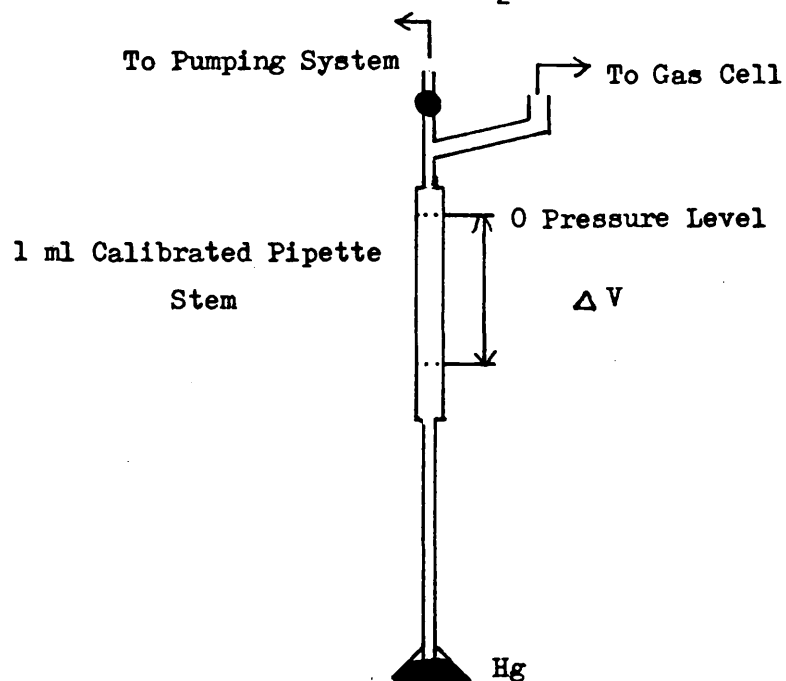


FIGURE 3 - 9

APPARATUS USED TO CALIBRATE CO₂ CELL FOR VOLUME



$$n = \frac{v}{P_1 (RT)}$$

Where

v = cell volume (cm^3)

R = gas constant (6240 cm^3 cm Hg/mol K)

T = absolute temperature K.

T was easily obtained from the average of the two thermometer readings T_1 and T_2 at the storage manifold. During the experiment, T differed by a maximum of $\pm 0.2^\circ\text{C}$ from its mean value of 24.5°C . However, v was more difficult to obtain. The cell used was one of the new type with displaced cold finger. It was therefore difficult to measure its volume by filling with solvent. In any case polar solvents contain water which tends to fog the cell windows while non-polar solvents attack the glue affixing the salt plates to the cell. A new procedure was developed to determine the volume of the i.r. cell by an application of Boyles Law.

(iii). Small Volumes By Gas Expansion.

Work was carried out using the apparatus depicted in fig. 9. The assembly was thoroughly evacuated and the zero pressure level on the calibrated stem P_0 was estimated. Gas was then admitted to the assembly to a pressure P_1 . The i.r. cell was isolated and the remainder of the gas was pumped away to bring the mercury column back to P_0 level.

The assembly was isolated from the manifold and the gas contained in the i.r. cell was allowed to expand into the assembly to achieve a final pressure P_2 .

By Boyles Law

$$P_1 v = P_2 (v + V + \Delta V_2)$$

Where

v = volume of the gas cell (ml)

V = volume outside of the i.r. cell and above the zero pressure level of the mercury (ml).

Δv_2 = extra volume generated in the calibrated manometer
to achieve pressure P_2 .

By rearrangement

$$\frac{P_1}{P_2} = \left(1 + \frac{v}{\bar{v}}\right) + \frac{1}{\bar{v}} \Delta v_2$$

If all readings are obtained on the calibrated portion of the manometer

$$\frac{\Delta v_1}{\Delta v_2} = \left(1 + \frac{v}{\bar{v}}\right) + \left(\frac{1}{\bar{v}}\right) \Delta v_2$$

Where

Δv_1 = volume generated in the calibrated manometer to
achieve pressure P_1

The data points $\left(\Delta v_2, \frac{\Delta v_1}{\Delta v_2}\right)$ were subjected to a linear least
squares analysis to determine the gradient $\left(\frac{1}{\bar{v}}\right)$ and the intercept
 $\left(1 + \frac{v}{\bar{v}}\right)$ of the graph.

Before the procedure was used to calibrate the i.r. gas
cell for volume, it was first tested for accuracy by using it to
obtain the volume of a glass storage bulb of similar dimensions.
The volume obtained by gas expansion was then compared with the
volume of the bulb as measured by the weight and hence volume of
water required to completely fill it. Volumes so obtained are
tabulated below.

TABLE 3 - 3

CELL VOLUMES (ml) BY GAS EXPANSION AND TITRATION.

	GAS EXPANSION		TITRATION
	v	V	v
GLASS BULB	12.25	7.24	12.21
i.r. CELL	11.00	9.86	/

It can be seen from TABLE 3 that the volume of the
storage bulb as measured by gas expansion differs by much less than
1% from the volume as measured by titration. Because of this the
method was assumed to be accurate enough to justify its usage.

Of interest are the relatively large differences of the V values for the glass bulb and the i.r. cell. This presumably arises because the two objects contain different volumes in the space between the stopcock and the connecting B14 cone. It can be seen that even a small volume, constant volume manometer would have to be recalibrated for each system because of the relatively large change in V between systems.

During the course of the experiment the top of the mercury column deviated by a maximum of 0.002 ml from its mean position. If it is assumed that the v value for the storage bulb is correct then so too must be its V value of 7.24 ml. The relative error in V introduced by this volume fluctuation is therefore shown to be much less than 0.1%.

(iv). Conditions of Degradation.

Oxalic acid quantitatively sublimes upon heating. It was therefore necessary to trap it in the hot zone to produce quantitative decompositions.

This was achieved by degrading the material in small breakseal vessels of the type illustrated in fig.10 which could be completely contained in the oven.

Samples were warmed at a programmed rate of $10^{\circ}\text{C}/\text{min}$ to 300°C then cooled to room temperature.

(v). Product Separation and Analysis.

The breakseal vessel was attached to the assembly shown in fig. 11 . The breakseal was broken and the products of degradation were allowed access to the liquid nitrogen trap to remove condensable material. After a few minutes, stopcocks 2 and 3 were opened and the noncondensable product fraction was allowed access to the molecular sieve held at -196°C in the cell for noncondensables. After a pressure of 10^{-3} torr had been achieved, as measured by the

FIGURE 3 - 10

BREAKSEAL FLASK FOR CLOSED SYSTEM WORK

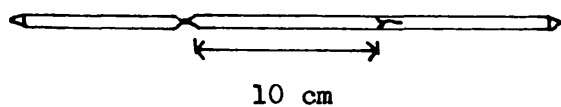
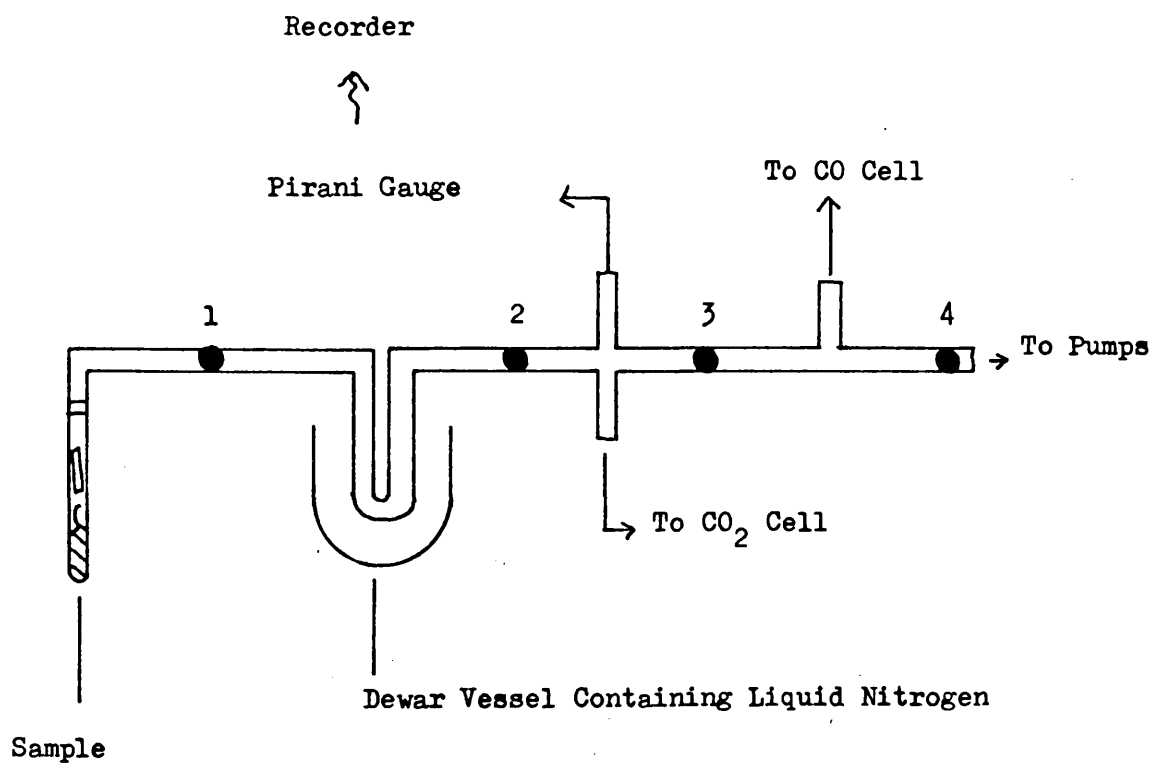


FIGURE 3 - 11

APPARATUS USED TO OBTAIN SPECTRA OF CONDENSABLE AND NONCONDENSABLE
PRODUCTS FROM CLOSED SYSTEM DEGRADATION



Pirani gauge, residual noncondensable material was pumped away and the cell was isolated from the manifold.

After removal of the cold trap condensable material was collected in the cold finger of the cell calibrated for carbon dioxide.

The i.r. spectra of both fractions were obtained.

(vi). Cell Calibration.

The relevant experimental results are tabulated below.

TABLE 3 - 4

CARBON DIOXIDE ASSAY IN OXALIC ACID DECOMPOSITIONS.

SAMPLE WEIGHT (mg)	MOLES CO ₂ ($\times 10^4$) (EXPECTED)	MOLES CO ₂ ($\times 10^4$) (FOUND)
11	1.22	1.23
16	1.78	1.84
20	2.22	2.33
25	2.78	2.72
30	3.33	3.29

TABLE 3 - 5

CARBON MONOXIDE ABSORBANCE AT 2150 cm⁻¹

SAMPLE WEIGHT (mg)	(ASSUMED) MOLES CO ($\times 10^4$)	%ABSORBANCE
11	1.23	2
16	1.84	6
20	2.33	10
25	2.72	15
30	3.29	22

The gas calibration chart depicted in fig. 13 was constructed from the above data.

Of interest is the nonlinearity for small n values. This is best explained by proposing that the molecular sieve in the cell concentrates the gas with the result that the free gas

FIGURE 3 - 12

GAS CELL CALIBRATION CURVE FOR CO₂ AT 3710 cm⁻¹

$$n = P \left(\frac{V}{RT} \right)$$

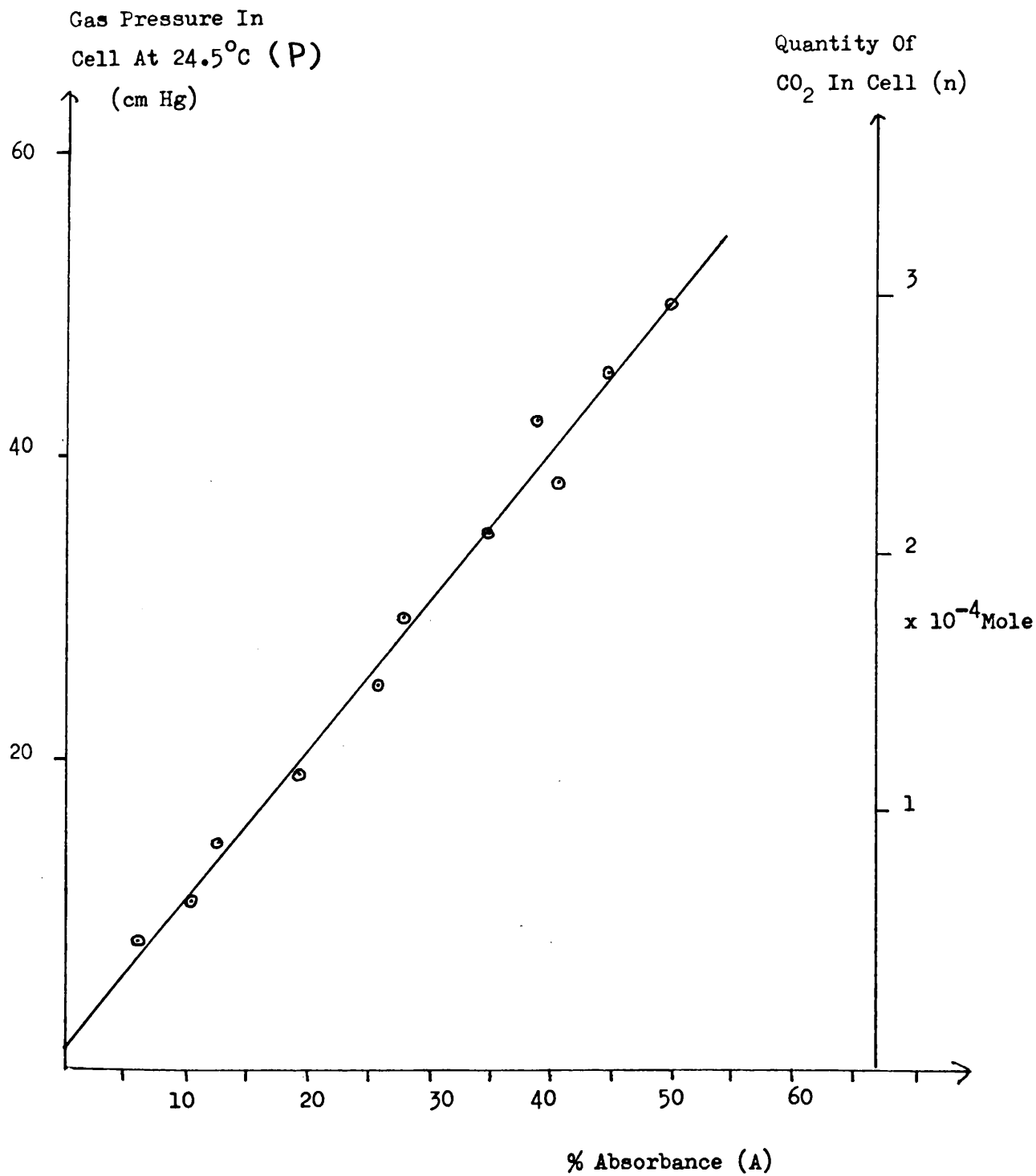
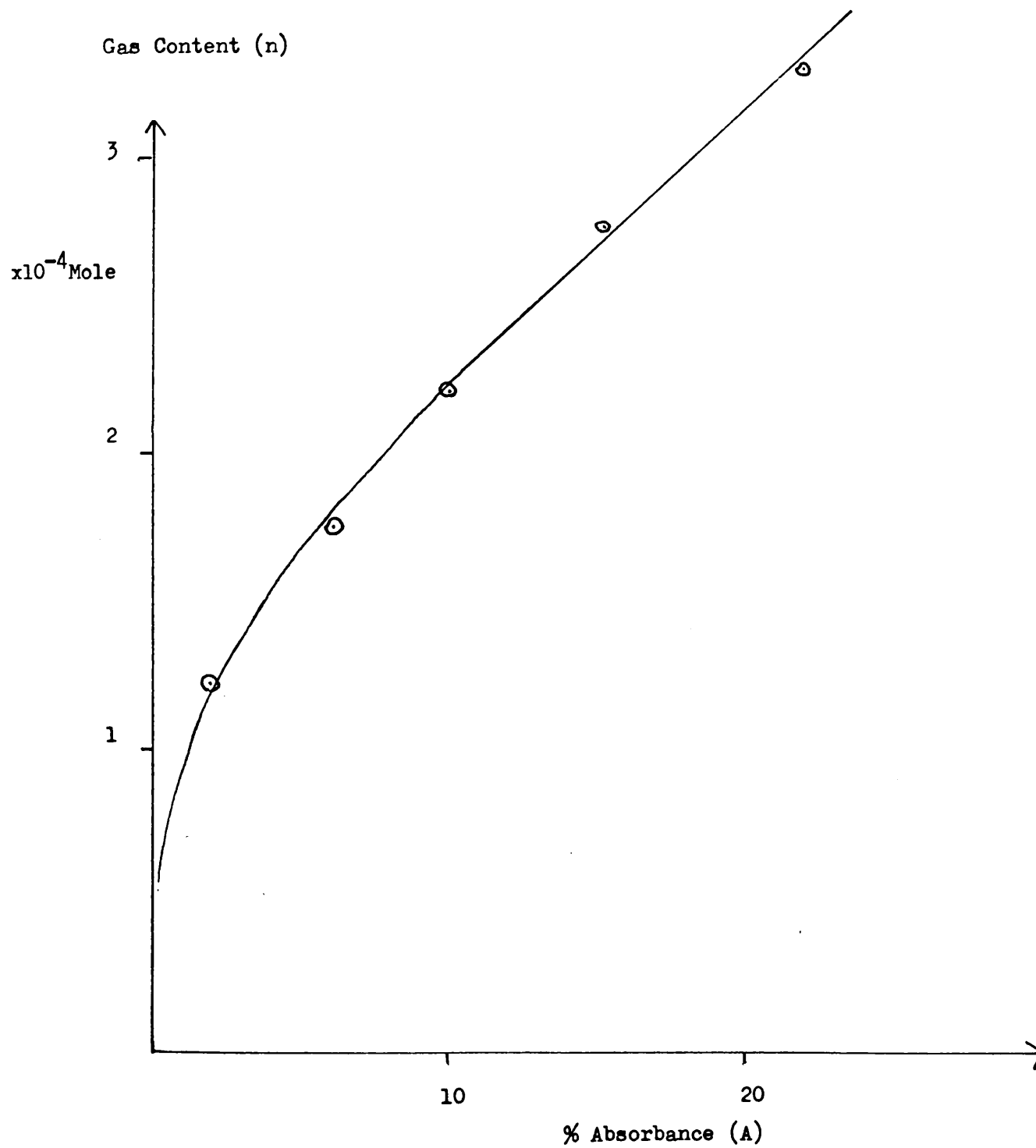


FIGURE 3 - 13
CALIBRATION CURVE FOR CO AT 2150 cm^{-1}



content in the cell is reduced. At higher gas contents the sieve is saturated and the graph becomes linear.

This process which is reversible in nature must be distinguished from adsorption at -196°C which is irreversible.

From the above considerations it becomes obvious why the cell for noncondensables (above) could not first have been calibrated for CO_2 then for CO by condensation into the cell of the complete volatile degradative product content of the breakseal vessel. Firstly, n values for CO_2 in the cell during calibration would always be low because of the very large equilibrium capacity of 5A sieve for the material at room temperature. Secondly, carbon dioxide and water would displace carbon monoxide from its equilibrium concentration in the sieve at room temperature producing high absorbance readings for the noncondensable material. The adsorption of water into the sieve would ruin the cell for further work.

B 6 ATVA CURVES FOR NONCONDENSABLES, USING 5A MOLECULAR SIEVE.

ATVA curves corresponding to pure fluxes of hydrogen, oxygen, nitrogen, carbon monoxide and methane can be inspected in fig. 14 - 18 respectively.

Throughout this discussion, we will use as a criterion to measure the capacity of the sieve for a substance, the smallest molar gas loading (n) required to produce a Pirani Y reading distinguishable from zero. It can be seen that sieve capacity increases in the order hydrogen ($< 10^{-6}\text{MOLE}$), oxygen ($\doteq 10^{-5}\text{MOLE}$), to nitrogen ($\doteq 10^{-5}\text{MOLE}$).

Carbon monoxide and methane seem to exhibit much higher capacities of adsorption. The capacity for methane seems to be of the order of $5 \times 10^{-4}\text{MOLE}$ while that for carbon monoxide may be as high as 10^{-3}MOLE (by reference to its enormously high \bar{S} value of TABLE 2).

The most striking feature of the ATVA curves of hydrogen gas shown in fig. 14 is the relatively small X and Y Pirani readings obtained throughout. Because of its high random velocity, static gas pressures of hydrogen produce a very large Pirani output (manufacturer's data). It may therefore be that very same property of the gas which allows it to diffuse very rapidly to the pumping system to produce a low dynamic pressure in the system. The same effect is observed in normal sub-ambient warm up experiments for condensable volatiles, when the collecting trap is moved closer to the sub-ambient trap to produce an enhanced pressure gradient.

It remains true, however, that small amounts of hydrogen generated in, for example, the carbon fibre forming reaction, give a very large noncondensable response in the normal TVA experiment when compared with the response generated by a similar quantity of condensable material.

A comparison of curves B and D of fig. 14 indicates that hydrogen does not interact with 5A molecular sieve at -196°C , in fact hydrogen can not be trapped by this system. Of interest also is the gas "hold up" effect illustrated in fig. and discussed more fully in section B 2 of this chapter.

Fig. 15 illustrates the low adsorptive capacity of the material for oxygen gas. A comparison between curves C and D, however, indicates that some interaction with the sieve takes place. When the experiment with sieve at -196°C which produces curve C is repeated with sieve at 0°C to give curve D this pumping effect disappears to give enhanced Pirani X and Y outputs.

Nitrogen, as depicted in fig. 16 is adsorbed to a larger extent than oxygen. Its static Pirani response is identical to that of the latter as therefore should be its speed of diffusion to the pumping system. The reduced Pirani X and Y outputs (cf . oxygen) must therefore arise from the pumping action of the sieve

trap to the gas.

Simple rules can therefore be drawn up to identify qualitatively a single component noncondensable gas flux. Carbon monoxide (fig 17) and methane (fig. 18) are easily distinguished from the other three gases by their large capacities for adsorption and from each other by their distinctive i.r. spectra. Hydrogen is the only gas which will produce a Pirani Y output distinguishable from zero for Pirani X outputs of less than 1 mv. If the choice can be narrowed by elimination to nitrogen and oxygen the situation becomes more complex and is best resolved by a consideration of the nature of the degrading sample and the temperature range in which the flux is evolved. Nitrogen tends to be produced in high temperature decompositions ($> 500^{\circ}\text{C}$) while oxygen is formed (if at all) usually in low temperature peroxide decompositions in the temperature range $150 - 200^{\circ}\text{C}$.

The interpretation of the behaviour of a multicomponent gas flux will obviously be more difficult and will require a knowledge of the nature of the degrading sample immediately prior to the temperature range of gas generation and of accompanying products of degradation (if any).

Dynamic adsorptive behaviour can be summarised as follows. The capacity of a 5A molecular sieve towards adsorption of noncondensable gases most likely to be produced in a degrading polymer matrix is in the order $\text{H}_2 \ll \text{O}_2 < \text{N}_2 \ll \text{CH}_4 < \text{CO}$.

For the gases H_2 , O_2 , N_2 , and CH_4 this ordering parallels the ordering of β - the molecular dimensions of the gas at -196°C (section B 1 of this chapter). As β increases, so does the activation energy for diffusion of gas throughout the sieve. Carbon monoxide retains its position most likely because of its permanent dipole moment which will allow it to complex strongly with the "naked" mobile cation in activated molecular sieve.

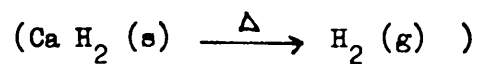
An extended TVA assembly of the type illustrated in fig. 19 should for the first time enable a complete volatile product analysis of a degrading polymer to be carried out in a single experiment.

FIGURE 3 - 14

ATVA OF HYDROGEN CURVE A

Heating Rate $10^{\circ}\text{C}/\text{min}$

Sample Size (n) = 2.4×10^{-4} Mole



Sieve Trap At -196°C

Key

— Pirani Output (X)
 - - - Pirani Output (Y)

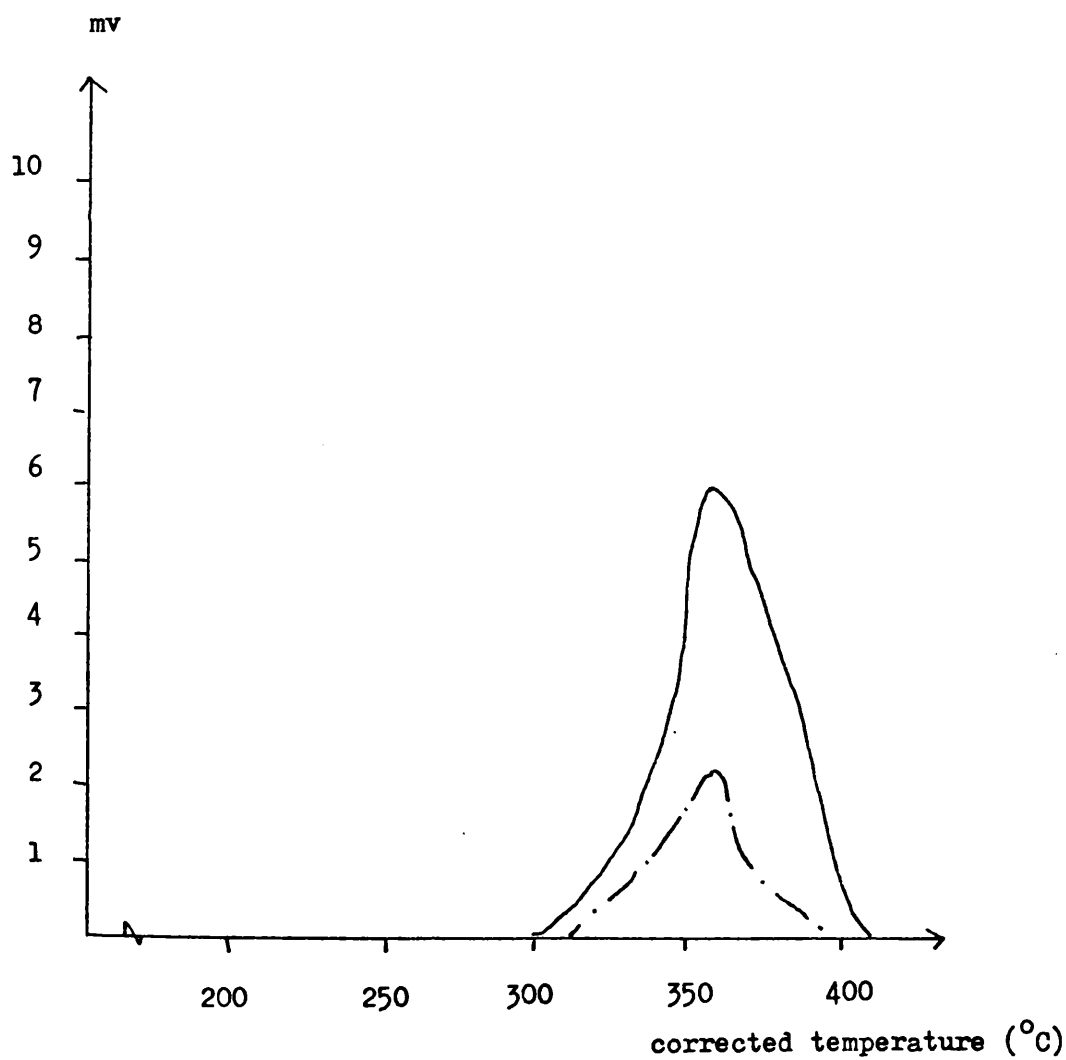
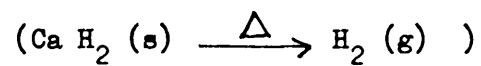


FIGURE 3 - 14

ATVA OF HYDROGEN CURVE B

Heating Rate $10^{\circ}\text{C}/\text{min}$

Sample Size (n) = 4.8×10^{-5} Mole



Sieve Trap At -196°C

Key

Pirani Output (X)

Pirani Output (Y)

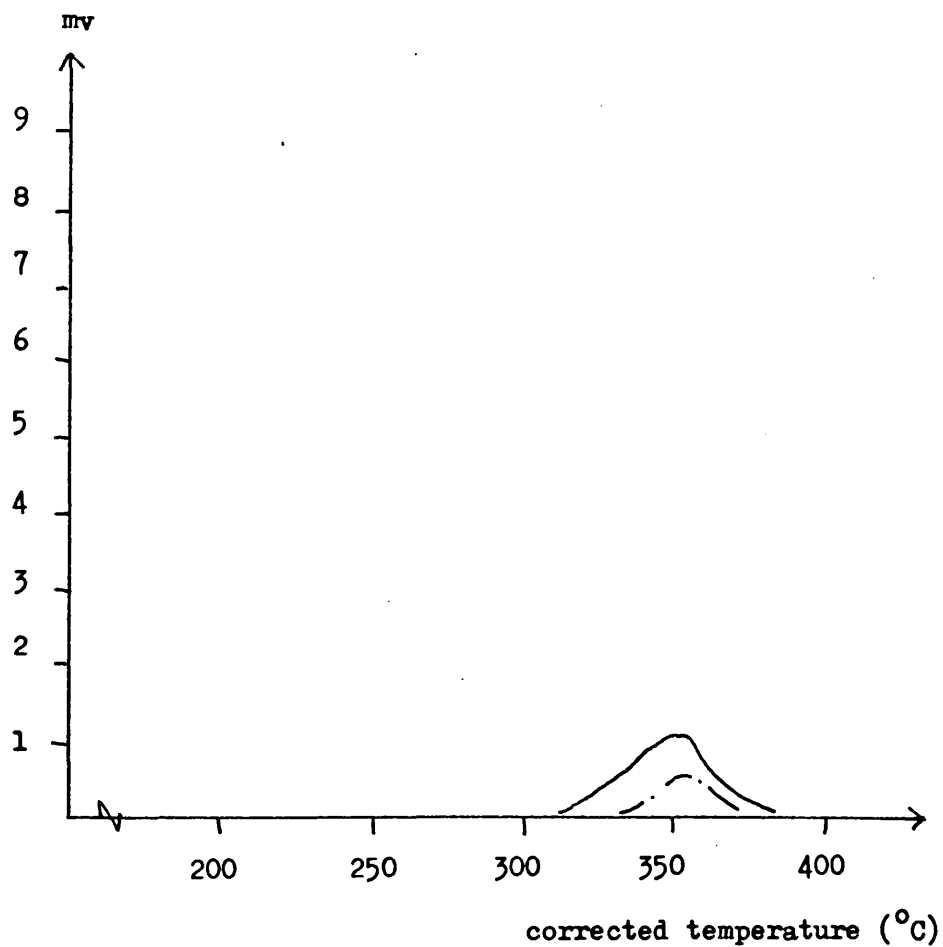
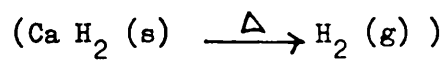


FIGURE 3 - 14

ATVA OF HYDROGEN CURVE C

Heating Rate $10^{\circ}\text{C}/\text{min}$

Sample Size (n) $\dot{=} 10^{-6}$ Mole



Sieve Trap At -196°C

Key

— Pirani Output (X)

- - - Pirani Output (Y)

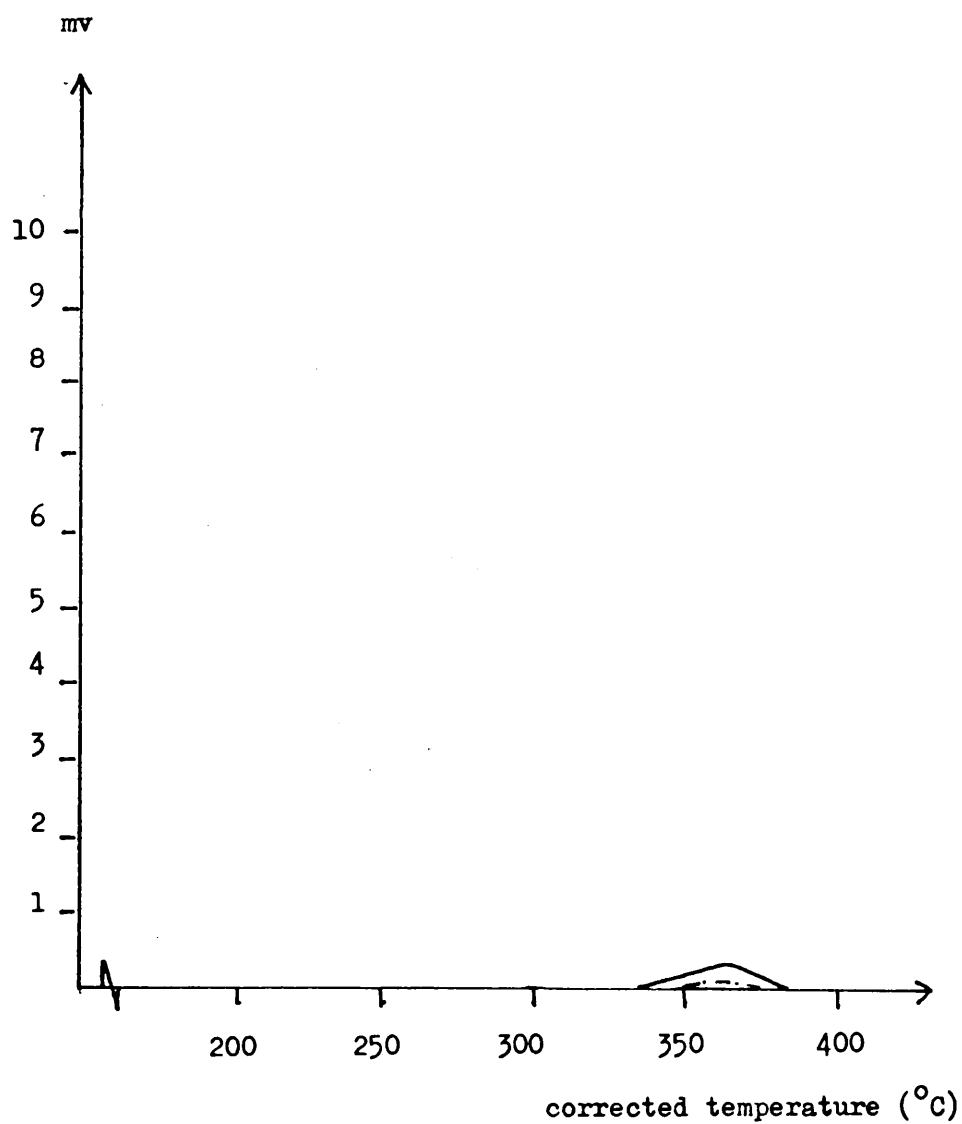


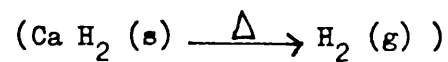
FIGURE 3 - 14

ATVA OF HYDROGEN CURVE D

Heating Rate $10^{\circ}\text{C}/\text{min}$

Sample Size (n) = 4.8×10^{-5} Mole

Sieve Trap At 0°C



Key

— Pirani Output (X)

- - - Pirani Output (Y)

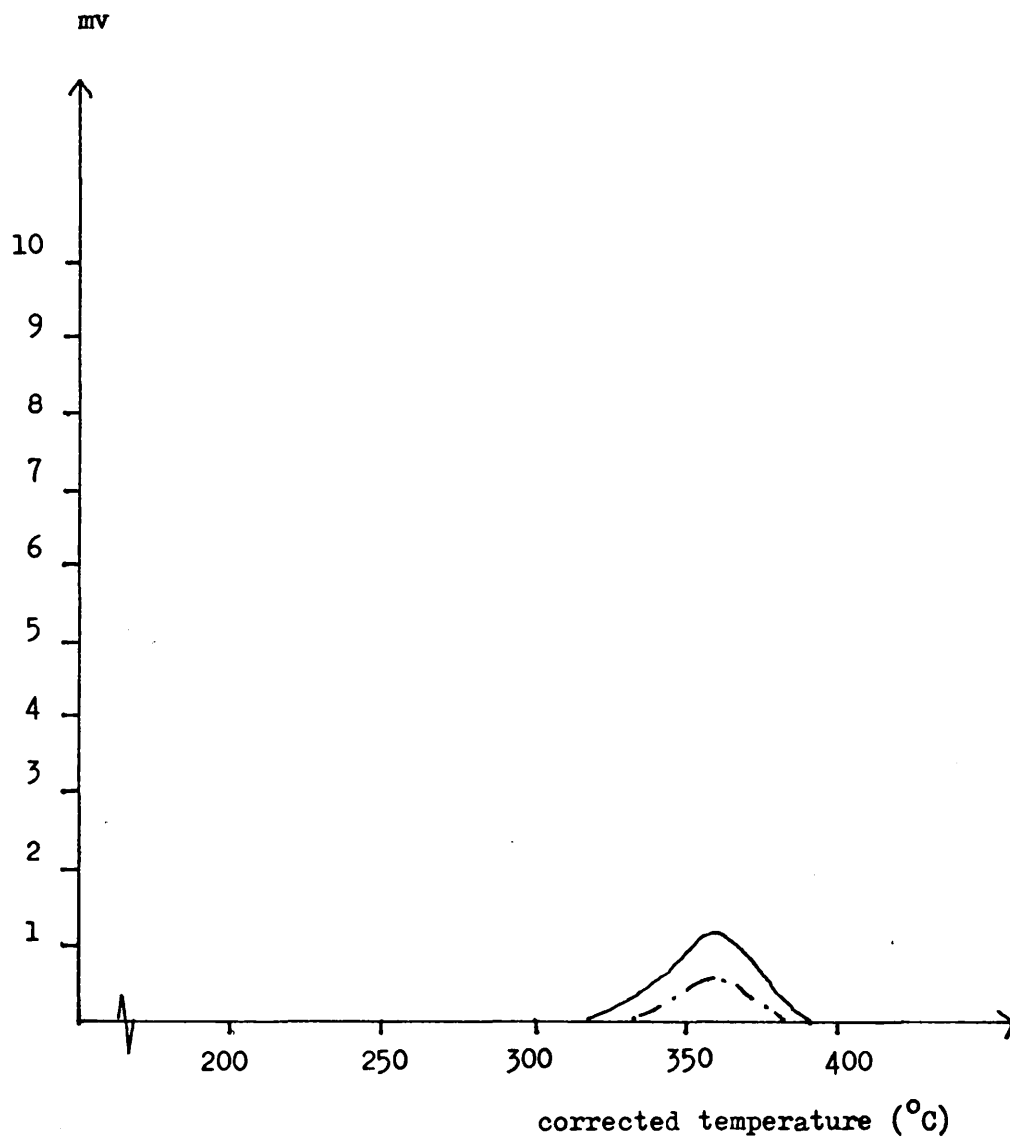
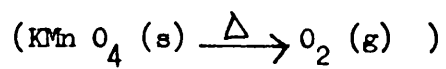


FIGURE 3 - 15

ATVA OF OXYGEN CURVE A

Heating Rate $10^{\circ}\text{C}/\text{min}$

Sample Size (n) = 3.1×10^{-6} Mole



Sieve Trap At -196°C

Key

— Pirani Output (X)

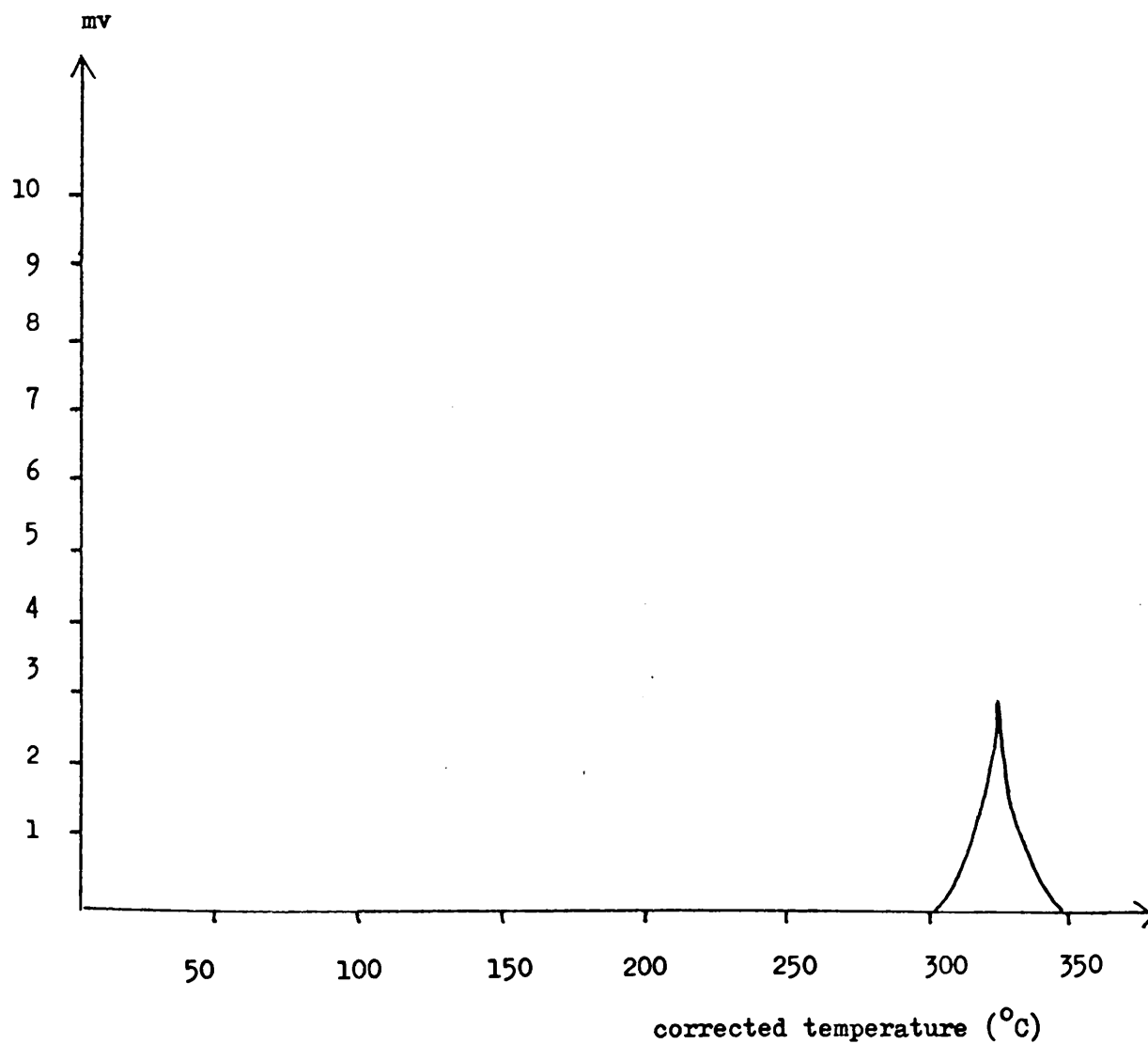
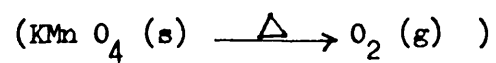


FIGURE 3 - 15

ATVA OF OXYGEN CURVE B

Heating Rate $10^{\circ}\text{C}/\text{min}$

Sample Size (n) = 9.5×10^{-6} Mole



Sieve Trap At -196°C

Key

— Pirani Output (X)
 - - - Pirani Output (Y)

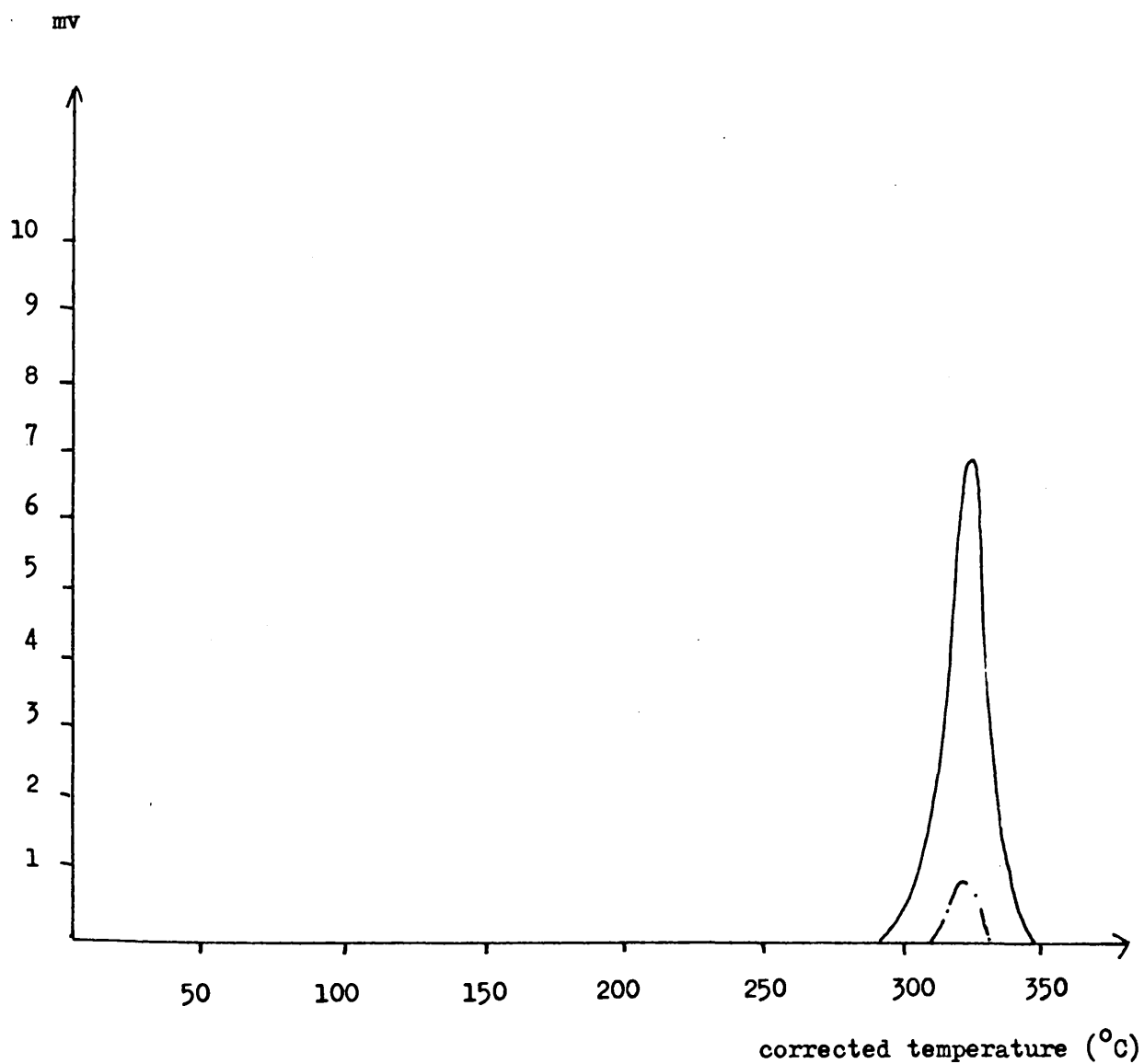
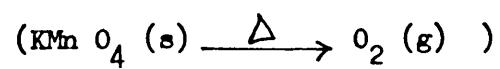


FIGURE 3 - 15

ATVA OF OXYGEN CURVE C

Heating Rate $10^{\circ}\text{C}/\text{min}$

Sample Size (n) = 3.1×10^{-5} Mole



Sieve Trap At -196°C

Key

— Pirani Output (X)

- - - Pirani Output (Y)

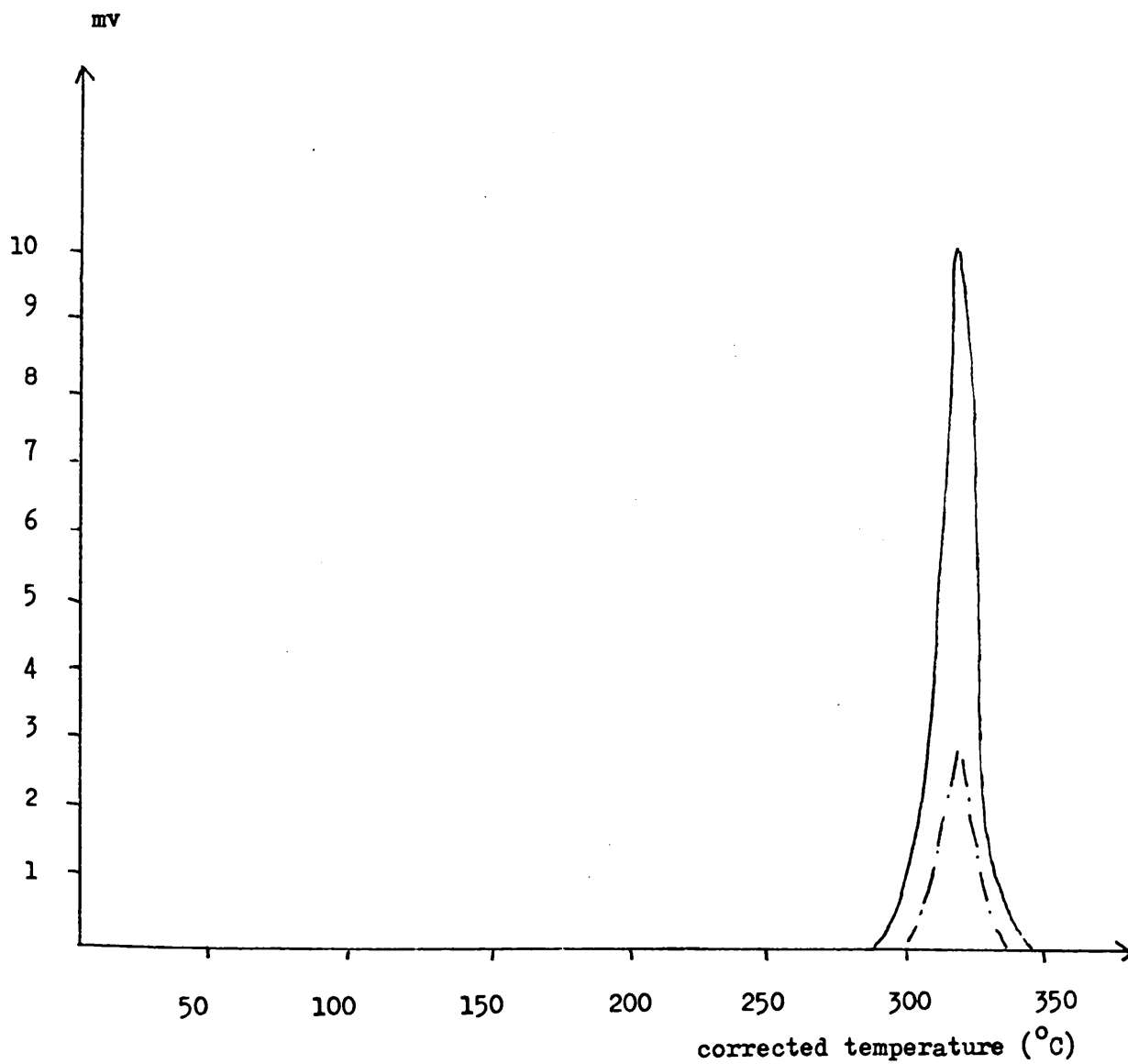
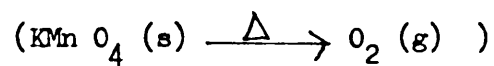


FIGURE 3 - 15

ATVA OF OXYGEN CURVE D

Heating Rate $10^{\circ}\text{C}/\text{min}$

Sample Size (n) = 3.1×10^{-5} Mole



Sieve Trap At 0°C

Key

Pirani Output (X)

Pirani Output (Y)

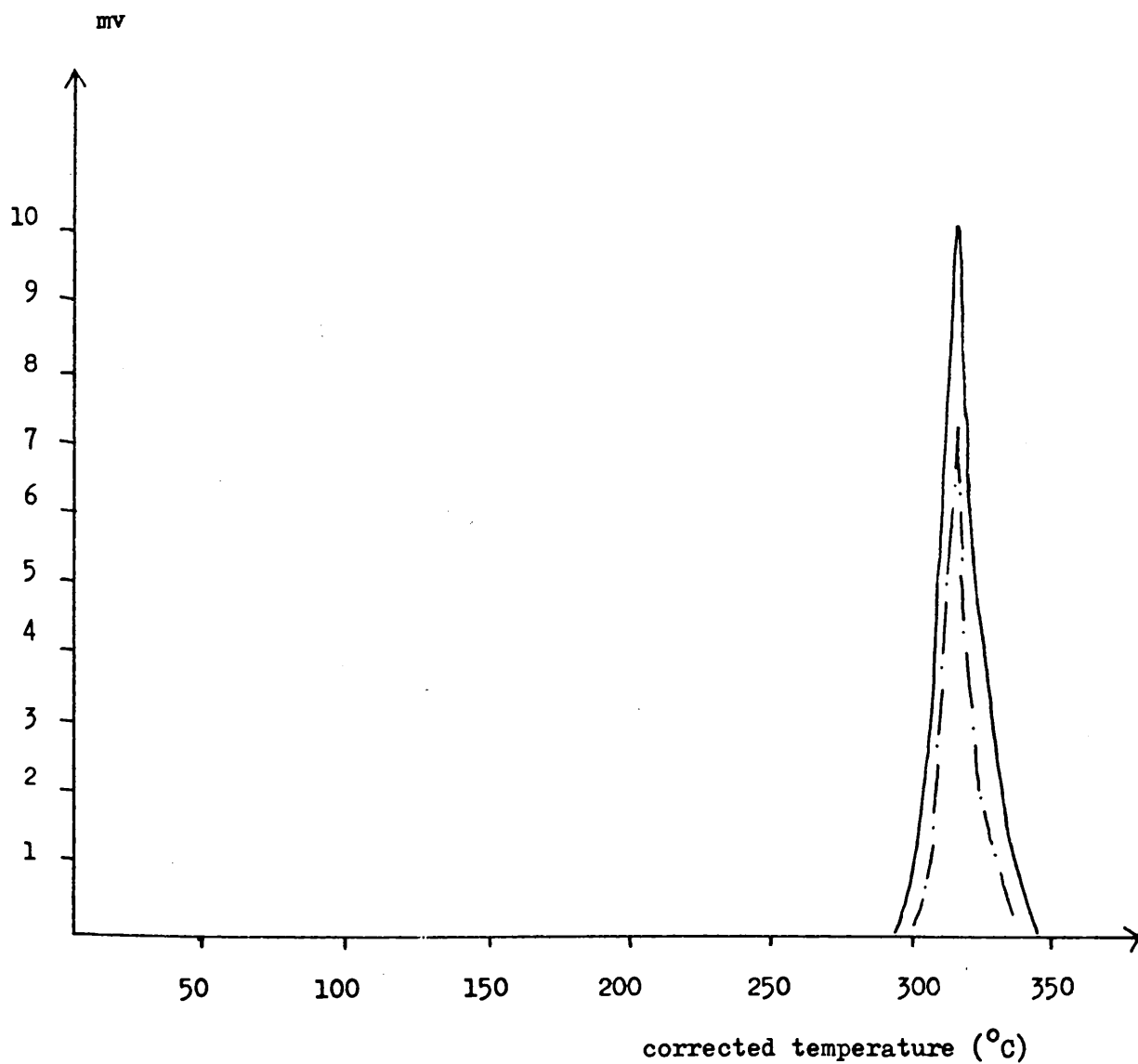


FIGURE 3 - 16

ATVA OF NITROGEN CURVE A

Heating Rate $10^{\circ}\text{C}/\text{min}$

Sample Size (n) = 1.2×10^{-5} Mole

(AIBN $\xrightarrow{\Delta}$ N_2 (g))

Sieve Trap At -196°C

AIBN Encapsulated In 13X Sieve

Key

— Pirani Output (X)
- - - Pirani Output (Y)

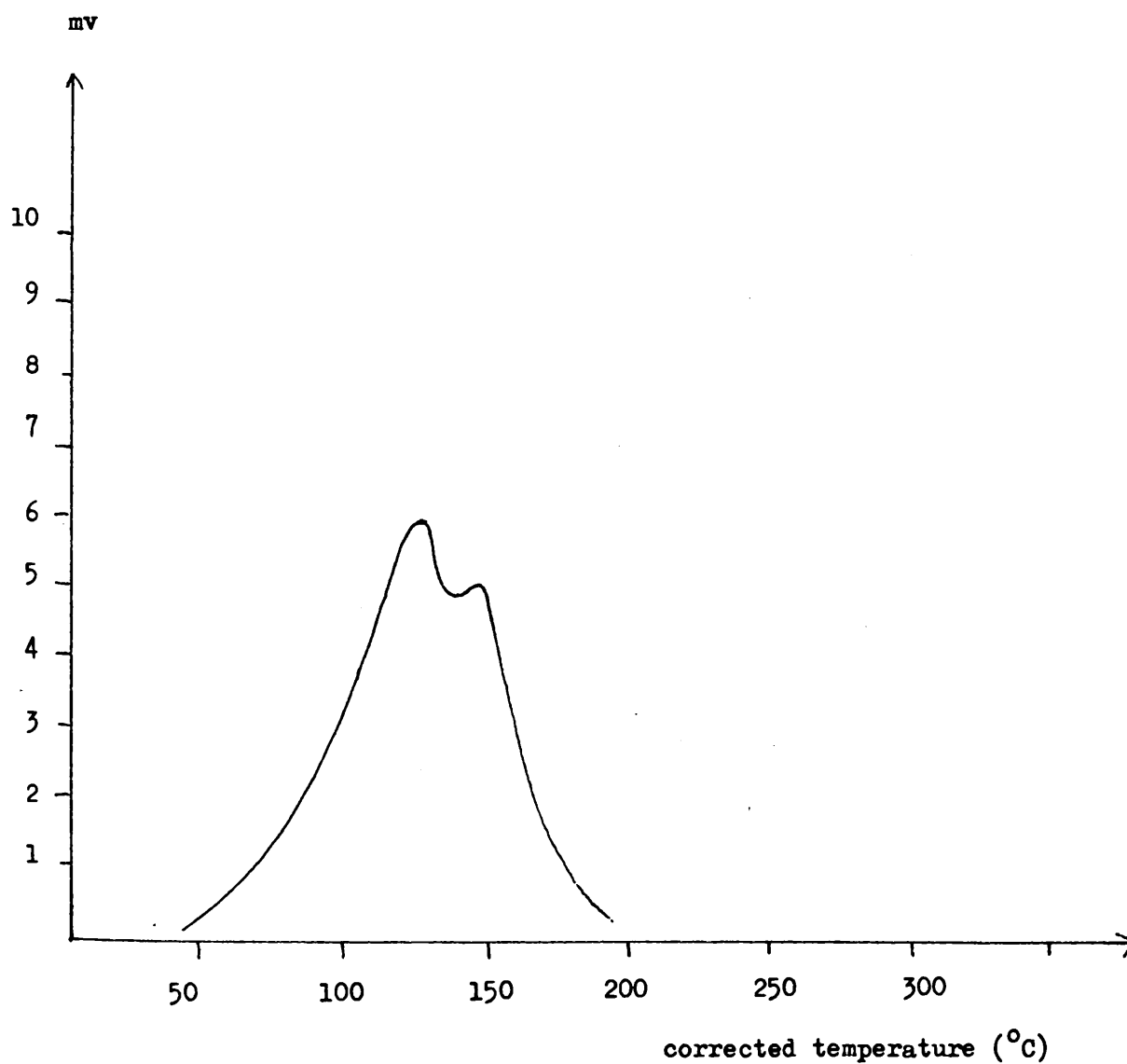
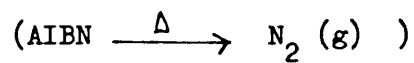


FIGURE 3 - 16

ATVA OF NITROGEN CURVE B

Heating Rate $10^{\circ}\text{C}/\text{min}$

Sample Size (n) = 3.7×10^{-5} Mole



Sieve Trap At -196°C

AIBN Encapsulated In 13X Sieve

Key

— Pirani Output (X)

- - - Pirani Output (Y)

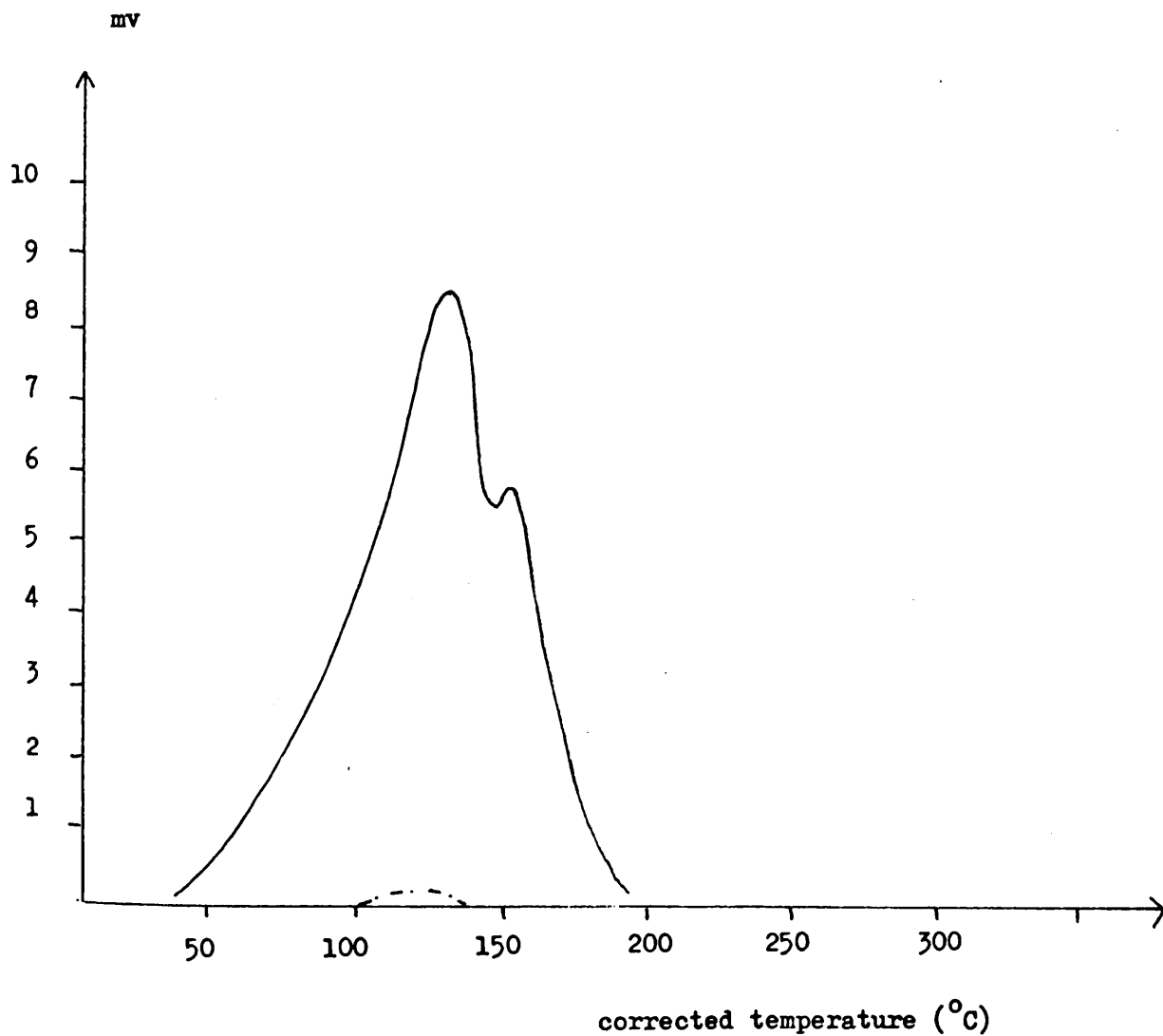


FIGURE 3 - 16

ATVA OF NITROGEN CURVE C

Heating Rate $10^{\circ}\text{C}/\text{min}$

Sample Size (n) = 7.9×10^{-5} Mole

(AIBN $\xrightarrow{\Delta}$ N_2 (g))

Sieve Trap At -196°C

AIBN Encapsulated In 13X Sieve

Key

— Pirani Output (X)
- - - Pirani Output (Y)

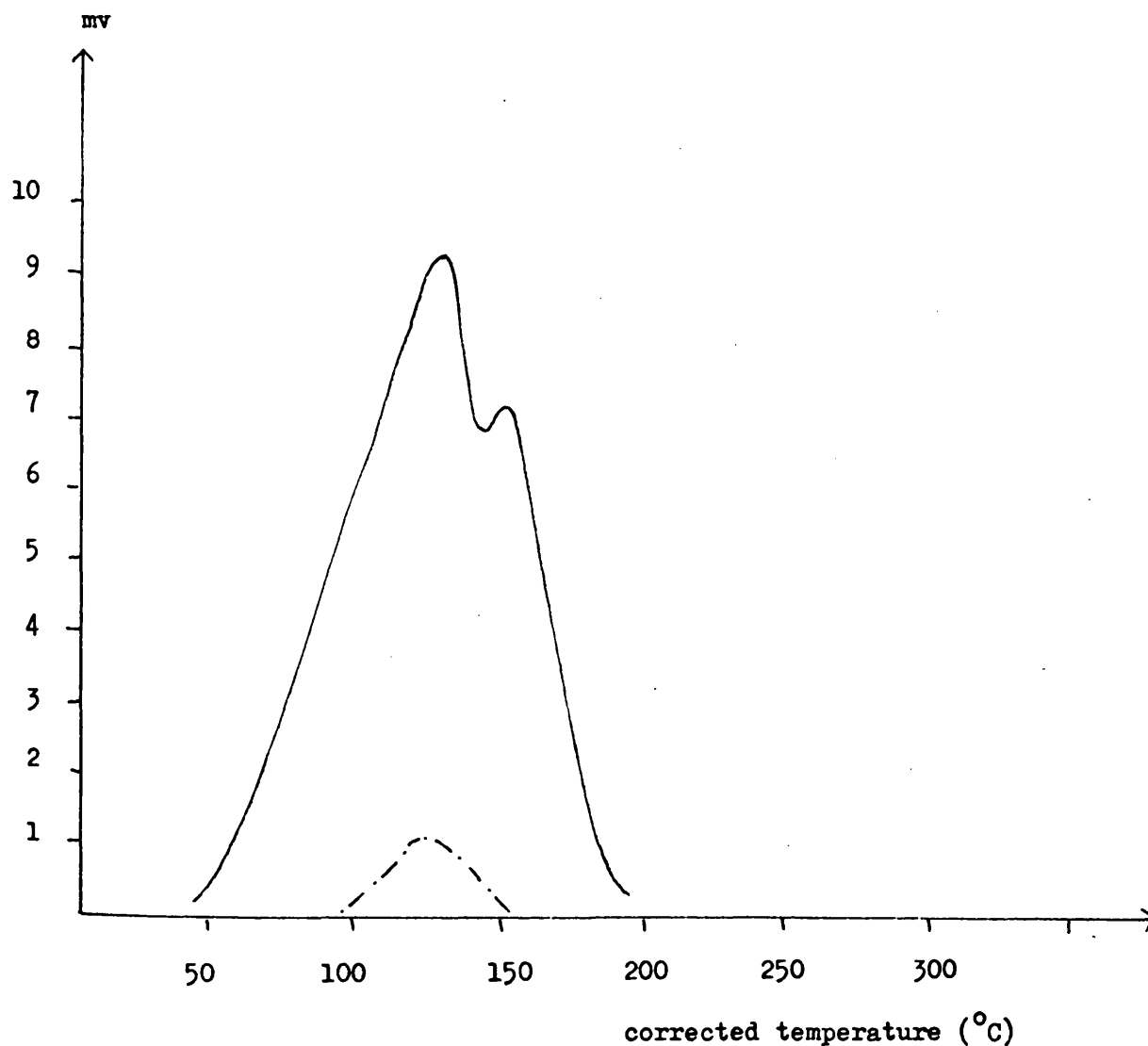
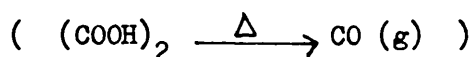


FIGURE 3 - 17

ATVA OF CARBON MONOXIDE

Heating Rate $10^{\circ}\text{C}/\text{min}$

Sample Size (n) = 1.1×10^{-4} Mole



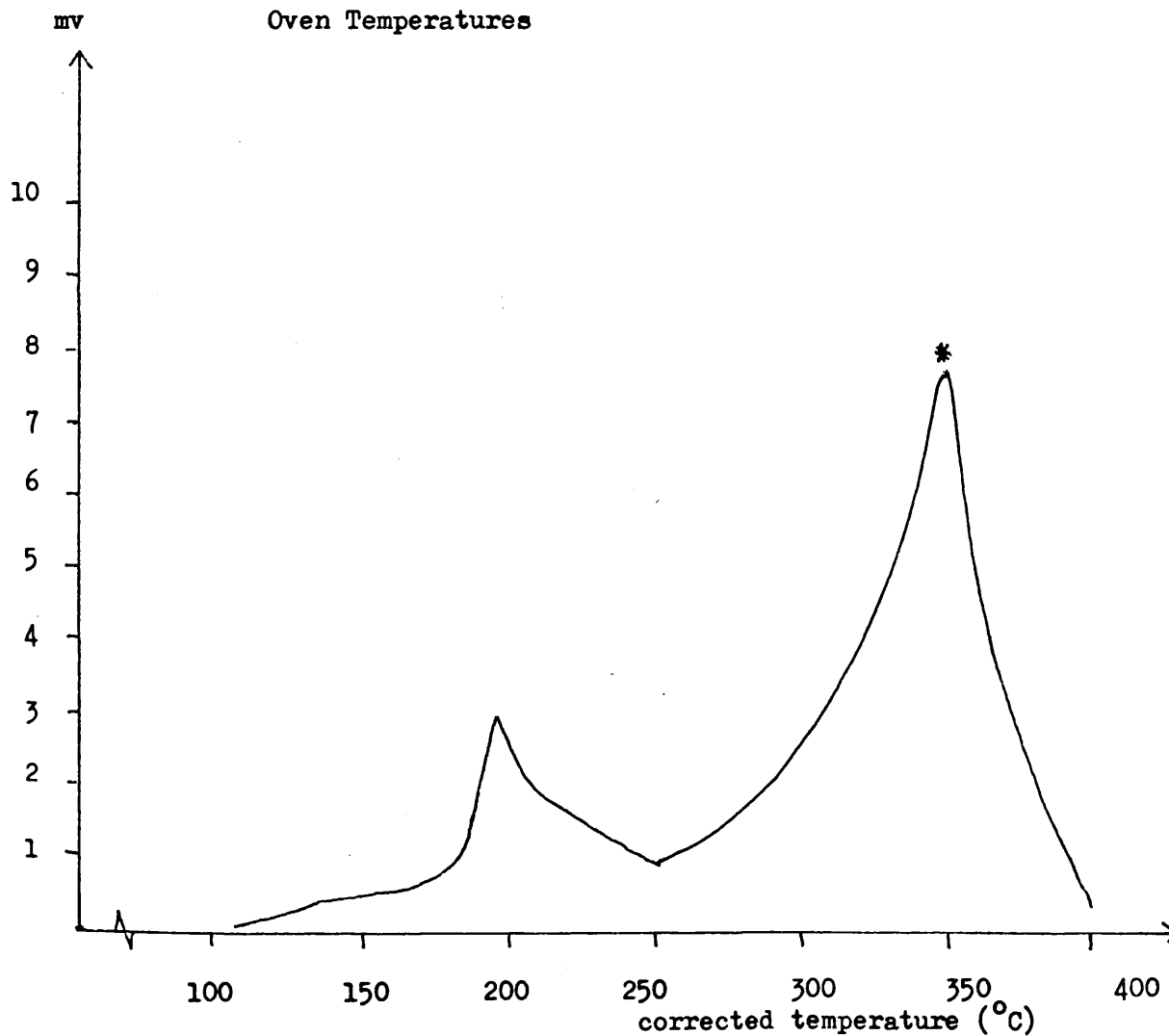
Sieve Trap At -196°C

Oxalic Acid Encapsulated In 13X Sieve

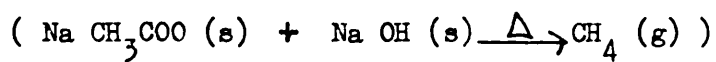
Key

— Pirani Output (X)
 - - - Pirani Output (Y)

* Degradation Of Sublimed Oxalic Acid Effected By Blackbody
 Radiation Incident At The Top Of The TVA Tube At High
 Oven Temperatures



ATVA OF METHANE

Heating Rate $10^{\circ}\text{C}/\text{min}$ Sample Size (n) = 6.2×10^{-4} MoleSieve Trap At -196°C Key

— Pirani Output (X)

- - - Pirani Output (Y)

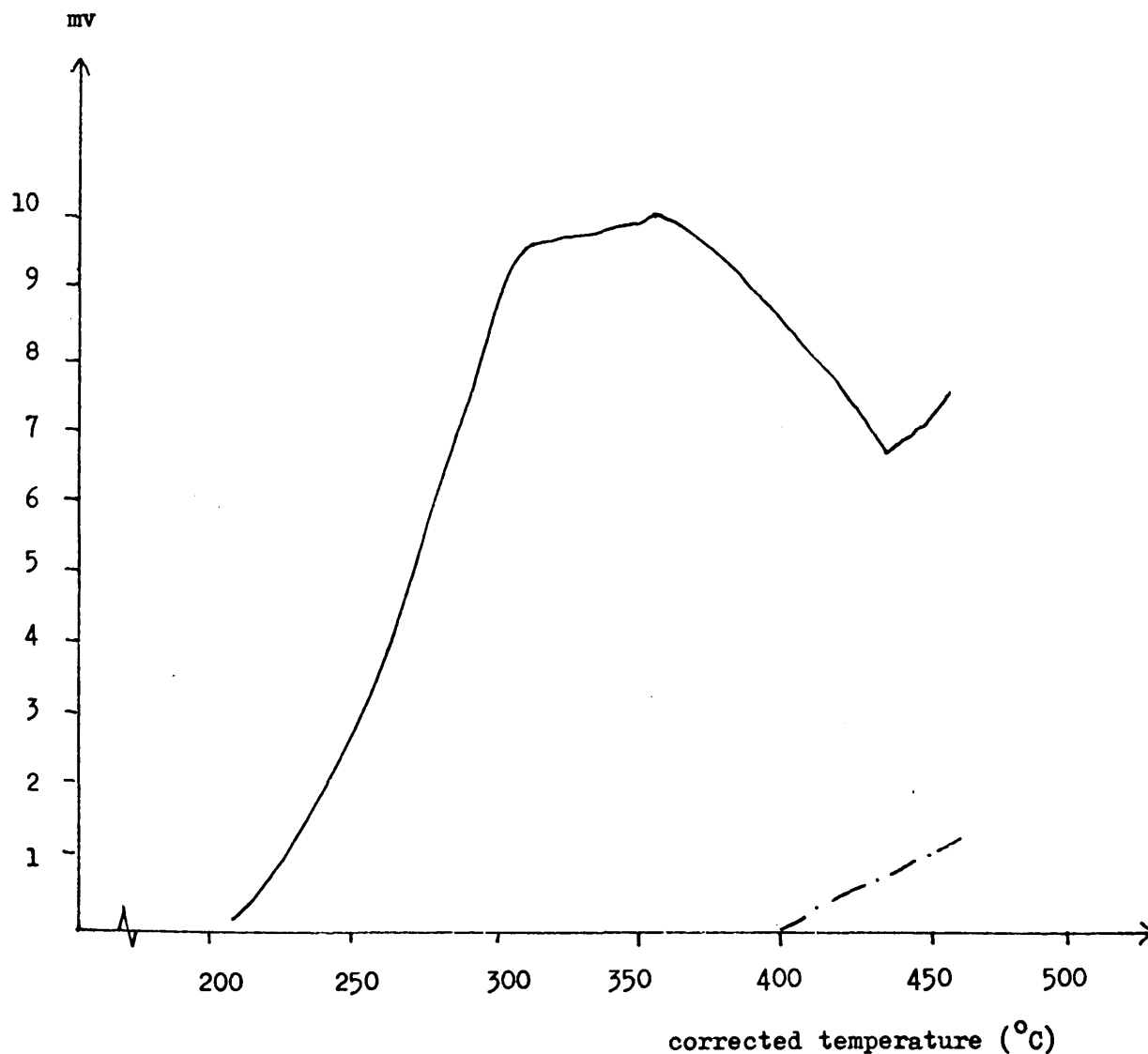
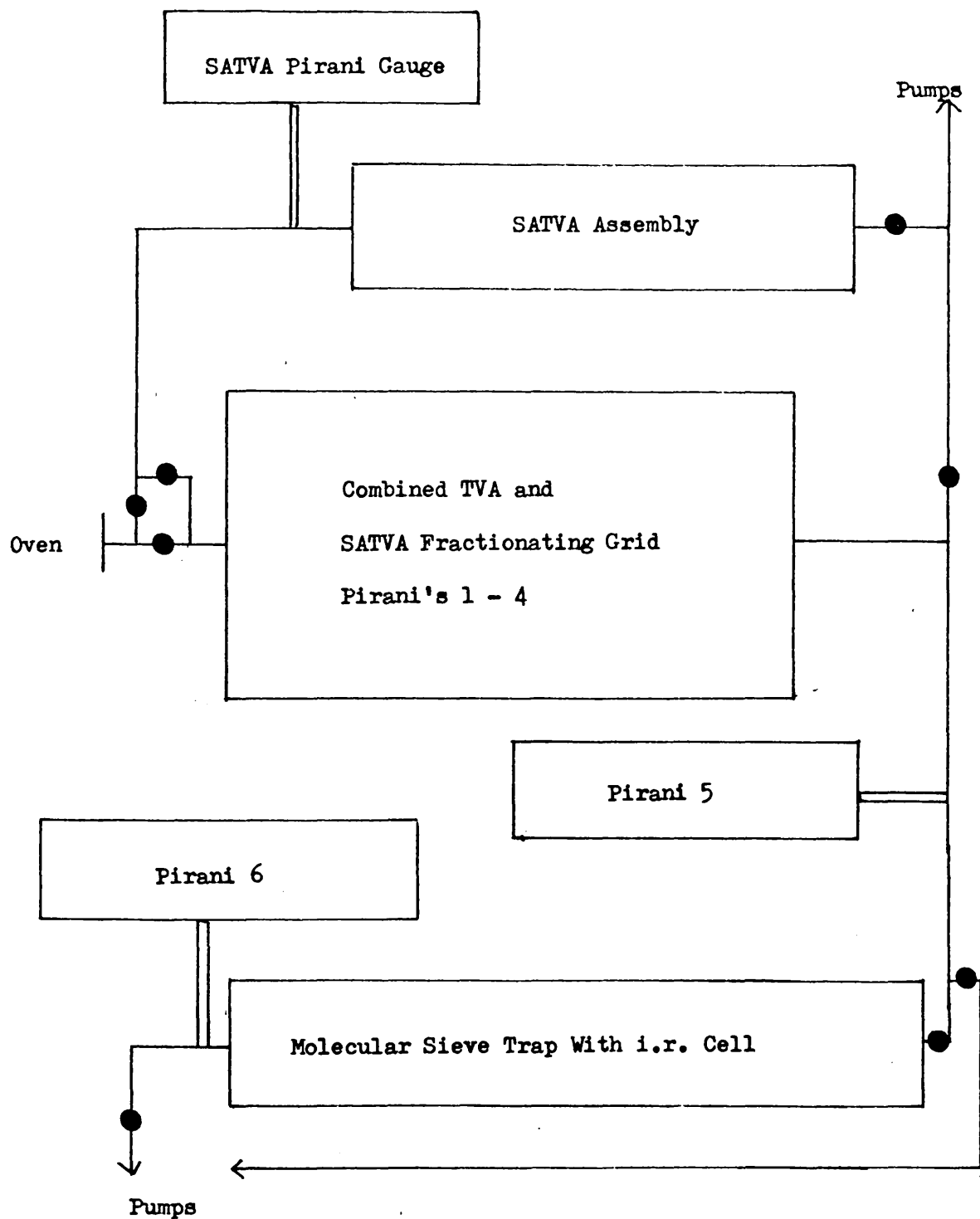


FIGURE 3 - 19
EXTENDED TVA ASSEMBLY



CHAPTER 4.

POLYMER PREPARATION AND CHARACTERISATION.

A INTRODUCTION AND LITERATURE REVIEW.

The materials under investigation in this work were the homopolymers and diblock copolymer of butadiene and styrene, all of which were best prepared anionically. The literature review is concerned mainly with those characteristics of the system which determine the optimum conditions of preparation. There follows a description of the apparatus developed in this laboratory to this end and an outline of the procedure followed in the purification and polymerising steps. Finally, techniques for characterisation of the polymers are considered.

The mechanism involved in the anionic polymerisation of vinyl monomers was first elucidated by Szwarc and co-workers ⁽²⁶⁾. The absence of a termination step ^(27,28) made the system resemble the glycol-initiated polymerisation of ethylene oxide, The molecular weight distribution of which was shown by P.J. Flory ⁽²⁹⁾ to be Poisson in nature. The most important characteristic of this type of distribution is that the heterogeneity index, defined as $\frac{M_w}{M_n}$, can be made very close to one in polymers taken to a high conversion per initiating site. It has been shown statistically ^(27,28) that to minimise the heterogeneity index of the material, batch addition of monomer to catalyst is preferable to slow or dropwise addition, provided that polymerisation is slow enough to enable reagent homogeneity to be attained before quantitative consumption of monomer. The depropagation reaction ⁽²⁷⁾ and reactive impurities in the monomer ⁽²⁸⁾ have also been shown to enhance the "most probable" character of the polymer more effectively in a continuous as opposed to batch process.

Of more specific relevance to the butadiene system was the realisation ⁽³⁰⁾ that colour in the living polystyrene system could be attributed to u.v. absorbance of the living chain end chromophore. The ease with which the u.v. technique can be adapted to leak-tight systems has made it a widely used tool as shown below.

Termination by isomerisation was followed ⁽³⁰⁻³²⁾ by changes in the u.v. absorbance of the living end group. Isomerisation has been found to be irreversible, to involve hydride expulsion, and to increase in rate with the size of the counterion, the dielectric constant of the solvent and the temperature of the solution ^(30,31). Isomerisation in the butadiene end group has been shown ⁽³²⁾ to be reversible upon addition of further monomer but to depend in a qualitative manner upon the same experimental conditions as the polystyryl system.

Rates of initiation in hydrocarbon solvents have been found to be first order in monomer concentration with respect to both styrene and butadiene but one sixth order in n-butyllithium concentration ^(33,34). It has been argued ⁽³⁵⁾ that this indicates that initiator exists as a hexamer in hydrocarbon solvents, in dynamic equilibrium with a small quantity of unassociated active material able to react on a 1 : 1 basis with monomer.

Rates of polymerisation were again found to be first order with respect to both monomers, but one half order in polystyryl-lithium and one sixth order in polybutadienyl-lithium. These features have been interpreted as indicating that living polystyryl and polybutadienyl chain end groupings exist as dimer and hexamer complexes respectively, in solution. This assumption is backed by light-scattering molecular weights of the polymers, which were found to decrease by factors of two and six respectively, after termination.

U.V. absorption has been used ^(36, 37) to measure the rates of crossover monomer additions during polymerisation.

Although styrene homopolymerises more rapidly than butadiene, anomalously high butadiene contents have been obtained with copolymers taken to low conversions, because of the very rapid addition of butadiene to the polystyryl-lithium chain end. An explanation on the grounds of preferential solvation of the styryl-lithium grouping by butadiene (38) was disproved by Morton and co-workers (39), who gave evidence to show that the driving force in the crossover reaction is a preferential pairing of the lithium cation to the polybutadienyl anion.

Difficulties in separating the initiation from the propagation reaction when n-butyllithium, vinyl monomers, and hydrocarbon solvents are used, were first noted by Worsfold and Bywater (33). Not only does this behavior result in an increased heterogeneity index, but if initiation is sufficiently slow, block copolymers so prepared can incorporate large quantities of homopolymer contaminant. Subsequent work has provided three main methods of overcoming this difficulty, all of which are outlined below.

Initiation can be made instant by polymerising in ether solvents such as tetrahydrofuran (THF) at low temperatures. Disadvantages of this approach are as follows. Firstly, homogeneity problems arise due to greatly enhanced rates of polymerisation. Secondly, ether complex formation with the active chain-end was found to enhance rates of pseudotermination (30) and the 1, 2-content of the polybutadiene segment (39). The most important disadvantage, however, is the well known reactivity of ether towards organo-lithium compounds and its difficulty of purification to the degree required for this type of work.

For the above reasons, hydrocarbon media are preferred. Rates of initiation using n-butyllithium have been found to be greatly enhanced by adding to the hydrocarbon small quantities of phenyl

ethers, which were found to affect neither the rate of polymerisation of the system nor the rubber block microstructure. The ether can be added to the polymerising mixture either by direct addition of a millimolar quantity to the reactor or by distilling the ether into the reactor as a very dilute solution in the solvent. The former is difficult to achieve because of the difficulties involved in the quantitative handling under high-vacuum conditions of such small quantities of material, while the latter is difficult to achieve because the differing boiling points of ether and solvent produce a fractionating effect in distillations which are performed with top and bottom "cuts". Such distillations form an essential part of the solvent purifying process. As such, the final concentration of ether in the reactor is difficult to estimate.

Perhaps the simplest solution to the problem is the use of isomers of n-butyllithium, of which sec-butyllithium has been found to be the most useful (42). Its effectiveness, especially with styrene which because of its high rate of homopolymerisation was found to suffer particularly from molecular weight broadening, was assumed to arise from its low degree of association in hydrocarbon media, estimated as tetrameric by Worsfold and Bywater (43).

B EXPERIMENTAL.

All purification steps and polymerisations were carried out under high vacuum conditions. The low concentrations of active species required to produce a high polymer precluded the use of inert atmosphere techniques. Of special relevance is a series of elegant papers by Morton and co-workers (44 - 47).

B 1 VACUUM MANIFOLD DESIGN AND OPERATION.

The manifold designed for this work is shown in fig. 1 . Because of its resistance to solvent vapour and wide operative temperature range, Kel F grease was used on all stopcocks placed to the right of "X" in fig. 1 . Because of its low vapour pressure and reliability under clean conditions, Apiezon L grease was used on all other stopcocks.

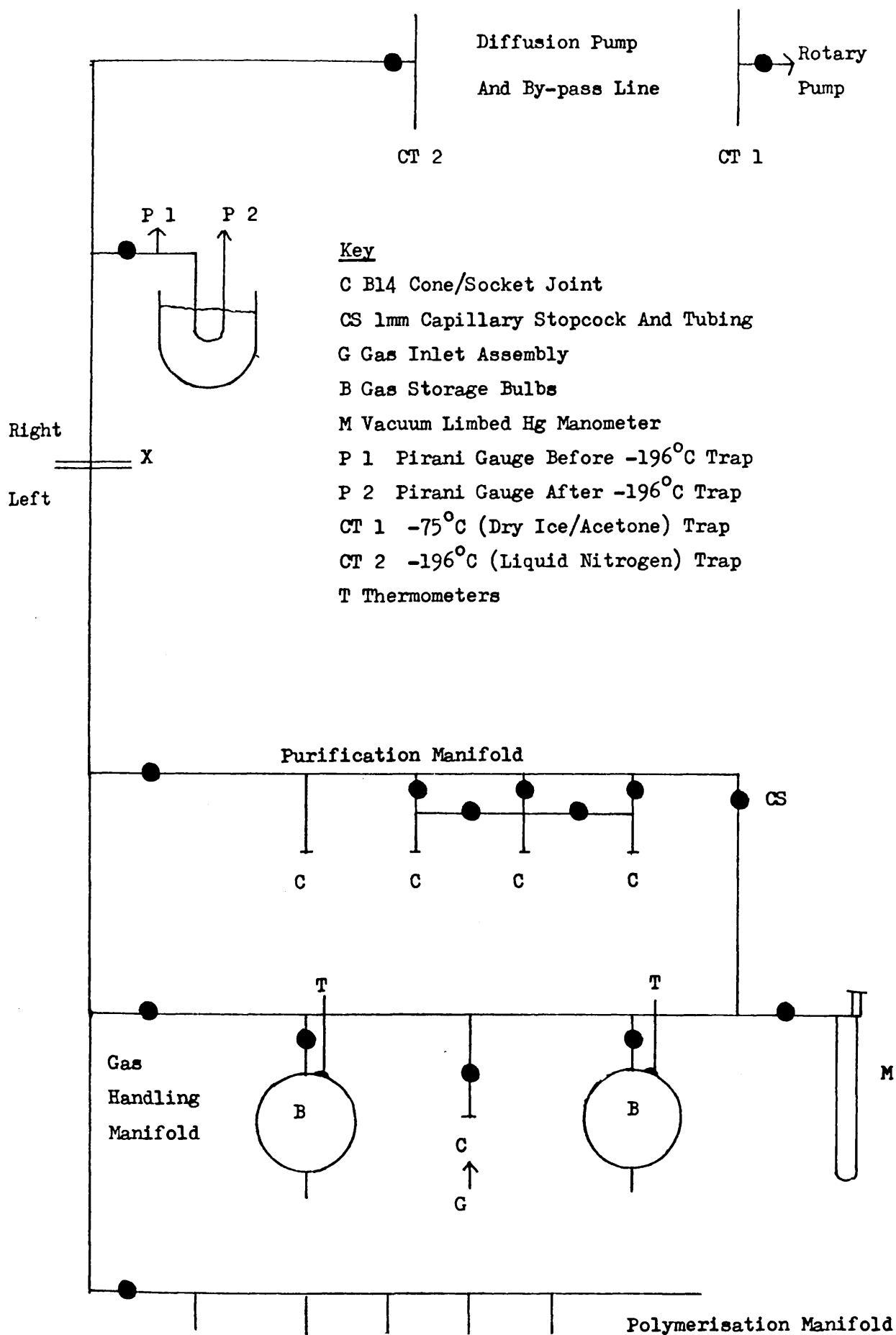
The Pirani gauge arrangement shown enabled the contributions of condensable and noncondensable gas towards the total pressure to be roughly estimated. This facility proved valuable in the identification of real as opposed to "virtual" leaks. The latter situation arises when condensable material slowly volatilises at a limiting rate to the pumping system and is often encountered after the flash distillation of large quantities of material.

Because of the high reactivity of water towards organo-lithium compounds, its level in the manifold had to be minimised. This was effected by continuously operating the rotary pump in conjunction with a dry-ice/acetone cold trap at -75°C in position CT1 (fig. 1). Such a trap isolated the line from pump vapours and maintained a low water content in the system, with none of the attendant risks of gas condensation exhibited by a liquid nitrogen trap.

Before the manifold was used, cold trap 2 was filled with liquid nitrogen to pump carbon dioxide and residual water

FIGURE 4 - 1

POLYMERISATION MANIFOLD



from the system, and used thereafter with the oil diffusion pump to achieve an ultimate pressure of 10^{-4} - 10^{-5} torr.

B 2 CLEANING OF GLASSWARE.

Before use all glassware was heated in air with a hot gas-oxygen flame to remove carbonaceous deposits. After cooling the glassware was further cleaned by immersion in "Pyronex" alkaline cleaning solution, followed by several rinses in distilled water, which was finally removed by rinsing with AR acetone followed by pumping under vacuum.

B 3 REMOVAL OF CHEMICALLY ADSORBED WATER.

Because of its high polarity, a small quantity of water is bound to a glass surface under high vacuum. To maintain reagent purity it was essential that this be removed before contact of the reagent with the glass. This was achieved by heating the glass under vacuum with a soft blue gas-oxygen flame until the yellow sodium line was emitted from the glass. It is the author's opinion that passage of reagent vapour over flamed out glassware results in the removal of trace quantities of water from the reagent by adsorption onto the glass surface. To this end, the polymerisation manifold was so treated between each distillation.

B 4 REAGENT AGITATION.

Whenever possible, in the purification steps, mixing of the reagent with the solid drying agent was achieved by mechanical shaking of the purification ampoule (fig. 2). Along with its highly random nature, the process resulted in a scrubbing action which continuously exposed new surface to the reagent. The large solvent ampoules and the polymerisation reactor could not be so treated and were agitated by a magnetic stirrer.

Because of the required flaming out procedure, Teflon-covered stirrers could not be used. Commercial glass-covered stirrers were found to be badly sealed and fragile. For this reason all stirrers were made by the standard procedure of sealing small bar magnets and glass wool into heavy walled capillary tubing under vacuum.

B 5 LEAK DETECTION.

Leaks in the manifold were pinpointed by the usual methods - Tesla coil testing and chamber by chamber isolation from the pumping system. Leakage into the reagent ampoules was detected as follows. Several days after sealing of the ampoule, its contents were frozen and a Tesla coil applied to the neck of the flask. A spark was found to be generated only in perfectly sealed flasks. All other ampoules and their contents were discarded.

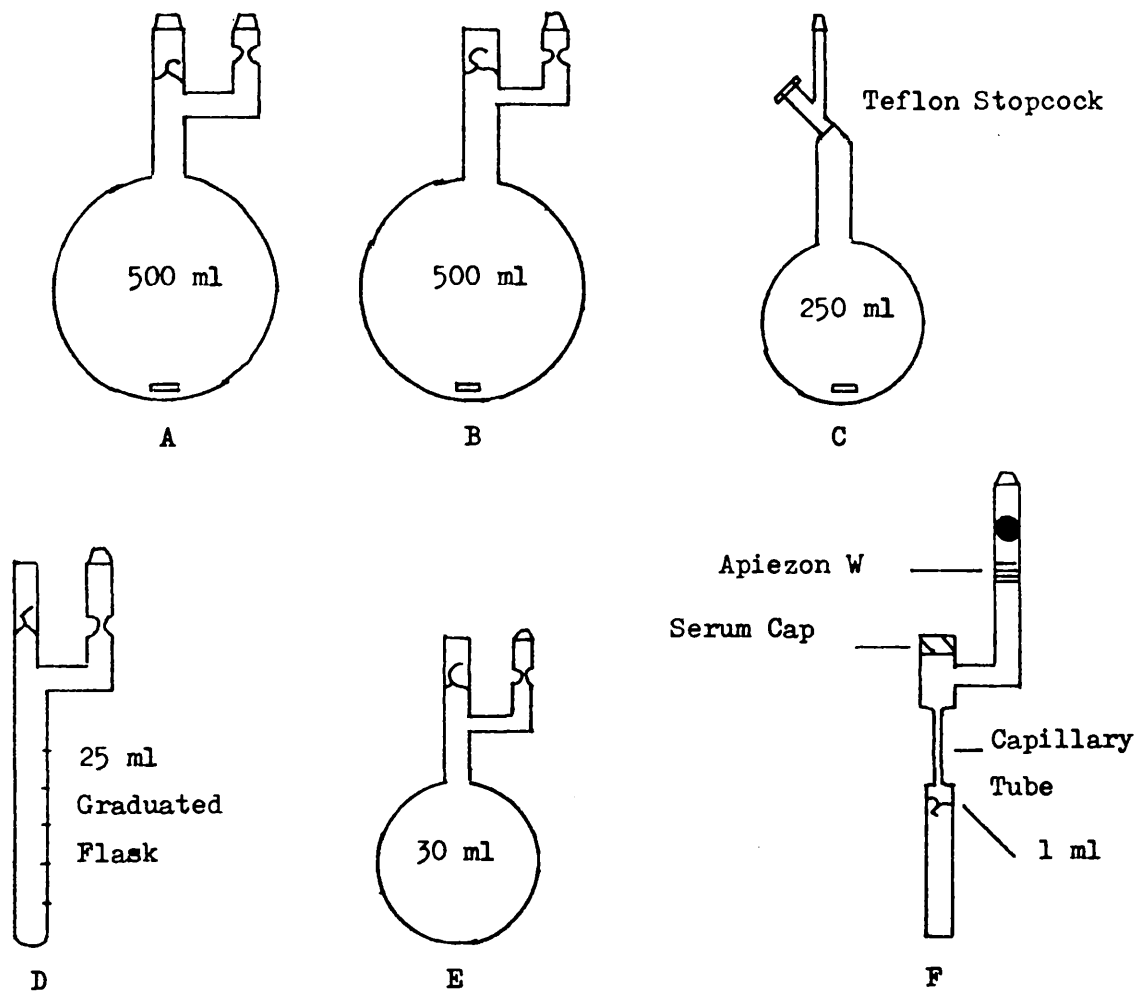
B 6 n-HEXANE MANIPULATION.

For reasons mentioned in the literature review, a non-polar solvent was used in the polymerisation. Cyclic solvents such as benzene and cyclohexane which form highly ordered crystalline solids when frozen tend to crack containers in the warm up process following distillation and degassing cycles. For this reason acyclic hydrocarbon solvents were preferred, of which n-hexane, with its low boiling point and subsequent ease of manipulation, was selected.

" Spectrosol " n-hexane (130 ml), used because of its low olefinic and aromatic content, was added to AR sulphuric acid (90 ml) in flask A of fig. 2 . The mixture was thoroughly degassed and sealed at the constriction. Stirring was maintained for a few days during which a brown to black colour developed in the acid phase. During this period the bulk of the water in the n-hexane was extracted, basic impurities were protonated, olefins were cracked

FIGURE 4 - 2

REAGENT AMPOULES



Key

- A,B n-Hexane Ampoules
- C,D Styrene Ampoules
- E Butadiene Ampoule
- F sec-Butyllithium Ampoule
- G Styrene Top Cut Bulb

and ionised and aromatic material was sulphonated. All of these derivatives are involatile.

Flask A was then opened to the vacuum line via its breakseal, degassed, and the n-hexane distilled with cuts onto 3-4 g of freshly ground lithium aluminium hydride in flask B of fig. 2 . The distillate was thawed, stirred for a few minutes, degassed and the flask was sealed at the constriction. After it had been stirred for a few days , the flask was stored until required. In this step the lithium aluminium hydride was used to ionise and make involatile all residual acidic impurities (including water) able to terminate the organolithium grouping.

B 7 STYRENE MANIPULATION.

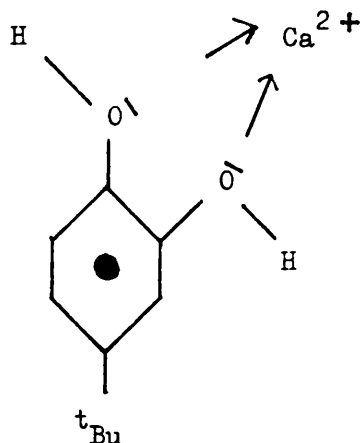
When selecting a purification scheme for styrene monomer it is necessary to consider carefully its chemical reactivity towards the drying agent. For example, violent polymerisation is effected by contact with strong acids such as phosphorus pentoxide and strong bases such as lithium aluminium hydride, while rapid polymerisation occurs in the presence of sodium metal.

Styrene monomer was bulk dried over anhydrous calcium chloride during storage. Finely crushed white calcium sulphate 5-10 g was added to flask C of fig.2 and activated by heating with a silicone oil bath to 200°C under vacuum until Pirani indicated complete activation of the salt by the reaction



Approximately 75 ml of styrene was added to the flask which was degassed and stirred overnight. The action of calcium sulphate is twofold. Its main function is that it efficiently removes the bulk of the water in the monomer. It also reduces the

volatilisable p - tert - butylcatechol inhibitor present in the monomer by complex formation as shown below.



Styrene (middle cut) was flash distilled to flask D of fig. 2 which contained 2-3g of freshly ground calcium hydride. The mixture was degassed and after the flask had been sealed the mixture was agitated by mechanical shaking. Calcium hydride - the most endothermic simple hydride and one which does not polymerise the monomer - was used as a scavenger for water and other residual acidic material which it irreversibly ionises to produce hydrogen, which is removed in the subsequent degassing cycle.

Because of the tendency of pure styrene to polymerise, an optimum exposure time of three days was chosen. Even a small degree of polymerisation results in "skin" formation with resultant sample bumping in the subsequent distillation.

B 8 BUTADIENE MANIPULATION.

Butadiene reacts with drying agents in a manner similar to that of styrene and the choice therefore required the same care. Gas phase i.r. and sealed tube n.m.r. spectra indicated a high level of purity, approaching the 99%, claimed by the manufacturer. In

view of this the predrying step was omitted.

At room temperature the ideal gas laws hold for butadiene up to pressures of approximately two atmospheres (48). To maintain a leak tight system and prevent any dangerous pressure buildup, however, it was necessary to contain the gas in a high volume manifold under low pressures.

Gas pressure was measured with a simple vacuum-limbed mercury manometer. It was felt that a constant volume manometer was an unnecessary refinement when using a manifold of volume greater than six litres.

The gas manifold volume, \bar{V} , was obtained by expanding gas at pressure P_1 in a bulb of known volume, v , placed at point G of fig. 1 , into the manifold and noting the final pressure P_2 .

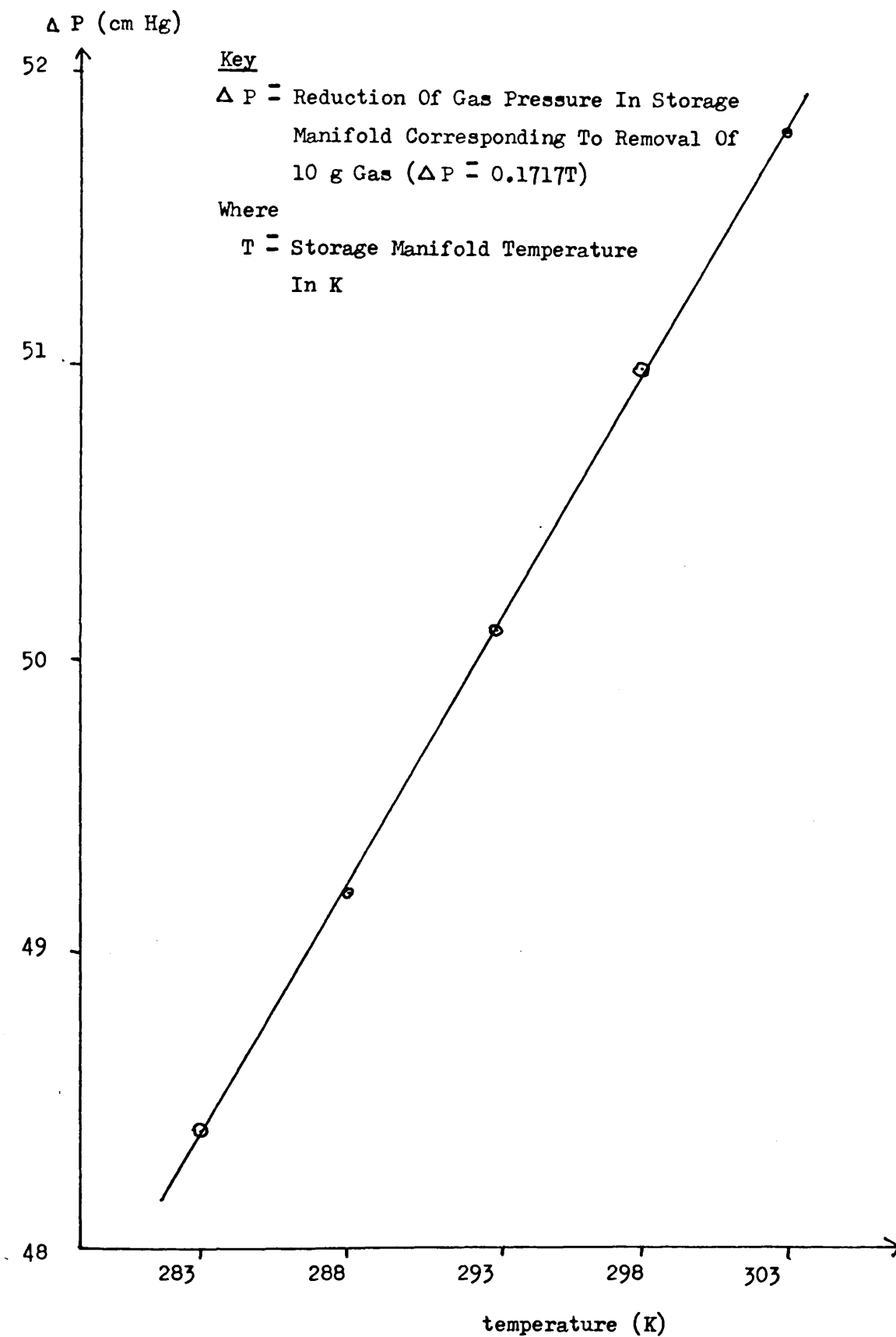
Assuming Boyles Law to hold for this system, \bar{V} was obtained by an average of six \bar{V} readings obtained from the relationship

$$\bar{V} = \frac{v(P_1 - P_2)}{P_2} \quad \text{and had the value } 6730 \pm 50 \text{ cm}^3.$$

To remove a molar quantity of gas Δn from the storage manifold the following procedure was followed. A graph such as that of fig. 3 was constructed. Immediately before the withdrawal, the temperature was read from the thermometers T_1 and T_2 which were found to differ by at most $\pm 0.2^\circ\text{C}$. The appropriate pressure change, indicated by the graph, was effected by removal of gas via the capillary stopcock of fig. 1 , to be condensed into the breakseal ampoule E, positioned in the purification manifold, containing 2-3g of finely crushed calcium hydride. After the mixture had been degassed, the flask was sealed and mechanically shaken for a maximum of three days. This minimised as far as possible the wastage of uninhibited monomer by thermal polymerisation. The complete volatile contents of the ampoule were distilled into the polymerisation reactor without cuts. Any loss of butadiene as such would reduce its mass ratio to styrene in the block copolymer.

FIGURE 4 - 3

PRESSURE VERSUS TEMPERATURE CURVE FOR 10 g BUTADIENE
IN STORAGE MANIFOLD



For reasons outlined in the literature review, sec-butyllithium was selected as initiator. It was supplied by Aldrich, nominally one molar in cyclohexane in a serum-capped bottle. Because of the reactivity towards oxygen and moisture, its composition was checked before use by the Gilman double titration method (49).

Depending upon its history, any organolithium compound contains proportions of lithium hydroxide and alkoxide by reaction with moisture and oxygen respectively. Because of its unselectivity, a simple titration with acid will always give a high level of organolithium by reacting also with hydroxide and alkoxide.

In the Gilman method, total base was estimated by a simple acid - base titration using phenolphthalein as indicator. The alkyllithium compound was removed from an equal quantity of the initiator solution by reaction with 1, 2 - dibromoethane and the unreacted hydroxide and alkoxide were determined by acid - base titration. The pure organolithium compound was then estimated by difference.

The procedure followed was identical to that outlined in (49). All steps were carried out under research grade nitrogen dried over blue silica gell, in glassware dried by heating in the same gas flow. Seals were maintained by the use of serum caps through which material was manipulated by the "three needle" technique (50).

Three double titrations were carried out, with the results as shown below.

[sec-butyllithium]	= 1.09 ± 0.05 M
[impurity]	= 0.30 ± 0.03 M

The lithium hydroxide level in the polymerising medium affects the tacticity of anionic polystyrene (51). In low temperature weak link decomposition studies, the tacticity of

the polymer has been found to affect the bond scission rate (52). However work carried out in this laboratory has shown that the rate of quantitative high temperature conversion of pure polymer to monomer and cold ring as measured by TGA and TVA is independent of sample origin. For this reason the initiator was not purified by , for example, distillation (43) before use.

Initiator was transferred to ampoule F of fig. 2 by the following procedure. The ampoule was placed on the vacuum line, dried by pumping and isolated by the stopcock shown. Injection of the initiator solution into the evacuated ampoule was found to result in fouling of the capillary tubing with organolithium compound which decomposed on heating to yield a fragile vitrified glass seal. For this reason a positive pressure of predried nitrogen was introduced via a syringe inserted through the serum cap. The required quantity of initiator was then cleanly injected into the bulb through the serum cap using a 500 μ L gas tight syringe equipped with stainless steel plunger and extra long needle (18 cm). The ampoule was degassed, sealed off at the capillary tube and glassblown onto the polymerisation reactor to produce the assembly shown in fig.4.

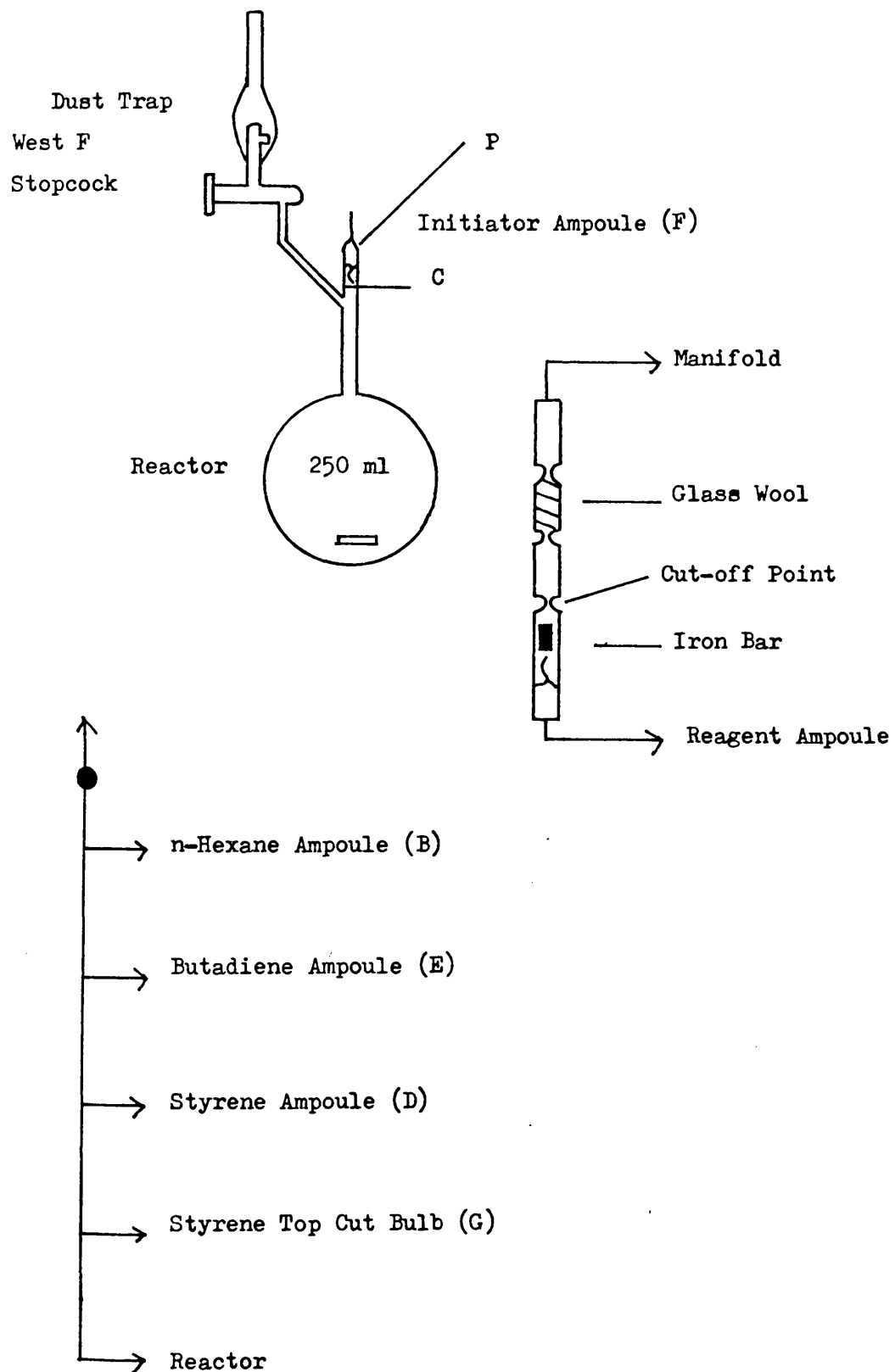
B 10 POLYMERISATION PROCEDURE.

All polymerisations were carried out in the reactor shown in fig. 4 , which was connected to the manifold via an ultra high vacuum West F greaseless stopcock protected by the dust trap shown. Styrene polymerisations had to be carried out above its θ temperature of 35°C. The reactor was constructed with all components above the "bulb". This eliminated the problem of reagent loss by distillation to other parts of the assembly.

Reagent ampoules were fused onto the manifold via the assembly shown in fig. 4 . After degassing, the complete contents

FIGURE 4 - 4

POLYMERISATION REACTOR AND MANIFOLD SCHEMATIC DIAGRAM



of a flask were distilled through the glass wool plug, also shown, into the polymerisation reactor. The flask was then removed at the constriction. A variation in this procedure was required for styrene which was initially purified by the removal of a first "cut" into bulb G of fig. 2 , which was subsequently removed. The middle cut to the reactor was then estimated volumetrically.

Styrene and n-hexane were distilled from flasks held at room temperature by a water bath. The butadiene ampoule was, however, kept at -75°C by a dry ice/acetone bath during distillation to ensure a smooth transfer of contents.

After addition of solvent to the reactor, initiator was introduced by the following procedure. Using a bar magnet, the breakseal was broken and initiator was allowed to drip into the flask . A cold surface (a beaker containing dry ice) was applied to point P of fig. 4 and the initiator ampoule was allowed to fill with solvent, which was expelled by raising its vapour pressure with a warm air blower. This process was repeated several times after which monomer was distilled into the bulb and the polymerisation was allowed to proceed.

When polymerisation was complete, a few millilitres of AR methanol were distilled into the reactor to terminate the chain ends. Methanol and n-hexane were removed by back distillation to the purification manifold and the reactor was removed from the line and cut open at point C of fig. 4 .

The polymer was dissolved in a minimum quantity of AR carbon tetrachloride. The solution was freed of glass fragments from the breakseal, and insoluble polar material by filtration, and the polymer was recovered by dripping the filtrate onto agitated methanol. After a subsequent filtration the coagulated polymer was freeze-dried under vacuum.

Because of the susceptibility of polybutadiene towards oxidation, rubber-containing polymers were stored in small sample bottles which were sealed into glass storage tubes under high vacuum conditions, to be stored at approximately -20°C . The "batch" currently in use was stored in a serum capped vessel under a positive pressure of nitrogen at 0°C .

The molecular weight of the finished polymer was assumed to be related to the quantities of initiator and monomer used by the equation

$$\bar{M}_n = \frac{\text{Weight monomer (g)}}{\text{Moles initiator}}$$

The maximum polymer yield in these experiments was set at 10 g. To ensure that the monomer/solvent ratio never exceeded 10% by weight, approximately 110 ml of n-hexane were used.

As stated previously, styrene was polymerised above 35°C . Butadiene was polymerised at room temperature to minimise its vinyl content. For this reason, and to ensure a maximum block integrity even if some of the first monomer were still present when the second monomer was added, the diblock polymer was formed by first polymerising butadiene then styrene (36, 37). The subsequent development of colour provided a useful qualitative check that the solution was active throughout the polymerisation.

Polymers were characterised by osmometry, infrared, nuclear magnetic resonance and ultra-violet spectrometry as outlined in section C of this chapter.

C POLYMER CHARACTERISATION.

C I OSMOMETRY.

Number average molecular weights \bar{M}_n were obtained using a Mechrolab high speed osmometer with cellophane membrane and using toluene as solvent at 25 °C.

The data points (concentration (c), $\frac{\text{Osmotic pressure } (\pi)}{c}$) were subjected to a linear least squares cycle to determine the intercept on the y axis ($\frac{\pi}{c}$)₀ which was assumed to be equal to $\frac{RT}{\bar{M}_n}$.

By simple rearrangement, \bar{M}_n was given as $\frac{RT}{(\frac{\pi}{c})_0}$.

Where :- R = gas constant

T = temperature, K.

C 2 INFRARED SPECTROMETRY.

Homopolymer spectra complete with peak assignments are given in fig. 5,6 . The block copolymer spectrum was found to be a simple superposition of the two homopolymer spectra.

A quantitative investigation of rubber microstructure was made, based upon the method of Silas, Yates and Thornton (53). The above reference is one of a series of papers in which rubber microstructure has been determined by estimation of the relative intensities of the olefinic out of plane deformation vibrations of the polymer. To maximise the reproducibility of the procedure, solution spectra were obtained in carbon disulphide which was used for its optical window in the i.r. fingerprint spectral region.

The situation is complicated in that each of the bands under investigation is made up of contributions of the three groupings shown below.

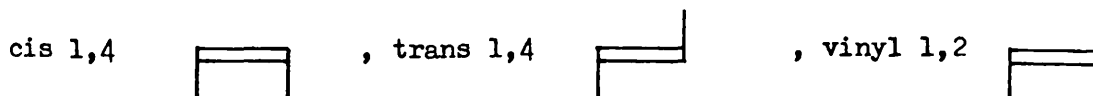
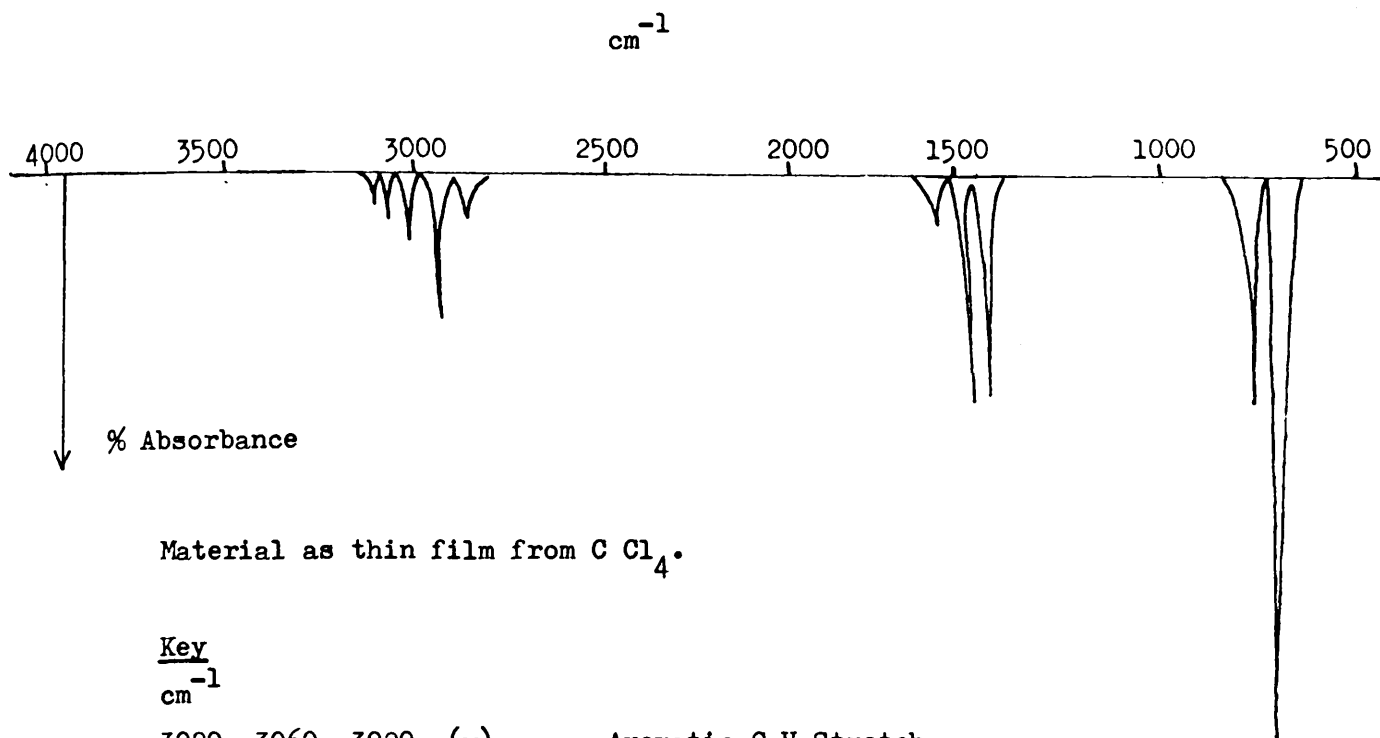


FIGURE 4 - 5

POLYSTYRENE HOMOPOLYMER INFRARED (i.r.) SPECTRUM



Material as thin film from C Cl_4 .

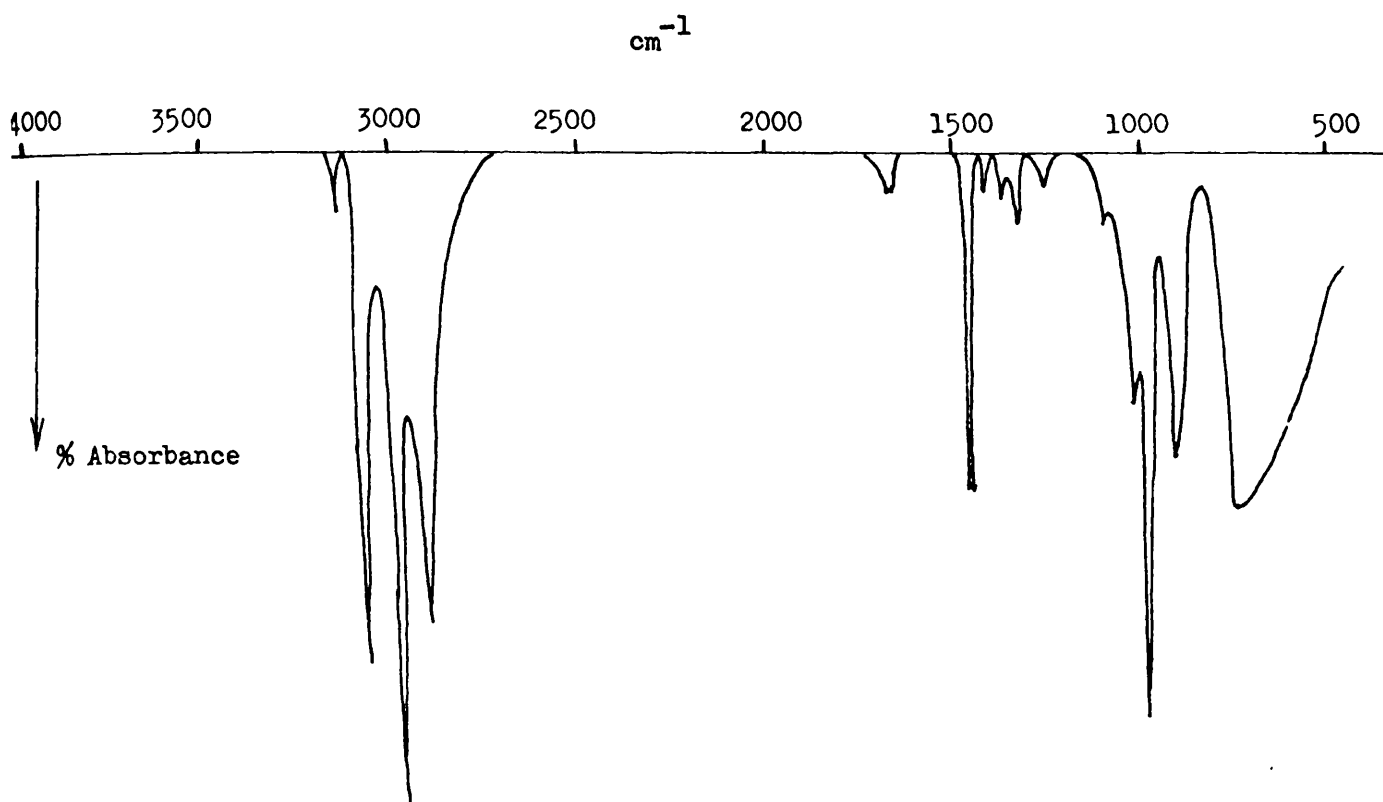
Key

cm^{-1}

- | | |
|-----------------------|----------------------------------|
| 3080, 3060, 3020, (w) | Aromatic C-H Stretch |
| 2920, 2840, (m) | Saturated C-H Stretch |
| 1600, 1490, (m) | Aromatic C-C Ring Vibrations |
| 1450, (m) | Saturated C-H Rock |
| 750, 690, (s) | Out Of Plane C-H Ring Vibrations |

FIGURE 4 - 6

POLYBUTADIENE INFRARED (i.r.) SPECTRUM



Material as thin film from C Cl_4 .

Key

cm^{-1}

3080, 3000, (w,s) Olefinic C-H

2910, 2840, (s) Saturated C-H

1655, 1640, (w) $\text{C}=\text{C}$ Stretch

1450, 1430, (m) Saturated C-H Rock

990, 910, (m) vinyl 1,2 Out Of Plane Deformation

960, (s) trans 1,4 Out Of Plane Deformation

Envelope centred on 730 cm^{-1} - mainly cis 1,4 out of plane deformation

but with contributions from vinyl and trans groupings.

In spite of this complication, the 960 cm^{-1} vibration is mainly due to the trans 1,4 while the 910 cm^{-1} vibration is mainly due to vinyl 1,2. On the other hand, the $830 - 630\text{ cm}^{-1}$ band contains significant contributions from all three groupings. Because of its variable shape for different polymer samples, no single wavenumber could be assigned to the latter band, the intensity of which was represented by the fraction α , made equal to the expression

$$\log \frac{\int_{630\text{ cm}^{-1}}^{830\text{ cm}^{-1}} I_0 d\lambda}{\int_{630\text{ cm}^{-1}}^{830\text{ cm}^{-1}} I d\lambda}$$

Where

- (1). $\int_{630\text{ cm}^{-1}}^{830\text{ cm}^{-1}} I_0 d\lambda$ represents the area integral in the infrared chart between 630 cm^{-1} and 830 cm^{-1} .
- (2). $\int_{630\text{ cm}^{-1}}^{830\text{ cm}^{-1}} I d\lambda$ represents the area integral of spectral transmission in the infrared chart between 630 cm^{-1} and 830 cm^{-1} .

By iterative methods Silas et al. obtained the following relationship :-

$$S_a = MX$$

Where

- (1). S_a is a 3×1 column matrix representing the specific absorbances in $\text{LM}^{-1}\text{cm}^{-1}$ at 960 cm^{-1} (1,1), 910 cm^{-1} (2,1) and the $830 - 630\text{ cm}^{-1}$ band (3,1) respectively.
- (2). X is the 3×1 column matrix representing the mole fractions of vinyl 1,2 (1,1) - trans 1,4 (2,1) and cis 1,4 (3,1) groupings in the polymer, assuming 100% unsaturation.

(3). M is a 3 x 3 operative matrix.

The expression can be rewritten in the form

$$X = M^{-1} s_a$$

Where M^{-1} is defined as $\left| \frac{1}{M} \right| \text{ adj } M$.

It was felt by this author that the application of the method would be improved if it were made concentration independent. This modification was performed as follows.

Absorbance (a) can be related to specific absorbance (s_a) by the expression $a = cl s_a$ where c is concentration in ML^{-1} and l is the path length (0.5 mm). If cl is denoted by K, then by a simple application of matrix algebra it can be seen that

$$M^{-1} a = K (M^{-1} s_a).$$

If we denote the matrix $M^{-1} a$ as A, then it can be seen that $A = KX$.

Similarly, it can be seen that $\sum A_i = K \sum X_i = K$.

By simple equating of terms

$$\begin{bmatrix} X_{1,2} \\ X_{t\ 1,4} \\ X_{c\ 1,4} \end{bmatrix} = \begin{bmatrix} \frac{A_{1,2}}{K} \\ \frac{A_{t\ 1,4}}{K} \\ \frac{A_{c\ 1,4}}{K} \end{bmatrix}$$

Throughout this work the 3 x 3 operative matrix M^{-1} took the form

$$\begin{bmatrix} 9.2217 \times 10^{-5} & 5.4633 \times 10^{-3} & 9.8759 \times 10^{-4} \\ 7.5432 \times 10^{-3} & 1.9165 \times 10^{-4} & 3.2501 \times 10^{-3} \\ 5.9939 \times 10^{-4} & 2.5258 \times 10^{-3} & 9.9746 \times 10^{-2} \end{bmatrix}$$

Using this approach the polymer microstructures can be directly obtained from the spectral absorbances.

Because of interference from the polystyrene segment, this method could not be used to characterise the rubber component of the block copolymer.

The above procedure may prove useful in the determination of the microstructure of the soluble fraction of polybutadiene samples containing a proportion of insoluble material, as the final solution concentration of extracted material is often inconvenient to measure. This was, however, not attempted in this work.

Before the method is used, it must be ascertained that the gel-forming process does not lead to either a quantitative reduction in unsaturation or to structures which produce significant interference in the $1000 - 600 \text{ cm}^{-1}$ range.

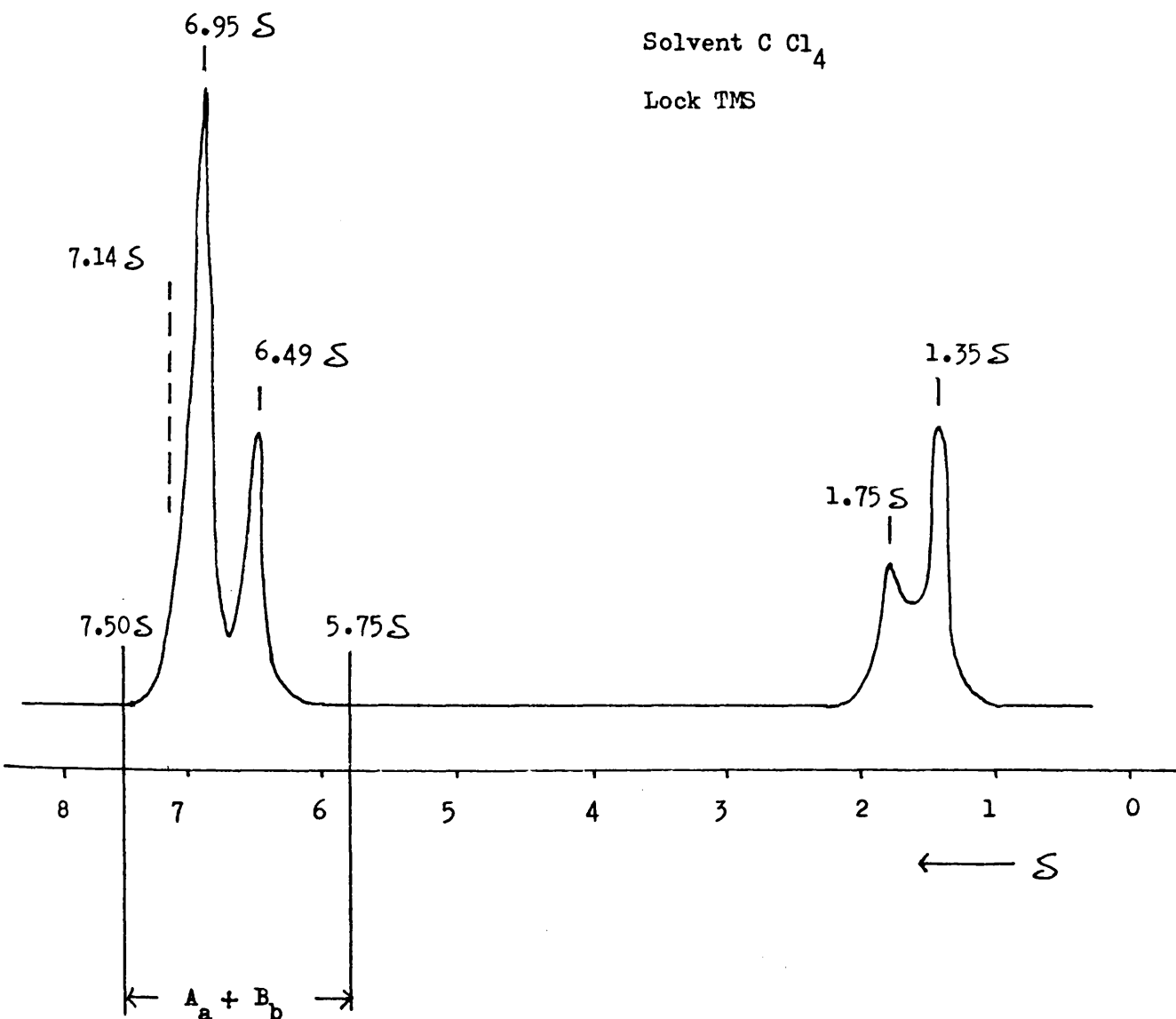
C 3 PROTON MAGNETIC RESONANCE SPECTROMETRY.

A simple yet effective way of characterising styrene/butadiene block copolymers is by proton n.m.r. spectrometry. Fig. 7,8 illustrates the ability of this approach to separate the proton signals due to aromatic polystyrene from those of the olefinic polybutadiene. Because the method is self-calibrating, peak sizes can be directly compared and the relative abundances of the groupings present then determined.

In addition the method allows a distinction to be made between block and non-block or copolymer styrene, the latter of which is represented by a sharp peak at 7.14δ (fig. 7). This effect is explained as follows. In polystyrene, each benzene ring exists in a permanent though changeable magnetic flux caused by the intrinsic aromatic currents of its neighbours. This effect, which is additive, shields the ring protons and separates the ortho from the meta and para ring proton signals. If the polystyrene sequences are interrupted by butadiene spacers the ring current effect is negated

FIGURE 4 - 7

POLYSTYRENE HOMOPOLYMER NUCLEAR MAGNETIC RESONANCE (n.m.r.) SPECTRUM



Key

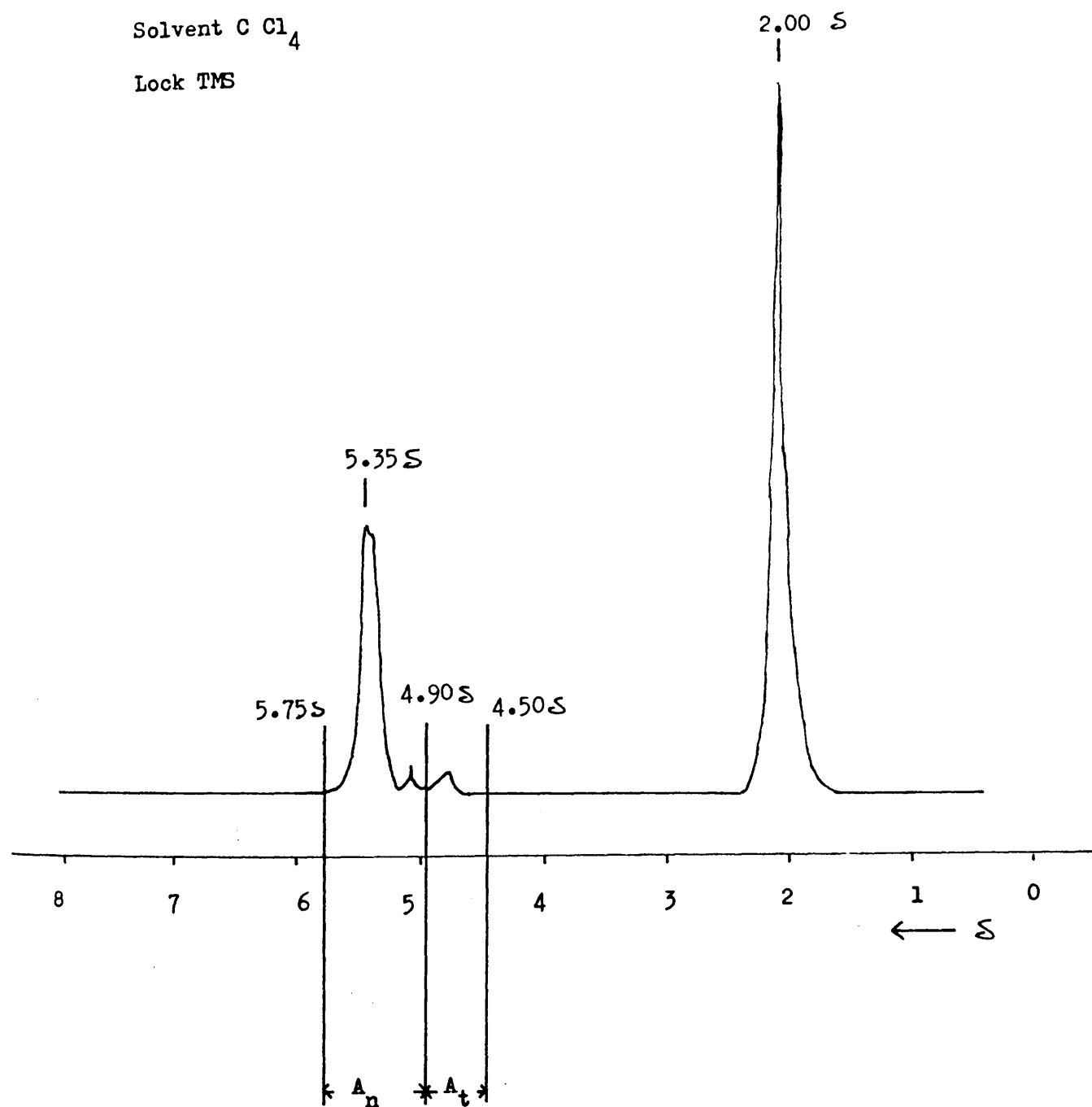
- 1.35 -CH₂-
- 1.75 -CH-
- 6.49 o-Aromatic Protons
- 6.95 m,p-Aromatic Protons
- 7.14 Isolated Benzene Type Protons

FIGURE 4 - 8

POLYBUTADIENE HOMOPOLYMER NUCLEAR MAGNETIC RESONANCE (n.m.r.) SPECTRUM

Solvent C Cl₄

Lock TMS



Key

δ

2.00 Saturated C-H α To Olefin Group

5.35 1,4 Olefin

and a toluene type signal is produced.

Copolymer styrene could be produced if the styrene monomer is introduced to the polymerisation reactor before complete consumption of the butadiene.

This effect, which, though qualitative, is very sensitive to the presence of copolymer styrene due to the sharpness of the accompanying aromatic signal. Its absence in the block copolymer under study confirmed that a pure block structure was present.

The method also allows a distinction to be made between the vinyl and the 1,4-repeat units of the rubber block because of the observable chemical shift between the signals generated by the two types of protons. Unfortunately, no such distinction could be made between the respective 1,4-isomers. There exists, however, no reason to suppose that the cis/trans ratio in the rubber section in the block copolymer differs in any way from that of the rubber homopolymer prepared under identical conditions.

The limits of signal integration can be inspected in fig.7,8 . These limits along with the mode of data manipulation were taken from work by Mochel (54).

Assumptions.

1. Block styrene content > 3 Mole% .
2. Vinyl content < 15 Mole% of rubber segment.

TABLE 1.

EQUATIONS FOR n.m.r. SPECTRA DATA MANIPULATION.

STRUCTURAL UNIT	RELATIVE MOLE CONTENT (Fig.7,8)
BLOCK STYRENE	$0.2 (A_a + A_b)$
1,2 BUTADIENE	$A_t/2.5$
1,4 BUTADIENE	$\frac{1}{2} (A_n - 0.2A_t)$

Peak weights were substituted for areas in the above equations.

C 4 ULTRA-VIOLET (u.v.) SPECTROMETRY.

The weight percentage of styrene in the block copolymer was determined by u.v. spectrometry, mainly as a check on results obtained by n.m.r. spectrometry. Use was made of the method of Meehan (55) in which the specific absorbance (E^*) of the polymer determined in chloroform solution at 262 nm (in units of absorbance/g cm) is related to the polystyrene weight fraction by the expression $E^* = xE_s^* + (1 - x)E_b^*$ where E_s^* is the specific absorbance of pure polystyrene, E_b^* is the corresponding value for pure polybutadiene, and x is the weight fraction of polystyrene in the copolymer. The method is made possible by the non-interaction of the two chromophores and is used in this work in the form $x = 0.476E^* - 0.019$.

C 5 POLYMER CHARACTERISATION.

(i). POLYSTYRENE

CONDITIONS OF POLYMERISATION

MONOMER CHARGE 10 ml

INITIATOR CHARGE 200 μ l (2×10^{-4} M)

TEMPERATURE 35 - 40°C

TIME OF POLYMERISATION 24 hr

CHARACTERISATION

\bar{M}_n (EXPECTED) = 50000

\bar{M}_n (FOUND) = 56000

i.r. and n.m.r. spectra can be seen in fig. 5 and 7 respectively.

The polymer was found to be microstructurally pure.

ULTRA-VIOLET SPECTROMETRY.

WT% POLYSTYRENE (BLANK) = 98.5

(ii). POLYBUTADIENE - LOW MOLECULAR WEIGHT LATEX.

CONDITIONS OF POLYMERISATION.

MONOMER CHARGE 5g

INITIATOR CHARGE 500 μ l (5×10^{-4} M)

TEMPERATURE 20 - 25°C

TIME 24 hr

CHARACTERISATION.

\bar{M}_n (EXPECTED) = 10000

Because of the expected diffusion of material through the membrane,
its osmometric molecular weight was not measured.

INFRARED SPECTROMETRY.

MOLE% cis 1,4 = 84.3, MOLE% trans 1,4 = 12.9, MOLE% vinyl 1,2 = 2.9

NUCLEAR MAGNETIC RESONANCE SPECTROMETRY.

MOLE% 1,4 = 96.6, MOLE% 1,2 = 3.4

(iii). POLYBUTADIENE - MODERATE MOLECULAR WEIGHT.

CONDITIONS OF POLYMERISATION.

MONOMER CHARGE 10g

INITIATOR CHARGE 100 μ l (10^{-4} M)

TEMPERATURE 20 - 25°C

TIME 24 hr

CHARACTERISATION.

\bar{M}_n (EXPECTED) = 100000

\bar{M}_n (FOUND) = 94400

INFRARED SPECTROMETRY (fig. 6)

MOLE% cis 1,4 = 81.7, MOLE% trans 1,4 = 13.2, MOLE% vinyl 1,2 = 5.1

NUCLEAR MAGNETIC RESONANCE SPECTROMETRY (fig. 8)

MOLE% 1,4 = 95.1, MOLE% vinyl 1,2 = 4.9

ULTRA-VIOLET SPECTROMETRY.

WT% POLYSTYRENE (BLANK) = -0.9

(iv). DIBLOCK COPOLYMER

CONDITIONS OF POLYMERISATION.

FIRST MONOMER - BUTADIENE.

MONOMER CHARGE 4.6g

INITIATOR CHARGE 400 μ l (4×10^{-4} M)

TEMPERATURE 20 - 25°C

TIME 24 hr

SECOND MONOMER - STYRENE.

MONOMER CHARGE 5ml

TEMPERATURE 35 - 40°C

TIME 24 hr

CHARACTERISATION.

\bar{M}_n (EXPECTED) = 25000

\bar{M}_n (FOUND) = 28000

INFRARED SPECTROMETRY.

The block copolymer spectrum consisted of a superposition of the two homopolymer spectra.

NUCLEAR MAGNETIC RESONANCE SPECTROMETRY.

WT% POLYSTYRENE = 53.8

RUBBER MICROSTRUCTURE.

MOLE% 1,4 = 97.8, MOLE% vinyl 1,2 = 2.2

ULTRA-VIOLET SPECTROMETRY.

WT% POLYSTYRENE = 51.4

POLYSTYRENE DEGRADATION.A LITERATURE REVIEW.

The first systematic study of polystyrene degradation was attempted by Staudinger and Steinhofer (56). The products they obtained convinced them of the head-tail addition nature of polystyrene.

Jellinek (57) pyrolysed polystyrene to differing extents of degradation and obtained a molecular weight versus extent of conversion curve. This coupled with the large quantities of monomer produced in the process convinced him that monomer was being formed not as a product fraction of a random scission process but by an unzipping process initiated at active sites formed upon random weak-link scission in the material.

At about the same time Madorsky and co-workers were perfecting the isothermal TG technique as applied to polymer thermolysis. The rate of polymer volatilisation was found (58) to reach a maximum at 30 - 40% weight loss. This was assumed to be consistent with an end-unzipping process.

Bradt and co-workers (59) attempted a volatile product analysis for polystyrene degradation using mass spectrometry. The composition of the volatile and cold ring product fractions taken together was found to be independent of conversions. This further discredited the random theory of degradation and suggested that intramolecular transfer may play a major role in the degradation process. Grassie and co-workers (60 - 64) further investigated the characteristics of polystyrene degradation, concentrating especially upon the early stages of degradation.

Rates of volatilisation at 298°C were found (60)

to be proportional to the chain end concentration of the system. This supported Madorsky's arguments. The volatilised product ratio was found to be independent of conversion by a more satisfactory method (by weight) than that employed previously (59). This again emphasised the importance of intramolecular transfer in the process. It was argued that intermolecular transfer, even with long zip lengths, would prevent the molecular weight "plateau" observed in the later stages of degradation from being formed.

An attempt was made (61) to associate weak links with one or more of the polymerisation variables. In fact, the weak link concentration was found to be dependent only upon the temperature of polymerisation. Some possible unstable structures were discussed and examined more fully (63 , 64).

The radical population in the early stages of degradation was greatly reduced (62) by pyrolysis in the inhibitor tetralin. The initial molecular weight drop was not affected in any way. This was taken as convincing proof of the weak link theory. Experimental errors inherent in the technique were discovered, however, (65) which cast doubts on the validity of the assertion. Until recently, nevertheless, this experiment remained the most convincing piece of work in support of the weak link theory of degradation.

Artificially high head-head concentrations in polystyrene were achieved (63) by copolymerising the material with trace quantities of stilbene. The copolymers so produced did not possess any marked instability at small percentage conversions. The weak link content estimated by the initial molecular weight drop in the early stages of thermolysis, however, was found (64) to approximate to that of main chain unsaturation as measured by ozonolysis. Main chain unsaturation increases with the temperature of polymerisation. For these reasons weak links were initially

associated with main chain unsaturation.

More recent work has suggested that neither head-head linkages nor main chain unsaturation contribute to the rate of initial (instant) scissions in the polymer. They have both, however, been found to contribute to the instability of the material in the period immediately following that occupied by weak link scission.

The most plausible alternative approach to the system under discussion was developed by Madorsky and co-workers (66-68) who asserted that the initial precipitous molecular weight drop in the system was caused by intermolecular transfer reactions which produced random scissions in the polymer backbone.

These authors (66) supported Grassie's view that depropagation was an end initiated process. They made no distinction, however, between the processes operative in the initial and final stages of degradation. The gentle molecular weight drop observed in the latter stages of degradation was explained by postulating long kinetic zip lengths of depropagation.

A computer programme was compiled (67) based upon the kinetic scheme assumed to be operative within the degrading polymer. The simulated volatilisation curves so produced, best approximated those of the real system when a large value of σ , the intermolecular chain transfer constant, and a small value of μ , the ratio of the random to end initiation rate constants, was used.

Central to the kinetic approach of the Madorsky group was that termination in the system was a second order process. This was in opposition to the Grassie approach which assumed a mechanism of first order termination. The effect of the order of the termination process upon the molecular weight distribution of the material was discussed (68) with special reference to the degradation of monodisperse anionic polymers. If termination is first order and

brought about by a process of small radical ejection from the system, then a most probable molecular weight distribution should be rapidly achieved with initially monodisperse polymers. This was not found to be the case. This evidence was taken as supporting the predominance of second order termination in the system. Of interest was the complete absence of volatilisation in the early stages of degradation of these polymers. This effect can not be satisfactorily explained using a kinetic scheme which does not take into account the existence of a small concentration of thermolabile bonds in the polymer molecule.

Richards and Salter induced the degradation of polystyrene at abnormally low temperatures by introducing radical sources into the system. The polymer was blended with poly(α -methyl styrene) (69) which produces monomer radicals on unzipping. It was also blended (70 , 71) with anionic polystyrene terminated in such a manner as to contain a known concentration of head-head weak linkages which decompose on heating to provide a radical source.

The destabilising effect observed (69) showed that the polymer was susceptible to intermolecular transfer.

The weak link concentration of the sample was elegantly varied (70) by blending pure polystyrene with the weak link-containing material. A short zip length of about six monomer units was estimated and a kinetic scheme was developed which indicated that the ratio of bulk/cage recombinations increased with the radical concentration in the sample.

The first direct evidence for intermolecular transfer was obtained by tracer methods (71). Labelled, anionic polystyrene was, however, found to be more stable than corresponding radical polystyrene with respect to emission of volatiles, at the abnormally low temperatures used in these studies.

Perhaps the most plausible degradation scheme to date (78),

is based upon work described by Cameron and co-workers (72 - 77). The weak link theory was declared unsound (72) because the weak link concentration in the sample (β) apparently varied with the temperature of degradation.

A simple, elegant, kinetic treatment (73) emphasised that first order termination is the predominant process in polystyrene degradation. The proposed mechanism of termination by small radical ejection from the sample was, however, proved invalid by a consideration of its effect on the molecular weight distribution of the sample (68). The proposal made that random scission in the polymer backbone is immediately accompanied by a process of disproportionation, however, remains valid.

M^CNeill and co-workers (74 , 75) measured main chain unsaturations by tracer methods. Their degradation results did not associate weak links with unsaturation.

The effect of the degradation temperature on β was removed (76 , 77) by degrading the material at sub-volatilisation temperatures. Weak link concentrations in radical polystyrene were found to increase with the temperature of polymerisation, but β was found to approach zero for anionic polystyrene. Head to head groupings were shown not to be sources of weak links but were shown to contribute to the early instability of the polymer.

Cameron et al (78) drew these observations into the following kinetic scheme. Initial scissions in radical polymers occur at weak linkages of unknown composition in the material. Degradation immediately afterwards is initiated at abnormal linkages such as main chain unsaturations and head to head groupings. Afterwards and until the end of the degradation, initiation is at unsaturated chain ends formed by the immediate disproportionation reactions which follow normal random scissions. Termination is

a first order process. A plausible (though unsubstantiated) mechanism was proposed.

Volatilisation is completely absent in the initial stages of breakdown of anionic polystyrene due to an absence of weak links in the material. Random scissions followed by disproportionation, however, efficiently build up the terminal unsaturated content of the polymer, with the result that the shape of the volatilisation curve in the later stages of degradation is indistinguishable from that for radical polystyrene.

B PROGRAMMED DEGRADATIONS.

B 1 THERMOGRAVIMETRY UNDER NITROGEN ($10^{\circ}\text{C}/\text{min}$).

The single rate maximum of fig. 1 confirms the single step nature of the volatilisation process which begins at approximately 300°C , achieves a rate maximum at 420°C and is complete at 460°C , leaving no residue.

B 2 DIFFERENTIAL SCANNING CALORIMETRY UNDER NITROGEN ($10^{\circ}\text{C}/\text{min}$).

Both the shape and position of the DSC maximum at 420°C (fig. 2) agree well with the TG rate curve. This confirms the endothermic nature of the bond scission process and eliminates the possibility that quantitative sub-volatilisation processes are occurring in the polymer.

B 3 TVA.

It can be seen from the 0°C TVA curve of fig. 3 that volatilisation under high vacuum conditions commences at approximately 300°C , proceeds to a rate maximum at 415°C and is complete at 450°C . The small discrepancy between the TVA and TG rate trace maxima is best accounted for by a more efficient product removal under vacuum.

The "limiting rate" effect observed in the -45°C curve indicates that a single condensable volatile material is being produced in the degradation reaction. This is confirmed by a sub-ambient TVA fractionation of the products.

FIGURE 5 - 1

POLYSTYRENE TG UNDER NITROGEN

Heating Rate $10^{\circ}\text{C}/\text{min}$

Sample Size 5 mg

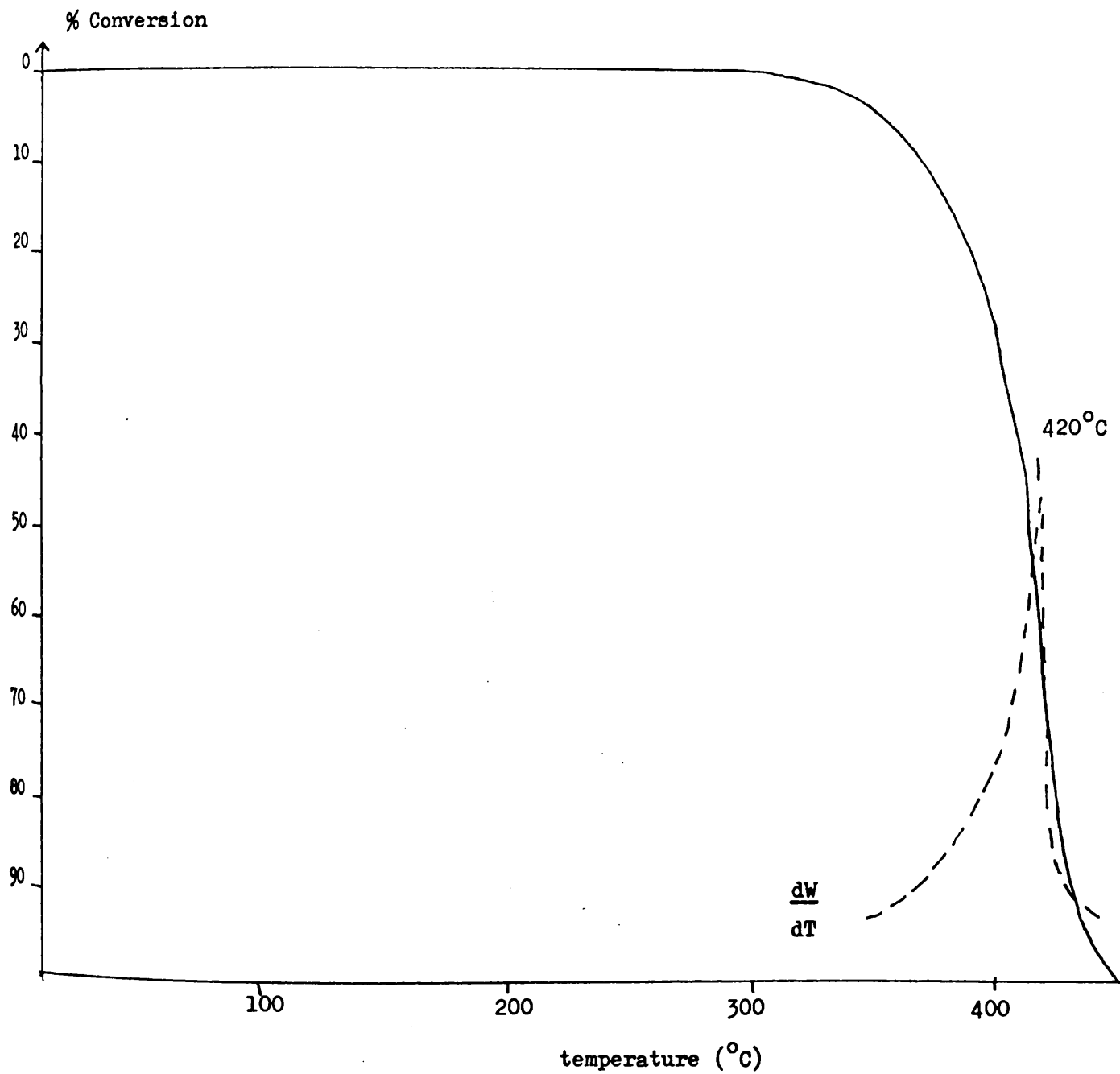


FIGURE 5 - 2

POLYSTYRENE DSC UNDER NITROGEN

Heating Rate $10^{\circ}\text{C}/\text{min}$

Sample Size 2.5 mg

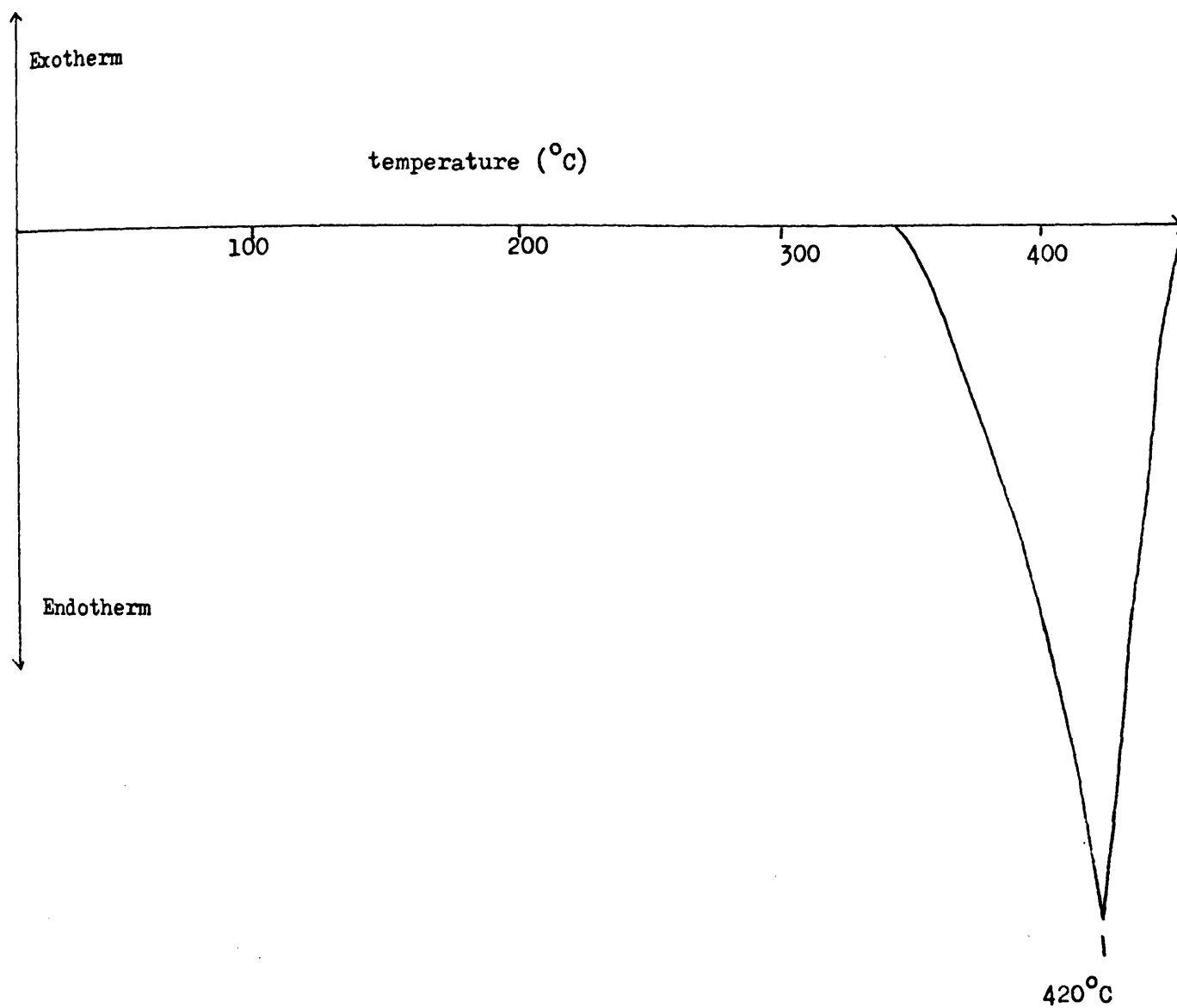
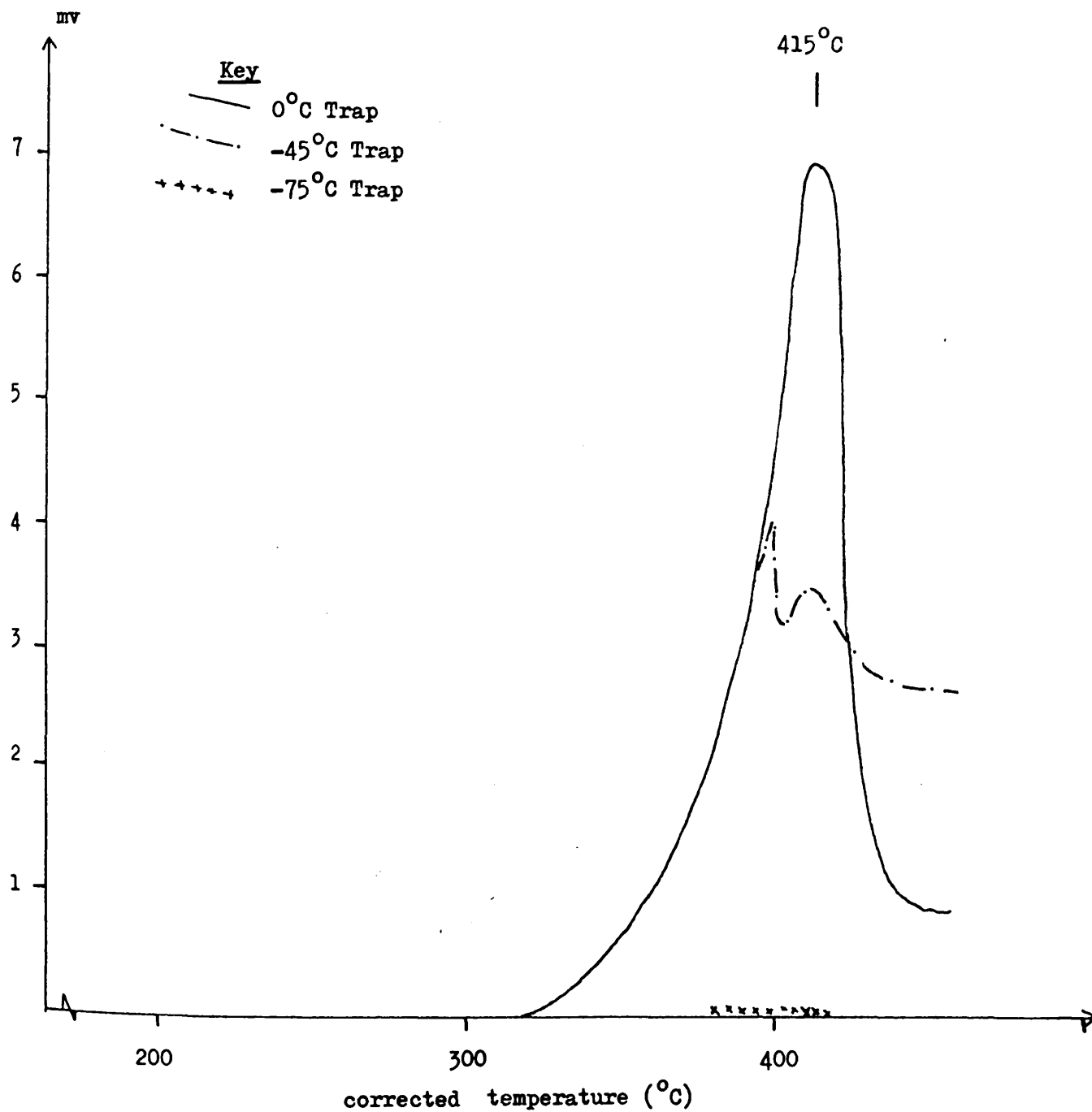


FIGURE 5 - 3

POLYSTYRENE TVA

Heating Rate $10^{\circ}\text{C}/\text{min}$

Sample Size 100 mg



Volatile material corresponding to both programmed ($10^{\circ}\text{C}/\text{min}$) and isothermal (380°C) degradations to completion was subjected to sub-ambient TVA fractionation and the fractionated material was identified spectroscopically.

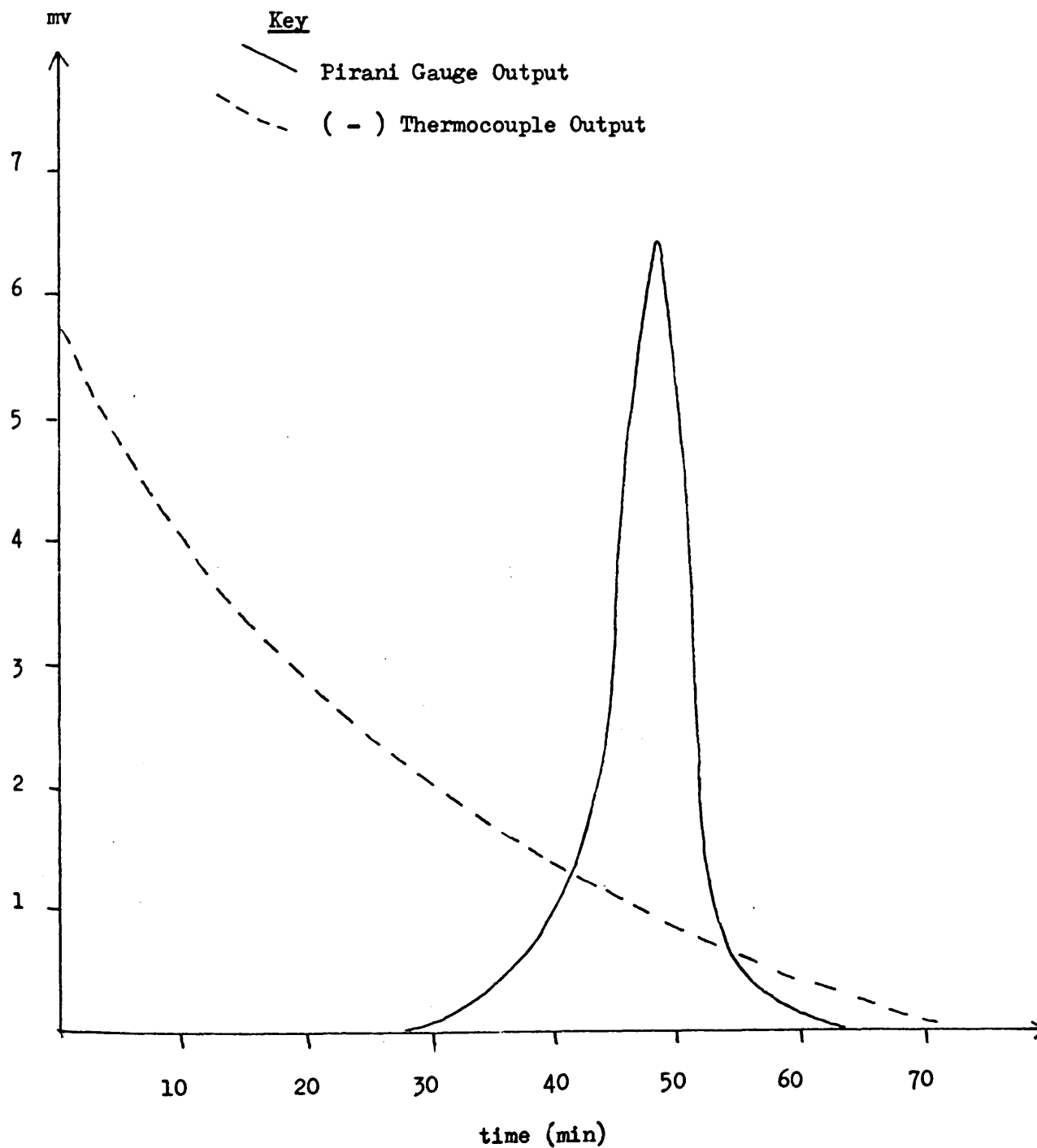
The shape of the sub-ambient TVA curve of the condensable volatile fraction of degradation (fig. 4) suggested that either a pure material or a mixture of substances of very similar volatility was being produced. The material was directed to the fractionating grid and distilled under closed system conditions to a collecting vessel for subsequent spectroscopic analysis. The n.m.r. and solution phase i.r. spectra of the material were indistinguishable from those of pure styrene.

Madorsky and Straus (79) showed that styrene oligimers were involatile under vacuum at room temperature. For reasons which become obvious in section D of this chapter it was necessary to confirm the absence of a proportion of oligameric material in the volatile fraction of degradation. Such material may elude detection by the above tests in two ways. First of all it may be sufficiently involatile to be retained in the sub-ambient trap until it reaches ambient temperatures and to be subsequently distilled from it at a limiting rate. A "long time scale" sub-ambient separation would not be able positively to identify this material for the following reason. A Pirani gauge zeroed with a neighbouring cold trap at -196°C suffers considerable baseline drift when the trap is warmed to room temperature. It may therefore be difficult to distinguish between the two effects. Secondly, high molecular weight material may be lost in the closed system distillation to the collecting vessel.

FIGURE 5 - 4

SATVA CURVE FOR TOTAL CONDENSABLES FROM PROGRAMMED AND
ISOTHERMAL POLYSTYRENE DEGRADATION

Sample Size 15 mg



To eliminate this uncertainty, the following experiment was performed. A sample of polystyrene (100 mg) was degraded to completion at 380°C for one hour in an oven assembly directly connected to a removable cold trap at -196°C. The oven was cooled and the cold ring fraction of degradation on the upper portion of the degradation tube was pumped continuously through the cold trap for another hour. The trap was isolated from the vacuum manifold, opened to the atmosphere, and its complete contents were carefully transferred with solvent to an n.m.r. tube for analysis. Oligomeric material was not detected. Toluene as measured by the n.m.r. signals corresponding to its saturated protons, was estimated as comprising 1 - 2% of the distillate (81).

C 2 COLD RING PRODUCT ANALYSIS.

Polystyrene was degraded to completion as above and the cold ring fractions of degradation were subjected to spectroscopic analysis.

The i.r. spectrum differed from that of the homopolymer only in the appearance of an extra band at 1625 cm⁻¹ (m) attributable to olefinic/aromatic conjugations and in the splitting of the band at 1580 cm⁻¹ associated with the polymer into a weak doublet of unknown origin.

N.m.r. spectra of the fraction both before and after the application of preparative thin layer chromatography using n-hexane are shown in figs. 5 and 6 respectively. The fractions produced by this technique will be referred to as F_n with the stationary fraction taking the value F₁.

F₁, F₂ (fig. 6A)

These spectra are consistent with that of the structures

FIGURE 5 - 5

n.m.r. SPECTRUM OF POLYSTYRENE COLD RING FRACTION
OF DEGRADATION

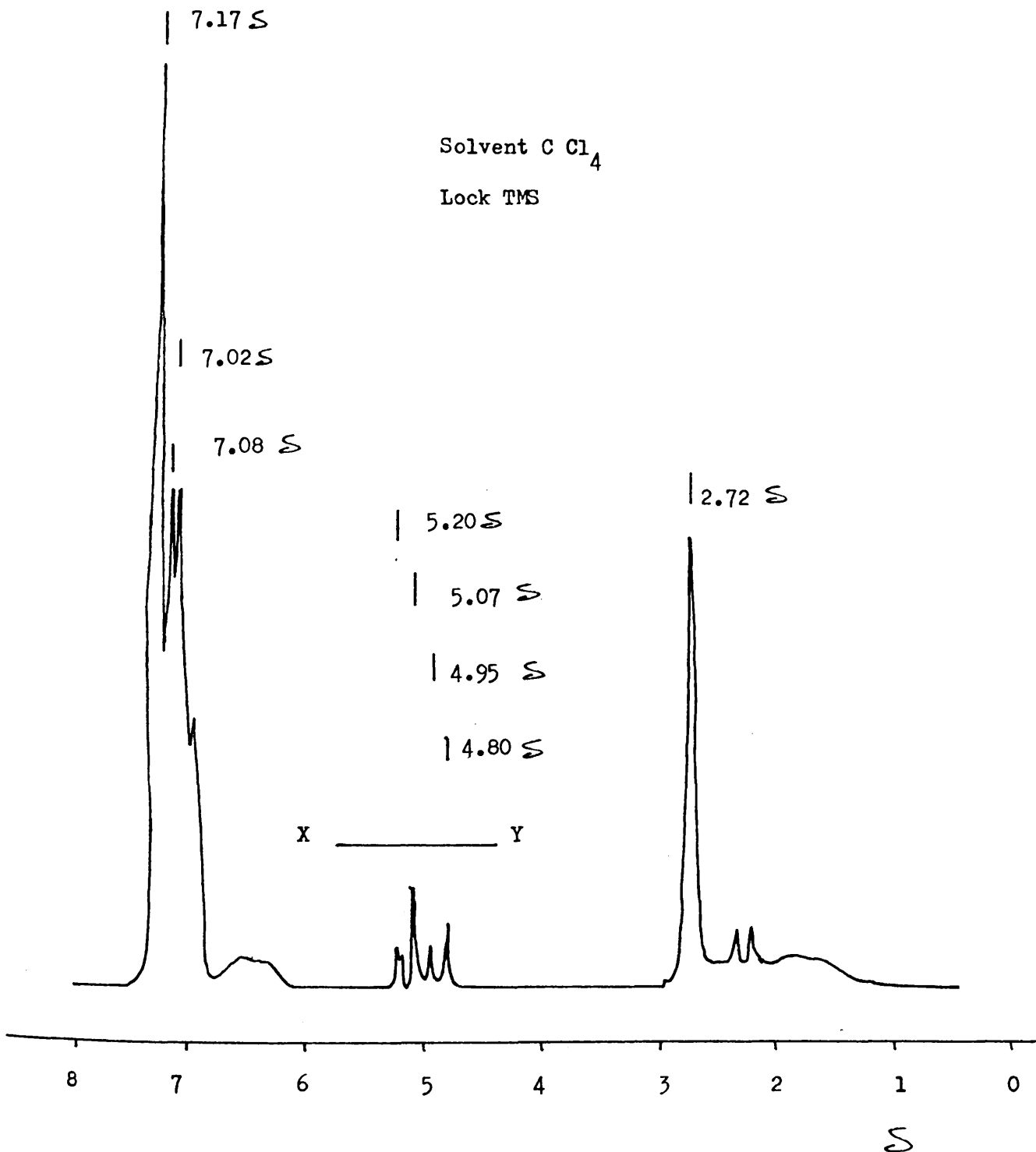


FIGURE 5 - 6 A

n.m.r. SPECTRA OF POLYSTYRENE COLD RING FRACTION OF DEGRADATION AFTER
FRACTIONATION BY PREPARATIVE THIN LAYER CHROMATOGRAPHY

250 mg Sample

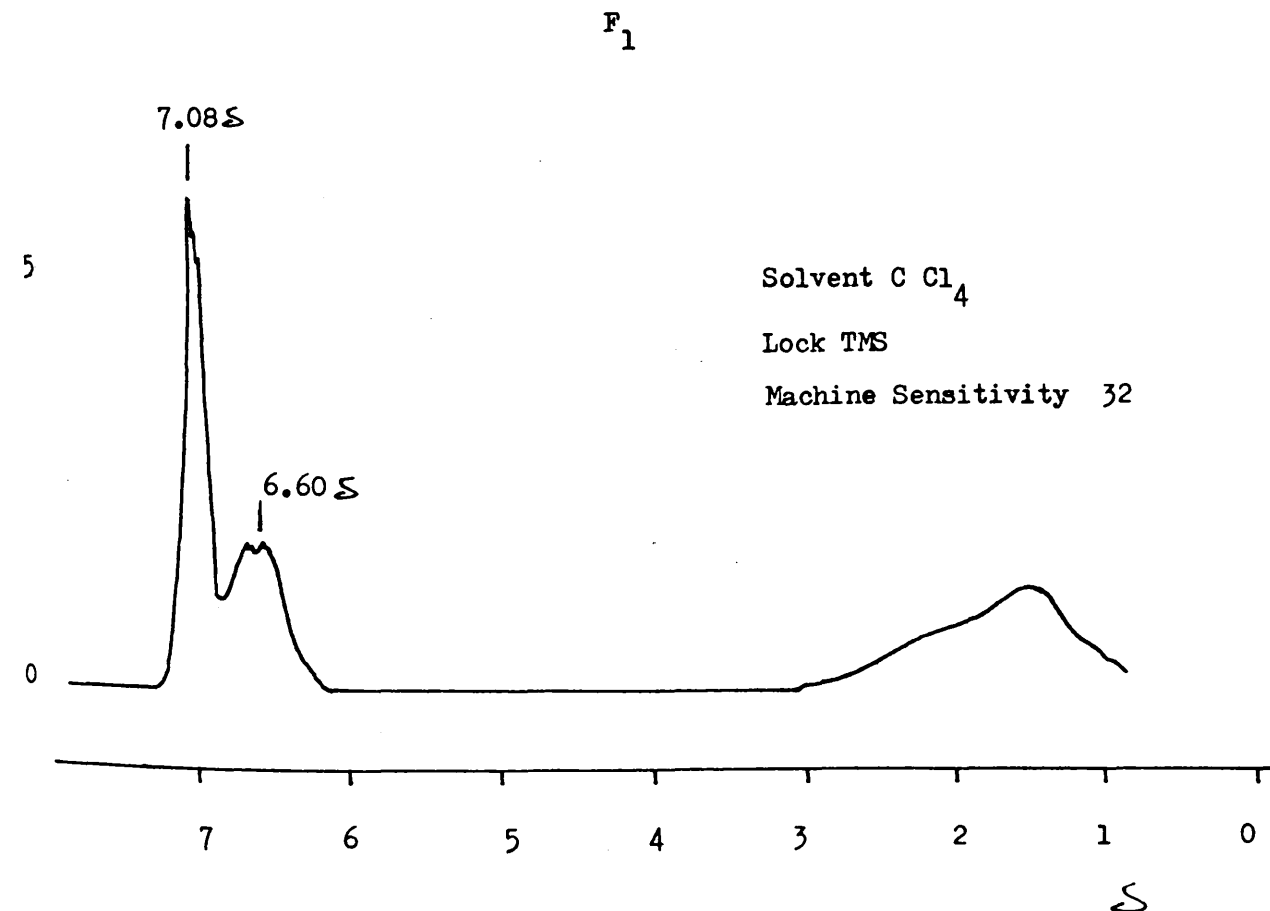
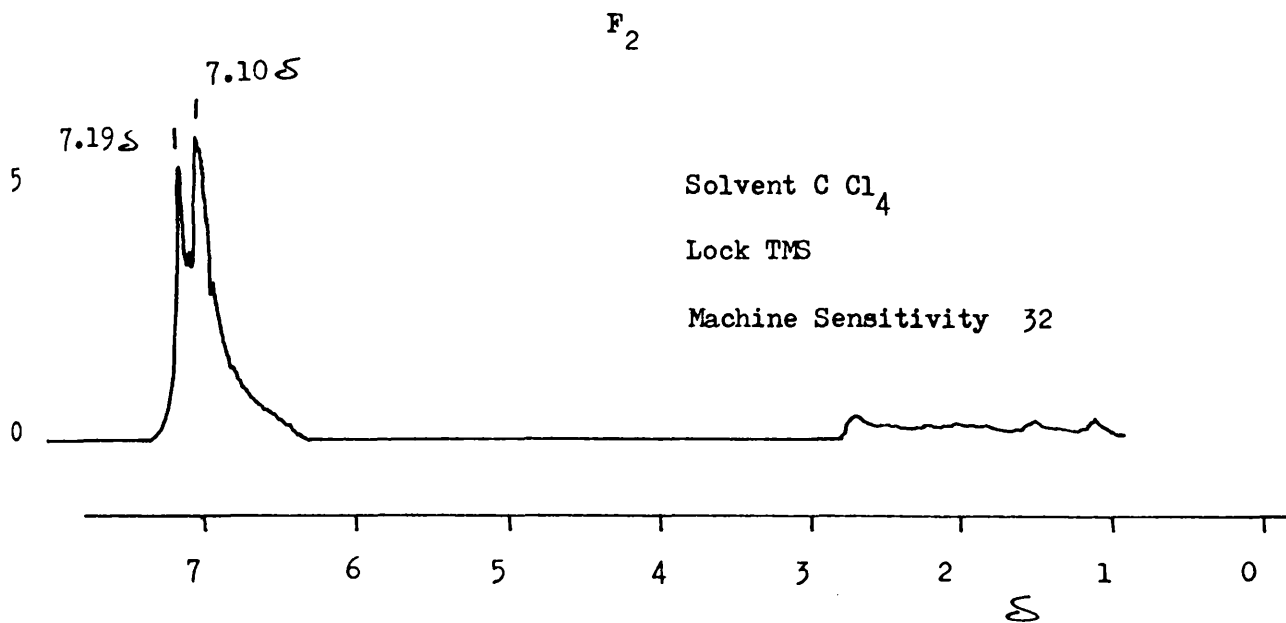


FIGURE 5 - 6 B

n.m.r. SPECTRA OF POLYSTYRENE COLD RING FRACTION OF DEGRADATION AFTER
FRACTIONATION BY PREPARATIVE THIN LAYER CHROMATOGRAPHY

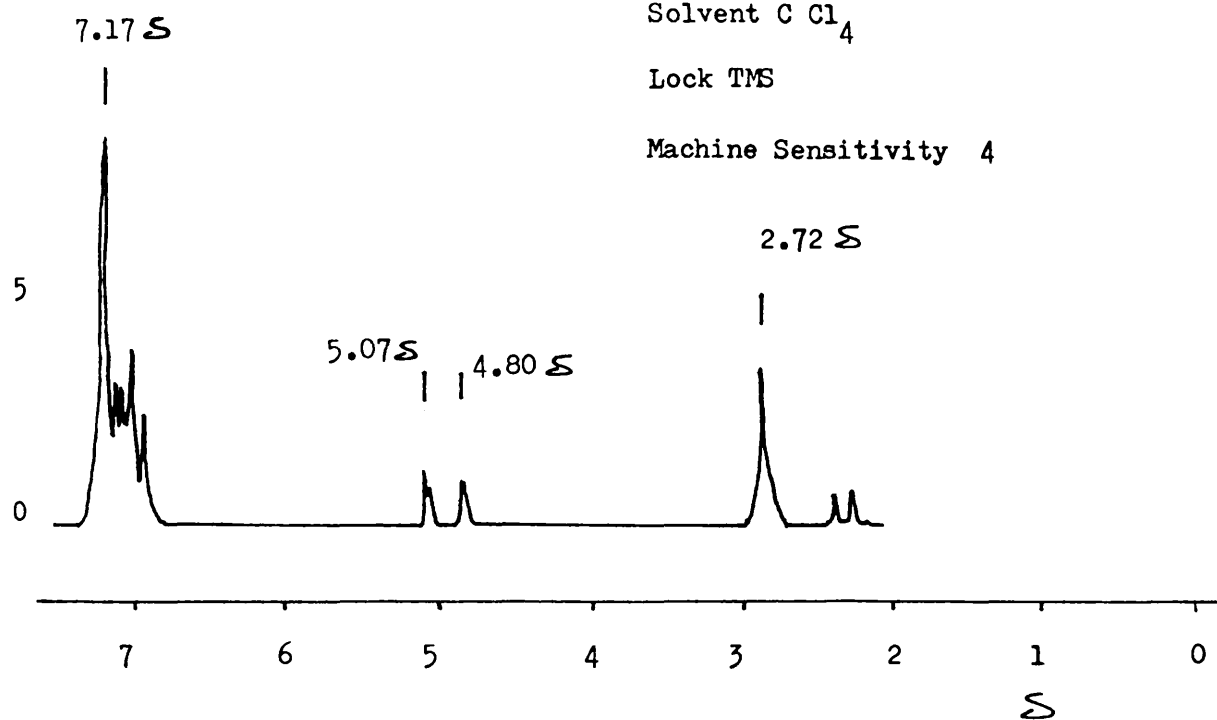
250 mg Sample

F₄

Solvent C Cl₄

Lock TMS

Machine Sensitivity 4

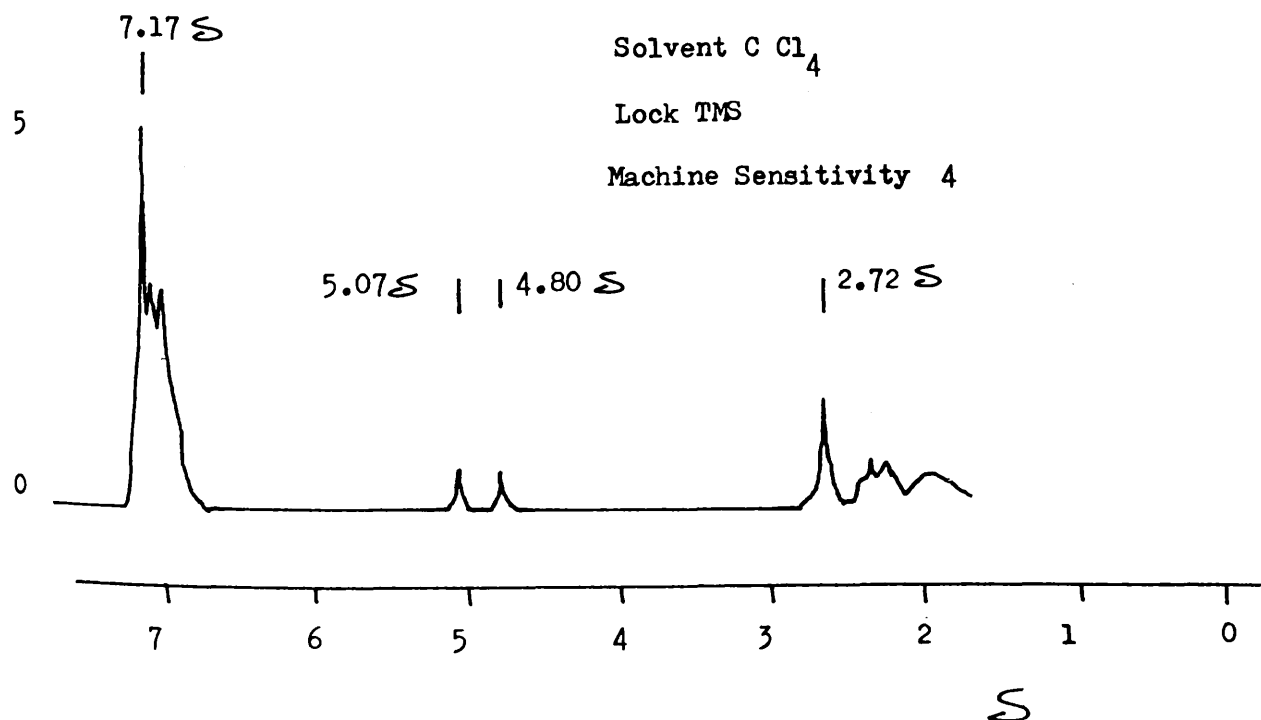


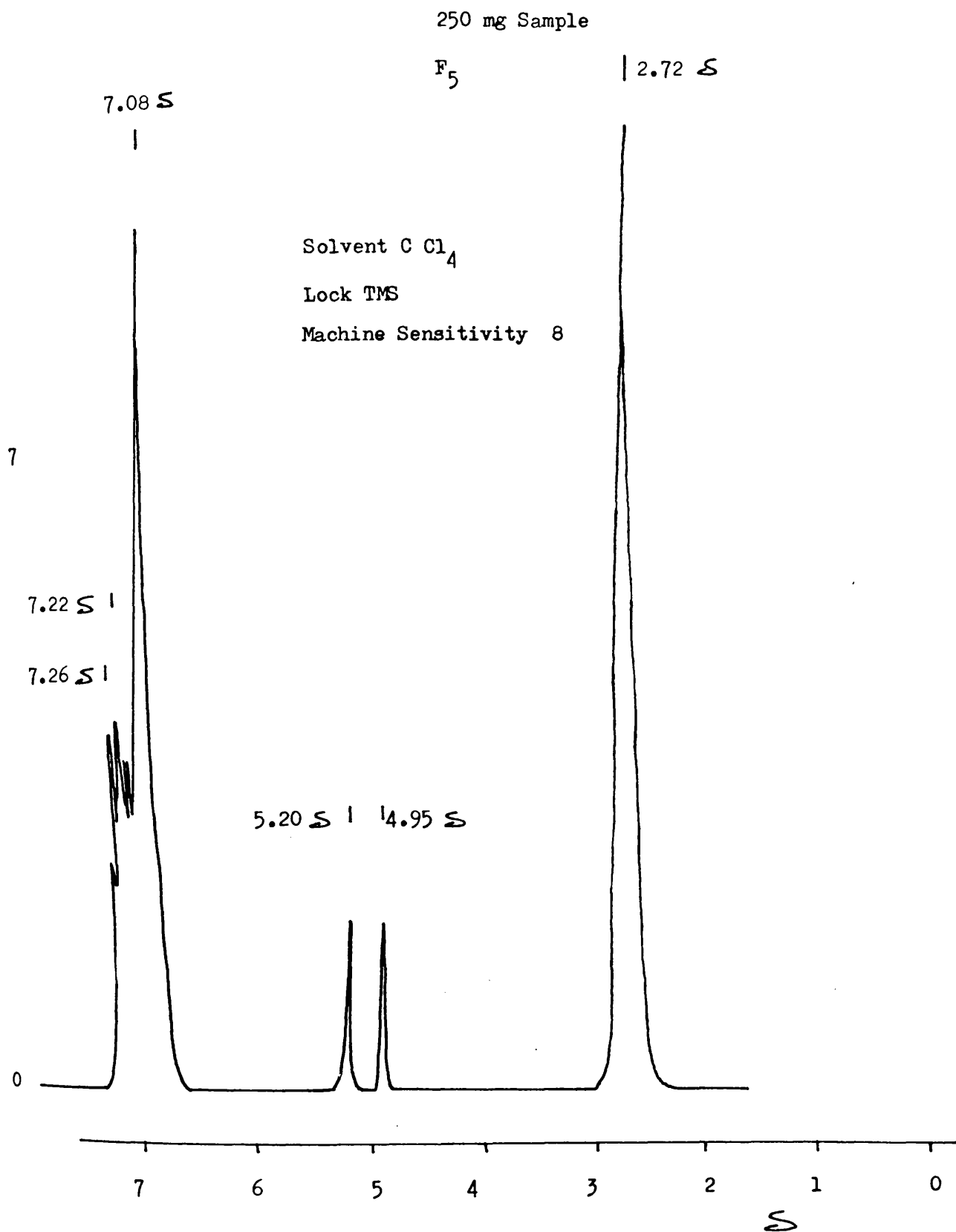
F₃

Solvent C Cl₄

Lock TMS

Machine Sensitivity 4

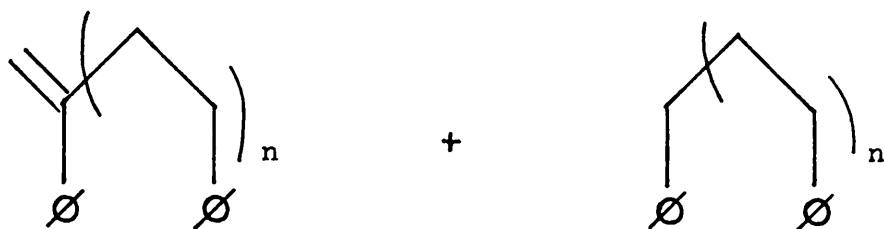


n.m.r. SPECTRA OF POLYSTYRENE COLD RING FRACTION OF DEGRADATION AFTER
FRACTIONATION BY PREPARATIVE THIN LAYER CHROMATOGRAPHY

$-(CH_2 CH\emptyset)_n-$ of molecular weight approaching the limit of volatilisation ($\frac{1}{2}$ 900).

F₃, F₄ (fig. 6B)

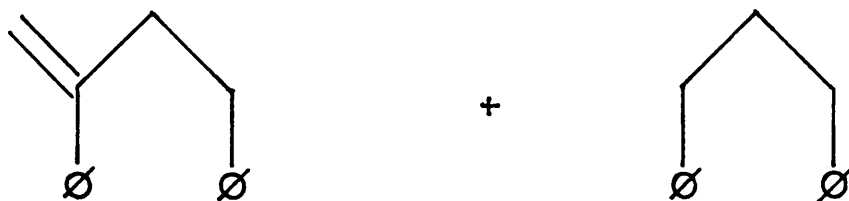
These spectra are consistent with those expected from a mixture of the structures shown below.



Where $n = 2, 3, 4, \dots$

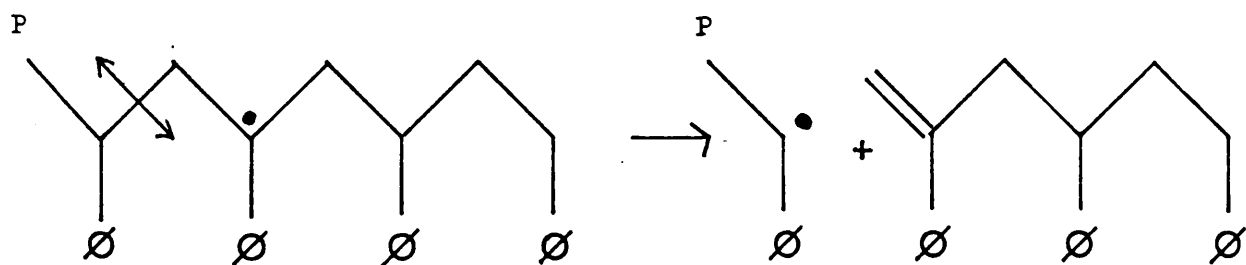
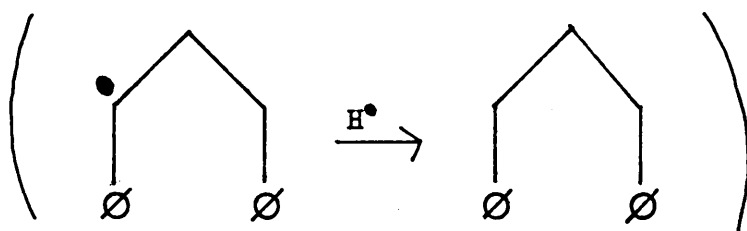
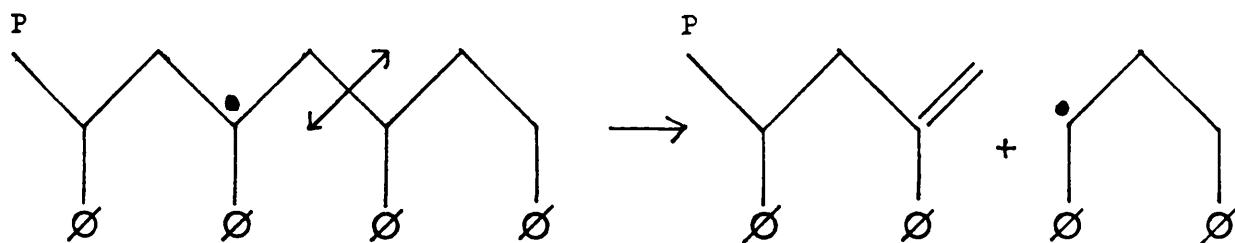
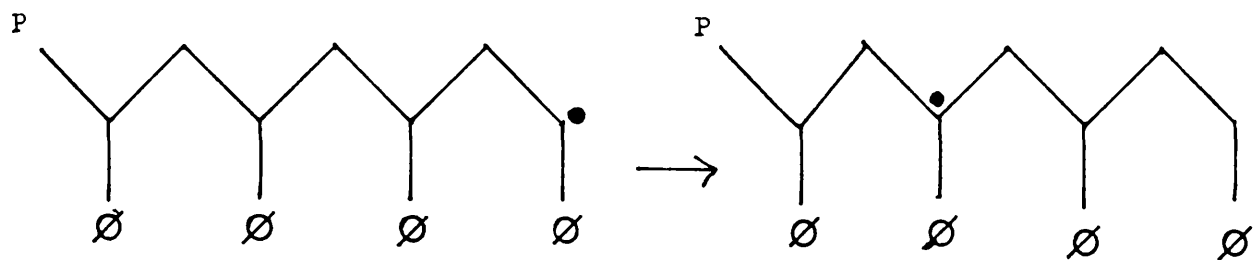
F₅ (fig. 6C)

This spectrum is consistent with that of a mixture of the dimeric structures shown below.



The mole ratio of the terminally unsaturated dimer/higher oligomer can be obtained by integration of the peak area between X and Y of fig. 5 . It was found to have a value of approximately 0.5.

The above structures are those expected in products of intramolecular transfer reactions of the following type.



Where P = Polymer Residue

D ISOTHERMAL DEGRADATIONS AT 380°C.

D 1 INTRODUCTION AND DESCRIPTION OF APPARATUS.

Polystyrene was degraded isothermally at 380°C and the percentage conversion to monomer and cold ring material was estimated gravimetrically. Similar measurements were performed with polybutadiene and the two were used in conjunction to estimate the stability of a 1 : 1 by weight homopolymer mixture assuming no interaction.

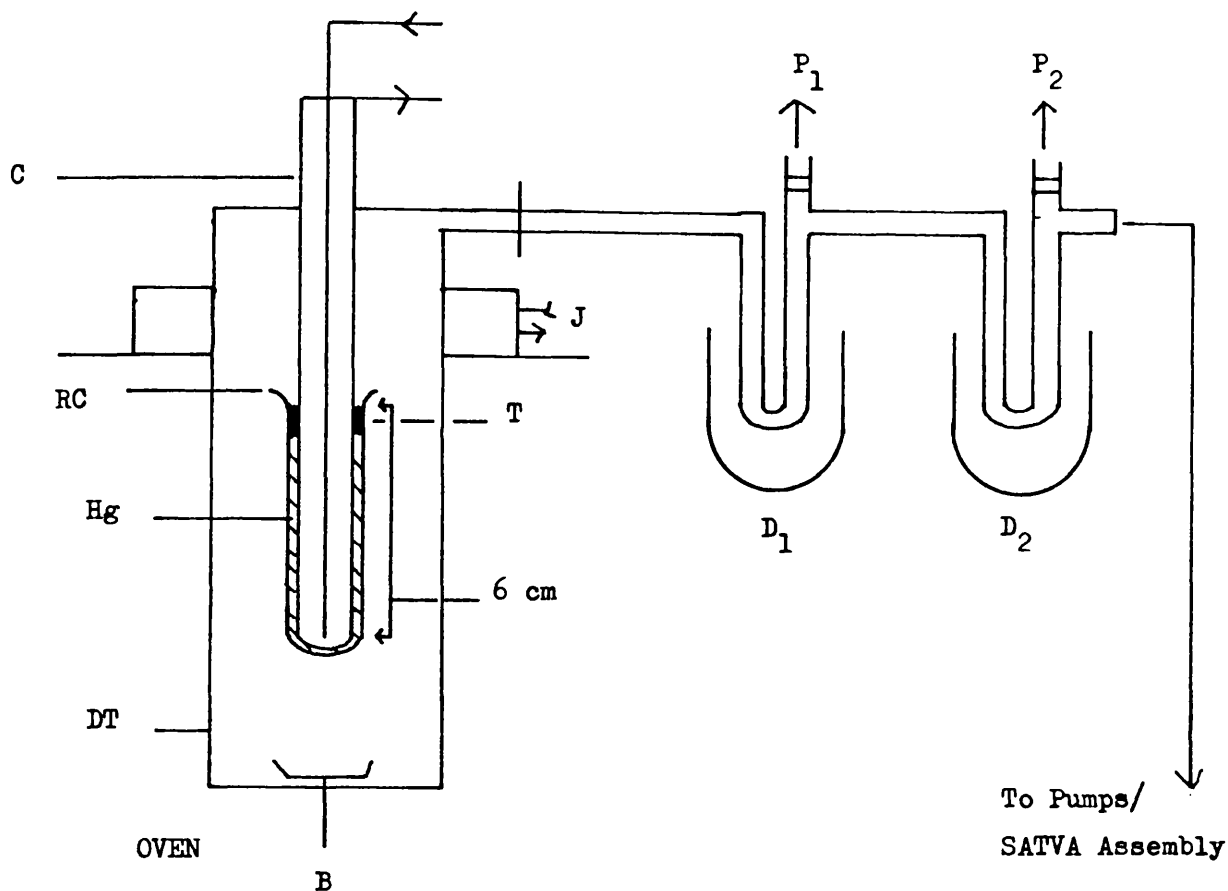
M^CNeill and co-workers (80) used thin-walled TVA tubes which were sectioned after use to weigh directly the cold ring and residue fractions of degradation. It was felt that large mass ratios of glass/product may introduce uncertainties into such measurements. For this reason an alternative gravimetric procedure was developed.

The oven assembly illustrated in fig. 7 was temperature-calibrated by the procedure outlined in Chapter 2 and was used in conjunction with a single-limbed differential condensation TVA and sub-ambient TVA assembly when required.

A good thermal contact between the internal and external cold fingers was effected by a thin film of mercury. Other contact materials such as glass beads and silica powder did not achieve an efficient enough thermal contact with the internal cold finger to prevent excessive overheating of the external cold finger via black-body radiation from the oven. In these cases cold ring material was deposited at the water jacket. When mercury was used the cold ring fraction of degradation was completely condensed onto the tip of the cold finger.

The mass of the cold ring fraction was obtained as follows. The external cold finger was removed from the assembly and carefully emptied of mercury. The opening was sealed with sellotape to prevent

DEGRADATION ASSEMBLY FOR ISOTHERMAL WORK

Key

- DT Degradation Tube
- B Pyrex Sample "Boat"
- C Internal Cold Finger
- RC Removable Cold Finger
- T Teflon Tape Plug
- Hg Mercury Film
- D₁ Dewar Vessel Containing Ice/Water
- D₂ Dewar Vessel Containing Liquid Nitrogen
- P₁ Pirani Gauge For Total Volatiles
- P₂ Pirani Gauge For Noncondensables
- J Water Jacket (Cold Ring)

residual droplets of mercury from running onto the balance pan and the tube was weighed. It was then wiped clean with a solvent moistened tissue and reweighed to obtain the mass of the cold ring fraction.

Residue weights were estimated as the weight difference obtained by flaming clean the degradation boat after the degradation. The mass of volatile material so produced was obtained by difference.

The accuracy of the technique should increase with sample size. Polymer, however, can "sputter" during degradation and cold ring material can drop back into the hot-zone, especially when samples of mass greater than 100 mg are used. With this in mind a compromise sample size of 50 mg was used.

A major problem in all isothermal work of this type is that of deciding upon a "zero time" of degradation. The criterion used in work performed on the blend system was that the degradations were assumed to commence upon the emission of volatile material from the sample. With the degradation assembly used for the previous work this entailed shifting the time axis by 5 min, in other words removing 5 min from all time readings. To facilitate a comparison with the blend system the same criterion was employed in this work. The time shift required was found to be 5 min as before.

D 2 EXPERIMENTAL RESULTS.

(i). TG Under Nitrogen.

An isothermal TG trace of the material at 380°C under nitrogen is shown in fig. 8 . This indicates that the polymer is completely removed from the hot zone after approximately 60 min degradation at 380°C.

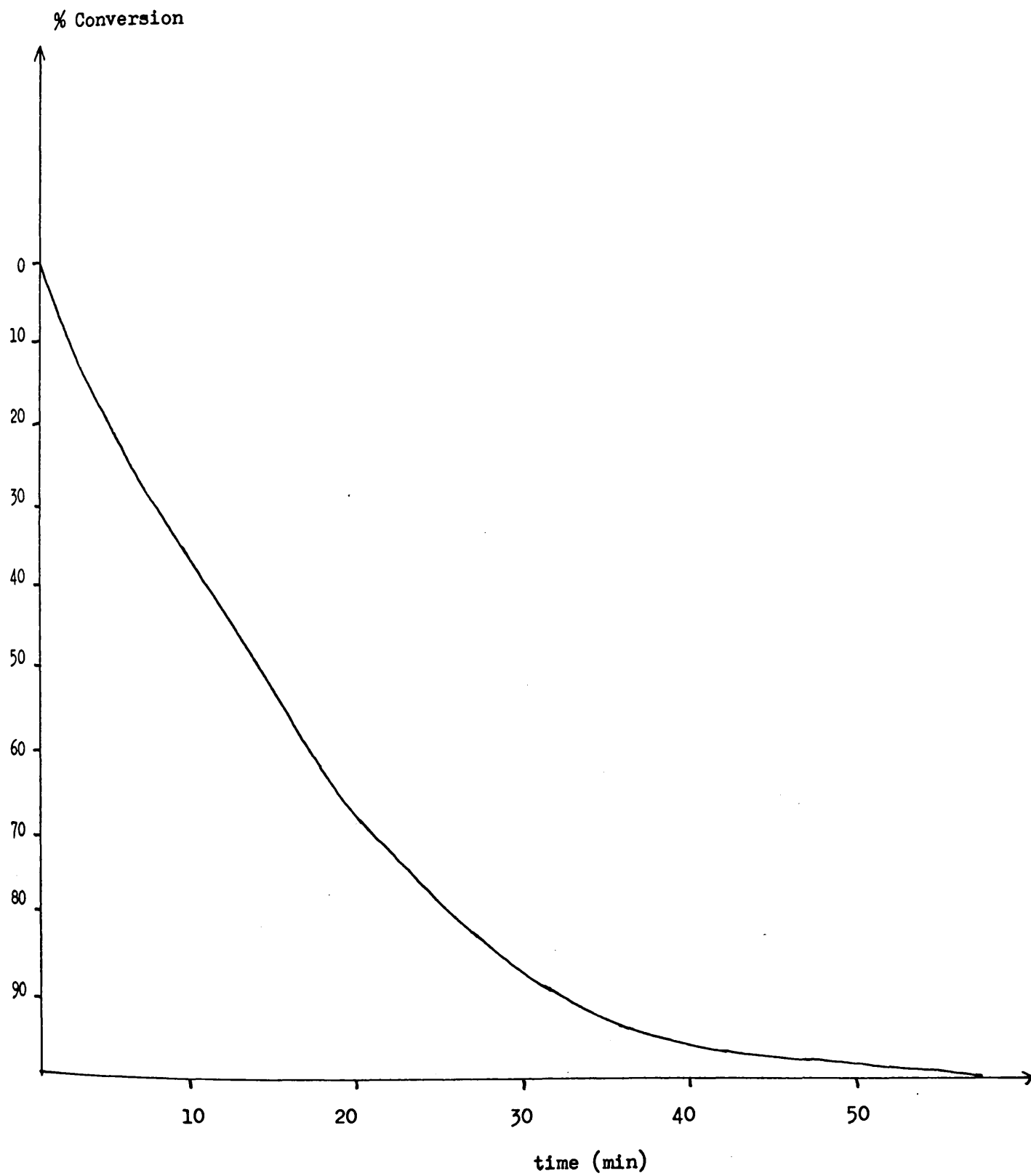
(ii). TVA.

An isothermal TVA trace for the material can be inspected

FIGURE 5 - 8

POLYSTYRENE ISOTHERMAL TG AT 380°C UNDER NITROGEN

Sample Size 6 mg



in fig. 9 . It can be seen that the low molecular weight material used in this work produces a sharper TVA trace than that exhibited by the higher molecular weight material used in previous work (80). This effect was observed by Madorsky et al (66) who attributed it to an enhanced chain end concentration present during the degradation of lower molecular weight material.

(iii). Gravimetric Analysis Under Vacuum.

Percentage conversions for polystyrene under vacuum are tabulated below and plotted graphically in fig. 10 .

TABLE 5 - 1

POLYSTYRENE CONVERSION DATA UNDER VACUUM

CORRECTED TIME	N ^o OF RUNS	WT.OF POLYMER(mg)	WT% RESIDUE	WT% COLD RING FRACTION	WT% MONOMER	MONOMER COLD RING
0	3	50	99.0 \pm 0.1	0.3 \pm 0.1	0.7 \pm 0.2	2.3
10	3	50	73.7 \pm 1.2	5.1 \pm 1.1	21.2 \pm 2.3	4.2
20	3	50	31.4 \pm 2.1	23.5 \pm 1.8	45.1 \pm 3.9	1.9
30	3	50	11.2 \pm 1.1	31.4 \pm 3.0	57.4 \pm 4.1	1.8
50	3	50	3.5 \pm 1.0	35.4 \pm 2.5	61.1 \pm 3.5	1.7

D 3 DISCUSSION.

If we neglect the second product ratio of Table 1 it can be seen that the mass ratio of monomer to cold ring material is fairly constant throughout the degradation. This is expected for a mechanism involving monomer formation by unzipping and cold ring fraction formation by intramolecular transfer. The average product ratio of 1.9, obtained by neglecting the second measurement of Table 1 differs from the previously reported value of 0.67 (60). It agrees well, however, with the value obtained by McNeill (80) and with the value of 1.8 - 1.9 obtained by estimation by GLC of the monomer yield in degradation to completion at 350°C (Chapter 8).

FIGURE 5 - 9

POLYSTYRENE ISOTHERMAL TVA AT 380°C

Sample Size 50 mg

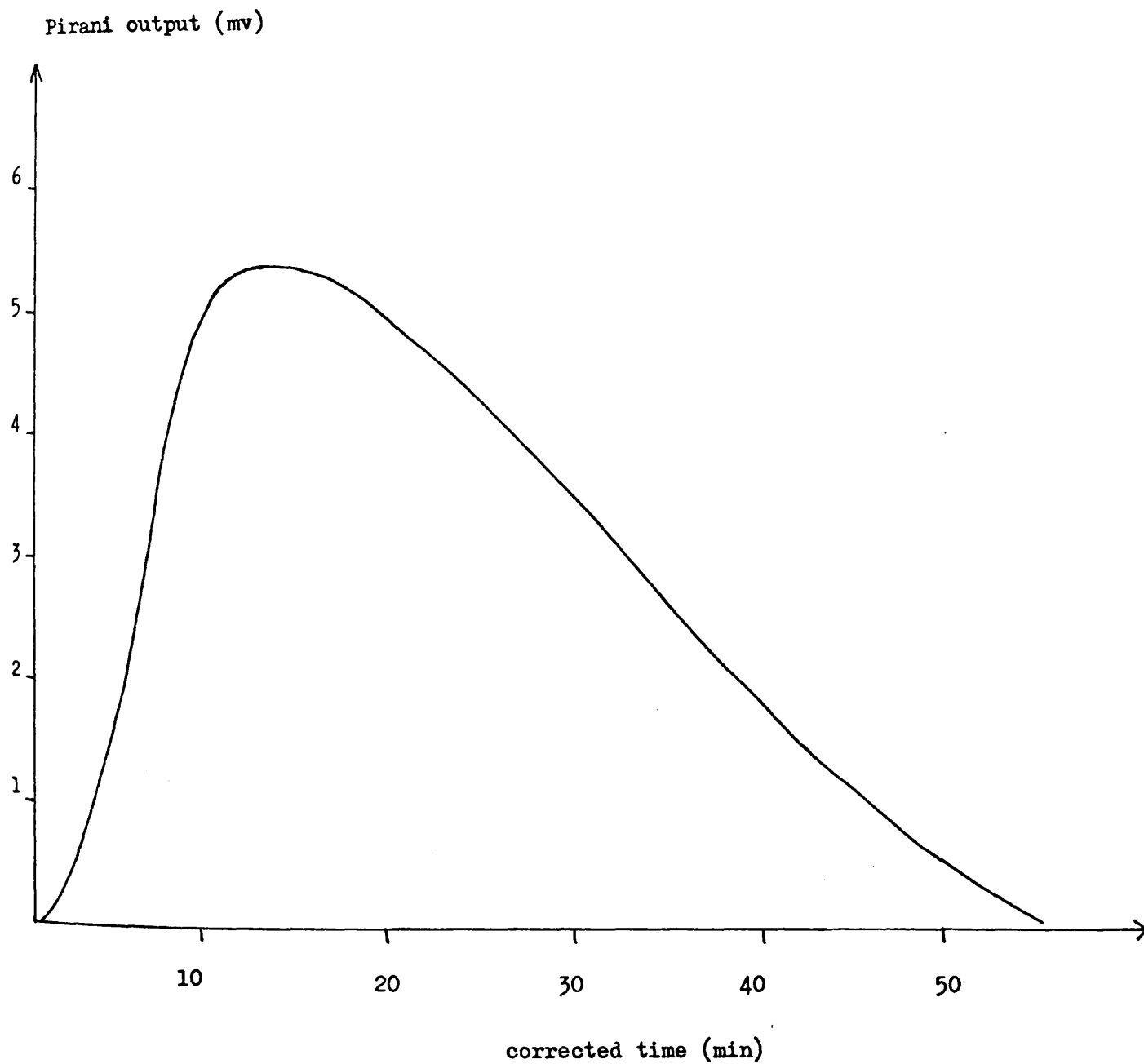
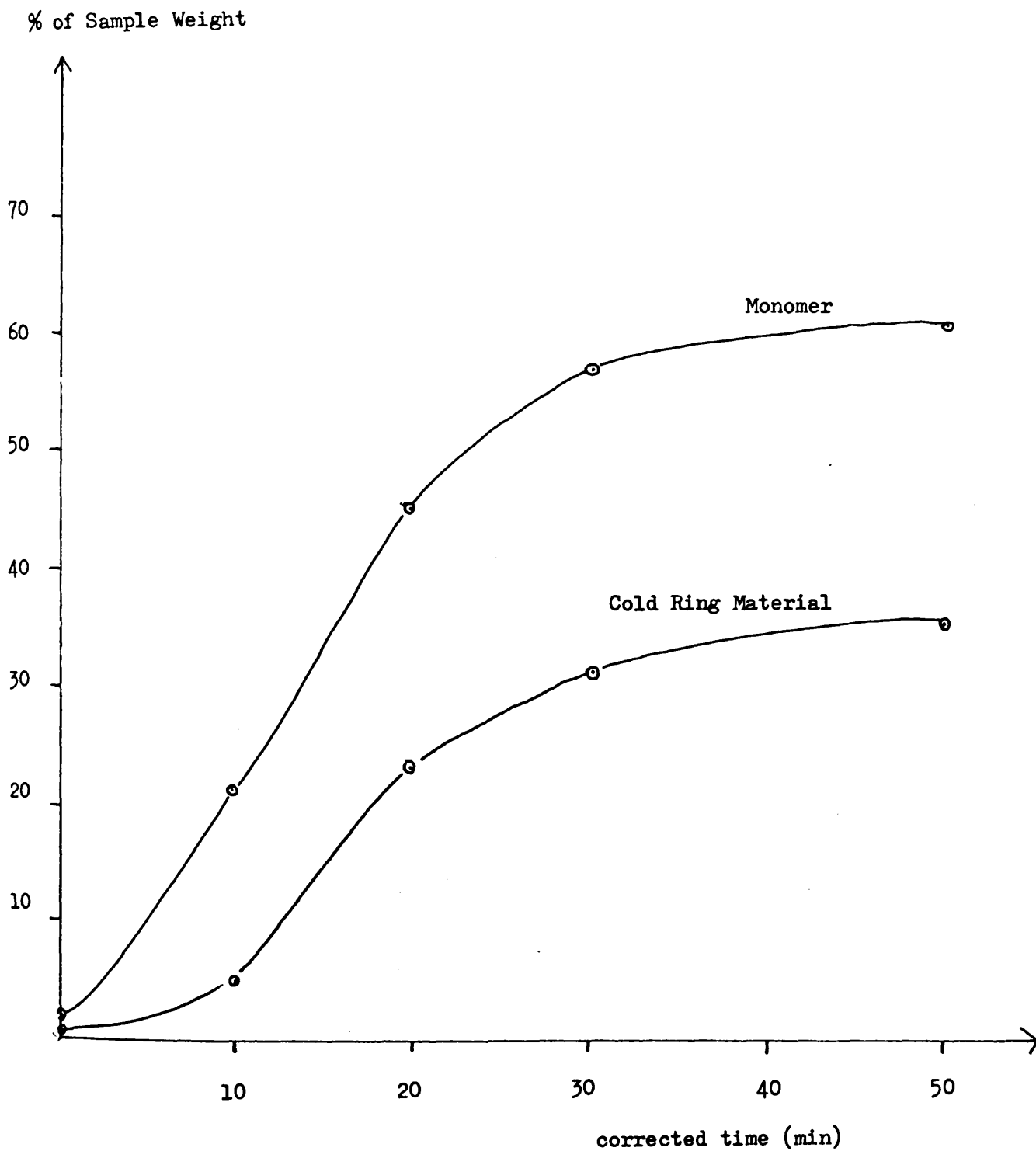


FIGURE 5 - 10

PERCENTAGE CONVERSIONS IN POLYSTYRENE DEGRADATION AT 380°C

UNDER VACUUM

Sample Size 50 mg



More work will clearly have to be done to identify the reason for this discrepancy.

From fig. 8 it can be seen that degradation at 380°C is complete after 50 min and so the final weight percentages of the monomer and cold ring fractions can be taken as 61.1% and 35.4% respectively. By comparing figs. 9 and 10 it can be seen that the volatilisation rate maximum occurs at 24% conversion to monomer or at 39.3% of the reaction to completion. This is expected of an end-initiated reaction (60).

POLYBUTADIENE DEGRADATION.A. INTRODUCTION AND LITERATURE REVIEW.

Polybutadiene samples were degraded under isothermal conditions at 380°C and in programmed warm up experiments at 10°C/min to provide reference for assessing the stability of the polystyrene/polybutadiene system if there were no interaction between the components. On this basis, the extra stability generated in the real system could be estimated.

Extra work was performed, firstly to obtain a more complete picture of the mechanisms operative in the exothermic decomposition reaction of polybutadiene, and, secondly to elucidate the mechanisms operative in the higher temperature endothermic decomposition reaction which to date has not been the subject of any systematic study.

Polybutadiene was degraded under isothermal conditions at temperatures in the range 325 - 400°C under vacuum and the volatile products of degradation were separated into product fractions according to their volatility (5, 83). The cold ring fraction of the TVA experiment, (V_{pyr}), was in all cases found to be the major product fraction of degradation. Its average molecular weight (by cryoscopy) was estimated as 739. The noncondensable product fraction, V_{-190} , accounted for much less than 1% of the mass of the total products of degradation, and consisted mainly of methane. The condensable volatile fraction of degradation was found to be a complex mixture of hydrocarbons. It was separated into two fractions by distillation. The fraction V_{-80} consisted of a mixture of $C_2 - C_6$ hydrocarbons the major component of which was found to be 1,3 butadiene. Higher molecular weight material was not subjected to analysis because of experimental difficulties. Its major constituent, however, was

correctly assumed to be 4-vinylcyclohexene (4VCH). Monomer was assumed to be formed by an unzipping reaction which could follow a main chain scission in the polymer. It was suggested that the low yields of monomer obtained in all experiments were the result of a radical deactivation by a facile hydrogen transfer reaction between the macroradicals formed by chain scission, to produce a conjugated double bond and a terminal methyl group at the chain ends. After an initial rapid but small weight drop, the remainder of the sample was volatilised in a slow but linear manner.

Samples of cis- and trans-polybutadiene were degraded under programmed warm-up conditions under nitrogen in a TG assembly to 50% weight loss and the residue of degradation was examined by i.r. and n.m.r. spectrometry (84). Both spectroscopic methods showed that the polymer was undergoing a process leading to a loss of unsaturation. I.r. spectra showed this by a reduction in intensity of the characteristic out of plane deformation vibrations of the olefinic groups in the polymer. The appearance of peaks at 1370 cm^{-1} (methyl rock) and at 1600 cm^{-1} (conjugated double bonds) confirmed that the disproportionation reaction, first suggested by Madorsky, was taking place. N.m.r. spectra of the soluble fraction of degradation confirmed that double bonds were being consumed and suggested that polycondensed rings were being formed in their place. The occurrence of a disproportionation reaction was again confirmed by the presence of signals which would be produced by methyl groups in the polymer.

Microstructural changes and volatilisation were assumed to be initiated by that portion of the products of the main chain scission events which escape the disproportionation reaction. A shift of the radical position by π -allyl isomerisation would produce an assembly susceptible to depropagation. The radical,

however, could attack the polymer chain by an intramolecular process to form 4VCH, or cyclised rubber by a chain process termed "Type 1" cyclisation. Of interest was the observation that 1,4-polybutadiene undergoes a process of thermal isomerisation to the thermodynamically most stable cis/trans ratio at pre-volatilisation temperatures in the range 200 - 300°C.

Catalysed Cyclisation Of Polybutadiene.

It has been known for some time that polybutadiene can be chemically reacted to form a polycyclic material, usually by acid catalysis (85, 86). Shelton et al (85) isolated a tricyclic acid from the products of a sample of oxidatively degraded pre-cyclised rubber. The rubber initially contained 20 mole% vinyl groupings which were shown to give on average a 1,4 sequence length of three units. It was suggested that the predominance of a tricyclic material indicated that vinylic groups interrupted the cyclisation process.

Binder (87) cyclised 1,2-polybutadiene using POCl_3 . The product produced an n.m.r. spectrum identical to that of thermally cyclised rubber. It was suggested that cyclic structural abnormalities are accumulated by polybutadiene polymers on storage.

Kossler et al (88) followed the course of H_2SO_4 catalysed cyclisations by i.r. spectroscopy. A kinetic scheme (89) was simplified and used to estimate the effect of reaction conditions on the lengths of polycondensates formed in the early stages of the reaction. Substituted polybutadienes such as polyisoprene and poly (2,3-dimethylbutadiene) were found to give a predominantly monocyclic product. It was suggested that the concentration of structural abnormalities in the chain determined the maximum length of the polycondensed segments. It was concluded that polycondensates containing more than 25 units could be produced from polybutadiene.

Shagov et al (90) partially cyclised polybutadiene using Ti Cl_4 . The product was subjected to ozonolysis to show the presence of two types of double bonds in the material, one of which could be identified as residual linear unsaturation and the other as a disubstituted double bond. This was convincing evidence in support of the accepted mechanism of cyclisation which necessitates the formation of a disubstituted double bond in the end ring which initiated the cyclisation.

Golub and Sung (91) examined by i.r. and n.m.r. spectrometry the microstructural changes which took place when a sample of 1,2-polybutadiene was degraded to 60% weight loss. A very plausible degradation pathway was postulated to account for the formation of polycyclic material, 1,3-butadiene and 4VCH.

A second order process of cyclisation was reported to take place in samples of 1,2-polybutadiene warmed to sub-volatilisation temperatures (92). No specific mechanism was proposed to account for this process.

Grassie and Heaney (93) identified a non-radical process, first order in vinyl content, which was operative at sub-volatilisation temperatures; this consumes vinyl but not 1,4 groupings in the polymer by cross linking the material. The consumption of vinyl groupings was monitored by i.r. spectroscopy while increases in \bar{M}_n were followed by osmometry. It was concluded that a concerted molecular rearrangement was taking place to form a carbon - carbon bond between a vinyl group (which became saturated) and a carbon atom in a position α to a 1,4 double bond.

Samples of normal and cross-linked 1,4- and 1,2-polybutadienes were flash pyrolysed at 380°C , 480°C and 600°C and the products of degradation were separated by GLC. In samples of

normal (uncross-linked) polybutadiene the monomer yield decreased as the temperature of degradation was raised. It was found, however, not to vary with the microstructure of the polymer. The yield of 4VCH as a product of the degradation of 1,4 polybutadienes also decreased as the temperature of degradation was raised. The yield of 4VCH did not seem to vary with the cis/trans content of predominantly 1,4- polymers. It was, however, enormously reduced as a product of degradation of 1,2-polybutadienes. Cross-linked 1,4-polybutadienes degraded to give a product distribution similar to that of normal 1,4-polybutadienes. However the 1,3-butadiene yield of 1,2-polybutadiene was greatly reduced when the polymer was cross-linked. (94)

Tamura and Gillham (95), using a recently developed on-line system of analysis for polymer degradations (96), studied the influence of the cis/trans ratio of high 1,4-polybutadienes on the course of the reaction. The degradation reaction was treated as a two step process. Programmed degradations were performed to 15% weight loss of the sample and the products of degradation were analysed in an attempt to elucidate the mechanisms operative in the first stage of degradation. In short, their findings reaffirmed those of Golub (84). Both 1,3-butadiene and 4VCH yields were found to be decreased as the trans content of the polymer was raised. This was at variance with results obtained by pyrolysis - GLC (94) and also with work by Golub (84) which suggested that samples of rubber attained their thermodynamically most stable cis/trans ratio at sub-volatilisation temperatures. Products of degradation from 15% weight loss to complete volatilisation of the sample were qualitatively examined. The only conclusion reached from this work was that 4VCH was not present among the products of degradation.

This review is perhaps best ended by a discussion of work reported by Brazier and Schwartz (82, 97). The degradation of

polybutadiene under programmed conditions was shown to be a two stage process. The first stage of decomposition was exothermic in nature and resulted in a small weight loss in the polymer. The second stage of degradation was endothermic and completely volatilised the remainder of the sample. By an examination of the volatile products of the two processes it was concluded that the low temperature process corresponded to the cyclisation/depolymerisation reaction reported by Golub (84) while the high temperature process corresponded to the breakdown of those cyclic structures formed in the low temperature process.

By varying the heating rate used in DSC and derivative TG experiments it was shown that the exothermic and endothermic processes occur in competition. The cyclisation process was shown to gain in importance as the heating rate was increased. This effect probably accounts for the decreased monomer and dimer yields which have been reported in flash pyrolysis experiments (94).

B. PROGRAMMED DEGRADATIONS.

B 1. TG UNDER NITROGEN.

A TG curve for the high 1,4-content anionic polybutadiene (A) used in this work can be inspected in fig. 1 . It can be seen that the weight loss process commences at approximately 350°C and accelerates to a small rate maximum at 380°C. The weight loss reaction decreases in rate to 410°C after which it begins to rise to a very prominent rate maximum at 480°C. The rate of the second process then decreases to zero as the sample approaches complete volatilisation.

The shape of the rate curve suggests that there exists a considerable range of temperatures in which both weight loss processes occur at a measurable rate. If so, then it is not possible to treat them as completely separate events in programmed work at 10°C/min. In fact, the two may be regarded as occurring in competition at all temperatures in the range 380 - 480°C.

B 2 DSC UNDER NITROGEN.

A DSC curve for polybutadiene A is shown in fig. 2 . It can be seen that the process which results in the low temperature weight loss reaction is exothermic in nature while the high temperature weight loss reaction is endothermic in nature. Both rate maxima, 380°C (Exo) and 480°C (Endo), agree well with the corresponding weight loss maxima. This indicates that processes which do not lead to the production of volatile material occur (if at all) in tandem with the volatile-producing reactions.

Of interest is the fact that exothermic reactions are taking place in the material at sub-volatilisation temperatures. These are most probably accounted for by cis/trans isomerisations in the material along with the various reported double bond rearrangements (98).

FIGURE 6 - 1

POLYBUTADIENE A, TG UNDER NITROGEN

Sample Size 6 mg

Heating Rate 10°C/min

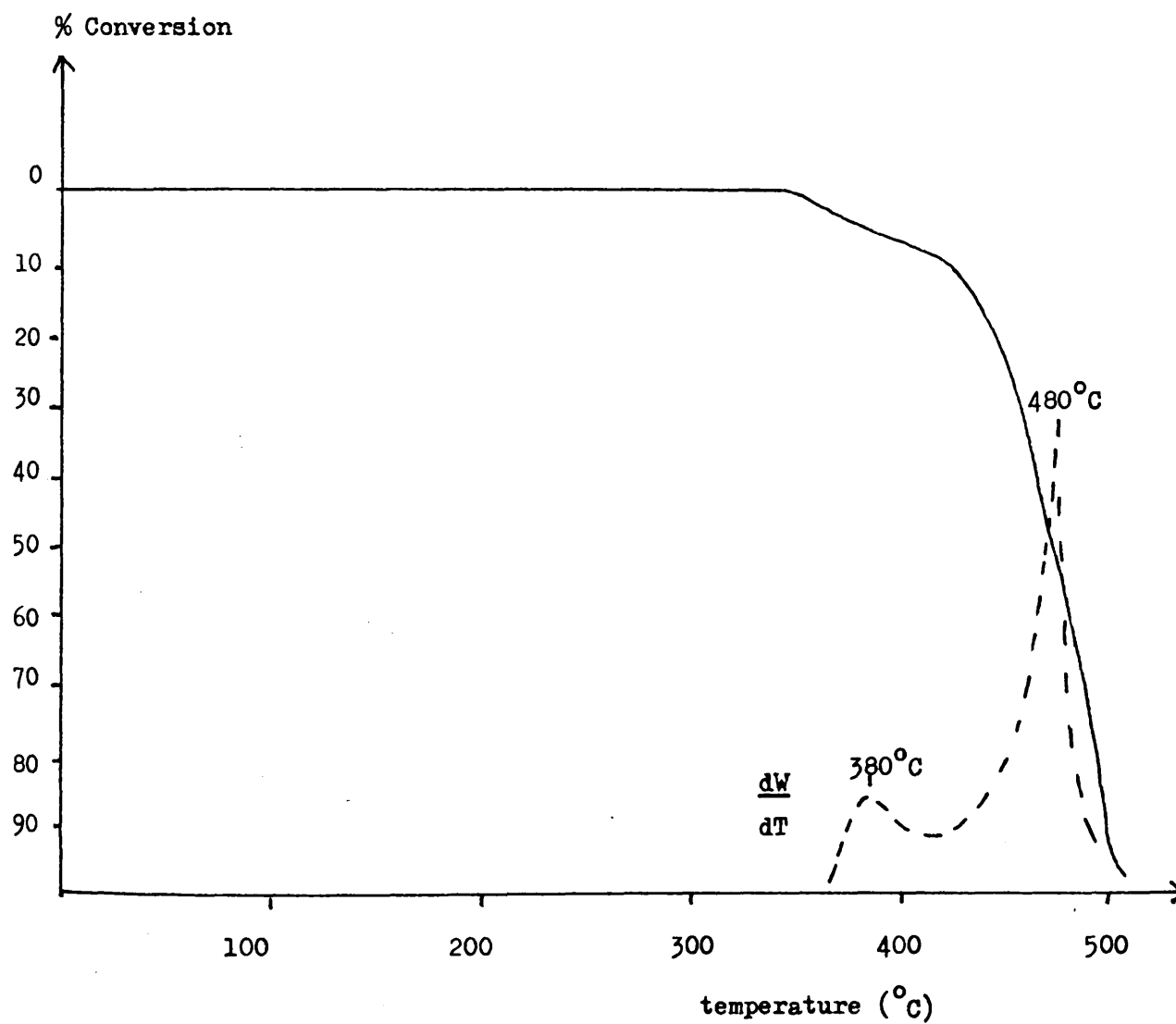
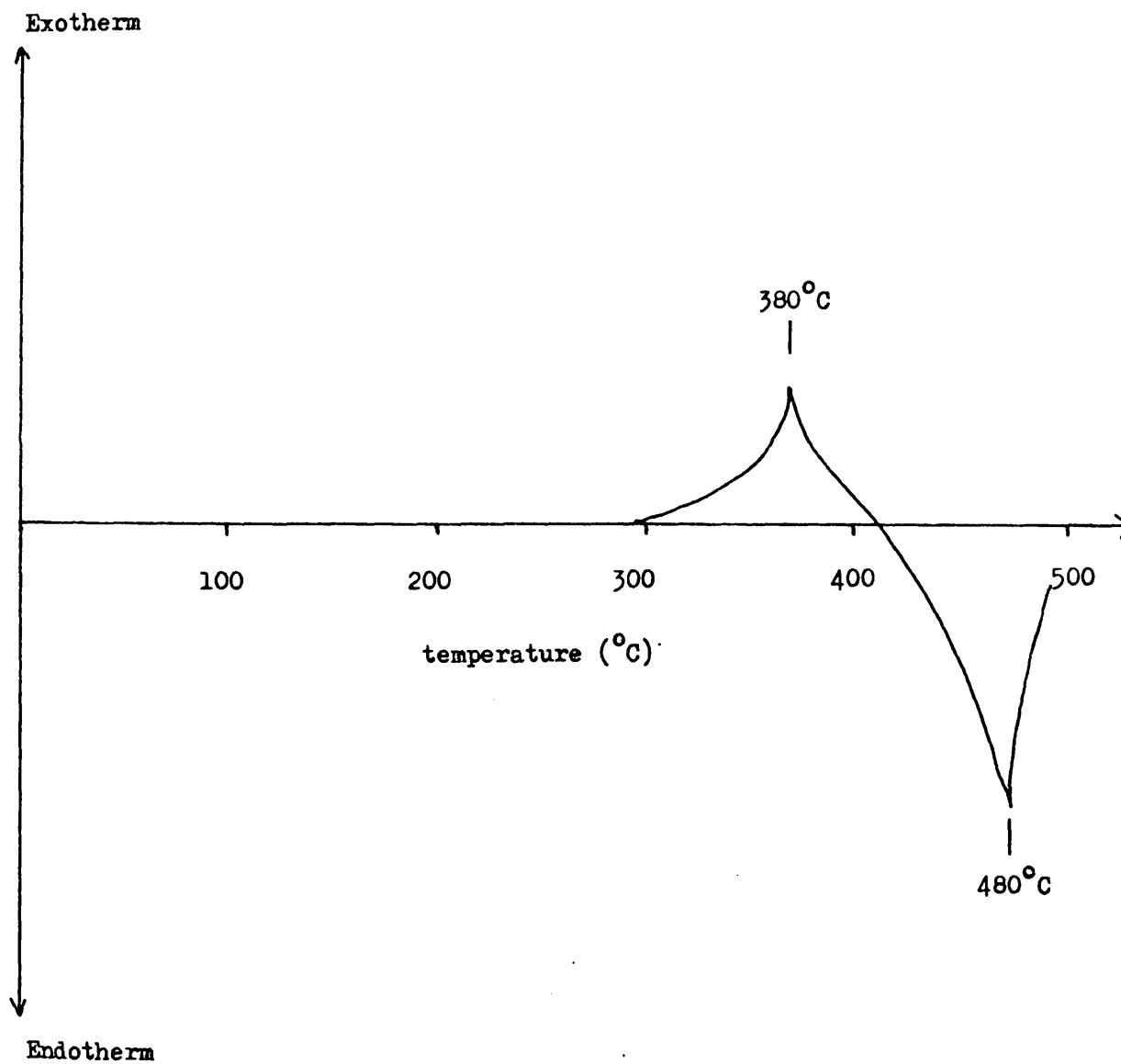


FIGURE 6 - 2

POLYBUTADIENE A, DSC UNDER NITROGEN

Sample Size 6 mg

Heating Rate $10^{\circ}\text{C}/\text{min}$



A TVA trace for polybutadiene A is shown in fig. 3 . The evolution of volatile material commences at 325°C and reaches a rate maximum at 450°C. It must be assumed that this corresponds to the DSC endotherm peak at 480°C. If this is the case then it can be seen that the volatiles produced in the exothermic process form the low temperature "shoulder" of the TVA peak.

The trace also shows that both processes produce products of a wide range of volatility. Of interest is the appearance of noncondensable material at a rate profile which corresponds to that of the high temperature process. If this is so then the TVA experiment provides proof of a considerable overlap between the low and high temperature processes, the latter of which is seen to commence at 350°C.

There exists a considerable discrepancy between temperatures corresponding to the endothermic rate maximum under nitrogen (TG and DSC) and under vacuum (TVA). This effect has been encountered before during similar work performed with polyisoprene polymers (99). When it is considered that the cold ring fraction of polybutadiene degradation is the major product fraction then it becomes apparent that the discrepancy probably arises because of the more efficient removal of high molecular weight material under vacuum as opposed to under a nitrogen atmosphere.

To conclude this discussion it must be noted that the TVA trace corresponding to polybutadiene A differs somewhat from the TVA trace obtained by degrading the commercial sample of polybutadiene used in earlier work on the blend system (80). The latter can be inspected in fig. 4 , from which it can be seen that while the evolution of volatile material commences at the same threshold temperatures (325°C and 350°C) to achieve the same rate maxima (380°C and 450°C), such material is produced in smaller quantities from this polymer than from the material presently under study.

FIGURE 6 - 3

POLYBUTADIENE A, TVA

Sample Size 50 mg

Heating Rate $10^{\circ}\text{C}/\text{min}$

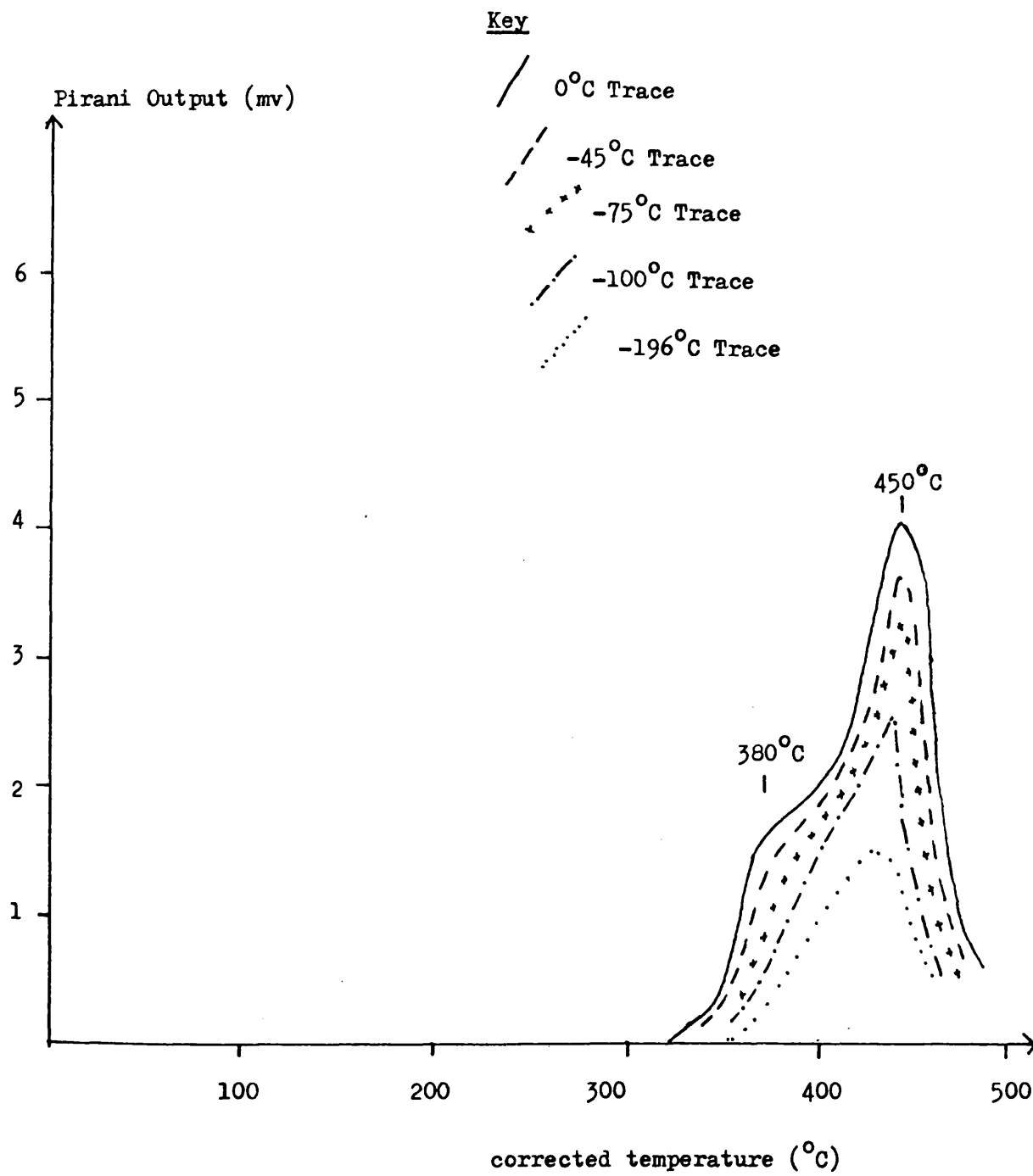
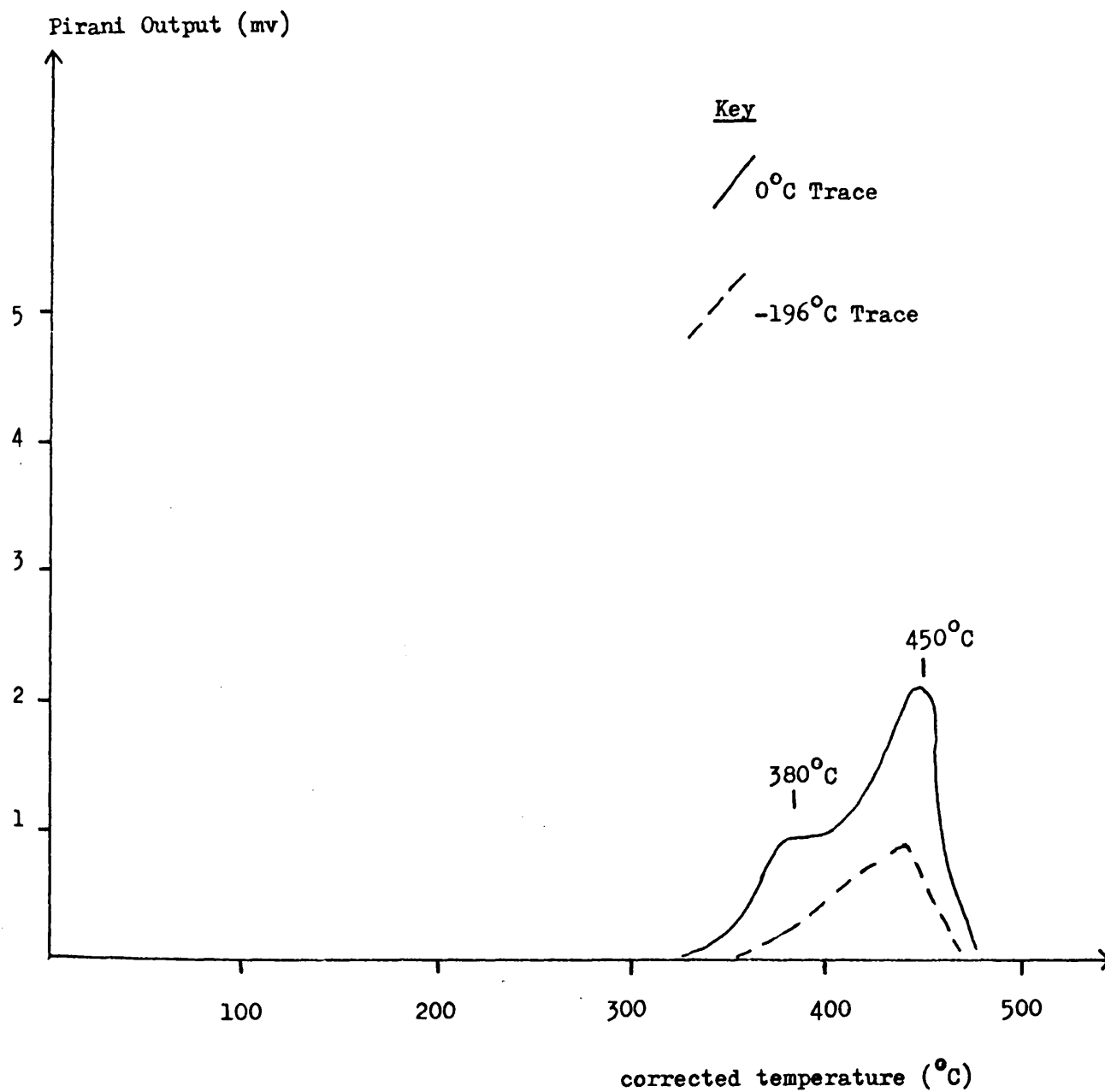


FIGURE 6 - 4

POLYBUTADIENE (COMMERCIAL SAMPLE) TVA

Sample Size 60 mg

Heating Rate $10^{\circ}\text{C}/\text{min}$



POLYBUTADIENE CHARACTERISATION

	ANIONIC POLYBUTADIENE A	CATIONIC POLYBUTADIENE "AMERIPOL CB221"
\bar{M}_n	94400	100000
cis 1,4	81.7 mole%	98 mole%
trans 1,4	13.2 mole%	
vinyl 1,2	5.1 mole%	trans 1,4 + vinyl 1,2 = 2mole%

From Table 1 it would appear that the only differences between the two polymers are the small but measurable contents of trans 1,4 and cis 1,2 groupings in the anionically prepared polymer. However the author is of the opinion that this can not account for the differences in the TVA trace shapes of the two polymers. It will be shown in Chapter 11 that the TVA traces of samples of anionically prepared polybutadiene which have been subjected to low temperature oxidative degradation are similar to that shown in fig. 4. The assertion that the commercial polymer was oxidised to a small extent was substantiated by the identification of CO_2 as a volatile product of thermal degradation (see Chapter 11).

B 4 ATVA OF POLYBUTADIENE.

An ATVA curve corresponding to polybutadiene A is shown in fig. 5. The polymer contains only carbon and hydrogen. The only possible noncondensable products of degradation are, therefore, methane and hydrogen. Using the criteria developed in Chapter 3 it can be seen that the noncondensable product fraction contains hydrogen which is produced at a threshold temperature of $350 - 360^\circ\text{C}$ to reach a rate maximum of production at 450°C .

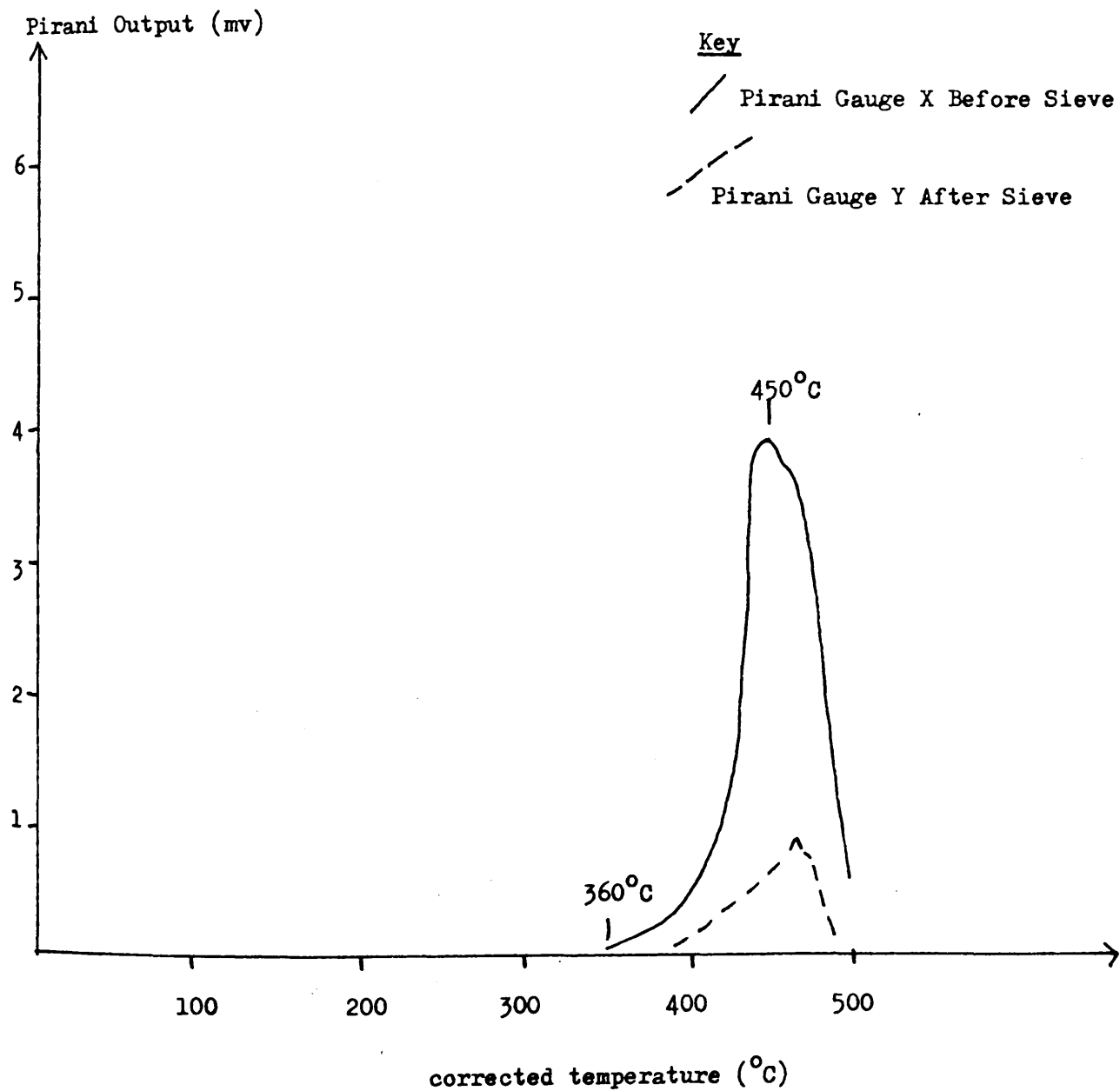
If a comparison is made between the relative sizes of the X and Y Pirani outputs for this material and for materials known to produce only hydrogen, then it can be seen that large quantities of a second noncondensable material are being produced. Such material

FIGURE 6 - 5
POLYBUTADIENE A, ATVA

Sample Size 50 mg

Heating Rate $10^{\circ}\text{C}/\text{min}$

Sieve Trap At -196°C



was retained by the molecular sieve trap and was shown to be methane by i.r. spectroscopy.

The close similarity between the shape of the Pirani X and Y curves suggests that both gases are being produced in a concerted process.

C PRODUCT DISTRIBUTION IN PROGRAMMED DEGRADATIONS.

C 1 VOLATILE PRODUCT DISTRIBUTION IN PROGRAMMED DEGRADATIONS.

(i). SATVA Of Volatile Products Of Programmed Degradations.

SATVA separations of successive volatile fractions produced in the TVA experiment were performed as follows. The sample under study was degraded under programmed conditions in an oven assembly connected to the SATVA manifold discussed in Chapter 2. Volatile fractions 1,2, and 3, which were produced in the first three temperature ranges of interest, were condensed successively into three limbs of the TVA assembly. Fraction 4 was directly routed to the sub-ambient TVA assembly. Stopcocks were manipulated to allow fractions 1,2 and 3 to be maintained under high vacuum conditions by pumping through a liquid nitrogen trap positioned at the fourth limb of the TVA assembly. Fraction 4 was then subjected to sub-ambient volatilisation in part to the pumping system and in part to the liquid nitrogen trap on limb 4 of the TVA assembly (figs. 2 - 7, 8). Fractions 1,2, and 3 were then successively volatilised by direct through pumping to the pre-cooled SATVA trap and from it to produce the other three SATVA curves. Using this procedure it was possible to completely eliminate possibilities of sample contamination either by each other or by leakages into the system of atmospheric contaminants (CO_2 , H_2O etc.). It was not possible to separate the materials which produced these SATVA curves for spectroscopic analysis. This was achieved by collecting and separating the product fractions in four separate experiments.

SATVA separations of the four fractions of degradation corresponding to the temperature ranges, room temperature - 380°C , $380 - 410^\circ\text{C}$, $410 - 450^\circ\text{C}$, $450 - 500^\circ\text{C}$, can be seen in figs. 6 - 9.

Peak assignments were made by the use of gas and liquid phase i.r. spectroscopy, proton n.m.r. spectroscopy and mass spectrometry where applicable. Products corresponding to region 4 of figs. 8, 9 were identified by GLC.

FIGURE 6 - 6

POLYBUTADIENE A, SUB-AMBIENT TVA OF PRODUCTS OF PROGRAMMED
DEGRADATION TO 380°C

Sample Size 50 mg

Key

— Pirani Gauge Output

- - - (-) Thermocouple Output

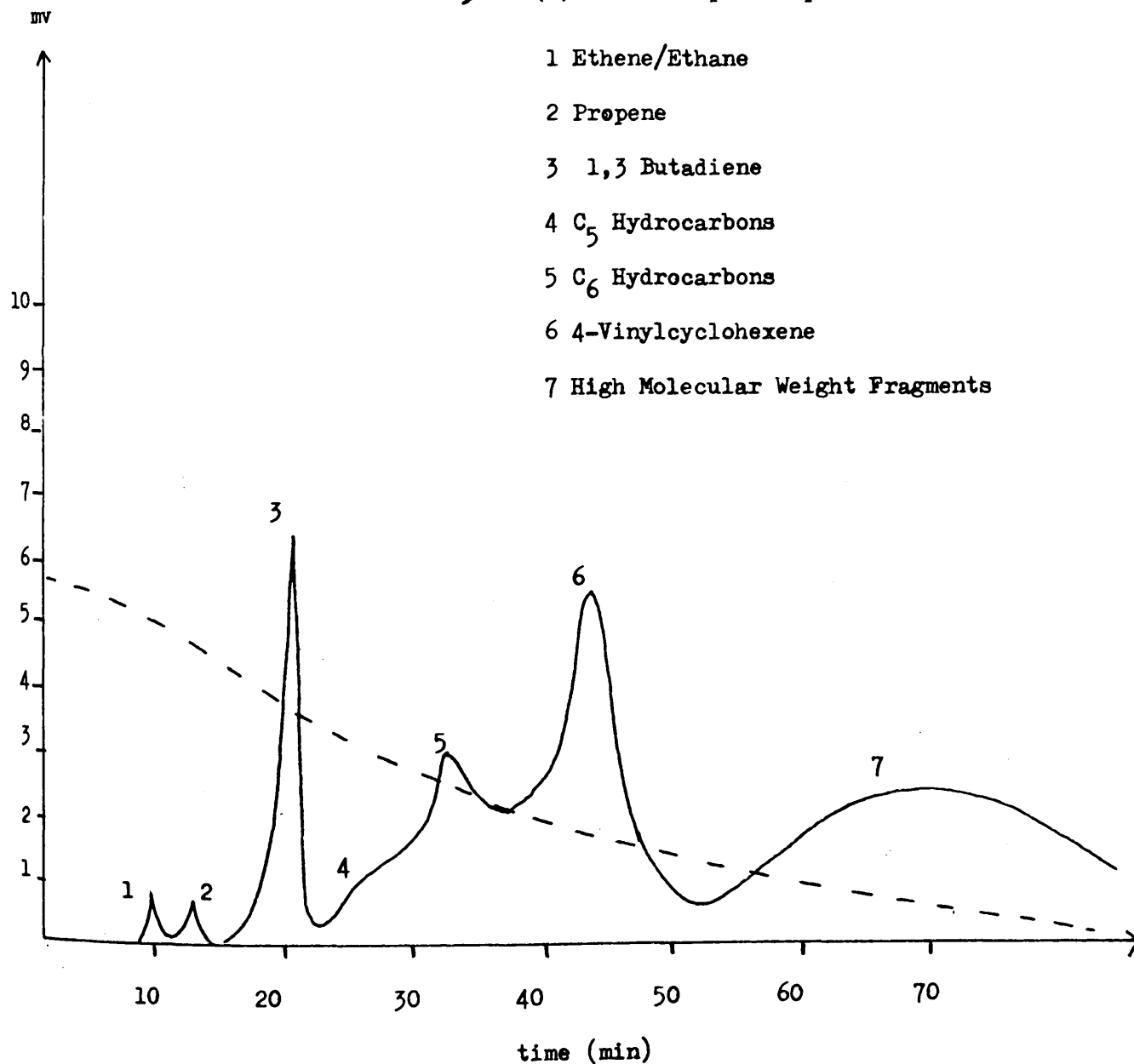


FIGURE 6 - 7

POLYBUTADIENE A, SUB-AMBIENT TVA OF PRODUCTS OF PROGRAMMED

DEGRADATION, 380 - 410°C

Sample Size 50 mg

Key

— Pirani Gauge Output

- - - (-) Thermocouple Output

1 Ethene/Ethane

2 Propene

3 1,3 Butadiene

4 C₅ Hydrocarbons

5 C₆ Hydrocarbons

6 4-Vinylcyclohexene

7 High Molecular Weight Fragments

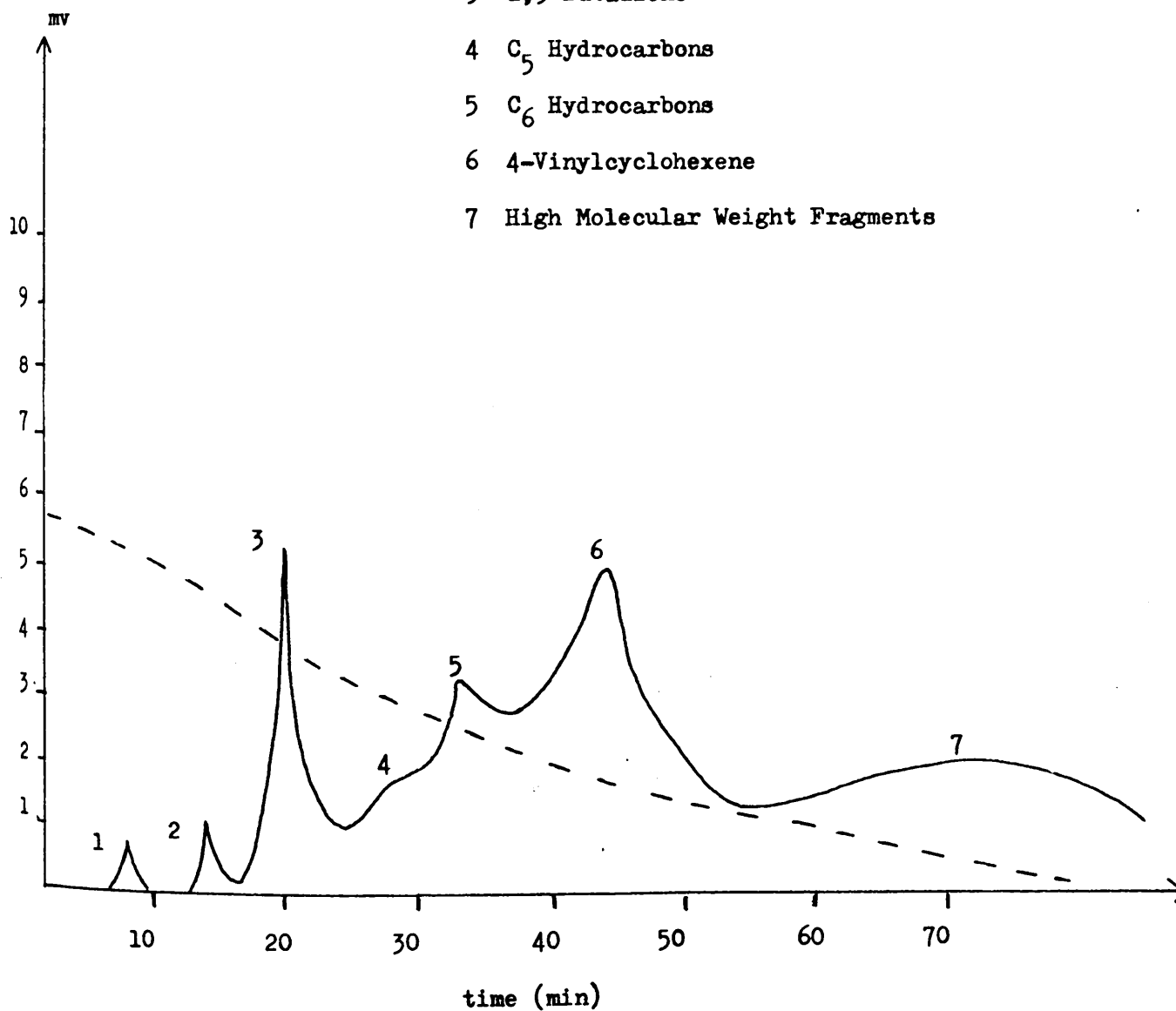


FIGURE 6 - 8

POLYBUTADIENE A, SUB-AMBIENT TVA OF PRODUCTS OF PROGRAMMED

DEGRADATION, 410 - 450°C

Sample Size 50 mg

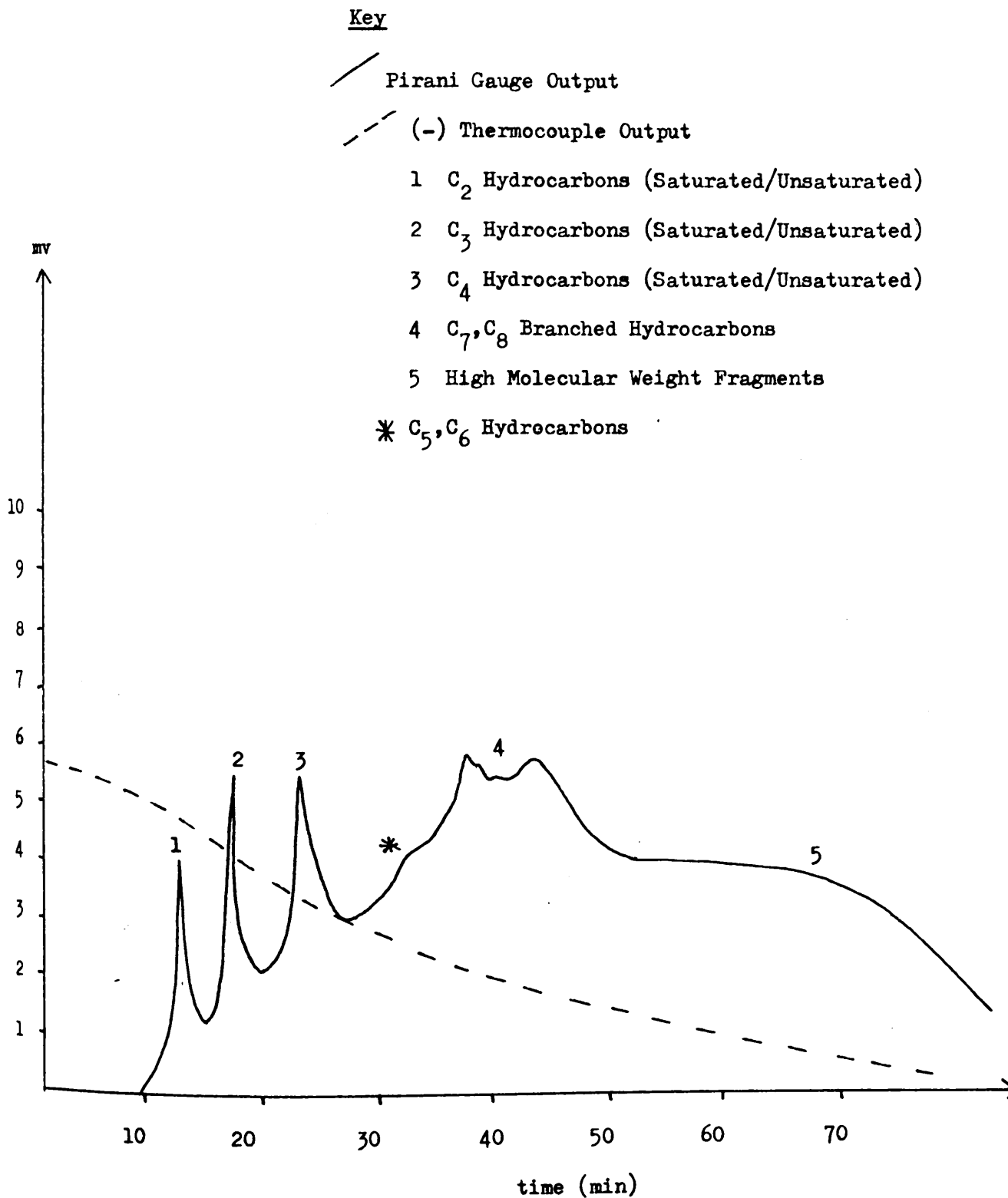


FIGURE 6 - 9

POLYBUTADIENE A, SUB-AMBIENT TVA OF PRODUCTS OF PROGRAMMED

DEGRADATION, 450 - 500°C

Sample Size 50 mg

Key

— Pirani Gauge Output

- - - (-) Thermocouple Output

1 C₂ Hydrocarbons (Saturated/Unsaturated)

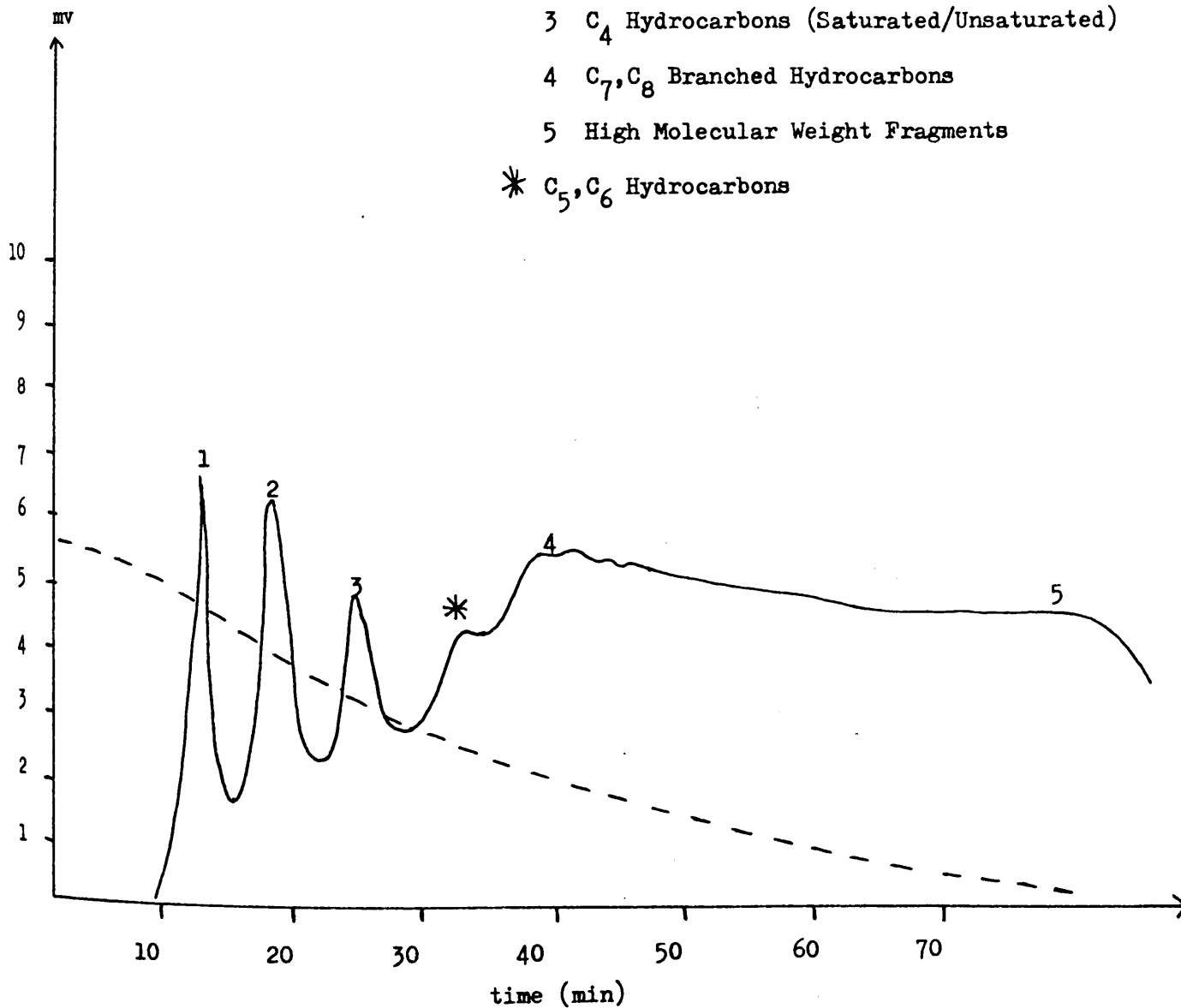
2 C₃ Hydrocarbons (Saturated/Unsaturated)

3 C₄ Hydrocarbons (Saturated/Unsaturated)

4 C₇, C₈ Branched Hydrocarbons

5 High Molecular Weight Fragments

* C₅, C₆ Hydrocarbons



(ii). GLC Separation Of Volatile Products Of Programmed Degradation.

GLC traces corresponding to separations of the four volatile fractions of programmed degradation (above) are shown in figs. 10, 11, 12 and 13 . Fraction 1 of figs. 10, 11 was identified by the use of reference material. The identification of fractions 1 and 2 of figs. 12 and 13 was more difficult. It was found that the column in use separated classes of hydrocarbon material purely on a boiling point basis. All volatile aromatic, cycloaliphatic and all available aliphatic materials up to C₈ were tested and the peak assignments shown were made on a retention time basis.

(iii). Volatile Product Identification By n.m.r. Spectroscopy.

The material causing the high molecular weight "tail" of the volatile product distributions shown in figs. 6 - 9 could not be separated for analysis by sub-ambient fractionation. Although it can be separated by GLC (figs. 12, 13) , the complexity of the structures involved would make even GCMS measurements of limited value.

For these reasons n.m.r. spectrometry was used to monitor the relative quantities of the various saturated, olefinic and aromatic functional groupings in the volatile product mixtures, on a "fingerprint" basis.

N.m.r. spectra of the complete volatile product distributions of the temperature ranges of interest can be inspected in figs. 14 - 16.

They must be compared on an internal basis and not with each other because each spectrum has been obtained with the spectrometer operating at a different sensitivity.

C 2 COLD RING FRACTION OF PROGRAMMED DEGRADATIONS.

N.m.r. spectra of cold ring material produced in programmed

FIGURE 6 - 10

POLYBUTADIENE A, GLC SEPARATION OF VOLATILE PRODUCTS OF

PROGRAMMED DEGRADATION TO 380°C

Sample Size 100 mg

Column - 6', $\frac{1}{4}$ ", 10% Microwax On Chromosorb At 100°C

Key

1 4-Vinylcyclohexene

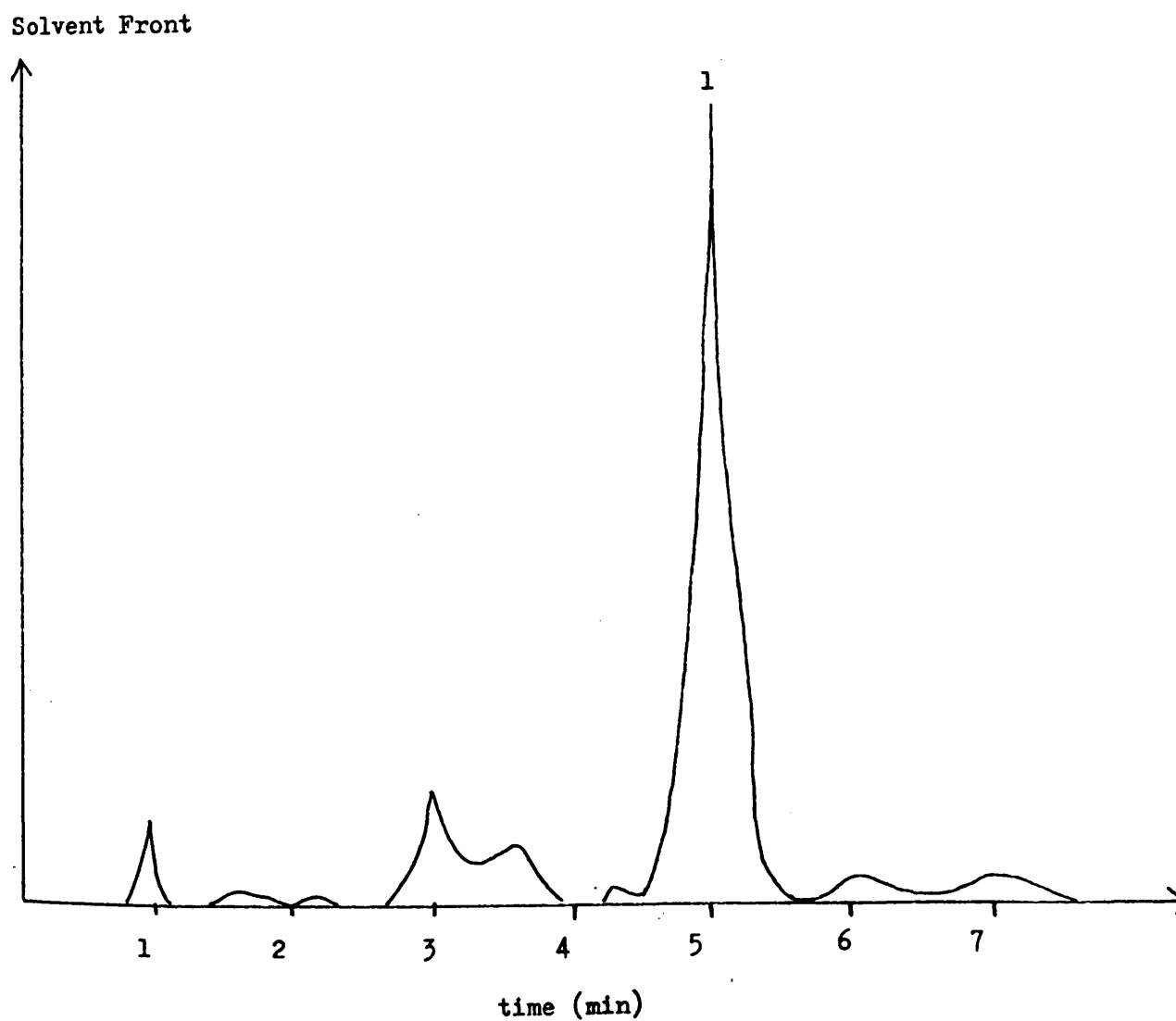


FIGURE 6 - 11

POLYBUTADIENE A, GLC SEPARATION OF VOLATILE PRODUCTS OF
PROGRAMMED DEGRADATION, 380 - 410°C

Sample Size 100 mg

Column - 6', $\frac{1}{4}$ ", 10% Microwax On Chromosorb At 100°C

Key

1 4-Vinylcyclohexene

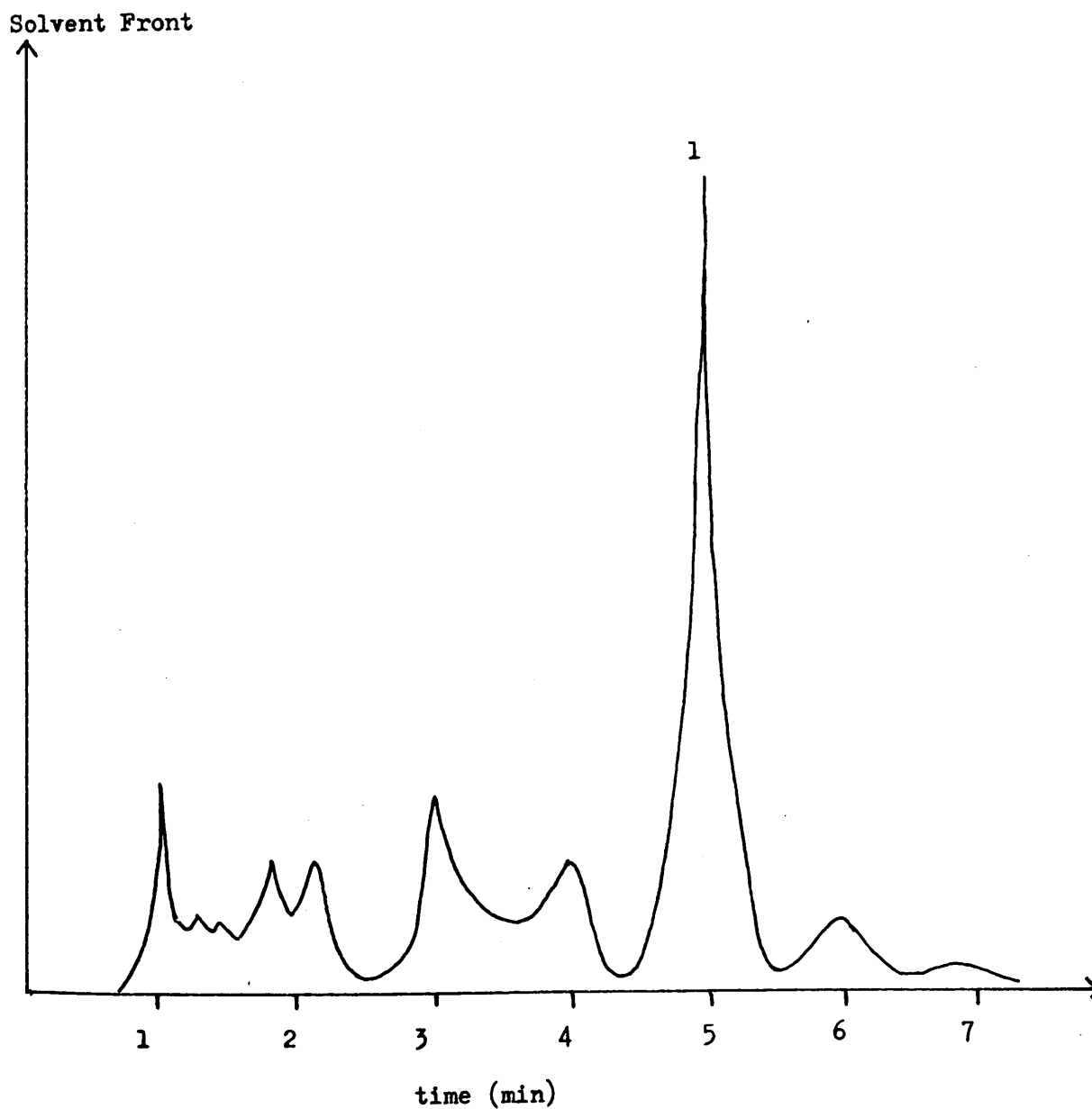


FIGURE 6 - 12

POLYBUTADIENE A, GLC SEPARATION OF VOLATILE PRODUCTS OF
PROGRAMMED DEGRADATION, 410 - 450°C

Sample Size 100 mg

Column - 6', $\frac{1}{4}$ ", 10% Microwax On Chromosorb At 100°C

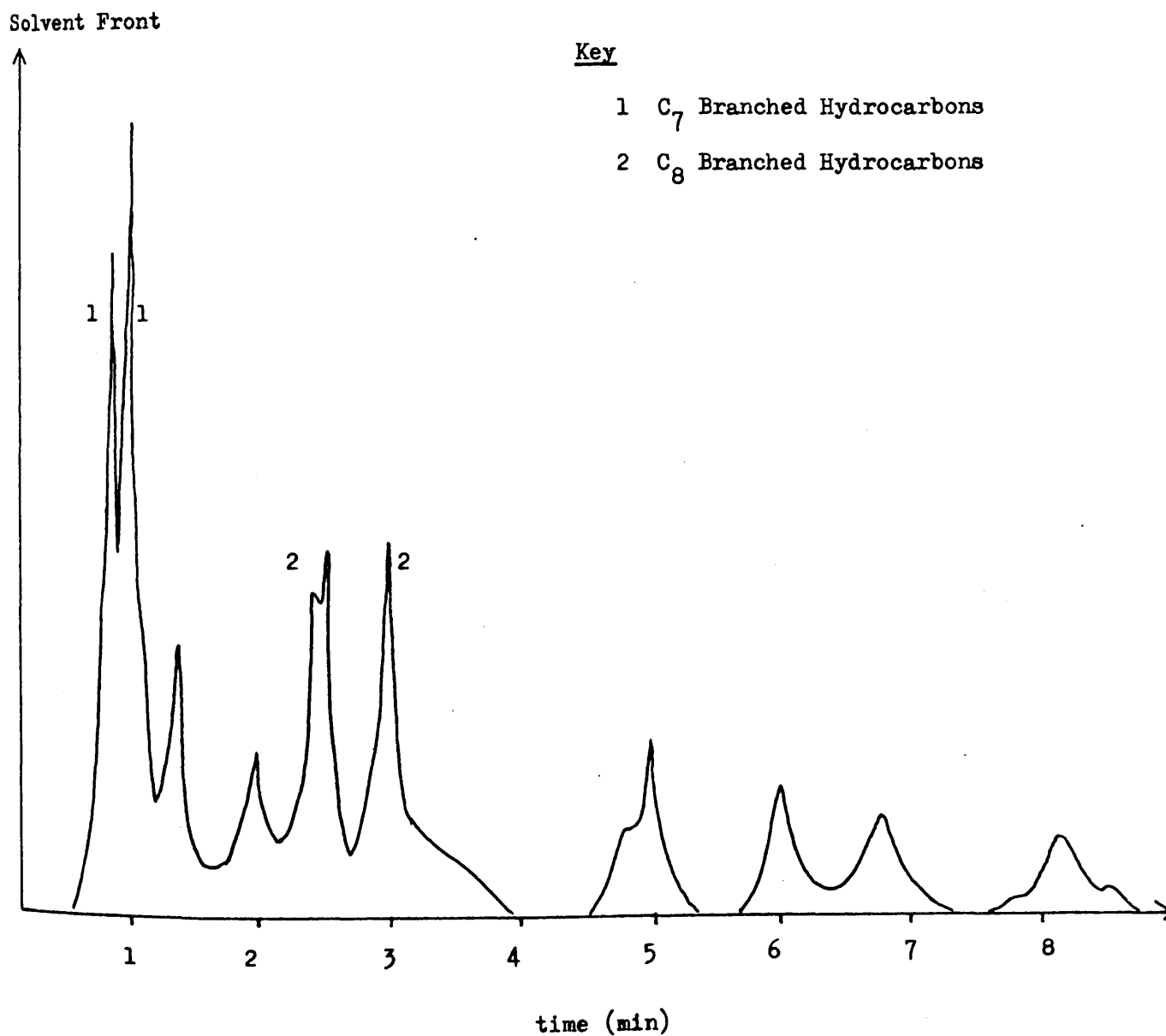


FIGURE 6 - 13

POLYBUTADIENE A, GLC SEPARATION OF VOLATILE PRODUCTS OF
PROGRAMMED DEGRADATION, 450 - 500°C

Sample Size 100 mg

Column - 6', $\frac{1}{4}$ ", 10% Microwax On Chromosorb At 100°C

Solvent Front

Key

- 1 C₇ Branched Hydrocarbons
- 2 C₈ Branched Hydrocarbons

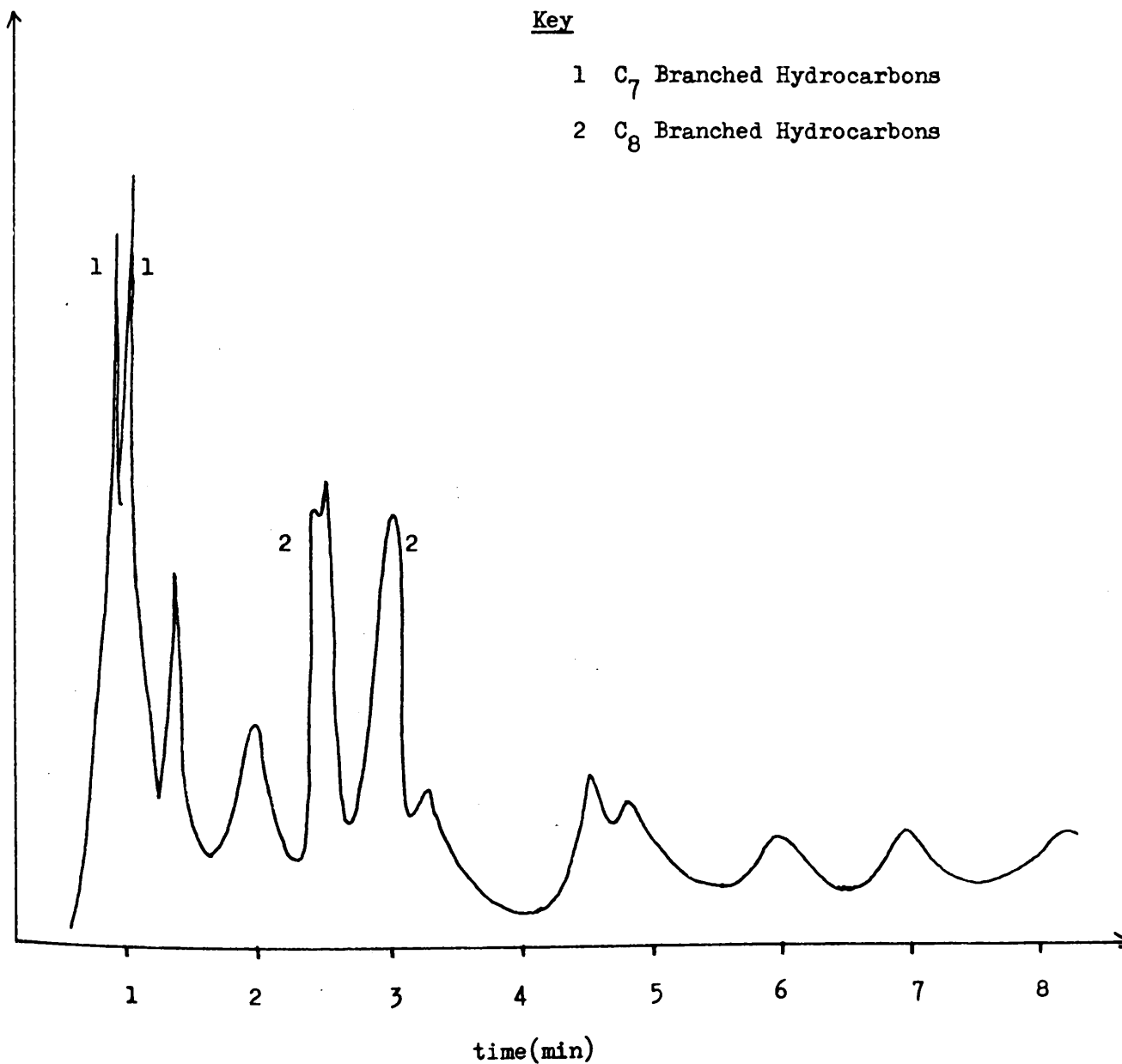


FIGURE 6 - 14

POLYBUTADIENE A, n.m.r. SPECTRUM OF VOLATILE PRODUCTS OF PROGRAMMED

5.60S

DEGRADATION TO 380°C

Key

*4-Vinylcyclohexene

Solvent C Cl₄

Lock TMS

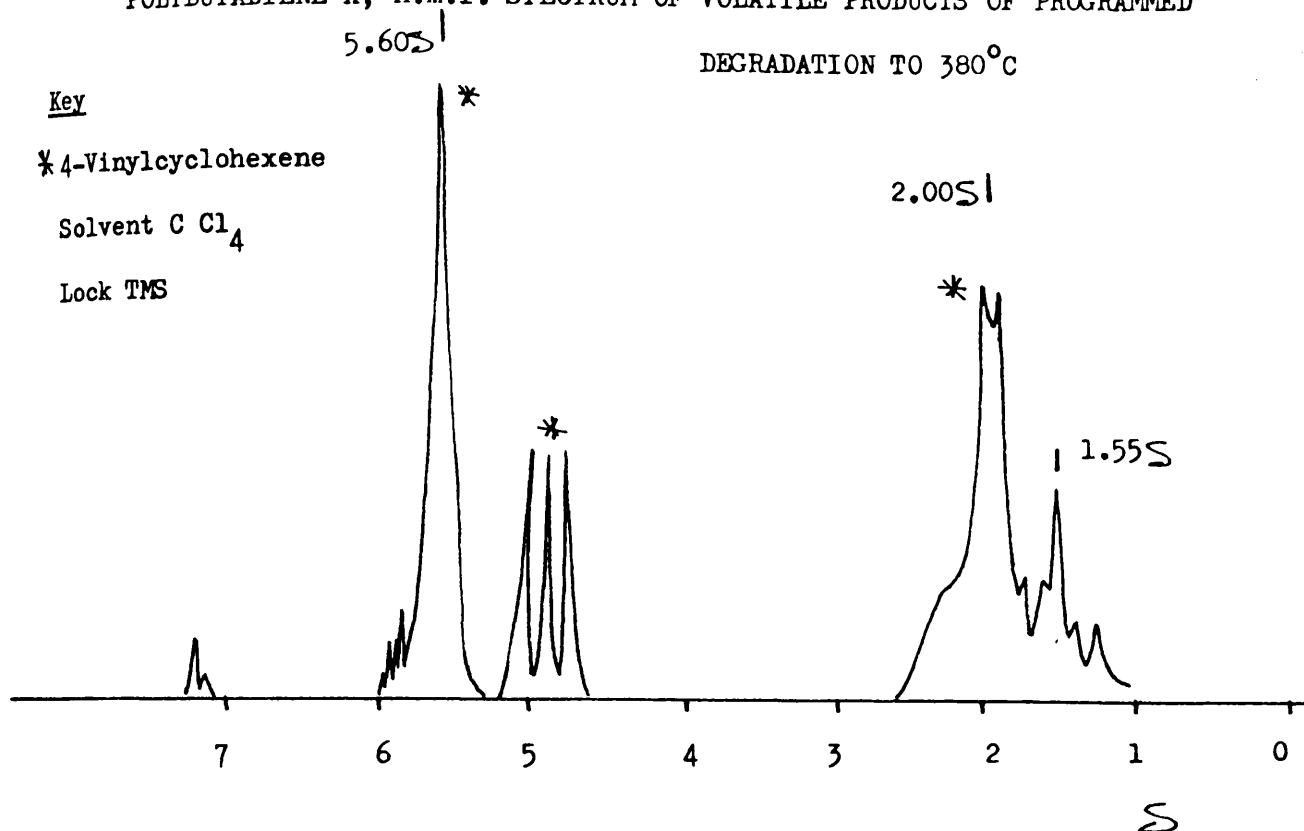


FIGURE 6 - 15

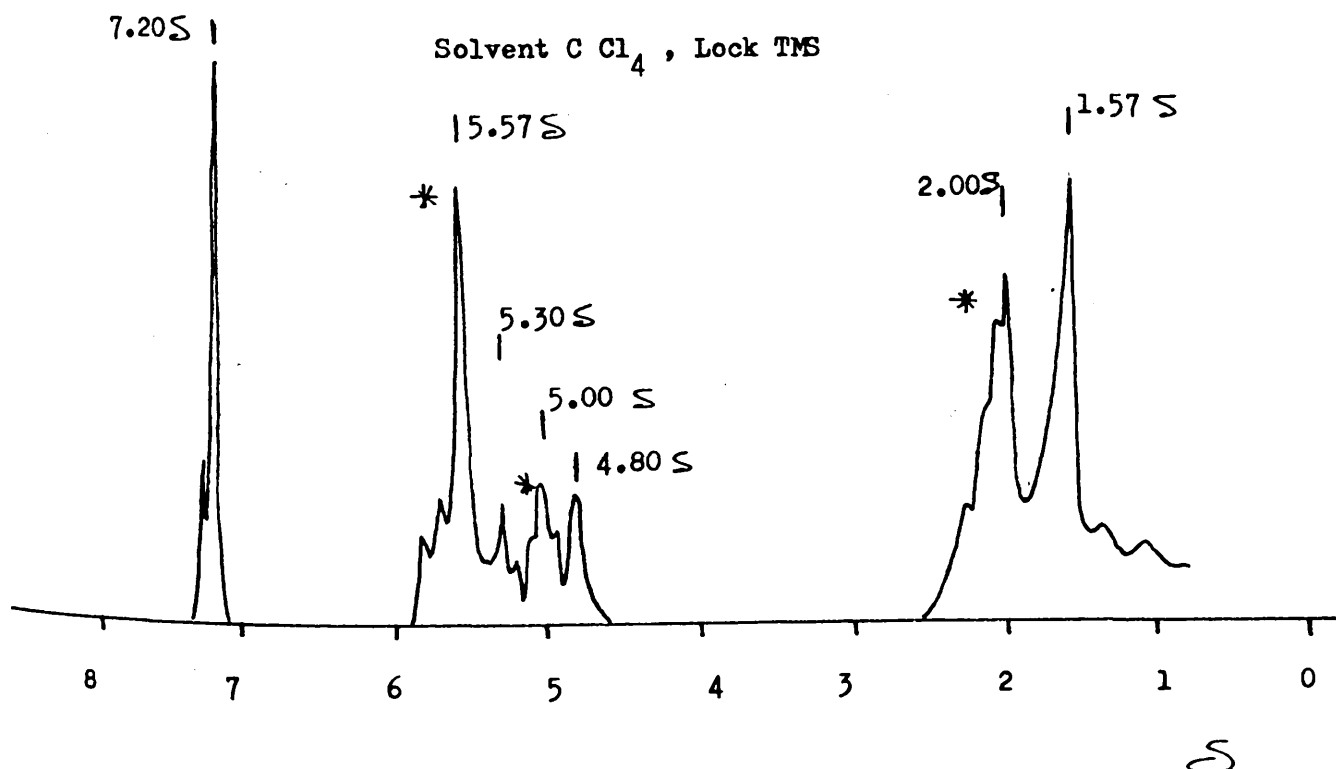
POLYBUTADIENE A, n.m.r. SPECTRUM OF VOLATILE PRODUCTS OF PROGRAMMED

DEGRADATION, 380 - 410°C

Key

*4-Vinylcyclohexene

Solvent C Cl₄, Lock TMS

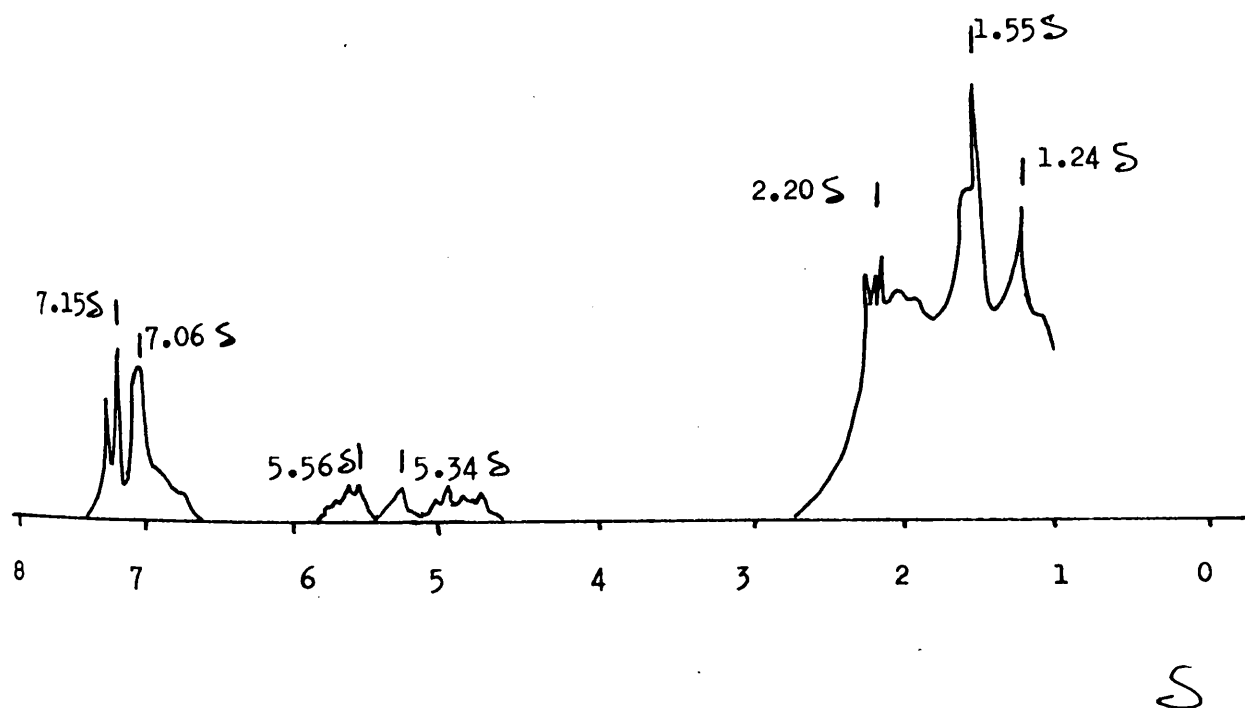


POLYBUTADIENE A, n.m.r. SPECTRUM OF VOLATILE PRODUCTS OF PROGRAMMED

DEGRADATION, 410 - 500°C

Solvent C Cl₄

Lock TMS



degradations to completion of polybutadiene A, before and after its separation by preparative TLC, can be inspected in figs. 17, 18 while the n.m.r. spectrum corresponding to programmed degradation to 400°C can be seen in fig. 19 .

C 3 RESIDUES OF PROGRAMMED DEGRADATIONS.

In order to complete a description of the processes operative in the programmed degradation of polybutadiene it was essential that n.m.r. spectra be obtained of polymer residues of partial degradation. Samples of normal polybutadiene polymers rapidly become insoluble at pyrolysis temperatures and so can only be examined by i.r. spectroscopy. It was discovered during the course of this work that polybutadiene of a very low initial molecular weight retains its solubility throughout programmed degradations. A sample of such material - the low molecular weight "latex" referred to in Chapter 4 - was subjected to TVA, TG and DSC and found to degrade in an identical manner to its higher molecular weight analogue (A). N.m.r. spectra corresponding to the residues of programmed degradation to 400°C and 450°C are shown in fig. 20 . Spectra corresponding to degradation to 425°C and to 425°C (+ 5 min isothermal heating at 425°C) are illustrated in figs. 21 and 22 respectively.

FIGURE 6 - 17

POLYBUTADIENE A, n.m.r. SPECTRUM OF COLD RING FRACTION OF PROGRAMMED
DEGRADATION TO 500°C

Sample Size 250 mg

Solvent C Cl₄

Lock TMS

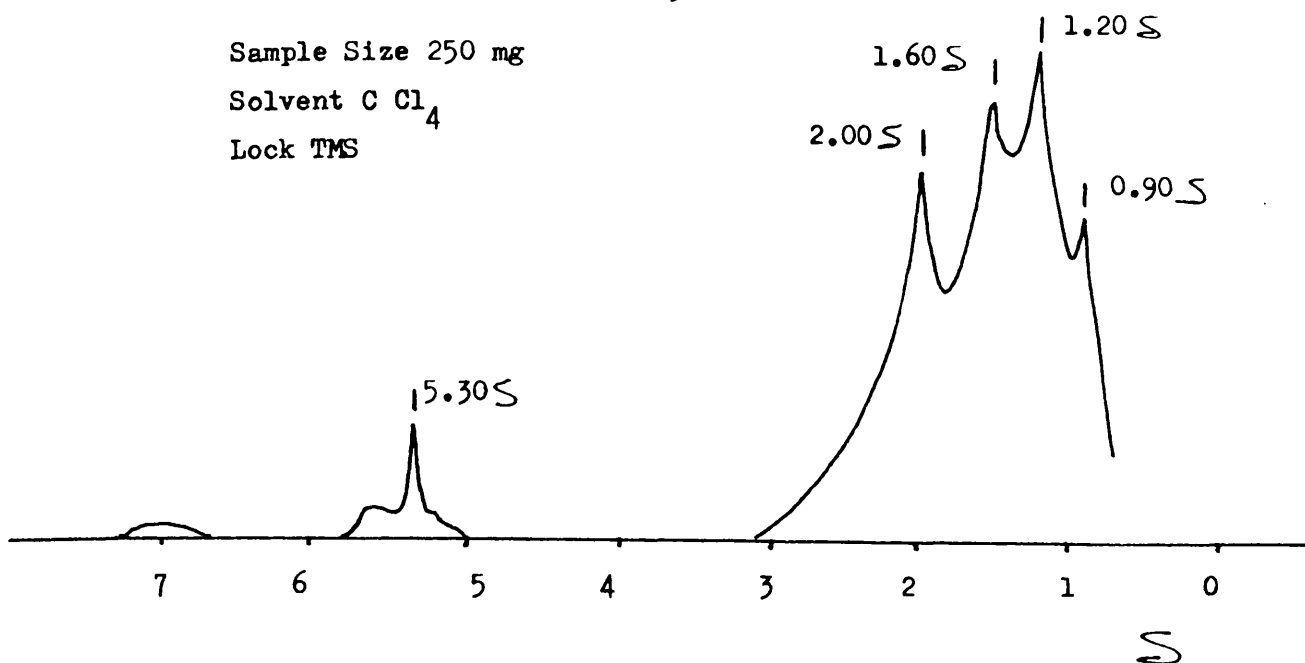


FIGURE 6 - 18

POLYBUTADIENE A, n.m.r. SPECTRUM OF COLD RING FRACTION OF PROGRAMMED
DEGRADATION TO 500°C AFTER PREPARATIVE TLC

USING n-HEXANE

Solvent C Cl₄

Lock TMS

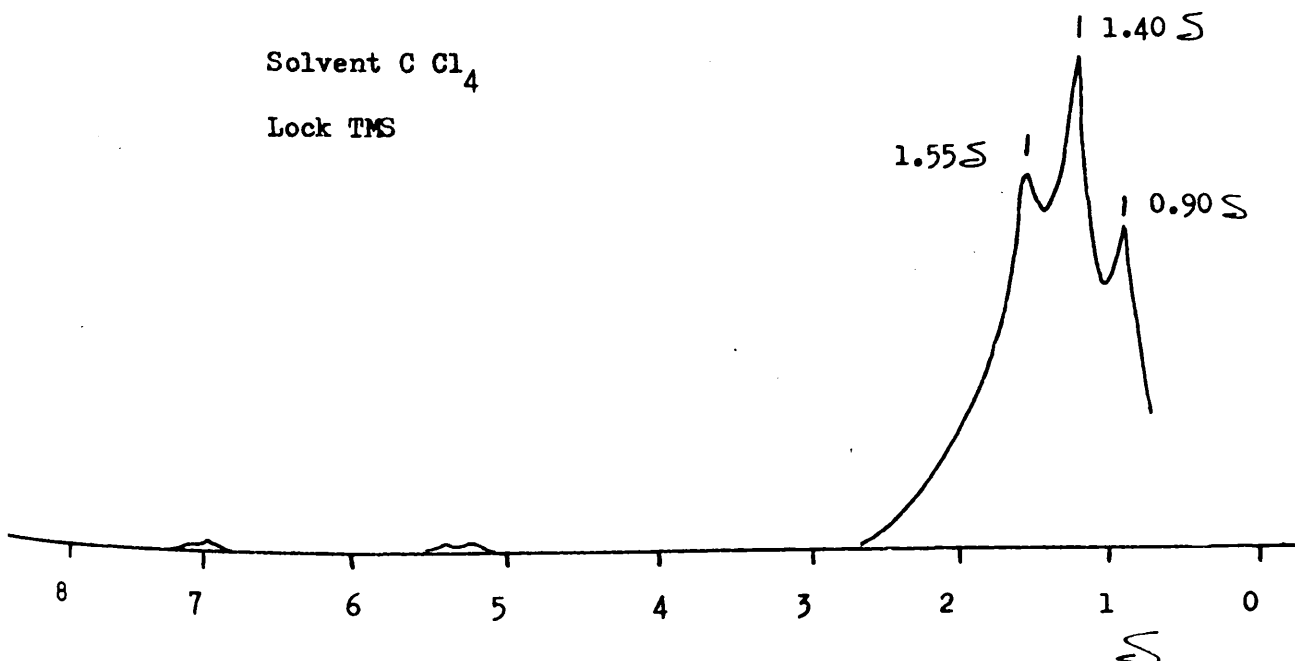


FIGURE 6 - 19

POLYBUTADIENE A, n.m.r. SPECTRUM OF COLD RING FRACTION OF PROGRAMMED
DEGRADATION TO 400°C

Key

* Signals Associated With Undegraded Polybutadiene

Solvent C Cl₄

Lock TMS

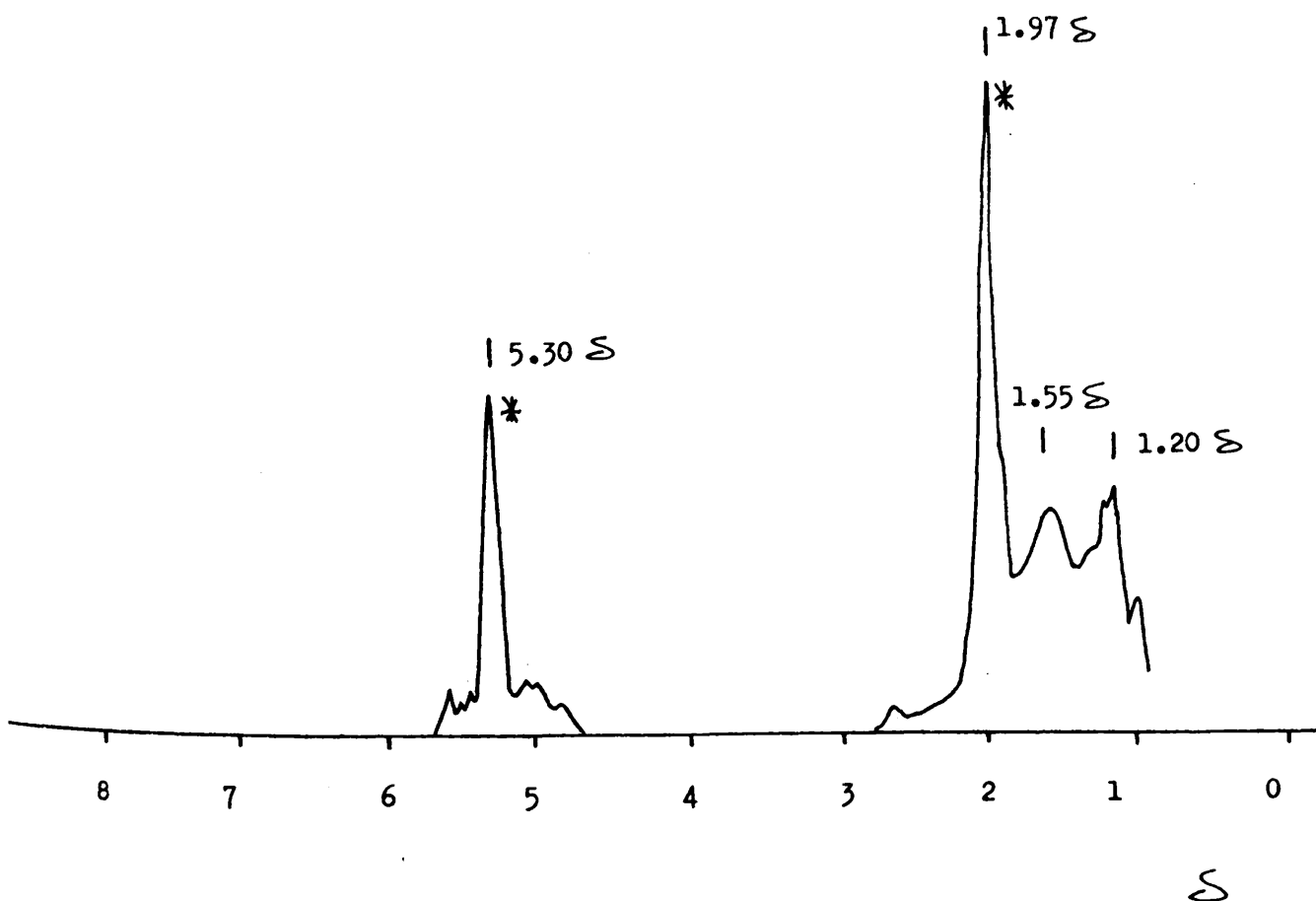


FIGURE 6 - 20

POLYBUTADIENE A, n.m.r. SPECTRUM OF RESIDUE OF PROGRAMMED DEGRADATION
TO 400°C AND 450°C

Key

--- 450°C

Solvent C Cl₄

Lock TMS

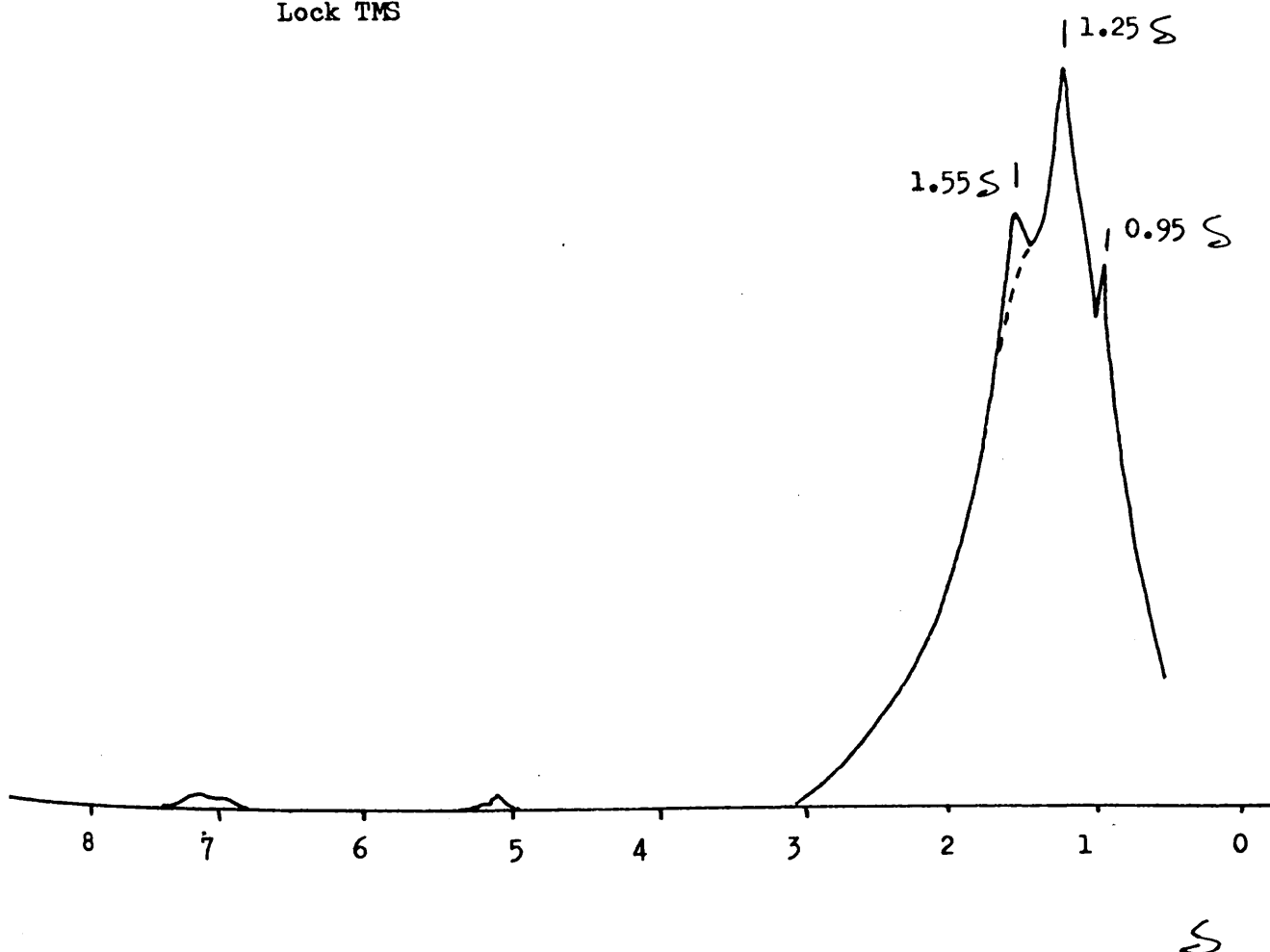


FIGURE 6 - 21

POLYBUTADIENE A, n.m.r. SPECTRUM OF RESIDUE OF PROGRAMMED DEGRADATION

TO 425°C

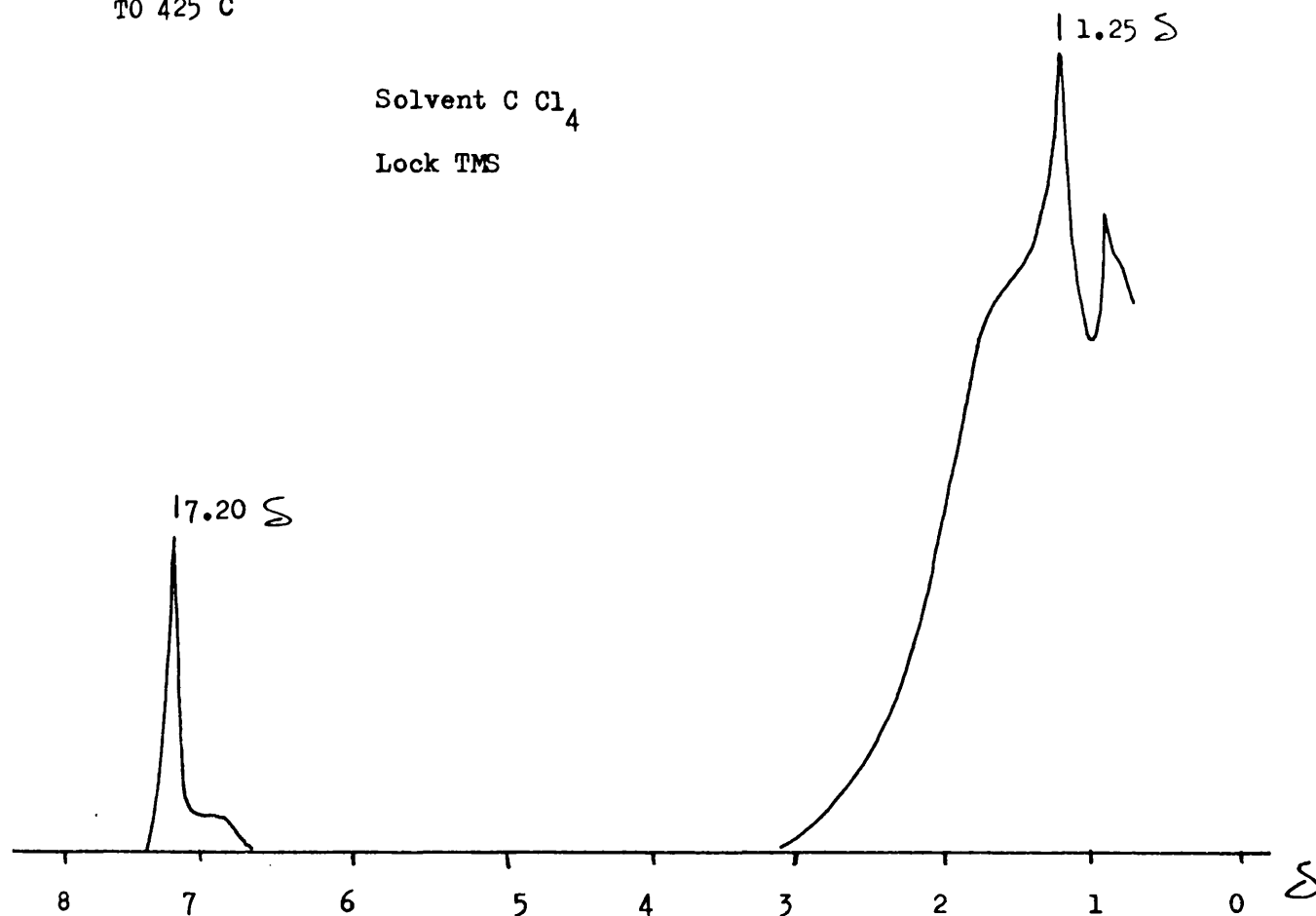
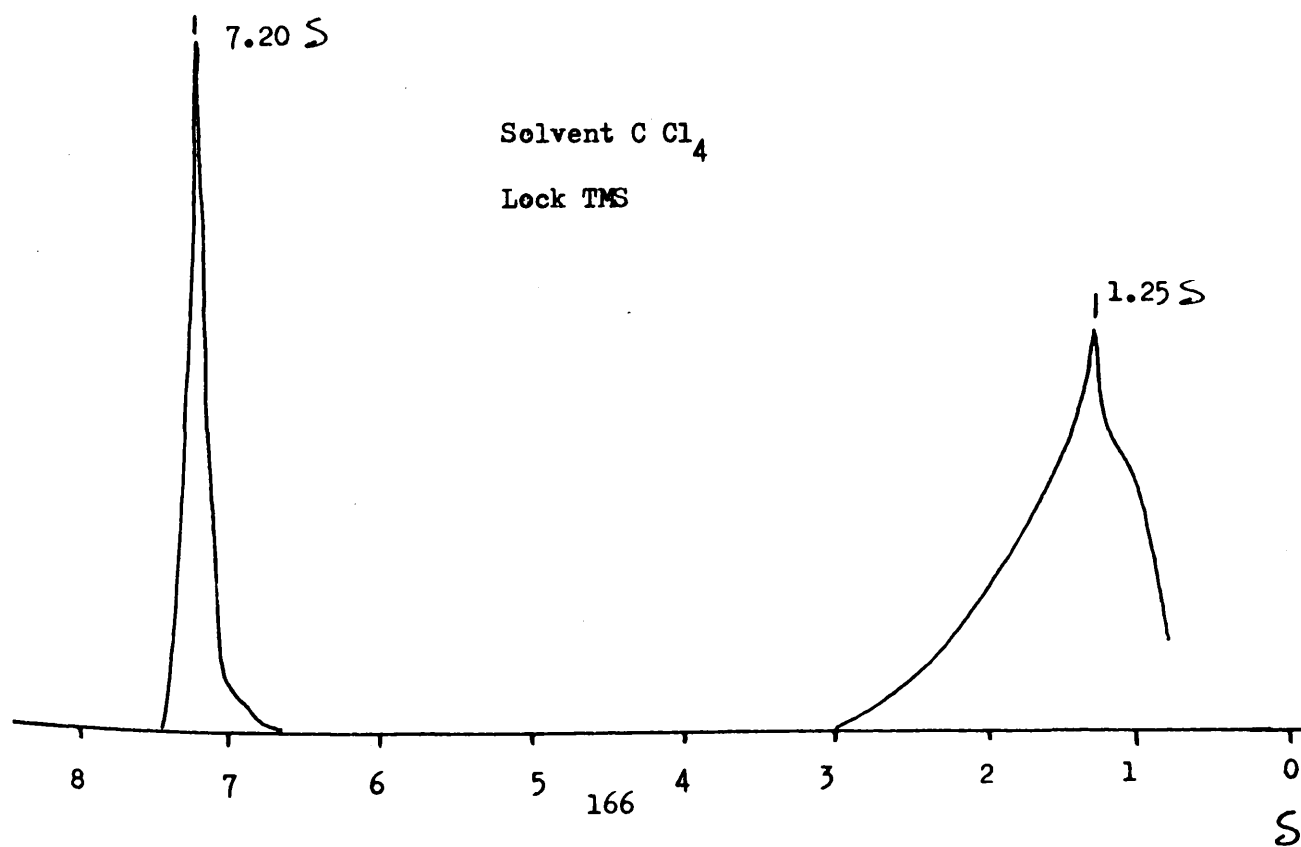


FIGURE 6 - 22

POLYBUTADIENE A, n.m.r. SPECTRUM OF RESIDUE OF PROGRAMMED DEGRADATION

TO 425°C FOLLOWED BY ISOTHERMAL DEGRADATION AT 425°C FOR 5 min



D MECHANISMS OF DEGRADATION.

In this discussion an attempt will be made to bring together the results obtained in sections B and C to elucidate the mechanisms operative in polybutadiene degradation.

The DSC, TVA and TG traces corresponding to the material (figs. 1, 2, 3) all indicate that the degradation reaction is a two step process. The low temperature process is exothermic in nature and results in a small weight loss in the polymer. The high temperature process is endothermic in nature and completely volatilises the sample. The shape of the -196°C TVA trace indicates that there is a considerable temperature region of overlap between the two processes. The TVA trace for the material indicates that the high temperature decomposition reaction produces methane and hydrogen in a concerted process.

D 1 THE EXOTHERMIC DECOMPOSITION REACTION.

It will be assumed throughout the discussion that this process corresponds to the cyclisation/depolymerisation reaction first postulated by Golub (84).

The n.m.r. spectrum of the residue of programmed degradation to 400°C (fig. 20) shows that the material is completely cyclised and almost completely saturated, containing only trace quantities of unsaturated and aromatic material. The peaks at 1.25δ and 1.55δ are produced by CH_2 and CH groupings respectively in polycondensed ring segments. The peak at 0.95δ is produced by terminal methyl groups which are thought to be produced by disproportionation reactions in the polymer.

The n.m.r. spectrum of the cold ring fraction of degradation to 400°C (fig. 19) shows that it consists mainly of segments of uncyclised polybutadiene which are accompanied by appreciable

quantities of saturated, condensed ring fragments. No aromatic material was detected. The small quantity of material generated in this process prevented its analysis by preparative TLC, and so its origin must be speculated upon. The uncyclised material was probably generated at the onset of volatilisation as the product fraction of the random scission/disproportionation reaction able to volatilise from the hot zone. The condensed ring material was probably produced at higher temperatures as a product fraction of the ring decomposition reaction which begins at approximately 350°C. The possibility that some incompletely cyclised, condensed ring end-capped polybutadiene is formed by the interruption of the polycyclisation reaction by volatilisation can not be discounted.

The sub-ambient TVA separations corresponding to volatile material generated in the temperature ranges room temperature - 380°C and 380 - 410°C show that the major volatile products of degradation to 410°C are 1,3-butadiene and 4-vinylcyclohexene (figs.

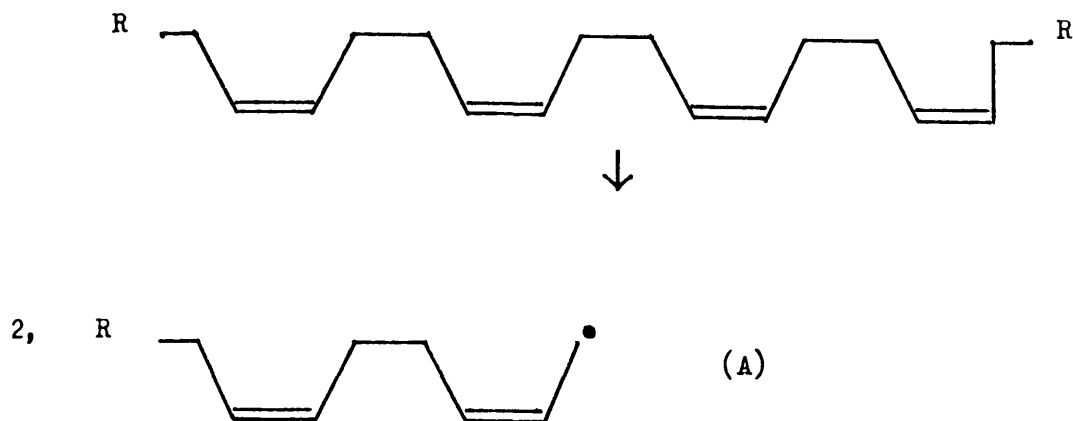
6, 7). The presence of 4-vinylcyclohexene but not 1,3-butadiene (which is lost during transfer) was reaffirmed by GLC (figs. 10, 11). The presence of such material confirms that a fraction of the radicals generated by main chain scissions in the polymer take part in depropagation reactions (1,3-butadiene) and cyclisation/depropagation reactions (4-vinylcyclohexene).

Benzene and monosubstituted aromatic material was detected in trace quantities in the volatile fraction of degradation to 380°C (fig. 14) and in much larger quantities in the volatile fraction of degradation 380 - 410°C (fig. 15), where it is accompanied by significant quantities of saturated monocyclic ring structures. It is assumed that this material is produced by the overlapping ring decomposition reaction.

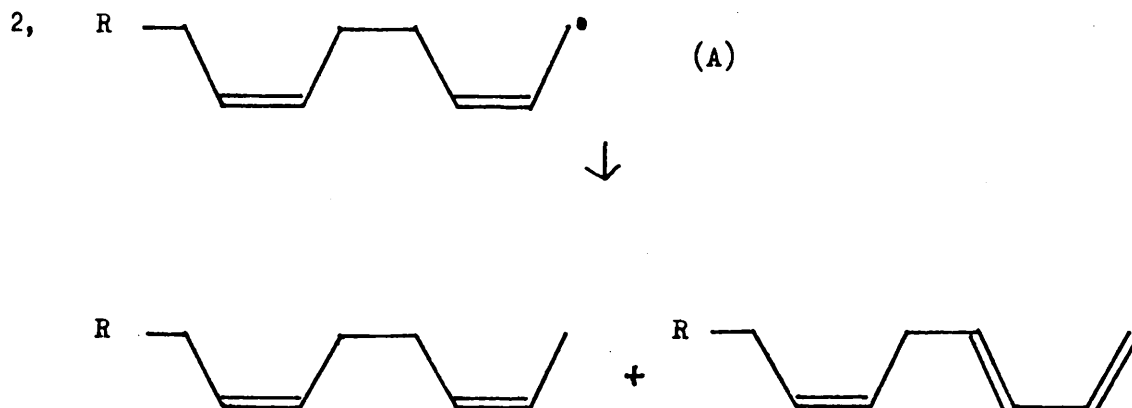
The processes thought to be operative during the exothermic

decomposition process are summarised below. In all cases the symbol R is used to represent a polymeric residue.

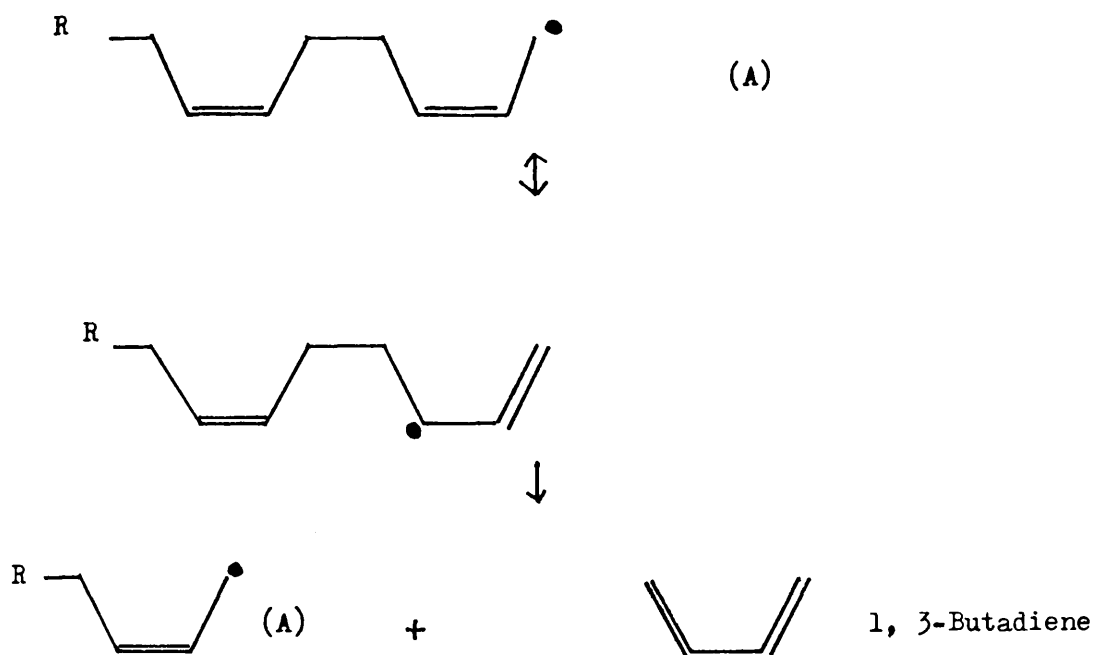
(i). Main Chain Scission (Major)



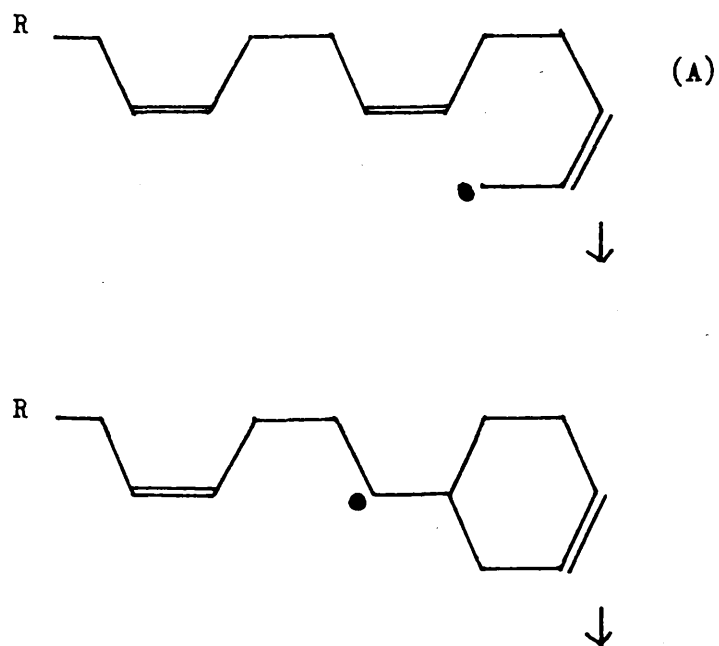
(ii). Disproportionation (Major)

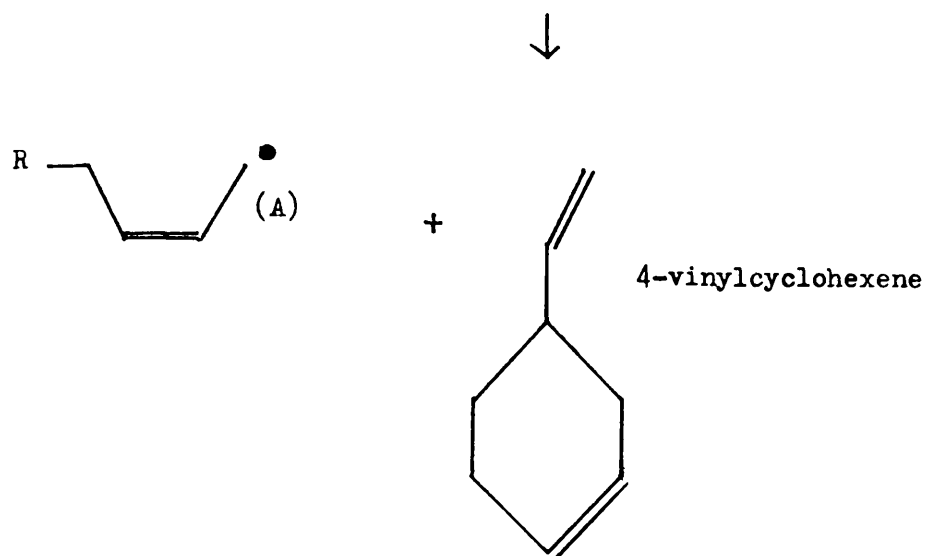


(iii). Depropagation (Major)

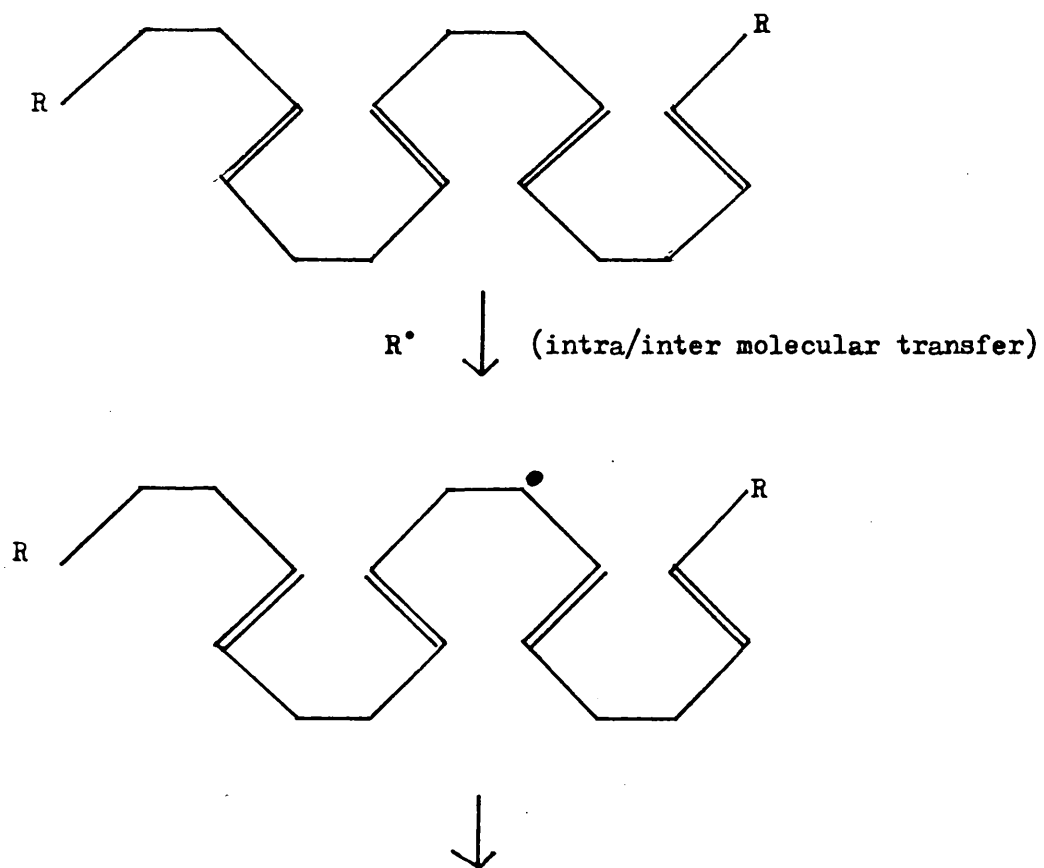


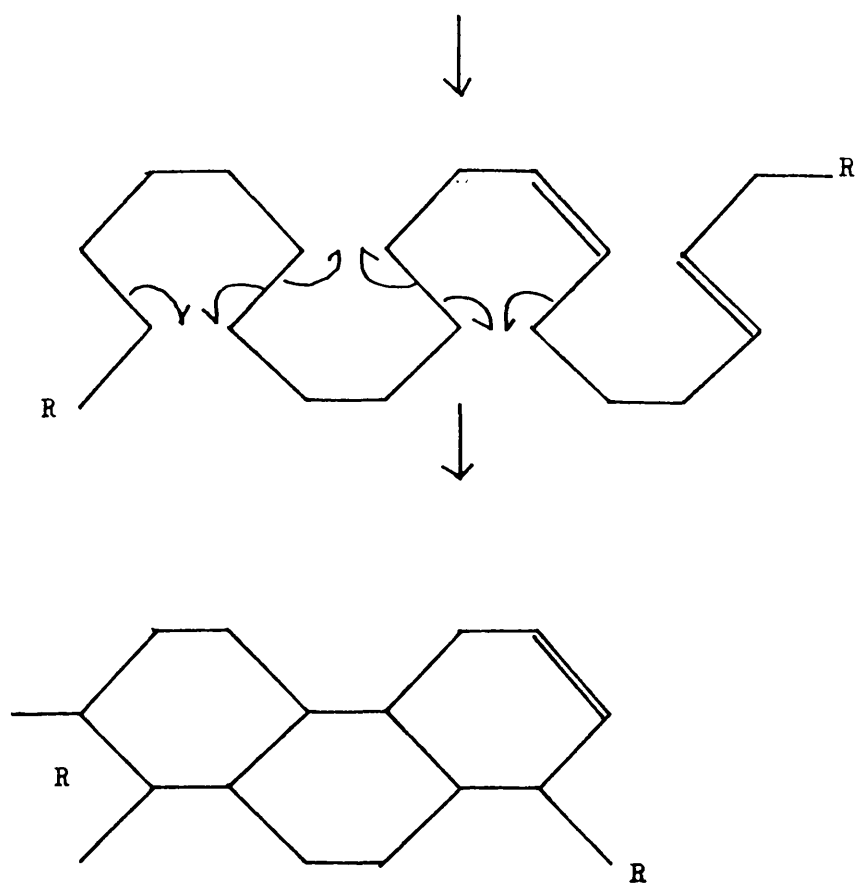
(iv). Cyclisation/Depropagation (Major)



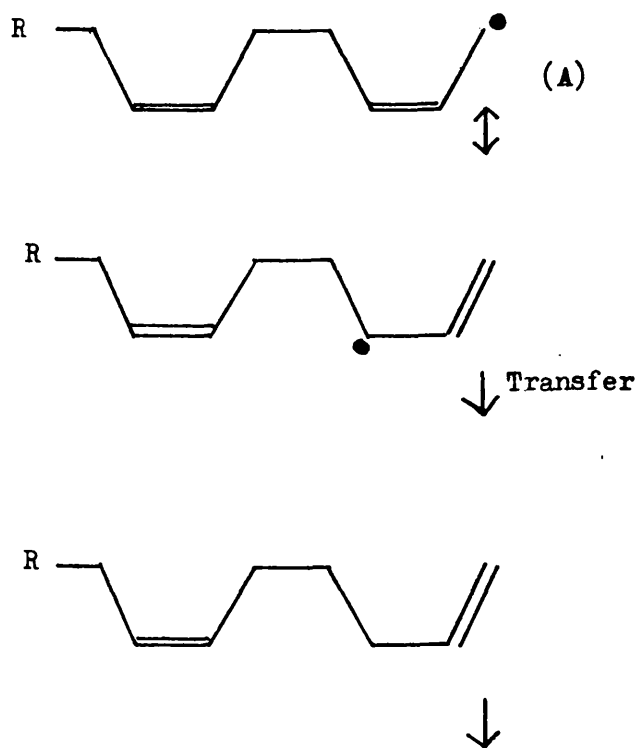


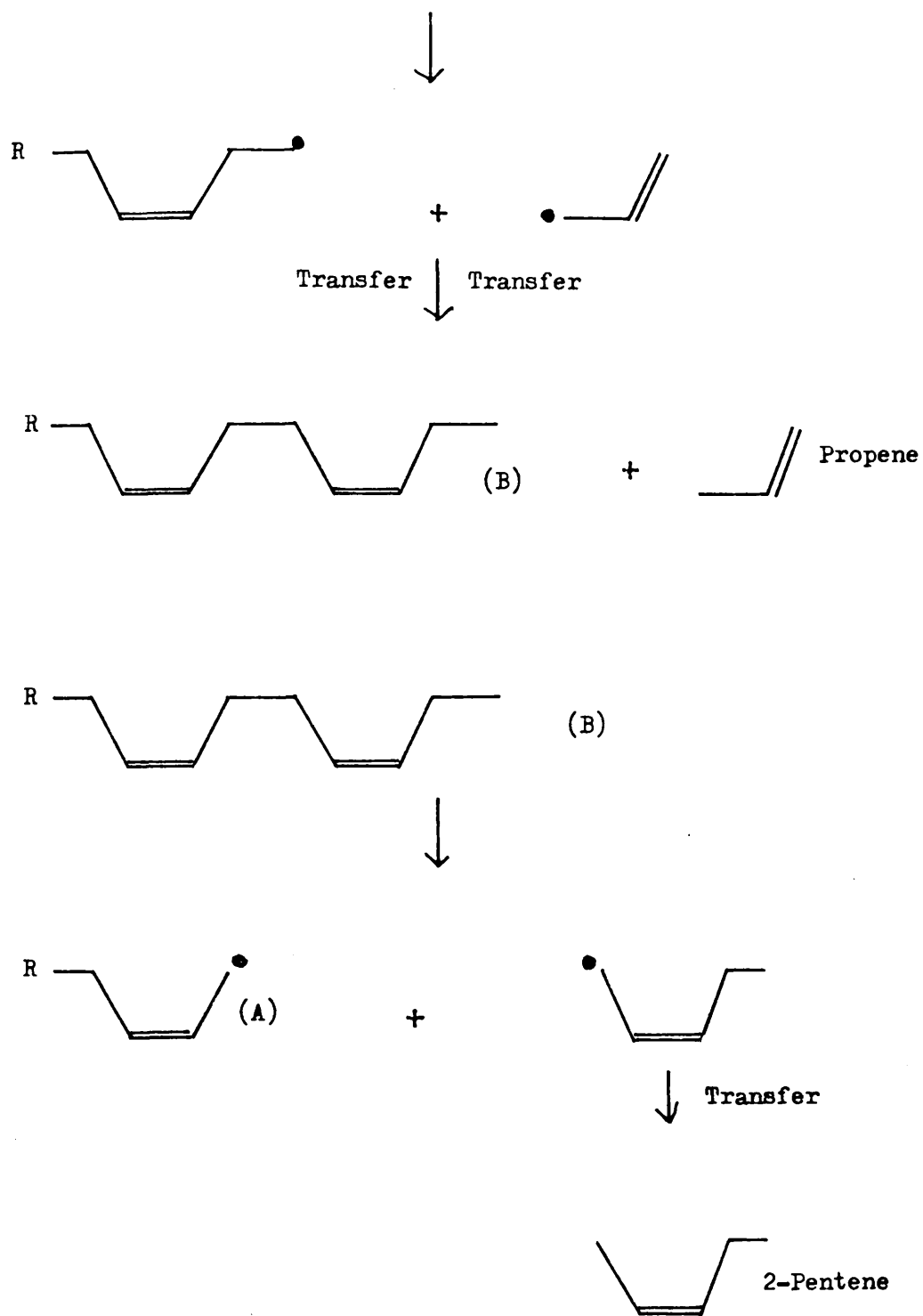
(v). Polycyclisation (Major)





(vi). Scissions to Form $\dot{\text{R}}$ - Allyl Radicals (Minor)





It will be assumed throughout the discussion that this process corresponds to the thermal decomposition of the polycondensed ring structures which are formed in the exothermic decomposition reaction.

The volatile products of degradation generated in the temperature ranges 410 - 450°C and 450 - 500°C were collected and separated by SATVA (figs. 8, 9) and GLC (figs. 12, 13). It can be seen that the major volatile products of lower temperature decompositions, 1,3-butadiene and 4-vinylcyclohexene, are completely absent from the product distribution and are replaced by large quantities of C₂, C₃, C₄, C₇ and C₈ acyclic hydrocarbons. Acyclic C₅ and C₆ hydrocarbons, if present, would be masked by the solvent used in GLC work. They are, however, the only hydrocarbon materials able to be volatilised at point * of figs. 8 and 9 and so were assumed to be present, (saturated cyclic and aromatic material would be detected by GLC).

The n.m.r. spectrum of the volatile product fraction of degradation in the temperature range 410 - 500°C (fig. 16) indicates that it also contains saturated and aromatic ring fragments. Aromatic material similar to that produced in the temperature range 380 - 410°C (fig. 15) is accompanied by what can only be described as a wide range of polysubstituted and conjugated unsaturated aromatic material.

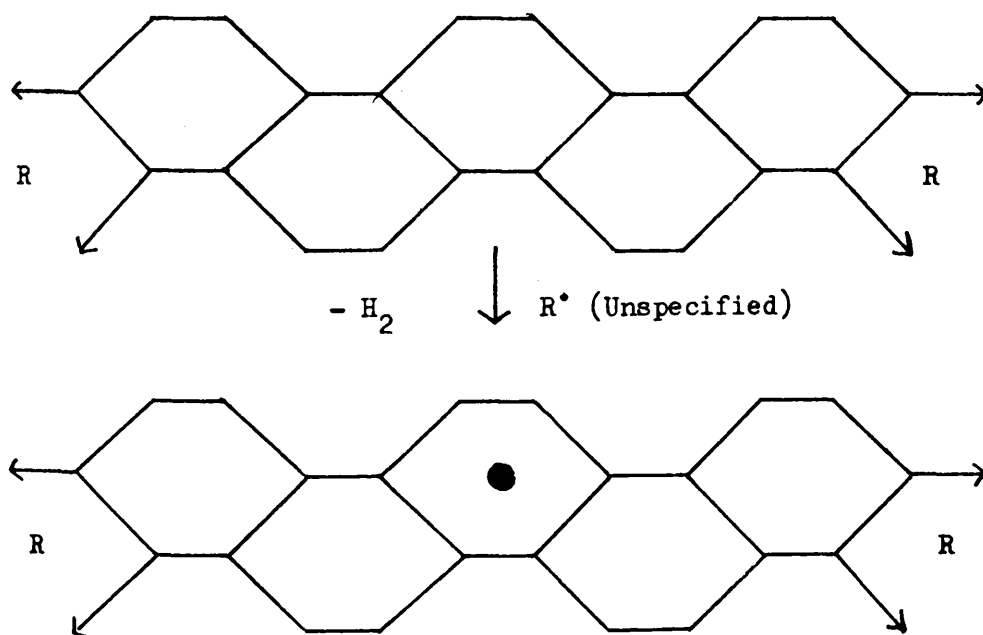
The n.m.r. spectrum of the cold ring fraction of degradations to completion (fig. 17) indicates that it consists predominantly of polycondensed saturated ring structures along with material very similar to that produced in the exothermic decomposition reaction (fig. 19). Such material was removed by preparative TLC to confirm that the cold ring fraction produced in the

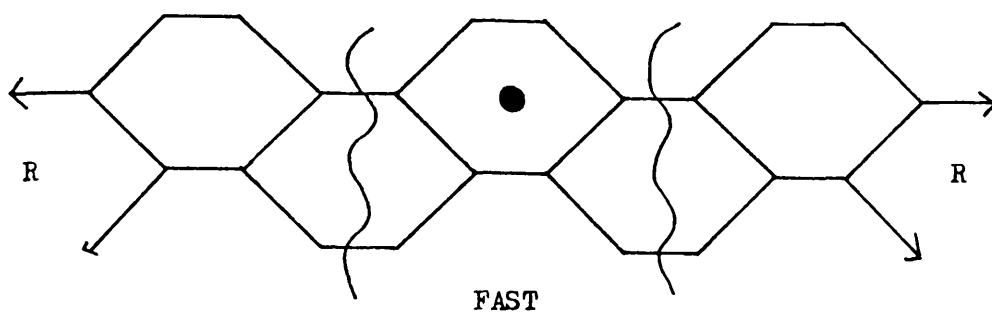
endothermic reaction consists only of polycyclic saturated hydrocarbons. No aromatic material was detected.

Large quantities of volatile aromatic material are generated in the endothermic decomposition reaction of polybutadiene. The rate of aromatisation of the polymer should therefore be a maximum at 350°C. The stationary concentration of such material in the polymer at this temperature was examined by n.m.r. spectroscopy (fig. 20) and found to be very low. This indicated that such material was unstable at this temperature and was rapidly volatilised after formation. The residue of degradation to an intermediate temperature of 425°C contained a small but measurable concentration of aromatic material (fig. 21) which was enhanced by isothermal heating at this temperature (fig. 22).

The mechanisms thought to be operative during this stage of degradation are outlined below.

(R = Polymer Residue)





↙
 Benzene, Mono, Di, Tri, Substituted Benzenes,
 Styrene "Type" Material

↘
 $C_1 - C_8$ Hydrocarbons

↓

Condensed Rings Of Degree n


Small n

Volatile Material

Large n

Cold Ring Material

Aromaticity is assumed to be generated at random along the polycondensate and to destabilise neighbouring rings, which fragment to give the products shown above.

It has been shown (100) that the development of unsaturation during the thermal degradation of organic material is a facile process. It has also been shown (101) that aromatic groupings encourage the disruption of neighbouring bonds by their ability to stabilise  radicals, and to encourage the formation of low molecular weight hydrocarbon fragments as products of degradation (102).

The process was assumed to be accelerated by the presence of free radicals in the system (R°) which are able to abstract hydrogen from tertiary carbons in the polycondensate. This is supported by the shape of the emission curve of noncondensables for the material degraded at 380°C (fig. 23). If the reaction is insensitive to the radical population in the material and dependent only upon concentrations of polycondensed material then it should rise to a rate maximum after approximately 20 min degradation at this temperature. On the contrary, it rises to a small but distinct rate maximum after 6 min degradation at which point the cyclisation/depropagation reaction has achieved a rate maximum.

E ISOTHERMAL DEGRADATIONS AT 380°C.

Samples of polybutadiene A were subjected to isothermal degradation under vacuum for various periods of time in the degradation assembly outlined in Chapter 5. The various fractions of degradation were subjected to spectroscopic analysis to determine the mechanisms operative at this temperature. TG and TVA rate measurements were made and the fractions of degradation were estimated gravimetrically.

E 1 TVA.

A differential condensation TVA trace for polybutadiene A is shown in fig. 22 . The rate of production of volatile material rapidly attains a maximum at 6 min degradation, after which it decays to a small limiting rate. Of interest is the production of noncondensable material which comprises a significant fraction of the product mixture after 30 min degradation.

E 2 TG UNDER NITROGEN.

An isothermal TG curve for polybutadiene A degraded under nitrogen at 380°C is shown in fig. 24 . The shape of the curve conforms with that predicted by Straus and Madorsky (83). After an initial rapid but small weight loss, the sample weight drops in a slow linear manner.

E 3 THE RESIDUE OF DEGRADATION.

Polybutadiene rapidly forms a glassy insoluble residue when degraded at 380°C. This prevented its analysis by n.m.r. spectroscopy. For this reason microstructural changes in the polymer were followed by i.r. spectroscopy.

Thin films of polymer were deposited on disposable salt

FIGURE 6 - 23

POLYBUTADIENE A, ISOTHERMAL TVA AT 380°C

Sample Size 50 mg

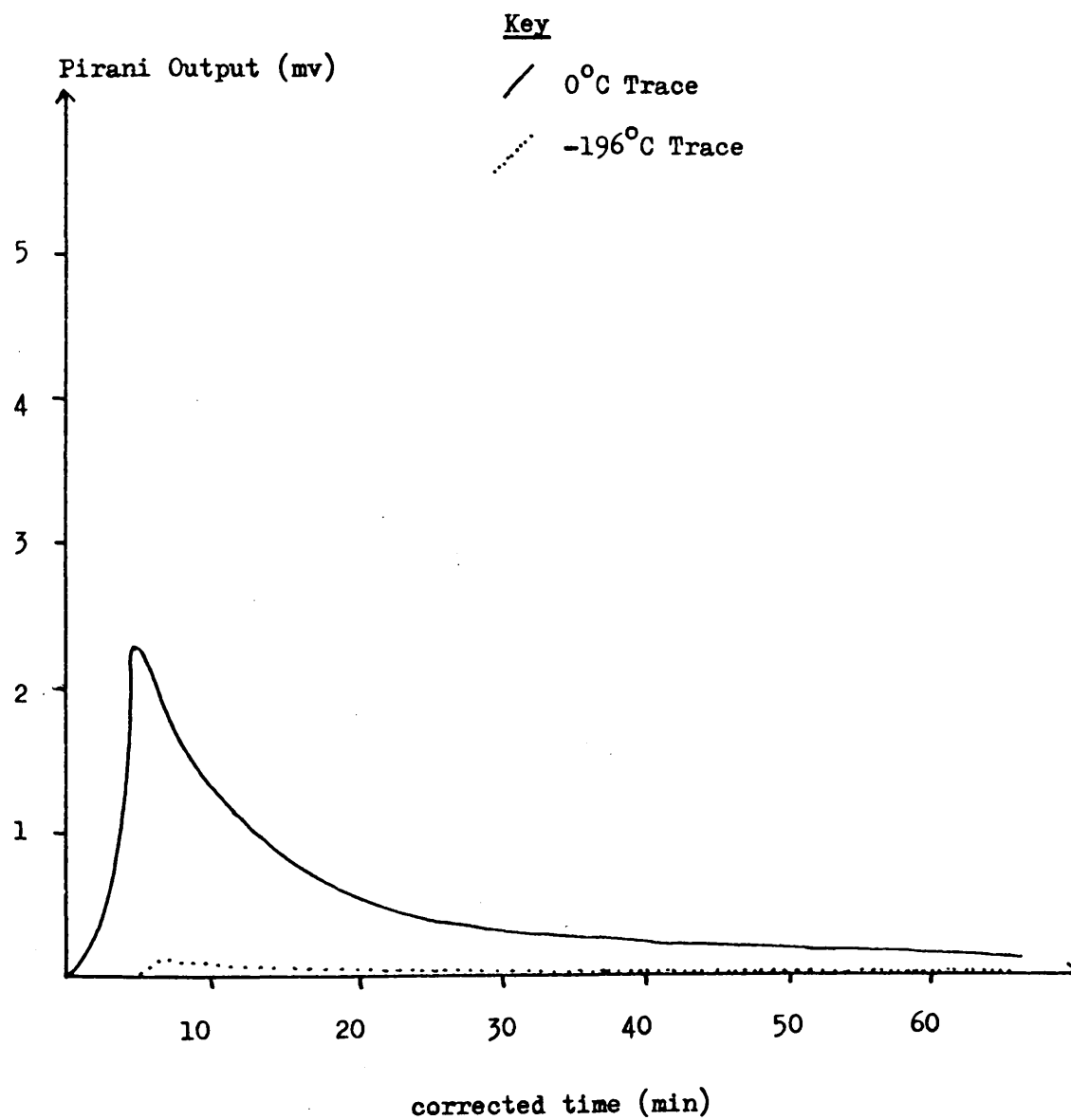
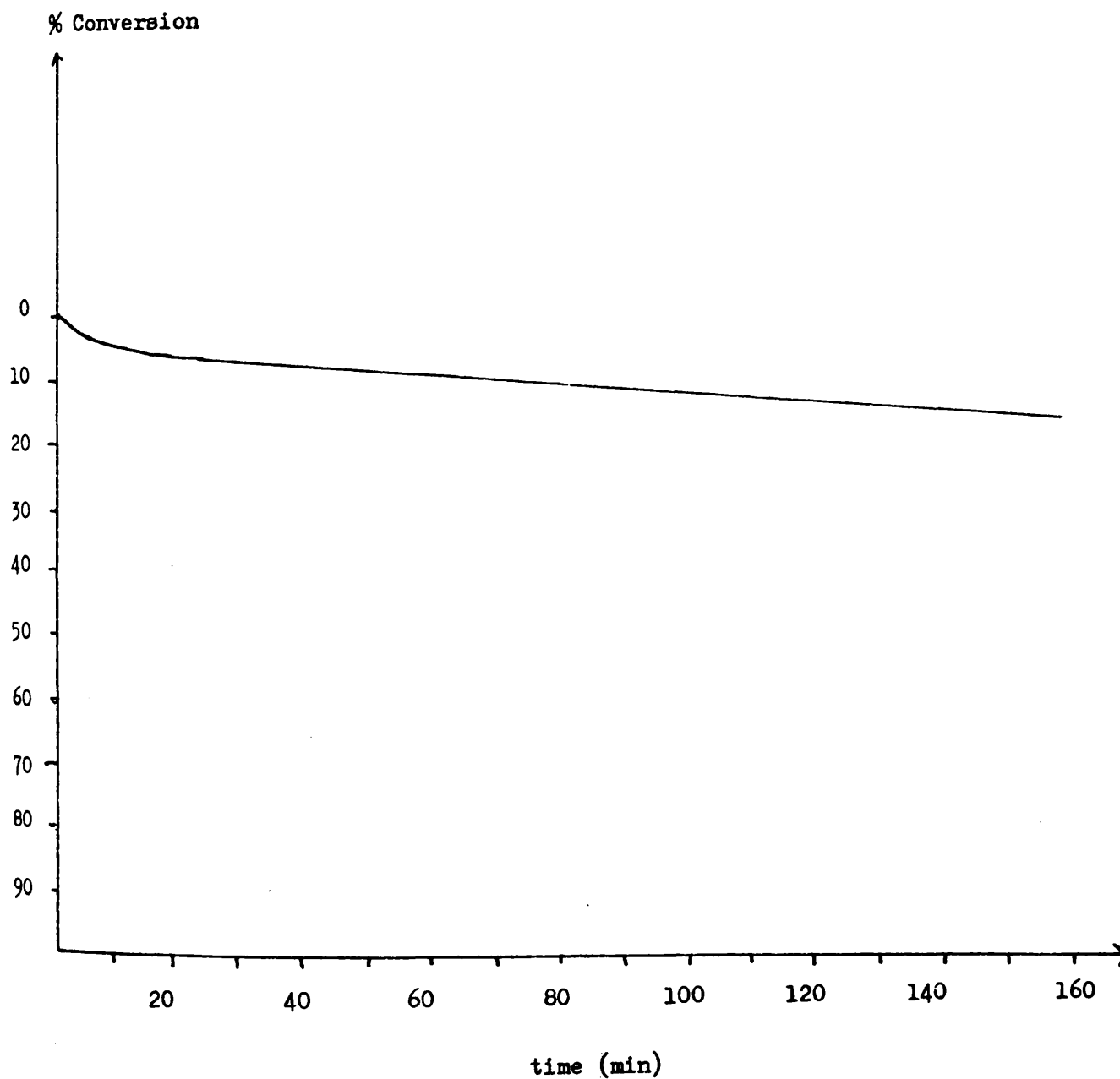


FIGURE 6 - 24

POLYBUTADIENE A, ISOTHERMAL TG UNDER NITROGEN AT 380°C

Sample Size 9 mg



plates and degraded for 10, 20, 30, 40 and 60 min at 380°C under vacuum. Each spectrum was normalised by the factor required to adjust the absorbance of the 1440 cm⁻¹ band of the undegraded polymer to 50%. Removal of unsaturated material was indicated by a reduction in intensity of its corresponding i.r. vibrations. This is best observed in the fingerprint regions of the spectra shown in fig. 25. Methyl groupings (1370 cm⁻¹) were the only detectable functional groupings formed during this process (84). Of interest is the observation that small but detectable quantities of linear unsaturated groupings are present in the polymer even after 60 min degradation at this temperature. These are probably "frozen into" the lattice in a configuration difficult to cyclise.

E 4 VOLATILE PRODUCTS OF DEGRADATION.

A sub-ambient TVA trace corresponding to the volatiles produced in the first 60 min of degradation is shown in fig. 26. It can be seen that appreciable quantities of "high molecular weight" fragments are produced along with 1,3-butadiene and 4-vinylcyclohexene. This material is shown by n.m.r. spectroscopy (fig. 27) to consist mainly of saturated ring fragments and some aromatic material.

E 5 THE COLD RING FRACTION OF DEGRADATION.

The n.m.r. spectrum of the cold ring fraction of degradation (fig. 28) indicates that it is a mixture of polybutadiene oligomers and polycondensed saturated material. No aromatic material was detected.

E 6 MECHANISMS OF DEGRADATION.

It is clear from the above that both the exothermic cyclisation/depolymerisation and the endothermic ring decomposition reactions are facile processes at 380°C. They do, however, proceed

FIGURE 6 - 25

POLYBUTADIENE, NORMALISED i.r. SPECTRA OF RESIDUE OF ISOTHERMAL
DEGRADATION AT 380°C

(Material As Thin Films On Disposable Salt Plates)

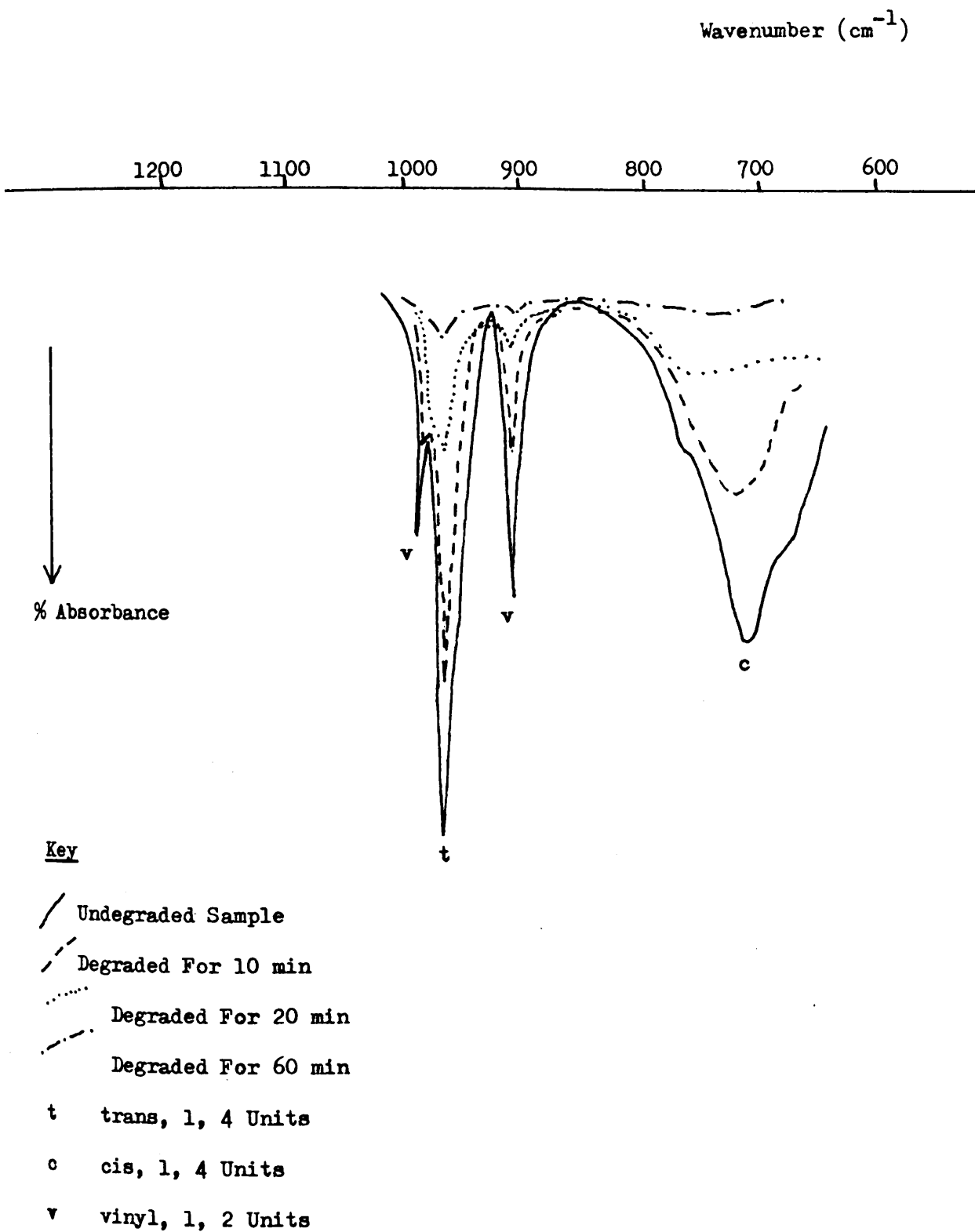


FIGURE 6 - 26

SUB-AMBIENT TVA OF PRODUCTS OF ISOTHERMAL DEGRADATION AT 380°C FOR 1 hr

Sample Size 50 mg

Key

Pirani Gauge Output

(-) Thermocouple Output

1 Propene

2 1,3-Butadiene

3 C₅ Hydrocarbons

4 C₆ Hydrocarbons

5 4-Vinylcyclohexene

6 High Molecular Weight Fragments

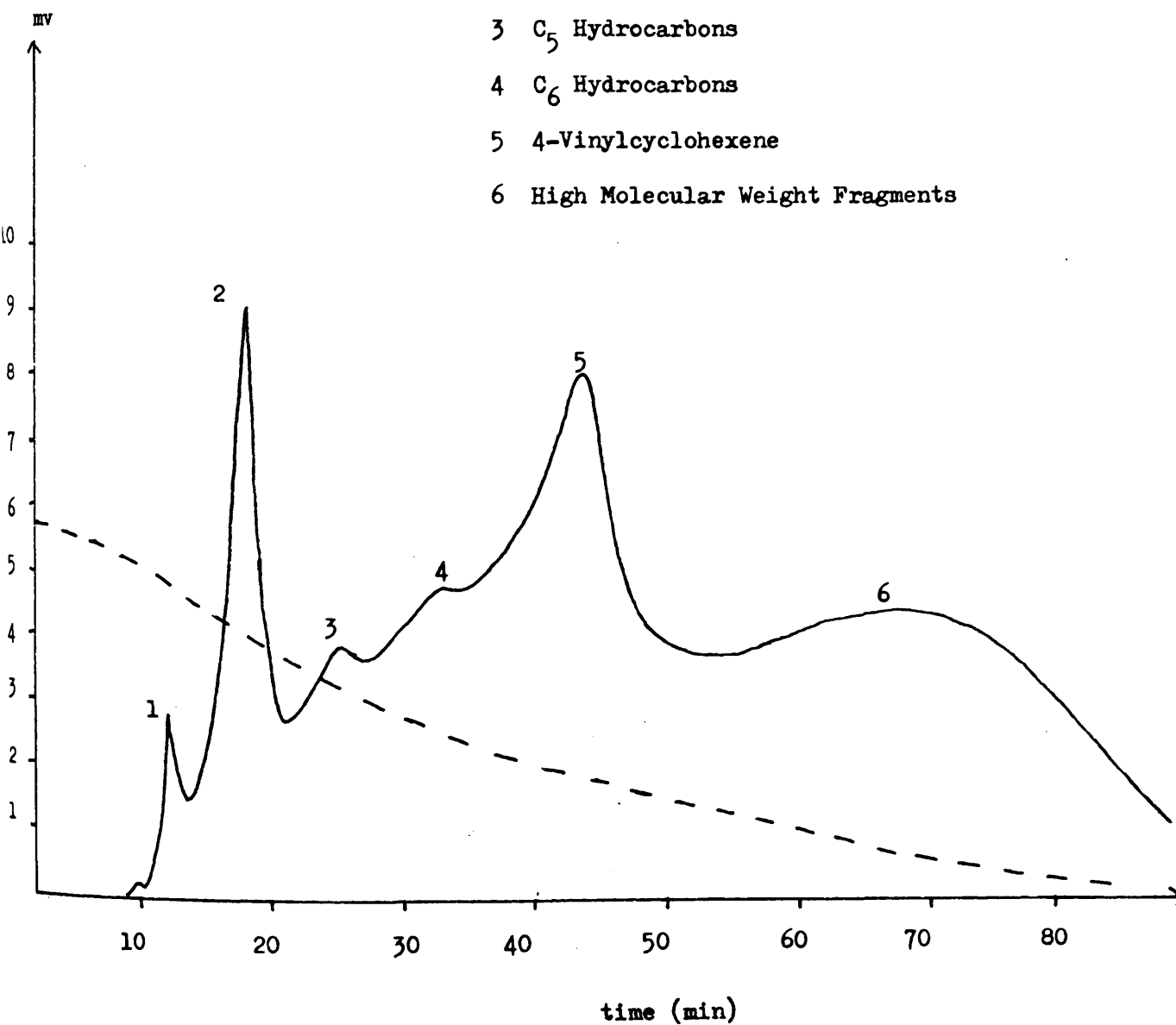


FIGURE 6 - 27

POLYBUTADIENE A, n.m.r. SPECTRUM OF VOLATILE PRODUCTS OF ISOTHERMAL
DEGRADATION AT 380°C FOR 1 hr

Solvent C Cl₄

Lock TMS

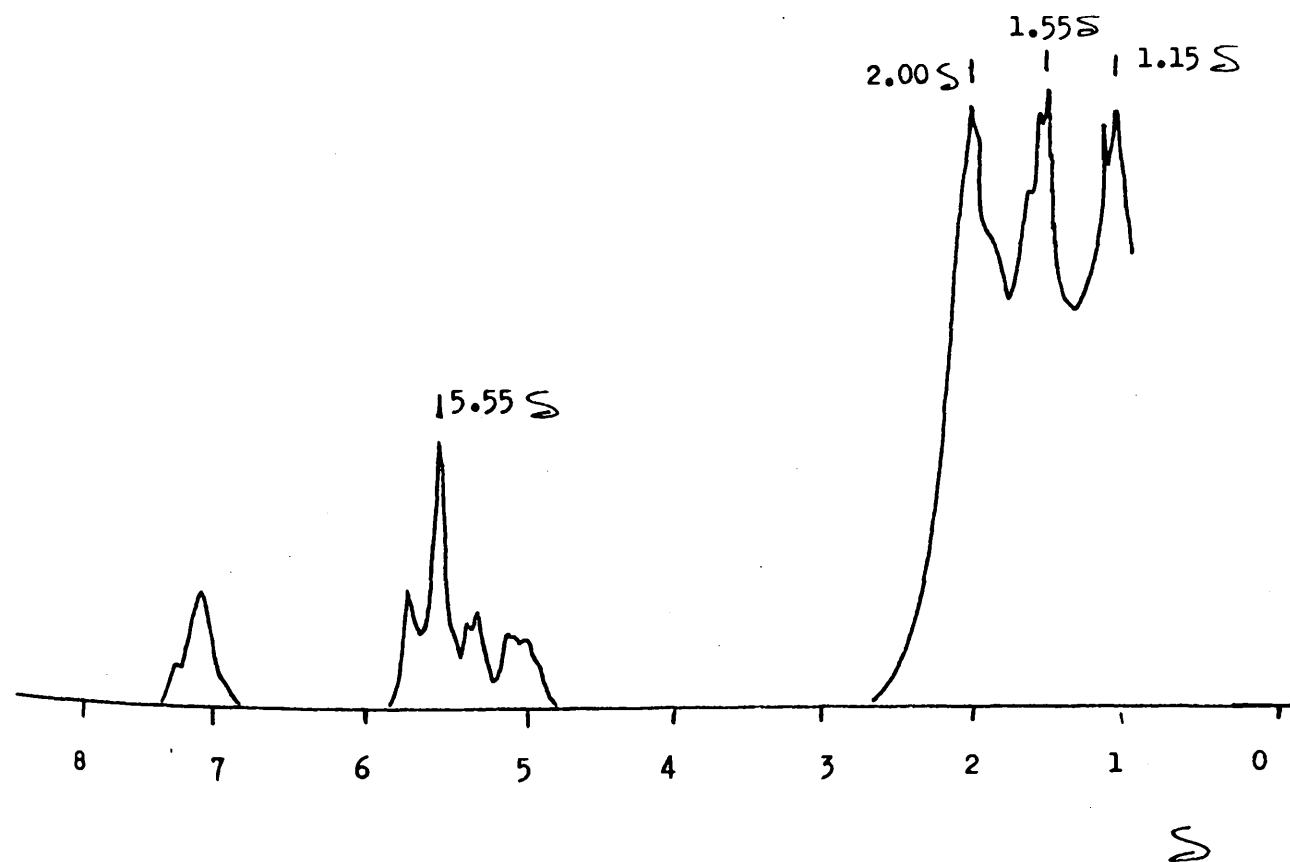
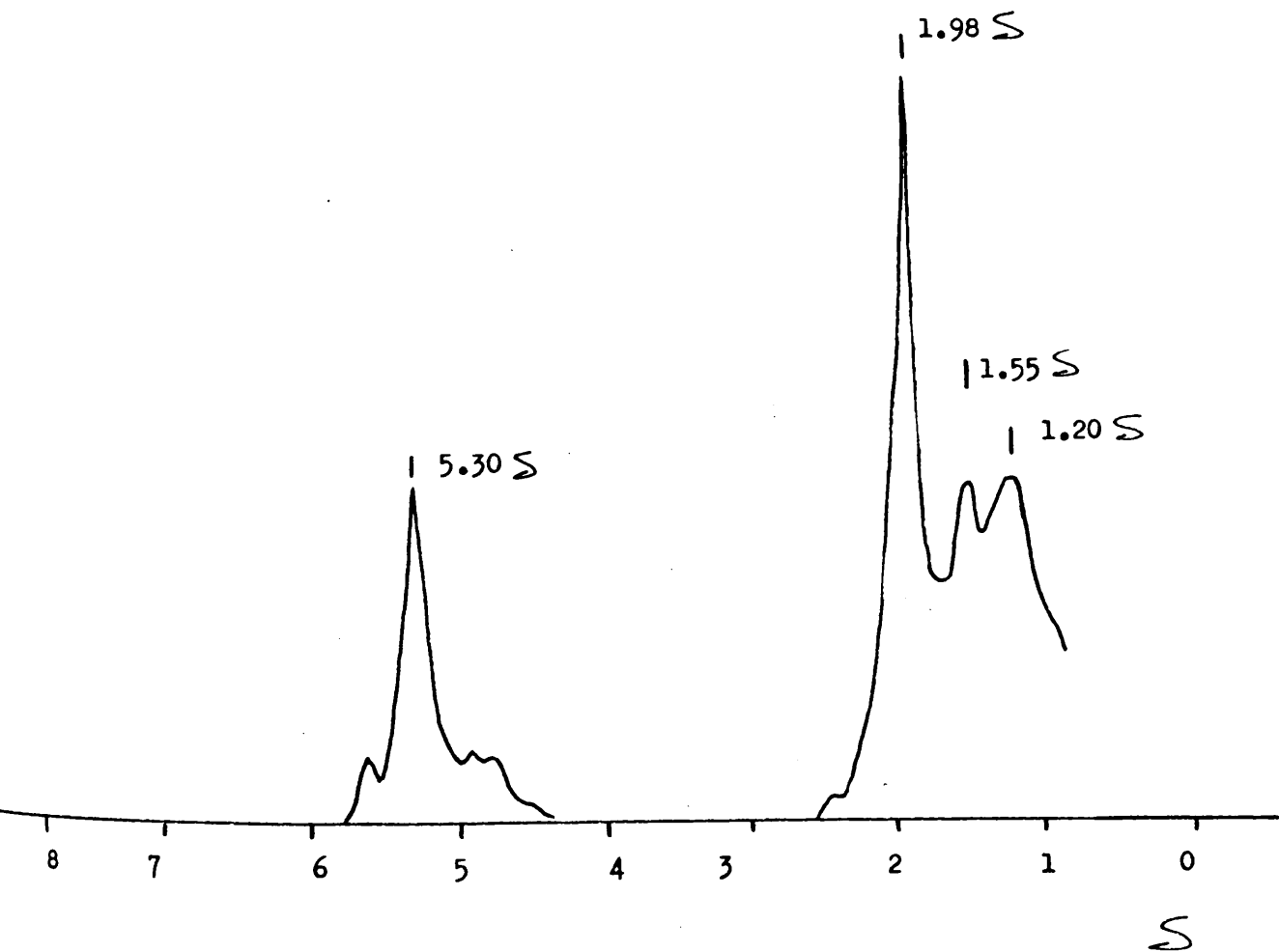


FIGURE 6 - 28

POLYBUTADIENE A, n.m.r. SPECTRUM OF COLD RING FRACTION OF ISOTHERMAL
DEGRADATION AT 380°C FOR 1 hr

Solvent C Cl₄

Lock TMS



at very different rates. The exothermic reaction is driven almost to completion during the first 10 min of degradation while the endothermic reaction occurs throughout at a small but measurable rate and probably accounts for the eventual volatilisation of the bulk of the sample.

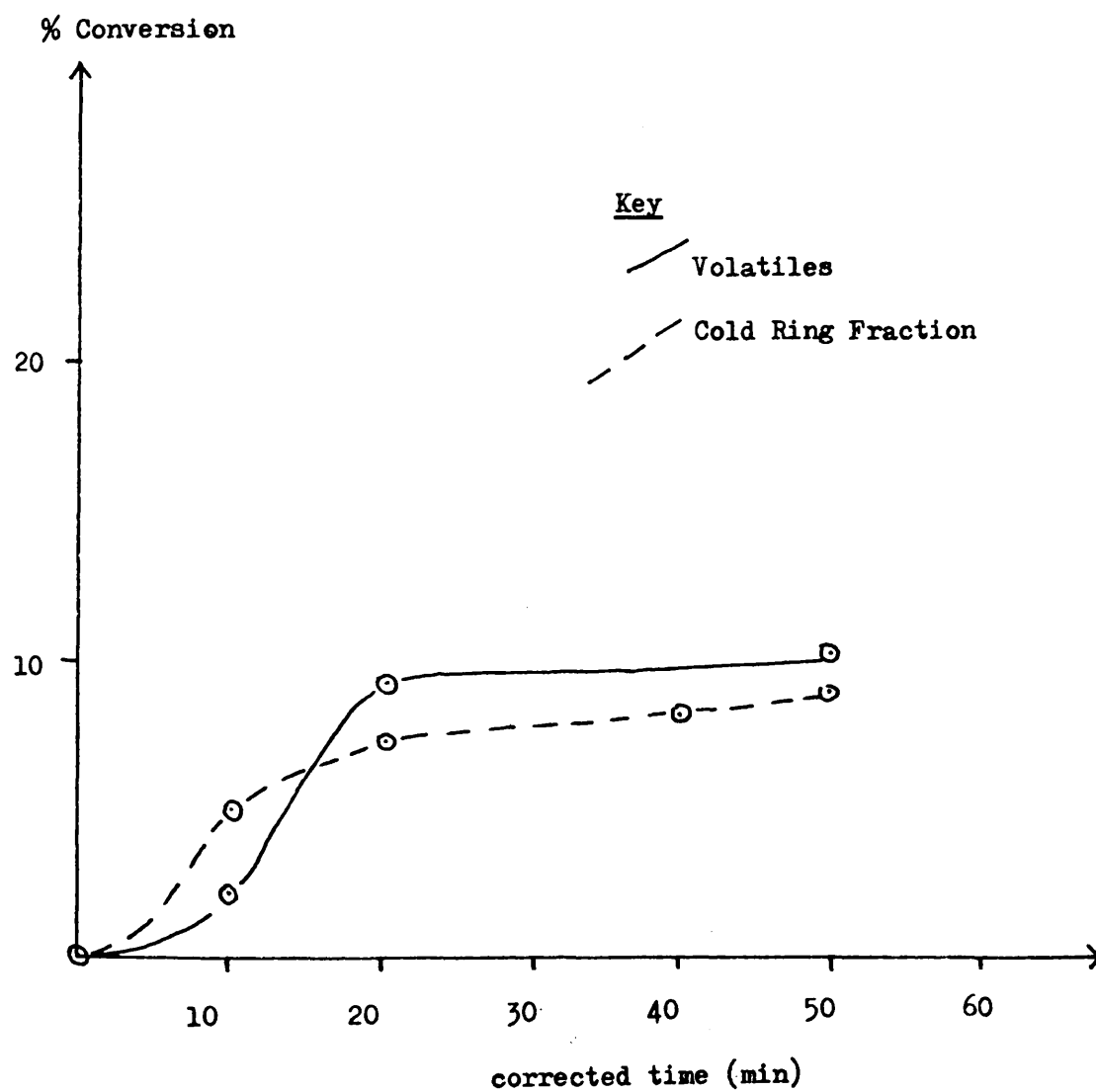
E 7 GRAVIMETRIC ANALYSIS UNDER VACUUM.

Yields of volatile and cold ring material generated during isothermal degradations of polybutadiene A at 380°C were obtained using the procedure outlined in Chapter 5. It can be seen (fig. 29) that during the time interval in which the exothermic decomposition reaction takes place both product fractions are formed at a high rate which decays to a small limiting rate corresponding to endothermic decompositions upon exhaustion of this process.

FIGURE 6 - 29

POLYBUTADIENE A, GRAVIMETRIC CONVERSION CURVES AT 380°C

Sample Size 50 mg



CHAPTER 7.

THERMAL DEGRADATION OF BLOCK COPOLYMER.

INTRODUCTION.

The 50/50 by weight styrene/butadiene block copolymer (characterised in Chapter 4) was subjected to programmed (at 10°C/min) and isothermal (at 380°C) degradation in an attempt to achieve the following aims. First of all, it was necessary to determine whether or not the homopolymer segments degrade in a cooperative manner. Secondly, if such interactions exist, it was necessary to estimate quantitatively the extra stability (or instability) generated in the material with respect to the volatilisation process. Finally, it was essential to elucidate the mechanisms of homopolymer interactions, if such processes occur in the material.

Whenever possible, the degradative behaviour of this polymer was compared with that of the blend system in an attempt to illustrate the effect of polymer morphology - more specifically the effect of the degree of domain dispersion, on the efficiencies of the interactive processes. Much of the data relating to the blend system has been drawn from published work (80) and will be distinguished from original work by associating with it the above reference.

7 - I PROGRAMMED DEGRADATION.

A 1 TG UNDER NITROGEN.

TG curves corresponding to degradation of the block copolymer, the blend system and the system with no interaction are shown in fig. 1 . It can be seen that the block copolymer is more stable with respect to weight loss than either of the other two systems.

A comparison was also made (fig. 2) between the TG rate curves which correspond to the block copolymer, the blend system (calculated) and the system with no interaction (calculated), after normalising them to similar peak areas.

As expected, the distinctive rate maximum at 420°C which corresponds to the volatilisation of polystyrene homopolymer is well separated from the broad rate maximum at 480°C which corresponds to the bulk of the volatilisation of polybutadiene homopolymer in the "no interaction" curve.

When the two homopolymers are degraded as a blend the magnitude of the rate maximum at 420°C is greatly reduced and broadened as (presumably) the polystyrene segment is stabilised with respect to its conversion to volatile material.

This effect is most strikingly observed in the block copolymer system in which the polystyrene homopolymer rate maximum is completely absent and is replaced by a broad, fine structured and enhanced rate maximum centred on 475°C .

A 2 DSC UNDER NITROGEN.

A comparison is made in fig. 3 between DSC curves which correspond to the block copolymer and the polymer blend system. In both systems the position and shape of the part of the curve which corresponds to the temperature interval in which the rubber component is undergoing the process of cyclisation is indistinguishable

FIGURE 7 - 1

TG UNDER NITROGEN OF THE BLOCK COPOLYMER, THE 50/50 POLYMER BLEND
SYSTEM, AND A 50/50 MIXTURE WITH NO INTERACTION

Heating Rate 10°C/min

Key

- 50/50 Block Copolymer - 5 mg
- · - 50/50 Blend System - 10 mg (80)
- - - 50/50 Mixture With No Interaction (Calculated) (80)

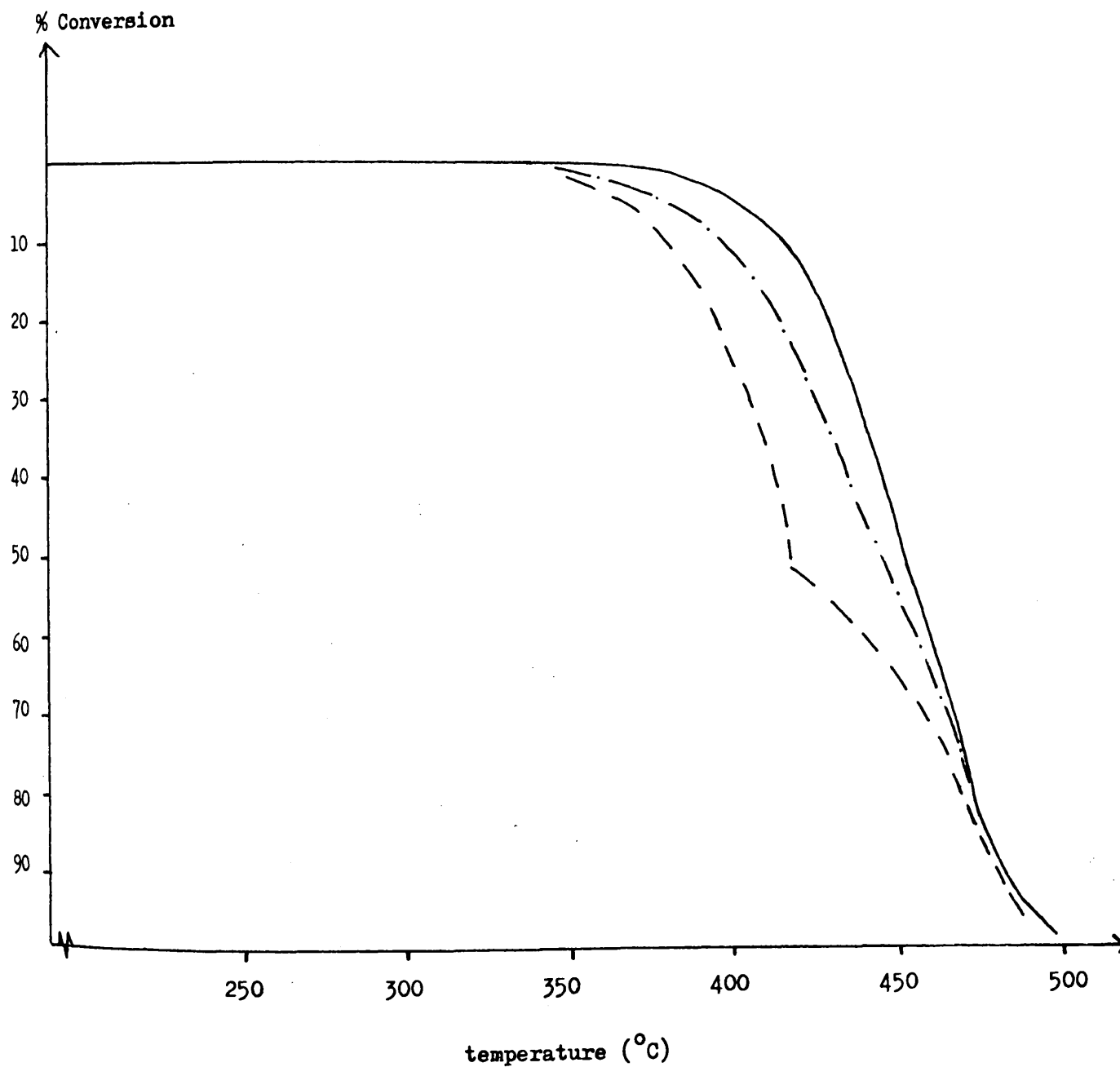


FIGURE 7 - 2

TG RATE CURVES CORRESPONDING TO DEGRADATION UNDER NITROGEN OF THE
BLOCK COPOLYMER, THE 50/50 POLYMER BLEND SYSTEM, AND A
50/50 MIXTURE WITH NO INTERACTION

Heating Rate $10^{\circ}\text{C}/\text{min}$

Key

— 50/50 Block Copolymer

- - - 50/50 Blend System

- · - · 50/50 Mixture With No Interaction (Calculated)

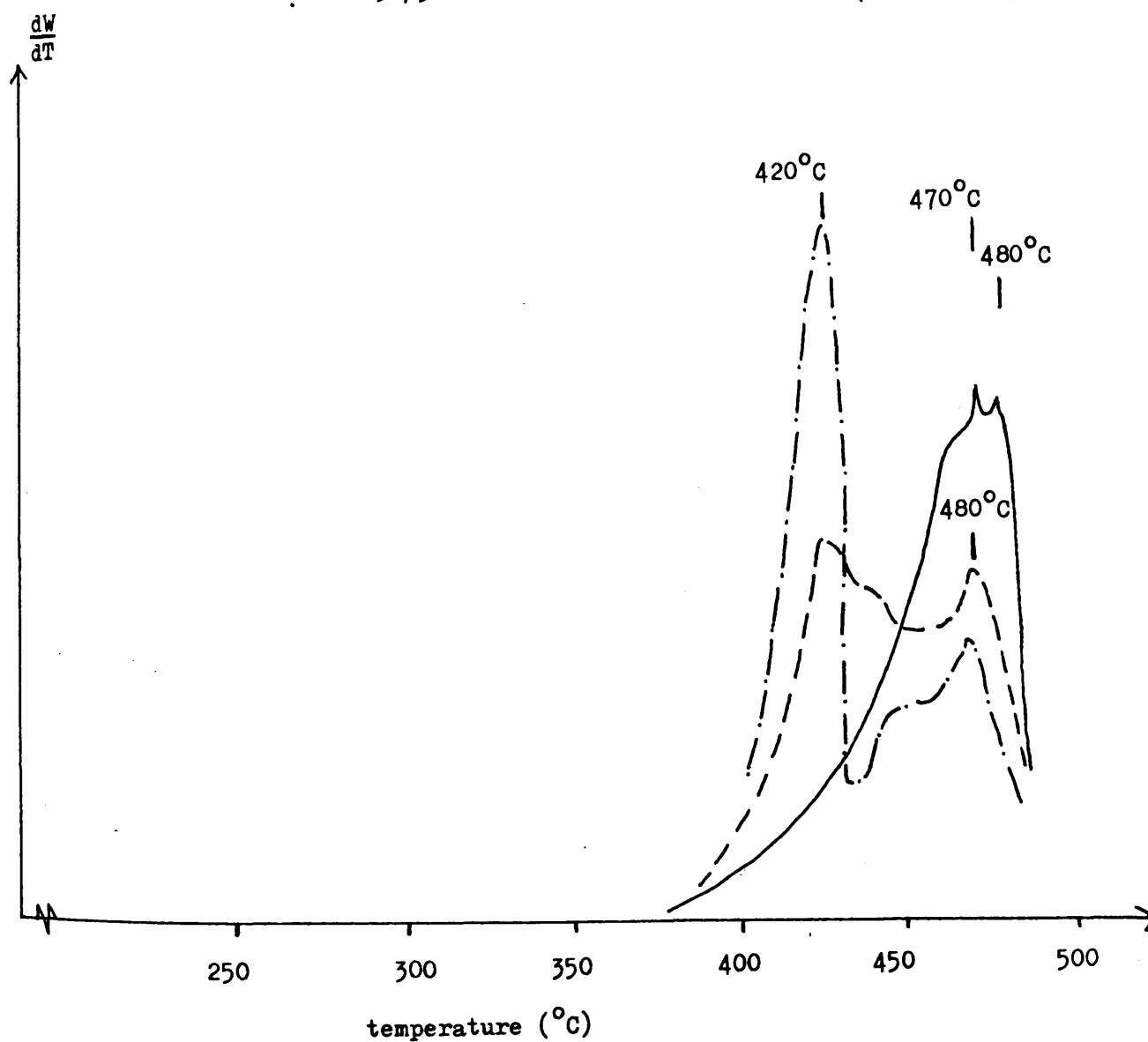


FIGURE 7 - 3

DSC UNDER NITROGEN OF BLOCK COPOLYMER AND POLYMER BLEND SYSTEM

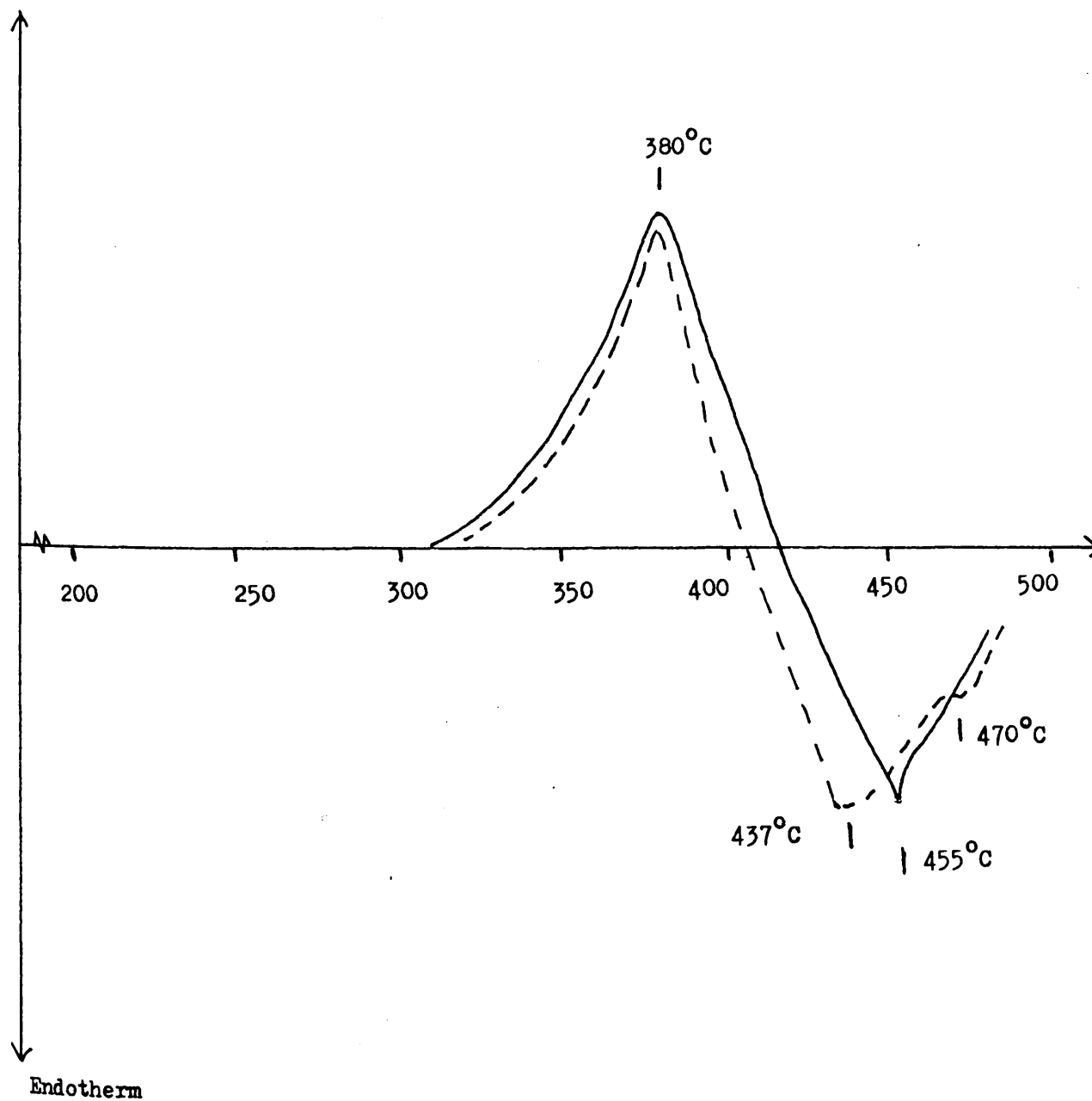
Heating Rate $10^{\circ}\text{C}/\text{min}$

Key

— 50/50 Block Copolymer

- - - 50/50 Polymer Blend (80)

Exotherm



from that obtained using pure rubber. This shows that the polystyrene component of the system does not interfere in this process. The endothermic rate maxima at 437°C and 470°C which can be attributed to volatilisation of the polystyrene and polybutadiene components, respectively, of the blend system are absent in the curve which corresponds to the block copolymer and are replaced by a common rate maximum at 455°C .

A 3 TVA.

The TVA curve produced by programmed degradation at $10^{\circ}\text{C}/\text{min}$ of the block copolymer is shown in fig. 4. From the 0°C curve it can be seen that the evolution of volatile material commences at approximately 310°C and reaches a broad rate maximum at 430°C . It is of interest to note that the TVA curves which correspond to lower trap temperatures are broadened towards higher oven temperatures. This effect is most strikingly observed in the -196°C curve which exhibits a double rate maximum at 440°C and 455°C .

A comparison between the total volatile and noncondensable volatile curves which are produced by programmed degradation of the block copolymer, the polymer blend system, and the system with no interaction, is made in fig. 5.

(i). Total Volatile Material (0°C Curve).

It can be seen that the block copolymer is more stable than the polymer blend system which is in turn more stable than the system with no interaction.

As expected, the system with no interaction displays two distinct rate maxima, at 415°C and 450°C , which correspond to volatilisation of the polystyrene and polybutadiene homopolymers respectively.

In the blend system the low temperature peak is made broader and is shifted to a higher oven temperature (425°C), while

FIGURE 7 - 4

TVA OF BLOCK COPOLYMER

Sample Size 120 mg

Heating Rate 10°C/min

Key

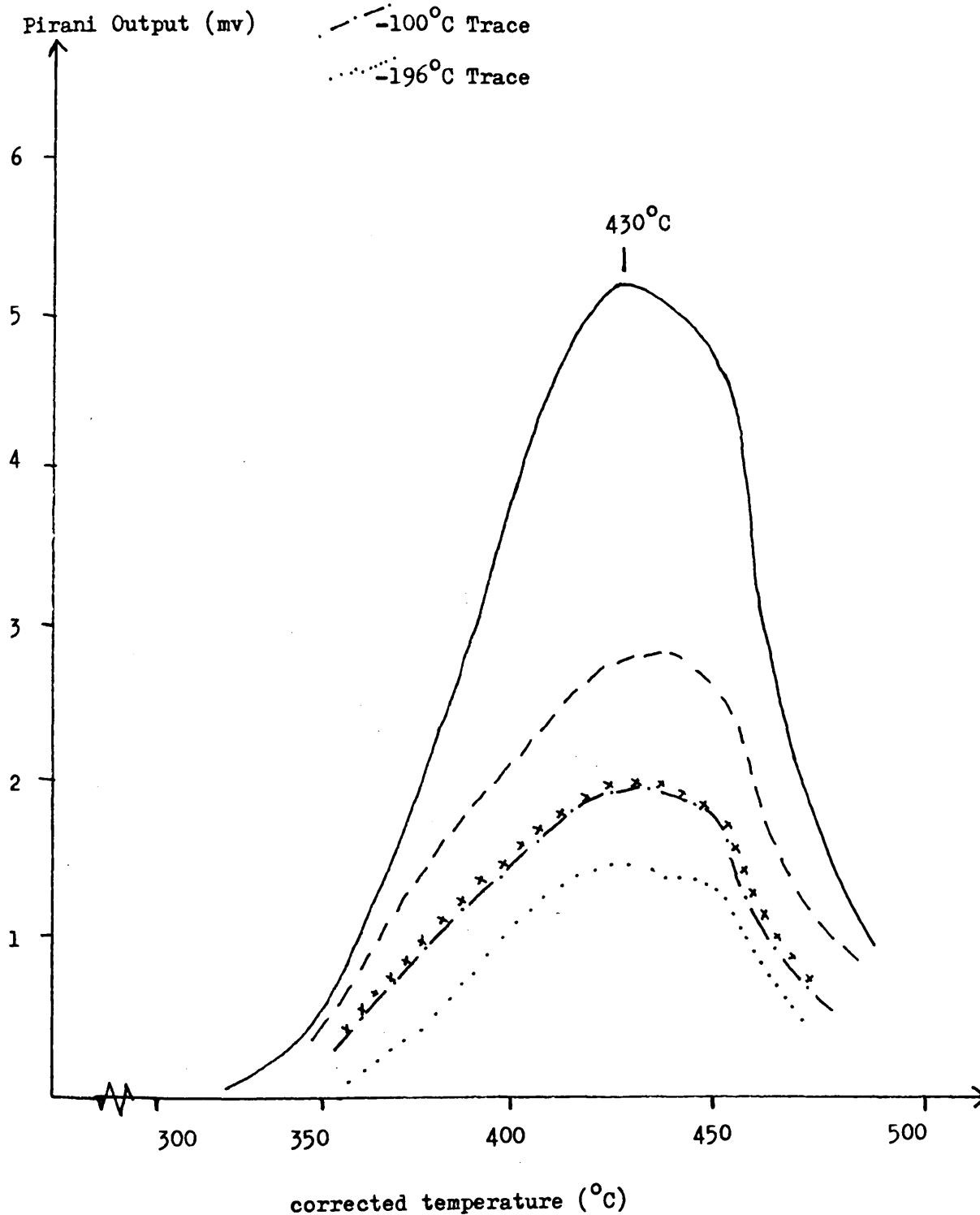
— 0°C Trace

- - - -45°C Trace

x x x -75°C Trace

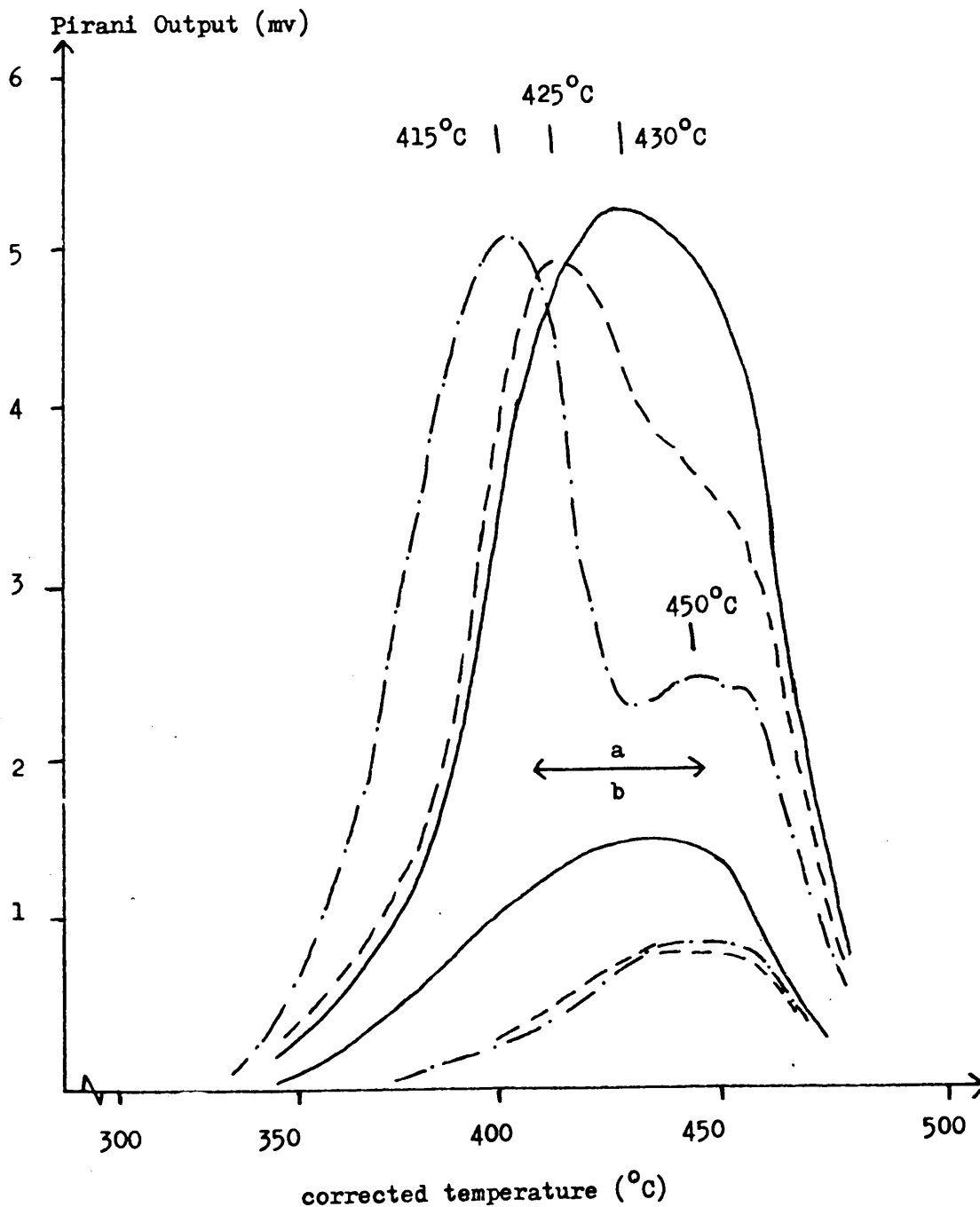
. . . -100°C Trace

... -196°C Trace



COMPARISON BETWEEN TVA TRACES FOR THE BLOCK COPOLYMER, THE 50/50
POLYMER BLEND SYSTEM, AND A 50/50 MIXTURE WITH NO INTERACTION

Key
 --- 50/50 Polymer Blend System (80)
 .-. 50/50 Homopolymer Sample Degraded Unmixed
 In Trouser Tube (103)
 — 50/50 Block Copolymer
 a Total Volatile Material
 b Noncondensable Material



the high temperature peak disappears to be replaced by a high temperature shoulder on the 425°C peak.

All traces of both homopolymer rate maxima are completely absent from the 0°C trace produced by the degradation of the block copolymer and are replaced by the broad symmetric peak already discussed.

(ii). Noncondensable Volatile Material (-196°C Curve).

The shape of the noncondensable emission curve for the blend system is indistinguishable from that produced by rubber homopolymer. On the other hand the curve which corresponds to the block copolymer is broadened towards lower oven temperatures and indicates that noncondensable material is formed in higher yields from the block copolymer than from the systems discussed above.

A 4 ATVA.

ATVA curves which correspond to the polymer blend system and the block copolymer are shown in figs. 6 and 7 respectively.

The shape and position of the ATVA curve which is produced by the blend system is indistinguishable from that for the rubber homopolymer. Using the criteria developed in Chapter 3 it can be shown that hydrogen and other noncondensable material (identified as methane by i.r. spectroscopy) are produced concurrently at a threshold temperature of 350°C to reach a rate maximum of production at 450°C .

As suggested in section A 3 of this chapter, the noncondensable emission curve for the block copolymer achieves two rate maxima one at 440°C and the other at 455°C . Using the same procedure as above both sections of the curve were found to be produced by a mixture of hydrogen and methane.

FIGURE 7 - 6

ATVA OF 50/50 POLYMER BLEND SYSTEM

Sample Size 50 mg - Cast From Toluene

Heating Rate 10°C/min

Sieve Trap At -196°C

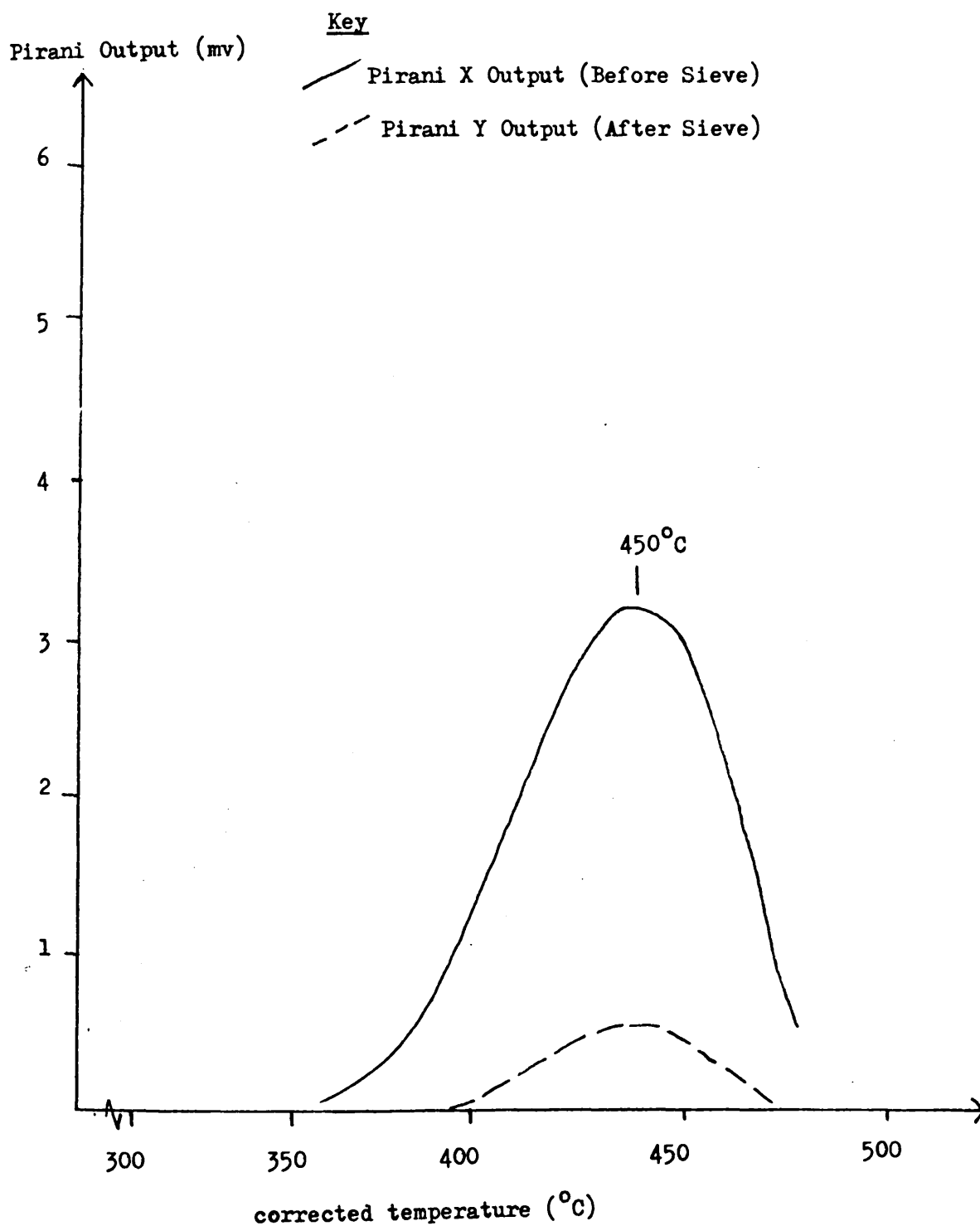


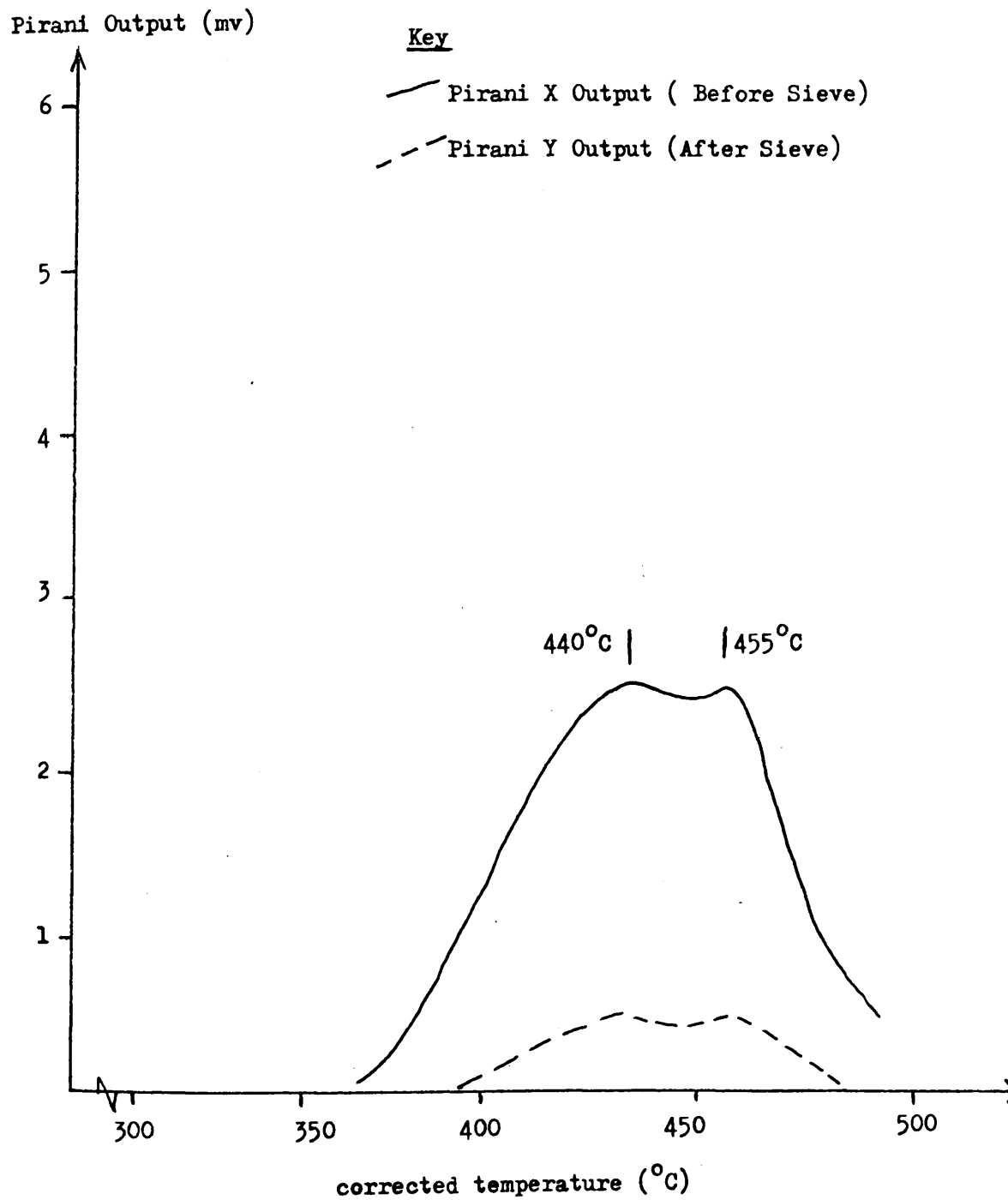
FIGURE 7 - 7

ATVA OF BLOCK COPOLYMER

Sample Size 50 mg

Heating Rate $10^{\circ}\text{C}/\text{min}$

Sieve Trap At -196°C



B VOLATILE PRODUCT FORMATION IN PROGRAMMED DEGRADATIONS.

B 1 SUB-AMBIENT TVA FRACTIONATION OF THE CONDENSABLE VOLATILE PRODUCT FRACTION OF DEGRADATION.

The SATVA curve which corresponds to the condensable volatile product fraction of programmed degradation to completion of the block copolymer is shown in fig. 8. From the shape of the curve it can be seen that the major volatile product of degradation is styrene.

The relatively small quantities of volatile materials which are produced by the degradation of the rubber block are not sufficient to be detected spectroscopically. When the volatile fraction of degradation was examined by n.m.r. spectroscopy, it was shown to consist of styrene (89 mole%) and toluene (11 mole%) along with a small quantity of ethyl benzene.

B 2 YIELDS OF STYRENE DURING PROGRAMMED DEGRADATIONS (BY GLC).

Samples of the block copolymer were degraded under programmed conditions ($10^{\circ}\text{C}/\text{min}$) to predetermined even cut out temperatures, and the corresponding yields of styrene were determined by the application of GLC to the condensable volatile fraction of degradation.

Separations were performed on a 10% microwax on Chromosorb column using toluene as internal reference material under conditions of operation which are outlined in Chapter 8, to produce the cumulative styrene yield plot illustrated in fig. 9.

From the curve it can be seen that the temperature which corresponds to the rate maximum of styrene production is shifted from 415°C (homopolymer styrene) to 440°C .

The situation is complicated by the fact that toluene is present as a product of degradation. If the volume of toluene so produced is assumed to be one tenth of the volume of styrene (Y) - a reasonable assumption, then the volume ratio of styrene/toluene

FIGURE 7 - 8

SUB-AMBIENT TVA CURVE OF VOLATILE PRODUCTS OF PROGRAMMED DEGRADATION TO 500°C
OF BLOCK COPOLYMER

Sample Size 20 mg

Key

- - - (-) Thermocouple
Output

— Pirani Response

* Styrene

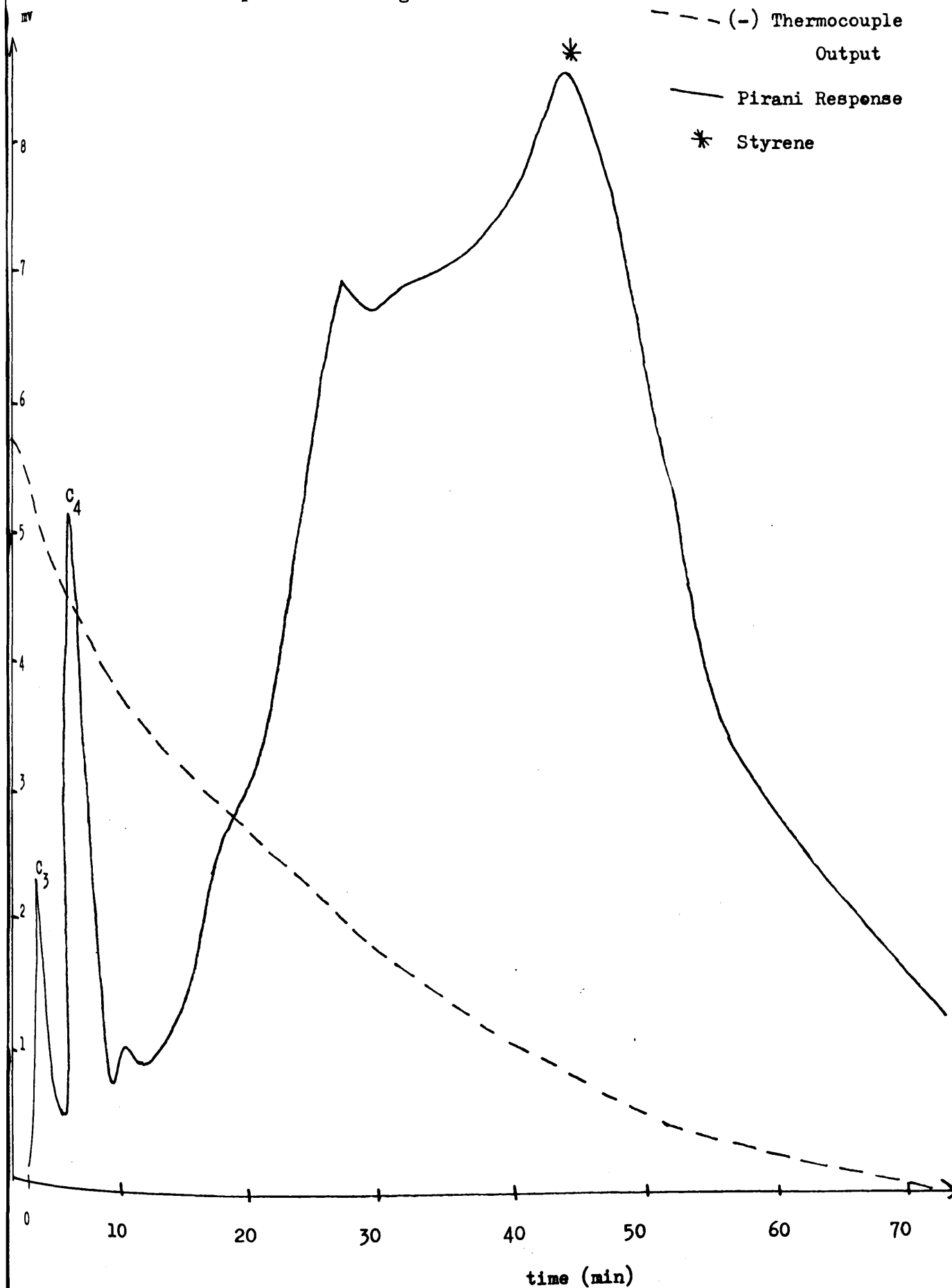


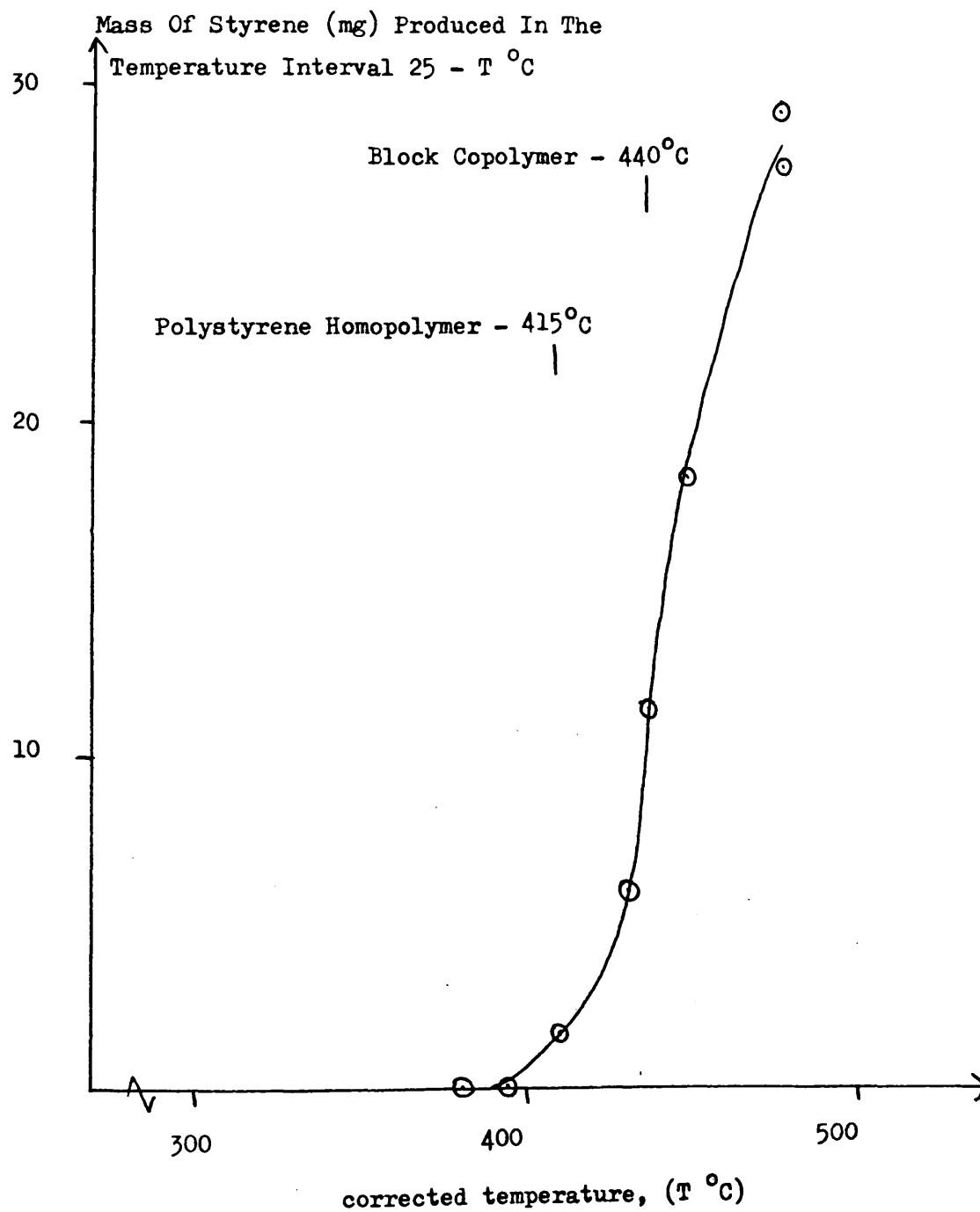
FIGURE 7 - 9

CUMULATIVE STYRENE EMISSION PLOT FOR BLOCK COPOLYMER

Sample Size 150 mg

Heating Rate $10^{\circ}\text{C}/\text{min}$

GLC Reference Material - Toluene



can be rewritten as $\frac{Y}{50 + \frac{Y}{10}}$, where 50 (μ l) is the volume of toluene which is added to the collecting vessel before separation. The relative error in the volume ratio of styrene/toluene can be expressed in the form

$$\frac{\frac{Y}{50} - \frac{Y}{50 + \frac{Y}{10}}}{\frac{Y}{50}}$$

and can be seen to vary from a maximum of 5.5% ($Y = 30 \mu$ l) to a minimum of 0.2% ($Y = 1 \mu$ l).

C COLD RING PRODUCT FRACTION OF PROGRAMMED DEGRADATIONS.

An n.m.r. spectrum which corresponds to the cold ring fraction of programmed degradation to completion of the block copolymer is shown in fig. 10. It can be seen that the spectrum is similar in many ways to that which would be produced by a superposition of the two homopolymer cold ring fraction spectra. For example, the signals at 2.00 δ and 5.30 δ are most probably produced by polybutadiene oligimers which are volatilised during its exothermic decomposition reaction, while the signals at 0.90 δ , 1.25 δ and 1.55 δ are identical to those which are produced by the saturated condensed ring segments which comprise the cold ring fraction of degradation formed in the endothermic decomposition reaction of polybutadiene (Chapter 6).

On first inspection, the aromatic proton signals of fig. 10 would appear to originate from protons contained in the polystyrene cold ring fraction of degradation (Chapter 5). On more detailed inspection it can be seen that this is not the case. Firstly, the corresponding signal at 2.72 δ is greatly reduced from its expected value (see dotted line). Secondly, the corresponding multiplet signal centred on 5.0 δ is completely absent from the spectrum. Finally, the signal at 7.17 δ which is characteristic of the bulk of the polystyrene cold ring fraction of degradation is accompanied by a stronger broad signal at 7.10 δ . From the above it would appear that the bulk of the aromatic material in the sample is best associated with the polybutadiene portion of the polymer.

In order to clarify the situation, a sample of the above material was subjected to preparative thin layer chromatography using n - hexane and the fractions so produced were examined by n.m.r. spectroscopy. The results of this experiment can be inspected in figs. 11a, b and c.

The n.m.r. spectrum produced by F_2 is consistent with that of the major component of the normal polystyrene cold ring fraction of degradation (Chapter 5). All other spectra are, however, best assigned to material which originates in the polybutadiene polymer block. The spectra which correspond to F_1 , F_3 and especially F_4 , are best assigned to condensed ring structures with a high loading of isolated aromatic groups, while the spectra of F_5 and F_6 (which correspond to the bulk of the mixture) show that they also are partially aromatised. It is of interest to note that aromaticity is not detected in the cold ring fraction of polybutadiene degradation. (Chapter 6).

FIGURE 7 - 10

n.m.r. SPECTRUM OF COLD RING FRACTION OF PROGRAMMED DEGRADATION AT
10°C/min TO 500°C OF BLOCK COPOLYMER

Solvent C Cl₄

Lock TMS

Sample Size 50 mg

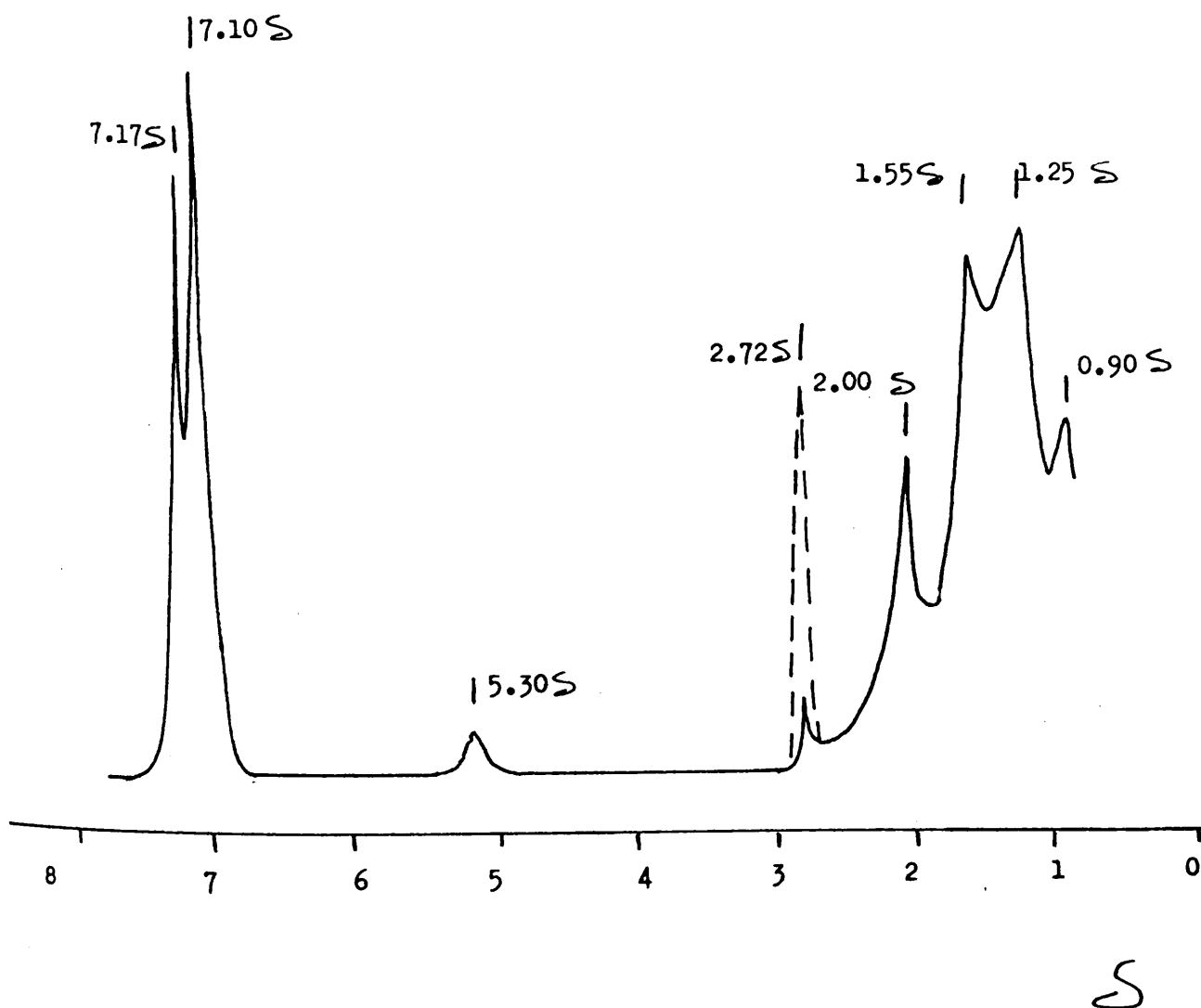


FIGURE 7 - 11a

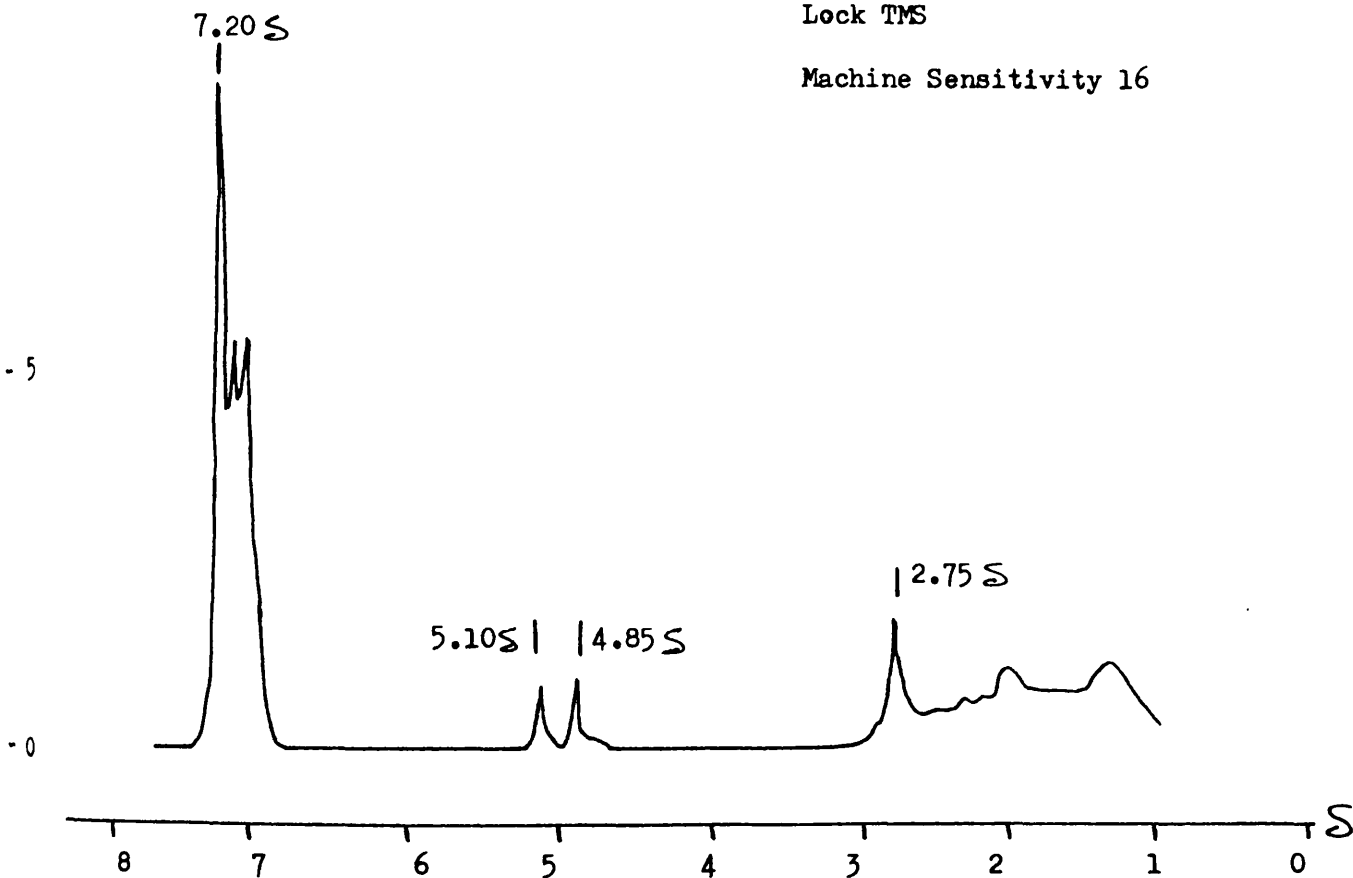
n.m.r. SPECTRA OF COLD RING FRACTION OF PROGRAMMED DEGRADATION AT $10^{\circ}\text{C}/\text{min}$
TO 500°C OF BLOCK COPOLYMER AFTER SEPARATION BY PREPARATIVE TLC

F₂

Solvent C Cl₄

Lock TMS

Machine Sensitivity 16



F₁

Solvent C Cl₄

Lock TMS

Machine Sensitivity 32

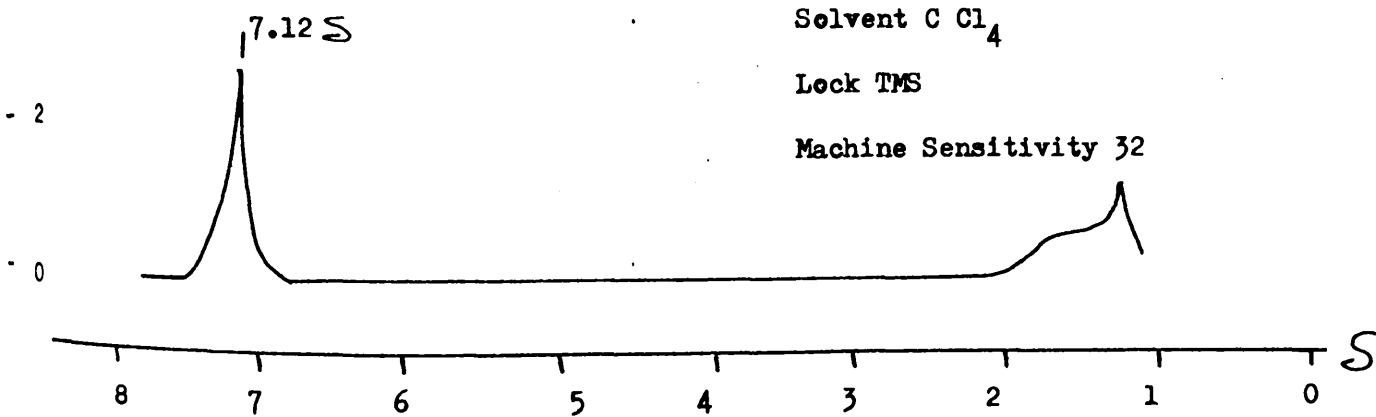


FIGURE 7 - 11b

n.m.r. SPECTRA OF COLD RING FRACTION OF PROGRAMMED DEGRADATION AT $10^{\circ}\text{C}/\text{min}$
TO 500°C OF BLOCK COPOLYMER AFTER SEPARATION BY PREPARATIVE TLC

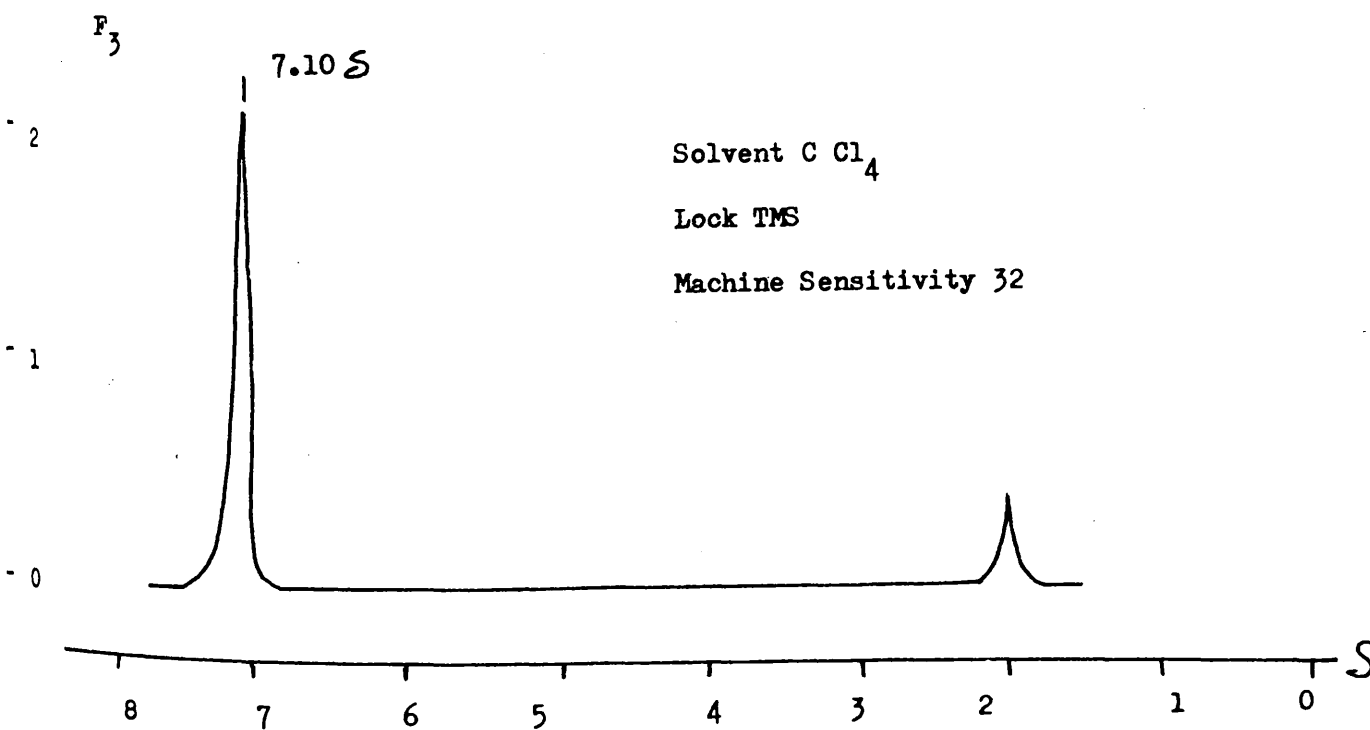
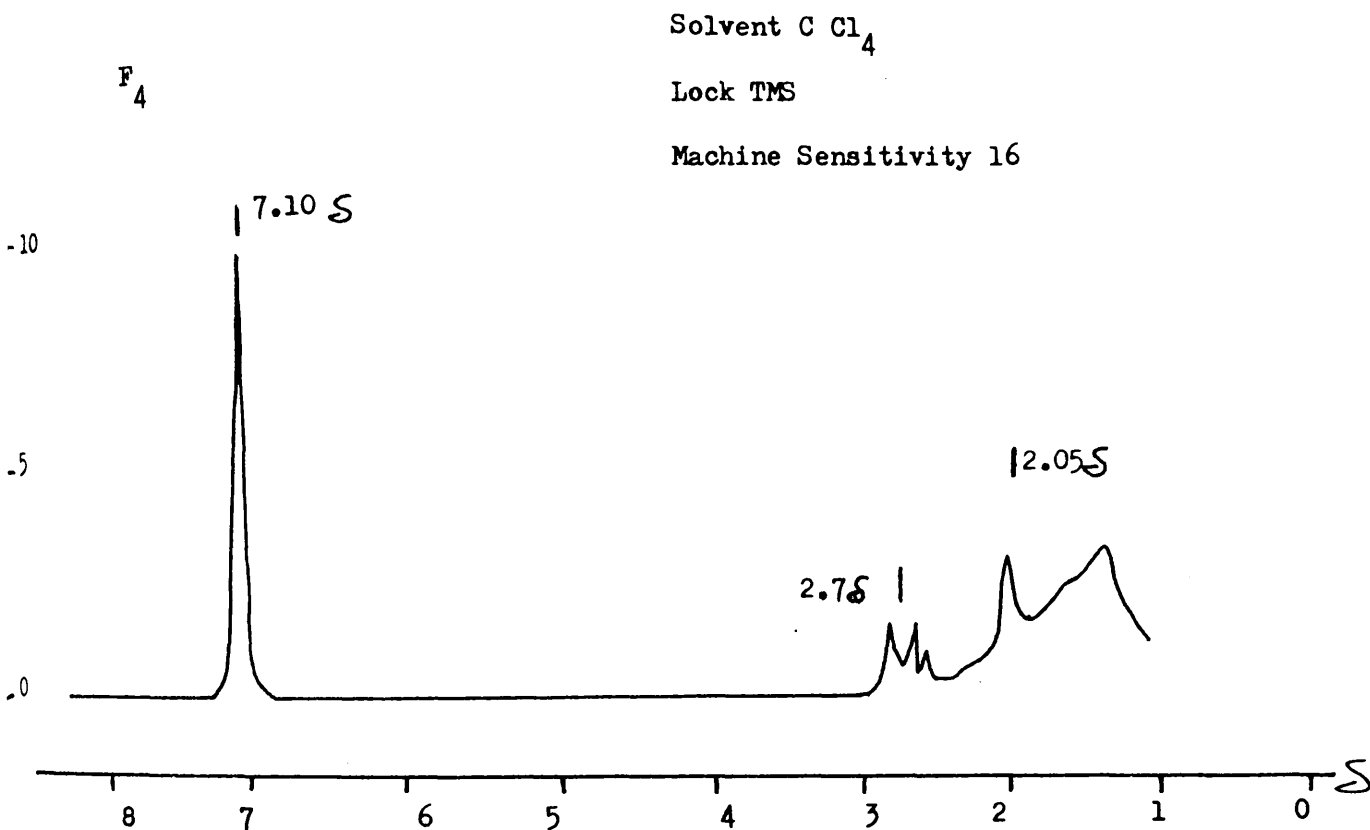
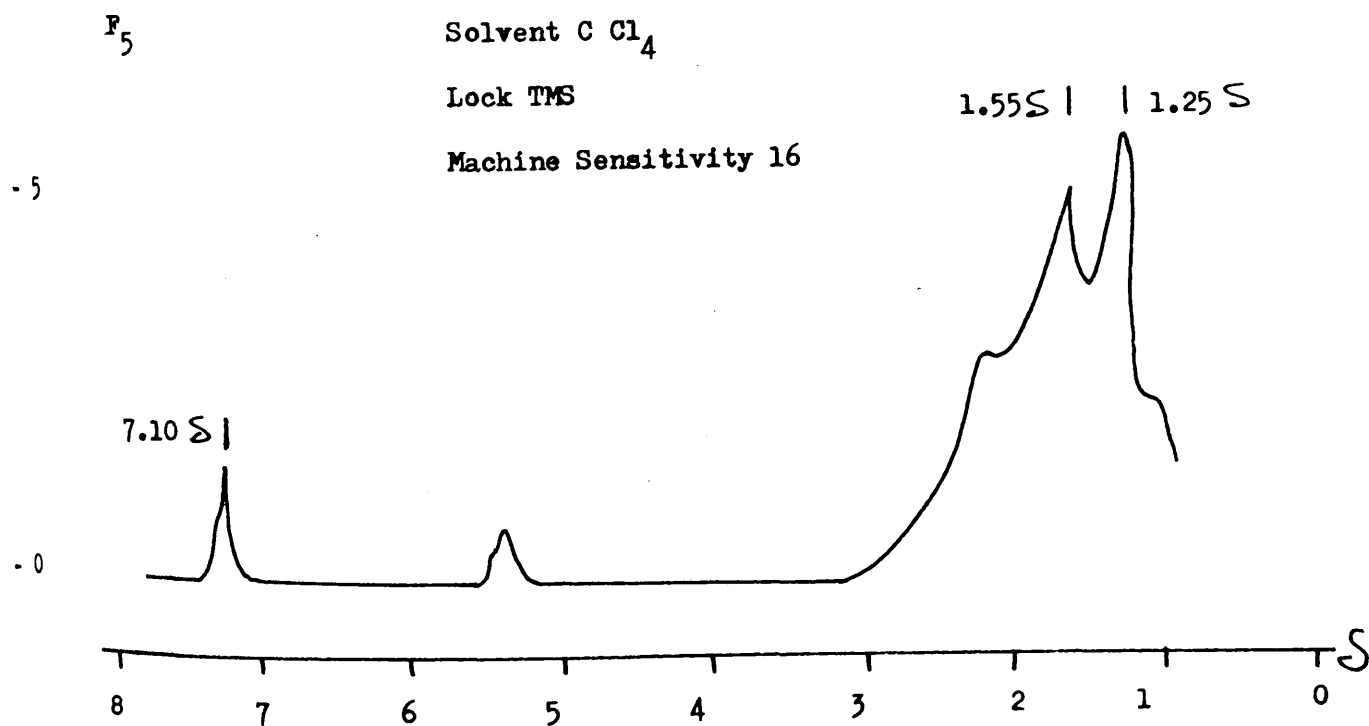
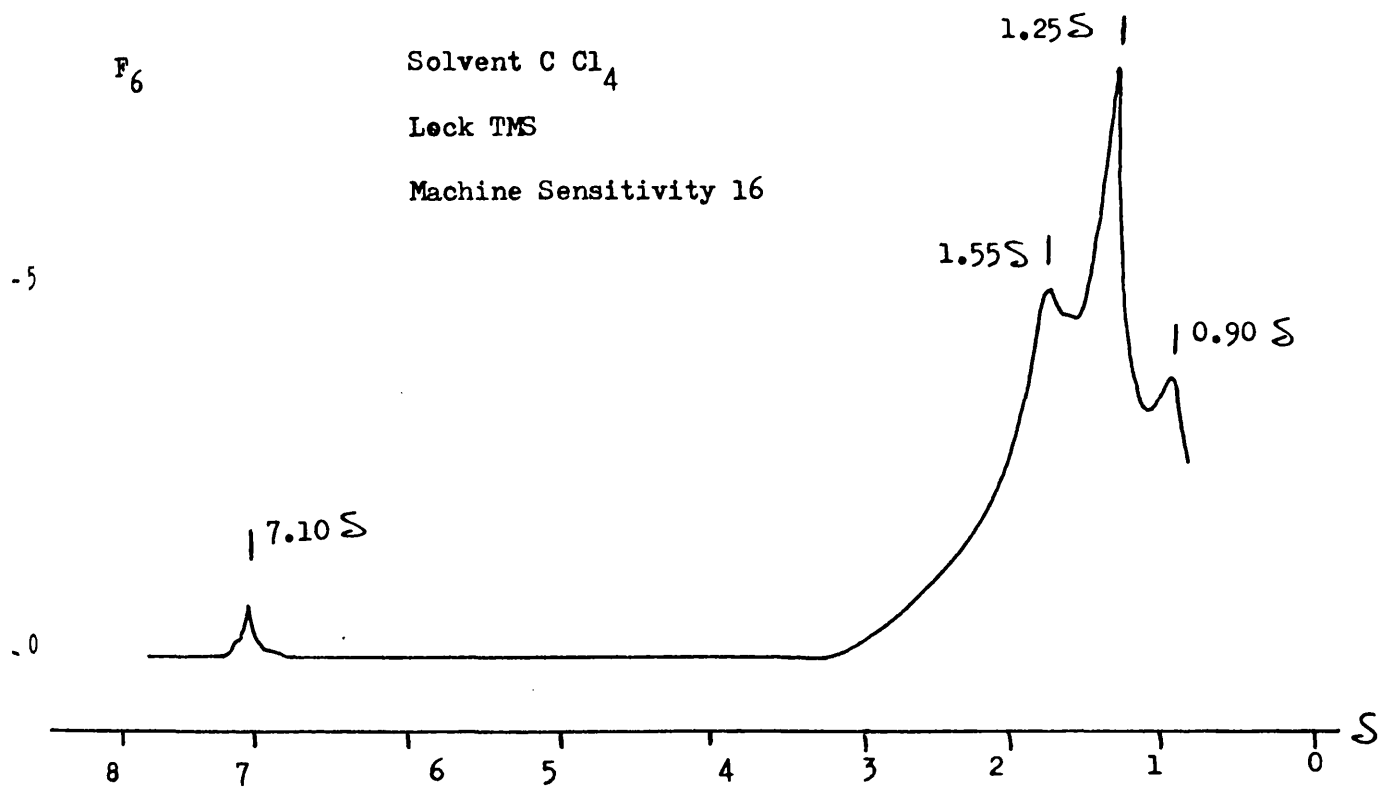


FIGURE 7 - 11c

n.m.r. SPECTRA OF COLD RING FRACTION OF PROGRAMMED DEGRADATION AT 10°C/min
TO 500°C OF BLOCK COPOLYMER AFTER SEPARATION BY PREPARATIVE TLC



D RESIDUE OF PROGRAMMED DEGRADATION TO 450°C.

A sample of the block copolymer was partially volatilised by warming it under vacuum to 450°C at 10°C/min. The residue of degradation and its soluble fraction were then analysed by i.r. and n.m.r. spectroscopy respectively (fig. 12).

As expected, the i.r. spectrum shows the material to be composed of a mixture of polystyrene and cyclised polybutadiene.

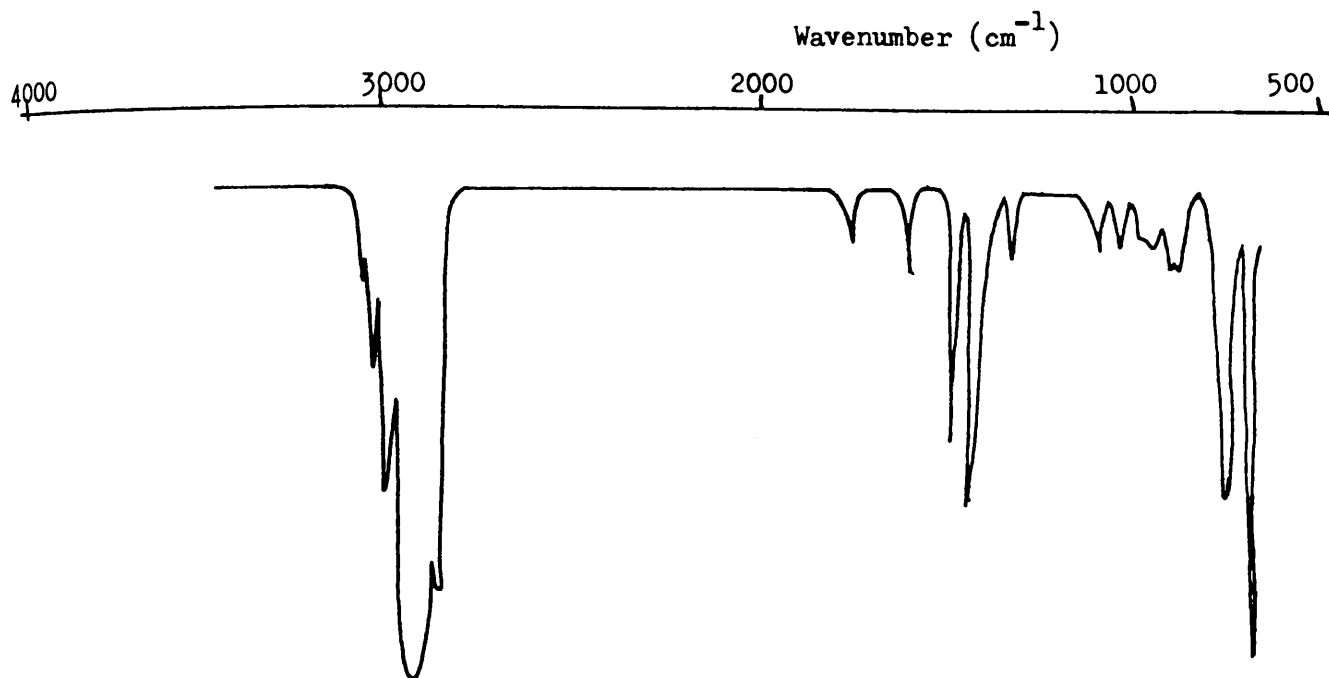
The n.m.r. spectrum confirms that polystyrene is present in the residue at 450°C and shows that a fraction of the cyclised polybutadiene is soluble.

FIGURE 7 - 12

SPECTRA OF THE RESIDUE OF ISOTHERMAL DEGRADATION AT 380°C FOR 1 hr
AND OF PROGRAMMED DEGRADATION AT 10°C/min TO 450°C OF

BLOCK COPOLYMER

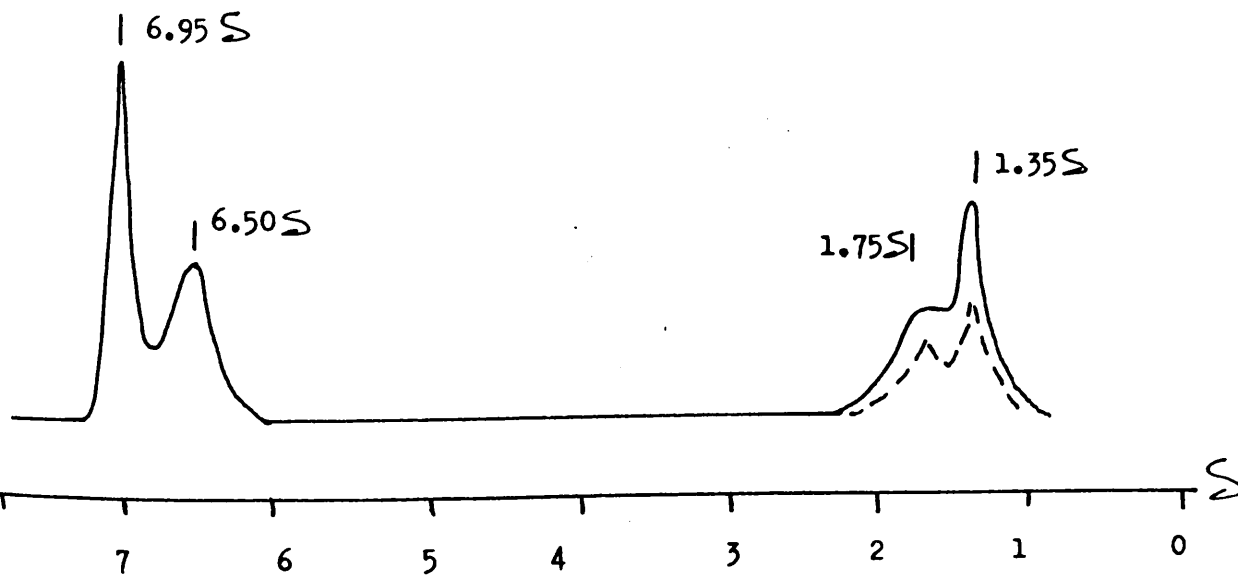
i.r. Spectrum (K Br Disc)



n.m.r. SPECTRUM OF SOLUBLE FRACTION OF RESIDUES AFTER EXTRACTION AND
FILTRATION

Solvent C Cl_4

Lock TMS



E DISCUSSION.

The TG curves of fig. 1 indicate that the block copolymer is more stable with respect to the volatilisation process than either the blend system or the system with no interaction. This behaviour was reflected in the TG rate curve of fig. 2 which suggested that the extra stability is due to a suppression of volatilisation of the polystyrene component of the system. The shapes of both the TG rate curve and the DSC curve for the material suggest that the polystyrene and polybutadiene components degrade in concert.

The extra stability of the system and the concerted nature of the volatilisation process is confirmed by the shape and position of the TVA curve for the polymer (figs. 4, 5) While the ATVA curve for the material (fig. 7) shows that the polybutadiene portion of the system has been destabilised with respect to the reaction forming noncondensables, which has developed a low temperature rate maximum at 440°C.

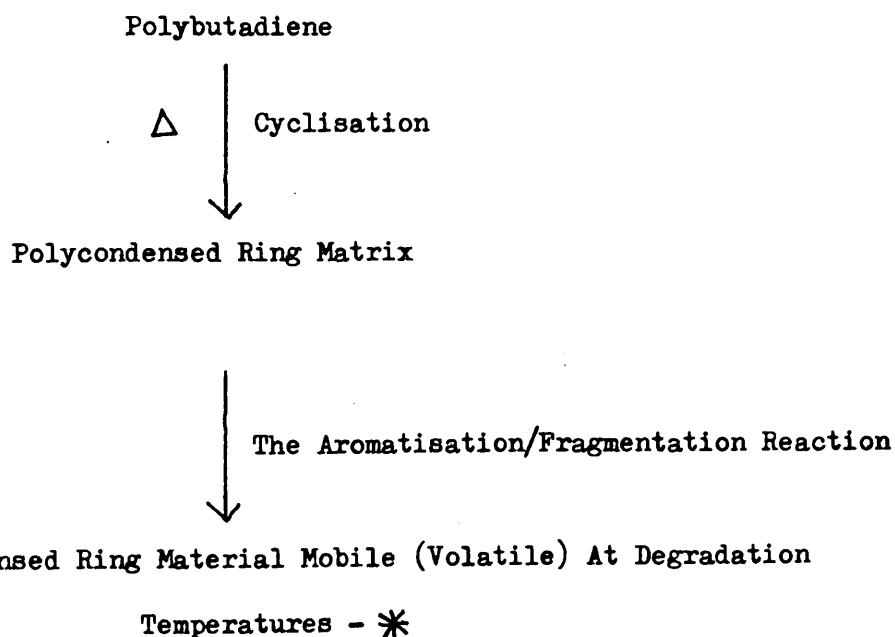
More direct evidence to show that the polystyrene component of the system is stabilised can be obtained by analysis of the residue of programmed degradation to 450°C (fig. 12) - a temperature at which polystyrene homopolymer is completely volatilised under vacuum. Such work shows that a considerable quantity of polystyrene is present in the residue of degradation at this temperature. This behaviour is also reflected in the styrene evolution curve for the material (fig. 9) which shows that the production of styrene is completely suppressed until the system reaches 400°C after which it is evolved to reach a rate maximum of production at 440°C.

In conclusion it must be noted, firstly, that the cold ring fraction of degradation to completion of the polybutadiene portion of the block copolymer, in contrast to its homopolymer analogue, contains a large proportion of aromatic material. Secondly, it

must be noted that the volatile product fraction produced in the polystyrene portion of the block copolymer contains a (relatively) massive quantity of toluene and ethyl benzene.

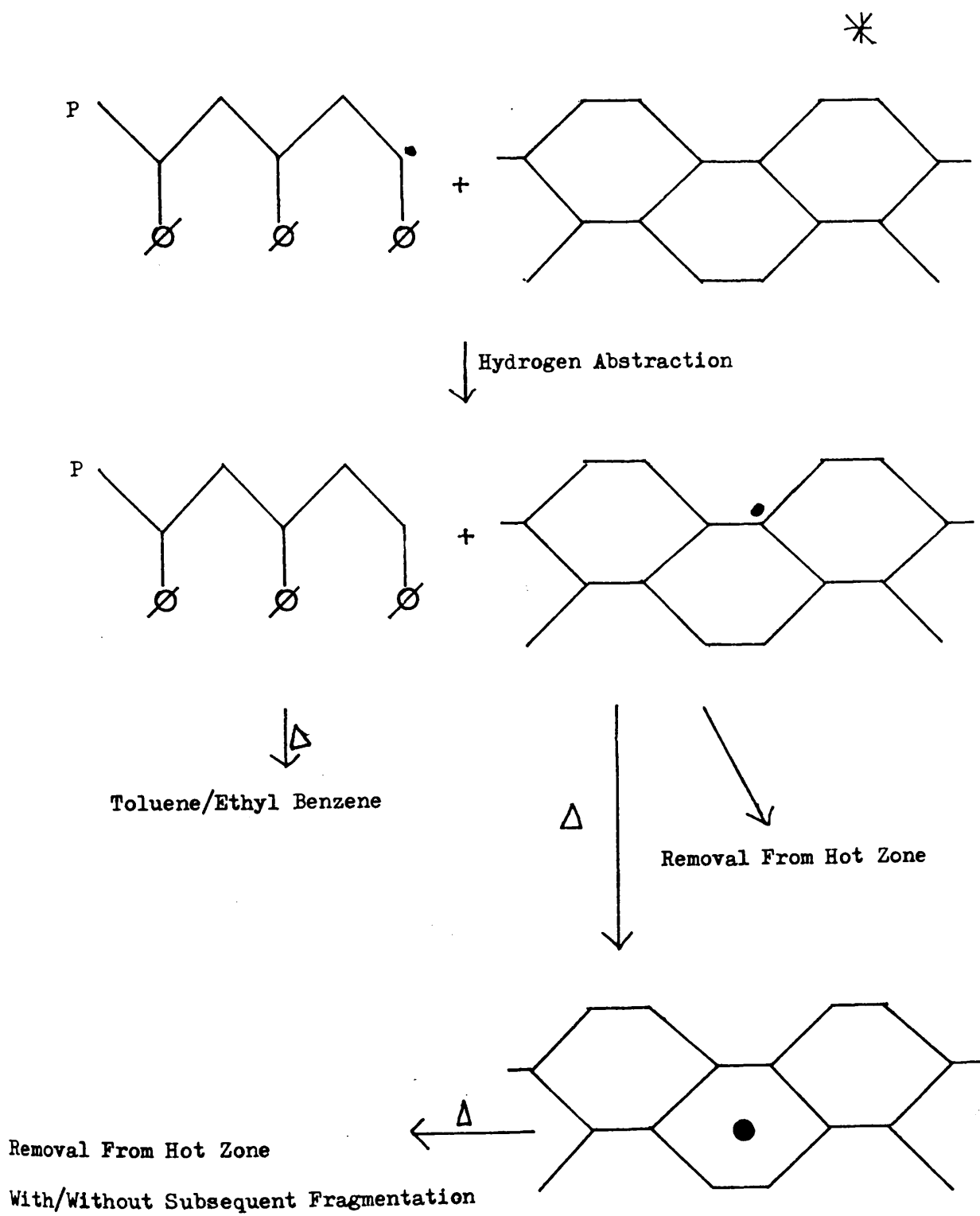
The above observations have been used as evidence in support of the existence of the following proposed interactive process which is assumed to be operative in the temperature range in which polycyclic cold ring material is produced in quantity. Additional mechanisms of stabilisation which are operative at low temperatures ($< 400^{\circ}\text{C}$) will be discussed in section II of this chapter.

(i).



(P = Polystyrene Residue)

(ii).



It has been shown in Chapter 9 that the saturated polycyclic material which comprises the polybutadiene cold ring fraction of degradation at high temperatures is capable of terminating polystyrene radicals by a chain transfer process. The close agreement between the temperatures which correspond to the rate maximum of formation of styrene (or radical centres in the polystyrene) and noncondensable material (440°C), support the existence of a subsequent aromatisation reaction. The condensed ring aromatic groupings which are detected in the cold ring fraction of degradation most probably arise from the product fraction of the reaction which is volatilised before it can fragment.

7 II ISOTHERMAL DEGRADATION AT 380°C.

A 1 ISOTHERMAL TG UNDER NITROGEN.

A TG curve which corresponds to isothermal degradation at 380°C of the block copolymer is shown in fig. 13 . It can be seen that the expected extra stability of the system with respect to its conversion to material volatile at degradation temperatures is operative over a prolonged time period. This suggests that the stabilising processes proposed by McNeill et al (80) are accompanied by other such processes which are operative throughout the decomposition reaction at this temperature.

A 2 ISOTHERMAL TVA.

Isothermal TVA curves at 380°C which correspond to the emission of volatile material from the block copolymer, the polymer blend system and the system with no interaction are shown in fig. 14. As expected, the block copolymer is more stable with respect to this process than either of the other two systems. The (massive) degree of stability imparted to the system and the (long) time period over which it is operative support the observation which is made in A 1 (above).

A 3 GRAVIMETRIC ANALYSIS UNDER VACUUM.

In semi-quantitative terms the cold ring fraction of degradation of the block copolymer can be assigned to the polybutadiene portion of the system, while the volatile fraction of degradation can be assigned to the polystyrene portion of the system, if both assignments are made on a weight% basis. Gravimetric conversion curves which relate to the formation of volatile and cold ring material could therefore be used as a probe to determine which if any of the two components of the system was subject to stabilisation with

respect to the volatilisation process.

To this end, samples of the block copolymer were degraded under vacuum in the experiment described in Chapter 5 Section D 1, and the mass% conversion to cold ring and volatile material was estimated gravimetrically. The results of this experiment are shown in fig. 15 . It can be seen that the system is stabilised with respect to the formation of volatile material but not to the formation of cold ring material. This suggests that, as expected, the extra stability is associated with the polystyrene component of the system.

ISOTHERMAL TG AT 380°C UNDER NITROGEN OF BLOCK COPOLYMER

Key

1 50/50 Block Copolymer - 6 mg

2 50/50 Mixture With No Interaction (Calculated)

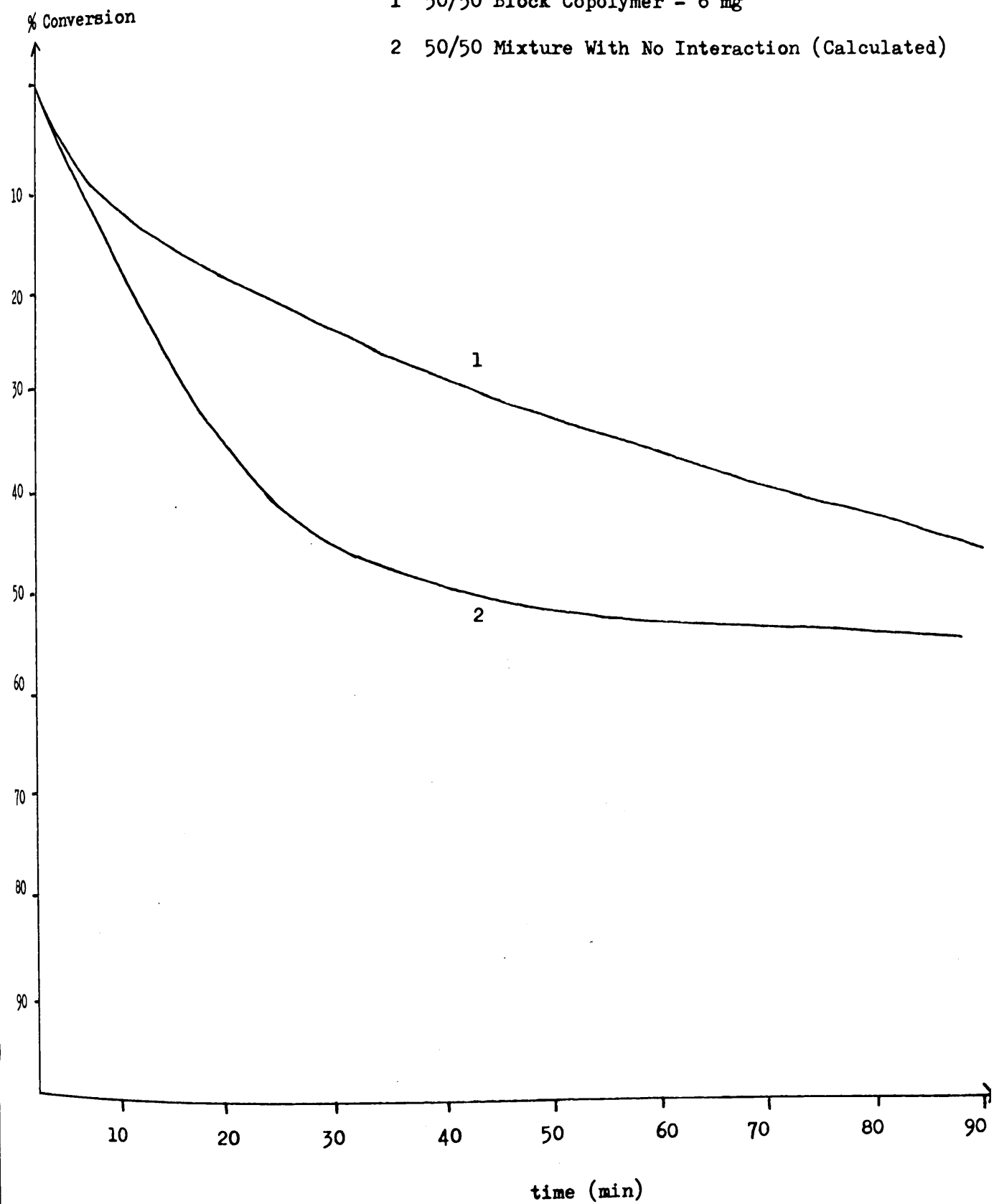
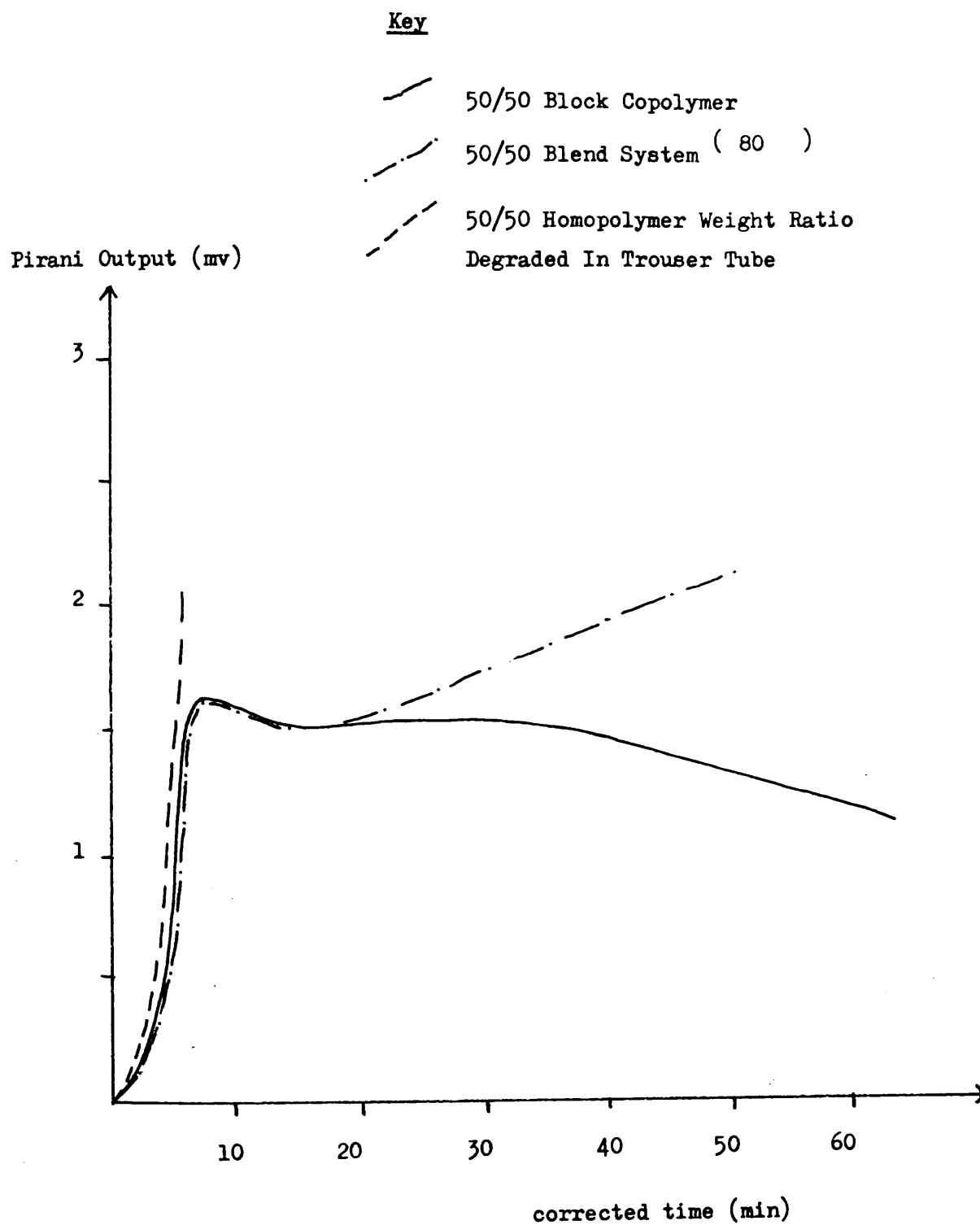
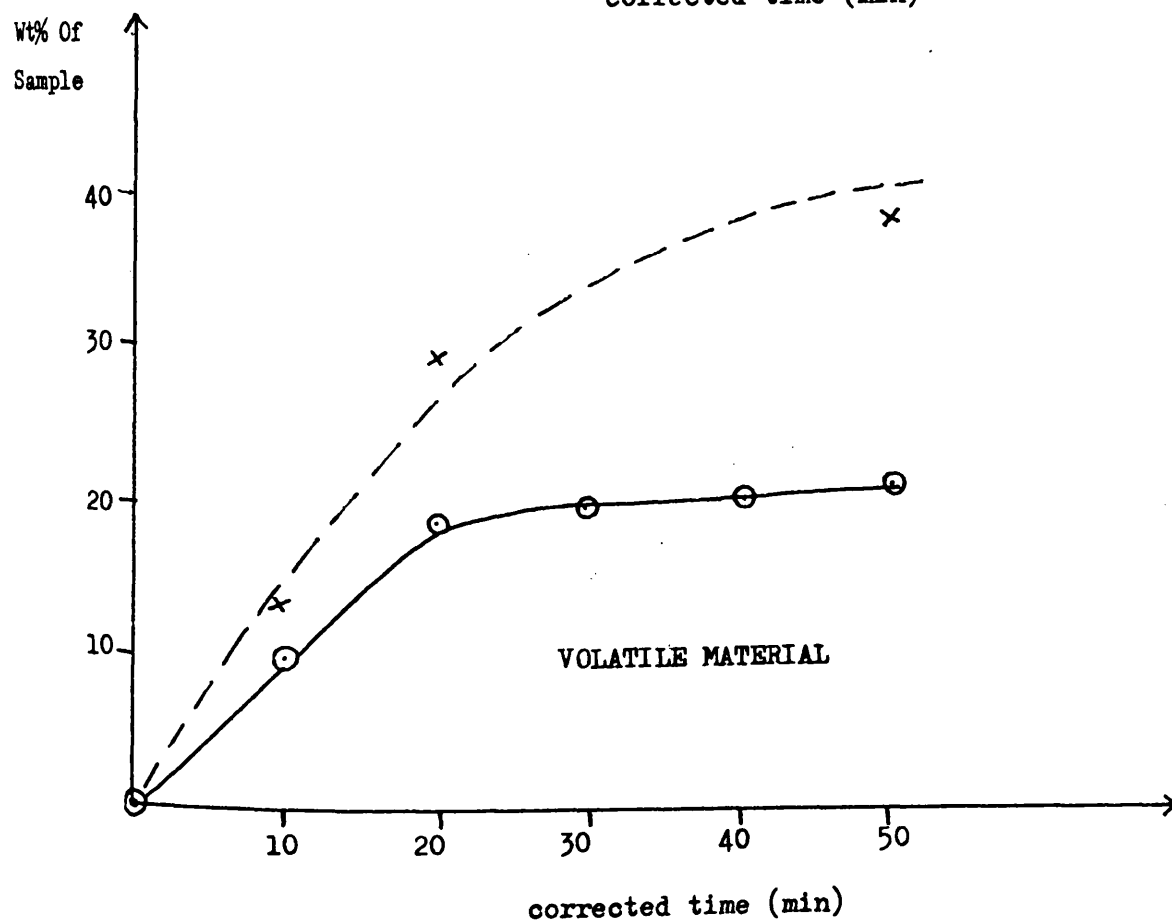


FIGURE 7 - 14

ISOTHERMAL TVA AT 380°C OF BLOCK COPOLYMER, 50/50 POLYMER BLEND SYSTEM
AND 50/50 MIXTURE WITH NO INTERACTION



ISOTHERMAL CONVERSION CURVES AT 380°C TO COLD RING AND VOLATILE MATERIAL
FOR BLOCK COPOLYMER UNDER VACUUM



B VOLATILE PRODUCTS OF ISOTHERMAL DEGRADATION AT 380°C.

The condensable volatile product fraction of degradation at 380°C for one hour was collected and subjected to fractionation by sub-ambient TVA to yield the pressure curve shown in fig. 16 . Liquefiable products of degradation - the material which corresponds to peak "A" - were examined by n.m.r. spectroscopy and shown to consist of a mixture of styrene (92 mole%) and toluene (8 mole%).

The volatile products of isothermal degradation at 380°C which are produced in the time intervals 0 - 15 min, 15 - 30 min, 30 - 45 min, and 45 - 60 min were collected separately and analysed consecutively by the sub-ambient TVA technique using the procedure developed in Chapter 6. The results of this experiment are shown in figs. 17, 18, 19 and 20 . Components of the mixtures were labelled by the use of i.r. and n.m.r. spectroscopy.

It can be seen that the production of styrene is almost completely suppressed in the time period (0 - 15 min) in which the polybutadiene portion of the polymer is subject to the exothermic cyclisation/depolymerisation reaction. After this process has been completed styrene begins to be evolved from the polymer though at a rate smaller than that which is expected of unstabilised polystyrene at this temperature.

FIGURE 7 - 16

SUB-AMBIENT TVA OF VOLATILE PRODUCTS OF ISOTHERMAL DEGRADATION AT 380°C
FOR 1 hr OF BLOCK COPOLYMER

Key

— Pirani Response

- - - (-) Thermocouple Output

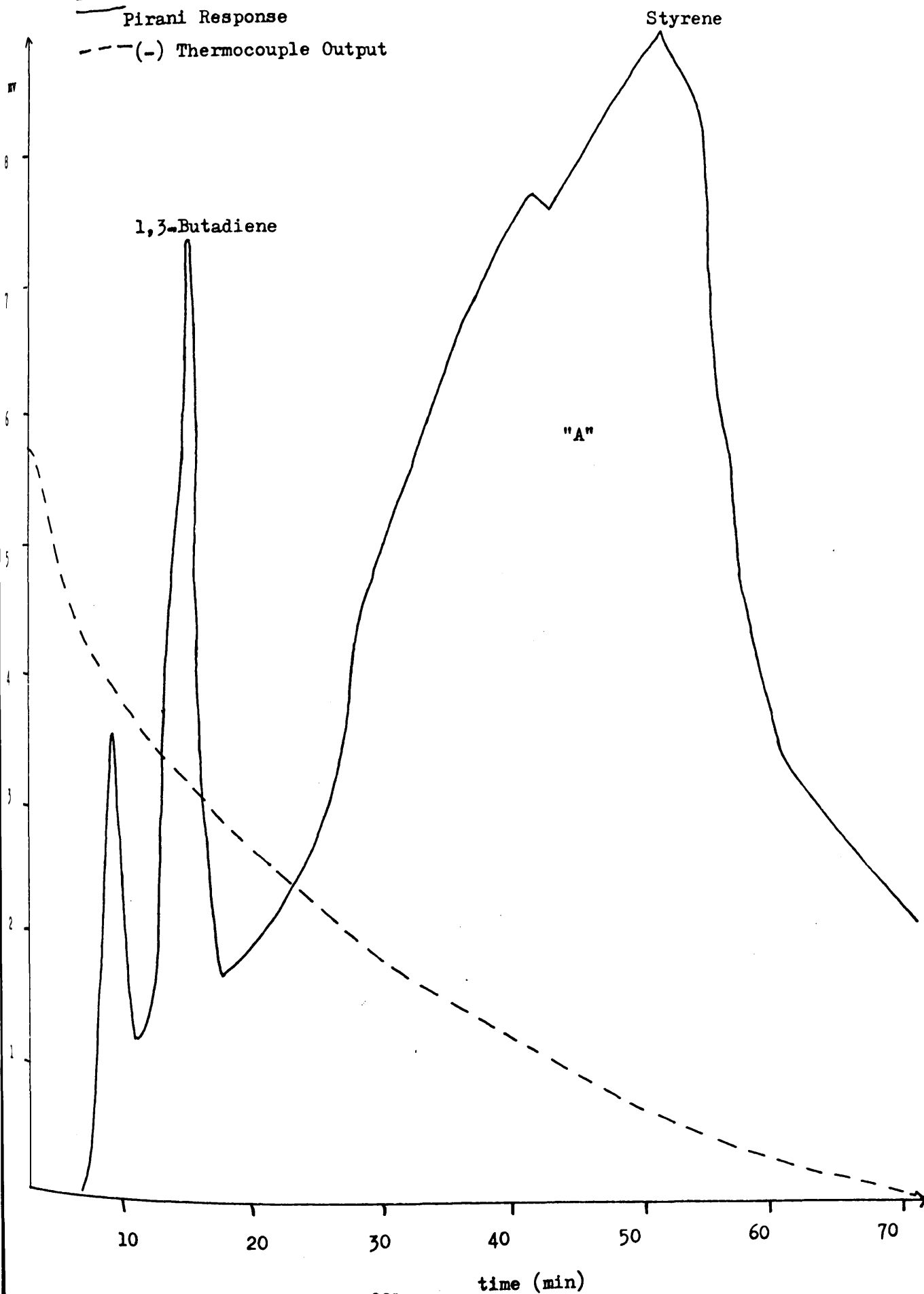


FIGURE 7 - 17

SUB-AMBIENT TVA OF VOLATILE PRODUCTS OF ISOTHERMAL DEGRADATION AT 380°C
OF BLOCK COPOLYMER, 0 - 15 min

Key

— Pirani Response - 50 mg Sample 50/50 Block Copolymer

--- Pirani Response - 25 mg Sample Polystyrene (0 - 15 min)

- - - (-) Thermocouple Output

1 1,3-Butadiene

2 4-Vinylcyclohexene

3 Styrene

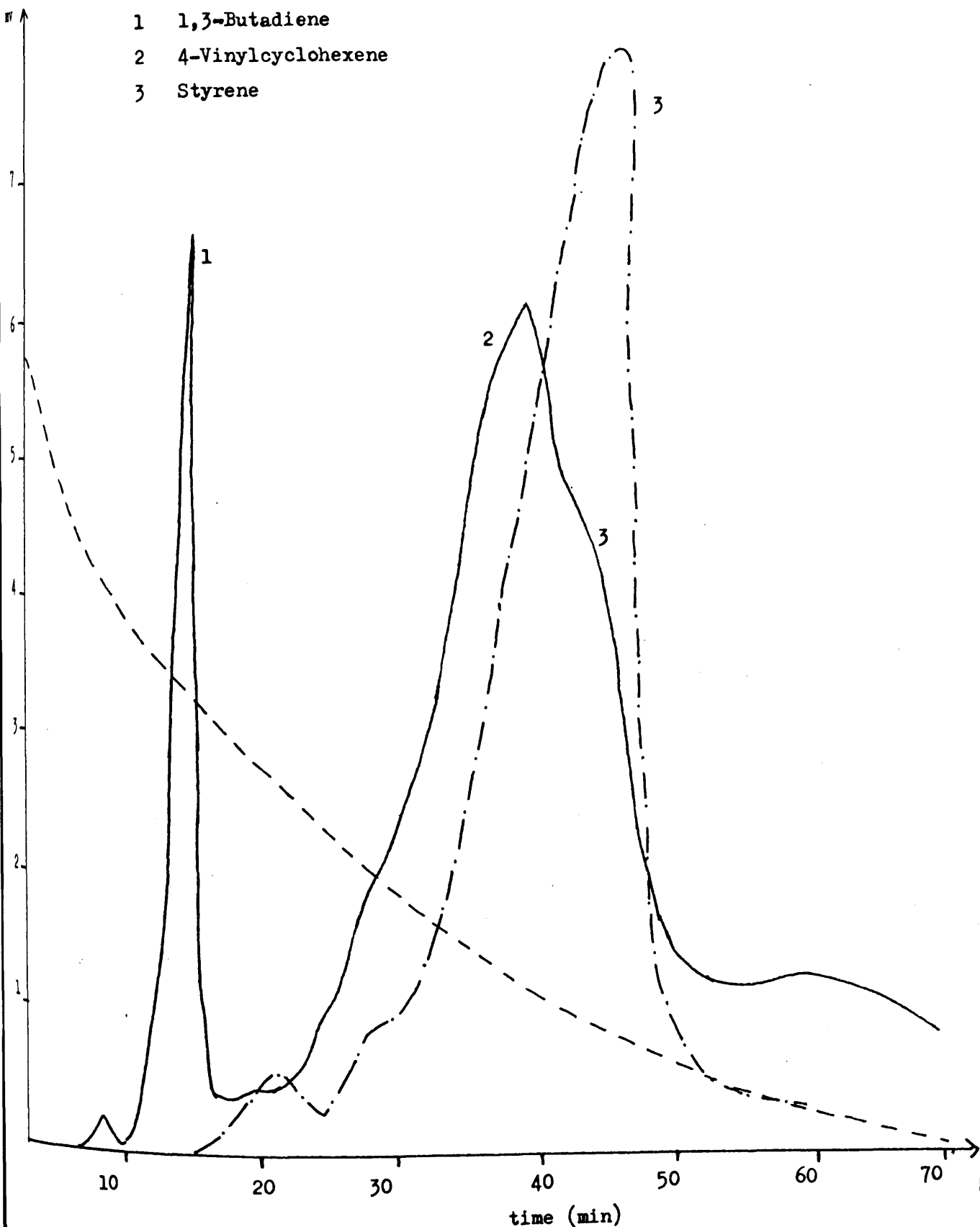


FIGURE 7 - 18

SUB-AMBIENT TVA OF VOLATILE PRODUCTS OF ISOTHERMAL DEGRADATION AT 380°C
OF BLOCK COPOLYMER, 15 - 30 min

Sample Size 50 mg

Key

— Pirani Response

- - - (-) Thermocouple Output

- 1 1,3-Butadiene
- 2 4-Vinylcyclohexene
- 3 Styrene

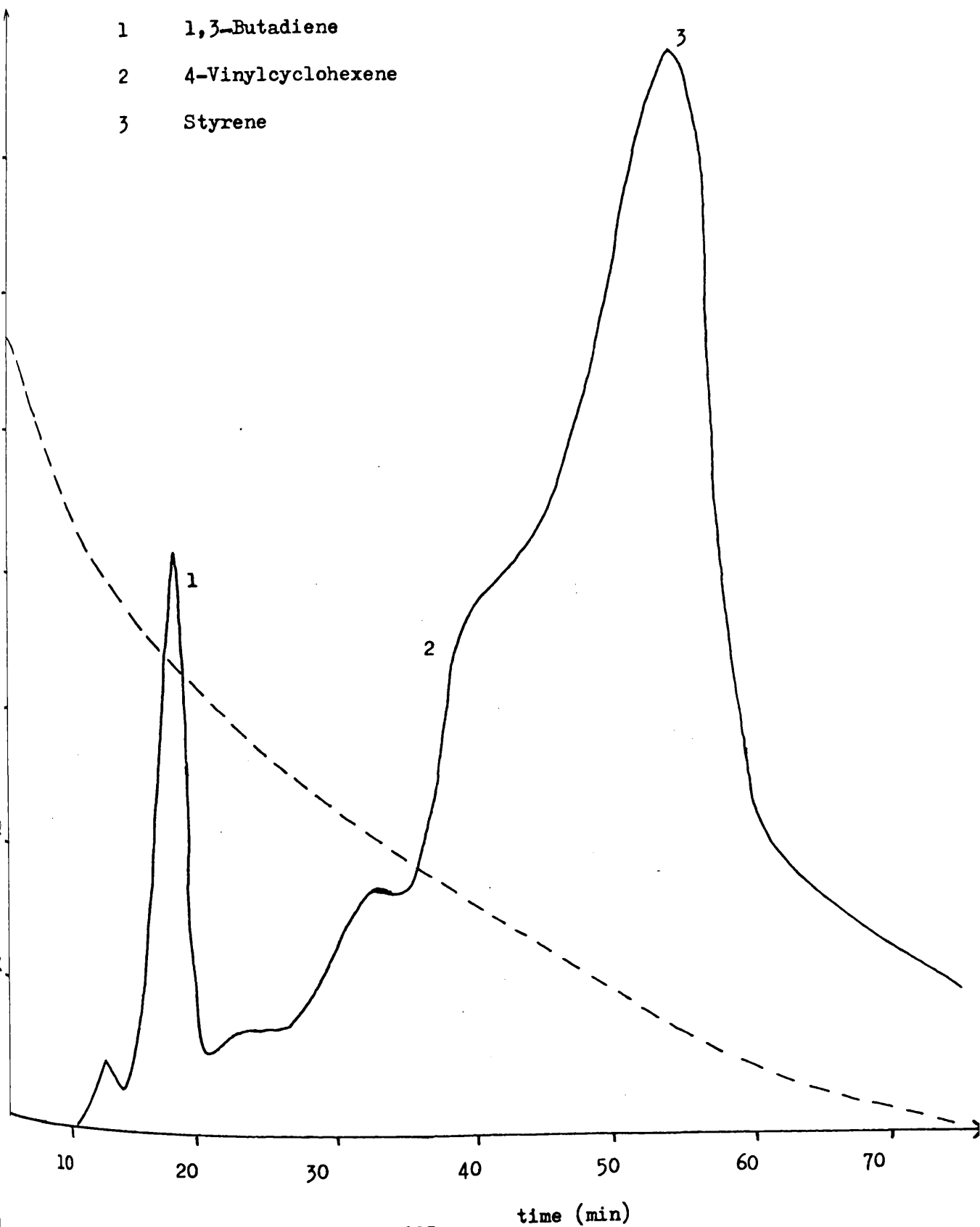


FIGURE 7 - 19

SUB-AMBIENT TVA OF VOLATILE PRODUCTS OF ISOTHERMAL DEGRADATION AT 380°C
OF BLOCK COPOLYMER, 30 - 45 min
Sample Size 50 mg

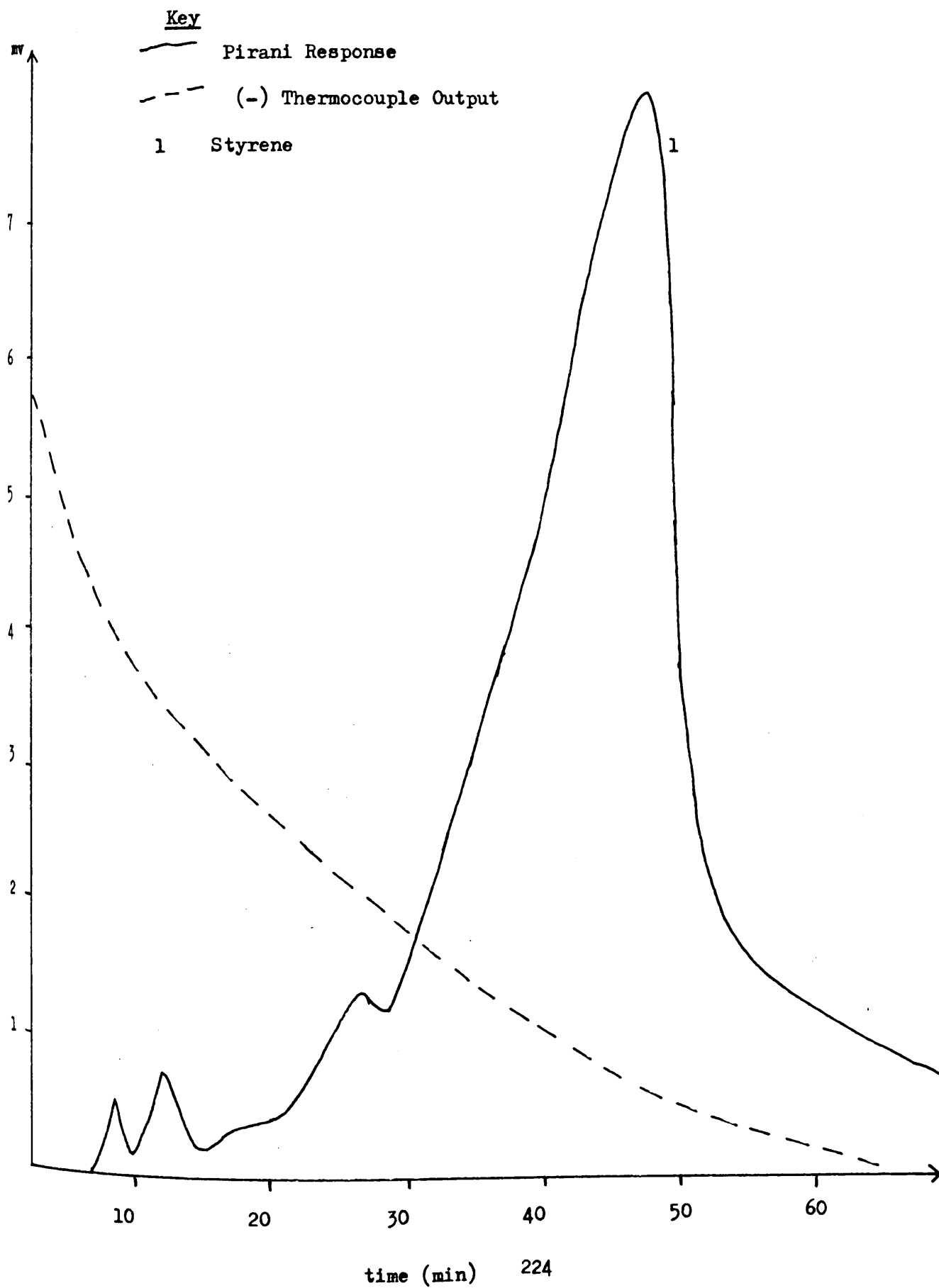
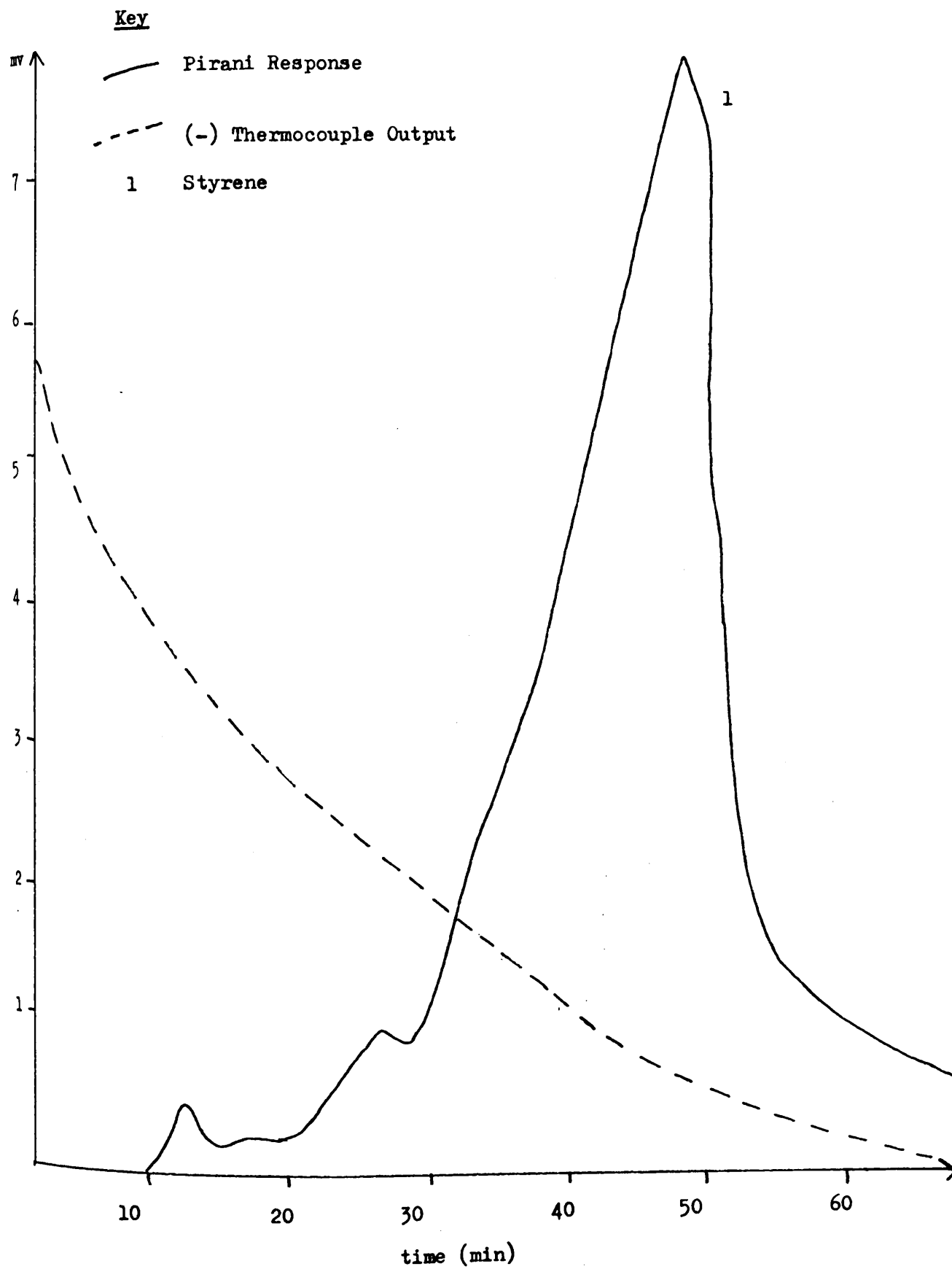


FIGURE 7 - 20

SUB-AMBIENT TVA OF VOLATILE PRODUCTS OF ISOTHERMAL DEGRADATION AT 380°C
OF BLOCK COPOLYMER, 45 - 60 min
Sample Size 50 mg



C COLD RING PRODUCT FRACTION OF ISOTHERMAL DEGRADATION AT 380°C.

The cold ring product fraction produced by isothermal degradation of the block copolymer at 380°C for one hour was examined by n.m.r. spectroscopy to yield the spectrum illustrated in fig. 21 . As expected, signals at 2.00 δ and 5.30 δ which are produced by polybutadiene oligimers formed during the exothermic decomposition reaction of polybutadiene are accompanied by signals at 1.55 δ and 1.25 δ which are due to saturated condensed ring material which is formed as a product fraction of the endothermic decomposition reaction of polybutadiene. It can be shown, by the same argument as that outlined in Chapter 7 I, that the material which produces the signals at 7.10 δ is not a component of the polystyrene cold ring fraction of degradation but is present as a product fraction which is derived from the polybutadiene portion of the block copolymer.

The cold ring fraction of isothermal degradation at 380°C for one hour of the block copolymer was separated on a polarisability basis by preparative thin layer chromatography using n - hexane. The fractions so produced were examined by n.m.r. spectroscopy to yield the spectra illustrated in fig. 22a and b . With the exception of F₃ which is identifiable as the major component of the polystyrene cold ring fraction of degradation, all other spectra can be attributed to material which must be produced in the polybutadiene component of the system.

It is surprising to note that F₁, F₂, F₄ and F₅ are all aromatised to some extent. Perhaps the most interesting spectrum is that which is produced by the most heavily aromatised fraction - F₄. It can be seen that the signal at 1.55 δ which corresponds to saturated tertiary condensed ring protons is almost completely absent from the spectrum. In contrast, the signal at 1.25 δ which corresponds to saturated secondary ring protons is strong.

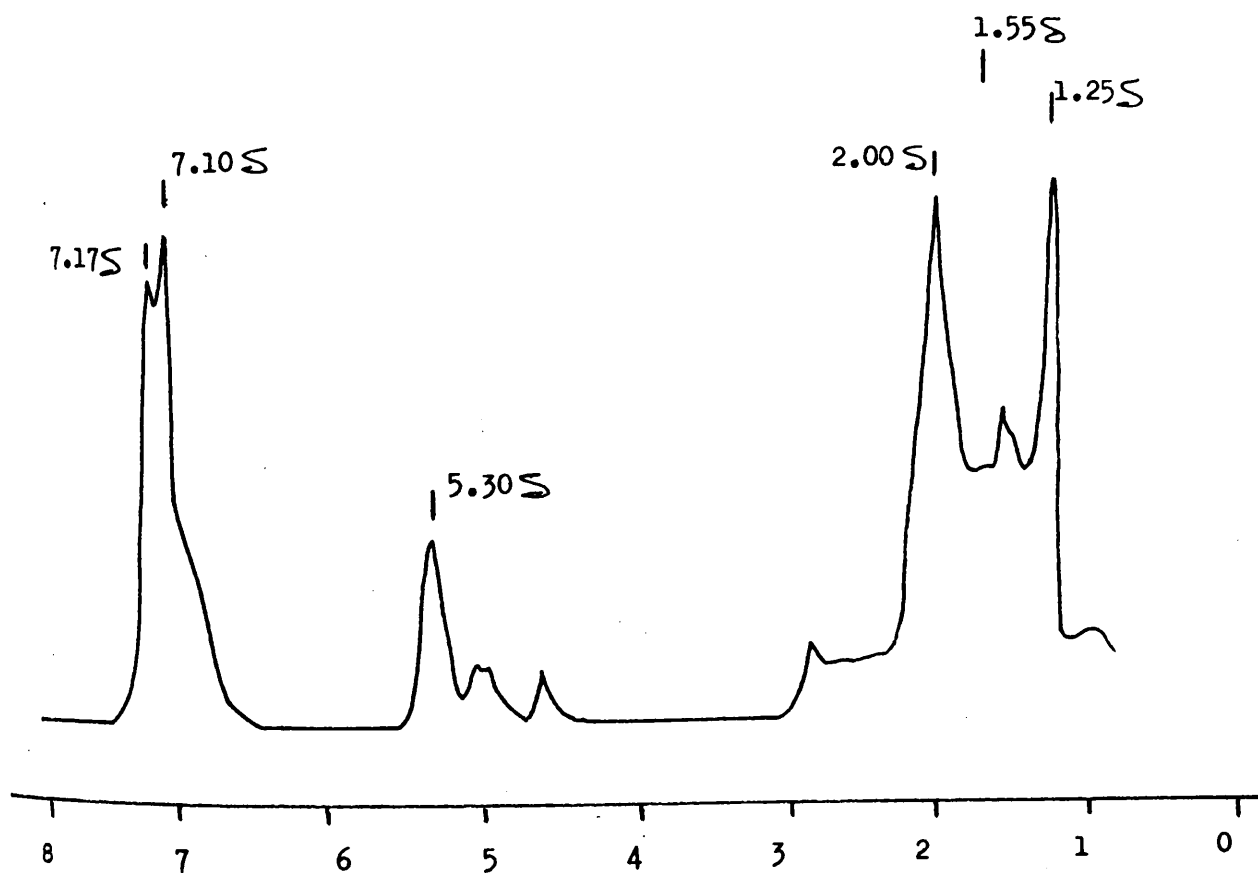
This shows that such material is present in quantity. Material in the molecular weight range of the cold ring fraction of degradation (200 - 800) is possessed of a high concentration of chain end groups. In the case of polycyclic material, the chain end group is a saturated ring which contains a higher proportion of CH_2 groups than the bulk of the material. The preferential elimination of tertiary C - H groupings is positive proof that aromatisation is produced throughout the polycondensate.

FIGURE 7 - 21

n.m.r. SPECTRUM OF COLD RING FRACTION OF ISOTHERMAL DEGRADATION AT 380°C
FOR 1 hr OF BLOCK COPOLYMER

Solvent C Cl₄

Lock TMS



S

FIGURE 7 - 22a

n.m.r. SPECTRA OF COLD RING FRACTION OF ISOTHERMAL DEGRADATION AT 380°C
FOR 1 hr OF BLOCK COPOLYMER, AFTER SEPARATION BY PREPARATIVE TLC

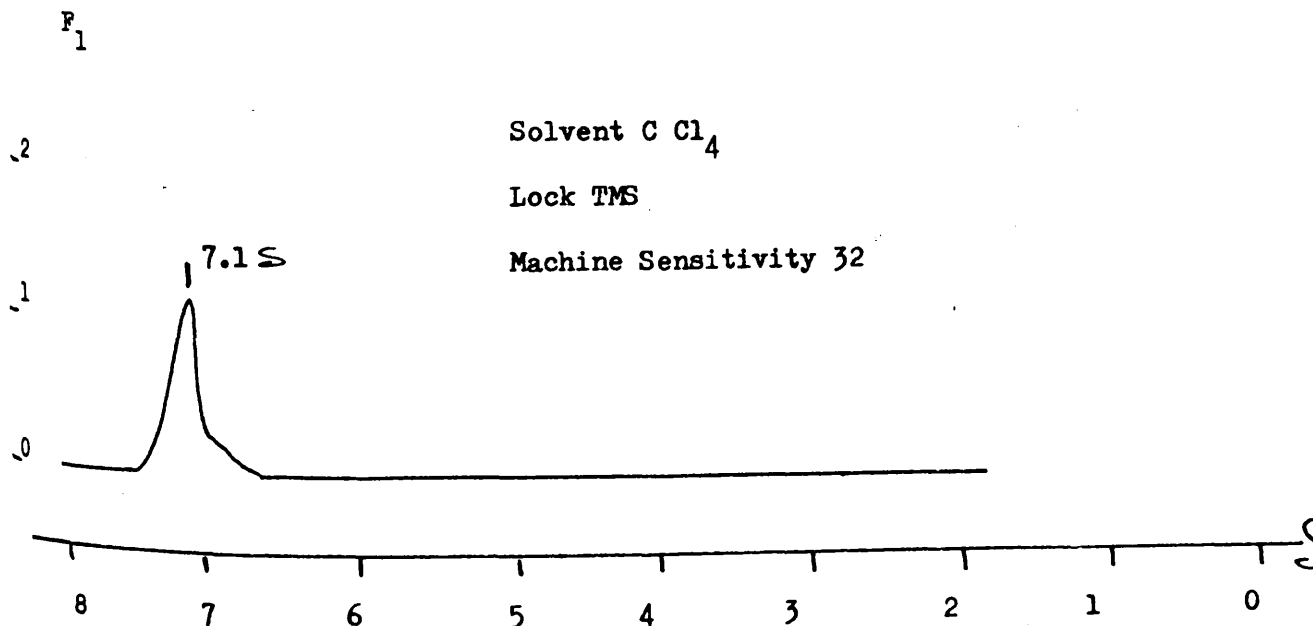
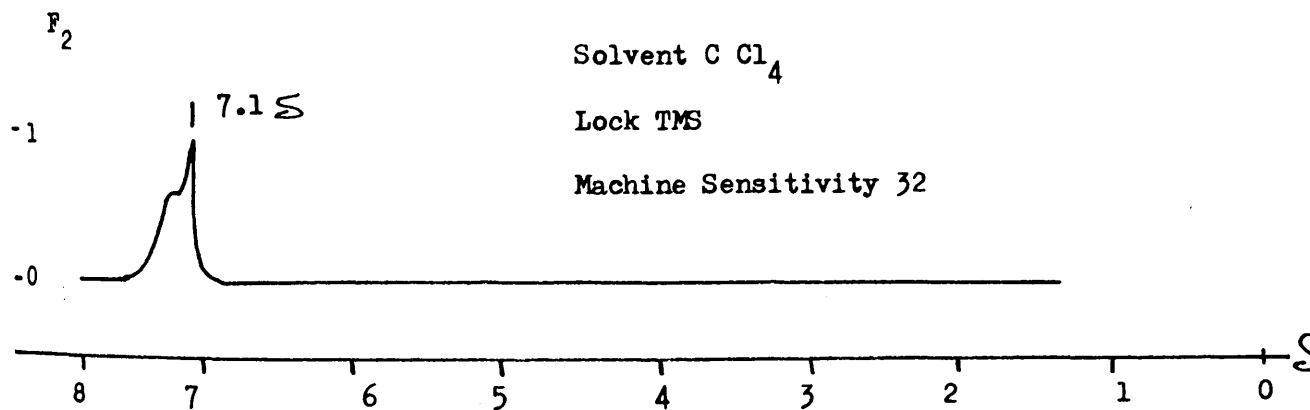
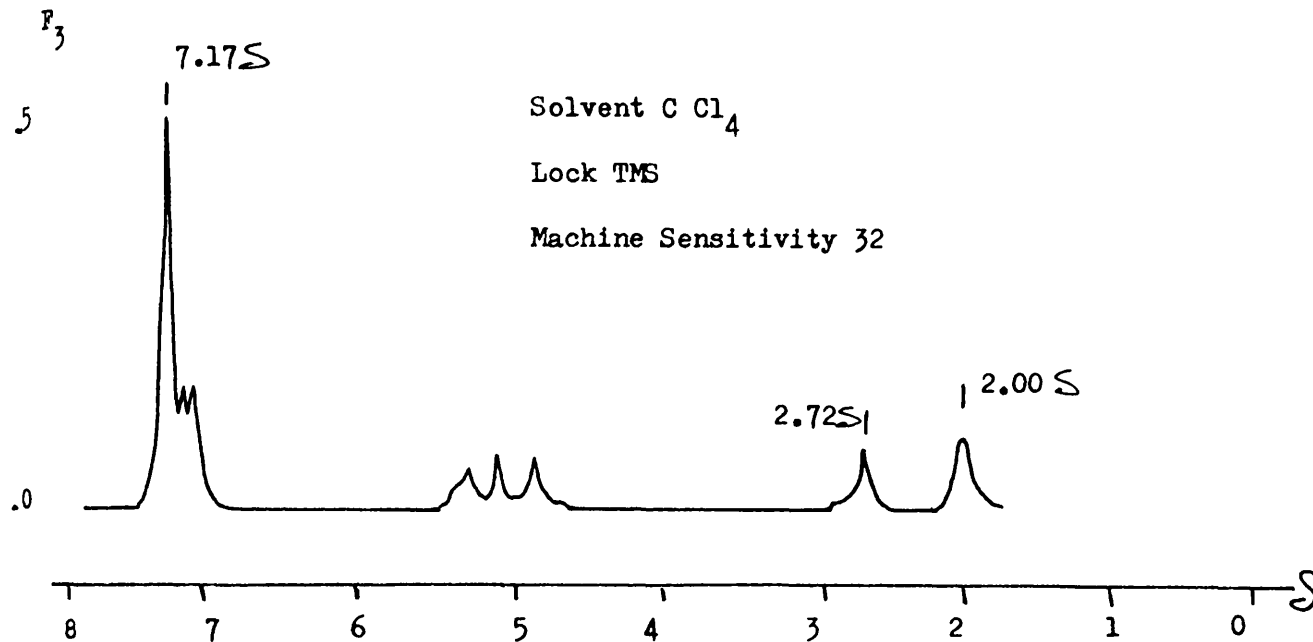
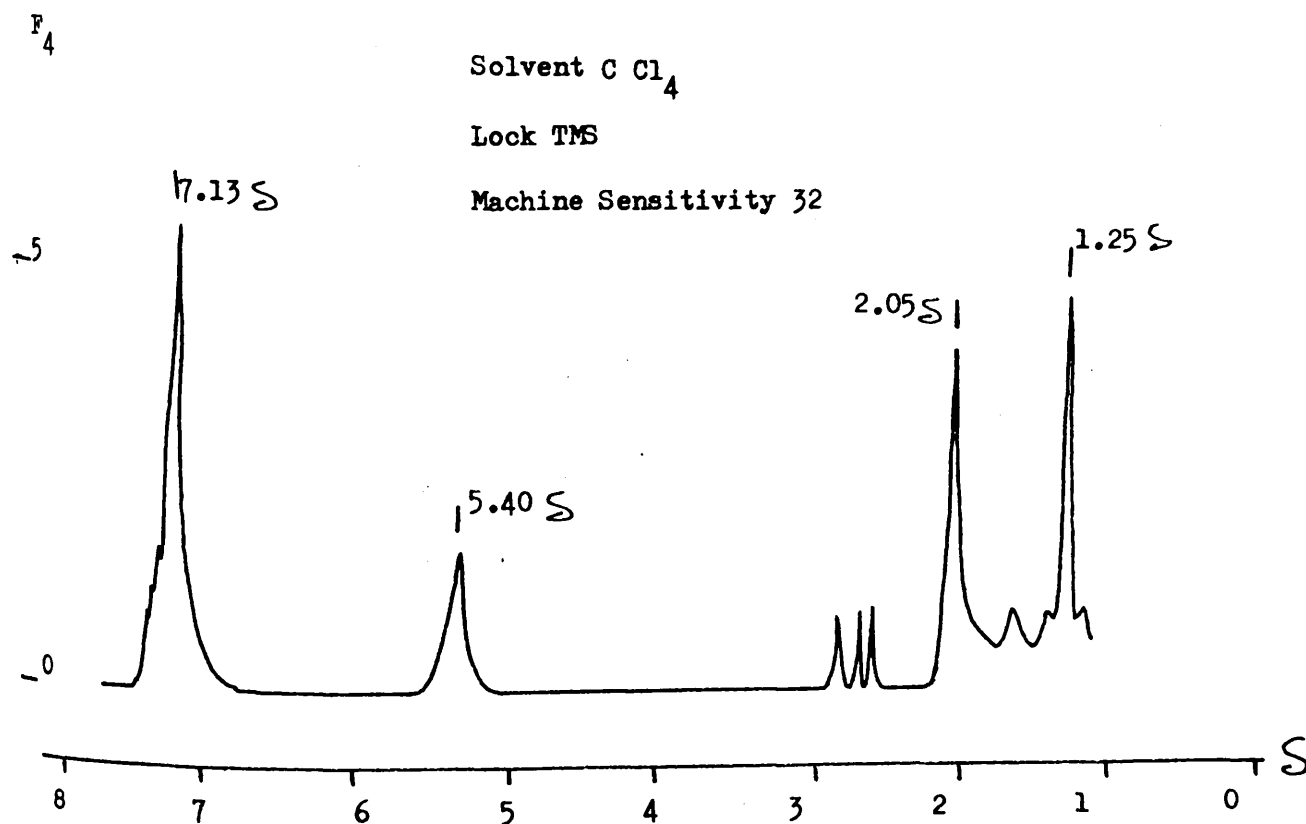
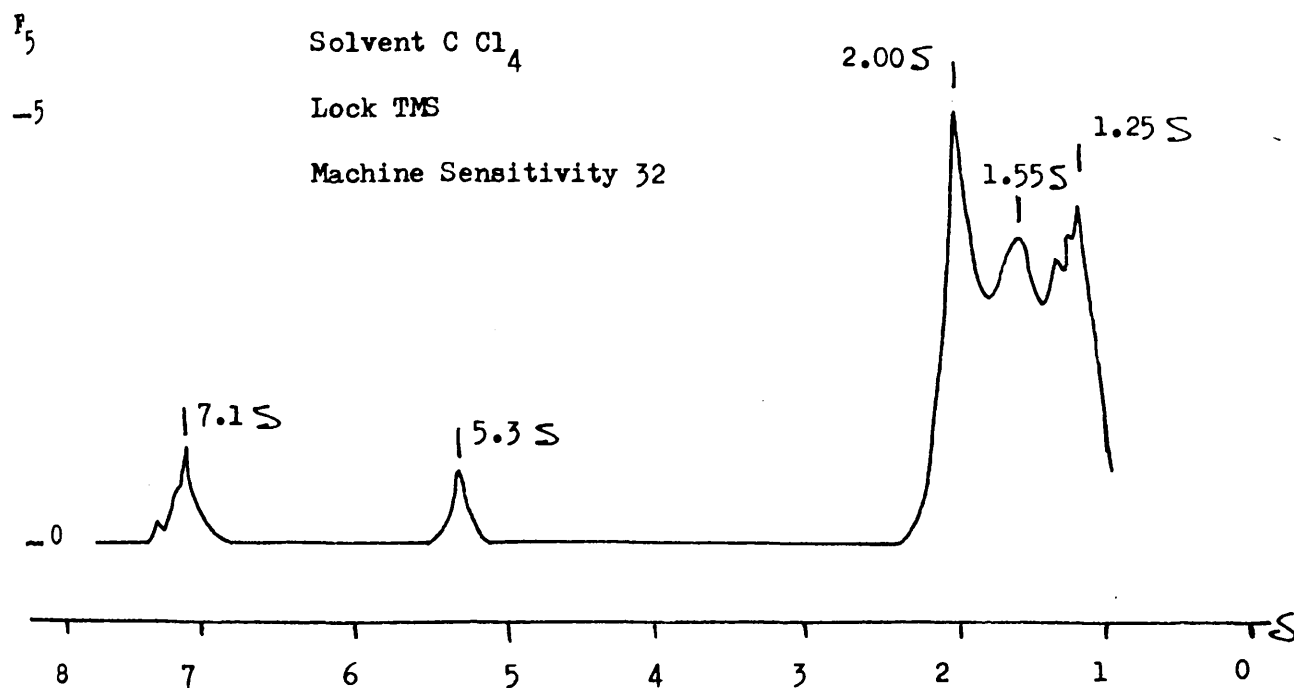


FIGURE 7 - 22b

n.m.r. SPECTRA OF COLD RING FRACTION OF ISOTHERMAL DEGRADATION AT 380°C
FOR 1 hr OF BLOCK COPOLYMER, AFTER SEPARATION BY PREPARATIVE TLC



D RESIDUE OF ISOTHERMAL DEGRADATION AT 380°C.

A sample of block copolymer was degraded under vacuum at 380°C for one hour, and the residue of degradation was examined by i.r. spectroscopy. Soluble material was extracted and filtered and was subjected to analysis by n.m.r. spectroscopy. The spectra so obtained were almost identical to those shown in fig. 12 . The i.r. spectrum shows that the residue of degradation is composed of a mixture of polystyrene and cyclised polybutadiene. The n.m.r. spectrum confirms the presence of a quantity of soluble polystyrene. It is of interest to note that unstabilised polystyrene is completely removed from the hot zone after one hour degradation at 380°C (Chapter 5).

E DISCUSSION.

The isothermal TG curve (fig. 13) and the isothermal TVA curve (fig. 14) for the block copolymer indicate that the material is stabilised with respect to weight loss over a prolonged time period at 380°C .

When the volatile and cold ring fractions of degradation are estimated separately by gravimetry (fig. 15), it becomes apparent that extra stability is concentrated within the polystyrene and not within the polybutadiene component of the system. This is supported by the detection of large quantities of polystyrene in the residue of degradation at 380°C for one hour.

When the volatile fraction of degradation is subjected to sub-ambient TVA it is shown to consist of styrene along with a (relatively) large quantity of toluene (fig. 16). The evolution of styrene is almost completely suppressed in the time interval during which the polybutadiene component of the system is undergoing its exothermic cyclisation/depropagation reaction. Styrene is thereafter evolved at a rate much reduced from that expected of unstabilised polystyrene.

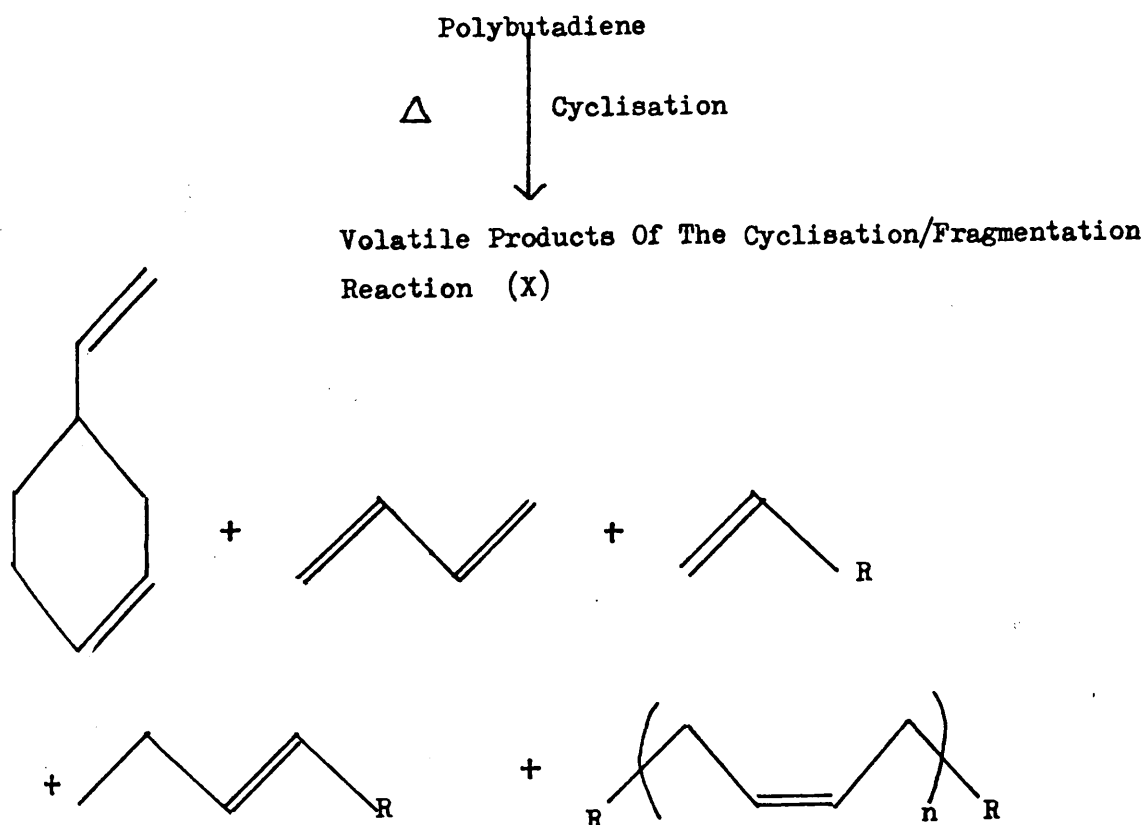
The cold ring fraction of degradation at 380°C for one hour was shown to consist of a mixture of the normal polystyrene cold ring fraction of degradation which is accompanied by a heavily aromatised version of the normal polybutadiene cold ring fraction of degradation.

The above evidence is cited in support of the existence of two distinct processes by which the polystyrene component of the system is stabilised with respect to the volatilisation process at 380°C .

Prolonged stability of the polystyrene component is achieved by radical transfer to mobile condensed ring material which is formed during the degradation of cyclised polybutadiene. The stability

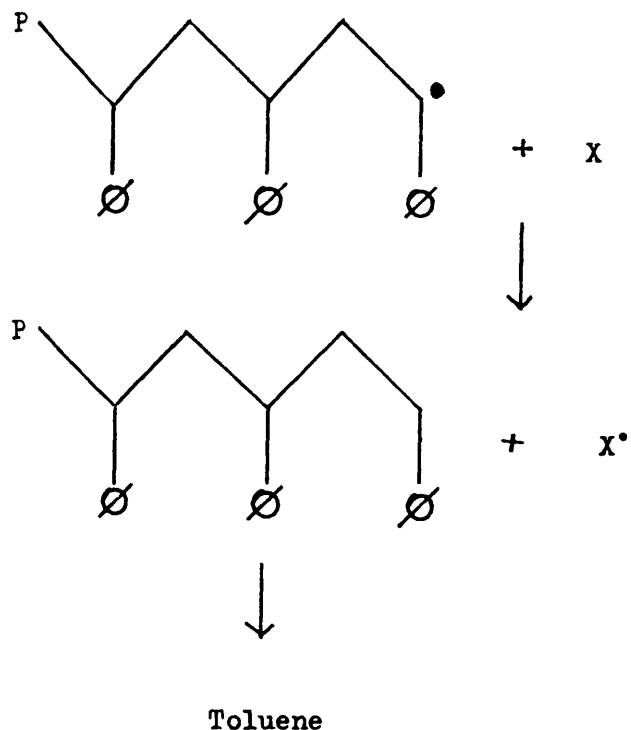
of the polystyrene component in the early stages of breakdown is further increased by the presence in the system of mobile products of the exothermic cyclisation/depropagation reaction of polybutadiene, many of which are capable of hydrogen abstraction/chain transfer reactions to form π - allyl radical centres. Many radical sites would be removed from the system by a subsequent volatilisation of the π - allyl complex while others would be removed by the bimolecular termination reactions to which such material is particularly susceptible. The stabilising reaction which is operative in the presence of condensed ring material has already been discussed (Chapter 7 I). The other process is outlined below.

(i).



(P = Polystyrene Residue)

(ii).



It has been shown that 4 - vinylcyclohexene is able to operate as a degradative chain transfer agent (Chapter 9). It has been found (104) that mono-olefins can act in a similar manner. Isoprene oligomers and polymers, which should react with radical centres in a manner similar to that of polybutadiene, have also been shown (105, 106) to be able to participate in hydrogen abstraction processes.

POLYSTYRENE DEGRADATIONS IN THE PRESENCE OF 4-VINYLCYCLOHEXENE.

A INTRODUCTION.

It has been established in Chapter 7 that 4-vinylcyclohexene (4VCH) is able to stabilise polystyrene with respect to conversion to cold ring and volatile fractions at degradative temperatures by a hydrogen abstraction process. The existence of a stabilising effect, though not its nature, has been tested by direct interaction of degrading polystyrene with 4VCH under closed system conditions. As in Chapter 7, extra stability (if any) in the polymer was measured with respect to its conversion to monomer and oligomeric fragments, volatile at degradation temperatures.

It must be emphasised that the closed system measurements discussed in this chapter should be examined on a comparative and not an absolute basis because it will be shown that the behaviour of such a system is very dependent upon the precise conditions under which the experiment is undertaken.

B EXPERIMENTAL.

B 1 REACTOR DESIGN AND OPERATION.

The major design criterion of the apparatus to be discussed in this section was that it should allow degradation reactions to be performed in conditions as close as possible to those exhibited by the open-pumping TVA system. Most importantly, the product yield from secondary decompositions of the cold ring fraction had to be minimised. This was very simply achieved by extending the reactor outside the oven and therefore presenting to the cold ring fraction a cold surface upon which to condense.

Severe limitations were therefore placed upon the geometry of the reactor. For example to stop 4VCH quantitatively and permanently distilling from the hot zone all surfaces outside the oven had to be directly above it. This introduced the additional complexity that cold ring material was seen to be washed back into the hot zone by refluxing 4VCH when the limiting vapour pressure of the latter in the cold zone was exceeded. (Visible) refluxing of liquids was eliminated by, firstly, minimising the polystyrene and 4VCH charges in to the reactor, and, secondly, by warming the cold zone of the reactor to 40 - 50°C throughout the degradation by adjusting the oven top spacers to allow a small convection current of air to warm the upper portion of the reactor.

Contamination of the system by grease was avoided by the use of Teflon stopcocks which also provide an improved vacuum seal able to maintain a sticking vacuum in the apparatus for any length of time provided the other side of the stopcock is attached to an open-pumping vacuum system.

To compare the behaviour of polystyrene degraded alone and in the presence of 4VCH, degradations were performed isothermally for various periods of time. Errors of temperature and time may be

introduced into consecutive degradations. To eliminate this type of error from the experiment, mixed and unmixed degradations were performed simultaneously using the three limbed assembly shown in fig. 1 .

To facilitate a comparison between this experiment and the open-pumping isothermal work of Chapters 5, 6 and 7 degradations were initially performed at 380°C . However, conversion rates at this temperature were too high to enable accurate measurements to be made using the techniques outlined below. A compromise temperature of 350°C was therefore selected. It can be seen from the isothermal TVA and TG traces of figs. 2 and 3 that an open system degradation at this temperature is essentially complete after 90 min.

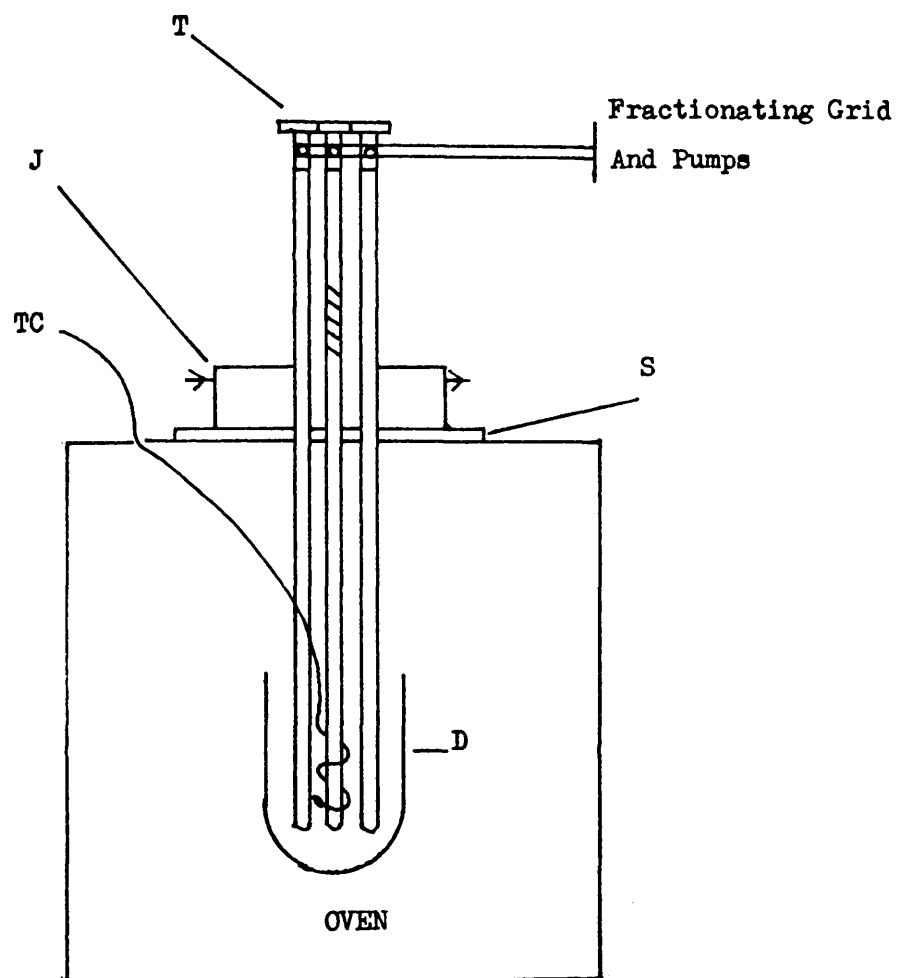
Samples were introduced into the assembly depicted in fig. 1 through the stopcock apertures. Low molecular weight polystyrene powder (100 mg) - see Chapter 4 - was introduced through a glass funnel while 4VCH (50 μl) was added by using a semimicro syringe.

To minimise 4VCH loss in the first degassing cycle the following procedure was observed. The reactor was charged , sealed and connected to the vacuum line as shown in fig. 1 . The tube ends were then immersed overnight in dry ice to ensure an efficient distillation of volatile material to the cold zone. While the tubes were still frozen, the dry ice was replaced by liquid nitrogen after which the first degassing cycle was carried out. Subsequent degassing cycles were performed more rapidly because the efficiency of collection of material in the cold zone was found to increase markedly after the bulk of the noncondensable material in the reactor had been removed. After three degassing cycles had been performed, the tubes were sealed and the degradation was carried out.

On completion of the degradation, the assembly was quickly

FIGURE 8 - 1

REACTOR FOR CLOSED SYSTEM DEGRADATIONS



Key

- J Water Jacket
- D Small Dewar Flask For Degassing Reactor
- T Teflon Stopcocks
- S Insulating Spacers
- TC Thermocouple
- //// Cold Ring Fraction Of Degradation

FIGURE 8 - 2

ISOTHERMAL TVA OF POLYSTYRENE AT 350°C

Sample Size 100 mg

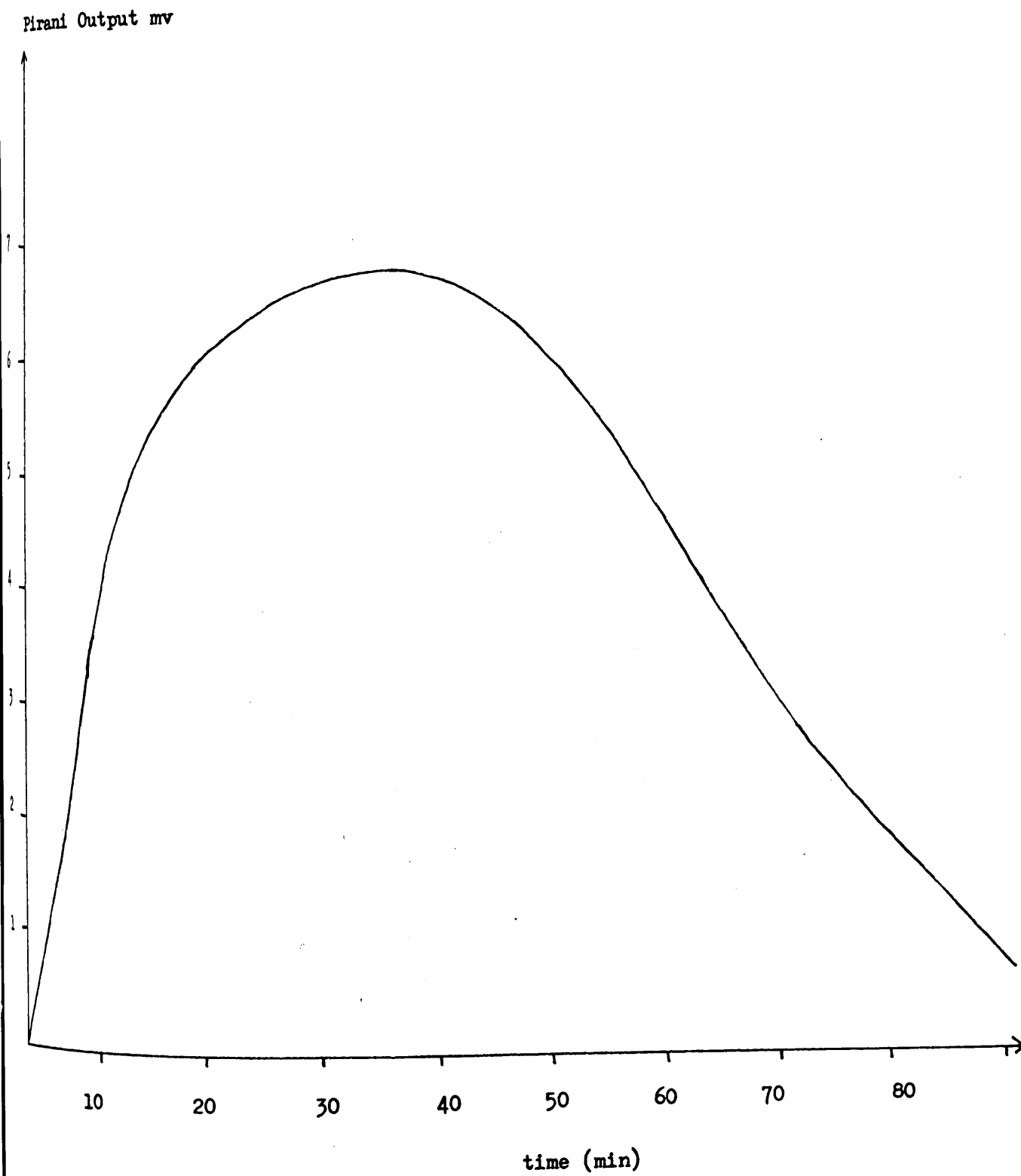
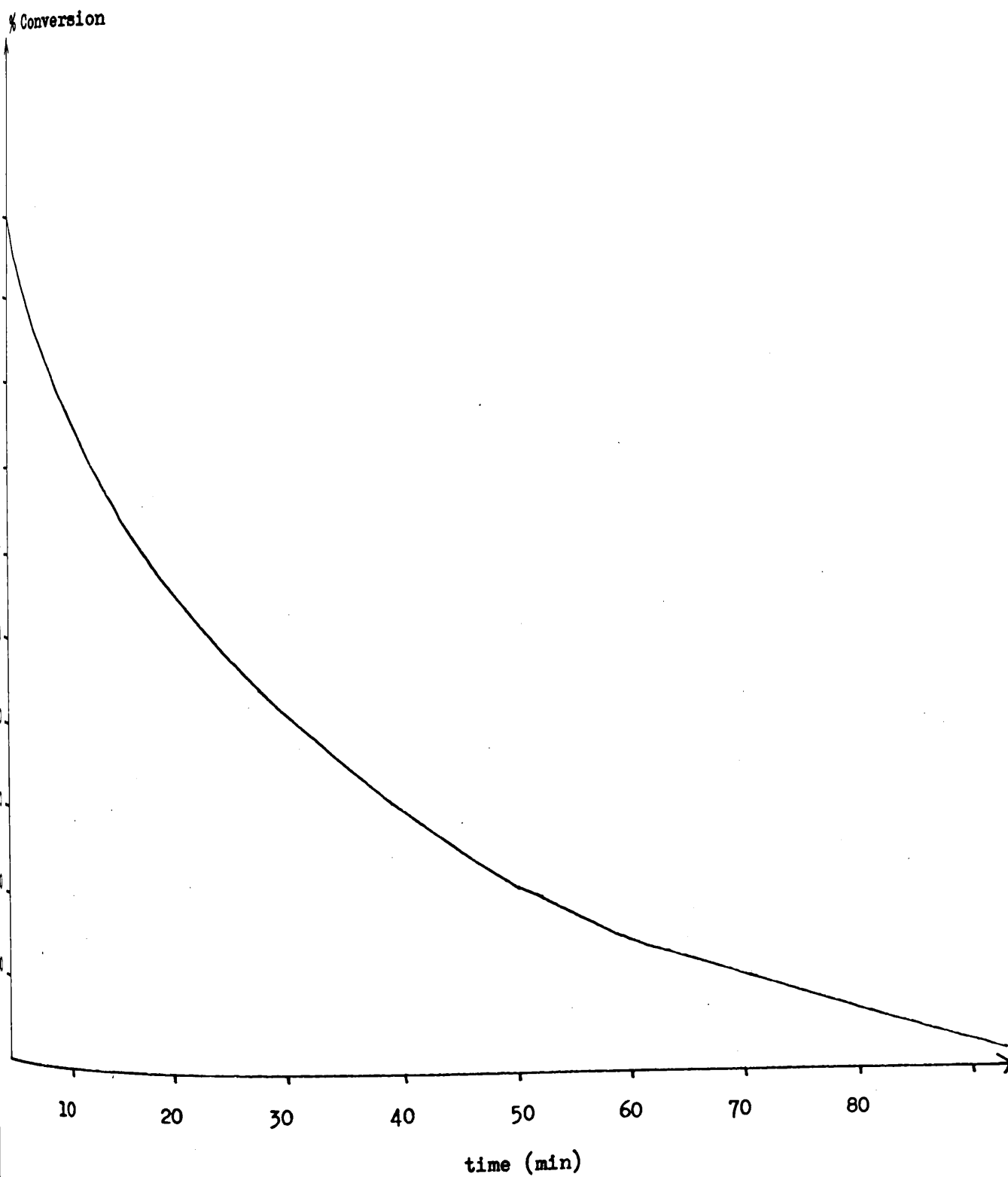


FIGURE 8 - 3

ISOTHERMAL TG OF POLYSTYRENE AT 350°C UNDER NITROGEN

Sample Size 6 mg



cooled and material volatile at room temperature was removed by distillation to the fractionating grid for analysis. Material involatile at room temperature, the residual fraction of degradation which contained both the cold ring and residue fractions of the normal TVA experiment, was dissolved in carbon tetrachloride and examined by proton n.m.r. spectroscopy.

The yield of styrene by GLC as a product of an open system degradation of polystyrene to completion at 350°C (fig. 4) agreed well with the corresponding yield to completion at 380°C as measured by weight difference (Chapter 5), to indicate that a high efficiency of product manipulation could be achieved in this system.

It must be emphasised that in this experiment the degrading polystyrene surface is exposed to a dynamic atmosphere of 4VCH and styrene by convection, while the interior of the polymer sample is exposed to concentrations of 4VCH and styrene determined by their respective degrees of solubility in the polymer at 350°C.

B 2 QUALITATIVE PRODUCT MANIPULATION.

The product distribution from the mixed and unmixed systems after isothermal degradation at 350°C for three hours was obtained using the procedure outlined below.

1. Noncondensable Volatile Material.

The condensable contents of the reactor were frozen in liquid nitrogen after the degradation. The reactor was then opened to an on-line Pirani gauge. A deflection of the gauge needle from the base line on the low pressure scale was taken as evidence of noncondensable formation.

2. Condensable Volatile Material.

The condensable volatile products of degradation were subjected to a sub-ambient TVA separation to test for the presence

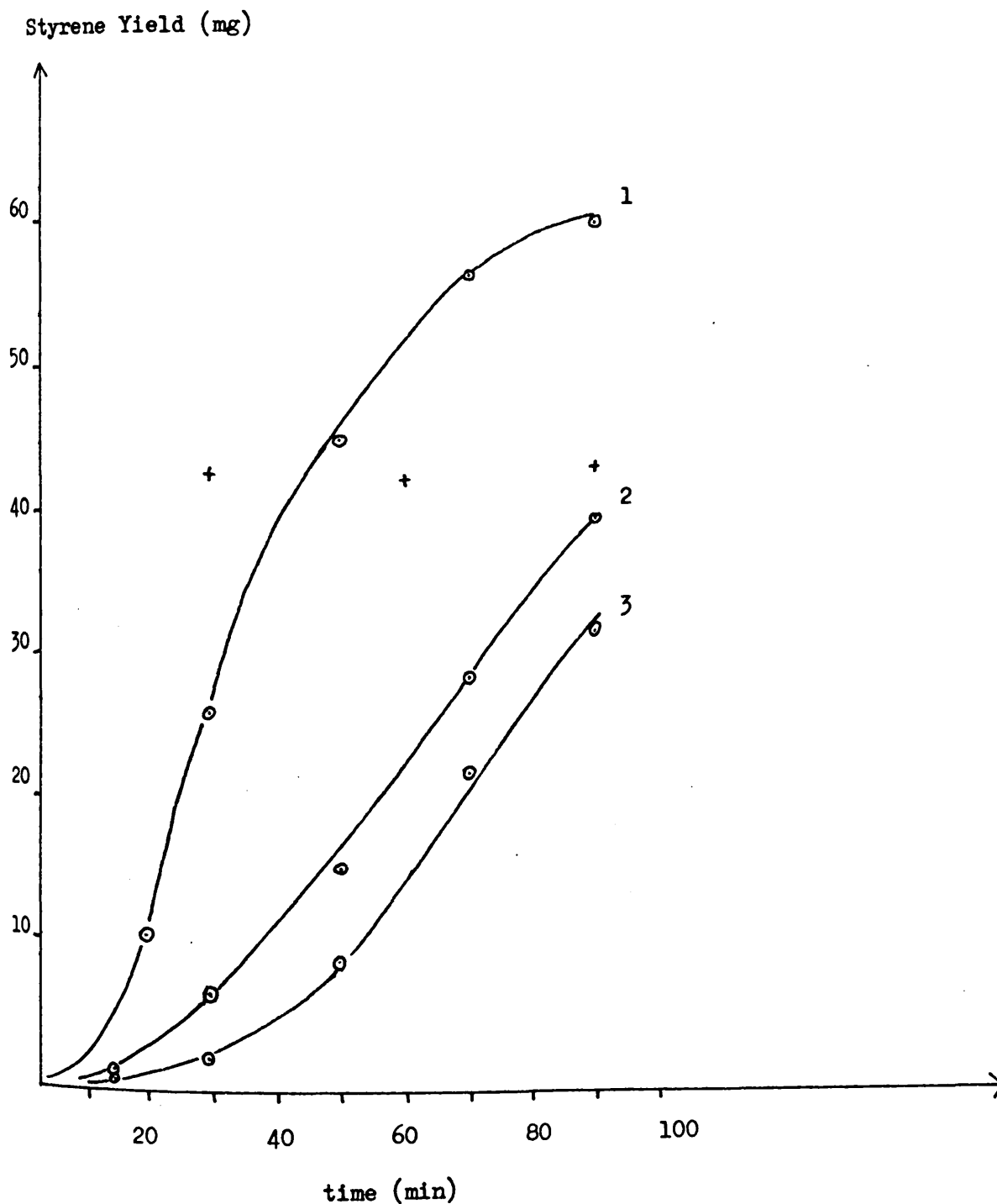
FIGURE 8 - 4

YIELDS OF STYRENE AS PRODUCT OF DEGRADATION OF POLYSTYRENE AT 350°C

Sample Size 100 mg

Key

- 1 Open System Degradation
- 2 Closed System Degradation
- 3 Closed System Degradation In The Presence Of 50 μ l, 4VCH
- + Yield Of Styrene Introduced Prior To Degradation



of low molecular weight fragments. The liquid fraction was then analysed by GLC and n.m.r. spectrometry.

3. Residual Material.

Material involatile under vacuum at room temperature was examined by n.m.r. spectrometry.

RESULTS

(i). 4VCH (50 μ l)

The material was found to be completely stable at 350°C.

(ii). POLYSTYRENE (100 mg)

The only detectable products of degradation were monomer and material with an n.m.r. spectrum identical to that of the normal cold ring fraction of degradation.

(iii). POLYSTYRENE (100 mg) + 4VCH (50 μ l)

The only detectable materials present at the end of the degradation were 4VCH, styrene monomer and the normal polystyrene cold ring fraction of degradation.

B 3 QUANTITATIVE VOLATILE PRODUCT ANALYSIS.

Styrene, 4VCH and the internal reference material, toluene, were separated on a 6 ft/ $\frac{1}{4}$ in diameter, 10% Microwax on Chromosorb column at 100°C. A typical GLC trace can be inspected in fig. 5 .

To reduce the time of analysis, volatiles from the separate tubes containing polystyrene and 4VCH were collected together before analysis. The quantities of styrene produced under open and closed system conditions determined by GLC, can be inspected in fig. 4 .

B 4 SEMI-QUANTITATIVE ANALYSIS OF RESIDUAL MATERIAL.

A typical n.m.r. spectrum of the product fraction involatile at 25°C is shown in fig. 6 . As expected, it consists of a

FIGURE 8 - 5

TYPICAL GLC SEPARATION OF TOLUENE 4-VINYLCYCLOHEXENE AND STYRENE

Column 6', $\frac{1}{4}$ " Diameter, 10% Microwax On Chromosorb (100-120)

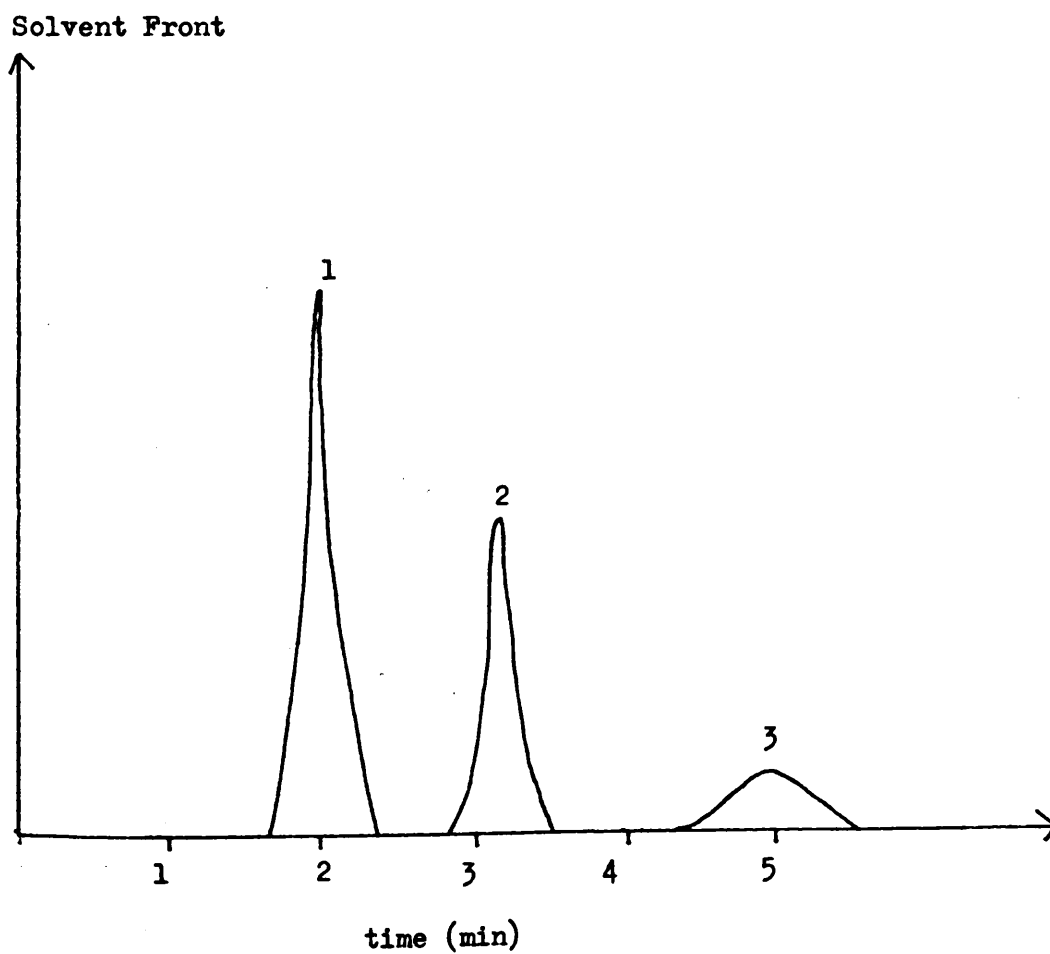
Temperature Of Operation 100°C

Key

1 Toluene

2 4-Vinylcyclohexene

3 Styrene



superposition of the broad saturated and aromatic signal bands generated by polymeric material and the sharp peaks at 2.72 δ (singlet), 7.17 δ (singlet) and 5.0 δ (multiplet) generated by oligameric material which would comprise the cold ring fraction of degradation in the TVA experiment.

The 2.72 δ peak appeared to be a particularly useful marker from which the quantity of cold ring material in the mixture could be estimated. It was first necessary, however, to check for spectroscopic interference by polymeric material. To this end, a sample of polystyrene was degraded for 40 min at 350°C to give a maximum chain-end concentration under open system conditions and the residue was examined by n.m.r. spectroscopy. The n.m.r. spectrum so produced was indistinguishable from that of the parent polymer. It was not possible to compare directly the size of the 2.72 δ peaks generated by the residual product fractions of the mixed and unmixed degradations for two reasons. Firstly, material is lost in each of the steps by which it is transferred to the n.m.r. tube, and, secondly, the sensitivity of the spectrometer changes between spectra even if the settings remain unaltered.

To overcome these problems the following procedure was developed. The n.m.r. spectrum of the residue of the unmixed degradation was obtained. The spectrum produced by the residue of the mixed degradation was then obtained on the same chart paper at a sensitivity which allowed the 1 - 2 δ band to coincide with that generated by the other sample. The heights of the two peaks at 2.72 δ were then reduced by the factor required to reduce the 1.4 δ peak to one tenth of full scale deflection on the paper. This procedure does not eliminate errors which will arise if the sample is incompletely dissolved in the solvent. This step was, therefore, carried out very carefully.

This procedure effectively measures the quantity of cold ring material per unit mass of polymer in the mixture. This function is non linear with conversion and is plotted in fig. 7 , where the quantity $\frac{b}{a}$ represents a ratio of the n.m.r. peak height generated by a unit mass of polymer (a) and by the cold ring product fraction derived from the conversion of unit mass of polymer (b).

The results of this procedure can be seen in fig. 8 .

TYPICAL n.m.r. SPECTRA OF THE PRODUCT FRACTIONS INVOLATILE AT 25°C

Conditions Of Degradation 50 min At 350°C

Solvent C Cl₄

Lock TMS

Key

- Polystyrene Degraded In The Absence Of 4-Vinylcyclohexene
- Polystyrene Degraded In The Presence Of 4-Vinylcyclohexene

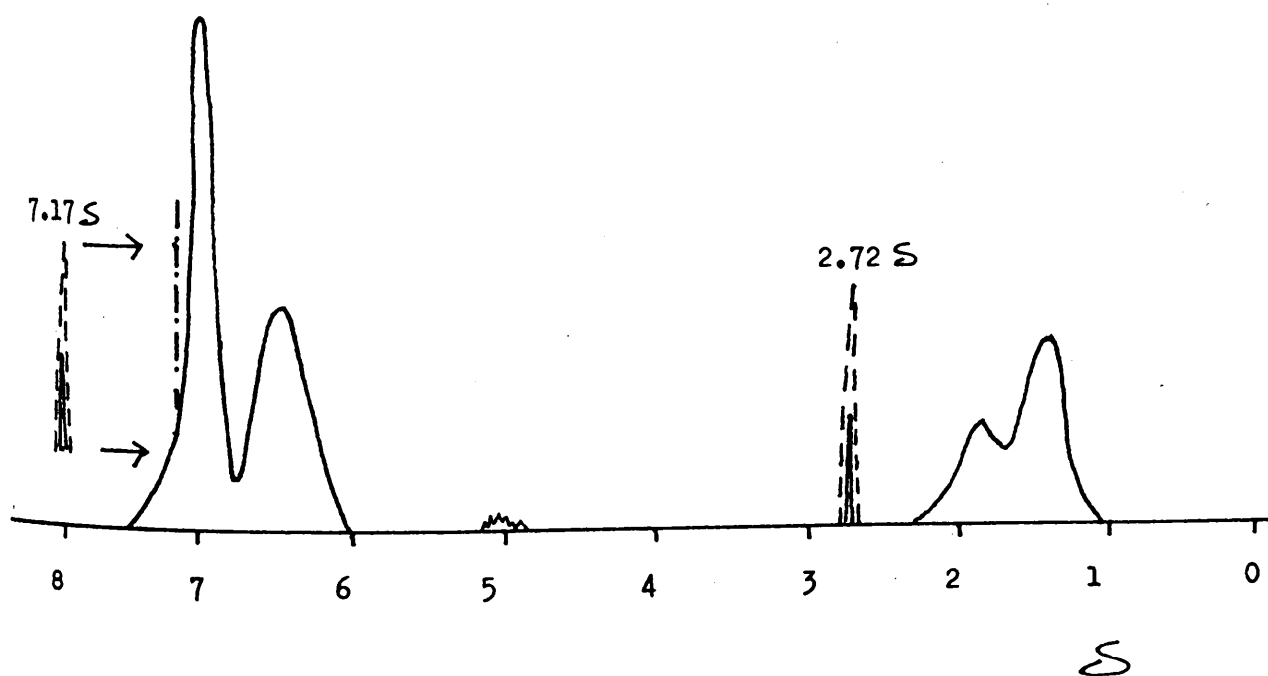


FIGURE 8 - 7

PEAK HEIGHT VERSUS CONVERSION CURVE FROM n.m.r. MEASUREMENTS

Key

- a Relative n.m.r. peak height generated by unit mass of polymer.
- b Relative n.m.r. peak height generated by the cold ring product fraction produced by the degradation of unit mass of polymer.

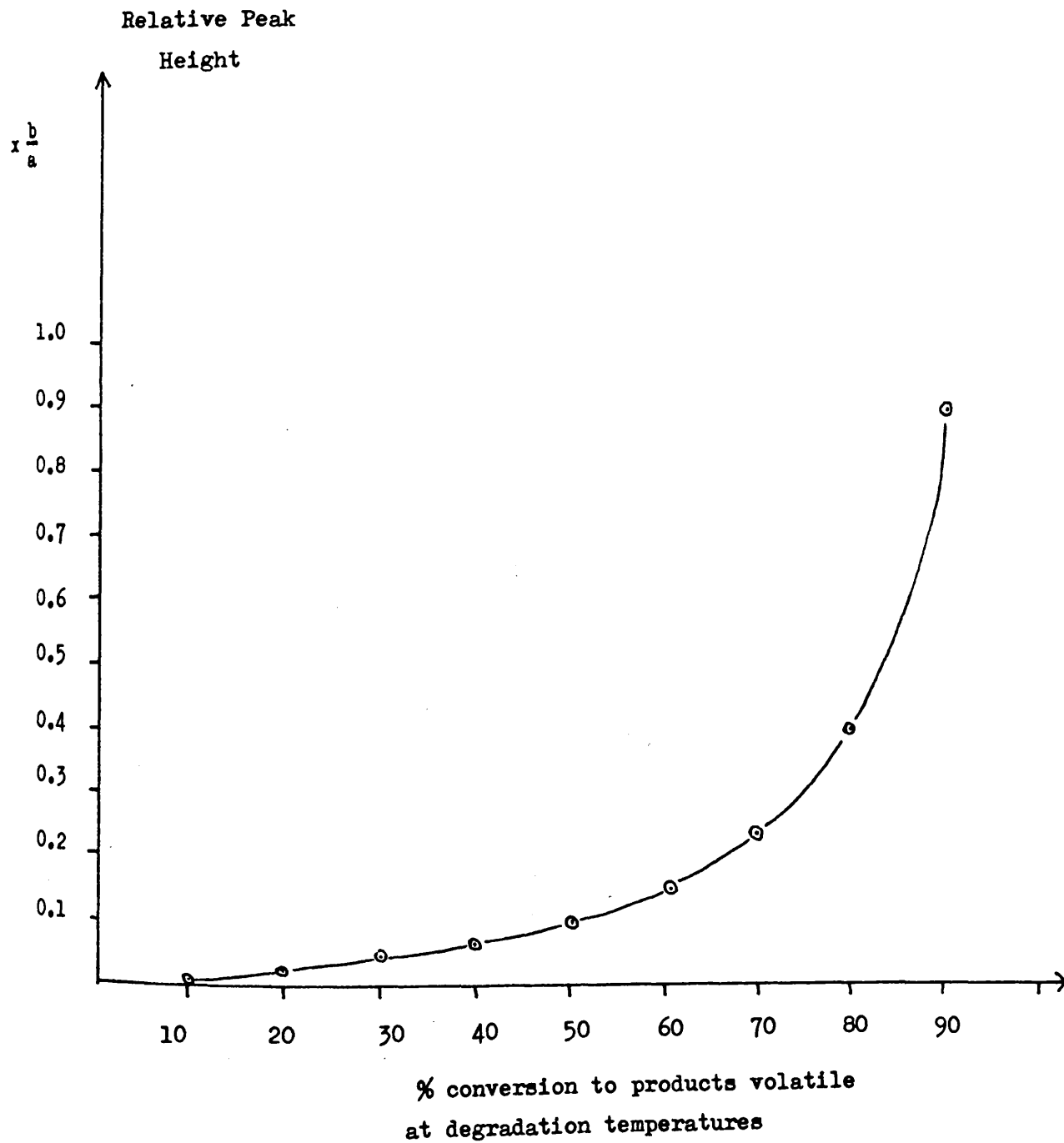


FIGURE 8 - 8

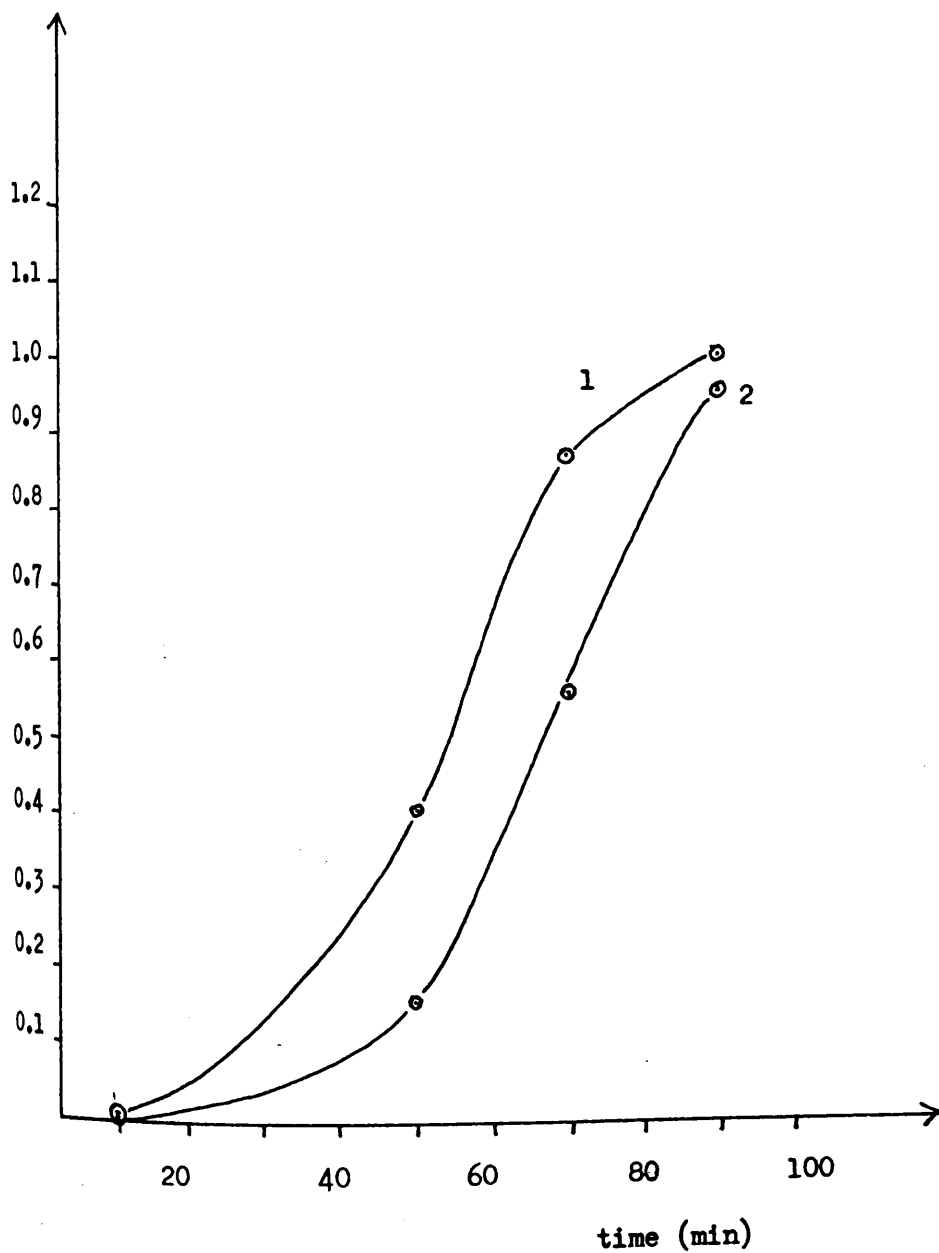
FORMATION OF COLD RING MATERIAL AT 350°C AS A FUNCTION OF TIME

BY THE n.m.r. METHOD

Key

- 1 Polystyrene Degraded In The Absence Of 4-Vinylcyclohexene
- 2 Polystyrene Degraded In The Presence Of 4-Vinylcyclohexene

Normal ised Peak Height At 2.72 δ



C DISCUSSION.

It is apparent from figs. 4 and 8 that the rates of formation of both the monomer and cold ring fractions from polystyrene degradation are depressed in the presence of 4VCH. Before this effect can be attributed to a chemical process it is first necessary to explain the apparent extra stability of polystyrene degraded alone under closed as opposed to open system conditions. This is indicated both by a depressed styrene content of the volatile fraction of degradation (fig. 4) and by the observation that appreciable quantities of polymeric material, as measured by n.m.r. spectrometry, are present after a closed system degradation of the polymer for 90 min. This fraction is completely absent when the degradation is performed under open system conditions. Possible explanations for this effect are listed below.

- (i). Styrene monomer may be absorbed quantitatively by the cold ring fraction, to be retained even with pumping.
- (ii). Styrene monomer may be undergoing the process of thermal polymerisation at the oven boundary (107) a part of which in theory must be subjected to temperatures in the range 150 - 200°C.
- (iii). By the principle of microscopic reversibility, an equilibrium of the form $R_n \rightleftharpoons R_{n-1} + M$ must be set up in a system in which products of the depropagation reaction are retained. Styrene monomer (M) may therefore be undergoing a measure of propagation at radical sites generated in the polystyrene sample. This would directly decrease the monomer yield and indirectly appear to decrease the yield of cold ring material by changing the normalising factor in the n.m.r. measurements.

The first explanation can be discounted because the distinctive AB_2 signals of styrene are completely absent from n.m.r. spectra of the involatile fraction of degradation.

The second was tested by subjecting 50 μ l samples of freshly distilled styrene to degradative cycles. The percentage recoveries of styrene monomer (fig. 4) and the complete absence of residual material in all degradations served to discount this assertion. The third reason was therefore assumed to be the process by which styrene was removed from the system. If this is the case then it is difficult to account for the extra stability of the system in the presence of 4VCH on anything other than chemical grounds.

CHAIN TRANSFER TO 4-VINYLCYCLOHEXENE.A INTRODUCTION AND LITERATURE REVIEW.

4-vinylcyclohexene (4VCH) has been shown to stabilise polystyrene with respect to its conversion to monomer and cold ring material at 350°C (Chapter 8) in an experiment which did not elucidate the mechanisms involved in the stabilising process. The following work was performed in an attempt to rectify this deficiency.

Radical sites in degrading polystyrene are identical in structure to those generated during the bulk polymerisation of the monomer at lower temperatures. Differences in behaviour of the radical in the two temperature ranges can be attributed to two major experimental variables :- the temperature of the system and the environment of the radical, which is surrounded by polymeric material during degradation and by monomer during polymerisation. As the temperature of the system is increased and the monomer concentration in the system is decreased the ratio $\frac{K_{\text{DEPROPAGATION}}}{K_{\text{PROPAGATION}}}$ is made larger to encourage the depropagation reaction.

If the assumption is made that the mode of interaction between the polystyryl radical and the additive is similar in the two temperature ranges then the very simple techniques used to classify additives according to their effect on the polymer forming radical can be used to predict qualitatively the nature of the interaction under degradative conditions.

Additives are classified below with particular reference to their effect upon the shape of the mass conversion curve of the polymerisation as measured by dilatometry and on the molecular weight of the polymer so produced.

Inhibitors.

Inhibitors efficiently remove radical centres from the polymerising medium. Stable radical inhibitors such as 2,2 - diphenyl, 1 - picrylhydrazyl (DPPH) do so by directly combining with the free radical (108). On the other hand metal salts such as ferric chloride, deactivate free radicals by a redox process involving the transfer of a halogen atom (109).

The rates and efficiencies of these processes are high enough to enable the inhibitor efficiently to scavenge radical fragments directly derived from the initiator, with the result that polymer formation is completely suppressed. When the initiator is completely consumed, polymerisation proceeds as in the absence of additive to produce a polymer of identical molecular weight to that of the polymer produced in the absence of inhibitor, provided that the products of the inhibition reaction are inactive towards radical species. A typical conversion curve for polymerisation in the absence of inhibitor is illustrated in fig. 1A, and in the presence of inhibitor, fig. 1 I.

Chain Transfer Agents.

Chain transfer agents remove radical centres in solution by allowing them to combine with a portion of the transfer agent, usually a hydrogen atom. This results in a transfer of the radical activity to the chain transfer agent which efficiently reinitiates polymerisation (fig. 1A). The rates at which these processes occur are usually low enough to allow polymeric material to be formed from the onset of polymerisation though at a reduced molecular weight.

The effect of a chain transfer agent on the molecular weight of the polymer is best described by the Mayo equation (110).

$$\frac{1}{\bar{x}} = \frac{1}{\bar{x}_0} + C_a \frac{[A]}{[M]} \quad \text{--- (i)}$$

Where :-

(1). \bar{x} = DEGREE OF POLYMERISATION IN PRESENCE OF TRANSFER AGENT.

- (2). x_0 = DEGREE OF POLYMERISATION IN ABSENCE OF TRANSFER AGENT.
 (3). $[A]$ = CONCENTRATION OF TRANSFER AGENT.
 (4). $[M]$ = CONCENTRATION OF POLYMERISING MONOMER.
 (5). C_a = A CUMULATIVE CONSTANT, $\left(\frac{\text{RATE CONSTANT FOR TRANSFER}}{\text{RATE CONSTANT FOR POLYMERISATION.}} \right)$.

Retarders.

Retarders in general, interact with radicals in solution to produce a radical centre which is reluctant to participate in further polymerisation. The distinction between this type of material and an inhibitor is often vague and is generally one of degree. Retarders, in general, do not react with radical centres with sufficient vigour to trap initiator fragments, with the result that polymeric material is formed from the onset of polymerisation though at a reduced rate (fig. 1R) and with a lower molecular weight than polymer prepared in the absence of retarder.

The "stable" radical centre may be formed in two ways. Usually it is formed by direct addition of the retarder to the chain end. An example of this type of retarder is p-benzoquinone (111) which approaches an inhibitor in the efficiency with which it traps radicals. Sometimes, however, it is formed by a chain transfer process to produce a radical centre on the chain transfer agent which inefficiently reinitiates polymerisation. Such additives are often termed degradative chain transfer agents.

It is usually impossible to predict the effect of additives such as p-benzoquinone on polymer molecular weights without detailed knowledge of the mechanism of termination of the chain end radical. However, the effect of degradative chain transfer agents on the molecular weight of the polymer can be completely described by a modified form of the Mayo equation (112).

$$\frac{1}{\bar{x}} = \frac{I}{2W} + C_m + C_a \frac{[A]}{[M]} \quad \text{--- (11).}$$

Where :-

- (1). I = RATE OF RADICAL FORMATION IN THE SYSTEM.
- (2). W = RATE OF MONOMER CONSUMPTION.
- (3). C_m = TRANSFER CONSTANT FOR MONOMER.

It can be seen from equation (ii). that great care must be taken to standardise the conditions of polymerisation if a precise value of C_a is to be obtained for the system. On the other hand it has been shown (113, 114) that, provided high polymeric material is being formed, the simple form of the Mayo equation can be used with a reasonable degree of accuracy.

FIGURE 9 - 1

CONVERSION CURVES FOR POLYMER FORMED IN THE PRESENCE OF RETARDER

AND INHIBITOR

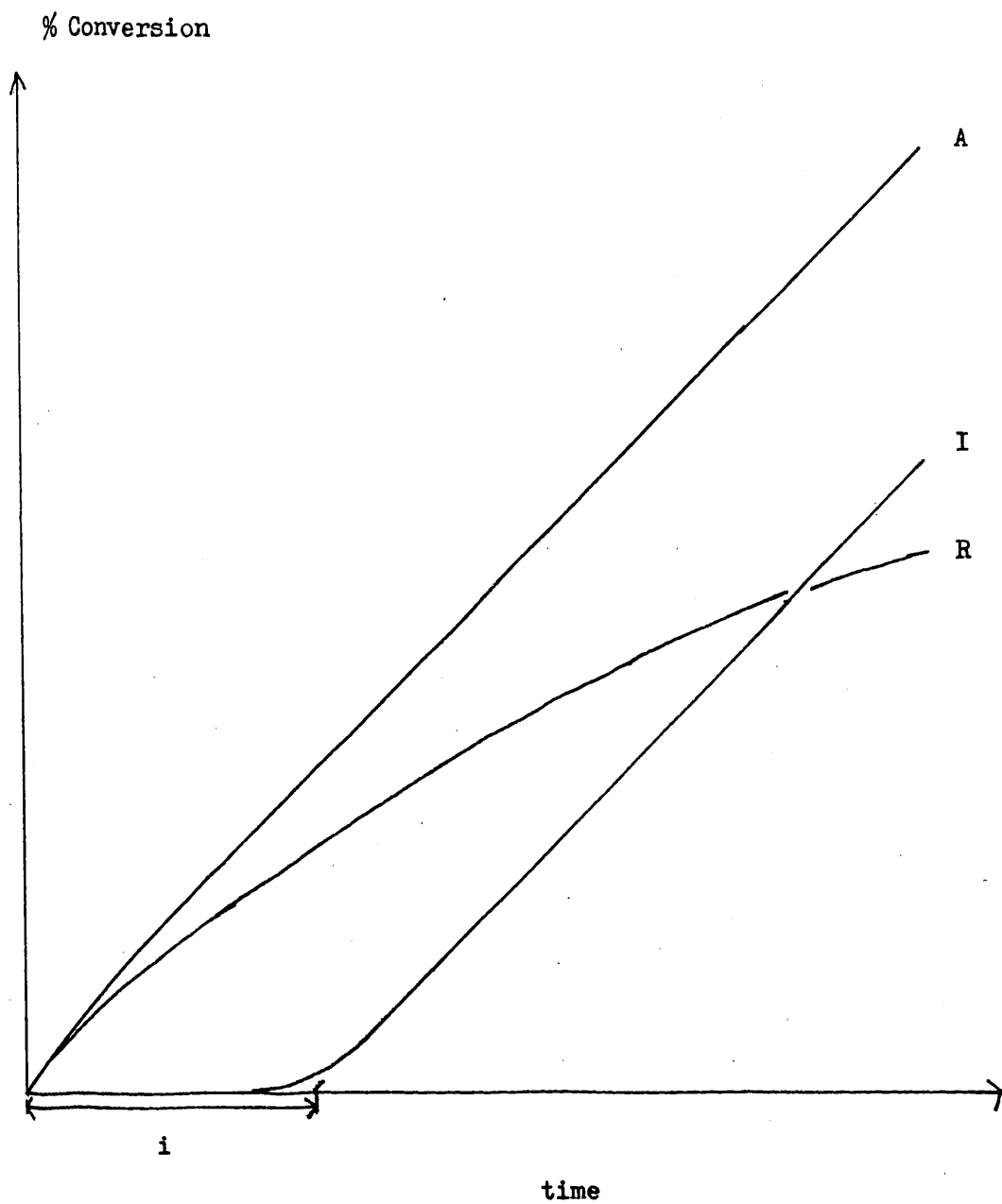
Key

A Conversion Curve In The Absence Of Additive Or In The Presence
Of A Normal Chain Transfer Agent

R Conversion Curve In The Presence Of A Retarder

I Conversion Curve In The Presence Of An Inhibitor

i Inhibition Period



B 1 REAGENT PREPARATION AND PURIFICATION.

(i). Styrene Monomer.

Monomer was stirred overnight over finely crushed and freshly activated calcium sulphate to reduce its inhibitor and water content. A middle cut was then flash distilled to a reservoir before its addition to the dilatometer.

(ii). 4-Vinylcyclohexene (4VCH).

4VCH was flash distilled before use.

(iii). Azobisisobutyronitrile (AIBN).

AIBN was recrystallised from warm ethanol after filtration and stored under refrigeration.

(iv). Cyclised Rubber Cold Ring Material.

A sample of polybutadiene was degraded isothermally under vacuum for one hour at 380°C to ensure its complete cyclisation. The assembly was cooled, opened, and the internal cold finger was wiped clean of the small quantity of cold ring material which accompanies this reaction. The assembly was evacuated and the sample was then degraded to completion by programmed heating from room temperature to 500°C at $10^{\circ}\text{C}/\text{min}$ to produce a sample of completely cyclised cold ring material, free of olefinic impurity.

B 2 CONDITIONS OF POLYMERISATION.

The conditions of polymerisation were selected so as to simplify the application of the Mayo equation (i) to the system. All polymerisations were performed in the same dilatometer the neck of which was reconstructed after each experiment. It was filled to the mark each time with the result that the Mayo equation could be rewritten in the form

$$\frac{1}{x} = \frac{1}{x_0} + C'_a v_a \quad \text{--- (iii).}$$

Where :-

(1). V_a = VOLUME OF 4VCH ADDED TO DILATOMETER (μ l).

$$(2). C_a' = C_a \times \left[\frac{\bar{M}_s \rho_{4VCH}}{\bar{M}_{4VCH} \rho_s V_s} \right]$$

And :-

(3). \bar{M}_s = MOLECULAR WEIGHT OF STYRENE 104

(4). \bar{M}_{4VCH} = MOLECULAR WEIGHT OF 4VCH 108

(5). $\rho_s^{20^\circ C}$ = DENSITY OF STYRENE 0.9060 g/ml

(6). $\rho_{4VCH}^{20^\circ C}$ = DENSITY OF 4VCH (115) 0.8299 g/ml

(7). V_s = VOLUME OF STYRENE (μ l) 21.55×10^3

It is assumed in the above equation that the volume of styrene used in each of the polymerisations is a constant. This is a reasonable assumption when it is considered that the maximum content of 4VCH used in the dilatometer of volume 21.55 ml was 0.05% by volume.

The equation can therefore be written and used in the form

$$\frac{1}{x} = \frac{1}{x_0} + (4.09 \times 10^{-5} C_a) V_a \text{ --- (iv).}$$

AIBN was chosen as initiator because of its low transfer constant (116). The polymerisation was carried out at $60^\circ C$ using 2.5 mg AIBN (117) to produce a polymer of number average molecular weight (in absence of additive) in the range $2 - 5 \times 10^6$ in order that all molecular weights could be measured by osmometry.

All polymerisations were carried out, not to the same conversion, but to the same time of reaction, in order that all batches of monomer be exposed to the same rates of initiation during polymerisation. The polymer formed in the absence of additive was taken to 6% conversion. Percentage conversions (C_v) were related to percentage contractions (C_t) of the system by the relationship (118)

$$C_v = 0.17 C_t \text{ --- (v).}$$

C DISCUSSION.

The conversion curves to polymer for the additive free system and for the system in the presence of approximately equal quantities of 4VCH and cyclised rubber are shown in fig. 2 . It can be seen that 4VCH retards but does not inhibit the polymerisation reaction.

The variations of the number average molecular weight and reciprocal number average molecular weight of the polymer with 4VCH concentrations are shown in figs. 3 and 4 , respectively. The connecting line in fig. 4 was obtained by a linear least squares cycle on the data points to give a $10^5 C$ value of 117. This is in good agreement with transfer constants (10^5) of additives thought to operate by the same mechanism of allyl radical formation.

TABLE 7.9 - 1

TRANSFER CONSTANTS TO POLYSTYRENE OF MATERIALS CAPABLE OF ALLYL
RADICAL FORMATION.

ADDITIVE	TEMPERATURE °C	$10^5 C$	REFERENCE
1-BUTENE	100	26	105
2-BUTENE	100	20	105
2-METHYL-1- - PROPENE	100	17	105

It was asserted in Chapter 7 that polycyclic material of the type generated by polybutadiene during its endothermic decomposition reaction can deactivate polystyryl radicals. To test this assumption a 10 mg sample of completely cyclised and saturated rubber cold ring material was added to AIBN and styrene monomer which was polymerised under the conditions previously outlined. The mass ratio of additive/styrene was approximately the same as that achieved in the system 10 μ l 4VCH/styrene (4.25×10^{-4} by weight). This enabled a comparison to be made between the two additives.

It can be seen (fig. 2) that both materials retard the conversion reaction with similar efficiencies. The polycyclic material, however, appears to be a more efficient chain transfer agent (by weight) than 4VCH (figs. 3 and 4).

CONVERSION CURVES FOR STYRENE POLYMERISED IN THE PRESENCE OF
4-VINYLCYCLOHEXENE AND CYCLISED RUBBER COLD RING MATERIAL

Key

- 1 Polystyrene Formed In The Absence Of Additive
- 2 Polystyrene Formed In The Presence Of 4.25×10^{-4} Weight %
4-vinylcyclohexene
- 3 Polystyrene Formed In The Presence Of 4.25×10^{-4} Weight %
Rubber Cold Ring Material

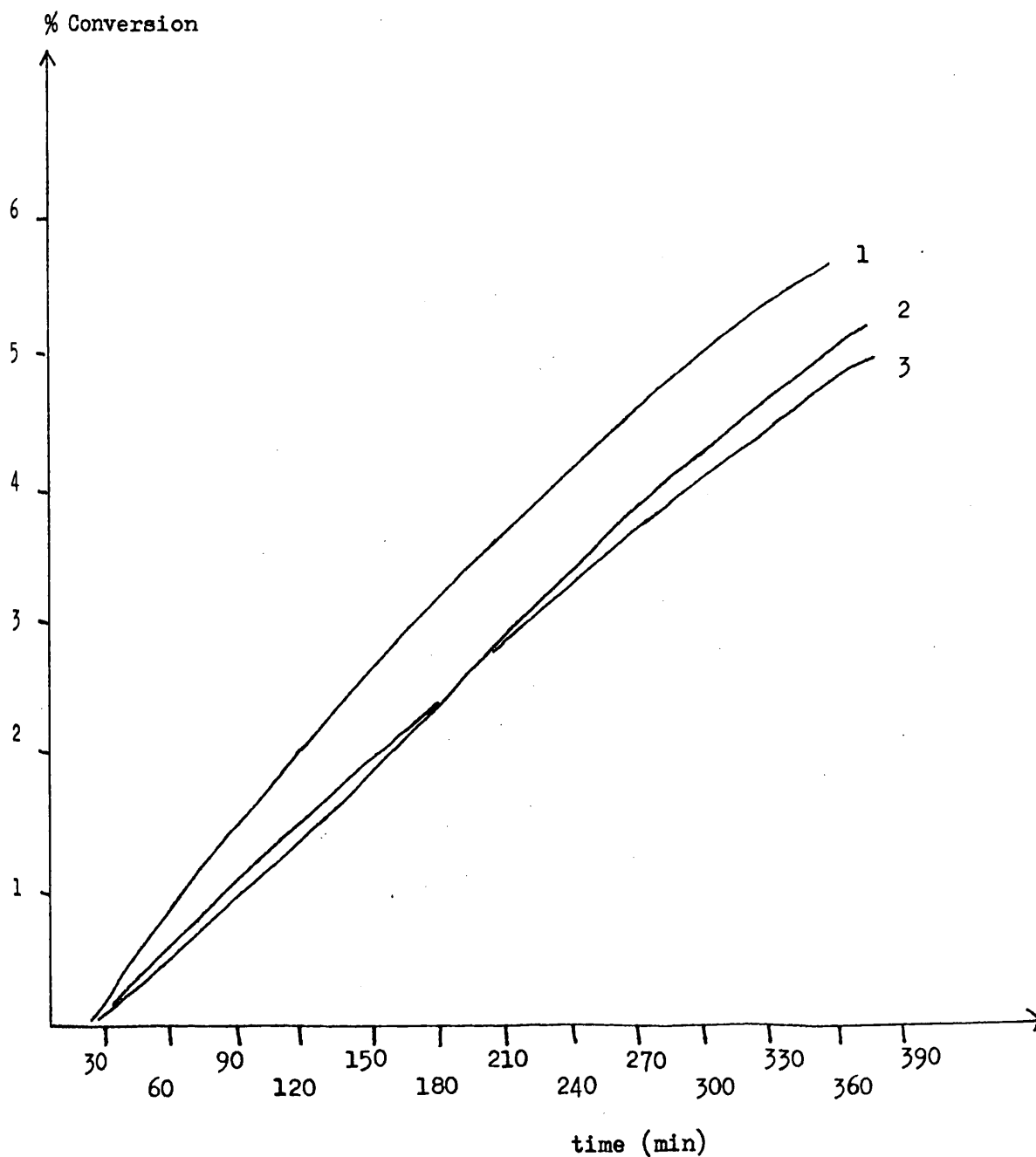


FIGURE 9 - 3

VARIATION OF NUMBER AVERAGE MOLECULAR WEIGHT OF POLYSTYRENE WITH
ADDITIVE CONCENTRATION

Key

4-vinylcyclohexene

Cyclised Cold Ring Material

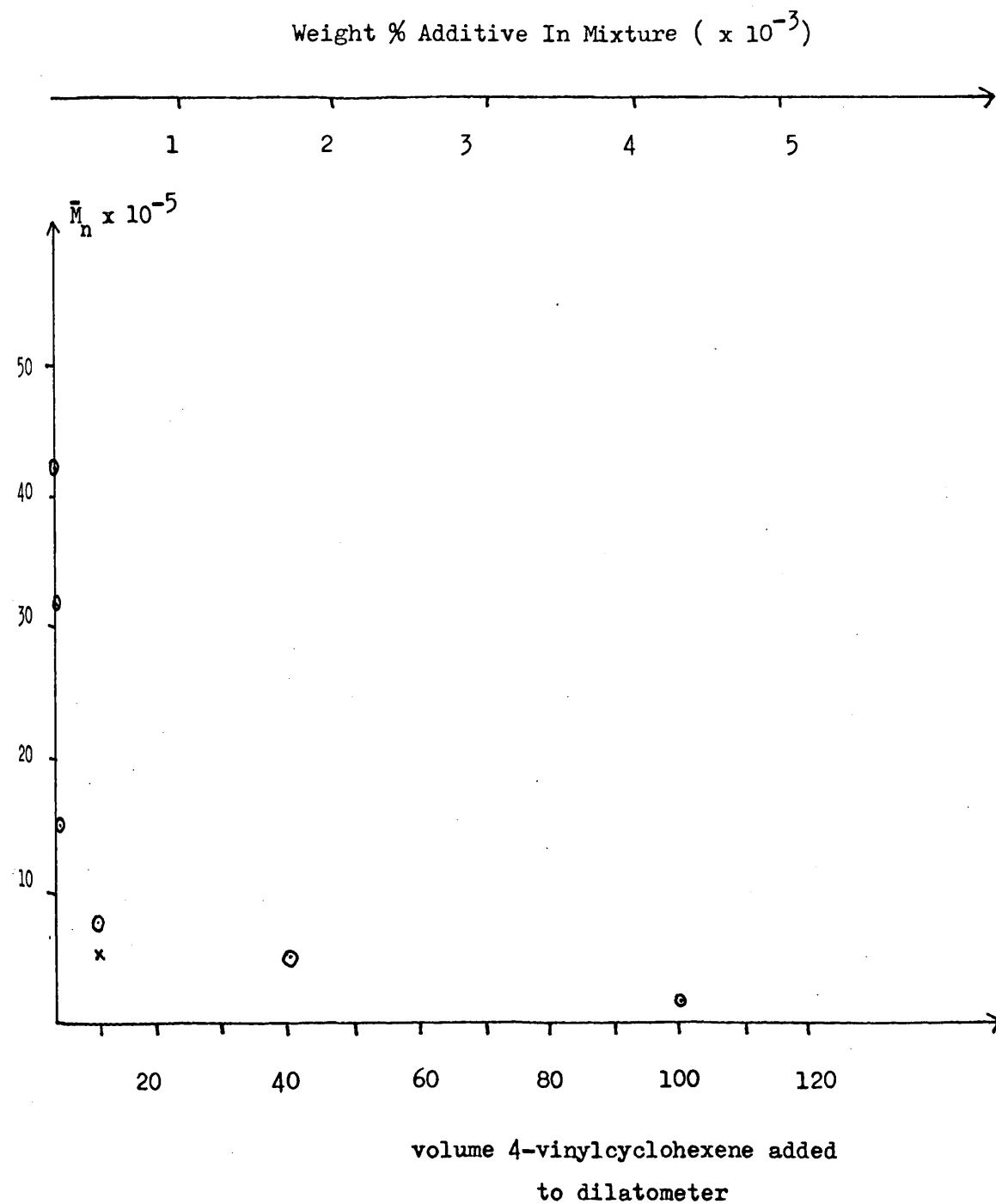


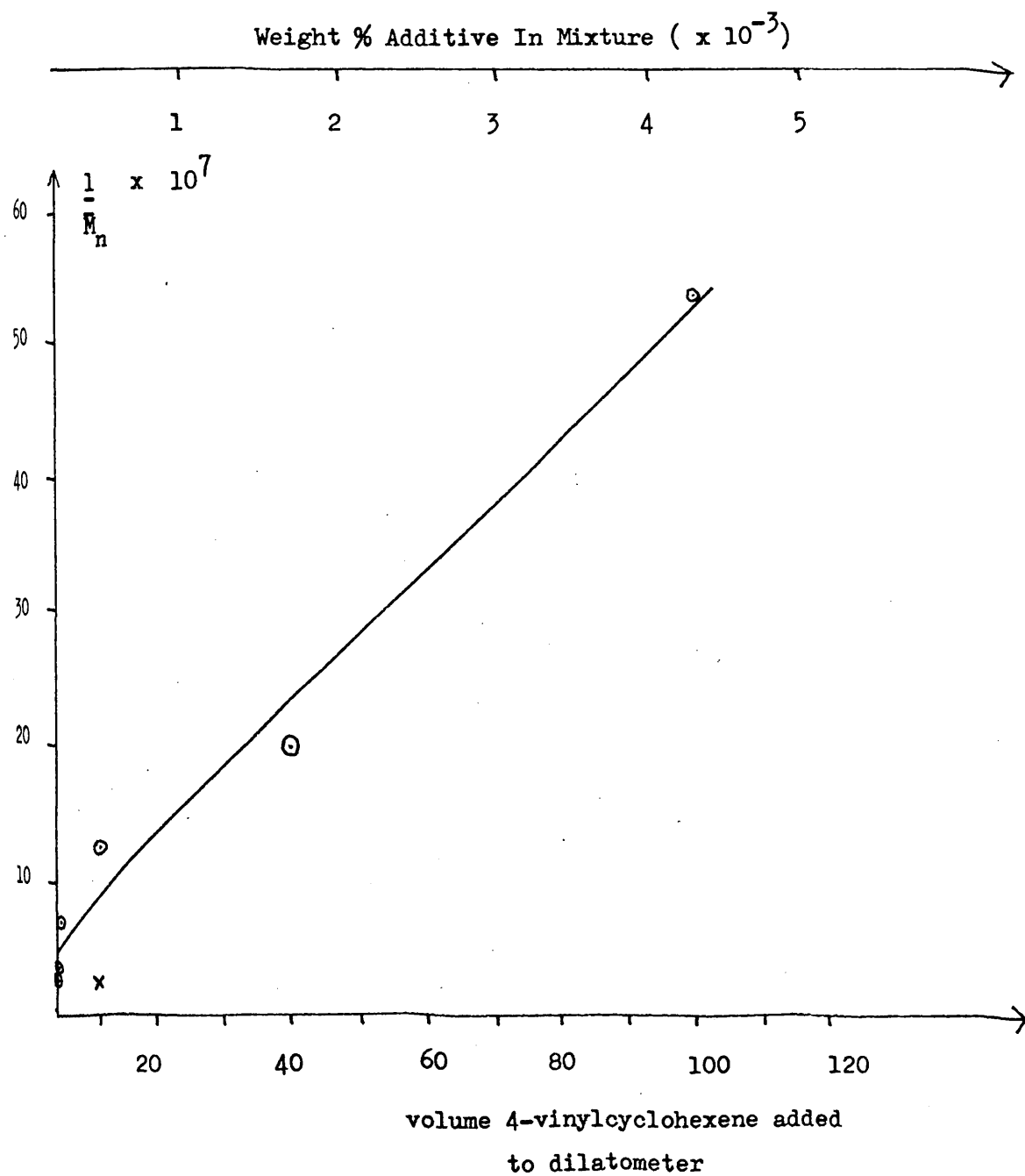
FIGURE 9 - 4

VARIATION OF RECIPROCAL NUMBER AVERAGE MOLECULAR WEIGHT OF POLYSTYRENE
WITH ADDITIVE CONCENTRATION

Key

4-vinylcyclohexene

Cyclised Cold Ring Material



BULK DECOMPOSITION OF AZOBISISOBUTYRONITRILEA INTRODUCTION AND LITERATURE REVIEW.

In Chapter 9, 4-vinylcyclohexene (4VCH) was termed a degradative chain transfer agent. By definition, a small fraction of this material in the presence of radicals will take part in hydrogen transfer and carbon - carbon bond forming reactions. It was felt that weight would be lent to the above statement if the products of such reactions could be directly detected. To this end, 4VCH was placed in intimate contact with an equal quantity of azobisisobutyronitrile (AIBN) which was subsequently thermolysed. After decomposition of the latter was complete, the products of degradation were separated by the usual vacuum line techniques and examined by spectroscopy and by GLC in an attempt, firstly, to identify adducts of isobutyronitrile (IBN) to 4VCH, 4VCH dimers, and, secondly, to detect an enhanced yield of isobutyronitrile as a product of hydrogen abstraction reactions in the mixture.

The experiments proved to be inconclusive, but some hitherto unpublished information relating to the bulk decomposition of AIBN was obtained. For this reason, the work has been included in the discussion.

Although some mention will be made of kinetic and mechanistic data obtained from, most notably, ultra-violet spectroscopy and the technique of radical scavenging, most of this review is concerned with information obtained by applying the very elegant ^{14}C tracer techniques of Bevington to the decomposition of AIBN.

The efficiency with which this material initiates the polymerisation of styrene is much less than 100% (119).

It has been assumed that this is because a proportion of the primary radicals recombine to yield tetramethylsuccinodinitrile (TMSDN) (112). The presence of IBN (120) indicated that a disproportionation reaction also takes place.

The detection of methacrylonitrile (MAN) as a product of disproportionation was hampered by its tendency to be removed from the polymerising medium as polymer or copolymer by its addition to radicals in solution. The concentration has been estimated, however, by isotope dilution (121) as approximately 10 - 12 mole% of the products of cage decomposition at 60°C. It was detected by Bevington (122) as a copolymerised impurity in polystyrene prepared with AIBN and by Grassie and Grant (123) as a low molecular weight polymer formed by refluxing AIBN with ethanol.

An unstable reactive intermediate was discovered by Talât-Erben and Bywater (124) who noticed that the decomposition of AIBN displayed a considerable deviation from first order kinetics when the process was followed by ultra-violet spectrometry. The material, assumed to be a ketenimine formed by an abnormal radical recombination, was later isolated and characterised by Hammond and co-workers (125).

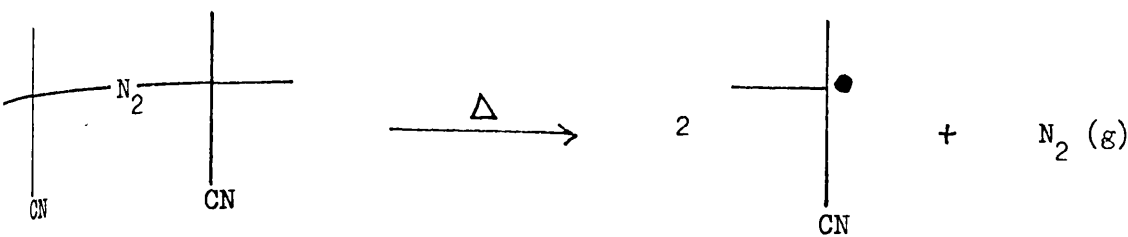
Talât-Erben and Isfendiyaroglu (126) showed that, in the absence of chemical interference, the intermediate quantitatively rearranged to TMSDN presumably by a molecular process. By an elegant kinetic argument normal and abnormal recombination were estimated as 28 mole% and 56 mole% , while disproportionation was estimated as producing 16 mole% of the products of decomposition at 80°C.

Hammond and co-workers, however, found that purified ketenimine could initiate the polymerisation of styrene (125) though with a lower efficiency than AIBN. This was supported by Bevington (122) who found that the polymerisation of styrene with AIBN was accelerated when the latter was contaminated by ketenimine. It was suggested that ketenimine decomposed by a radical mechanism, and that the lower efficiency with which this material can initiate polymerisation with respect to AIBN stems from the lower recoil energy of the products of decomposition. If it is assumed that the quantitative conversion to TMSDN is associated with this low "recoil energy" then an explanation is available to account for the increased yields of disproportionation products from AIBN as the temperature of decomposition is raised.

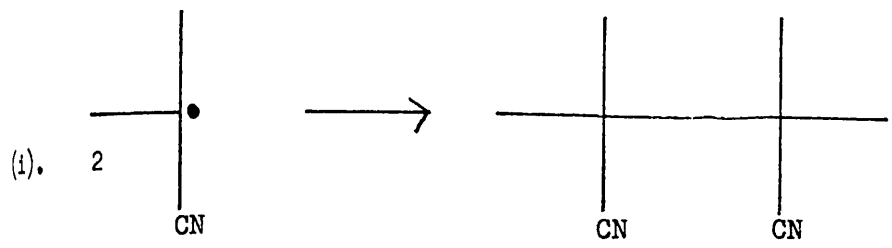
Hammond (127) found that ketenimine is formed by two processes one of which is inaccessible to inhibitor. Bevington (128) found that the efficiency with which AIBN initiates polymerisation was very variable in solutions of low monomer concentration. Ayrey (121) developed a method capable of analysing MAN formed by cage as opposed to bulk disproportionation of the products of AIBN decomposition. The above all point to the existence of cage and bulk processes in solution.

To end with it must be noted that although AIBN has been reported by Bevington (129) to possess a transfer constant "close to zero", it is in fact susceptible to induced decomposition. Prior and Fiske (117) using a modified form of Bevington's own method obtained a Mayo type transfer constant of approximately 10^{-2} . It was noted, however, that chain transfer to AIBN only becomes important at abnormally high concentrations of the inhibitor.

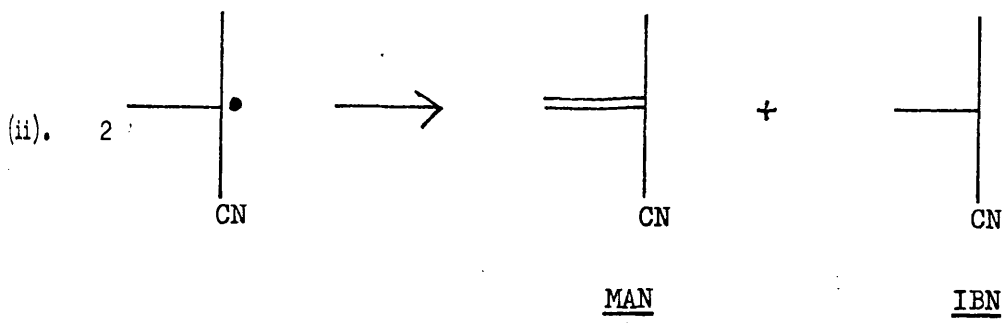
The mechanism by which AIBN is thought to decompose can be summarised as follows.



AIBN

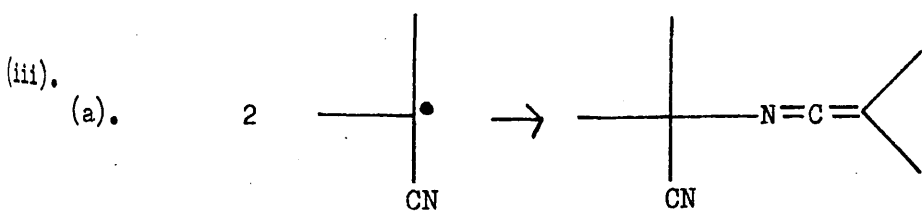


TMSDN



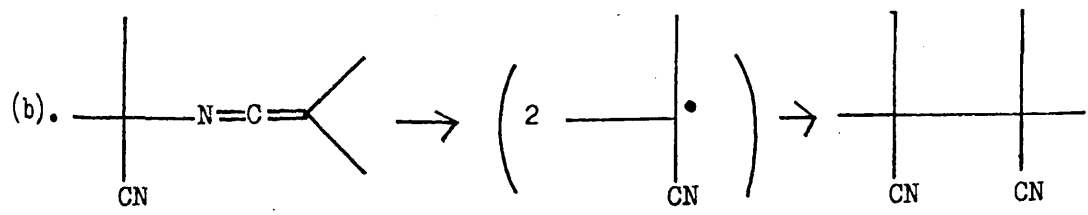
MAN

IBN



Dimethyl ketene cyano isopropylimine

DKCP



DKCP

TMSDN

B PROGRAMMED OPEN SYSTEM DEGRADATIONS.

B 1 DSC AND TG UNDER NITROGEN.

It can be seen from the DSC curve (fig. 1) that the processes of melting and decomposition overlap, with the latter achieving a rate maximum at 120°C . The close agreement between the DSC exotherm and the TG rate maximum (fig. 2) indicates that, at 120°C , the products of decomposition are efficiently removed from the hot zone.

B 2 TVA.

TVA curves showing the evolution of the noncondensable product fraction of AIBN decompositions are shown in fig. 3 . Curves a and b are of samples of AIBN which quantitatively sublimed to the top of the degradation tube on heating. The subsequent decomposition reaction was brought about by incident blackbody radiation. Curves c, d, e and f are of samples of AIBN which were encapsulated in finely ground 13X molecular sieve. It can be seen that provided the capacity of the sieve for AIBN at degradation temperatures is not exceeded the TVA trace so produced agrees well with the TG rate trace under nitrogen.

B 3 PRODUCT DISTRIBUTION.

The condensable volatile fraction of degradations carried out in the absence of molecular sieve was subjected to sub-ambient TVA fractionation and spectroscopic analysis to give a product distribution identical to that outlined in fig. 4 .

FIGURE 10 - 1

DSC OF AIBN UNDER NITROGEN

Heating Rate $10^{\circ}\text{C}/\text{min}$

Sample Size 2.5 mg

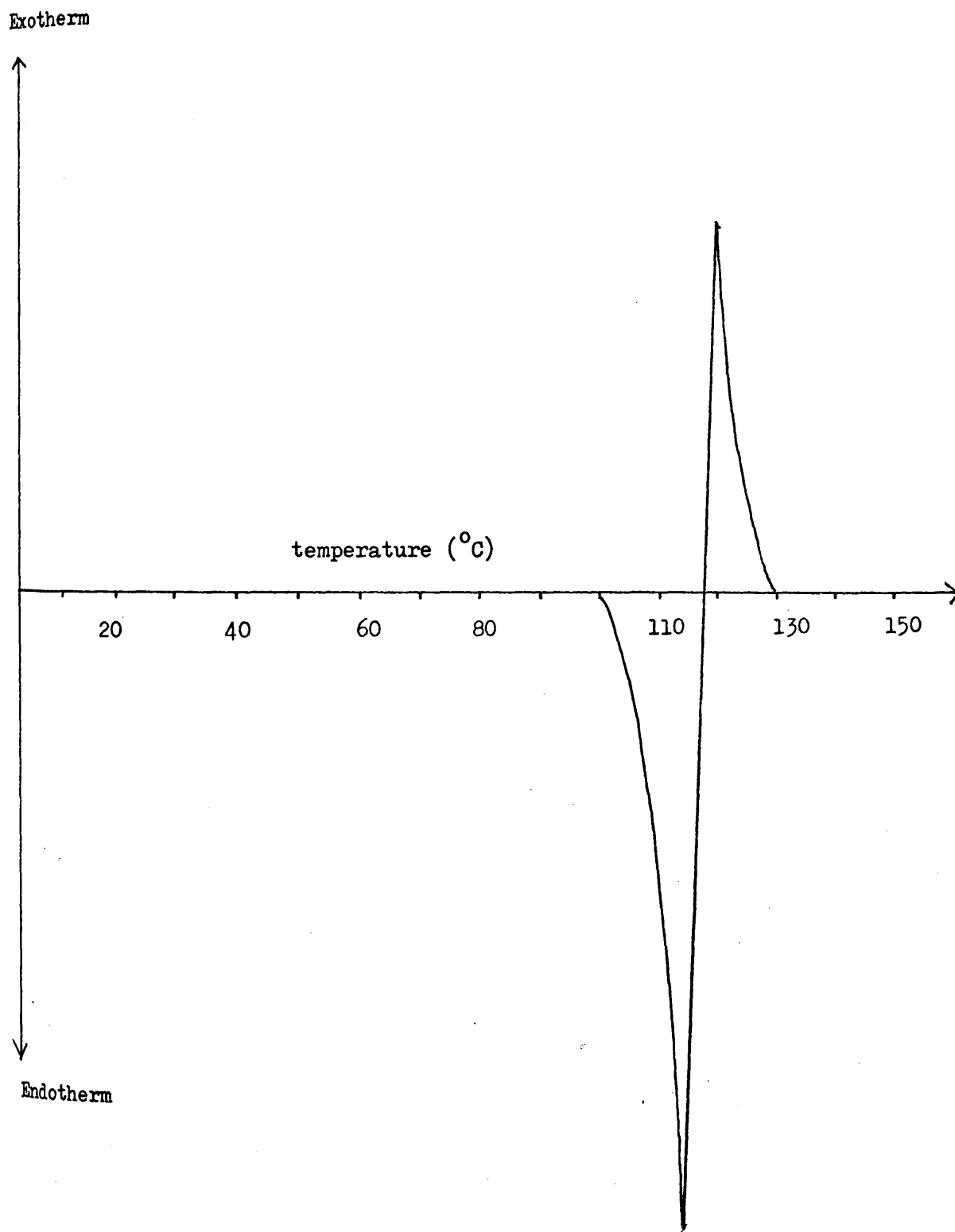


FIGURE 10 - 2
TG OF AIBN UNDER NITROGEN

Heating Rate $10^{\circ}\text{C}/\text{min}$

Sample Size 5 mg

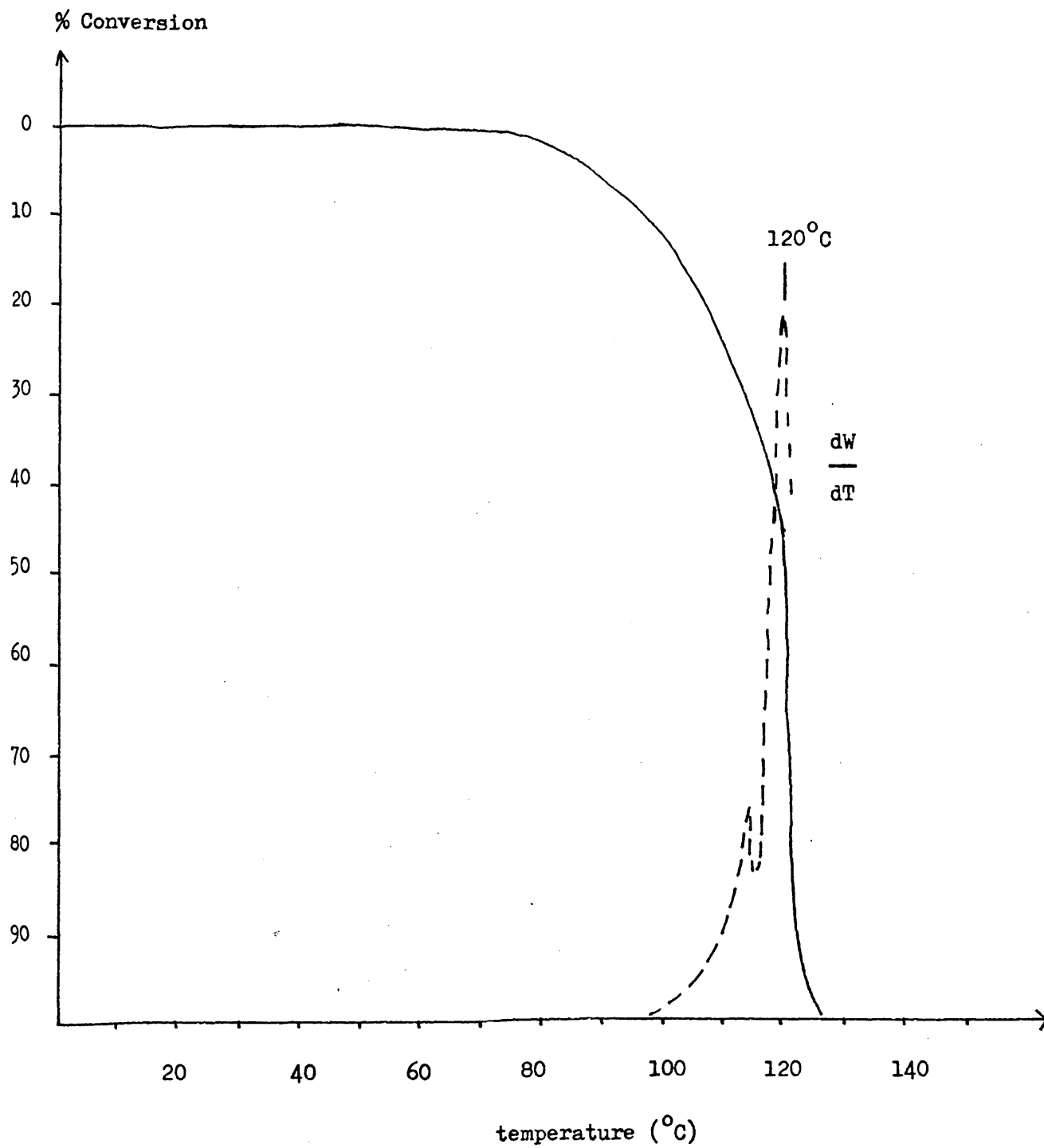


FIGURE 10 - 3

TVA CURVES SHOWING THE EVOLUTION OF THE NONCONDENSABLE PRODUCT

FRACTION OF AIBN DECOMPOSITION

Key

- a,b 10 mg Samples of AIBN Degraded In The Absence of 13X
Molecular Sieve In Different Oven Assemblies
- c 1 mg AIBN/400 mg 13X Sieve
- d 10 mg AIBN/400 mg 13X Sieve
- e 25 mg AIBN/400 mg 13X Sieve
- f 50 mg AIBN/400 mg 13X Sieve

Heating Rate 10°C/min

Pirani Output (mv)

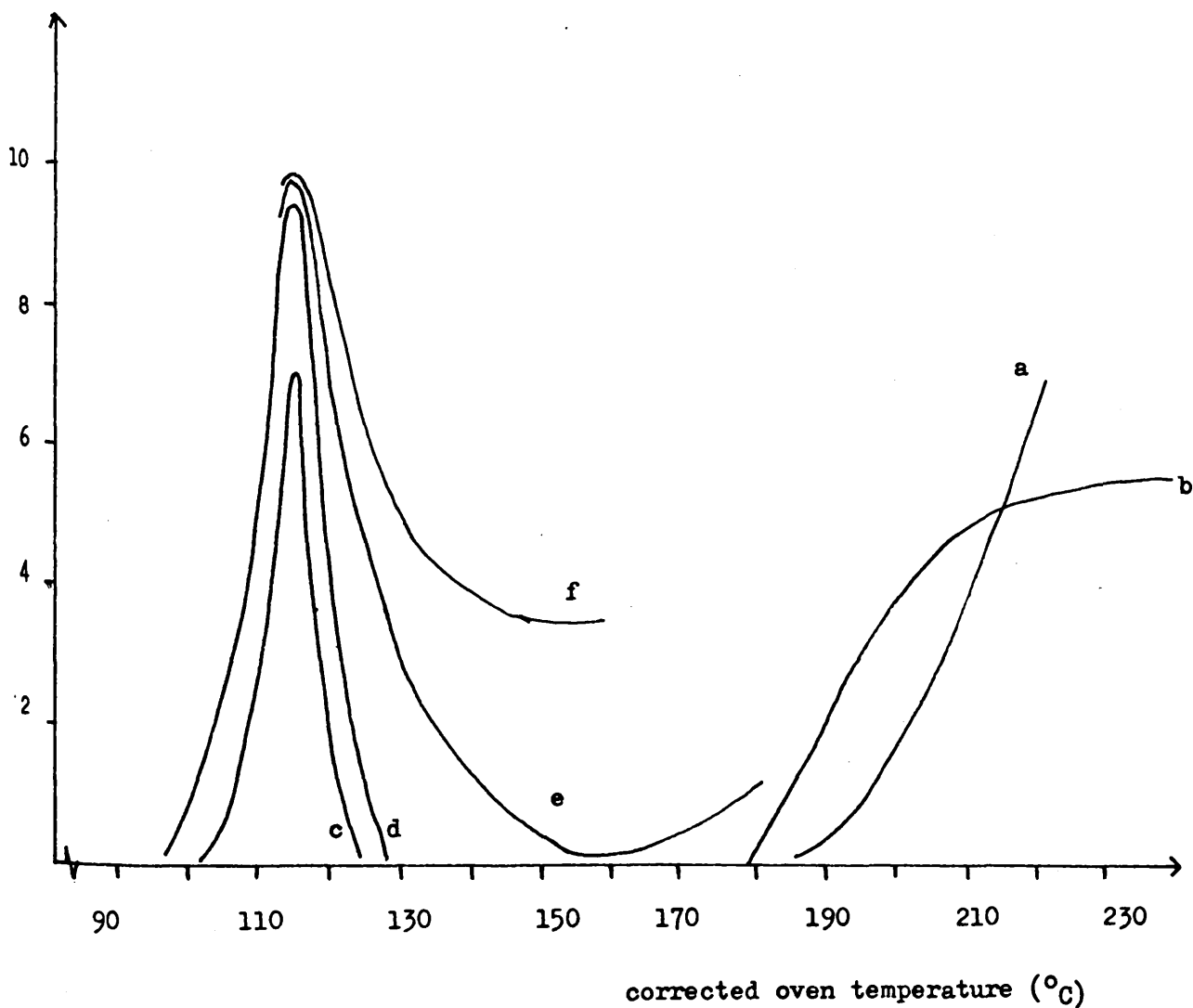


FIGURE 10 - 4

SUB-AMBIENT TVA OF PRODUCTS OF CLOSED SYSTEM AIBN DEGRADATION
TO COMPLETION AT 90°C

Sample Size 10 mg

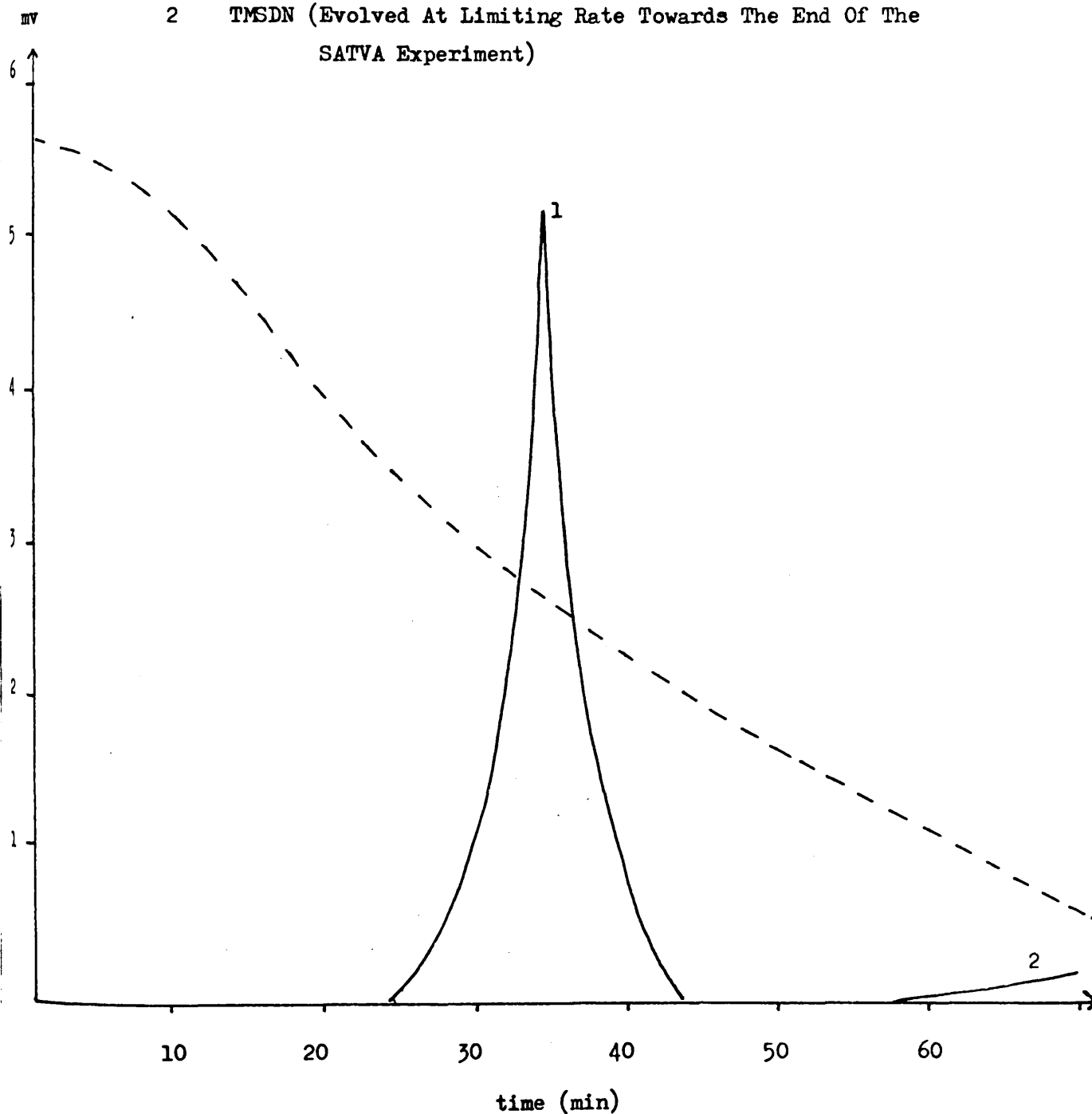
Key

(-) Thermocouple Output

— Pirani Gauge Output

1 MAN , IBN

2 TMSDN (Evolved At Limiting Rate Towards The End Of The
SATVA Experiment)



C ISOTHERMAL OPEN SYSTEM DEGRADATIONS AT 90°C.

C 1 TG UNDER NITROGEN.

It can be seen that the shape of the TG curve (fig. 5) deviates considerably from that expected from a first order decomposition reaction. If it is assumed that the products of the decomposition reaction are volatile at degradation temperatures then this behaviour can not be attributed to a measure of autocatalysis by the transient population of DKCP in the degradation medium and must be assumed to arise from sample "bubbling" effects. Weight is lent to this statement by the observation that the isothermal noncondensable emission curve at this temperature (discussed subsequently) does not display this anomalous behaviour.

C 2 TVA

An isothermal TVA curve for this reaction temperature can be inspected in fig. 6 . It can be seen that the primary decomposition reaction, as measured by nitrogen evolution, proceeds in the manner expected of a first order process. The reaction is complete after 40 min degradation at this temperature.

Provided it can be shown that 13X molecular sieve does not catalyse the decomposition of AIBN it may be possible to use the TVA method as a direct probe into the primary decomposition reaction of AIBN, with particular reference to obtaining rate constants for the reaction. The twin requirements of linearity of Pirani output and elimination of sample sublimation are easily achieved by using small samples of AIBN.

C 3 PRODUCT DISTRIBUTION.

This was found to be identical to that shown in fig. 4 .

FIGURE 10 - 5

ISOTHERMAL TG AT 90°C OF AIBN UNDER NITROGEN

Sample Size 5 mg

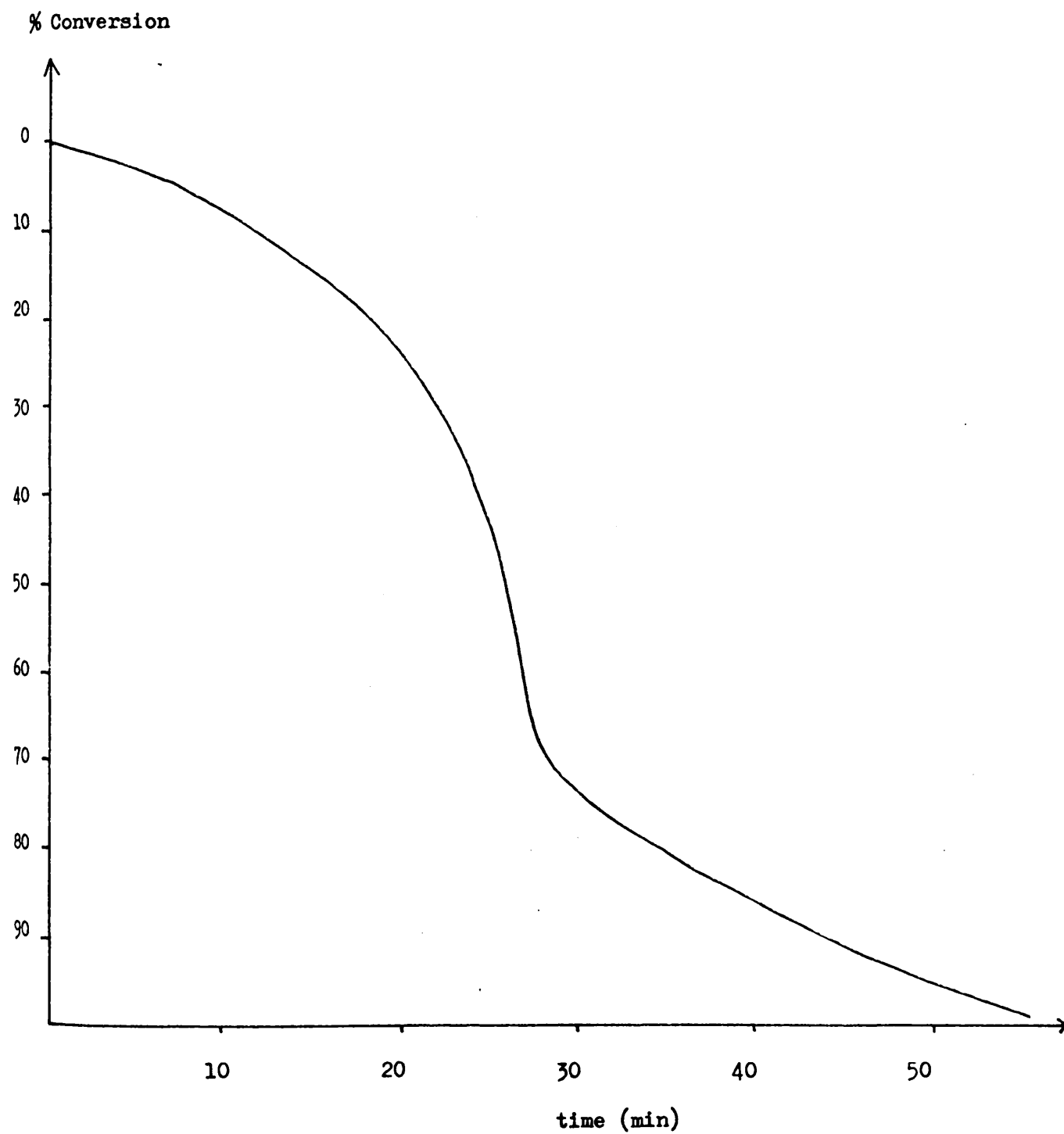
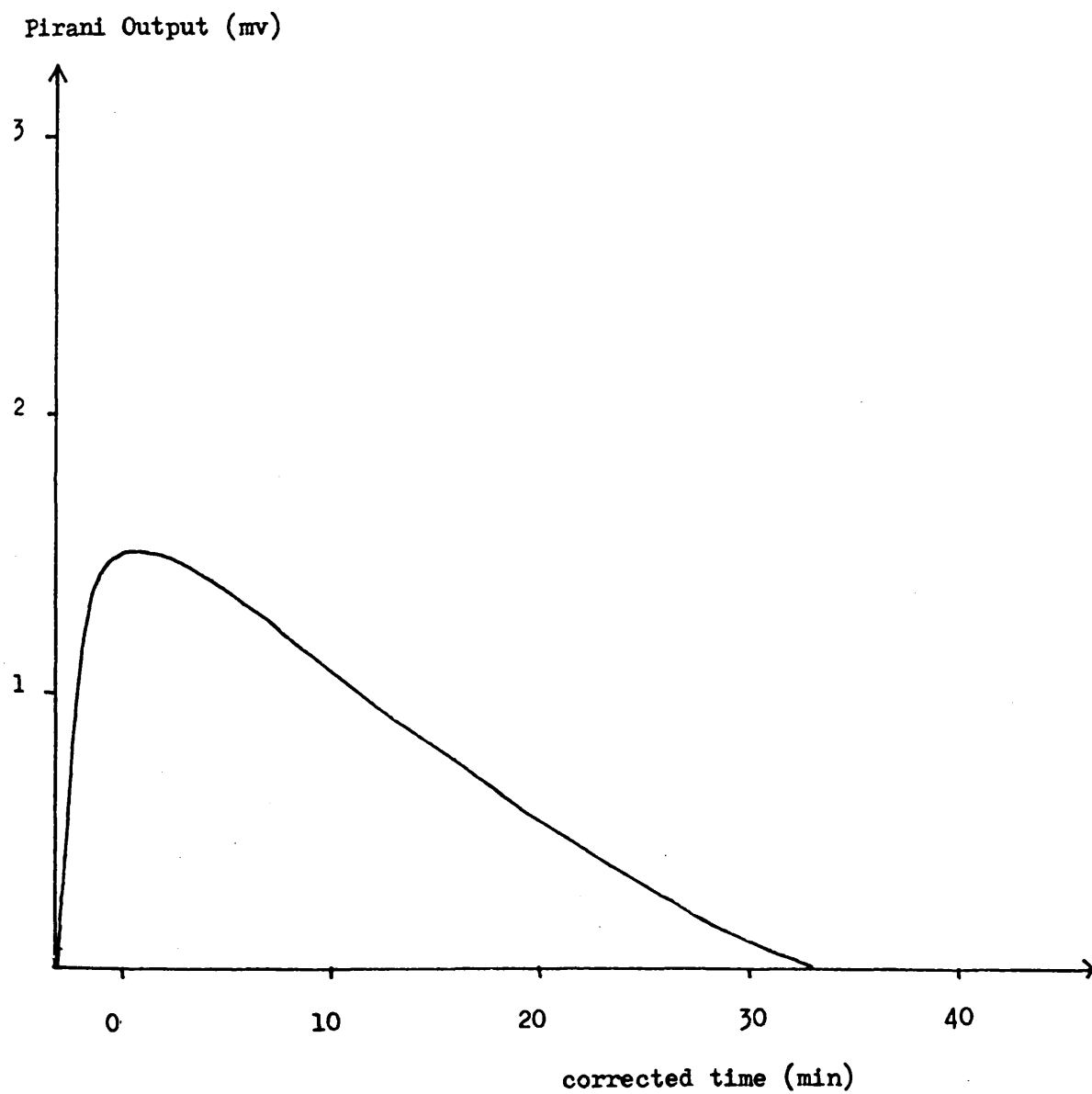


FIGURE 10 - 6

ISOTHERMAL TVA CURVE AT 90°C SHOWING THE EVOLUTION OF THE
NONCONDENSABLE PRODUCT FRACTION OF AIBN DECOMPOSITION

Sample Size 1 mg



D PYROLYSIS - GLC.

Solutions of AIBN in methylene chloride and acetone were flash pyrolysed in the injection block of a GLC assembly maintained at $\approx 300^{\circ}\text{C}$. The products of degradation were separated on a 6', $\frac{1}{4}$ " Chromosorb 103 column at 225°C to give a GLC trace of the type illustrated in fig. 7. The sharpness of peaks 1 and 2 indicate that degradation is very rapid, although the precise conditions under which it occurs can not be defined.

If we assume that the detector reacts linearly with mass then the following measurements can be made.

SOLVENT	MASS% DISPROPORTIONATION	MASS% COMBINATION
METHYLENE CHLORIDE	8.5 ± 0.3	91.5 ± 0.3
ACETONE	8.3 ± 0.2	91.7 ± 0.2

It can be seen that the solvent does not affect the product distribution of the reaction. Of greater interest is the observation that the relative quantities of MAN and IBN differ by less than 5%. This is apparently the first experiment to show this directly, though admittedly under badly defined conditions of reaction.

FIGURE 10 - 7

TYPICAL GLC SEPARATION OF PRODUCTS OF FLASH PYROLYSIS OF AIBN

Injection Block Assembly Held At 300°C

Column 6' , $\frac{1}{4}$ " Diameter, Chromosorb 103

Column Temperature 225°C

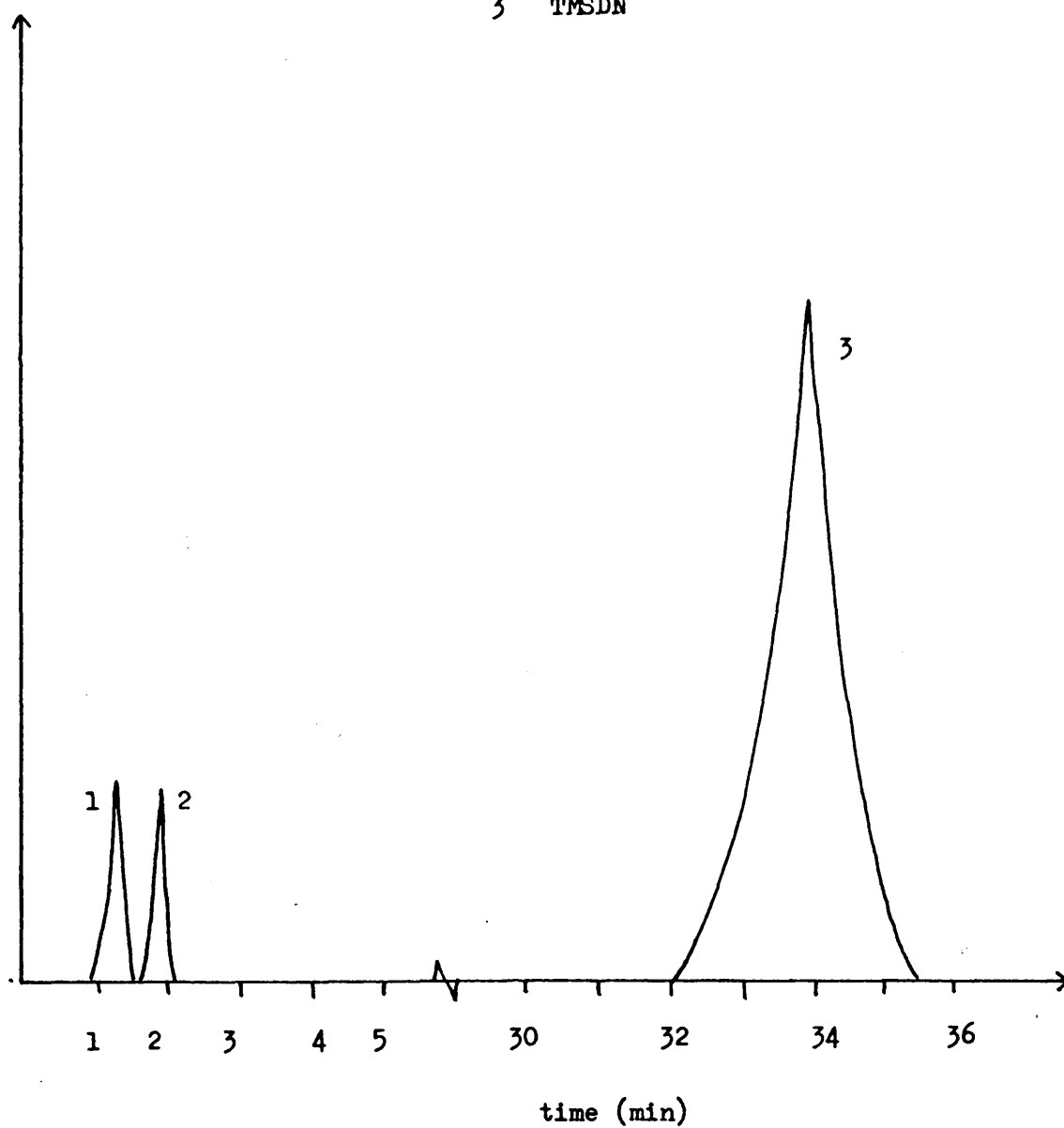
Key

1 MAN

2 IBN

3 TMSDN

Solvent Front



E ISOTHERMAL CLOSED SYSTEM DECOMPOSITIONS AT 90°C.

E 1 PROCEDURE.

Degradations were performed in the assembly shown in fig. 8 . Samples of AIBN (250 mg) and 4VCH (250 μ l) were degraded simultaneously, separately and as a mixture, using the three limbed assembly discussed in Chapter 8.

Degradations were performed under a nitrogen blanket to stop AIBN and 4VCH from quantitatively subliming and distilling, respectively, from the hot zone.

The reactor was exhaustively degassed. With its contents frozen it was then opened to a stream of nitrogen gas freed of condensable impurities by passage through a glass spiral held at -196°C. The assembly was then sealed and its contents were degraded to completion by heating to 90°C for one hour. The reactor was again degassed and its contents were transferred to the fractionating grid for analysis.

E 2 QUALITATIVE PRODUCT DISTRIBUTION (60 min/90°C).

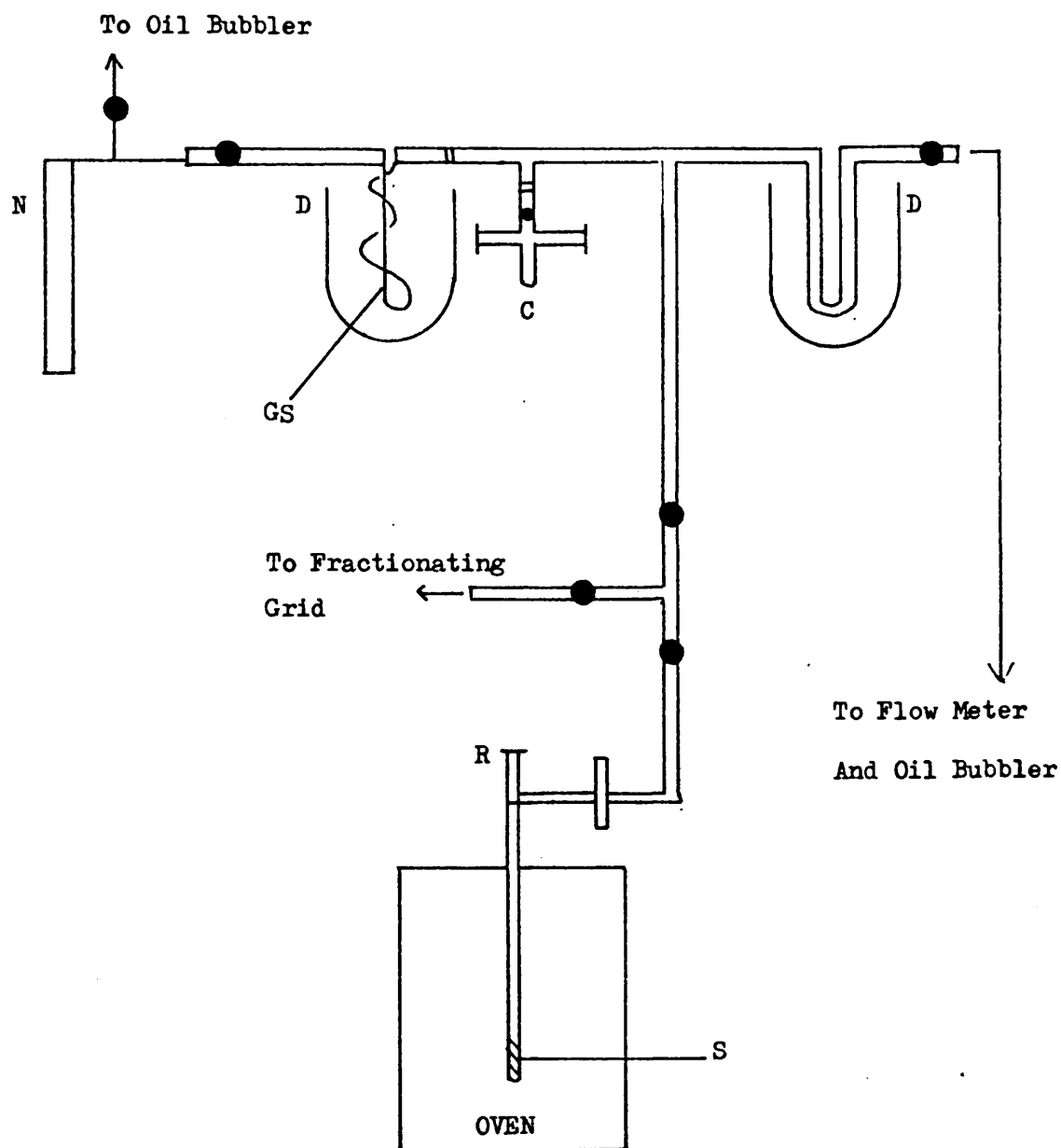
10 mg AIBN were degraded to completion and the condensable volatile product fraction of decomposition was subjected to a sub-ambient TVA separation. Subsequent spectral checks enabled the volatile peaks to be labelled as shown in fig. 4 . The addition of 10 mg 4VCH did not produce any new products. A mixed degradation using 250 mg AIBN and 250 μ l 4VCH produced the same result.

E 3 QUANTITATIVE PRODUCT DISTRIBUTION (60 min/90°C).

The volatile fractions of degradation were separated by GLC on a 6' , $\frac{1}{4}$ " Chromosorb 104 column at 220°C using toluene as the internal reference material. A typical GLC trace is shown in fig. 9 . Yields of MAN and IBN are tabulated below.

FIGURE 10 - 8

APPARATUS FOR CLOSED SYSTEM DEGRADATIONS UNDER NITROGEN



Key

- C i.r. Gas Cell Used To Check Purity Of Gas Flow
- D Dewar Vessels Containing Liquid Nitrogen
- S Sample To Be Degraded
- N Nitrogen Gas Cylinder
- R Closed System Reactor
- GS Glass Spiral

FIGURE 10 - 9

TYPICAL GLC SEPARATION OF PRODUCTS OF CLOSED SYSTEM AIBN

DEGRADATION

Column 6' , $\frac{1}{4}$ " Diameter, Chromosorb 104

Column Temperature 220°C

Key

1 MAN

2 IBN

3 Toluene (Internal Reference Material)

4 4VCH (Introduced Prior To Degradation)

Solvent Front

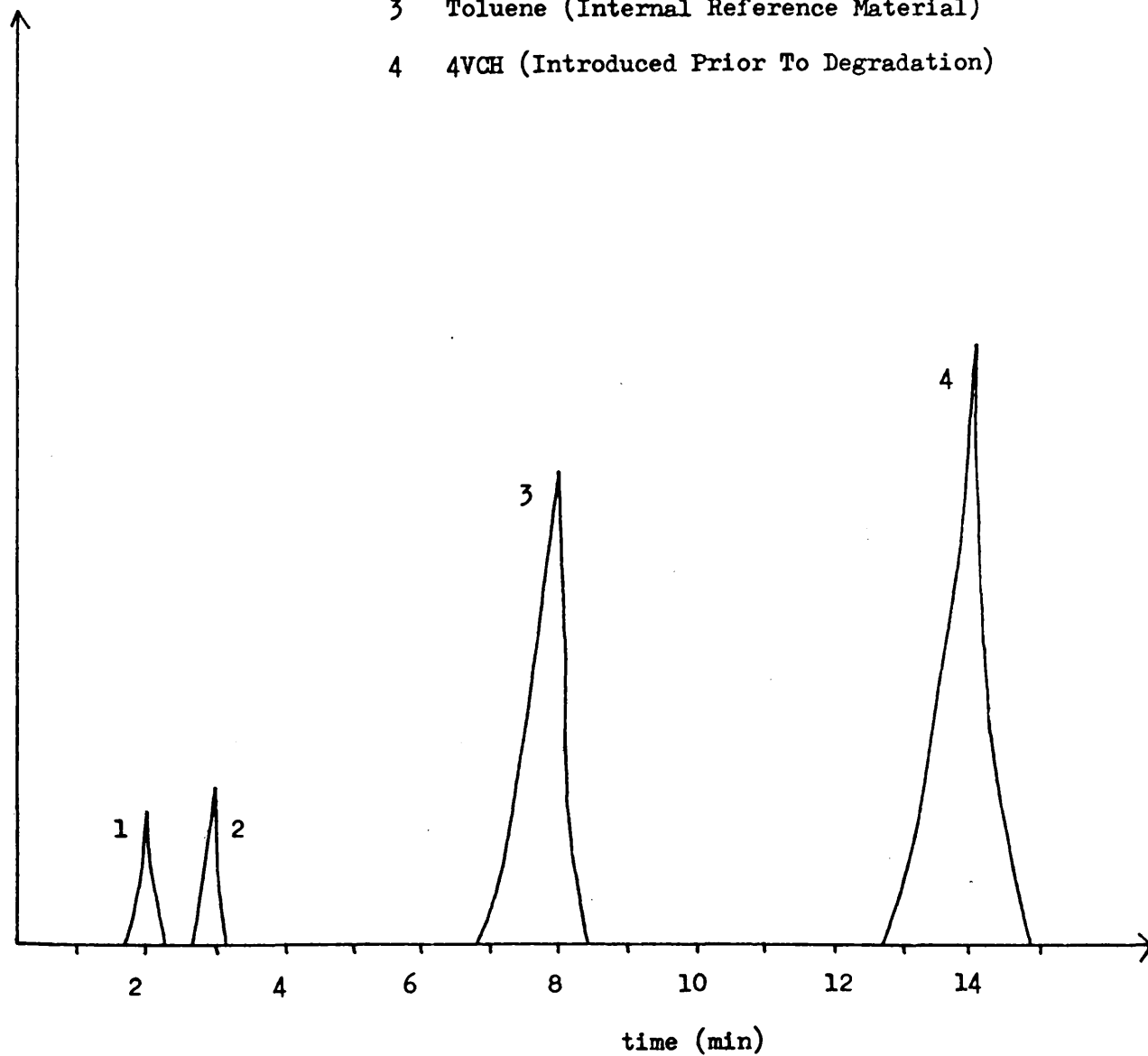


TABLE 10 - 1

YIELDS OF MAN AND IBN FROM AIBN DECOMPOSITIONS AT 90°C

RUN N°	AIBN (mg)	MAN (μ l)		IBN (μ l)	
		MIXED	UNMIXED	MIXED	UNMIXED
1	250	7.0	14.0	14.0	17.0
2	250	7.0	13.5	16.5	17.0
3	250	7.0	11.0	15.5	16.0
4	250	5.5	13.5	15.0	17.5
5	250	8.0	12.5	15.5	17.0
6	250	7.0	11.5	13.5	15.0
AVERAGE		6.9	12.7	15.0	16.6
MOLE% OF PRODUCTS *		5.3	9.6	11.5	12.5

* ASSUMING.

$$(i). \rho_{\text{IBN}}^{20^\circ\text{C}} = \rho_{\text{MAN}}^{20^\circ\text{C}} = 0.80 \text{ g/cc}$$

$$(ii). 250 \text{ mg AIBN} = 1.49 \text{ mmole}$$

F DISCUSSION.

It can be seen from Table 1 that the yield of IBN is almost unaffected by the presence of 4VCH. The yield of MAN as product, however, decreases in the presence of 4VCH. This effect is also observed when AIBN is degraded in the presence of n-decane and so must be purely physical in nature.

If MAN and IBN are assumed to be formed in equal quantities (12.5 mole%) then it would appear that AIBN decomposes to form 75 mole% combination and 25 mole% disproportionation products during isothermal degradations performed at 90°C under a nitrogen blanket.

A INTRODUCTION AND LITERATURE REVIEW.

The purpose of this discussion is to consider the effect of oxidative degradation of polybutadiene at temperatures below its flash point on the subsequent thermal degradation either under vacuum or under nitrogen.

This work was performed for two reasons. Firstly, it is impossible to suppress completely the oxidation of polybutadiene except under high vacuum conditions even after the addition of high concentrations of antioxidant. Such material is very rapidly exhausted in regions of high activity and the diffusion of fresh material to the site is hampered by the amorphous nature of the polymer. All fabricated rubbers must therefore be considered as partially oxidised. It is therefore essential that some insight be gained into the mechanisms of thermal degradation of oxidatively modified polybutadiene to enable predictions to be made concerning the thermal stability of "real" polymers.

Secondly, it must be realised that the mechanisms which are operative in polybutadiene oxidation are still only partially understood. This situation has arisen for a number of reasons. The reaction is of course heterogeneous and except in the case of very thin films of the material, is controlled by the rate of migration of oxygen into the sample. This effect is dependent not only upon the size and geometry of the sample but also upon its history and therefore its morphology. The problem of identifying products of the primary oxidation reaction has never been completely solved in practice as such material itself is susceptible to further oxidation. Oxidised polybutadiene rapidly

becomes insoluble. This effect renders useless or at best unreliable a whole range of "wet chemical" techniques which have been successfully applied to the study of mechanisms of oxidation of low molecular weight model compounds, and of polyisoprene, which, because of its susceptibility to chain scission reactions, retains its solubility to high extents of oxidation (130).

The techniques of thermal degradation were applied to oxidatively modified polybutadiene in an attempt to elucidate the thermal degradation mechanisms and therefore to be able to "work backwards" and gain some insight into the composition of the oxidised material prior to its modification by purely thermal processes.

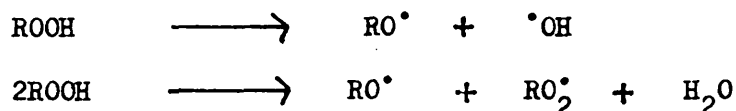
It must be noted that this work was not intended to be quantitative mainly because samples were not examined as films thin enough to eliminate effects of gas diffusion on the oxidation process (131).

It has been known for some time that oxygen is incorporated on storage into materials which contain mono-olefinic groupings. It was shown (132, 133) that this process does not lead to a reduction in unsaturation but gives a hydroperoxide grouping in a position α to the olefinic centre, which may or may not have been displaced. The formation of products attainable only through double bond shifting reactions (134) confirmed that the primary oxidation reaction proceeded via the abstraction of a proton in position α to the double bond by a (unspecified) radical, to produce a π -allyl complex which may or may not isomerise before the very rapid addition of the diradical oxygen molecule. The cycle was assumed to be completed by an α hydrogen abstraction by the peroxide group from a neighbouring molecule to continue the chain process.

The first detailed kinetic study of a homogeneous oxidation

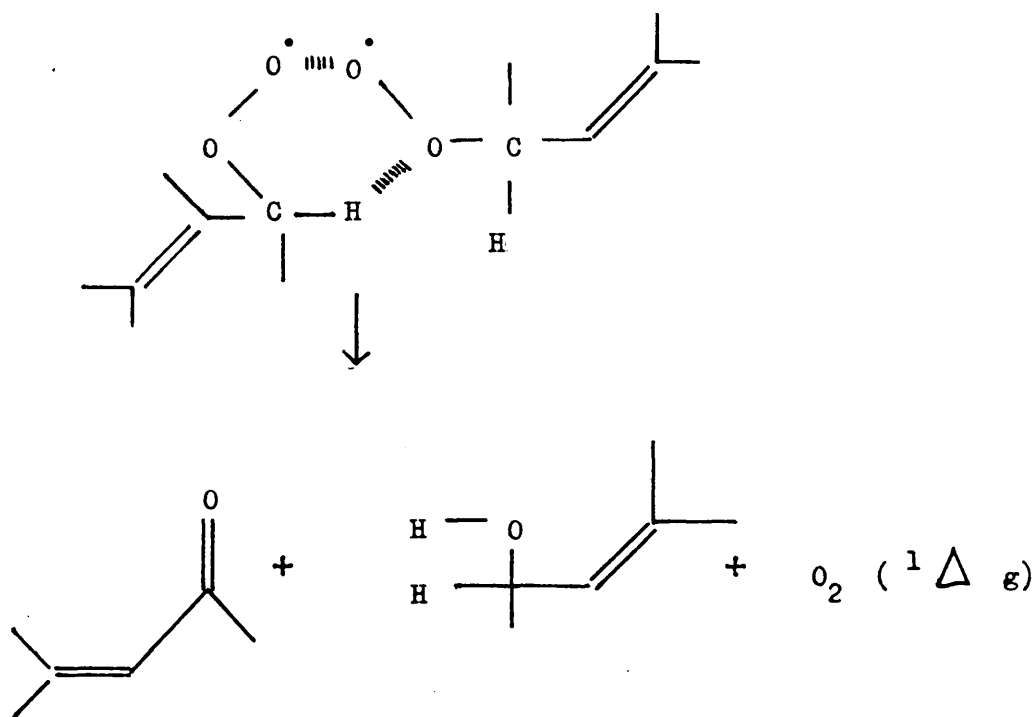
of a mono-olefin system (135) produced relationships which enabled a correlation to be made between olefin structure and ease of oxidation (136). As expected, oxidisability was found to increase with the lability of the α olefinic hydrogen atoms in the molecule. In normal olefin containing systems the rate of addition of oxygen to a radical centre is high enough to enable the corresponding expression to be removed from the kinetic scheme with the result that the rate of oxidation can generally be considered to be a function of only olefin concentration in homogeneous media subject to oxygen pressures above a few torr (137).

The nature of the reactions which are responsible for initiation and termination of the kinetic chain has been determined. In solutions of high hydroperoxide content the initiation reaction has been found to be second order in peroxide concentration (138). If the solution concentration of hydroperoxide is reduced it becomes possible to detect a first order process of decomposition (139). This contradiction was resolved by evidence which suggested that hydroperoxide groupings can exist as dimer complexes in equilibrium with uncomplexed material, the relative proportion of which depends upon the concentration of the solution (140). Hydroperoxide decompositions of the type outlined below are generally assumed to account for the autocatalytic nature of the olefin oxidation process.



The detection of water as a product of hydroperoxide decomposition under vacuum (140) is evidence in support of the existence of these mechanisms.

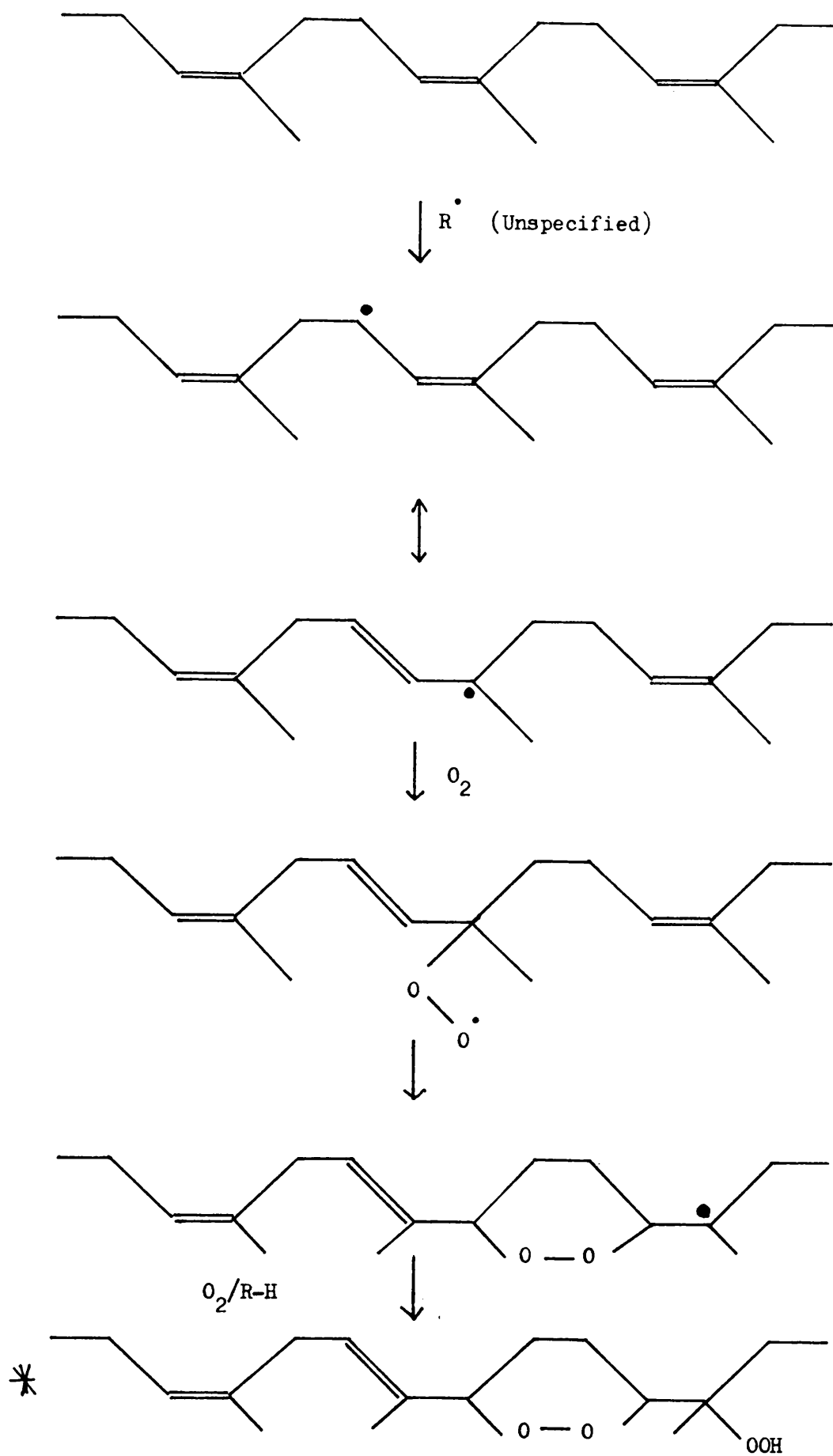
If it is assumed that the addition of oxygen to an allyl radical is a very fast process then it must follow that at any instant the concentration of ROO^\bullet is much larger than the concentration of R^\bullet in the reaction mixture. It must therefore follow that if the termination reaction is a biradical event then it most probably is effected by two peroxy radicals. Oxygen has been detected as a product of closed system hydroperoxide decomposition under vacuum (140) and has been shown to be produced in an excited singlet state (141). This has led to the generally accepted view that the mutual termination of hydroperoxide radicals proceeds via an intermediate tetroxide complex which decomposes to yield α β unsaturated carbonyl material, α hydroxy olefinic material and singlet oxygen (142) as shown below.



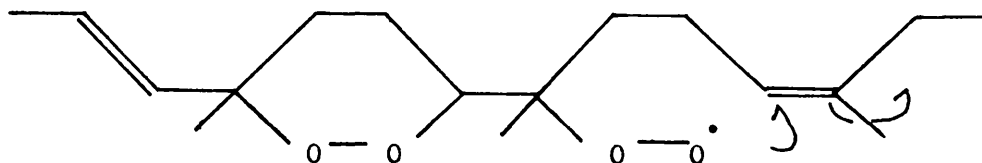
Di- and poly-olefin containing molecules in general exhibit more complex mechanisms of oxidation. Isolated olefinic groups which are separated by three or more saturated carbon atoms are oxidised in a manner which is identical to the mono-olefins depicted above. As the olefinic groups are brought closer together, for example in 1,4 and 1,5 diene containing molecules, basic departures from the above kinetic schemes are observed.

As expected, 1,4-dienes have been found to be very reactive towards oxygen (136) presumably because of the ease with which a hydrogen atom in a position α to both double bonds could be abstracted to initiate the kinetic chain. The product of the primary oxidation reaction has been found to be a hydroperoxide group (143). On theoretical grounds, the intermediate radical would be expected to isomerise before the addition of oxygen to produce a conjugated system (144). This has been found to be the case (143).

1,5 diene containing systems - model compounds for polybutadiene - have been found to oxidise in a complex manner. By an elegant analysis of the products formed during the oxidation of squalene (145) it was concluded that the oxidation reaction involved the formation of one cyclic-peroxide and one hydro-peroxide grouping. A plausible reaction scheme was postulated to account for this observation. Bevilacqua (146, 147) analysed the volatile products formed during the oxidation of polyisoprene and concluded that the reaction proceeds via a cyclic intermediate which is similar to that postulated above (145), differing only in the position of the hydroperoxide group. The postulated mechanism has relevance to the following discussion and has therefore been reproduced below.



It has been argued (148) that (*) will decompose in quantity only at temperatures above 100°C. It should therefore be possible to accumulate a large population of such groupings in rubber which is oxidised at low temperatures. The same author has argued (149) that adjacent cyclic peroxides could be formed by an intramolecular addition of the intermediate (shown below) to a neighbouring double bond.



A more thorough investigation of the volatile products of polyisoprene oxidation has been performed (150) and an additional mechanism of chain scission by radical exchange was proposed to account for products not obtainable from either (*) or from the further oxidation of the products of decomposition of (*).

The description of the processes of oxidative degradation of polyisoprene has been completed by further analysis of the residue and volatile products of degradation. The detection of residual epoxides (151) was viewed as evidence for the existence of a process of direct attack of peroxy radicals on olefinic groups in the polymer, while the identification of a range of high boiling point material (152) was cited in support of a mode of cycloperoxide decomposition competitive with that suggested by Bevilacqua (146, 147).

In contrast, the oxidative degradation of polybutadiene has been examined in less detail. It has been shown (153)

that polybutadiene is subject to a dramatic decrease of molecular weight during the very early stages of oxidation, after which the material rapidly cross-links to insolubility. It was also shown (153) that the ratio of chain scissions to cross-links formed increased with the temperature of oxidation. Microstructural changes in the polymer during low and high temperature oxidation have been examined by i.r. spectroscopy (153, 154) which has shown that the reaction is associated with the appearance of involatile carbonyl and hydroxyl containing material. It has also been shown by solid state ^{13}C n.m.r. spectroscopy (155) that epoxides are formed in high temperature oxidations of polybutadiene.

B PREPARATION OF OXIDISED MATERIAL.

B 1 MATERIAL OXIDISED AT 0°C AND ROOM TEMPERATURE.

Samples of high 1,4-polybutadiene (A) were oxidised at 0°C by the following procedure. Approximately 100 mg portions of the material were placed in small lidless sample bottles which were inserted into a large test tube which was sealed with a serum cap. The assembly was flushed with pure oxygen using the two needle technique. The exit needle was removed before the inlet needle to leave the assembly under a slight positive pressure of gas. The samples were stored at approximately 0°C under refrigeration and periodically flushed with oxygen. Samples were examined after approximately 2 and 6 months treatment.

Microstructural changes associated with low temperature oxidation were examined using samples of rubber oxidised at room temperature. I.r. and u.v. spectra were obtained of material as thin films, on a salt plate and a quartz window respectively, which were oxidised by air in the absence of light.

B 2 MATERIAL OXIDISED AT ELEVATED TEMPERATURES.

Samples of high 1,4-polybutadiene (A) were oxidised at temperatures in the range 50 - 300°C by the following procedure. Samples (50 mg) were introduced to the normal TVA oven assembly (Chapter 2) in small pieces. Material to be removed after treatment was introduced in a sample boat. In contrast, material which was subjected to subsequent thermal degradation under vacuum was directly added to the TVA tube.

A serum cap was attached to the oven head assembly which was made leak tight by evacuation at room temperature. The system was preheated under vacuum to the appropriate corrected temperature for 5 - 10 min, isolated from the pumps, and pure oxygen was

admitted via the serum cap. An exit needle connected to an oil bubbler was inserted and a flow rate of a few ml/min was maintained throughout the degradation reaction. On completion of the degradation the gas supply was removed and the sample was allowed to cool under vacuum. A disadvantage of this approach is the (very real) possibility that the peroxide population in the sample could be removed during the cooling process. It is however preferable to a procedure of cooling the sample under an oxygen atmosphere as in the latter situation the end product contains oxidised groupings which have been generated over a wide temperature range. When the system had reached room temperature the sample was either removed for analysis or subjected to degradation under vacuum after replacing the serum cap with a greased stopper.

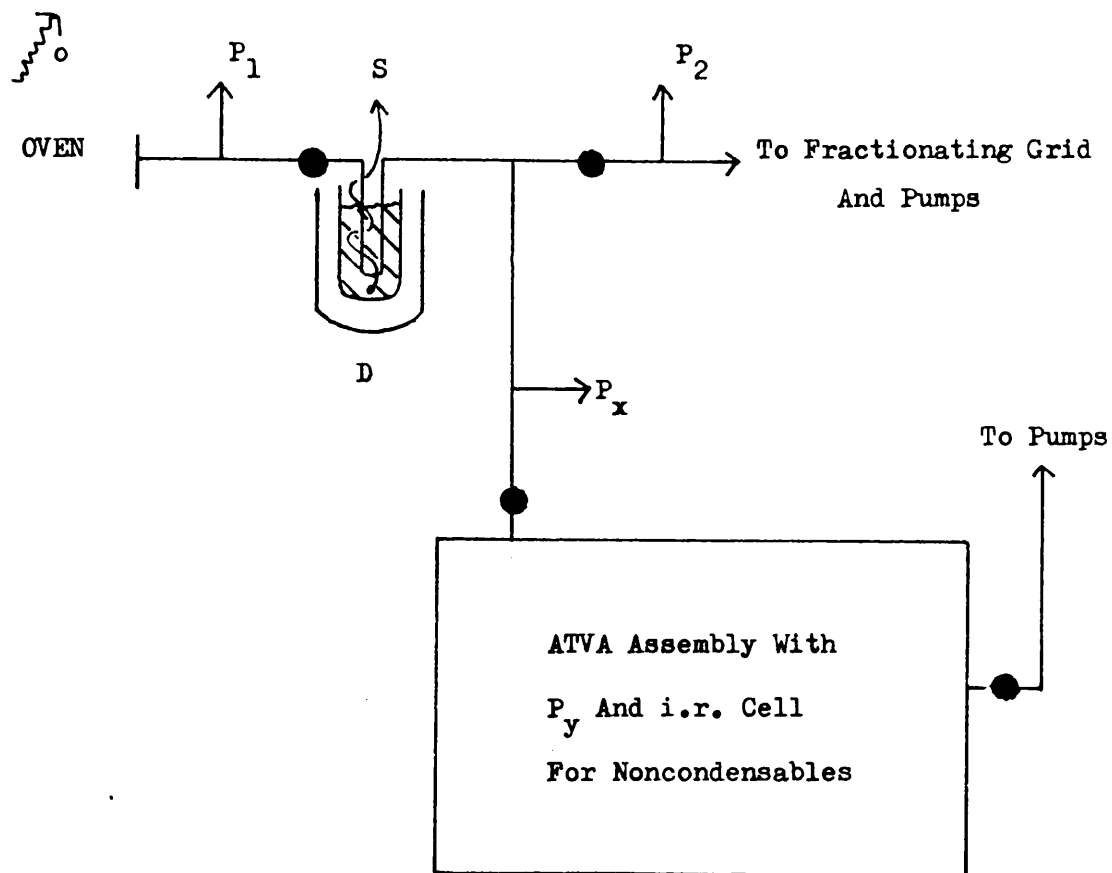
Samples of pure rubber were also degraded under an oxygen atmosphere in TG and DSC experiments at a programmed heating rate of $10^{\circ}\text{C}/\text{min}$.

C THERMAL DEGRADATION OF OXIDISED MATERIAL.

Samples of oxidised rubber were degraded under nitrogen in the normal TG and DSC experiments. Samples were also degraded in the combined TVA/ATVA/SATVA assembly shown in fig. 1 at a heating rate of $10^{\circ}\text{C}/\text{min}$. The total volatile flux was measured by Pirani P_1 , the total noncondensable flux was measured by Pirani P_x , and the gas fraction unadsorbed by molecular sieve was measured by Pirani P_y . The three Pirani outputs were recorded simultaneously with the oven thermocouple output to obtain a combined TVA/ ATVA trace for the material. On completion of the experiment the residue and cold ring fractions were examined by spectroscopy, material trapped by the molecular sieve was transferred to and analysed in the i.r. cell for noncondensables, while the condensable volatile fraction of degradation was subjected to SATVA fractionation to a collecting vessel or i.r. cell for analysis. Material was also subjected to analysis by the normal differential condensation TVA experiment.

FIGURE 11 - 1

APPARATUS FOR COMBINED TVA/ATVA/SATVA EXPERIMENT



Key

o Oven Thermocouple (To Recorder)

S Sub-ambient Thermocouple (To Recorder)

/// Sub-ambient Jacketing Material

D Dewar Vessel Containing Liquid Nitrogen

P_1 Pirani Gauge For Total Volatile Material From Oven (To Recorder)

P_2 Pirani Gauge For SATVA Experiment (To Recorder)

P_x Pirani Gauge For Total Noncondensables (To Recorder)

P_y Pirani Gauge For Noncondensables Unadsorbed By Molecular Sieve
At -196°C (To Recorder)

D TG AND DSC.

D 1 TG AND DSC UNDER OXYGEN AT 10°C/min OF PURE POLYBUTADIENE.

The TG curve associated with the programmed degradation under oxygen of polybutadiene is shown in fig. 2. It can be seen that the sample increases in mass in the temperature range 100 - 150°C presumably by the incorporation of oxygen into the polymer. This trend is reversed above 150°C and the sample returns to its original mass at approximately 300°C and continues to be volatilised until a temperature of 437°C is reached at which the sample ignites to produce a recoil force which disturbs the balance pan. The existence of a rate maximum at 380°C is proof that a portion of the sample is still able to take part in the cyclisation/depolymerisation reaction.

The corresponding DSC curve (fig. 3) shows that the processes responsible for oxygen absorption in the temperature range 100 - 200°C are exothermic in nature as are the processes operative in the temperature range 250 - 400°C. As expected, the burning process ($> 400^{\circ}\text{C}$) was also found to be exothermic in nature.

D 2 TG AND DSC UNDER NITROGEN AT 10°C/min OF POLYBUTADIENE MODIFIED BY OXIDATION AT 0°C.

The TG curve associated with the programmed degradation under nitrogen of polybutadiene modified by oxidation at 0°C for 6 months is shown in fig. 4 along with the TG curve associated with the corresponding degradation of pure rubber.

It can be seen that the microstructural changes associated with low temperature oxidation destabilise the polymer with respect to its conversion to volatile fragments which begin to be formed at 100°C. The TG experiment, however, does not provide any clues as to the origin of this material, which may either have been

formed by bond scission reactions in the TG experiment or by bond scissions during the oxidation process followed by volatilisation at elevated temperatures in the TG experiment. The latter situation seems unlikely when it is considered that the oxidised polymer is completely insoluble in all common laboratory solvents.

The situation is resolved by DSC (fig. 5). If material is simply volatilised at low temperatures then the corresponding enthalpy change associated with the process would be endothermic in nature. In fact an exotherm is detected. This can only arise from chemical reactions in the polymer which presumably disrupt the polymer matrix to produce material able to be volatilised. The only material in the polymer able to be decomposed in the temperature range 100 - 200°C is the resident peroxide and hydroperoxide population. The exotherm at 380°C is shown to be unaffected by the oxidation process while the endotherm of decomposition is lowered from 470 - 480°C to 450°C.

It can be seen that a close parallel exists between the behaviour of this system and the system depicted in fig. 3, at least in the temperature range 100 - 400°C.

FIGURE 11 - 2

POLYBUTADIENE, TG UNDER OXYGEN

Heating Rate $10^{\circ}\text{C}/\text{min}$

Sample Size 6 mg

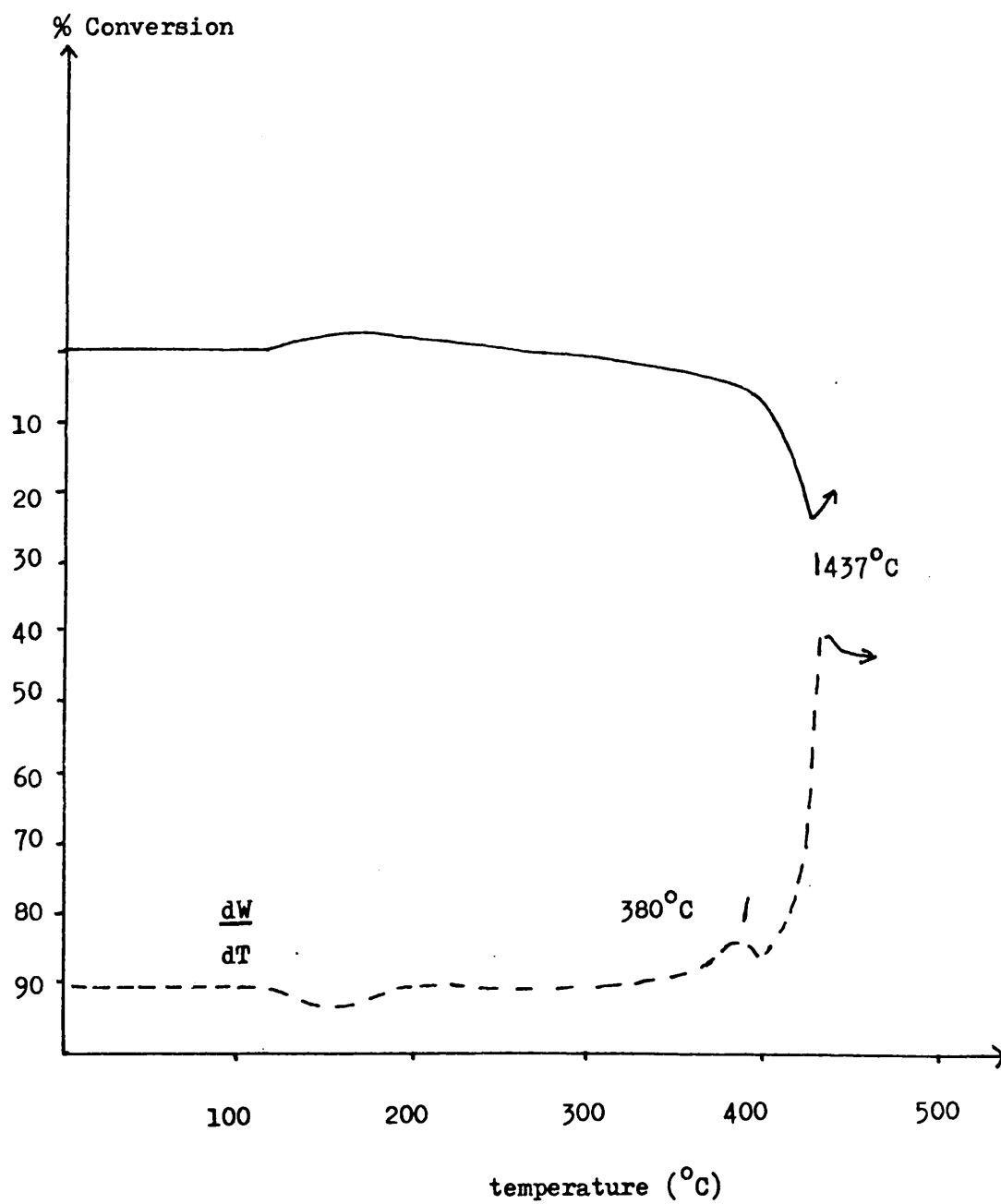


FIGURE 11 - 3

POLYBUTADIENE, DSC UNDER OXYGEN

Heating Rate $10^{\circ}\text{C}/\text{min}$

Sample Size 2.5 mg

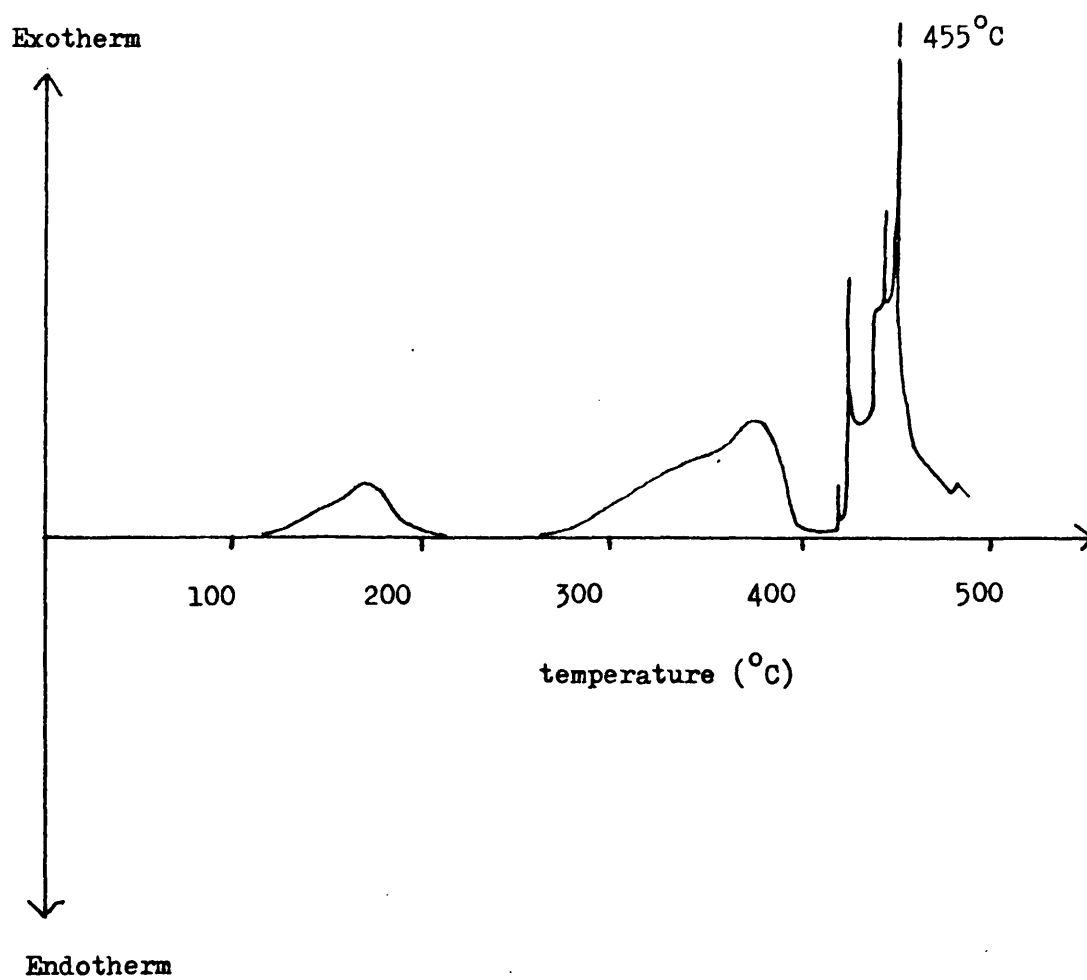


FIGURE 11 - 4

TG UNDER NITROGEN OF POLYBUTADIENE MODIFIED BY OXIDATION AT 0°C FOR
6 MONTHS

Sample Size 7 mg

Heating Rate 10°C/min

Key

— Oxidised Polybutadiene

- - - Unoxidised Polybutadiene

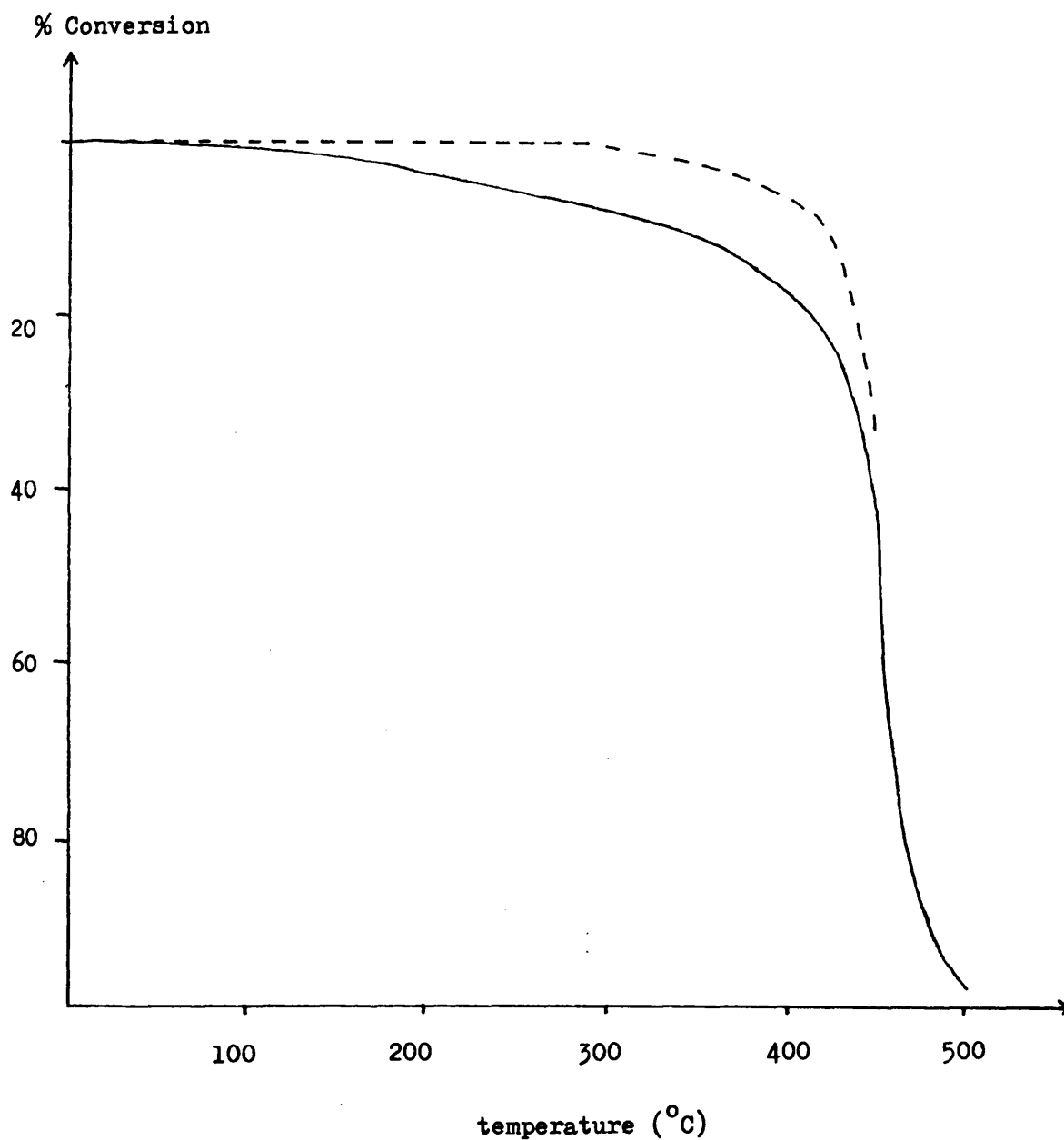
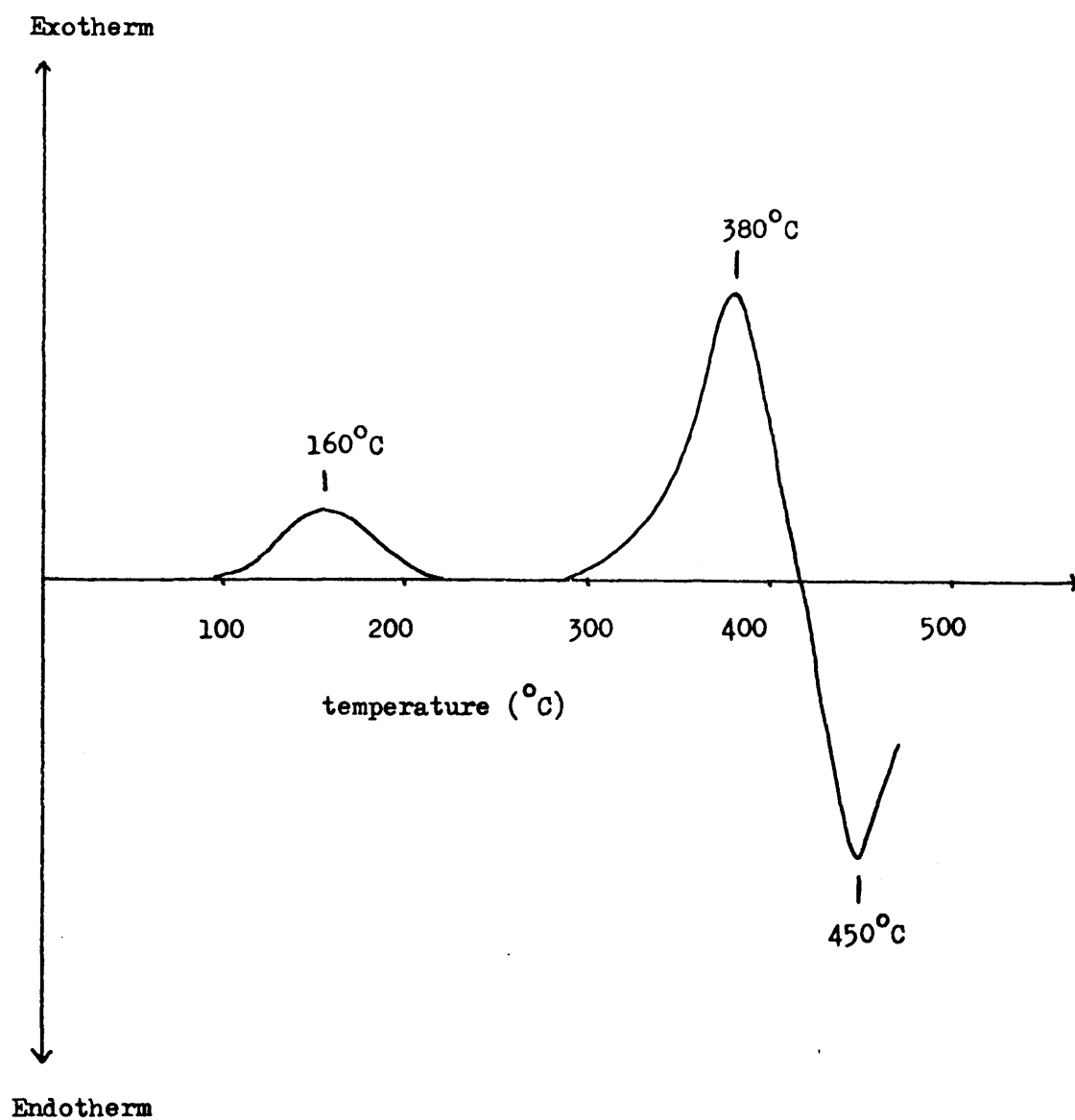


FIGURE 11 - 5

DSC UNDER NITROGEN OF POLYBUTADIENE MODIFIED BY OXIDATION AT 0°C FOR
2 MONTHS

Sample Size 3 mg

Heating Rate 10°C/min



OPERATIVE AT ROOM TEMPERATURE.

I.r. spectra of material oxidised at room temperature are shown in figs. 6 , 7 and 8 . Corresponding u.v. spectra are shown in fig. .

Infrared Spectroscopy.

4000 - 2000 cm^{-1} (fig. 6)

The development of a strong absorption band at 3400 cm^{-1} shows that the reaction is associated with the production of a large quantity of hydroxyl groupings in the polymer. It can also be seen that the absorbance at 3005 cm^{-1} which is associated with olefinic material is broadened, reduced in intensity but not eliminated.

2000 - 1500 cm^{-1} (fig. 7)

It can be seen that the reaction is also associated with the production of a large quantity of carbonyl material in the polymer. In the early stages of degradation three types of carbonyl material are produced. The development of an i.r. absorption at 1825 cm^{-1} is probably associated with the production of involatile anhydride or more likely acid peroxide material, while absorptions at 1720 cm^{-1} and 1695 cm^{-1} are probably associated with the production of saturated and $\alpha \beta$ unsaturated carbonyl groups. It is of interest to note that after 12 days exposure to the atmosphere the production of structures which absorb at 1825 cm^{-1} and 1695 cm^{-1} has ceased and carbonyl material which absorbs at 1720 cm^{-1} is the sole product of the oxidation reaction. The appearance of a C - H stretching vibration at 2680 cm^{-1} (fig. 6) suggests that a portion at least of the material is aldehydic in nature.

1500 - 600 cm⁻¹ (figs. 7 and 8)

The detection of material with i.r. activity in the region 1400 - 1000 cm⁻¹ was hampered by spectroscopic interference generated by the massive quantity of hydroxyl groupings and possibly water formed during oxidation. It will be shown subsequently that the broad absorption band at 1075 cm⁻¹ may be associated with polyether formation. It will also be asserted that the oxidation reaction involves the production of saturated acid groupings which absorb at 1270 cm⁻¹ and 1290 cm⁻¹.

It can be seen that the absorption bands at 965 cm⁻¹, 910 cm⁻¹ and 730 cm⁻¹, due to olefinic material in the polymer, are not eliminated but are reduced in intensity and broadened as a consequence of the oxidation process.

The above material was oxidised for 273 days at 0°C then placed in the TVA assembly which was evacuated and heated at 10°C/min to 200°C. The sample was re-examined by i.r. spectroscopy which showed it to be unaffected by this procedure. This proves that the i.r. absorbance at 3400 cm⁻¹ results mainly from alcoholic/acidic material and not hydroperoxide structures which are decomposed on heating. It also shows that the oxygenated groupings are bound to the polymer matrix and not attached to volatilisable material. As expected this procedure did not "sharpen up" absorption bands in the region 1400 - 1000 cm⁻¹. It is well known that acidic polymers and especially polyether polymers may require heat treatment under vacuum at temperatures above 200°C for several hours to dispel complexed water.

The above is placed on a more quantitative basis in fig. 9 in which the development of i.r. absorbance associated with groupings produced by the oxidation reaction is plotted on a time basis. It can be seen that both hydroxyl and carbonyl material are formed

by autocatalytic processes. The reaction is also shown to consume only a fraction of the olefinic population of the material.

Ultra-Violet Spectroscopy. (fig. 10)

It is again shown by the reduction in intensity of the 190 nm absorption band that the oxidation reaction is associated with a partial removal from the polymer of olefinic material. The development of u.v. absorbance at 235 nm is best attributed to the formation of $\alpha\beta$ unsaturated aldehyde material. As expected from a consideration of the corresponding i.r. spectra, the production of such material is shown to cease after the first seven days of degradation. The different time limits for this phenomenon as measured by i.r. and u.v. spectroscopy can be attributed to the different film thicknesses used in the two experiments.

The detection of an isasbestic point at 213 nm is proof that the above material is stable to further oxidation at room temperature.

FIGURE 11 - 6

i.r. SPECTRA OF POLYBUTADIENE OXIDISED AT ROOM TEMPERATURE, $4000 - 1800\text{cm}^{-1}$

(Material As Thin Film On Salt Plate)

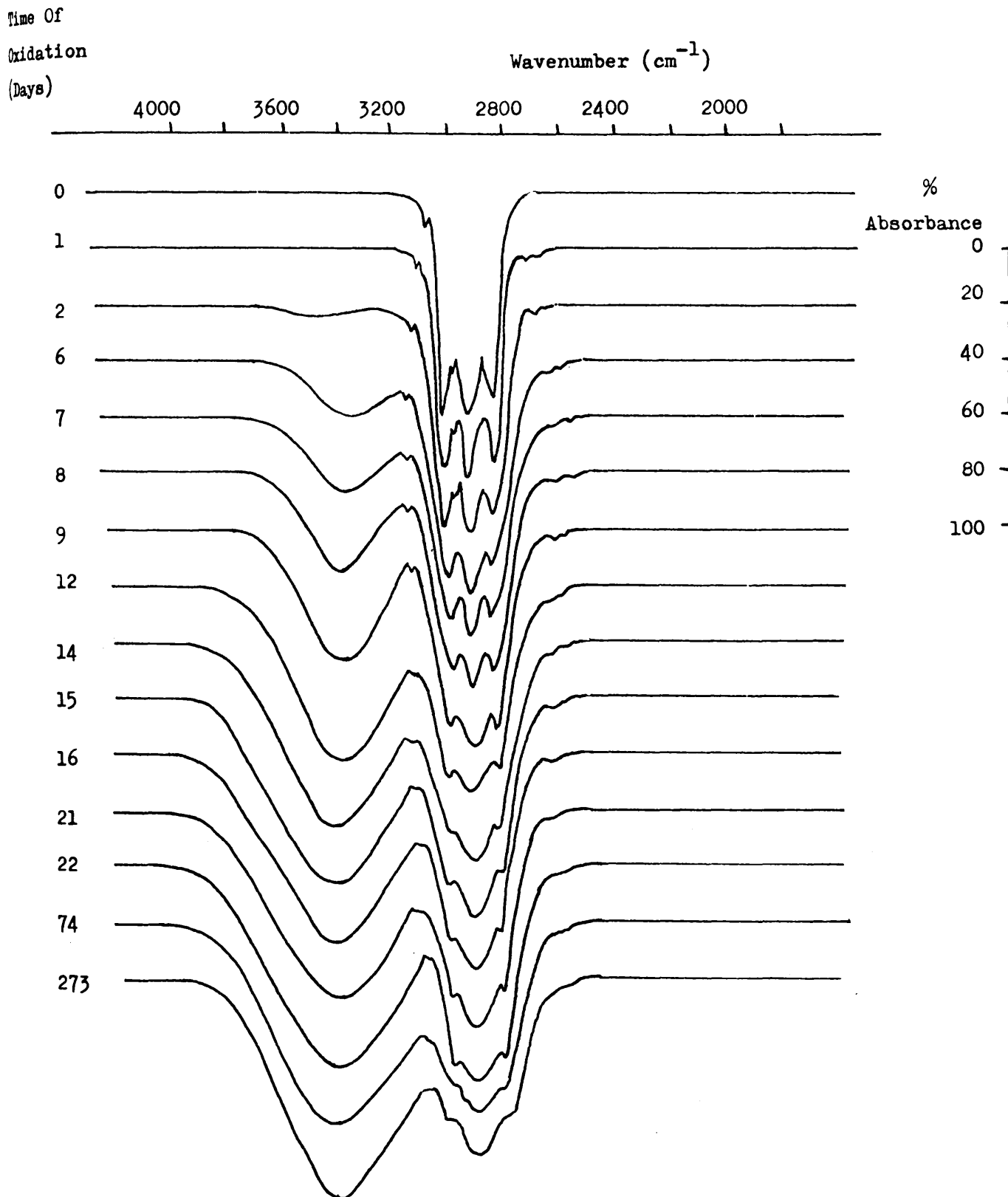


FIGURE 11 - 7

i.r. SPECTRA OF POLYBUTADIENE OXIDISED AT ROOM TEMPERATURE, 2000 - 1300 cm^{-1}
(Material As Thin Film On Salt Plate)

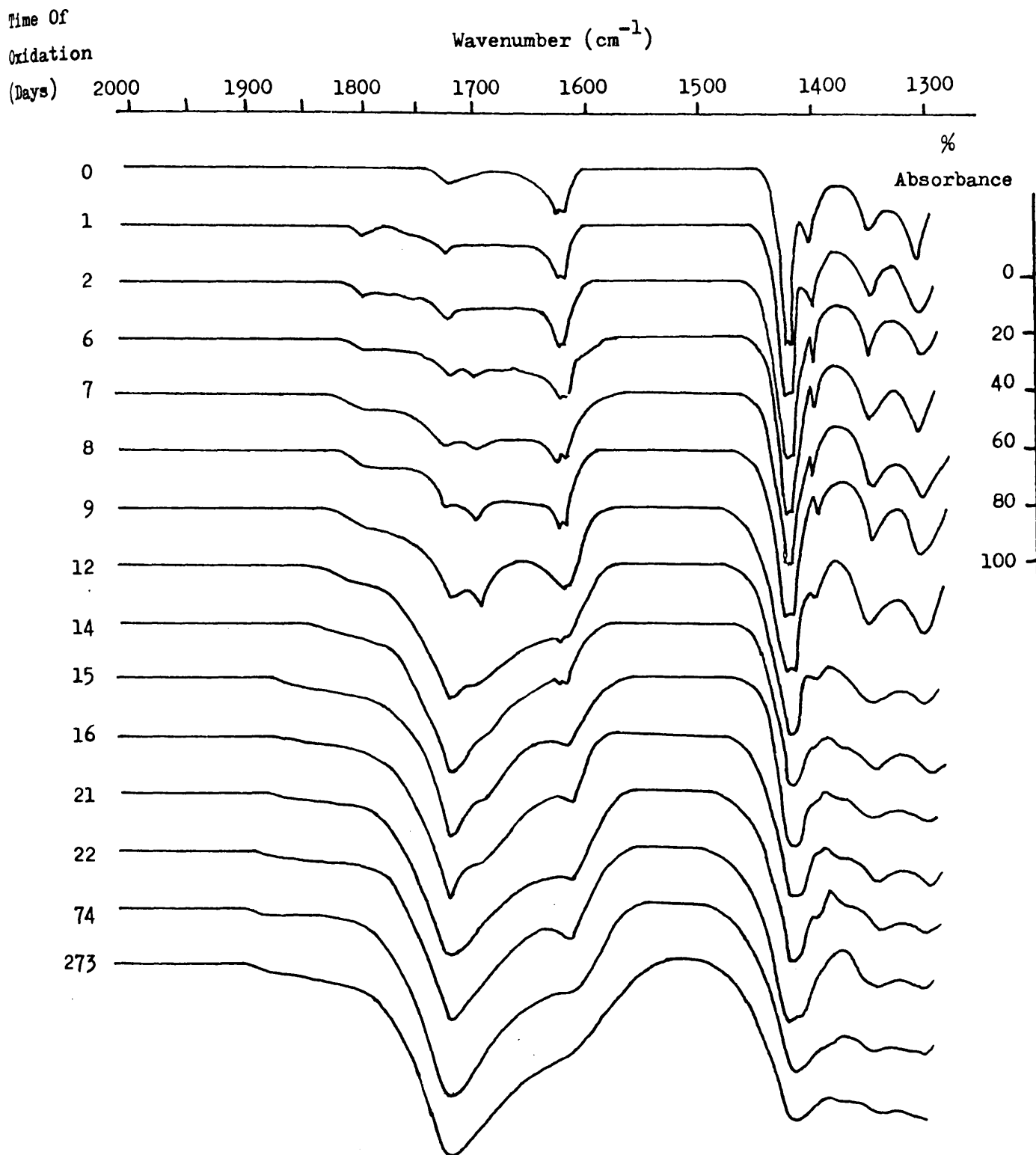


FIGURE 11 - 8

i.r. SPECTRA OF POLYBUTADIENE OXIDISED AT ROOM TEMPERATURE, 1300-600 cm^{-1}
(Material As Thin Film On Salt Plate)

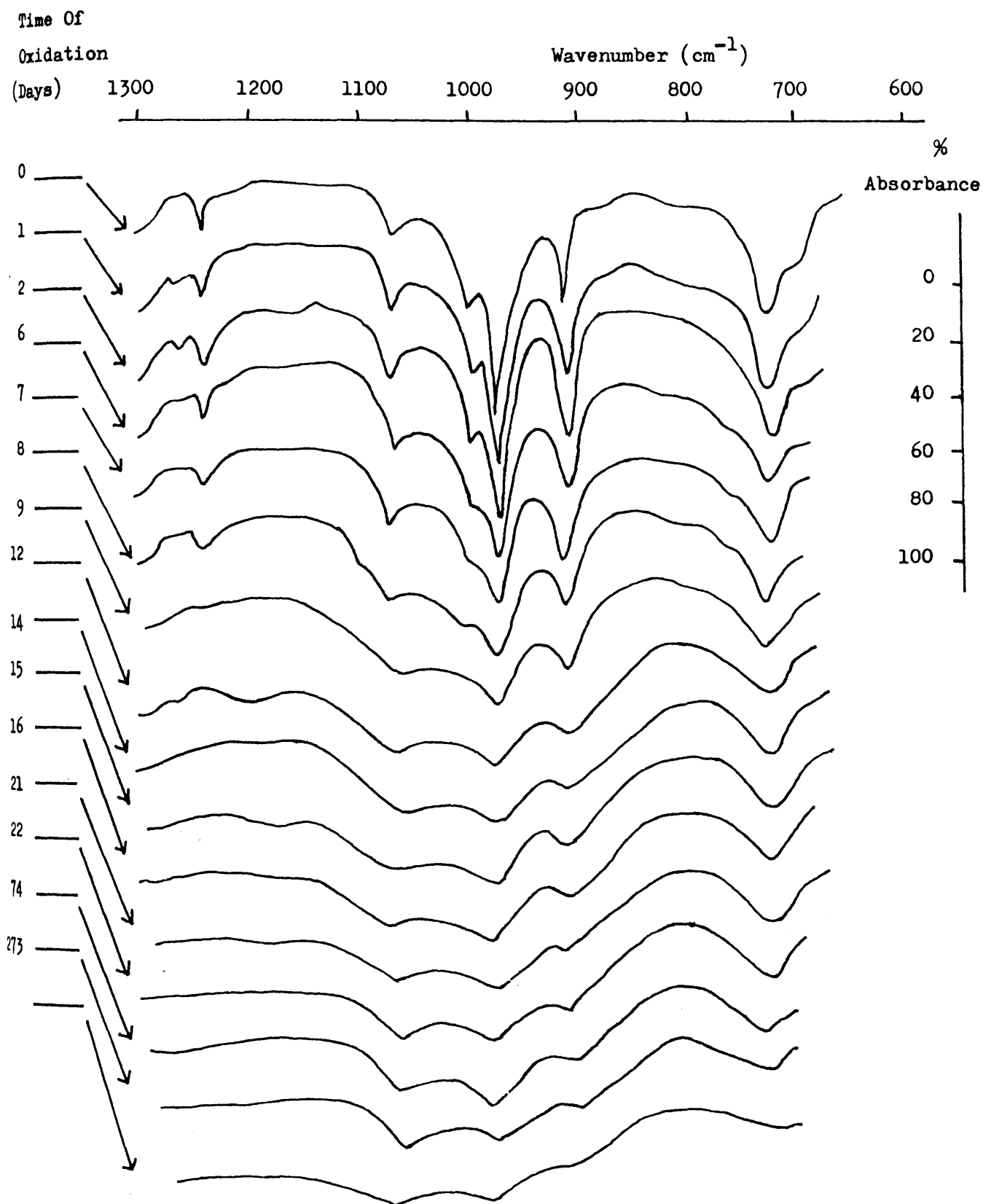


FIGURE 11 - 9

POLYBUTADIENE (AS THIN FILM), DEVELOPMENT OF i.r. ABSORBANCES ASSOCIATED WITH OXYGEN CONTAINING GROUPS DURING THE LOW TEMPERATURE OXIDATION REACTION

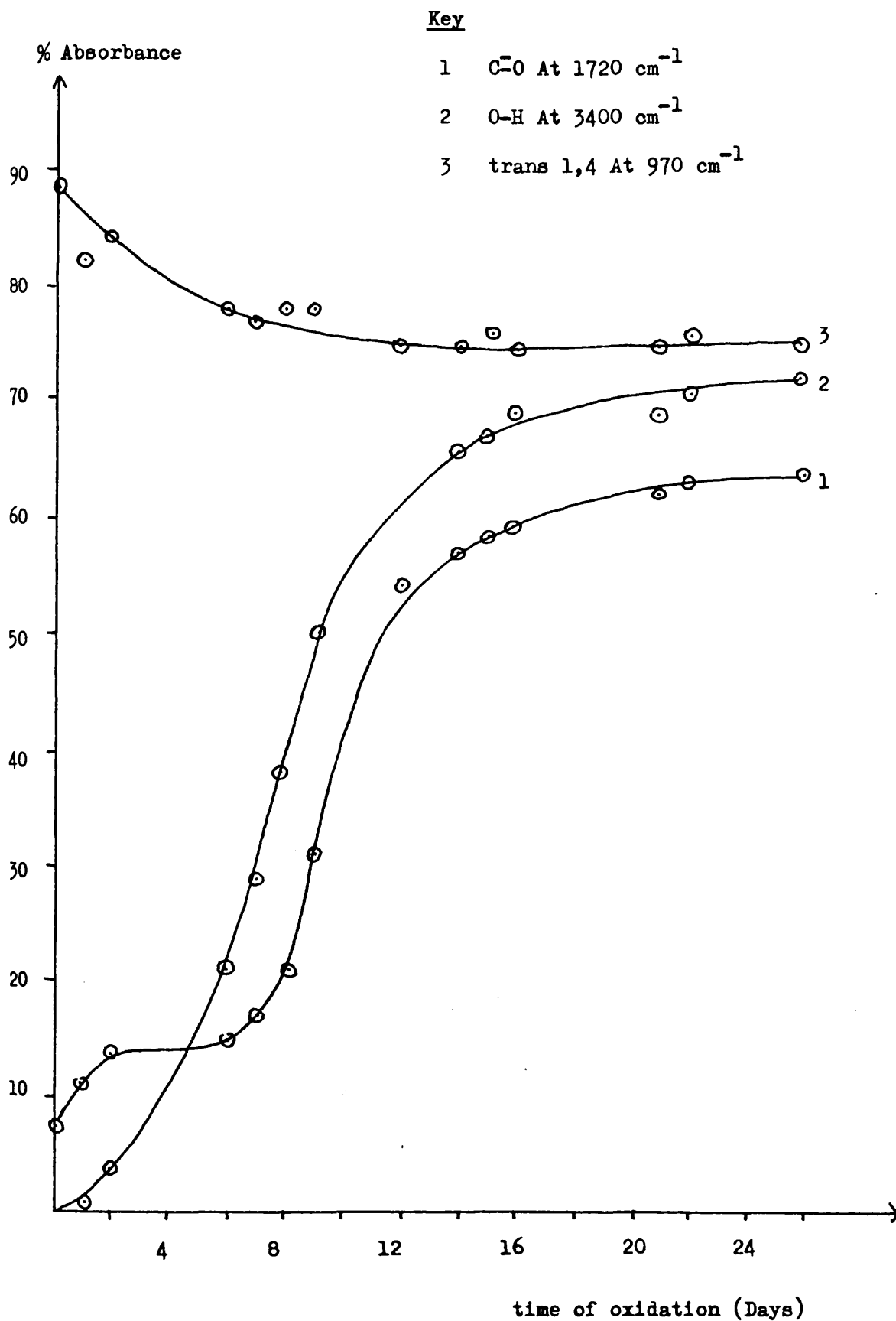


FIGURE 11 - 10

U.v. SPECTRA OF POLYBUTADIENE MODIFIED BY ATMOSPHERIC OXIDATION AT ROOM
TEMPERATURE
(Material As Thin Film On Quartz Window)

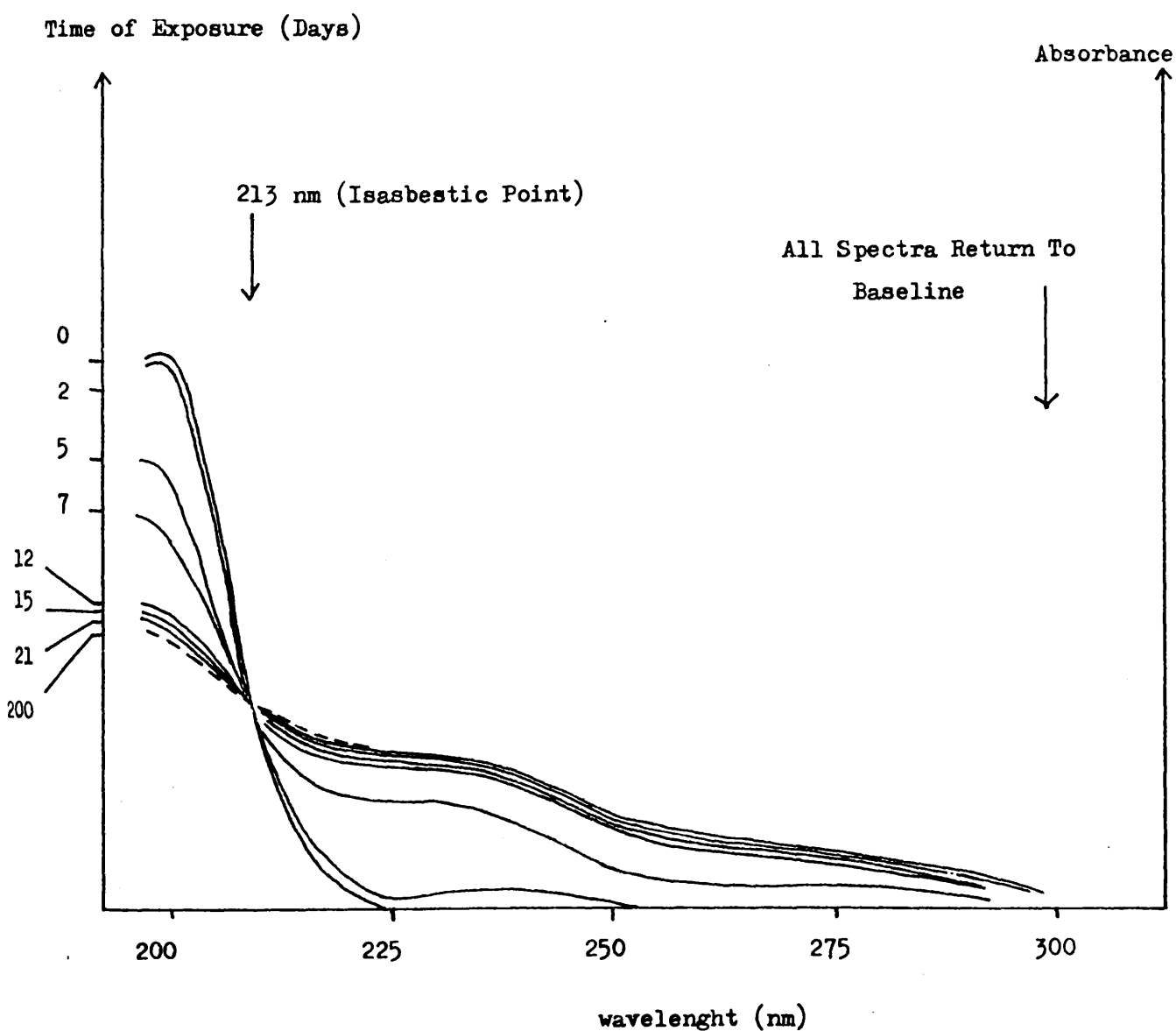


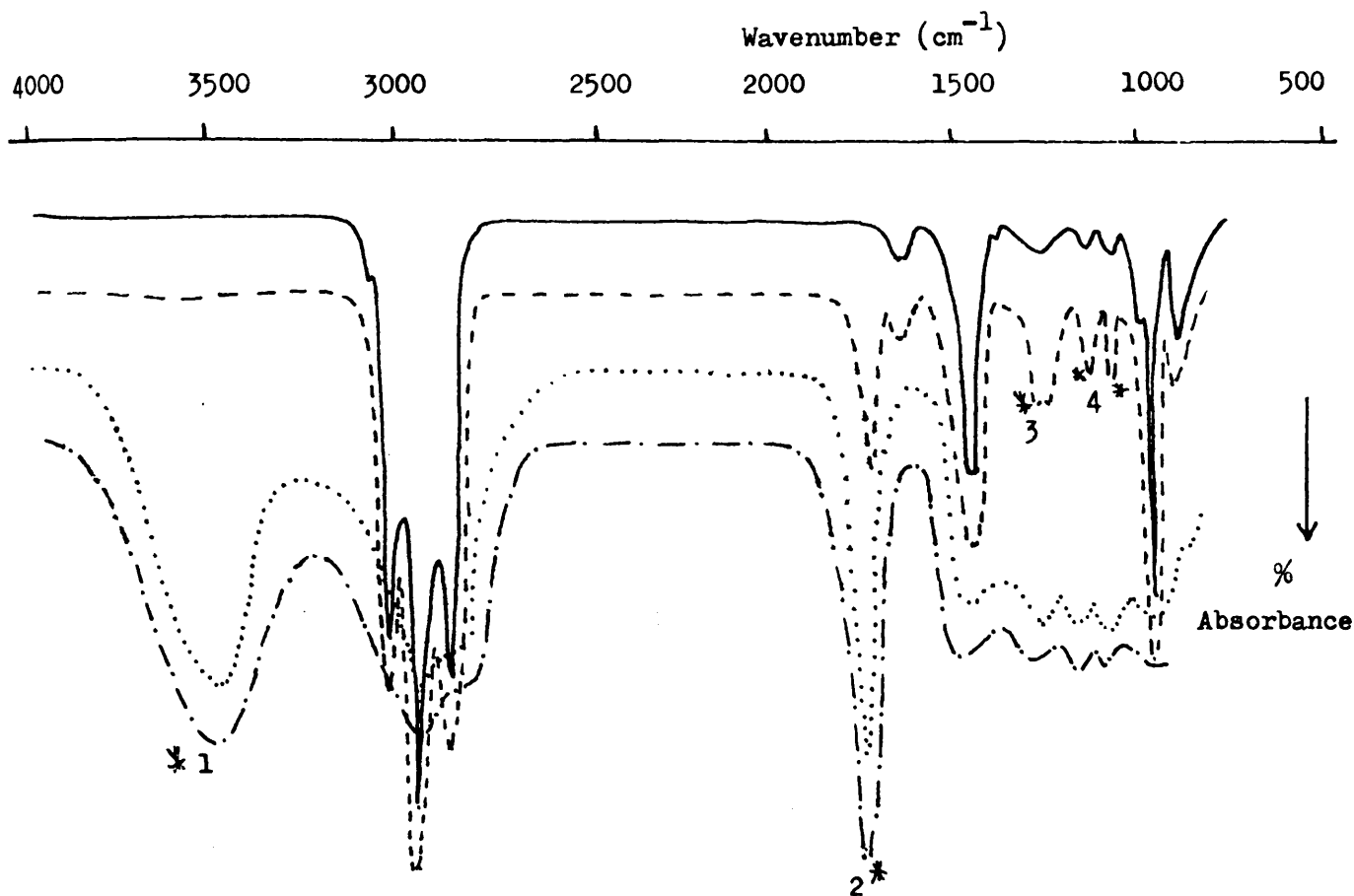
FIGURE 11 - 11

I.r. SPECTRA OF POLYBUTADIENE MODIFIED BY OXIDATION AT 100°C

(Material As Thin Film On Salt Plate)

Key

- Pure Rubber
- - - Material After 5 min Exposure To Oxygen At 100°C
- Material After 1 hr Exposure To Oxygen At 100°C
- Material After 2 hr Exposure To Oxygen At 100°C



* Absorptions Associated With Oxygen Containing Groups

Wavenumber (cm^{-1})

- 1 3400 (Broad) O-H
- 2 1720 (Broad) $\text{C}=\text{O}$ Of Saturated Acid Group
- 3 1270, 1290 C-O Of Saturated Acid Group
- 4 1120, 1070 C-O Of Ether Groups

F PROGRAMMED DEGRADATION UNDER VACUUM OF POLYBUTADIENE MODIFIED BY

OXIDATION AT 0°C

(i). TVA

A TVA trace which corresponds to the programmed degradation of rubber modified by oxidation at 0°C for 2 months is shown in fig. 12 .

It can be seen that low temperature decomposition produces a range of volatile materials a fraction of which is shown to be noncondensable in nature. It can also be seen that there is increased production of volatile material at higher temperatures. Considerable volatile material commences to be produced at 250°C (cf. 325°C for pure rubber, fig. 6 - 3) and there is a rate maximum of production at the same temperature as for pure rubber - 450°C. A prominent "shoulder" develops at the intermediate temperature of 390°C. Noncondensable material begins to appear at 300°C (cf. 350°C for pure rubber) also with a rate maximum at the same temperature as pure rubber - 450°C. It can be seen that the decomposition process, which achieves a rate maximum at 390°C, produces noncondensable volatile material.

(ii). ATVA

An ATVA trace which corresponds to the degradation of rubber which has been modified by oxidation at 0°C for 2 months is shown in fig. 13 .

It is evident that the noncondensable material produced by the low temperature decomposition processes is only partially condensed by passage through molecular sieve at -196°C. This indicates that it is not a pure flux of carbon monoxide and/or methane. It can also be seen that the process which achieves a rate maximum at 390°C produces noncondensable material which is completely adsorbed by molecular sieve at -196°C, while the process which achieves a rate maximum at 450°C gives noncondensable material

which is only partly adsorbed under the same conditions. It will be assumed that the latter process is associated with the endothermic condensed ring decomposition reaction of polybutadiene (Chapter 6). If this is the case then the noncondensable flux associated with the 450°C process is identified as a mixture of hydrogen and methane.

An ATVA curve which corresponds to the degradation of rubber which has been modified by oxidation at 0°C for 6 months is shown in fig. 14 , which shows that the sample has accumulated a very large quantity of material which decomposes in the temperature range 100 - 200°C. In addition it must be noted that noncondensable material associated with higher temperature decompositions in the material is produced at a lower threshold temperature of 210°C (cf. 300°C for the sample oxidised for 2 months) to achieve a single rate maximum of production at 425°C. As expected hydrogen, which is associated with the process which achieves a rate maximum at 450°C, is completely absent from the product mixture.

FIGURE 11 - 12

TVA OF POLYBUTADIENE MODIFIED BY OXIDATION AT 0°C FOR 2 MONTHS

Sample Size 50 mg

Heating Rate 10°C/min

Key

— 0°C Trace

--- -45°C Trace

xxxx -75°C Trace

..... -100°C Trace

..... -196°C Trace

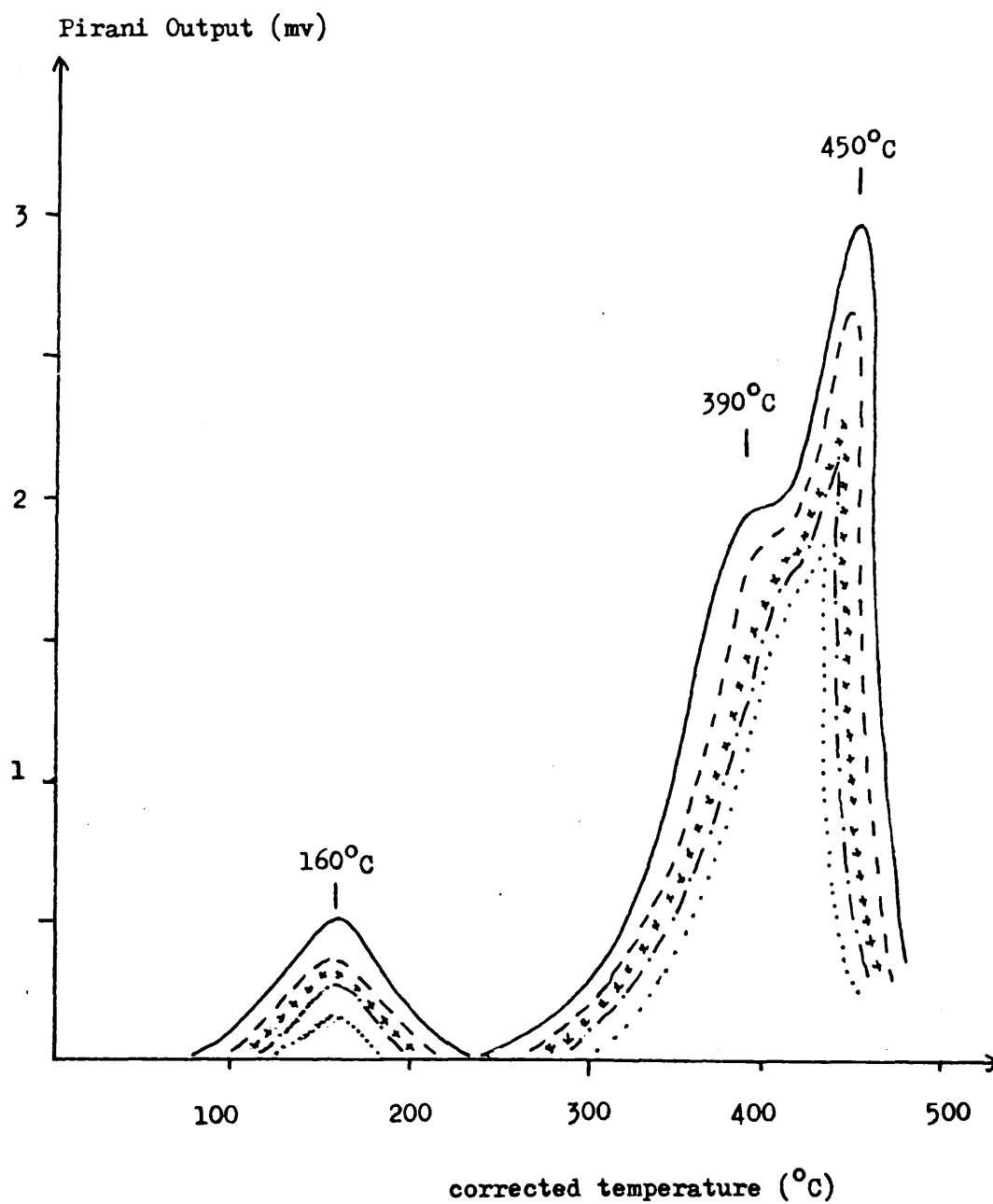


FIGURE 11 - 13

ATVA OF POLYBUTADIENE MODIFIED BY OXIDATION AT 0°C FOR 2 MONTHS

Sample Size 25 mg

Heating Rate 10°C/min

Sieve At -196°C

Key

— Pirani X Output (Before Sieve)

--- Pirani Y Output (After Sieve)

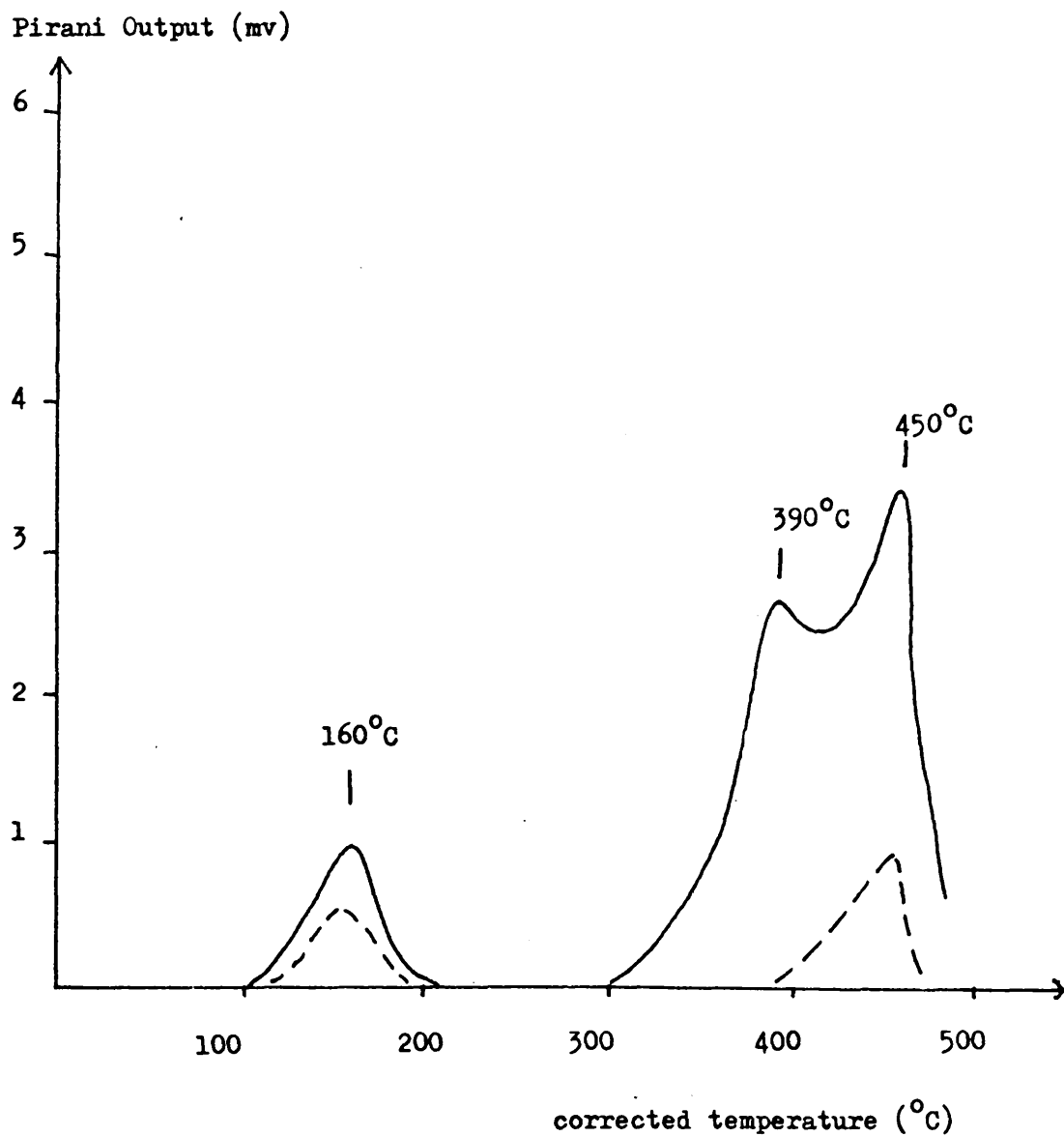


FIGURE 11 - 14

ATVA OF POLYBUTADIENE MODIFIED BY OXIDATION AT 0°C FOR 6 MONTHS

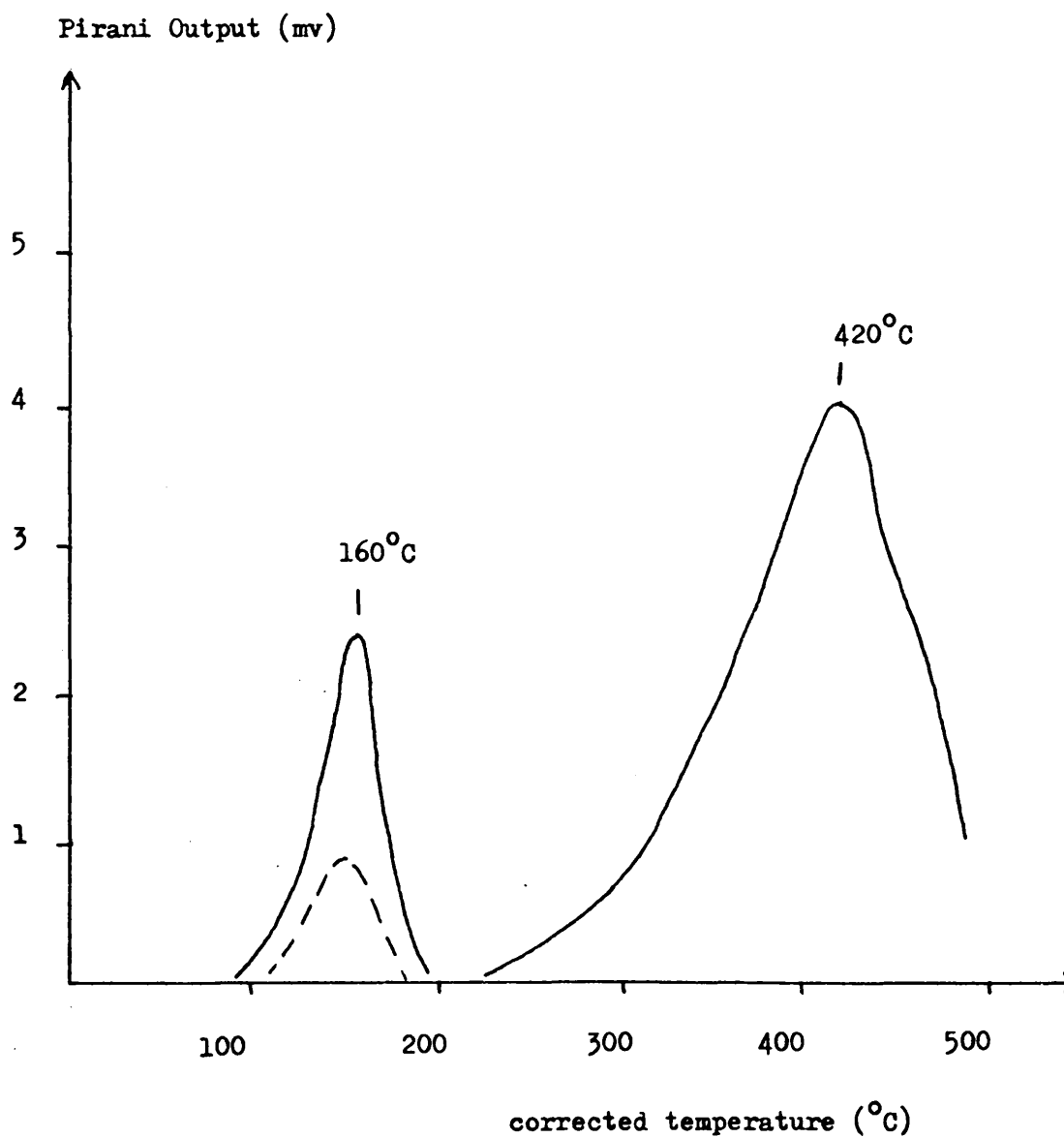
Sample Size 25 mg

Heating Rate 10°C/min

Sieve At -196°C

Key

— Pirani X Output (Before Sieve)
--- Pirani Y Output (After Sieve)



G PRODUCTS FORMED IN THE PROGRAMMED THERMAL DEGRADATION OF

POLYBUTADIENE MODIFIED BY OXIDATION AT 0°C.

G 1 IN THE TEMPERATURE RANGE 100 - 200°C.

(i). Noncondensable Volatile Material.

Oxidised polybutadiene contains carbon, oxygen and hydrogen atoms. The only possible types of noncondensable gas which can be formed are CH_4 , CO, O_2 and H_2 . It is very unlikely that H_2 gas, usually produced in high temperature processes, can be produced at such low temperatures. The ATVA curves of figs. 13 and 14 therefore suggest that oxygen is the major product of degradation in this temperature range. It is, however, possible that it is accompanied by fractions of CO and CH_4 . A large sample was therefore degraded as shown in fig. 15 and the condensed product fraction was examined by i.r. spectroscopy. No traces of CO or CH_4 could be detected. The noncondensable volatile fraction of degradation in this temperature range was therefore shown to consist of a pure flux of oxygen gas.

(ii). Condensable Volatile Material.

The condensable volatile fraction of degradation in this temperature range was collected and subjected to SATVA fractionation as shown in fig. 16. Peaks 1 and 5 were identified by i.r. spectroscopy while peak 4 was identified by i.r., n.m.r., and mass spectroscopy.

(iii). Cold Ring Material.

A small quantity of cold ring material was formed during this process. It was subjected to analysis by i.r. spectroscopy (fig. 18) and n.m.r. spectroscopy, on the basis of which it was tentatively assumed to be composed of a mixture of the structures shown below.

FIGURE 11 - 15

ATVA OF PRODUCTS OF PEROXIDE DECOMPOSITIONS IN RUBBER MODIFIED BY

OXIDATION AT 0°C FOR 6 MONTHS

Sample Size 250 mg

Heating Rate 10°C/min

Sieve At -196°C

Evolution/Condensation Curve For Gas

Transfer To i.r. Cell For

Noncondensables

Key

Key

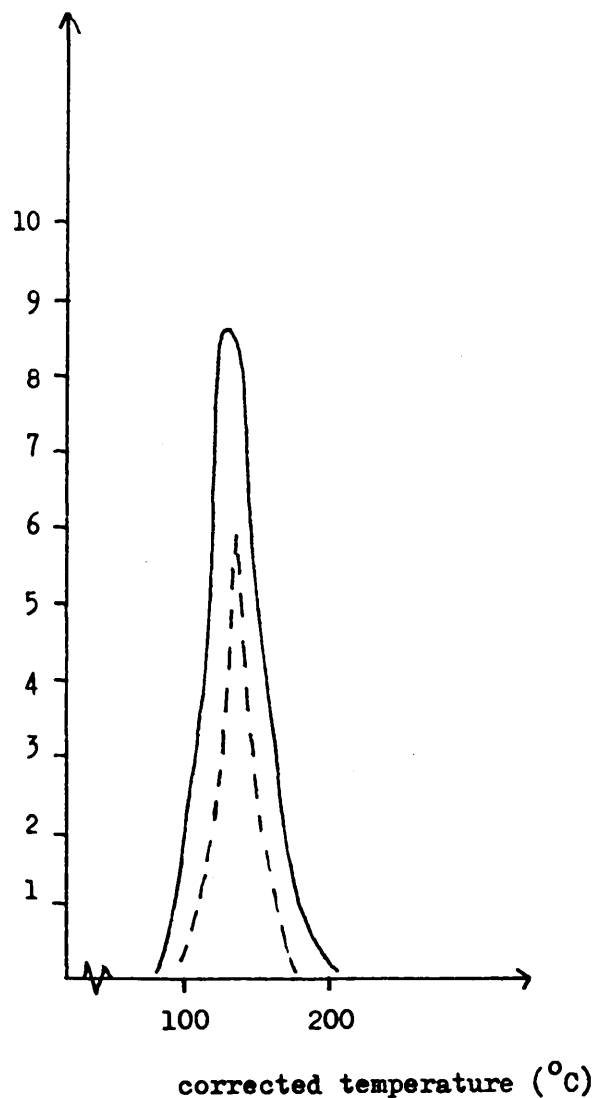
— Pirani X Output

- - - Pirani Y Output

— Pirani Y Output As Sieve Trap Is
Warmed To Room Temperature

* Point At Which Sieve In i.r. Cell
Is Cooled To -196°C

Pirani Output (mv)



Pirani Output (mv)

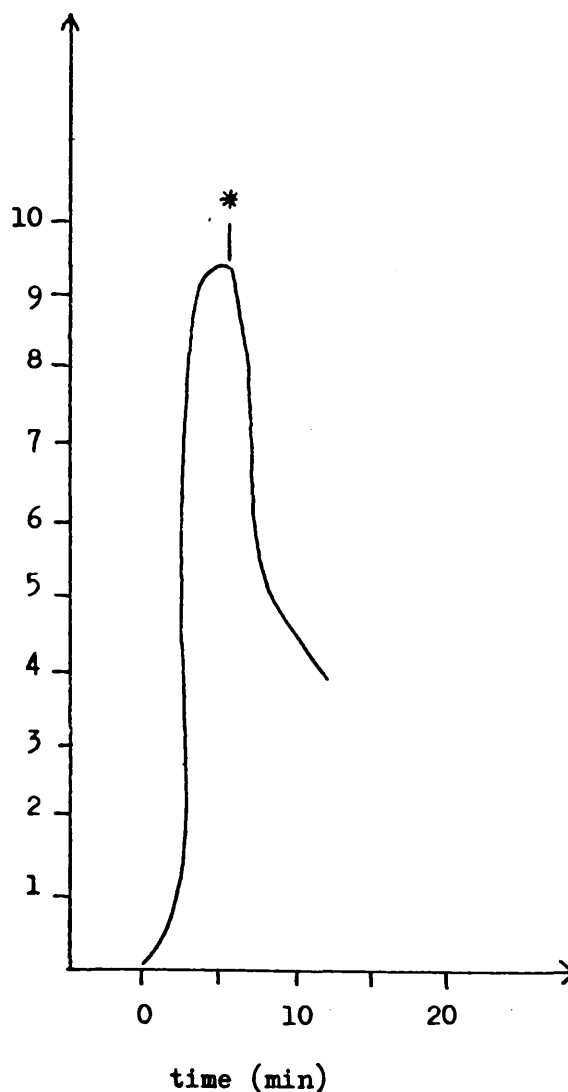


FIGURE 11 - 16

SUB-AMBIENT TVA OF CONDENSABLE VOLATILE FRACTION OF PEROXIDE DECOMPOSITION
REACTIONS IN RUBBER MODIFIED BY OXIDATION AT 0°C FOR 2 MONTHS

Sample Size 50 mg

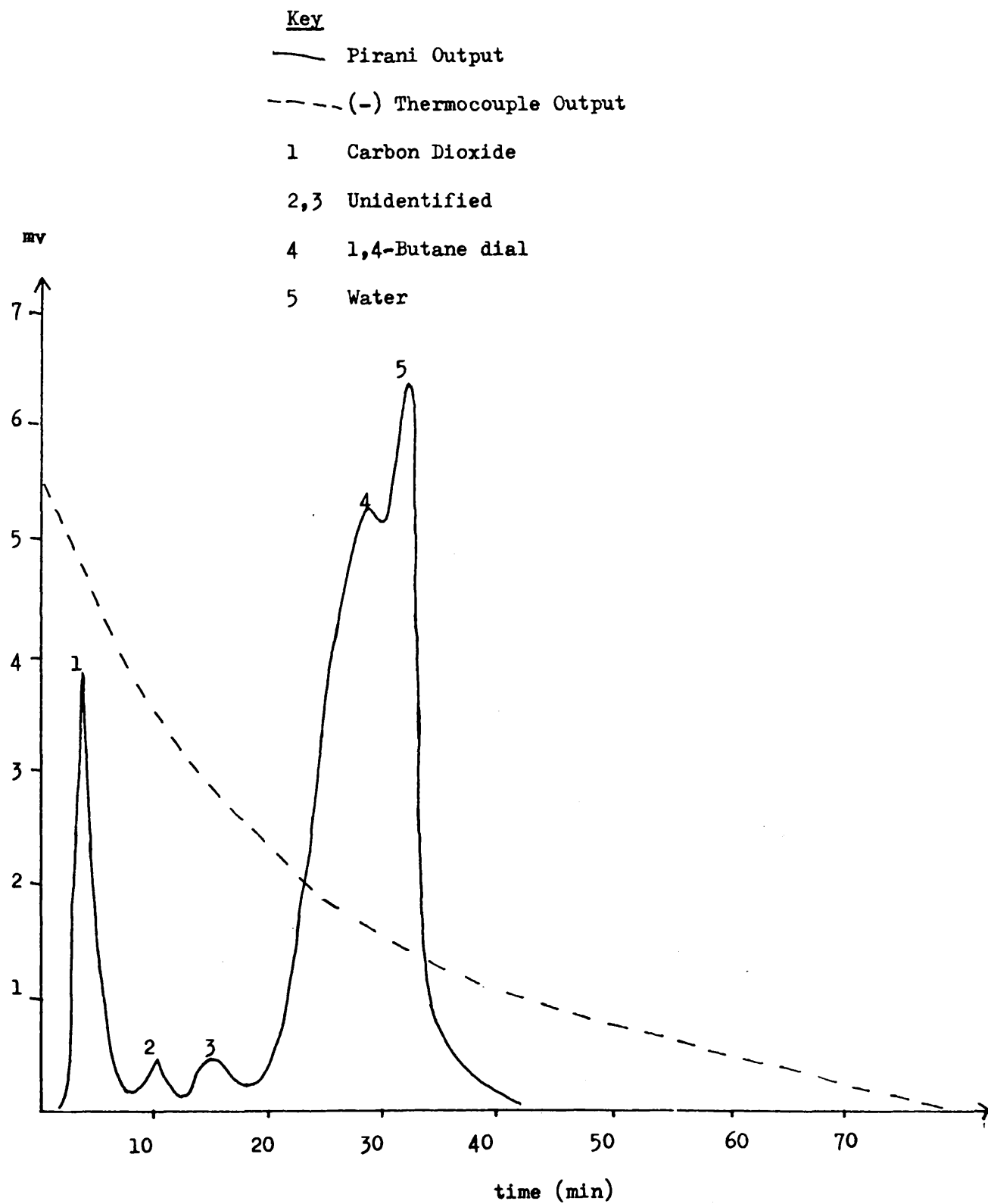


FIGURE 11 - 17

I.r. ABSORPTION BANDS ASSOCIATED WITH PRODUCTS OF THERMAL DEGRADATION
UNDER VACUUM OF POLYBUTADIENE MODIFIED BY LOW TEMPERATURE OXIDATION

Key

- (a) Gas Phase Spectrum Of Condensable Volatile Product Of Peroxide
Decompositions In Material
- (b) Solution Spectrum (C Cl_4) Of F_6 Of SATVA Of High Temperature
Decomposition Products
- (c) Solution Spectrum (C Cl_4) Of F_7 Of SATVA Of High Temperature
Decomposition Products

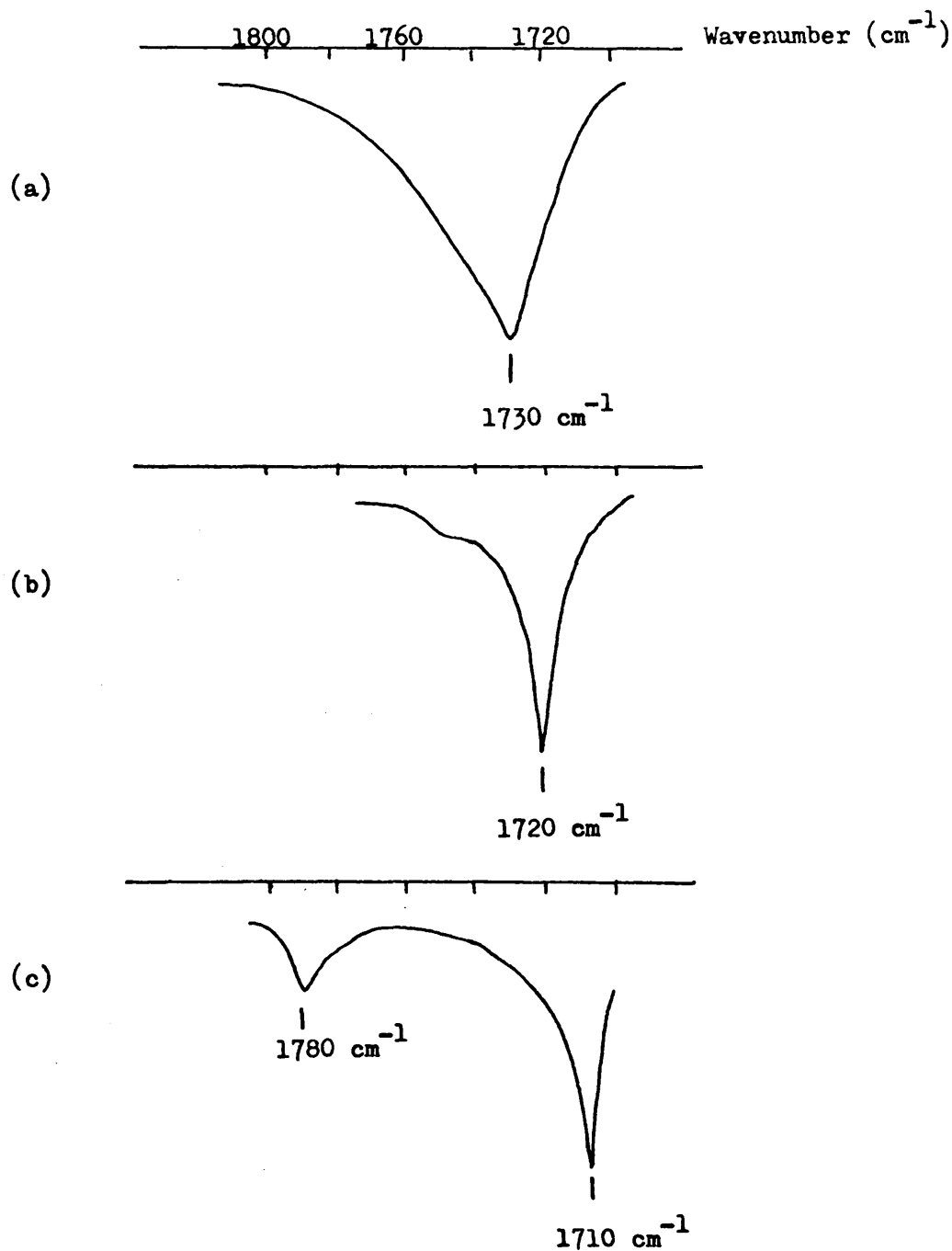
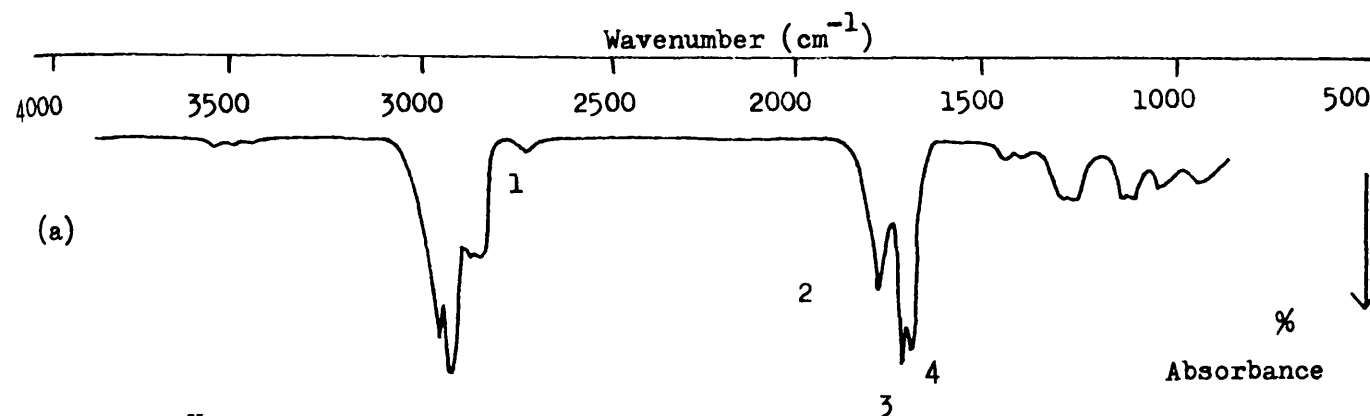


FIGURE 11 - 18

I.r. SPECTRA OF COLD RING PRODUCT FRACTION OF PEROXIDE DECOMPOSITIONS
UNDER VACUUM IN POLYBUTADIENE MODIFIED BY OXIDATION AT 0°C FOR 6 MONTHS

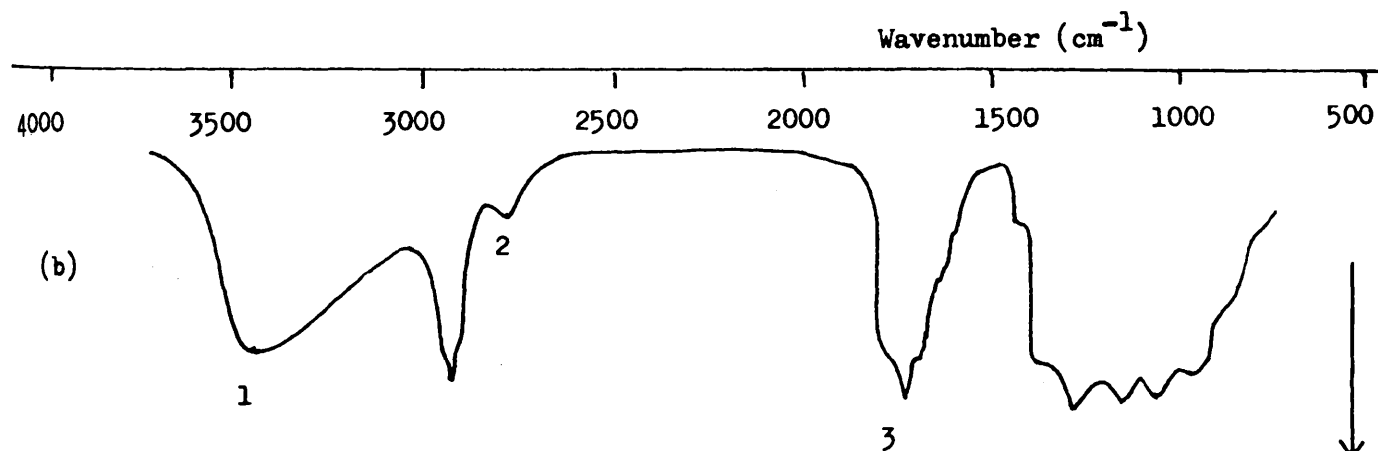
Key

- (a) Material As Solution With CHCl_3
(b) Material As Thin Film On Salt Plate



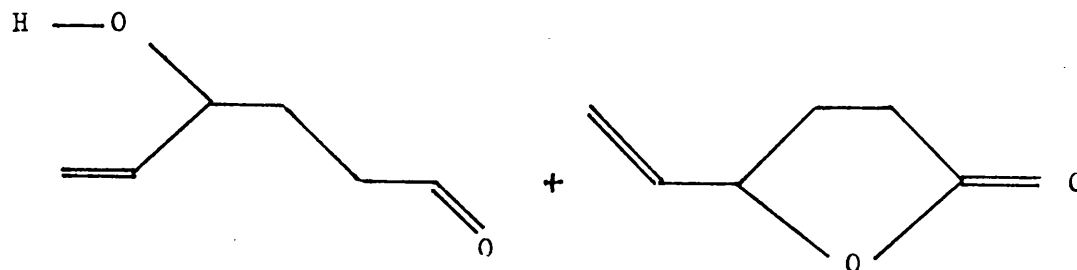
Key

- 1 2720 cm^{-1} Aldehyde C-H
2 1790 cm^{-1} 5 Ring Lactone C=O
3 1730 cm^{-1} Aldehyde C=O
4 1700 cm^{-1} (?)



Key

- 1 3400 cm^{-1} Hydroxyl O-H
2 2725 cm^{-1} Aldehyde C-H
3 1720 cm^{-1} (See Above)



(iv). Residual Material.

The effect of programmed degradation to 200°C under vacuum on polybutadiene modified by low temperature oxidation has already been discussed in section D of this chapter where it was shown to be minimal.

G 2 ABOVE 200°C.

(i). Noncondensable Volatile Material.

Noncondensable volatile material produced by thermal degradation of rubber modified by oxidation at 0°C for 6 months was trapped and analysed by i.r. spectroscopy to give the spectra outlined in fig. 19 . It can be seen that the low temperature "tail" of the degradation reaction produces only carbon monoxide and that higher temperature decompositions of the material produce a mixture of carbon monoxide and methane. It is of interest to note that methane is produced in larger quantities from this system than from the thermal degradation of pure rubber, even though the ATVA trace for this material (fig. 14) suggests that the aromatisation/fragmentation reaction - its mode of production in pure rubber - is quenched.

(ii). Condensable Volatile Material.

The condensable volatile products of programmed thermal degradation in the temperature range 200 - 500°C of rubber modified

by oxidation at 0°C for 6 months were collected and subjected to SATVA. The SATVA pressure curve was divided into seven regions as shown in fig. 20. Each region was examined by i.r. spectroscopy to yield the information outlined below.

F₁ (Gas phase i.r. spectroscopy)

F₁ was shown to be composed of a mixture of ethene and ethane.

F₂ (Gas phase i.r. spectroscopy)

F₂ was shown to be composed of a mixture of propene and carbon dioxide.

F₃ (Gas phase i.r. spectroscopy)

F₃ was shown to be composed of a mixture of C₄ hydrocarbons, carbon dioxide and unidentified carbonyl containing material, most probably aldehydic in nature (absorption at 2715 cm⁻¹).

F₄ (Gas phase i.r. spectroscopy)

F₄ was shown to be composed of a mixture of C₅ - C₆ hydrocarbons and an unidentified aldehyde compound.

F₅ (Gas phase i.r. spectroscopy)

F₅ was shown to be composed mainly of water.

F₆ (Liquid phase i.r. spectroscopy - fig. 17)

F₆ was shown to be composed of a mixture of hydrocarbon fragments at least one of which contains a saturated acid grouping.

F₇ (Liquid phase i.r. spectroscopy - fig. 17)

F₇ was shown to be composed of material a fraction of which could be described as cyclic anhydride in nature (159). It will, however, be shown that anhydride material (usually stable to volatilisation at high temperatures) is not detected in the residue of

partial degradation of this material. The high frequency carbonyl absorption could alternatively be assigned to 5 ring lactone groupings in the mixture.

(iii). Cold Ring Material.

The cold ring product fraction of programmed thermal degradation in the temperature range 200 - 500°C, of rubber modified by oxidation at 0°C for 6 months was examined by i.r. spectroscopy as shown in fig. 21 . It is of interest to note the close similarity between the oxygen-containing groups in this material and in the residue of rubber oxidised at 100°C for 5 min (fig. 11).

(iv). Residual Material.

The residues of programmed thermal degradations to 430°C and 440°C of rubber modified by oxidation at 0°C for 6 months were examined by i.r. spectroscopy with the results shown in fig. 22 . It can be seen that the processes of decomposition operative in the temperature range 200 - 440°C quantitatively remove oxygen-containing groupings from the polymer to leave material with i.r. activity similar to that of cyclised polybutadiene.

FIGURE 11 - 19

I.r. SPECTRA OF NONCONDENSABLE PRODUCT FRACTIONS OF PROGRAMMED DEGRADATION
UNDER VACUUM OF POLYBUTADIENE MODIFIED BY OXIDATION AT 0°C FOR 6 MONTHS

Sample Size 25 mg

Heating Rate 10°C/min

Key

(a) 200 - 320°C

(b) 320 - 500°C

(Room Temperature - 200°C, Blank Spectrum)

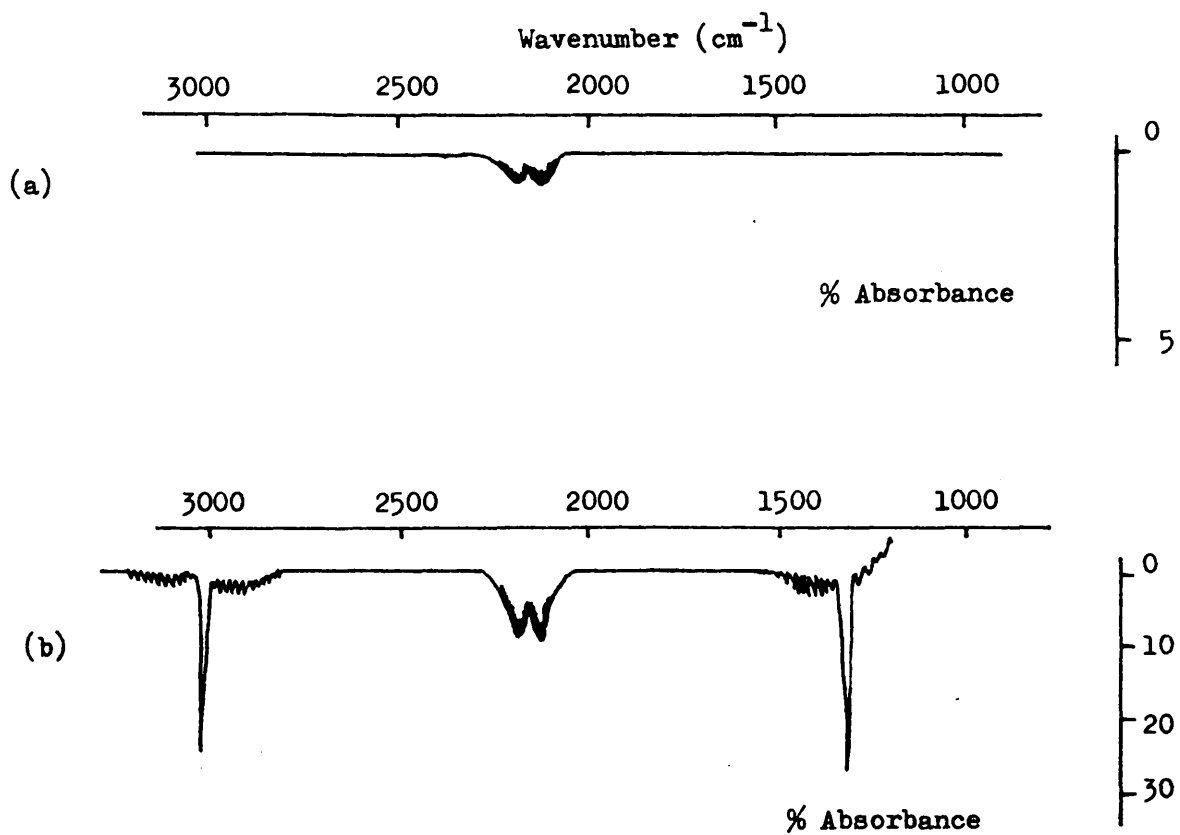


FIGURE 11 - 20

SUB-AMBIENT TVA OF PRODUCTS OF PROGRAMMED DEGRADATION ABOVE 200°C OF
 POLYBUTADIENE MODIFIED BY (a).OXIDATION AT 250°C FOR 1 hr
 (b).OXIDATION AT 0°C FOR 6 MONTHS

Sample Size 50 mg
 Heating Rate 10°C/min

Key
 .-.- Pirani Gauge Outputs
 - - - (-) Thermocouple Output
 F_n Regions Into Which The
 Pressure Curve Is Divided
 For Spectroscopic Analysis

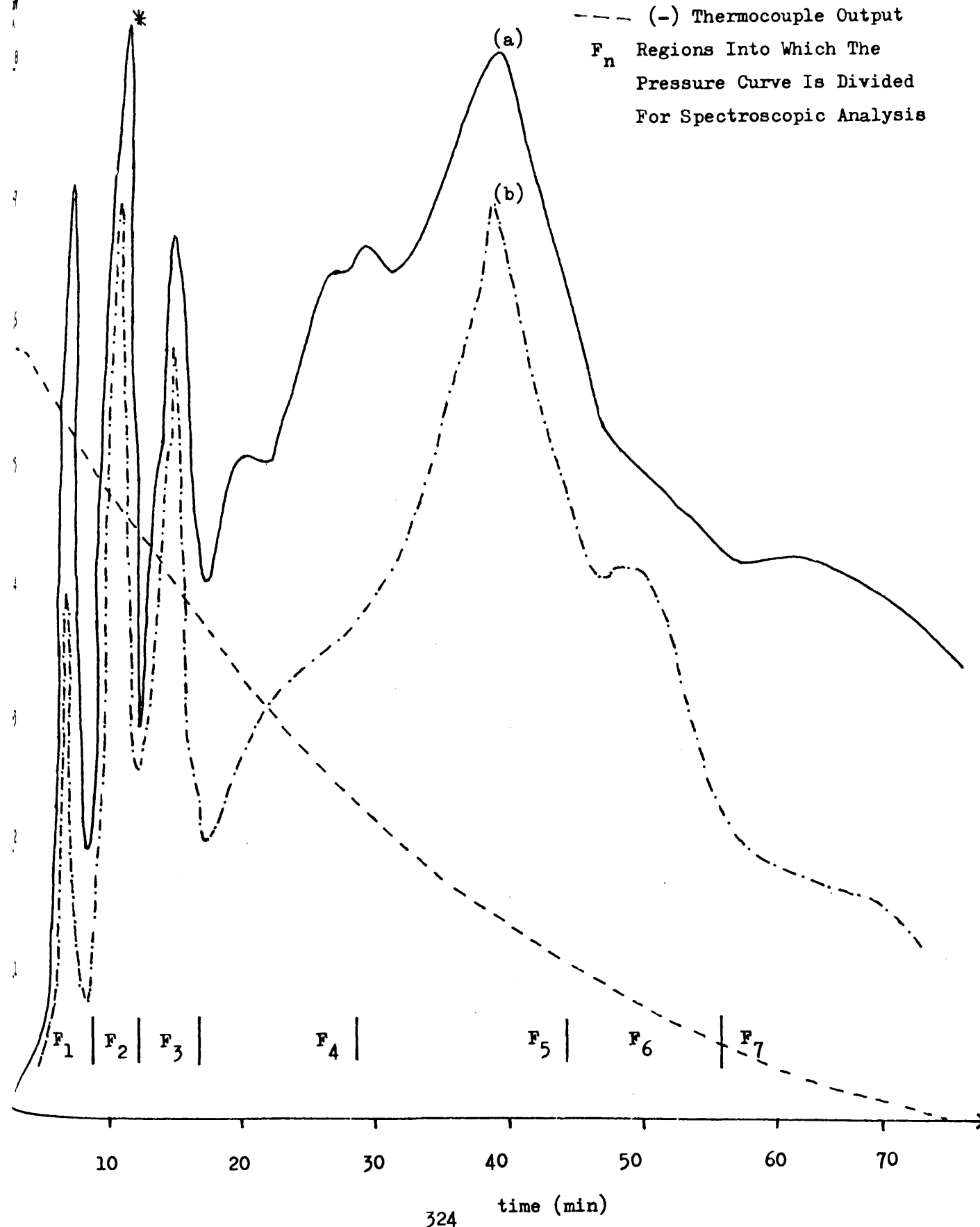


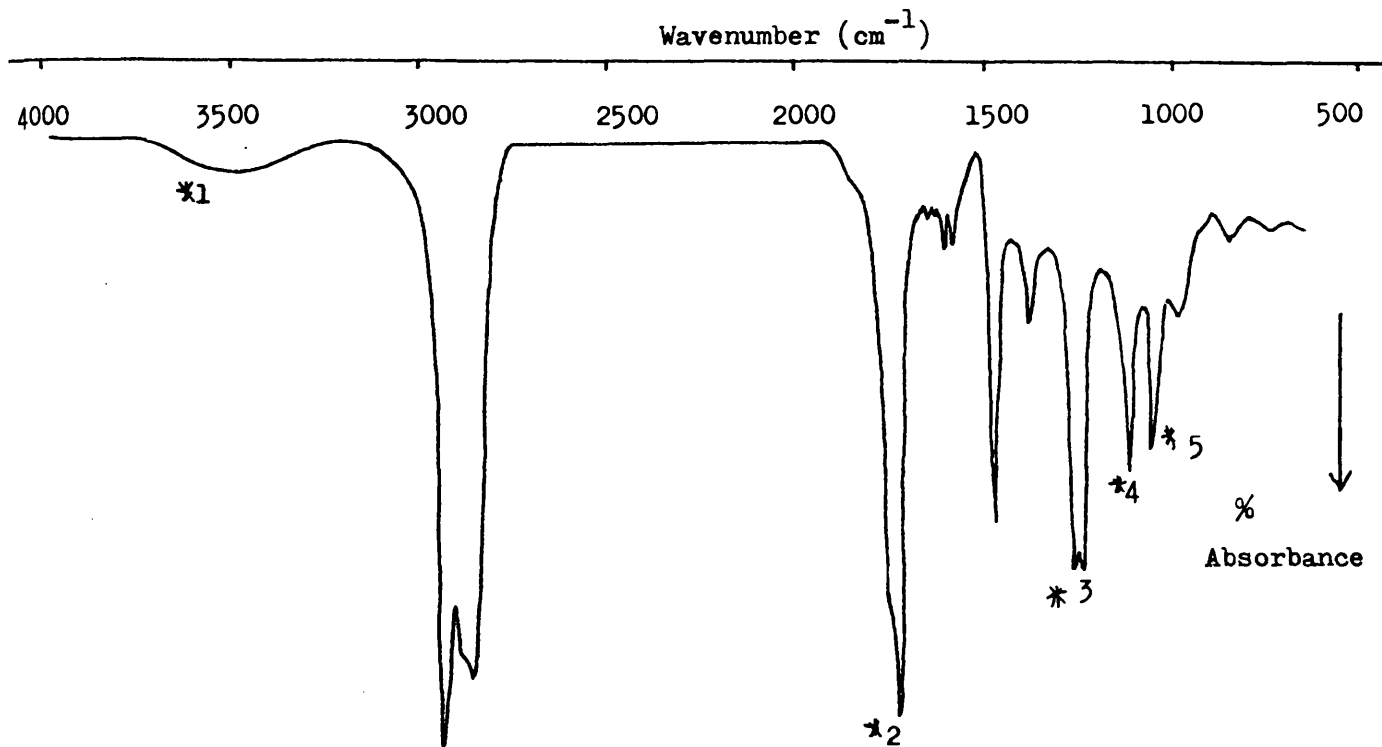
FIGURE 11 - 21

I.r. SPECTRUM OF COLD RING PRODUCT FRACTION OF PROGRAMMED DEGRADATION

ABOVE 200°C OF POLYBUTADIENE MODIFIED BY (a).OXIDATION AT 250°C FOR 1 hr

(b).OXIDATION AT 0°C FOR 6 MONTHS

(Material As Thin Film On Salt Plate)



* Absorptions Associated With Oxygen Containing Groups

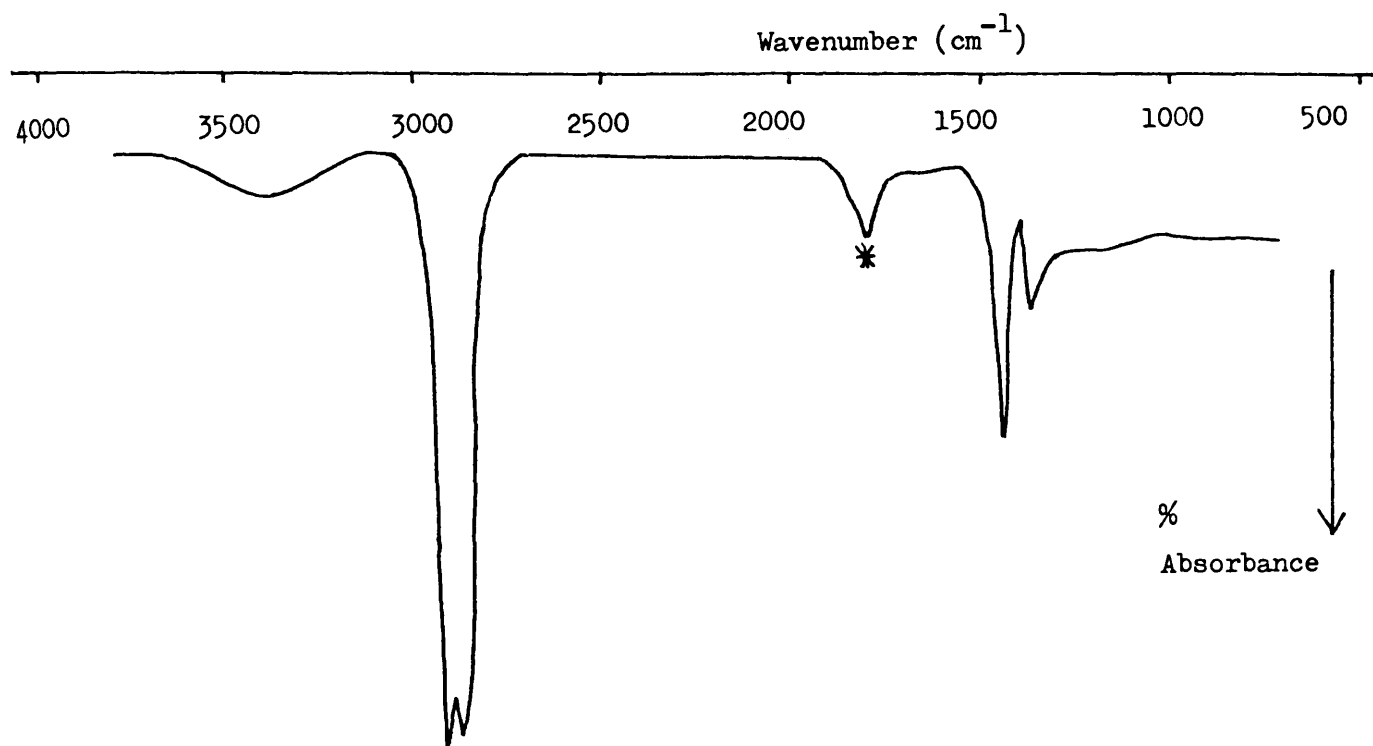
Wavenumber (cm⁻¹)

1	3400	O-H
2	1720	C=O Of Saturated Acid Group
3	1270,1290	C-O Of Saturated Acid Group
4	1120	C-O Of Polyether Group
5	1070	C-O Of Polyether Group

FIGURE 11 - 22

I.r. SPECTRUM OF RESIDUE OF PROGRAMMED DEGRADATION TO 440°C OF
POLYBUTADIENE MODIFIED BY OXIDATION AT 0°C FOR 6 MONTHS

(K Br Disc)



* C=O At 1710 cm⁻¹

OPERATIVE AT 100°C.

I.r. spectra of polybutadiene which has been subjected to oxidation at 100°C are shown in fig. 11. The development of a strong absorption band at 3400 cm^{-1} is proof that the reaction is associated with the production of alcoholic/acidic material which is bound to the matrix -volatile material would be removed either during oxidation or in the subsequent cooling process under vacuum. The development of i.r. absorptions at 1720 cm^{-1} , 1270 cm^{-1} and 1290 cm^{-1} is proof of the formation of involatile saturated acidic material while the appearance of absorption bands at 1120 cm^{-1} and 1070 cm^{-1} shows the presence of isolated polyether linkages (157, 158).

It is of interest that i.r. absorption bands in the region $1400 - 1000\text{ cm}^{-1}$ are absent in spectra which correspond to the later stages of the reaction. This can be caused only by complexation of oxygenated material with water which in turn can be introduced to the sample only as a product of the oxidation reaction.

Epoxide material is stable to decomposition at 100°C. Its absence from the residue of oxidation at this temperature suggested that such material was not formed in the oxidation process.

I PROGRAMMED DEGRADATION UNDER VACUUM OF POLYBUTADIENE MODIFIED
BY OXIDATION REACTIONS AT ELEVATED TEMPERATURES.

(i). ATVA

ATVA traces which correspond to the programmed thermal degradation of polybutadiene modified by oxidative degradation for 1 hr at 100°C, 150°C, 200°C and 250°C are shown in fig. 23 .

As expected, oxidised samples did not react to produce volatile material in the temperature range 100 - 200°C. This indicates that the stationary concentrations of peroxide groupings in polybutadiene oxidised at elevated temperatures are very small. This is not surprising when it is considered that these intermediates are quantitatively decomposed by purely thermal processes at temperatures in excess of 90°C (figs. 5, 12). This would appear to invalidate the claims made by some authors (155) that the presence of peroxide groups in the residue of accelerated oxidations of rubber could be detected by the less sensitive techniques of i.r. and n.m.r. spectroscopy.

All oxidised samples produce noncondensable material in larger quantities than the unoxidised rubber and at lower temperatures. Such material is quantitatively trapped by molecular sieve at -196°C. Samples oxidised at 100°C, 150°C and 200°C retain the 450°C rate maximum for emission of noncondensables as in pure rubber while at the same time displaying an extra rate maximum for noncondensable emission at 390°C. Both rate maxima are absent from the ATVA trace of rubber oxidised at 250°C and are replaced by a common rate maximum at 425°C.

A comparison between the Pirani Y outputs corresponding to degradation of pure rubber and rubber oxidised at 250°C (fig.23, 6-5) shows that the oxidation reactions operative in polybutadiene at elevated temperatures either produce material which inhibits the

aromatisation reaction or consumes material able to take part in it.

(ii). Combined TVA/ATVA

Combined TVA/ATVA traces corresponding to the programmed degradation of polybutadiene and polybutadiene oxidised at 250°C for 1 hr are shown in figs. 24 and 25. It can be seen that the threshold temperature for evolution of condensable and noncondensable products from the oxidised material (200°C and 250°C respectively) are much lower than the threshold temperatures for formation of noncondensable products in pure rubber (325°C and 360°C respectively).

FIGURE 11 -23

ATVA CURVES FOR POLYBUTADIENE MODIFIED BY OXIDATION AT ELEVATED TEMPERATURES

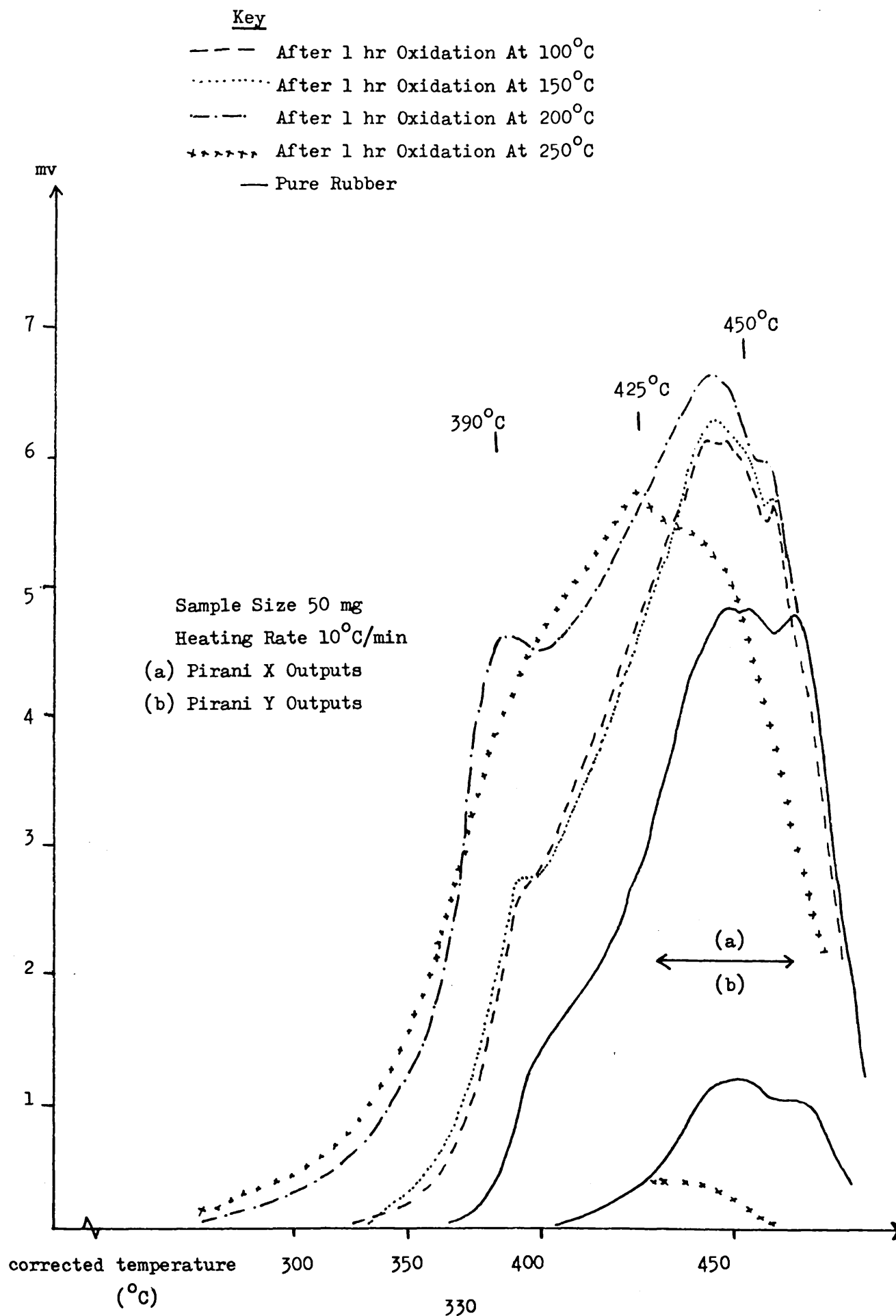


FIGURE 11 - 24

COMBINED TVA/ATVA TRACE FOR POLYBUTADIENE

Sample Size 50 mg
Heating Rate $10^{\circ}\text{C}/\text{min}$
Sieve Trap At -196°C

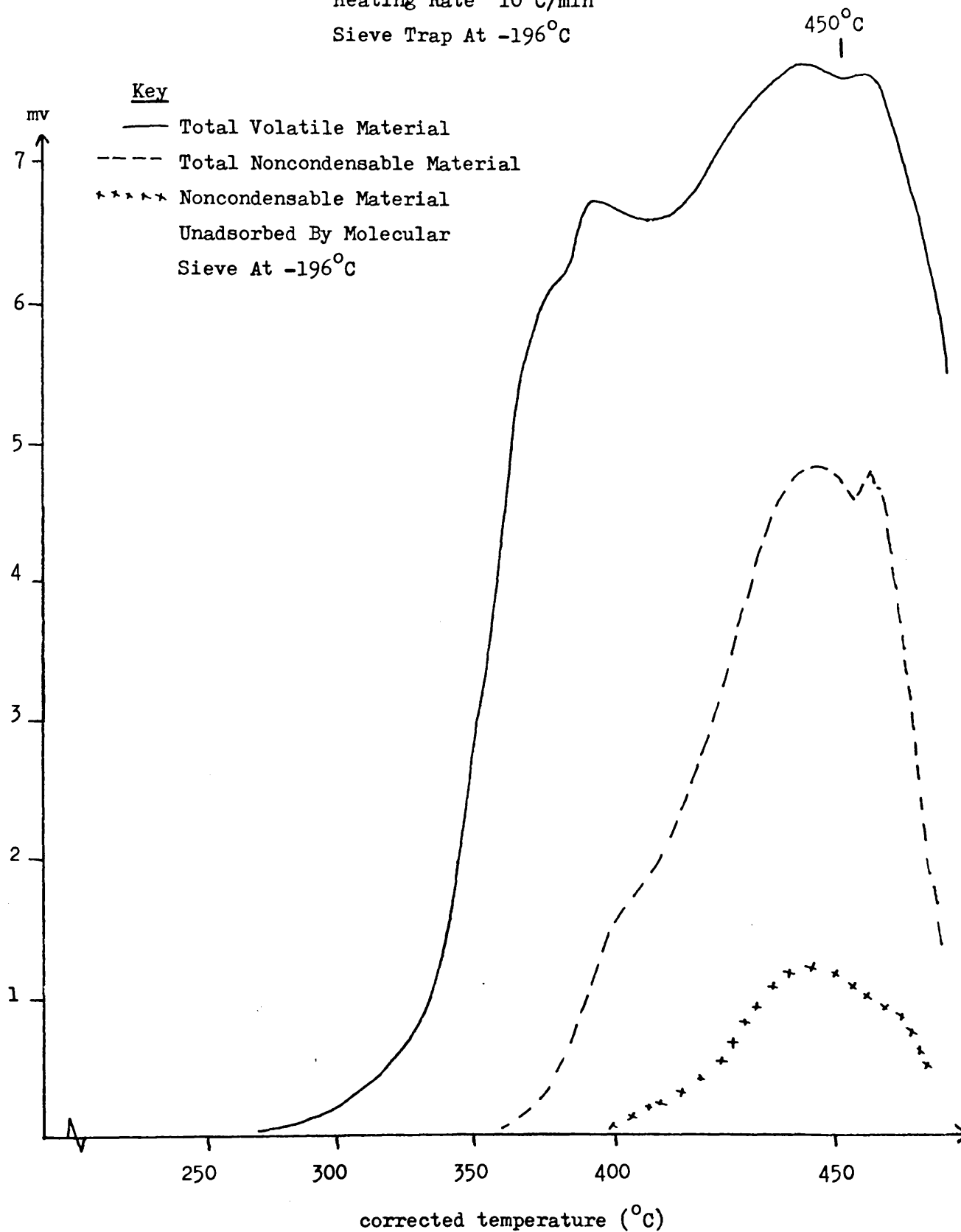


FIGURE 11 - 25

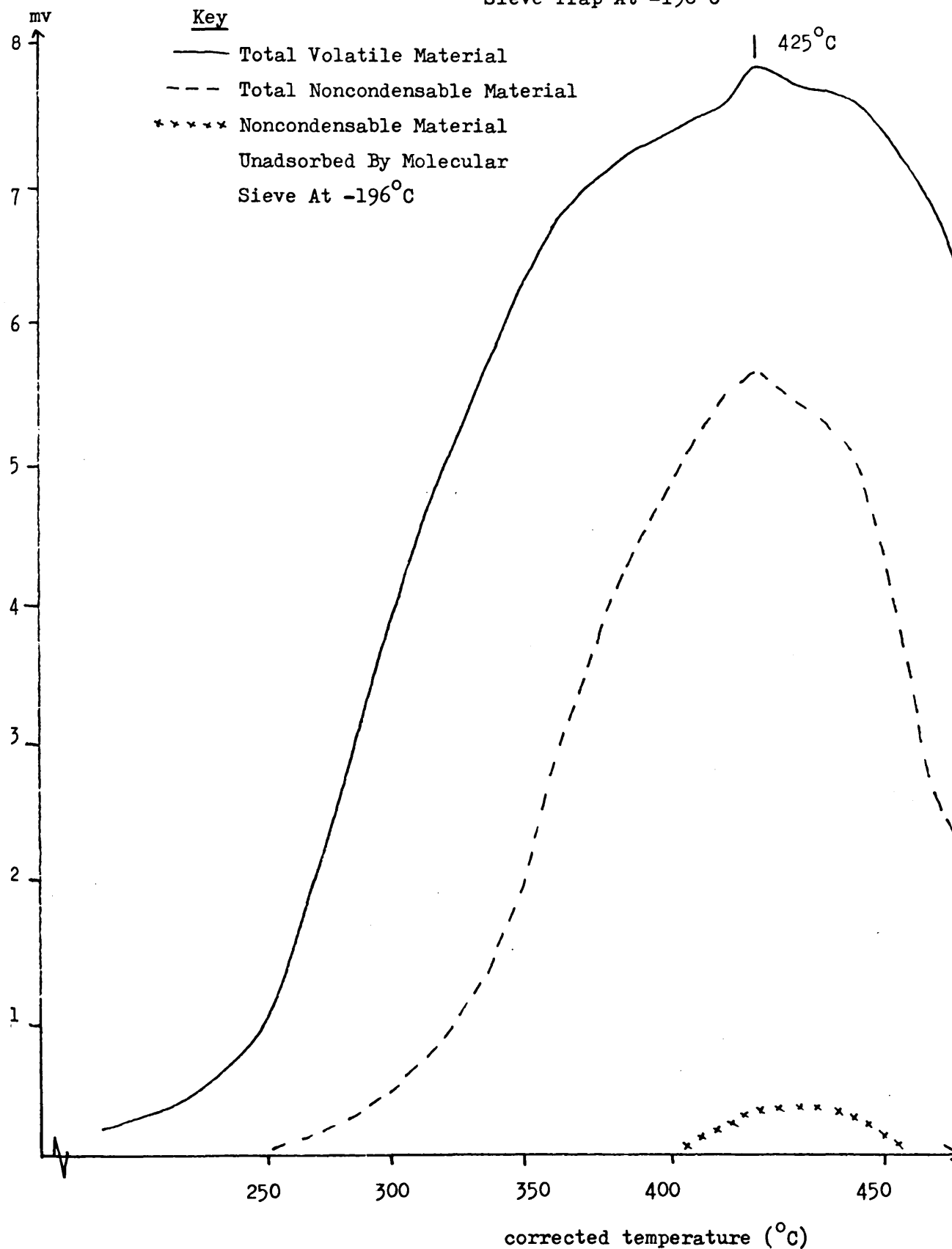
COMBINED TVA/ATVA TRACE FOR POLYBUTADIENE MODIFIED BY OXIDATION AT 250°C

FOR 1 hr

Sample Size 50 mg

Heating Rate 10°C/min

Sieve Trap At -196°C



J PRODUCTS FORMED IN THE PROGRAMMED THERMAL DEGRADATION OF POLYBUTADIENE
MODIFIED BY OXIDATION AT ELEVATED TEMPERATURES.

(i). Noncondensable Volatile Material.

The noncondensable volatile fraction of programmed degradation to 500°C of polybutadiene oxidised in the temperature range 100 - 300°C was shown to be composed of a mixture of carbon monoxide and methane. The yields of carbon monoxide from oxidised polymers are shown in Table 1.

TABLE 11- 1

YIELDS OF CARBON MONOXIDE AND CARBON DIOXIDE AS PRODUCT OF
PROGRAMMED DEGRADATION AT 10°C/min TO 500°C UNDER VACUUM OF
POLYBUTADIENE MODIFIED BY OXIDATION AT ELEVATED TEMPERATURES FOR 1 hr.

SAMPLE SIZE (mg)	TEMPERATURE OF OXIDATION (°C)	CO YIELD (mole x 10 ⁴)	CO ₂ YIELD (mole x 10 ⁴)
50	50	0	0
50	100	1.08	0.20
50	150	1.21	0.24
50	200	1.40	0.77
50	250	1.55	1.39
50	300	0	0.88

(ii). Condensable Volatile Material.

The condensable volatile fractions of programmed thermal degradations of polybutadiene modified by oxidation for 1 hr at 250°C and 300°C were subjected to SATVA. The pressure curves so produced were remarkably similar both to each other and to that for the condensable volatile products of thermal degradation of rubber modified by low temperature oxidation (fig. 20). In fact, fractions 1 - 5 were shown by i.r. spectroscopy to be very similar to the first 5 product fractions of the SATVA curve for polybutadiene oxidised at low temperatures (section G2 (ii)). Fractions 6 and 7 were not examined. The cell used for quantitative work with carbon dioxide in Chapter 3 was recalibrated at 2300 cm⁻¹ as shown in fig. 26 and used to obtain quantitative carbon dioxide yields from oxidised polymers (Table 1).

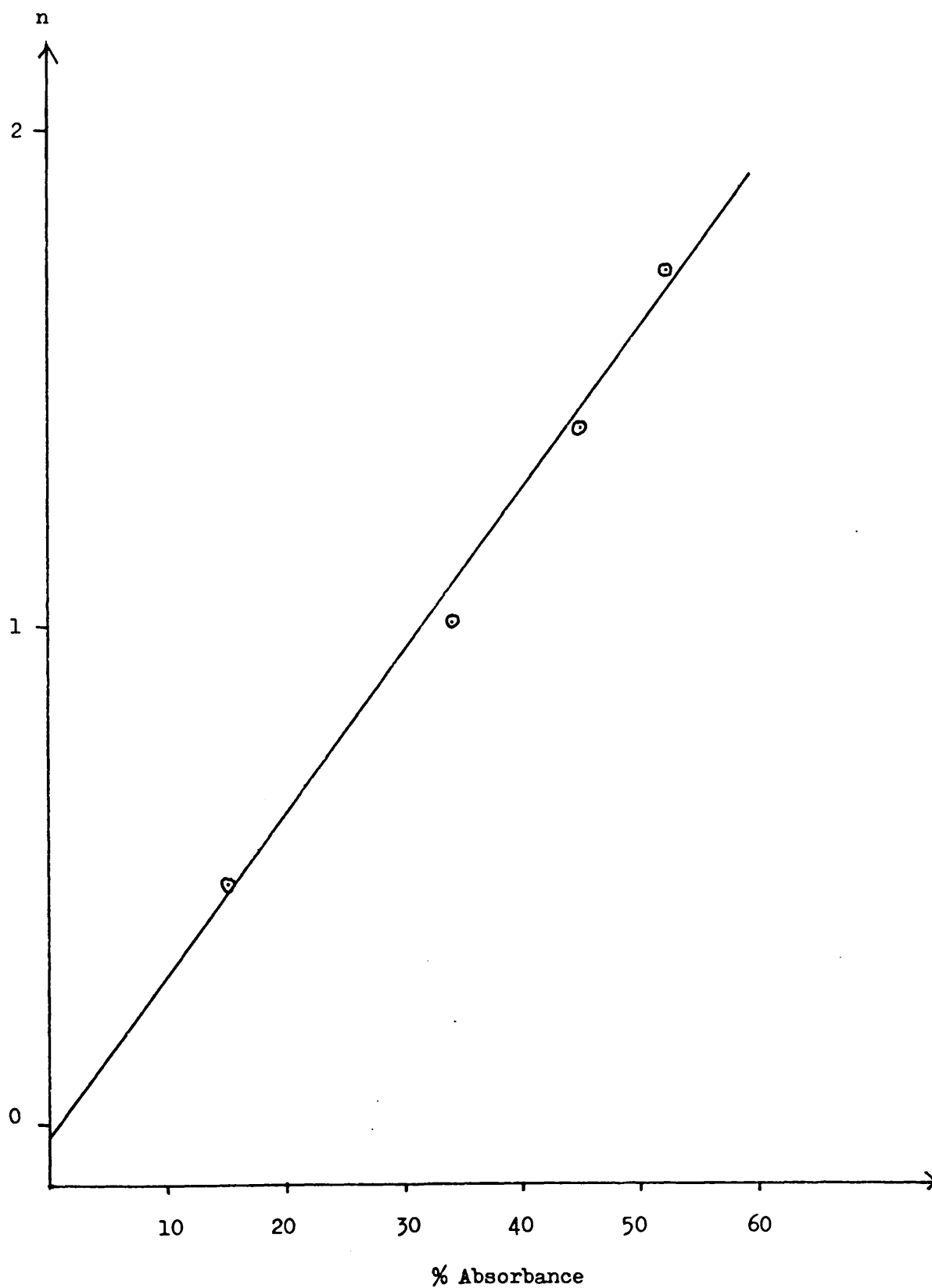
(iii). Cold Ring Material.

The cold ring fraction of programmed thermal degradation of polybutadiene modified by oxidation at 250°C was examined by i.r. spectroscopy and shown to be identical in structure to the residue of accelerated oxidation at 100°C for 5 min (fig. 11) and the cold ring fraction of programmed thermal degradation of polybutadiene modified by oxidation at 0°C (fig. 21).

FIGURE 11 - 26

I.r. GAS CELL CALIBRATION CURVE FOR CARBON DIOXIDE AT 2300 cm^{-1}

(Quantity Of Carbon Dioxide In Cell = $n \times 10^{-4}$ mole)



K DISCUSSION.

It has been shown (figs. 2 , 3) that polybutadiene is subject to exothermic oxidative processes which bind oxygen to the polymer residue at elevated temperatures below its flash point. It has also been shown (fig. 5) that it is possible to accumulate a large quantity of the reactive intermediates of oxidation at low temperature, and that this intermediate decomposes at elevated temperatures in an exothermic process with identical rate profile to the overall process of accelerated oxidation (fig. 3). These decompositions initiate processes of weight loss at abnormally low temperatures in the polymer (fig. 4).

The processes of low temperature oxidation (figs. 6, 7, 8) result in the production of carbonyl material, hydroxylic material from water, alcohol or carboxyl structures and do not remove olefinic material completely from the polymer (fig. 9).

$\alpha \beta$ - unsaturated aldehydic material was shown to be produced in the early stages of oxidation (figs. 7, 10).

Accelerated decompositions of the peroxide population generated by low temperature oxidation (figs. 12 , 13) produce a range of volatile material including oxygen, carbon dioxide, 1,4-butane dial, water and a small quantity of the material illustrated in section G1(iii) of this chapter.

Samples of rubber oxidised for 2 months at 0°C (figs. 12 , 13) retain the 450°C rate maximum of volatile production typical of unoxidised polybutadiene but develop a lower temperature rate maximum at 390°C. Both were found to be absent in traces corresponding to more heavily oxidised samples, to be replaced by a single rate maximum at 420°C (fig. 14).

Low temperature processes ($> 200^{\circ}\text{C}$) (fig. 22) remove oxygenated groups from the polymer residue producing carbon

monoxide (fig. 19), carbon dioxide, water and a range of volatile carbonyl containing material (fig. 20) along with a cold ring fraction containing saturated acids, and polyethers of the type $-O-(CH_2)_n-O-$ where n is large.

The processes of accelerated oxidation result (fig. 12) in the production of oxidised groupings identical to those detected in the cold ring fraction of thermal degradation of polybutadiene modified by low temperature oxidation (fig. 21).

Samples of polybutadiene oxidised to a small extent at elevated temperatures (fig. 23) also retain the 450°C rate maximum of volatile production associated with pure polybutadiene and develop a second rate maximum at 390°C. Both were again found to be absent in the case of more heavily modified samples for example those oxidised at 250°C (figs. 23 , 25) and 300°C (not shown) to be replaced by a single rate maximum at 425°C.

Peroxide groups are not accumulated in samples oxidised at above ambient temperatures, presumably because of their instability.

Polybutadiene modified by accelerated oxidation produces carbon monoxide and methane upon subsequent thermal decomposition, along with condensable volatile material similar to that produced in the thermal degradation of rubber modified by oxidation at low temperatures (fig. 20). The cold ring fraction of programmed thermal degradation of polybutadiene modified by accelerated oxidation (fig. 21) is identical to the oxidised polymer itself (fig. 11).

The carbon monoxide and carbon dioxide yields from thermal degradation of polybutadiene modified by accelerated oxidation (Table 1) both reach a maximum for samples oxidised at 250°C. It is not surprising that the product yield of these two gases from samples oxidised at 300°C is small when it is considered (fig. 25).

that oxygen-containing groups can be efficiently volatilised by purely thermal processes at this temperature during the oxidation process to place a limiting value on their concentration in the polymer.

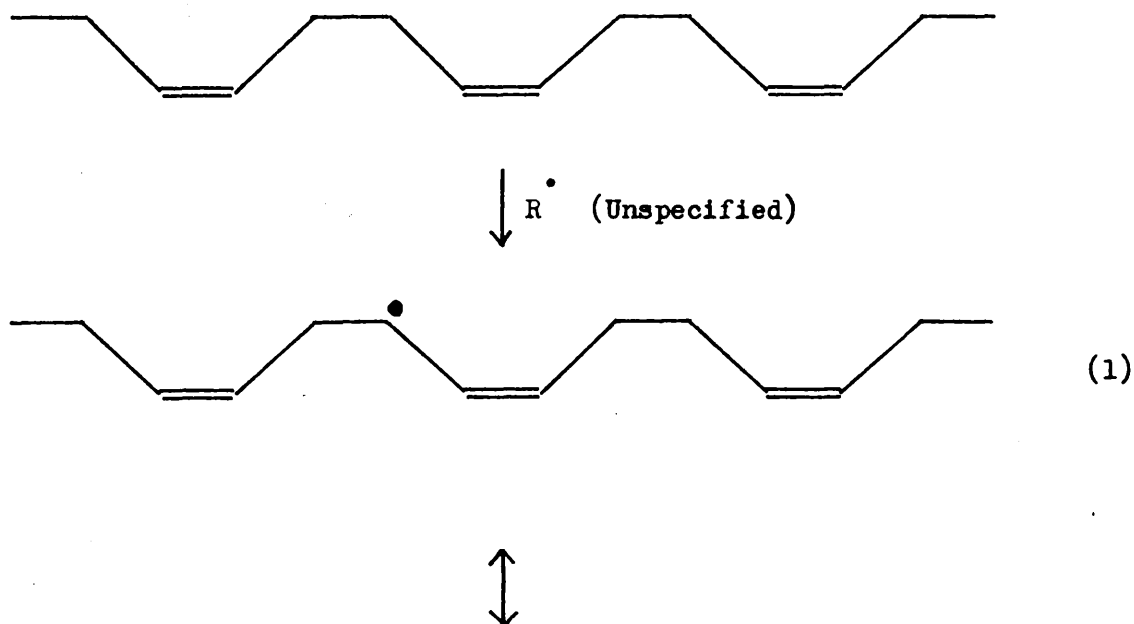
The above is seen as convincing evidence that similar mechanisms of polybutadiene oxidation are operative throughout the temperature range 0 - 250°C.

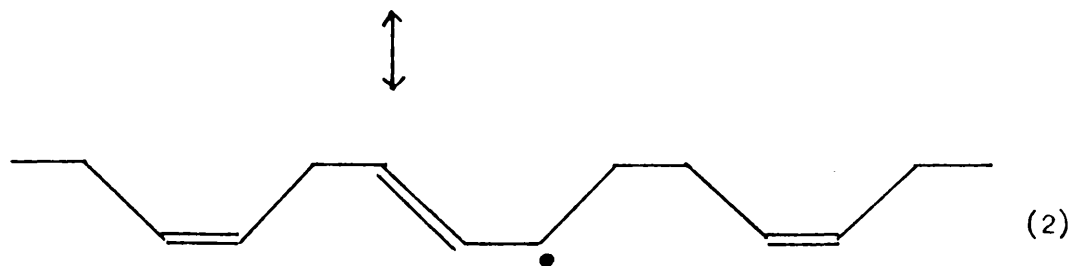
The product distribution obtained in the accelerated decompositions of intermediates of oxidation at 0°C suggests that they are similar to those thought to be formed during the oxidative degradation of polyisoprene (146, 147, 152). A possible reaction pathway for the primary oxidation reaction is postulated below.

MECHANISMS OPERATIVE IN THE PRIMARY OXIDATION REACTION.

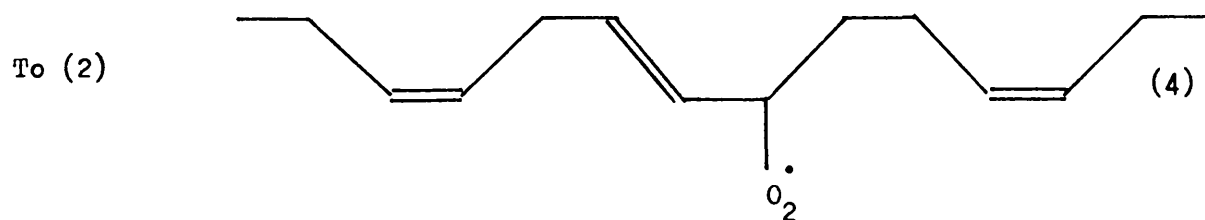
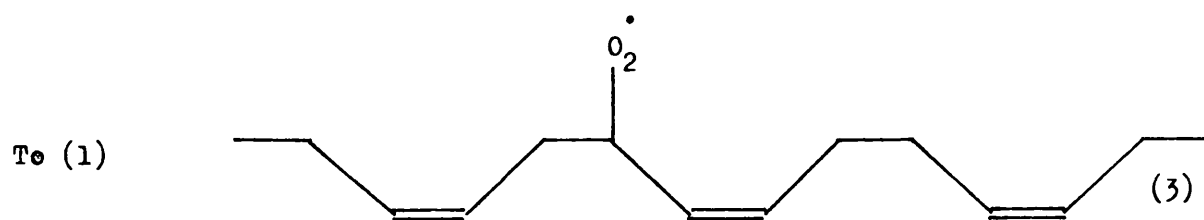
FORMATION OF REACTIVE INTERMEDIATES.

STEP 1 HYDROGEN ABSTRACTION

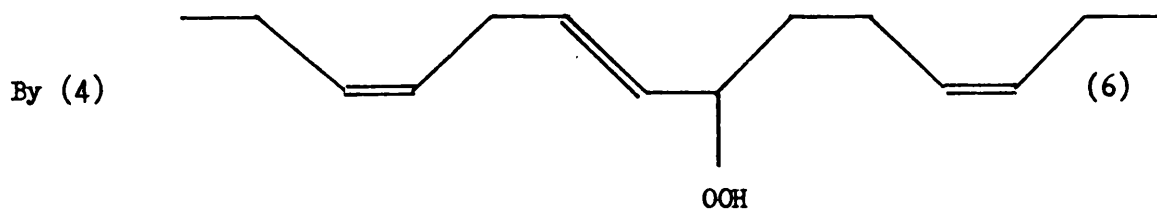
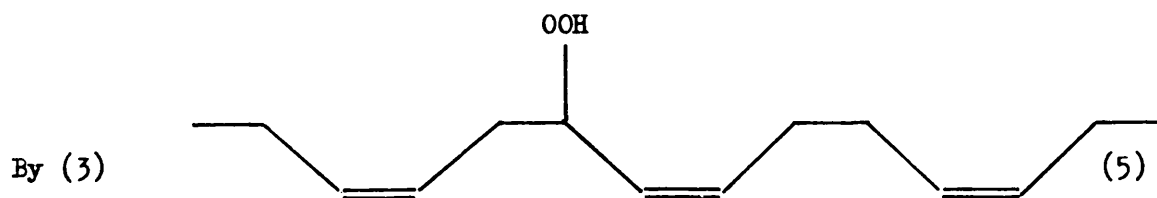




STEP 2 ADDITION OF OXYGEN

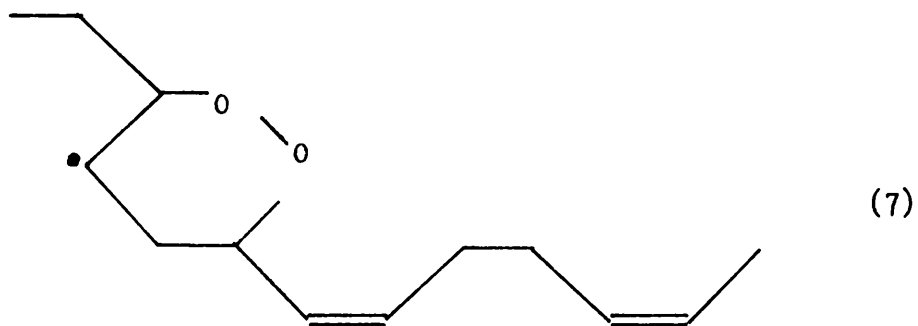


STEP 3 TERMINATION BY HYDROGEN ABSTRACTION

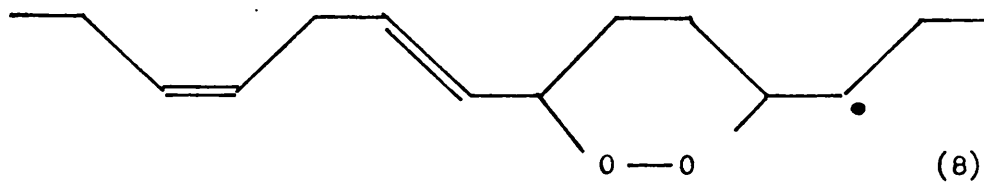


STEP 4 INTRAMOLECULAR CYCLISATION

of (3)

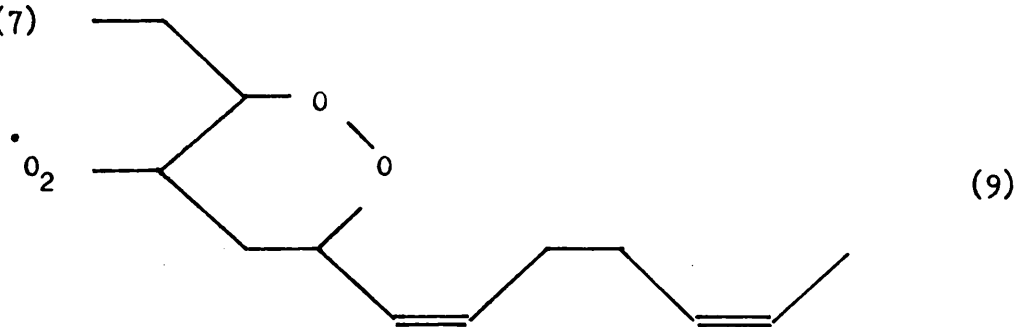


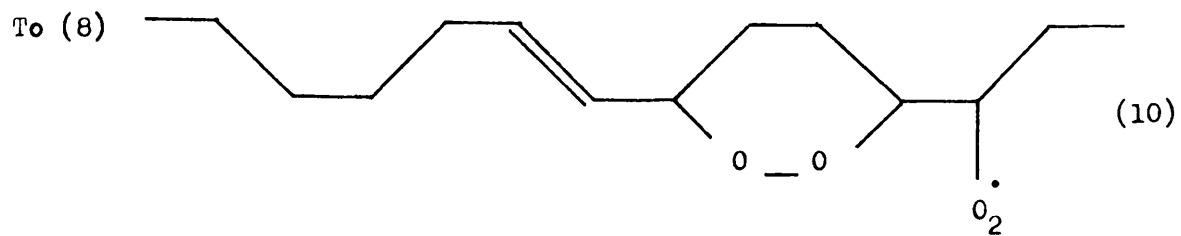
of (4)



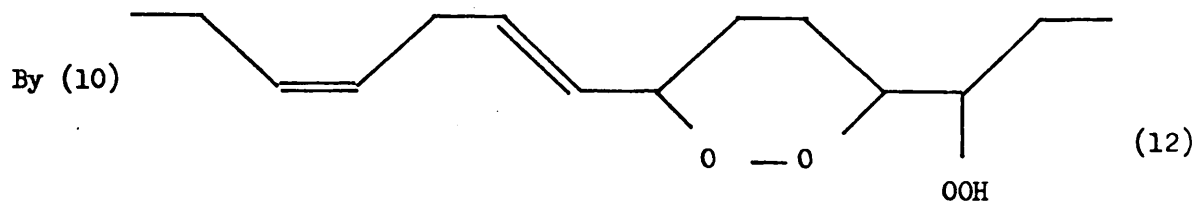
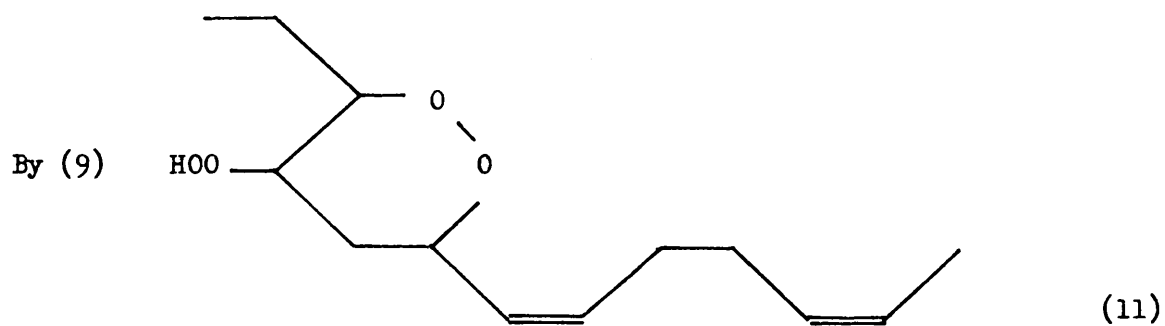
STEP 5 ADDITION OF OXYGEN

To (7)

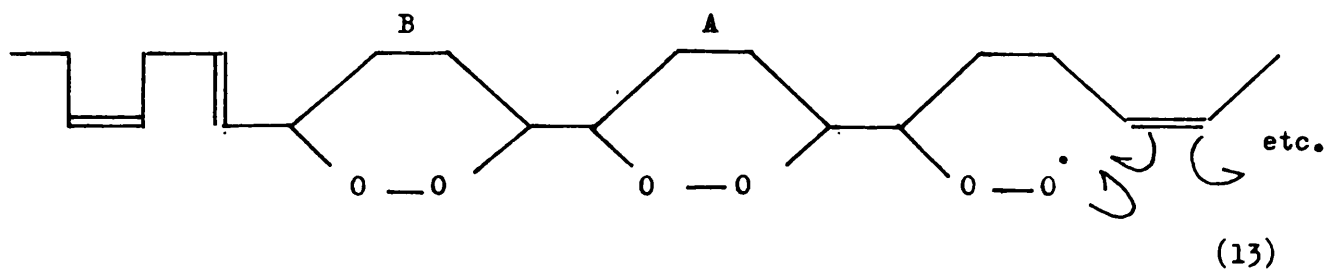




STEP 6 HYDROGEN ABSTRACTION



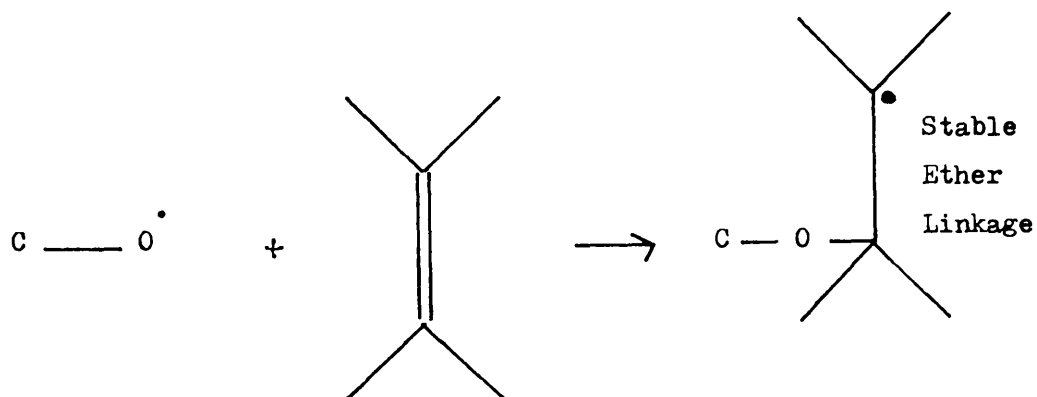
STEP 7 POLYCYCLISATION OF (10)



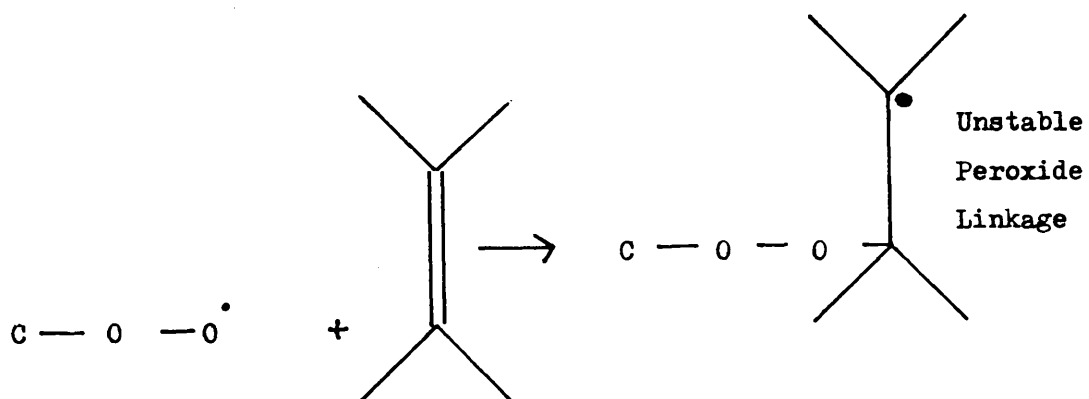
(Especially favoured at low temperatures)

STEP 8 FORMATION OF BRIDGING OXYGEN LINKS

(i). By Intermolecular Attack Of $C-O^\bullet$ (Formed By Peroxide Decomposition)
On Neighbouring Chain Vinyl Groups.



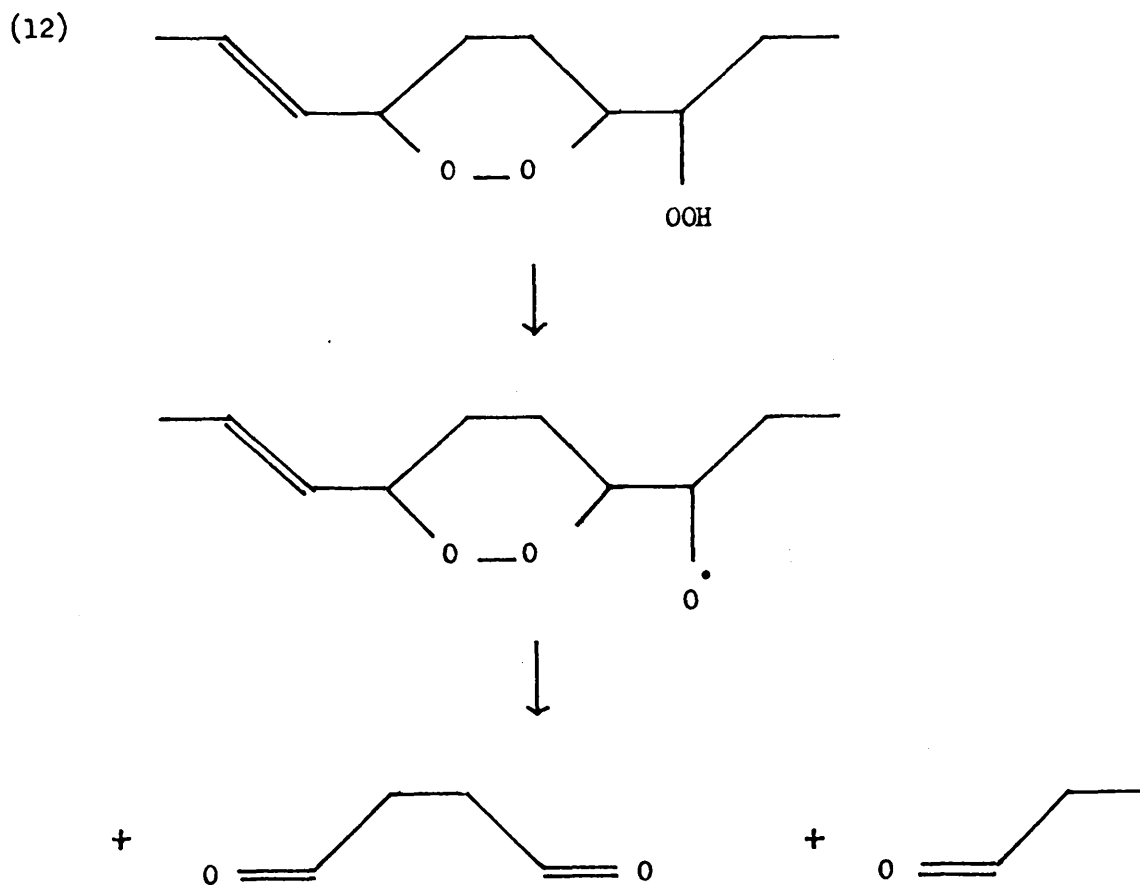
(ii). By Intermolecular Attack Of (3), (4), (9), (10) On Neighbouring
Chain Vinyl Groups.

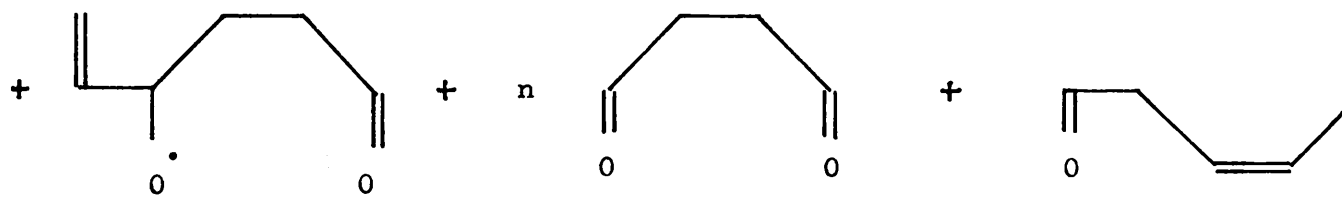
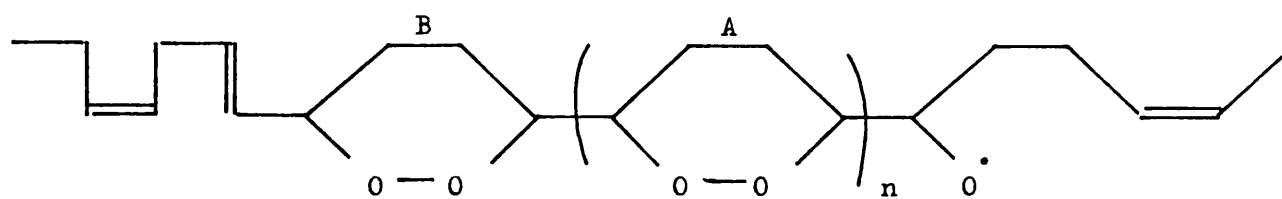
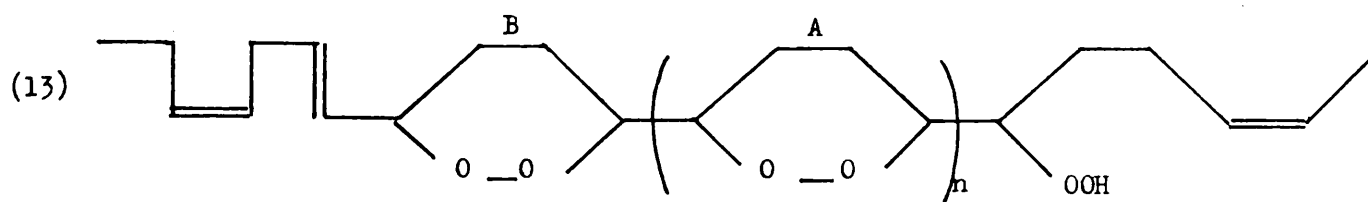


DECOMPOSITION OF REACTION INTERMEDIATES.

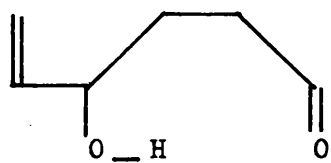
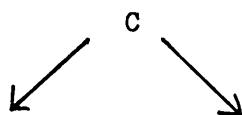
It is not implied (above) that each of the metastable reaction intermediates (5), (6), (11), (12), and (13) is present in equal quantities in the matrix. Mechanisms of decomposition (for which there is some experimental evidence) will now be discussed.

(i). Decomposition Of Cycloperoxide Structures.

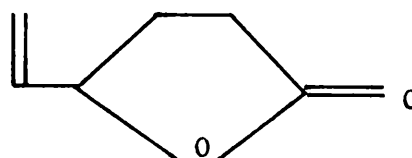




c

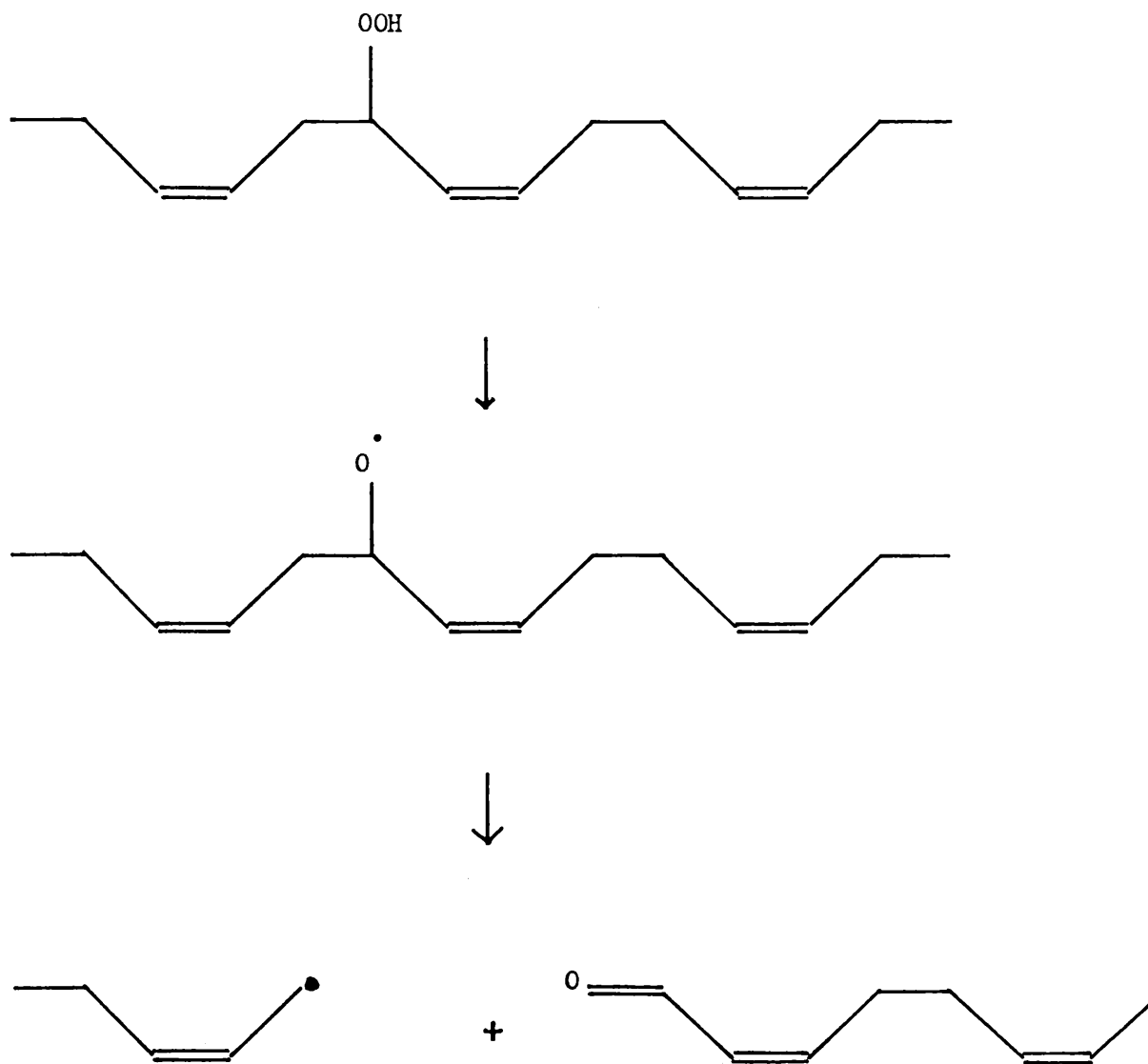


or



(ii). Decompositions Of Peroxide And Hydroperoxide Structures

Decomposition Of (5)



This process could account both for the decrease in molecular weight and for the formation of $\alpha \beta$ unsaturated aldehyde structures in the early stages of oxidation of polybutadiene.

The formation of water and oxygen in the accelerated decomposition of reaction intermediates of oxidation can be attributed to the usual first and second order decomposition reactions of hydroperoxide groups. It is of interest to note that this is possibly the first time that oxygen has been detected as a component of the volatile product fraction of anaerobic decompositions under conditions of efficient product removal which eliminate the possibility of its formation from secondary processes.

The formation of CO_2 as a product of anaerobic peroxide decompositions is more difficult to explain. It could be produced in abnormal decompositions of cycloperoxide species, but is more probably formed by the decarboxylation of acid peroxide groups (Section E of this Chapter).

From a consideration of the above it becomes obvious that the TVA rate maximum at 390°C is associated with the decomposition of residual oxygenated groups in the polymer. The detection of acidic groups in the residue of accelerated oxidation and in the cold ring fractions of degradation of oxidised polymer is proof that residual aldehydic material is further oxidised to its carboxylic acid derivative. The decarboxylation of isolated carboxylic acid groups would produce CO_2 while the concerted decarboxylation of adjacent acid groupings would produce CO_2 , CO and H_2O . Ether linkages are detected in all the cold ring fractions of degradation to show that they are thermally stable with respect to the bulk of the polymer.

CHAPTER 12.

GENERAL CONCLUSIONS.

The results of the present study may be summarised as follows :-

1. Noncondensable gases can be fractionated and quantitatively manipulated under high vacuum conditions by exposure to Linde type "A" molecular sieve held at -196°C . This effect may be used to study the hitherto intractable reactions which lead to the production of primary noncondensable material in substrates involatile under vacuum.
2. The generally accepted assertion that the monomer/oligimer product ratio of polystyrene is insensitive to the conditions of degradation may have to be re-examined in the light of this work which suggests that the proportion of monomer as product increases with the temperature of (isothermal) degradation.
3. A complete product analysis of polybutadiene in its various stages of thermal decomposition provided evidence in support of a two stage decomposition reaction. The lower temperature process was found to approximate closely to the cyclisation/depolymerisation reaction first postulated by Golub. The higher temperature process was shown to volatilise the polycondensate via a random scission reaction. A possible mechanism for this process was postulated.
4. The polystyrene/polybutadiene A : B block copolymer system was found to be more stable than the corresponding polymer blend system which was in turn found to be more stable than the unmixed polymers with respect to the production of material volatile at

degradation temperatures. The extra stability was found to be contained within the polystyrene component of the system and to be generated by its intimate contact with the volatile products associated with both stages of the degradation reaction of polybutadiene.

5. 4-Vinylcyclohexene was shown to interfere with the monomer forming process which is operative in the thermal degradation of polystyrene. 4-Vinylcyclohexene and cyclised polybutadiene were both classified as degradative chain transfer agents by virtue of their effect on the polymer forming radical of polystyrene.

6. It was established for the first time that in the thermal decomposition of AIBN in bulk under vacuum, MAN, IBN and TMSDN are all formed during the decomposition process. It was shown that the primary decomposition event could be monitored by the corresponding production of nitrogen gas under conditions of efficient product removal.

7. The mechanisms operative in the oxidative degradation of polybutadiene were found to be insensitive to the temperature at which the oxidation reaction was performed. The reaction was shown to proceed via a polyperoxide intermediate which decomposed to yield involatile aldehyde groups which were further oxidised to saturated carboxylic acid material. The detection of ether linkages in oxidised material suggested a possible route to its insolubilisation.

The introduction of oxygen into the polymer was found to reduce its thermal stability and to increase in complexity the degradation product distribution.

SUGGESTIONS FOR FURTHER WORK

The work outlined above would be best extended on two fronts. First of all, the analytical procedure which was applied to the polybutadiene polymer could be reapplied to polyisoprene to obtain a complete picture of the mechanisms operative in its thermal degradation. The process could be extended to a study of the thermal degradation of polystyrene/polyisoprene A : B block copolymer systems.

Secondly, polybutadiene could be oxidised in a sealed loop of glass under a dynamic atmosphere of oxygen produced by a sealed in magnetic pump. The volatile products of degradation could be collected in a cryozone in the loop and examined by SATVA and spectroscopy to ascertain whether or not the mechanisms of anaerobic cycloperoxide decomposition are duplicated under an atmosphere of oxygen.

REFERENCES

1. E. Simon, Ann. Chem.,31, 265 (1839).
2. J. Blythe and A.W. Hoffman, Ann. Chem.,53, 292 (1845).
3. E. Caventou, Ann. Chem.,127, 93 (1863).
4. G. Egloff and G. Hulla, Chem. Rev.,35, 279 (1944).
5. S. Straus, S.L. Madorsky, D. Thomson and L. Williamson, J. Res. Natl. Bur. Std.,42, 499 (1949).
6. W.J. Burlant and J.L. Parsons, J. Polym. Sci.,22, 249 (1956).
7. N. Grassie and J.N. Hay, J. Polym. Sci.,56, 189 (1962).
8. W.C. Geddes, Rubber Chem. Technol.,40, 177 (1967).
9. I.C. McNeill, Chapter 6, Developments In Polymer Degradation 1, (Ed) N. Grassie, Applied Science Ltd., London (1977).
10. I.C. McNeill, Europ. Polym. J.,3, 409 (1967).
11. I.C. McNeill, Europ. Polym. J.,6, 373 (1970).
12. I.C. McNeill, L. Ackerman, S.N. Gupta, M. Zulfigar and S. Zulfigar, J. Polym. Sci., Polym. Chem. Ed.,15, 2381 (1977).
13. D.W. Breck, J. Chem. Education,41(12), 678 (1964).
14. D.W. Breck W.G. Eversole, R.M. Milton, T.B. Reed and T.L. Thomas, J. Am. Chem. Soc.,78, 5963 (1956).
15. D.W. Breck, W.G. Eversole and R.M. Milton, J. Am. Chem. Soc.,78, 2338 (1956).
16. L. Broussard and D.P. Shoemaker, J. Am. Soc.,82, 1041 (1960).
17. T.B. Reed and D.W. Breck, J. Am. Chem. Soc.,78 5972 (1956).
18. S.A. Stern, F.S. DiPaulo, J. Vacuum Sci. Tech.,4(6), 347 (1967).
19. D.M. Ruthven, A. I. Ch. E. J.,22(4), 753 (1976).
20. S.A. Stern and F.S. DiPaulo, J. Vacuum Sci. Tech.,6(6), 941 (1969).
21. R. Dobrozemsky and G. Moraw, Vacuum,21(2), 587 (1971).
22. P. Vijendran and C.V.G. Nair, Vacuum,21(5), 159 (1971).
23. C.V.G. Nair and P. Vijendran, Vacuum,27(1), 549 (1977).
24. Y.C. Chan and R.B. Anderson, J. Catal.,50, 319 (1977).

25. I.C. McNeill and M.A.J. Mohammed, Europ. Polym. J. ,
8, 975 (1972).
26. M. Szwarc, L. Levy and R.M. Milkovich, J. Am. Chem. Soc.,
78, 2656 (1956).
27. W.B. Brown and M. Szwarc, Trans. Faraday Soc.,54, 416 (1958).
28. M. Szwarc and M. Litt, J. Phys. Chem.,62, 568 (1958).
29. P.J. Flory, J. Am. Chem. Soc.,62, 1561 (1940).
30. M. Levy, M. Szwarc S. Bywater and D.J. Worsfold,
Polymer,1, 515 (1960).
31. G. Spach, M. Levy and M. Szwarc, J. Chem. Soc., Pt.1,
355 (1962).
32. S. Bywater, A.F. Johnson and D.J. Worsfold, Canad. J.
Chem.,42, 1255 (1964).
33. D.J. Worsfold and S. Bywater, Canad. J. Chem.,38, 1891 (1960).
34. A.F. Johnson and D.J. Worsfold, J. Polym. Sci.,A3, 449 (1965).
35. T.L. Brown and M.J. Rogers, J. Am. Chem. Soc.,79, 1859 (1957).
36. J. Smid and M. Szwarc, J. Polym. Sci.,61, 31 (1962).
37. A.F. Johnson and D.J. Worsfold, Makromol. Chem.,85, 273 (1965).
38. I. Kuntz, J. Polym. Sci.,54, 569 (1961).
39. M. Morton R.D. Sanderson and R. Sakata, J. Polym. Sci.,
polym. Lett.,9, 61 (1971).
40. G.M. Burnett and R.N. Young, Europ. Polym. J.,2, 329 (1966).
41. M. Morton, J.E. McGrath and P.C. Juliano, J. Polym. Sci.,
C,26, 99 (1969).
42. H.L. Hsieh, J. Polym. Sci.,A,3, 163 (1965).
43. J. Worsfold and S. Bywater, J. Organomet. Chem.,9, 1 (1967).
44. M. Morton and R. Milkovich, J. Polym. Sci.,A,1, 443 (1963).
45. M. Morton, A.A. Rembaum and J.L. Hall, Ibid, 461.
46. M. Morton, E.E. Bostick and R.G. Clarke, Ibid, 475.
47. M. Morton, E.E. Bostick, R.A. Livigni and L.J. Fetters,
Ibid, 1735.
48. R.N. McCallum and J.J. McKetta, Hydrocarbon Process.
Petrol Refiner,42, 191 (1963).

49. H. Gilman and F.K. Cartledge, J. Organomet. Chem.,2, 477 (1964).
50. P.D. Bartlett and B. Seidel, J. Am. Chem. Soc.,83, 581 (1961).
51. D.J. Worsfold and S. Bywater, Makromol. Chem.,65, 245 (1963).
52. A. Nakajima, F. Hamada and T. Shimizu, Makromol. Chem.,
65, 245 (1963).
53. R.S. Silas, J. Yates and V. Thornton, Anal. Chem. ,
31, 529 (1959).
54. V.D. Mochel, Rubber Chem. Technology,40, 1200 (1967).
55. E.J. Meehan, J. Polym. Sci. ,1, 175 (1946).
56. H. Staudinger and A. Steinhofner, Annalen,517, 35 (1935).
57. H.H.G. Jellinek, J. Polym. Sci.,3, 850 (1948).
58. S.L. Madorsky, J. Polym. Sci.,2, 133 (1952).
59. P. Bradt, V.H. Dibeler and F.L. Mohler, J. Res. Natl.
Bur. Std.,50(4), 201 (1953).
60. N. Grassie and W.W. Kerr, Trans. Faraday Soc.,53, 234 (1957).
61. N. Grassie and W.W. Kerr, Trans. Faraday Soc.,55, 1050 (1959).
62. G.G. Cameron and N. Grassie, Polymer,2, 367 (1960).
63. G.G. Cameron and N. Grassie, Makromol. Chem.,51, 72 (1962).
64. G.G. Cameron and N. Grassie, Makromol. Chem.,51, 130 (1962).
65. G.G. Cameron, J. Appl. Polymer Sci.,9, 4025 (1965).
66. S.L. Madorsky, D. McIntyre, J.H. O'Mara and S. Straus,
J. Res. Natl. Bur. Std.,66,A, 307 (1962).
67. L.A. Wall, S. Straus, J.H. Flynn and D. McIntyre,
J. Phys. Chem.,70, 53 (1966).
68. L.A. Wall, S. Straus, R.E. Florin and L.J. Fetters,
J. Res. Natl. Bur. Std.,77,A, 157 (1973).
69. D.H. Richards and D.A. Salter, Polymer London,8, 127 (1967).
70. D.H. Richards and D.A. Salter, Polymer London,8, 139 (1967).
71. D.H. Richards and D.A. Salter, Polymer London,8, 153 (1967).
72. J.R. McCallum, Makromol. Chem.,83, 129 (1965).
73. G.G. Cameron, Makromol. Chem.,100, 255 (1967).

74. I.C. McNeill and S.I. Haider, Europ. Polym. J.,3, 551 (1967).
75. I.C. McNeill and T.M. Makhdumi, Europ. Polym. J.,3, 637 (1967).
76. G.G. Cameron and G.P. Kerr, Europ. Polym. J.,4, 709 (1968).
77. G.G. Cameron and G.P. Kerr, Europ. Polym. J.,6, 423 (1970).
78. G.G. Cameron , J.M. Meyer and I.T. McWalter, Macromolecules,11, 696 (1978).
79. S.L. Madorsky and S. Straus, J. Res. Nat. Bur. Std.40, 417 (1948).
80. I.C. McNeill, L. Ackerman and S.N. Gupta, J. Polym. Sci. Polym. Chem. Ed.,16, 2169 (1978).
81. S.L. Madorsky, Soc. Plastics Engineers J.,17, 665 (1961).
82. D.W. Brazier and G.H. Nickel, Rubber Chem. Technol.,48, 661 (1975).
83. S.L. Madorsky and S. Straus, J. Res. Natl. Bur. Std.,61, 77 (1958).
84. M.A. Golub and R.J. Gargiulo, J. Polym. Sci. Polym. Lett., 10, 41 (1972).
85. J.R. Shelton and L.H. Lee, Rubber Chem. Technol.,31, 415 (1958).
86. N.G. Gaylord, J. Kossler, M. Stolka and J. Vodehnal, J. Polym. Sci. A,2, 3969 (1964).
87. J.L. Binder, J. Polym. Sci. Polym. Lett. ,4, 19 (1966).
88. I. Kossler, J. Vodehnal, M. Stolka, J. Kalal and E. Hartlova, J. Polym. Sci.,C,16, 1311 (1967).
89. D.F. Lee, J. Scanlon and W.F. Watson, Proc. Roy. Soc. (London) A,273, 345 (1963).
90. V.S. Shagov, A.I. Yakubchik and V.N. Podosokorskaya, Vysokomol. Soyed,A,11(5), 968 (1969).
91. M.A. Golub and M. Sung, J. Polym. Sci. Polym. Lett., 11, 129 (1973).
92. M.A. Golub, J. Polym. Sci. Polym. Lett.,12,615 (1974).
93. N. Grassie and A. Heaney, J. Polym. Sci. Polym. Lett., 12, 89 (1974).
94. M. Host and D. Deur-Siftar, Chromatographia,5, 502 (1972).

95. S. Tamura and J.K. Gillham, J. Appl. Polym. Sci., 22, 1867 (1978).
96. E. Kiran and J.K. Gillham, J. Appl. Polym. Sci., 20, 931 (1976).
97. D.W. Brazier and N.V. Schwartz, J. Appl. Polym. Sci., 22, 113 (1978).
98. M.A. Golub, Rubber Chem. Technology, 51, 677 (1978).
99. I.C. McNeill and S.N. Gupta, Poly. Deg. And Stab., 2, 95 (1980).
100. A. Wall, Soc. Plast. Engrs. J., 8, 811 (1960).
101. A.A. Berlin, Pure Applied Chemistry, 36, 177 (1973).
102. A.A. Berlin, V.A. Grigorovskaya, V.P. Parini and K. Gafurov, Dokl. Akad. Nauk. SSSR, 156, 1371 (1964).
103. I.C. McNeill and D. Neil, Europ. Polym. J., 6, 143 (1970).
104. A.P. Titov and I.A. Livshits, Zh. Obshch. Khim., 29, 1605 (1959).
105. J. Scanlon, Trans. Faraday Soc., 50, 756 (1954).
106. F.M. Merrett, Trans Faraday Soc., 50 759 (1954).
107. W.I. Bengough and G.B. Park, Europ. Polym. J., 14, 889 (1978).
108. M.S. Matheson, E.E. Auer, E.B. Bevilacqua and E.J. Hart, J. Am. Chem. Soc., 73, 1700 (1951).
109. C.H. Bamford, A.D. Jenkins and R. Johnston, Proc. R. Soc. London, Ser A, 239, 214 (1957).
110. F.R. Mayo, J. Am. Chem. Soc., 65, 2324 (1943).
111. A.F. Bickel and W.A. Waters, Rec. Trav. Chim. Pays-Bas, 69, 1490 (1950).
112. W.H. Atkinson, C.H. Bamford and G.C. Eastmond, Trans. Faraday Soc., 66, 1446 (1970).
113. C.H. Bamford and E.F.T. White, Trans. Faraday Soc., 52, 716 (1956).
114. P.W. Allen, F.M. Merrett and J. Scanlon, Trans. Faraday Soc., 51, 95 (1955).

115. Beilstein,5,2, 81
116. W.A. Pryor and T.R. Fiske, *Macromolecules*,2, 62 (1969).
117. C.A. Baker and R.J.P. Williams, *J. Chem. Soc.*, 2352 (1956).
118. W. Patnode and W.J. Scheiber, *J. Am. Chem. Soc.*,61, 3449 (1939).
119. J.C. Bevington, J.H. Bradbury and G.M. Burnett, *J. Polym. Sci.*,12 469 (1954).
120. J.C. Bevington, *J. Chem. Soc.*, 3707 (1954).
121. G. Ayrey, K.L. Evans and D.J.D. Wong, *Europ. Polym. J.* 9, 1347 (1973).
122. J.C. Bevington and H.G. Troth, *Trans. Faraday Soc.*,58, 186 (1962).
123. D.H. Grant and N. Grassie, *J. Polym. Sci.*,42, 587 (1960).
124. M. Talât-Erben and S. Bywater, *J. Am. Chem. Soc.*,77, 3712 (1955).
125. G.S. Hammond, O.D. Trapp, R.T. Keys and D.L. Neff, *J. Am. Chem. Soc.*,81, 4878 (1959).
126. M. Talât-Erben and A.N. Isfendiyaroglu, *Canad. J. Chem.*, 37, 1165 (1959).
127. G.S. Hammond, C.H.S. Wu, O.D. Trapp, J.W. Warkentin and R.T. Keys, *J. Am. Chem. Soc.*,82, 5394 (1960).
128. J.C. Bevington, *Trans. Faraday Soc.*,51, 1392 (1955).
129. J.C. Bevington and T.D. Lewis, *Polymer*,1, 1 (1960).
130. E.M. Bevilacqua, *J. Am. Chem. Soc.*,77, 5394 (1955).
131. J.R. Shelton and W.L. Cox, *Ind. Eng. Chem.*,45, 392 (1953).
132. H. Hock and A. Neuwirth, *Ber.B.*,72 1562 (1939).
133. R. Criegee, H. Pilz and H. Flygare, *Ber.B.*,72 1799 (1939).
134. E.H. Farmer and D.A. Sutton, *J. Chem. Soc.*, 10 (1946).
135. J.L. Bolland, *Proc. Roy. Soc.*,A,186, 218 (1946).
136. J.L. Bolland, *Trans. Faraday Soc.*,46, 358 (1950).
137. J.R. Shelton, (Chapter) *Polymer Stabilisation*, (Ed). W.L. Hawkins, Wiley, New York (1972).

138. J.L. Bolland, Quart. Rev.,3, 1 (1949).
139. L. Bateman, H. Hughes, and A.L. Morris, Discuss. Faraday Soc.,14, 190 (1953).
140. L. Bateman and H. Hughes, J. Chem. Soc.,156, 4594 (1952).
141. P.D. Bartlett and G. Guaraldi, J. Am. Chem. Soc.,89, 4799 (1967).
142. G.A. Russell, J. Am. Chem. Soc.,79, 3871 (1957).
143. L. Bateman, Quart. Rev.,8, 147 (1954).
144. C.A. Coulson, Trans. Faraday Soc.,42, 265 (1946).
145. J.L. Bolland and H. Hughes, J. Chem. Soc.,153, 492 (1949).
146. E.M. Bevilacqua, Rubber Age New York,80, 271 (1956).
147. E.M. Bevilacqua, J. Am. Chem. Soc.,79 2915 (1957).
148. F.R. Mayo, Ind. Eng. Chem.,52, 614 (1960).
149. K. Egger, K.C. Irwin and F.R. Mayo, Rubber Chem. Technology, 41, 271 (1968).
150. E.M. Bevilacqua, E.S. English, J.S. Gall and P.M. Norling, J. Appl. Polym. Sci.,8, 1029 (1964).
151. M.A. Golub and M.S. Hsu, Rubber Chem. Technol.,48, 953 (1975).
152. J.L. Morand, Rubber Chem. Technol.,50, 373 (1977).
153. R.G. Bauman and S.H. Maron, J. Polym. Sci.,22, 203 (1956).
154. G.H. Miller, V.R. Larson and G.O. Pritchard, J. Polym. Sci.,61, 475 (1962).
155. R.V. Gemmer and M.A. Golub, p.79, Applications Of Polymer Spectroscopy, (Ed). E.G. Brame Jr. Academic Press Inc. (1978).
156. W.A. Patterson, Anal. Chem.,26, 823 (1954).
157. W.H.T. Davison, J. Chem. Soc., 3270 (1955).
158. D. Makino, M. Kobayashi and H. Tadokoro, Spectrochim. Acta,31A, 1481 (1975).
159. D.H. Grant and N. Grassie, Polymer,1, 125 (1960).